2016

On the bicyclic acids of petroleum

Wilde, Michael John

ON THE BICYCLIC ACIDS OF PETROLEUM

by

Michael John Wilde

A thesis submitted to Plymouth University

in partial fulfilment for the degree of

DOCTOR OF PHILOSOPHY

School of Geography, Earth and Environmental Sciences

December 2015

Acknowledgements

Author's Declaration

At no time during the registration for the degree of Doctor of Philosophy has the author been registered for any other University award without prior agreement of the Graduate Sub-Committee.

Work submitted for this research degree at the Plymouth University has not formed part of any other degree either at Plymouth University or at another establishment.

Relevant scientific conferences and workshops were regularly attended at which work was often presented and several papers prepared for publication.

Word count of main body of thesis: 70908

Signed: ……….*MfWilde*…………..

Date: …………09.05.2016…………..

Publications

1. **Wilde, M. J.** and Rowland, S. J. (2015) *Analytical Chemistry*, 87, 16, 8457-8465.

2. **Wilde, M. J.**, West, C. E., Scarlett, A. G., Jones, D., Frank, R. A., Hewitt, L. M. and Rowland S. J. (2015) *Journal of Chromatography A*, 1378, 74-87.

Related publications

3. Rowland, S. J., Pereira, A. S., Martin, J. W., Scarlett, A. G., West, C. E., Lengger, S. K., **Wilde**, **M. J.**, Pureveen, J., Tegelaar, E. W., Frank, R. A. and Hewitt, L. M. (2014) *Rapid Communications in Mass Spectrometry*, 28, 2352-2362.

4. West, C. E., Pureveen, J., Scarlett, A. G., Lengger, S. K., **Wilde**, **M. J.**, Korndorffer, F., Tegelaar, E. W. and Rowland, S. J. (2014) *Rapid Communications in Mass Spectrometry*, 28, 1023-1032.

Other publications

5. Coomber, R., Pavlidis, A., Santos, G. H., **Wilde**, **M. J.**, Schmidt, W. and Redshaw, C. H. (2015) *Journal of Performance Enhancement and Health*, In Press, available online 21st November.

6. Sutton, P. A., **Wilde**, **M. J.**, Martin, S. J., Cvačka, J., Vrkoslav, V. and Rowland, S. J. (2013) *Journal of Chromatography A*, 1297, 236-240.

Presentations

Oct 2015   Environmental and Food Analysis Special Interest Group Meeting of the British Mass Spectrometry Society (EFASIG/EMSSIG), Southampton, UK (prize for best lecture).

Jan 2015   6th Multidimensional Chromatography Workshop, Ministry of Environment and Climate Change, Toronto, CA.

Dec 2014   6th Annual Biogeochemistry Centre Conference (BGC), Plymouth, UK.

Nov 2014   Society of Environmental Toxicology and Chemistry Conference (SETAC), Vancouver, CA.

Aug 2014   Gordon Research Conference (GRC), Organic Geochemistry, Holderness, NH, USA (select as 1 of 3 for Hot Topics session).

Aug 2014   Gordon Research Seminar (GRS), Organic Geochemistry, Holderness, NH, USA. Poster presentation.

Jul 2014   25th Annual Meeting of the British Organic Geochemical Society (BOGS), Liverpool, UK (prize for best lecture).

Dec 2013   5th Annual Biogeochemistry Centre Conference (BGC), Plymouth, UK.

Jul 2013   24th Annual Meeting of the British Organic Geochemical Society (BOGS), Plymouth, UK.

Dec 2012   4th Annual Biogeochemistry Centre Conference (BGC), Plymouth, UK.

'I continue to have great troubles with the structure of the bicyclic naphthenic acid… everything that I have done with enormous expenditure of time and effort has led to too little… to recuperate, I have from time to time been working on other problems not connected with naphthenic acids.'

Prof Julius von Braun, 1931

x

On the bicyclic acids of petroleum

Michael John Wilde

Abstract

The identification of petroleum acids, also known as 'naphthenic' acids (NA), has been an analytical challenge for over 140 years. However, most recent interest in NA has arisen due to concerns over their presence and apparent associated toxic effect in oil platform produced waters and oil sands process waters (OSPW), respectively. Understanding the toxicity, transformations during biodegradation and remediation treatments and predicting the fate of NA in the environment will be aided by the identification of individual NA. However the elucidation of individual acid structures by standard chromatographic techniques, such as GC-MS, has so far been limited by the extreme complexity of the NA mixtures.

Recent analysis of NA as the methyl ester derivatives, by multidimensional gas chromatography-mass spectrometry (GC×GC-MS), has resulted in the identification of several tri- to pentacyclic, aromatic and sulphur-containing acids as well as tricyclic diacids. Therefore the current investigation focused on the identification of the abundant bicyclic acids in petroleum and OSPW acid extracts, utilising the unparalleled chromatographic separation and mass spectrometric detection offered by GC×GC-MS.

Analysis of fractionated NA as methyl esters, resulted in the first identification of several bicyclic acids in OSPW including several novel bridged bicyclic acids, several fused bicyclic acids, as well as some terpenoid-derived drimane and labdane acids. However, identifications were limited somewhat by a lack of reference mass spectra and lack of availability of reference compounds for co-chromatography.

A complementary method, based on an historical approach, involving reduction of NA esters to hydrocarbons, was modified and substantially improved. Analysis of the hydrocarbons resulting from the reduced acids, by GC×GC-MS, and comparison of the hydrocarbon mass spectra with the more abundant reference spectra available for petroleum hydrocarbons, resulted in the identification of over 40 individual bicyclic acids including fused, bridged and terpenoid-derived acids.

The study provides the most comprehensive analysis of one of the major classes of NA (the bicyclic acids) to date. The methods developed were applied to the structural elucidation of NA in commercial NA and OSPW NA and resulted in the identification of numerous alicyclic, aromatic and sulphur-containing acids, supporting and extending previous identifications.

There is clear potential for this method to be used for the identification of other unknown acids and functionalised biomarkers in complex matrices. The new knowledge of the acid structures in petroleum and OSPW NA can now be used to inform future research into the environmental monitoring and toxicity of NA.

Table of Contents

List of Tables

List of Figures

xxvii

consistent with condensed tricyclic, diaromatic sulphur-containing acid methyl esters,

Chapter 1

Introduction

1.1 Occurrences of carboxylic or 'naphthenic' acids

1.1.1 Crude oil and petroleum

Crude oil is an extremely complex mixture of compounds (Peters *et al.*, 2005b). The composition of petroleum can be categorised broadly into four major groups based on operational separations and solubility differences. These four groups are known as Saturates, Aromatics, Resins and Asphaltenes (SARA) (Waples, 1985; Hughey *et al.*, 2002). The most 'polar' constituents, which often contain nitrogen, sulphur or oxygen (NSO) are typically present in the Resin and Asphaltene fractions (Waples, 1985). An important class of 'polar' compounds in crude oil, despite being present at relatively low concentrations compared to the non-polar Saturate and Aromatic classes, is the carboxylic acids. The total acid content within a crude oil can vary between $0.1 - 3\%$, depending on geographical location, geological history and extent of biodegradation of the petroleum hydrocarbons (Lochte and Littmann, 1955; Hughey *et al.*, 2004). The carboxylic acids present in crude oils and bitumens have been the focus of much research since the early 1900s, mainly due to their importance in petroleum exploration, refining and processing, their industrial uses post-refining and more recently concerns over their fate and effects in the environment (Kennedy, 1939; Lochte and Littmann, 1955; Grewer *et al.*, 2010).

The carboxylic acids extracted from crude oils are also often termed 'naphthenic' acids (NA). The term is derived from 'naphthene', which is another name for alicyclic hydrocarbons (cycloalkanes), because the first identifications of NA were of monocyclic acids (Hell and Medinger, 1877). Later investigations showed some

petroleum acids were in fact aromatic and heteroatom-containing, so the term 'naphthenic' is not entirely accurate (Knotnerus, 1957; Seifert and Teeter, 1970a; b). Nonetheless the term is so embedded in use that it is retained by many petroleum scientists (Brown and Ulrich, 2015). Some authors differentiate between alicyclic, aromatic and heteroatom-containing acids, referring to the alicyclic acids as 'classical' NA, fitting the formula $C_nH_{2n+z}O_2$, where 'n' is carbon number and 'z' (a negative integer) is hydrogen deficiency due to cyclicity (Grewer *et al.*, 2010). The term 'petroleum acids', is also used, collectively referring to all types of acid in petroleum-related samples. Several other terms exist, mainly as a result of the increasing realisation by scientists of the actual complexity of so-called 'NA' mixtures (Headley *et al.*, 2013b; Grewer *et al.*, 2010). Thus, 'Acid-Extractable Organic' (AEO) fraction has been used to denote those acids extracted from oil sands process-affected waters (OSPW). High resolution mass spectrometric techniques have shown the presence of highly oxidized species or 'oxy-NA' and those containing other heteroatoms (e.g. N and S) in such materials. A recent, additional term used to describe the NA extracted from OSPW, agreed in an international workshop, was 'NA Fraction Components' (NAFCs) (Headley *et al.*, 2015). This was intended to encompass NA subclasses such as 'classical' NA, oxy-, aromatic and N or S-containing NA (Hindle *et al.*, 2013; Headley *et al.*, 2013b). The discovery of long-chain tetraprotic acids in petroleum and petroleum-related samples has seen the introduction of terms such as 'TPAs' or 'ARN' acids for this sub-class of acids (Smith *et al.*, 2007; Lutnaes *et al.*, 2007).

The total acidity of a crude oil is often expressed as a value of the Total Acid Number or 'TAN' value. This value reflects the mass of potassium hydroxide (KOH) in milligrams (mg) required to neutralise 1 g of oil at room temperature. Recorded TAN values for crude oils range from <0.1 to 8 mg KOH g^{-1} (Peters *et al.*, 2005b). The carboxylic acids present in crude oils are considered to be responsible for the main cause of this TAN

acidity. For instance, Meredith *et al.* (2000) showed a positive correlation ($r^2 = 0.91$) between the concentration of extracted acids and the TAN values of 33 different crude oils. The concentrations of carboxylic acids are generally highest in biodegraded crude oils and this is considered to be a result of the concurrent formation of the acids by the oxidation or microbial alteration of the non-polar or heteroatom-containing saturates and aromatics and the preferential removal of these hydrocarbons (Peters *et al.*, 2005a). Such observations are supported by the findings of Meredith *et al.* (2000), who also showed that higher extracted acid concentrations correlated strongly with crude oils with higher biodegradation levels ($r^2 = 0.86$). Despite this, the extent of biodegradation or the acid concentrations of oils cannot be directly inferred from the TAN values alone, as other compounds present in the crude oils, or acidic compounds not accounted for because they are not amenable with gas chromatographic methods, or are inefficiently extracted, may contribute to the TAN values (Meredith *et al.*, 2000; Peters *et al.*, 2005a).

The occurrence of organic acids in petroleum sometimes results in corrosive effects and deposition problems in refinery plant distillation units and pipelines (Derungs, 1956; Barrow *et al.*, 2003). NA corrosion has been shown to be dependent on several factors including temperature, fluid velocity and phase, and the specific composition of the NA (Derungs, 1956; Slavcheva *et al.*, 1999; Alvisi and Lins, 2011). The extent of corrosion has been shown to reach a maximum between operating temperatures of 200 – 400 °C, and typically occurs in areas where the acids are close to their boiling points (e.g. where concurrent vaporisation and condensing occurs in trays and walls of distillation columns and in bends and transfer lines which experience highest fluid velocities (Derungs, 1956; Alvisi and Lins, 2011)). Although oils or distilled fractions with higher TAN values generally show highest corrosivity, different crudes with the same TAN values have been reported to show different degrees of corrosion (Laredo *et al.*, 2004). The activity and corrosion rates of the acids has also been shown to vary with molar mass and

carbon number (Slavcheva *et al.*, 1999). Therefore, investigations into the nature and structures of NA are important areas of research into corrosion, with the aim of better understanding the mechanisms and key contributing factors.

Deposition problems caused by NA in crude oils reacting with cations (Ca^{2+}, Na^+ and K^+) present in formation or injected seawater within oil processing plants on production platforms, results in the formation of naphthenate soaps and deposits which cause flow assurance issues in oil pipelines and infrastructure (Dyer *et al.*, 2003). The incorporation of calcium can also reduce the market value of the produced crude oils (Turner and Smith, 2005). Sticky calcium naphthenate deposits trap other solids (e.g. sands and asphaltenes) in pipelines and when exposed to air they harden and cause blockages. A few studies investigating the composition of the resultant so-called 'calcium naphthenates' (CAN), report the presence of high molecular weight C_{80-82} acids containing 4-8 rings with four carboxylic acid groups ('ARN' acids) (Smith *et al.*, 2007).

Some of these higher molecular weight acids have been isolated and characterised by methods such as high temperature gas chromatography with a flame ionisation detector (HTGC-FID) of the permethyl esters, by electrospray ionisation-mass spectrometry (ESI-MS) and by nuclear magnetic resonance (NMR) spectroscopy of the acids or esters (Smith *et al.*, 2007; Lutnaes *et al.*, 2006; Lutnaes *et al.*, 2007).

1.1.2   Athabasca oil sands

The Athabasca oil sands in Alberta, Canada are a major oil reserve, with proven reserves of 175.2 billion barrels (Figure 1-1) (Rowling, 2012). Similar to the Orinoco Oil Belt, the bitumen in Alberta is contained within oil sands. The bitumen is extracted from the sand and clay by two main extraction processes; surface mining and Steam-Assisted Gravity Drainage (SAGD). Surface mining involves the extraction of bitumen from the ore mined at the surface using adaptations of the Clark hot water extraction

process. The mined ores are mixed with hot caustic water and the bitumen is extracted as the floating froth on the surface. Approximately 20% of the available bitumen within the oil sands region is recoverable by surface mining (Alberta-Energy, 2013). The remaining bitumen, deep below the surface requires other extraction techniques such as SAGD. This involves channelling two parallel pipelines deep into the bitumen rich sands. The upper pipeline carries hot steam down into the well which heats the bitumen within the sands, lowering its viscosity so it can be collected and pumped back to the surface.

Figure 1-1: Oil sands operation alongside the Athabasca River in Alberta, CA. (Image adapted from Droitsch (2015) and Frank *et al.* (2014)).

The process water from surface mining is recycled before being stored in large tailings ponds. The water soluble components of the ore or oil sands become concentrated within the so-called oil sands process-affected water (OSPW). The raw OSPW stored in the large lagoons has been shown to be toxic to bacteria (Jones *et al.*, 2011), plankton (Leung *et al.*, 2003), fish larvae (Scarlett *et al.*, 2013) and embryos (Marentette *et al.*, 2015a), fish (Kavanagh *et al.*, 2013), rats (Rogers *et al.*, 2002) and plants (Leishman *et al.*, 2013). The major class of compounds identified as causing the toxicity of the OSPW is the NA (Clemente and Fedorak, 2005; Grewer *et al.*, 2010).

Chapter 1

The rapid expansion of oil sands mining in Canada may be exemplified by a comparison of the predictions of Holowenko *et al.* (2002) with recent statistics given by the Government of Alberta. Holowenko *et al.* (2002) stated that the annual production of crude oil from oil sands was predicted to rise to 400 million barrels in a decade (e.g. by 2012). However, the Canadian Energy Research Institute released statistics for the daily production in 2013 of 1.98 million barrels which would approximately equate to an annual production of 723 million barrels per annum (CERI, 2014). Furthermore, daily production was predicted to double again in the next decade to 3.7 million barrels per day by 2020 and 5.2 million barrels per day by 2030 (CERI, 2014). The current area of the oil sands tailings ponds is approximately 176 km^2 (Alberta, 2011). Expanding production rates consequently means an increasing volume of toxic OSPW, resulting in a greater need to characterise the toxic pollutants such as NA in order to advance remediation plans.
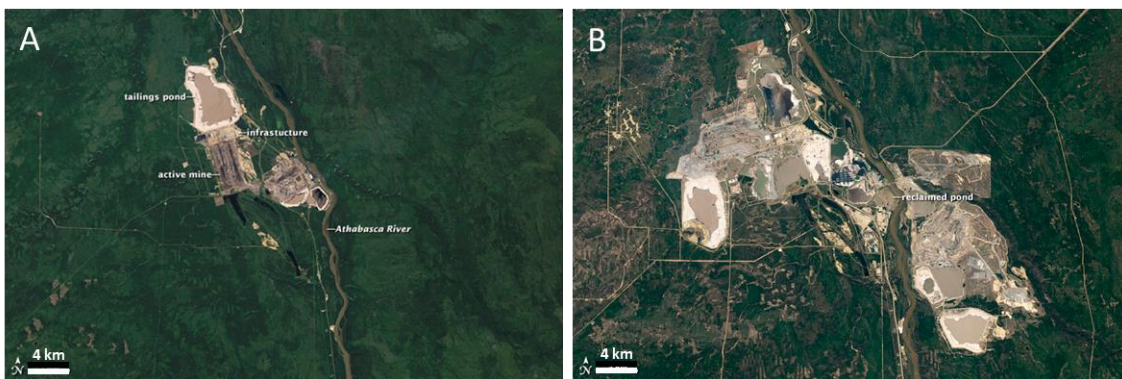
Figure 1-2: Satellite images of an area of oil sands mining industry showing the expansion between (A) 1984 and (B) 2011. (Images used from NASA Earth Observatory website (Riebeek, 2011)).

1.2 Early investigations of individual NA

The initial industrial interest in the isolation and characterisation of acid-extractable compounds from petroleum was due to the profitable uses to which the metal salts could be utilised (Seifert, 1975). Bulk crude mixtures of petroleum acid salts extracted and commercially isolated, were sold as additives in many products, such as drying agents in varnish and paints, as insecticides, as antifungals in wood preservatives and as dispersants in motor oils (Seifert, 1975; Lochte and Littmann, 1955). In World War II, the aluminium hydroxy soaps of NA were used to gelatinise petrol; when mixed with napalm in incendiary bombs the gelled petroleum stuck to targets such as buildings (Jolly, 1985; Lochte and Littmann, 1955).

In 1874, preliminary publications which are now recognised as the principal initial research into the characterisation of petroleum acids or NA, reported their isolation from Romanian oil (Hell and Medinger, 1874) and Baku petroleum (Lochte and Littmann, 1955; Ashumov, 1961). Hell and Medinger (1874) received a mixture of petroleum acids which they tried to separate by precipitation and fractional distillation, but both failed. However, after conversion of the acids to the ethyl esters, separation was achieved. Elemental analysis suggested three possibilities for the identity; that of a saturated $C_{11}H_{22}O_2$ compound, a monounsaturated $C_{11}H_{20}O_2$ compound or a di-unsaturated $C_{11}H_{18}O_2$ compound (Hell and Medinger, 1874). Further reactions with Br_2 and HBr showed substitution, not addition, ruling out unsaturated compounds. The reactions performed confirmed that the isolated product was unlike any known fatty acid, therefore the authors concluded that the isolated compound had a composition similar to oleic acid, but was cyclic (i.e. naphthenic). Thus the most probable formula was $C_{11}H_{20}O_2$, but due to the difficulties in purification, further confirmation was needed (Hell and Medinger, 1874; Lochte and Littmann, 1955).

The reported molecular formula gave the first structural information about the organic acids, suggesting they were cyclic structures following the general formula for monocyclic, monobasic NA of $C_nH_{2n-2}O_2$. The techniques utilised in early research to identify compounds may be considered primitive compared with the current instrumentation available, yet these early workers were able to deduce that the acids were cyclic (and not unsaturated) aliphatics by comparing the physical properties, such as refractive index with those of reference unsaturated acids with the same molecular formulae (Lochte and Littmann, 1955).

Eichler was involved in extracting 'illuminating oil' (i.e. lamp oil), from Baku petroleum when he was first challenged with acidic components in petroleum (cited by Henry (1905)). Eichler analysed a problematic sample of tinned oil which became colourised with time, changing from clear to dark brown after shipping: he deduced the colouration was due to organic acids within the oil reacting with iron, resulting in the oil having high iron content (Henry, 1905).

Whilst analysing Baku petroleum, Eichler was able to fractionate the organic acids and found that the molecular formula of one fraction matched the formula proposed by Hell and Medinger (1874) of $C_{11}H_{20}O_2$ (Lochte and Littmann, 1955). Markownikoff and Oglobin, in 1883 were also analysing Caucasian crude and confirmed the acidic components isolated previously by Hell and Medinger (1874) were carboxylic acids, after which they first proposed the term 'naphthenic acids' (cited by Jolly (1985)).

Interest in NA was not only spurred by industrial use; the acids also have importance in organic geochemistry. The origins of NA were thought to have potential links with the origins of other components in petroleum and thus might provide an insight into the origin of petroleum. The latter has often been a contentious subject. A key investigator during the early research of NA was von Braun, who believed that there was a genetic

relationship between the hydrocarbons and the organic acids (Lochte and Littmann, 1955). Identification of hydrocarbons had, up until then, progressed further than the identification of the organic acids, due to the difficulty of separating the more polar acids which relied on fractional distillation and recrystallization techniques.

Von Braun's approach involved the alteration of the acids by decarboxylation and reduction to hydrocarbons, as well as through degradation experiments, resulting in ketones and derivatives with lower carbon numbers (Lochte and Littmann, 1955). The degradation products were isolated and their physical properties used to determine structural detail. Accurate identification of the degraded compounds was then used to deduce the structures of the original acids. If the acids' carbon skeletons were found to be the same as those of the petroleum hydrocarbons, this was considered evidence for a genetic relationship between the acids and hydrocarbons.

Despite von Braun's rigorous work and unrelenting efforts, he struggled to identify the structure of any individual monocyclic or bicyclic acid (Lochte and Littmann, 1955). He was originally credited with isolating and identifying the first pure NA from petroleum, achieved by degrading a $C_{10}H_{18}O_2$ acid mixture to amines via the Schmidt reaction (Harkness and Bruun, 1940; Hancock and Lochte, 1939; Braun, 1938). He then degraded the amines to alkenes by Hofmann elimination and finally used ozonolysis to convert the alkenes to $C_8H_{14}O$ ketones. He isolated and purified what was believed to be an individual ketone and characterised its structure from its physical properties, such as the melting point of its semicarbazone and di-p-nitrobenzylidene derivatives, as well as logical deductions based on observed structures found in nature (Lochte and Littmann, 1955; Braun, 1938).

He identified the ketone as containing a five-membered ring, alkyl substituted at the 3 and/or 4 positions after comparing it with synthetic 3- and 4-ethylcyclohexanone

isomers, concluding it was 3,3,4-trimethylcyclopentanone (Figure 1-3; A) (Braun, 1938; Braun *et al.*, 1933). Braun et al. (1933) reported that this ketone, after similar degradation experiments, was found in Galician, Romanian, Californian, Texan and Venezuelan oils. He converted the ketone to 3,3,4-trimethylcyclopentylacetic acid and claimed this acid was a main constituent of Californian and Romanian acid fractions isolated between 148-155 °C at 12 mmHg (Lochte and Littmann, 1955; Braun *et al.*, 1933).

Afterwards, several attempts were made to replicate the isolation of von Braun's ketone and there were several efforts to synthesise 3,3,4-trimethylcyclopentanone (e.g. Buchman and Sargent (1942), Sargent (1942), Ruzicka *et al.* (1942), Ruzicka *et al.* (1947) and Baumgarten and Gleason (1951)) (Lochte and Littmann, 1955). After comparing the melting points of the synthesised 3,3,4-trimethylcyclopentanone semicarbazone and di-p-nitrobenzylidene derivatives with those of von Braun's ketone, it became quite apparent that von Braun's structural deductions were incorrect. Despite the misclassification of his ketone, von Braun's series of experiments were still important contributions to the advancement of organic geochemistry and natural product chemistry (Kraft *et al.*, 2005). Even Hancock and Lochte (1939) originally accepted von Braun's identification. Later, in the comprehensive report of petroleum acid history by Lochte and Littmann (1955), the authors devoted three chapters to von Braun's work and concluded the actual structure of von Braun's ketone was that of 3-ethyl-4-methylcyclopentanone (Figure 1-3; B).

Figure 1-3: Structures of (A) 3,3,4-trimethylcyclopentanone (von Braun's ketone) (Braun *et al.*, 1933) and (B) 3-ethyl-4-methylcyclpentanone (Lochte and Littmann, 1955).

The proposed link between the acids and hydrocarbons, led to the theory that such acids derived from hydrogenated aromatic structures and therefore also contained cyclohexyl rings; compounds in coal tar had been shown to be aromatic. However, the dehydrogenation of NA by 'Zelinsky's catalytic dehydrogenation' procedure, showed little or no evolution of hydrogen, suggesting no aromatic structures were formed (Zelinsky, 1924). Coupled with the observation that 3, 4, 7 and 8-membered rings were then uncommon in natural products, the next assumption was that the compounds mostly contained cyclopentyl rings, a theory reinforced by von Braun's work (Zelinsky, 1911; 1924; Zelinsky and Pokrowskaja, 1924).

Alteration of carboxylic acids to simpler or better understood compounds, such as hydrocarbons, was utilised during other early investigations (Goheen, 1940; Ashumov, 1961; Anbrokh *et al.*, 1972; Hoering, 1970; Harkness and Bruun, 1940). Seifert and co-workers, interested in the interfacial activity of carboxylic acids in Californian crude oil (Seifert and Howells, 1969; Seifert, 1969), developed an extensive extraction procedure to isolate the acids for subsequent GC-MS analysis of the fluoroalcohol derivatives (Seifert and Teeter, 1969). Key fragment ions of the fluoroalcohol esters, resulted in the partial elucidation of structural features such as the presence of saturated bicyclic acids with carboxylated side chains (Seifert and Teeter, 1969). Seifert *et al.* (1969) developed an alternative method for the identification of crude oil acids by conversion of isolated acids to their corresponding hydrocarbons, via alcohol and tosyl ester intermediates. At the time, the American Petroleum Institute (API) Project 6 had made significant advances in the structural identification of individual petroleum hydrocarbons (Rossini and Mair, 1958; Mair *et al.*, 1958a) contrasting with the few studies reporting the identification of acids, including some monocyclic and isoprenoid acids (Cason and Khodair, 1967a; b). This approach, adopted by Seifert and co-workers provided the first structural detail for many classes of NA including alicyclic, aromatic (Seifert and Teeter,

1970b), steroidal (Seifert *et al.*, 1972) and heteroatom-containing acid species (Seifert and Teeter, 1970a). However, in fact, only a few individual hydrocarbons (and thus acids) were identifiable due to insufficient chromatographic separation, which prevented assignable mass spectra from being obtained routinely.

The most common uses of NA up to the 1960s (e.g. as drying agents), did not necessitate the tedious and laborious challenge of isolating and characterising individual acids (Lochte and Littmann, 1955). Industry required no further development, so the research area became a quiet topic, despite having been a major topic of interest for many early researchers (e.g. Braun (1938); Lochte and Littmann (1955)). The lack of funds, coupled with continued difficulties in separation and purification of NA, meant progression in the elucidation of specific structures and determining the nature of individual NA was severely curtailed (Lochte and Littmann, 1955).

The beginning of mining in the Athabasca oil sands, coupled with the discovery of potassium naphthenates as plant growth stimulants, resulted in a brief revived interest in naphthenic acids in the 1970s (Seifert, 1975; Grewer *et al.*, 2010). However, few individual NA were identified and this has maintained ever since, until very recently.

In the last two decades, however, a combination of advancements in technologies, the increased exploitation of acid-rich crude oils (and consequentially the threat of toxic wastewaters) and increased pipeline corrosion problems, has resulted in an exponential increase and rapid expansion of publications investigating NA (reviewed by Grewer *et al.* (2010)). However, despite the power of modern techniques in helping to overcome some of the problems of the past, new difficulties have arisen.

1.3 The modern era of characterisation and structural identification of individual NA

The characterisation and structural identification of NA from different sources has been investigated utilising a vast range of different analytical techniques and instrumentation. The instrumentation used often includes an initial chromatographic separation by methods such as gas chromatography (GC) or high performance liquid chromatography (HPLC), followed by detection by mass spectrometry after ionisation by electron impact (EI) or electrospray ionisation (ESI). The ionisation technique used is dependent on its compatibility with the chromatographic eluents and the subsequent detectors, which may be high or low resolution mass spectrometers. Alternate ionisation techniques for the analysis of NA include fast atom bombardment (FAB-MS; now little used), or more commonly, atmospheric pressure chemical ionisation (APCI) or photoionisation (APPI). Many approaches involve extraction and preparative 'clean-up' or fractionations of the NA prior to analysis and include methods such as solid phase extraction (SPE), argentation chromatography (Ag-Ion) or ion exchange chromatography (IE). More involved preparation steps include preparative GC (prep-GC) and supercritical fluid extraction (SFE). Advanced chromatographic techniques include comprehensive multidimensional gas chromatography-mass spectrometry (GC×GC-MS), GC coupled with Fourier transform ion cyclotron resonance (FTICR) MS (e.g. GC-APCI-FTICR-MS and GC-TQ-FTICR-MS) and HPLC or supercritical fluid chromatography (SFC) coupled with Orbitrap MS (HPLC- or SFC-Orbitrap MS). Other techniques include direct infusion of the sample into a low or high resolution mass spectrometer without chromatographic separation (e.g. ESI-MS, ESI-FTICR-MS and ESI-Orbitrap MS), Fourier transform infrared spectroscopy (FT-IR) and field asymmetric ion mobility spectrometry (FAIMS). The extensive range of techniques, mainly involving mass spectrometry, have been summarised in numerous reviews published over the last

decade (Headley *et al.*, 2009b; Headley *et al.*, 2013b; Headley *et al.*, 2015; Grewer *et al.*, 2010; Zhao *et al.*, 2012; Brown and Ulrich, 2015).

The plethora of different methods for the identification and characterisation of NA all have advantages and disadvantages: currently there is no universal method which encompasses all that is desired for both qualitative and quantitative investigations. The natural variation between NA from different sources, coupled with the different extractions and sample preparations of NA or acid-extractable fractions, derivatisation methods, ionisation techniques, chromatographic conditions, mass spectrometer parameters and even presentation of data (Barrow *et al.*, 2009) are all factors which affect the apparent or actual, final compositions of NA and NA classes.

1.3.1 Gas chromatography and liquid chromatography with mass spectrometry

Gas chromatographic techniques usually require derivatisation of NA prior to analysis, if column lifetime is to be preserved and chromatographic resolution is to be maximised. Derivatisation of the polar carboxyl group improves the chromatographic properties and volatility of NA, making them more amenable for study. Numerous derivatisation options are available, the most common being production of methyl, trimethyl silyl (TMS) and *tert*-butyldimethylsilyl (tBDMS) esters; in earlier studies, particularly of acids in used cooking oils, picolinate esters were often studied (Gunstone, 2009).

One derivatisation procedure often adopted for GC-MS analysis of NA in modern times, including recently (e.g. Swigert et al., 2014 and Jie *et al.* (2015)) was that originally proposed by St. John *et al.* (1998), which involved reacting commercially available NA (sources undisclosed) with N-methyl-N-(*tert*-butyldimethylsilyl)-trifluoroacetamide (MTBSTFA) to produce the tBDMS esters. EI MS of such tBDMS esters of commercial NA usually results in spectra comprising abundant M-57 fragment ions, corresponding

to loss of the *tert*-butyl group from the molecular ion, which can then be monitored for the quantitation of each NA species (St. John *et al.*, 1998).

Holowenko *et al.* (2001) produced the tBDMS esters of NA extracted from OSPW for analysis by GC-MS. NA were suspected to be a source of substrate for methanogenic bacteria and thus thought to drive the methane production observed in OSPW tailings ponds (Holowenko *et al.*, 2000). Holowenko *et al.* (2001) suspected the OSPW NA were alicyclic, possessing 1 to 4 condensed cyclohexyl and cyclopentyl rings, with carboxylated alkyl side chains (Brient *et al.*, 2000). They suggested that β-oxidation of the carboxylated alkyl side chain would occur, resulting in the production of acetic acid and H_2, which are substrates used by methanogens in the production of methane (Holowenko *et al.*, 2001). However they eventually concluded that NA were an unlikely primary contributor to the production of methane in the OSPW tailings ponds (Holowenko *et al.*, 2001). They used their observations that certain 'surrogate' NA enhanced methane production with NA composition data obtained by GC-MS, to infer structural details about the NA. For example, n-hexadecanoic acid (z = 0) enhanced methane production, yet commercial NA did not, despite (according to the GC-MS selected ion monitoring data for the M-57 ions of the esters), the fact that the commercial NA contained 26% acyclic acids (z = 0) (Holowenko *et al.*, 2001). They suggested this correlation was evidence that the majority of acyclic acids in the commercial NA had branched alkyl chains, because these are more resistant to β-oxidation (Holowenko *et al.*, 2001).

The GC-MS method reported by Holowenko *et al.* (2001) showed significant differences between the compositions of a commercial NA mixture compared with NA extracted from OSPW. Therefore, Holowenko *et al.* (2002) applied the same GC-MS method for the analysis of NA extracted from nine different OSPW samples and a

sample of oil sands ore, in an attempt to differentiate samples from different sites based on NA composition. On the assumption that NA must fit the formula $C_nH_{2n+z}O_2$, plots of the relative abundance of each carbon number against 'z' value (hydrogen deficiency due to cyclicity), was used to produce a three dimensional bar chart (Figure 1-4) (Holowenko *et al.*, 2002). Such representations subsequently became a popular method of displaying NA 'profiles' (Figure 1-16; Section 1.5, page 47) (Bataineh *et al.*, 2006; Frank *et al.*, 2006; Martin *et al.*, 2008; Hindle *et al.*, 2013).
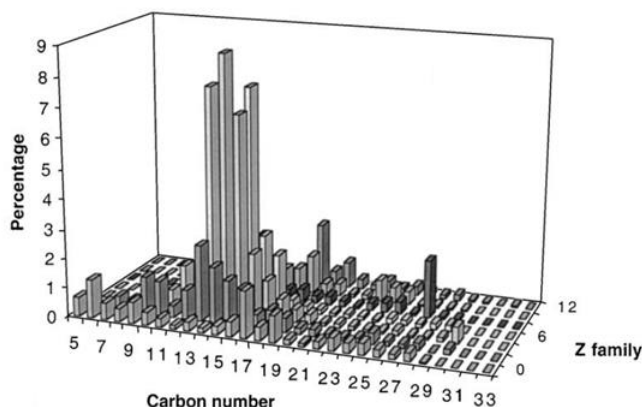
Figure 1-4: Example of a three dimensional bar chart showing the relative abundance of M-57 ions for compounds fitting the formula $C_nH_{2n+z}O_2$, suggested to show the NA distribution of OSPW from the Mildred Lake Settling Basin, by carbon number and z-value (Holowenko *et al.*, 2002).

The authors observed a bimodal acids distribution in several samples and identified two groups; $<C_{21}$ acids with a maximum at C_{13-17} and a '$C_{22}+$ cluster' with a maximum around C_{24-27}. The $C_{22}+$ cluster was the collective term used to describe the appearance of a group of purportedly higher molecular weight acids. The $C_{22}+$ cluster had a higher relative abundance in NA extracts from aged, heavily biodegraded OSPW samples, proposed to be due to the preferential removal of the lower molecular weight acids during ageing (Holowenko *et al.*, 2002). They suggested that the $C_{22}+$ cluster could be used as a parameter to distinguish between samples, since the relative abundance of the

$C_{22}+$ cluster appeared to correlate with the age of the OSPW and was higher in samples with lower total NA concentrations and lower toxicities (Holowenko *et al.*, 2002).

Clemente *et al.* (2004) were possibly the first to comment on a possible limitation of such derivatisations with unit resolution GC-MS methods. Whilst Holowenko *et al.* (2002) designated ions $\geq$ *m/z* 385 ([M-57] ion of a C_{22}, z = -12 acid) which fitted the formula $C_nH_{2n+z}O_2$, as part of the '$C_{22}+$ cluster', Clemente *et al.* (2004) noted that any hydroxy acids or di-acids present in the samples, might form the bis-derivatised tBDMS ether/ester or di-esters, respectively, with use of the MTBSTFA derivatisation reagent. This bis derivatisation would dramatically increase the mass of low molecular weight hydroxy acids or di-acids and would possibly result in their misclassification as high molecular weight acids as part of the '$C_{22}+$ cluster' (Figure 1-5).

C_{12} z = -6 diacid

m/z 395 possibly mis-assigned

as C_{22}, z = -2 acid
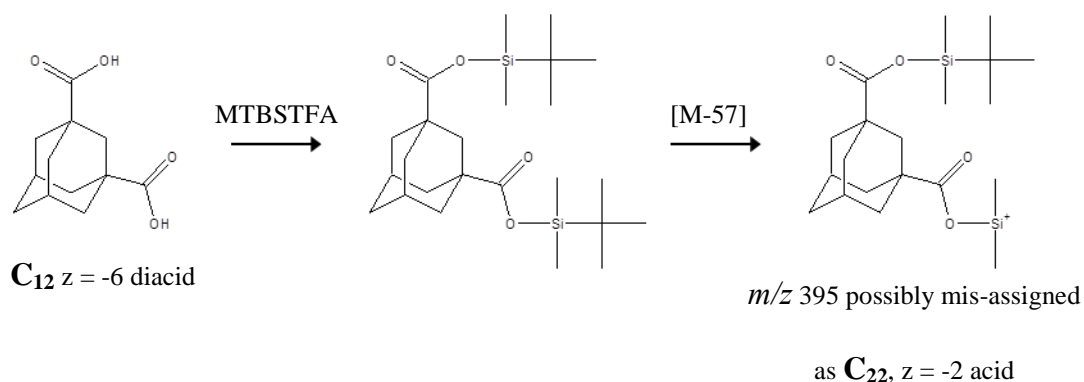
Figure 1-5: Example of a possible C_{12} z = -6 (tricyclic) tBDMS di-ester misclassified as a C_{22} z = -2 (monocyclic) monoester after derivatisation with MTBSTFA, as highlighted by Clemente *et al.* (2004). Diacids such as 1,3-adamantane-dicarboxylic acid were later shown to be present in an OSPW extract following bis-derivatisation with BF_3/methanol as the dimethyl esters, identified by GC×GC high resolution MS of the molecular and fragment ions and co-chromatography with authentic compounds (Lengger *et al.*, 2013).

Despite their acknowledged doubts surrounding the identification of the '$C_{22}+$ cluster', Clemente *et al.* (2004) still referred to this feature when comparing the extent of

biodegradation of two commercial acid samples, determining the relative abundance of different carbon number classes by GC-MS of the tBDMS derivatives.

Bataineh *et al.* (2006) developed a comprehensive HPLC-qTOF-MS method to monitor compositional changes in NA mixtures, and also for the characterisation of transformation products, after the microbial biodegradation of commercial and OSPW NA. Selected ion mass chromatograms showed that the use of HPLC prior to ESI-MS resulted in separation of the NA by carbon number and z-value, allowing quantification of individual NA isomer classes. Comparison of the quantification by this method to that obtained by direct infusion showed a significant increase in sensitivity and better linearity across a range of NA concentrations using the HPLC method (Bataineh *et al.*, 2006). They reported that the matrix effects of the tailings water on the model acids resulted in up to 21% suppression of ion formation for C_{12-24} model compounds. However, even this was relatively small compared with the suppression observed for a monocyclic C_8 model acid by 33% (Bataineh *et al.*, 2006). The matrix effects of tailings water reported by Bataineh *et al.* (2006) were significantly lower than the 50% enhanced responses reported by Lo *et al.* (2003) observed for similar model compounds analysed by direct infusion ESI-MS without HPLC separation in a simple six compound mixture.

Bataineh *et al.* (2006) also utilised the power of high resolution mass spectrometry (HRMS) (<10 ppm mass accuracy) to produce three dimensional NA profiles (relative abundance of carbon number vs. z-value) using their HPLC-MS method on the free acids and compared them with reproduced unit resolution GC-MS data using the method reported by Holowenko *et al.* (2002). Their HPLC-MS NA profile for refined Merichem NA (commercial sample) matched the GC-MS profile, which again was similar to the GC-MS profile reported by Clemente *et al.* (2003) for the same NA

supplier by the same method. The abundant acid classes in the refined Merichem NA were $z = 0$ to -4 acids (Bataineh *et al.*, 2006). The HPLC-MS profile for the NA extracted from OSPW however, was significantly different to the GC-MS profile; the GC-MS profile was significantly more complex, with a similar 'C$_{22}$+ cluster' to that reported previously by Holowenko *et al.* (2002) which was absent in the HPLC-MS profile (Figure 1-6). Bataineh *et al.* (2006) suggested the increased complexity and appearance of apparently 'high molecular weight acids' in the GC-MS profile was due to misclassification of nominally isobaric species (e.g. hydroxy acids with two derivatised functional groups), not distinguishable using low resolution mass spectrometry. Bataineh *et al.* (2006), using GC-HRMS confirmed the presence of more highly oxidised species misclassified as high molecular weight acids, previously highlighted by Clemente *et al.* (2004), showing that three ions originally classified as C$_{23-25}$ $z = 0$ acids had accurate masses corresponding to C$_{22-24}$H$_{43-47}$Si$_2$O$_3$ i.e. C$_{14}$ bis-derivatised acids (Bataineh *et al.*, 2006).
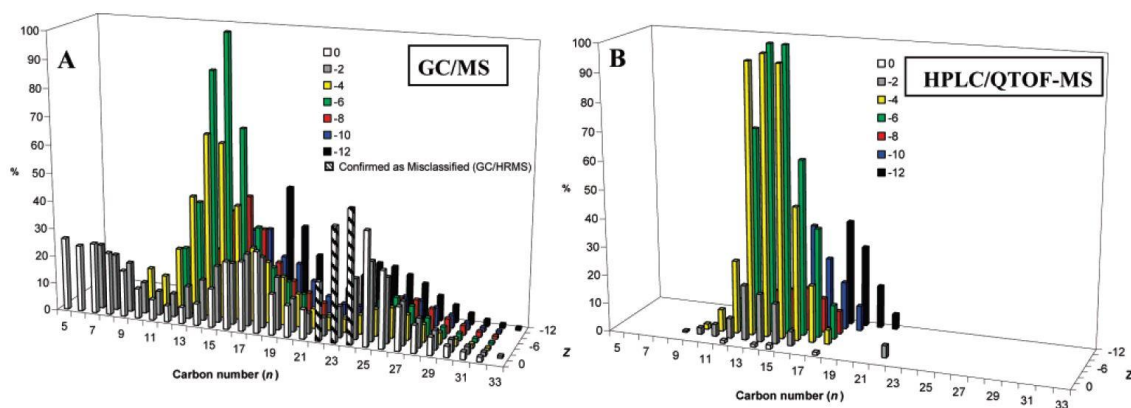
Figure 1-6: Naphthenic acid profiles produced by (A) unit resolution GC-MS of the tBDMS derivatives and (B) HPLC-qTOF-MS of the free NA. Hatched bars shown for the GC-MS-derived data were assigned to ions then confirmed by GC-HRMS to be indicative of bis-derivatised species (Bataineh *et al.*, 2006).

Despite showing the use of HRMS data to distinguish between nominally isobaric species from their mass spectra, Bataineh *et al.* (2006) were unable to further identify the O_3 species; their method lacked the ability to differentiate between isomers of the same molecular formula (e.g. between a C_{10} monocyclic hydroxy acid and a C_{10} acyclic keto acid). The structure of a monocyclic hydroxy acid could be substantially different to that of an acyclic keto acid, particularly for compounds with a higher carbon number, which may be important when considering the toxicity of acids.

The lack of structural information about the nature of the NA present in both commercial and OSPW NA also meant the quantification reported by Bataineh *et al.* (2006) of individual NA classes was not fully quantitative. Absolute concentrations were unattainable because no representative reference compounds for each NA class were available, the composition of NA isomers was unknown and the calibration curves were plotted using varying concentrations of commercial NA. Many investigations have shown that the composition of commercial NA is different to NA extracted from OSPW (Bataineh *et al.*, 2006; Grewer *et al.*, 2010; Barrow *et al.*, 2004). Lo *et al.* (2003) argued that model acids with substantially different structures to each other showed ion responses within 50% of each other. However Bataineh *et al.* (2006) acknowledged that the method was optimised on the non-biodegraded NA and that other acids and more oxidised acid species produced upon biodegradation, would likely show differences in electrospray ionisation efficiency.

Smith and Rowland (2008) investigated the derivatisation of naphthenic acids to their corresponding amides, prior to their analysis using HPLC/ESI-MS[n]. Conversion of the acids to the amides resulted in an increased detection response and reproducible fragment ions in sequential mass spectrometry studies (Smith and Rowland, 2008). The method required further development to produce quantitative results and definitive

structures for the NA could not be assigned. However the use of HPLC provided sufficient separation and the derivatisation proved effective for the identification of key structural details such as the presence and length of alkanoic chains, with acetic chains as the most abundant.

Wang and Kasperski (2010) developed an alternative HPLC-MS/MS method, using low resolution mass spectrometry. The use of HPLC prior to detection, afforded sufficient separation of NA classes based on carbon number and z-value within a commercial NA mixture, again allowing semi-quantitation of different isomer classes (Wang and Kasperski, 2010). To avoid misclassification of NA due to the unit mass resolution, Wang and Kasperski (2010) plotted z-value against retention times, producing curves for individual carbon numbers. They proposed that the retention times of peaks identified as NA within other environmental samples could then be compared with these curves, established using commercial NA (Wang and Kasperski, 2010). However, this method of checking the classification of NA without high resolution MS was not confirmed since these workers did not give an example of a compound previously or potentially misclassified as an NA being identifiable based on retention time. The carbon number curves they produced were not sufficiently separated to be reliable, especially for more complex environmental samples such as NA from OSPW, which had been shown previously to produce NA isomer classes with a wide range of retention times (Bataineh *et al.*, 2006). Also, the method relied on the assumption that the commercial NA contained only acids which fitted their assumed definition of NA (i.e. were saturated acids possessing the formula $C_nH_{2n+z}O_2$). Towards the higher z-values ($\geq$ z = -8) the curves overlapped; C_{17} and C_{18} z = -8 acids eluted before C_{14} and C_{15} z = -8 acids respectively and even C_{20} z = -10 acids eluted before C_{13} z = -10 acids. This was possibly due to the presence of aromatic species present in the commercial NA; aromatic acids often possess retention times different from those of alicyclic acids with

the same hydrogen deficiency, increasing the variation of retention times within the same isomer class.

Wang and Kasperski (2010) designed their HPLC-MS/MS method so that no sample pre-treatment was necessary, in order to eliminate alterations in the NA composition caused during extraction. They selected a C_8 column over the C_{18} column previously used by Bataineh *et al.* (2006) because process chemicals assumed likely to be in OSPW, such as benzalkonium chlorides, were difficult to elute through the C_{18} column and their mobile phase gradient started at 30% methanol, allowing sufficient solubility and subsequent elution of inorganic salts within the first 5 minutes, prior to any NA. However, Wang and Kasperski (2010) did not demonstrate their method using more complex environmental samples, such as NA in OSPW.

Shang *et al.* (2013) developed a HPLC-MS method for the rapid screening of NA in environmental surface water samples. Their method likewise involved no sample pre-treatment and similarly to the method described by Wang and Kasperski (2010), aimed to remove any salts and highly polar species prior to elution of the NA, achieved with an initially high aqueous mobile phase for the first 5 minutes. Salts can cause ion suppression and influence ion detection (e.g. sodiated ions can form instead of the deprotonated species, not seen in (-)ESI (Barrow *et al.*, 2010)). Shang *et al.* (2013) acknowledged the limitations of calibrating their method using commercial NA mixtures for quantifying NA concentrations within Athabasca River surface water samples, again showing there were significant compositional differences even between three different commercial NA mixtures. Shang *et al.* (2013) recorded full scan data over a limited scan range from *m/z* 150-350 and reported 90% of a commercial NA mixture was within this mass range. However, when developing a method for environmental samples, where the NA composition is unknown, limiting the scan range

could result in an unknown, possibly higher, proportion of components unaccounted for, giving overall unreliable quantitation of NA.

Hindle *et al.* (2013) and Brunswick *et al.* (2015) highlighted and summarised issues facing most HPLC-MS and ESI-MS methods for the quantification of NA (specifically $C_nH_{2+z}O_{2-4}$, termed 'oxy-NA' by these authors) in aqueous environmental samples such as OSPW. Hindle *et al.* (2013) showed that calibrations needed to be performed using complex mixtures of NA and for true quantification, the NA mixtures would have to possess a similar NA composition, distribution and structures to the NA sample being measured. They showed that the response factors of 39 'model' NA with differing structures varied considerably, contrary to the data reported by Lo *et al.* (2003). They therefore concluded that selecting small mixtures of 'model' NA to be representative of the vast number of isomers present in NA mixtures within environmental samples was impractical (Hindle *et al.*, 2013). They acknowledged that use of an average response factor for all the oxy-NA within an NA mixture might provide better quantification (Hindle *et al.*, 2013). They analysed four commercial acid mixtures which revealed distinct differences between suppliers and showed the NA concentrations of several 'real world' samples, calibrated with two different commercial NA mixtures, produced a 2-fold difference in final total NA concentrations (Hindle *et al.*, 2013). Martin *et al.* (2008) and Zhao *et al.* (2012) had suggested the reduced extent of branching and cyclicity assumed for the NA in the commercial NA made the commercial NA more hydrophobic in nature and therefore that they might preferably migrate to the surface of the droplets produced during ESI, resulting in a higher response of commercial NA in ESI-MS. The HPLC-MS method developed by Hindle *et al.* (2013) showed strong potential for the quantification of NA when representative OSPW NA reference mixtures of varying ages and levels of biodegradation eventually become available.

Brunswick *et al.* (2015) used a similarly comprehensive HPLC-MS method to Hindle *et al.* (2013), but used larger injection volumes of samples to improve detection limits for the analysis of trace concentrations of NA. Their method showed that some $C_nH_{2n+z}O_2$ species in both commercial Merichem NA (technical grade) and NA extracted from OSPW had similar retention times. For example, $C_{15}H_{26}O_2$ (z = -4) isomers in both Merichem NA and a fresh OSPW acid extract, eluted between 8.0 and 9.0 min. Differences between the commercial NA and NA from OSPW included the detection of 'polyoxy' or $C_nH_{2n+z}O_3$ and $C_nH_{2n+z}O_4$ species in OSPW samples, identified by the high resolution and mass accuracy of the mass spectrometer utilized. This highlighted both advantages and limitations of the method. They were able to detect and semi-quantify whole carbon number classes that would otherwise not have been reliably assignable by unit resolution mass spectrometry methods. However, even the NA classes that were supposedly similar in both OSPW NA and commercial NA based on their HPLC retention times, may have possessed different structures with varying response factors, meaning the method would remain 'semi'-quantitative until further knowledge of the structural nature of the NA in both mixtures became known.

Brunswick *et al.* (2015) stated that adamantane-1-carboxylic acid was absent or below the limit of detection in NA extracts from fresh, aged and raw OSPW despite being shown to be a component of OSPW, albeit a minor component, by other techniques which involved derivatisation with BF_3/methanol prior to analysis (Rowland *et al.*, 2011c). They showed their method was capable of measuring $C_{11}H_{16}O_2$ (z = -6) acids in full scan mode, producing a linear calibration with adamantane-1-carboxylic acid from 10 μg L^{-1}. Brunswick *et al.* (2015) acknowledged that other trace, almost absent, sulphur-containing NA, which had also been identified by other techniques requiring derivatisation (West *et al.*, 2014b), may be below their limit of detection but also suggested they could be artefacts introduced by sample clean-up or processing

procedures. Discrepancies between the methods therefore suggest that either some NA identified using techniques requiring derivatisation (e.g. GC×GC-MS) are artefacts of the sample preparation (as suggested by Brunswick *et al.* (2015)) or that techniques such as GC×GC following derivatisation are more sensitive and more specific than the HPLC-MS methods used to date.

1.3.2 Fourier transform ion cyclotron resonance mass spectrometry and Orbitrap mass spectrometry

Fourier transform ion cyclotron resonance-mass spectrometry (FTICR-MS) and Orbitrap-mass spectrometry (Orbitrap-MS) have been utilised for the analysis of complex NA mixtures in crude oils (Qian *et al.*, 2001; Barrow *et al.*, 2003; Stanford *et al.*, 2007), naphthenate deposits (Mapolelo *et al.*, 2011), OSPW (Barrow *et al.*, 2010; Headley *et al.*, 2009a), treated OSPW (Headley *et al.*, 2014; Pereira *et al.*, 2013b), contaminated environmental water samples (Yi *et al.*, 2015; Ahad *et al.*, 2013) and plant tissues (Headley *et al.*, 2011b) due to their inherent ultra-high mass resolution and mass accuracy.

Barrow *et al.* (2003) used FTICR-MS to analyse the NA content of two crude oils from West Africa. They focused on 'classical' NA and the ultra-high resolving power of FTICR-MS showed the presence of 'doublets', distinguishing between a z = -2 $C_{25}H_{48}O_2$ compound (theoretical mass: 379.35815 amu) and a z = -16 $C_{26}H_{36}O_2$ compound (theoretical mass: 379.26425 amu), which would otherwise have been misclassified. Plots of carbon number against relative intensity for each z-series showed both crude oil extracts were dominated by z = -2 (monocyclic), z = -4 (bicyclic) and z = -6 (tricyclic) acids. Subsequently, Barrow *et al.* (2004) applied their FTICR-MS method to the analysis of NA in two commercial acid mixtures and NA from a sample of OSPW. The composition of the NA in OSPW was again shown to be substantially more

complex (Barrow *et al.*, 2004). Whilst z = -2, -4 and -6 were abundant in all three samples, the Acros commercial NA was heavily dominated by z = 0 acids (acyclic) and the OSPW NA contained an abundant class of C_{15-20} z = -12 acids corresponding with the results reported by other techniques (Barrow *et al.*, 2004; Grewer *et al.*, 2010; Hindle *et al.*, 2013). FTICR-MS was unable to determine if the z = -12 acids were saturated hexacyclic or monoaromatic tricyclic acids.

Stanford *et al.* (2007) analysed the water soluble acidic, basic and neutral compounds from North and South American and Middle Eastern crude oils by FTICR-MS. They mainly focused on NSO-containing species within the basic and neutral fractions of water-soluble organics, but did note a low abundance of pyrrolic NO_x species and SO_3 species present in the acidic water-soluble organic fraction (Stanford *et al.*, 2007). They observed that the most abundant 'classical' NA (acidic $C_nH_{2n+z}O_2$ species) in the water-soluble acidic fraction were low molecular weight acyclic acids, as well as acids with a high number of double bond equivalents (DBE) and concluded the latter were most likely aromatic since aromatic acid solubility was shown to be greater than the solubility of 'naphthenic' non-aromatic acids (Stanford *et al.*, 2007).

Headley *et al.* (2007) investigated the effect of solvent on the relative abundance of $C_nH_{2n+z}O_2$ and $C_nH_{2n+z}O_4$ species in NA extracted from OSPW detected by FTICR-MS. The most abundant $C_nH_{2n+z}O_2$ NA observed in all the solvent systems were z = -4, -6 and -12, similar to the OSPW NA profile previously reported by Barrow *et al.* (2004). However, the relative intensity of all the $C_nH_{2n+z}O_2$ species when using ACN/octanol as the solvent, was significantly reduced and the use of ACN/DCM considerably enhanced the relative abundance of z = -12 $C_nH_{2n+z}O_2$ species (Headley *et al.*, 2007). Conversely, the most abundant $C_nH_{2n+z}O_4$ species were z = -6, -8 and -4 and their relative abundance was significantly greater when using ACN/octanol and were dramatically less, almost

absent, in ACN/DCM (Headley *et al.*, 2007). The ACN/1-octanol solvent system also showed an apparently higher proportion of higher molecular weight NA.

Headley *et al.* (2007) suggested the difference in the relative abundance of $C_nH_{2n+z}O_2$ and $C_nH_{2n+z}O_4$ species in the octanol and DCM solvent systems was due to differences in the solubility of certain NA species. They further inferred that as octanol was the most representative solvent of fatty tissue, the NA species observed in the ACN/octanol solvent system, such as $C_nH_{2n+z}O_4$ species (potentially diacids), were indicative of the most bioavailable NA structures (Headley *et al.*, 2007). However, the bioavailability and uptake of compounds by organisms is more complex and reliant on variables other than solubility alone. Frank *et al.* (2009) showed the toxicities of C_{4-10}, z = 0 to -2, dicarboxylic acids ($C_nH_{2n+z}O_4$) to be lower than those of monocarboxylic acids with similar overall structures. However these 'surrogate' acids were not representative of the abundant C_{11-18}, z = -6 $C_nH_{2n+z}O_4$ species detected by Headley *et al.* (2007) in ACN/octanol. Since these studies, some z = -6, $C_nH_{2n+z}O_4$ species such as adamantane-1,3-dicarboxylic acid have been identified in NA from OSPW, therefore representative reference compounds could now be used to quantify and study the bioavailability of such species (Lengger *et al.*, 2013).

Barrow *et al.* (2010) acknowledged that the toxicity of the OSPW may be attributed to more than the content of so-called 'classical' NA detectable by negative ion ESI-MS techniques. Therefore they used both APPI- and ESI-FTICR-MS, in positive and negative ion mode, to examine the complete composition of the organic constituents in OSPW. APPI in positive ion mode proved capable of detecting the broadest range of different compound classes, e.g. hydrocarbons, heteroatom-containing hydrocarbons, acids and heteroatom-containing acids (Barrow *et al.*, 2010). All four ionisation methods showed that O_x species were the most abundant species in OSPW with ESI in

negative ion mode showing the most intense signal for O_x species, highlighting its usefulness for analysing NA. The 'classical' NA ($C_nH_{2n+z}O_2$) profiles produced by ESI and APPI in negative ion mode again showed z = -6, -4 and -12 as the three major classes of NA with z = -12 NA dramatically enhanced in the APPI profile. The increased abundance of z = -12 acids was suggested to be due to the use of toluene in the solvent for APPI. However, interestingly, Headley *et al.* (2007) reported a similar NA profile when using ACN/DCM with ESI.

The challenge facing environmental monitoring, to determine to what extent OSPW stored within the large tailings lagoons or the surrounding bunds maybe leaking and contaminating the surrounding environment, is that the surrounding groundwater and rivers contain natural concentrations of similarly bitumen-derived organic components such as NA, due to the naturally high bituminous content of the land and river banks.

Headley *et al.* (2011a) attempted to use FTICR-MS (with negative ion ESI) to 'fingerprint' samples in order to differentiate OSPW from nearby river and lake sites. Use of Principal Components Analysis (PCA) data for all the compound classes detected, arguably differentiated between OSPW from two different industries and OSPW from Athabasca River water. The main differences were that both OSPW samples contained a smaller range of O_x species, with O_1-O_8 species detected in the OSPW samples as opposed to O_1-O_{14} species detected in the river and lake water (Headley *et al.*, 2011a).

Ahad *et al.* (2012) developed a unique isolation and separation method for the so-called acidic-extractable organic (AEO) fraction of OSPW and environmental samples. They used SPE and preparative GC prior to analysis by Orbitrap-MS and intramolecular isotopic characterisation ($\delta^{13}C_{pyr}$) (Ahad *et al.*, 2012). Ahad *et al.* (2013) showed this method could be used to distinguish between AEO from natural background substances,

such as humic acids, from bitumen-derived AEOs, since bitumen-derived AEO had substantially higher $\delta^{13}C_{pyr}$ values. Such a differentiation was also achieved by Ross *et al.* (2012) but instead using HPLC-HRMS to observe key differences between the NA profiles of environmental and industrial samples. However, the method of Ahad *et al.* (2013) could not distinguish between AEO from natural bitumen sources and OSPW. The structural identification of individual NA indicative of an OSPW source could aid such studies aimed at differentiating between AEO sources.

Frank *et al.* (2014) correlated Orbitrap-MS data with the presence or absence of specific monoaromatic compounds detectable by GC×GC-MS (Rowland *et al.*, 2011d), to differentiate between AEO from natural waters and OSPW. They proposed that a high $C_nH_{2n+z}O_2$: $C_nH_{2n+z}O_4$ ratio detected by Orbitrap-MS along with the presence of two groups of unidentified monoaromatic acids detected by GC×GC-MS, was indicative of AEO from OSPW. However, Yi *et al.* (2015) showed the $C_nH_{2n+z}O_2$: $C_nH_{2n+z}O_4$ ratios of AEO from snow and water samples collected near and far from OSPW storage sites varied considerably from the values reported by Frank *et al.* (2014). The discrepancy between the two methods could be due to the differences in sample pre-treatment and extraction of AEO.

High resolution HPLC-MS, FTICR-MS and Orbitrap-MS methods show good potential for the rapid, routine analysis of NA without sample pre-treatment since the data can be used to distinguish and detect a range of compound classes that might be misclassified by unit resolution techniques. The ability to perform analyses without sample pre-treatment avoids biasing the data; the extraction efficiencies of different NA being dependent on solvent (Headley *et al.*, 2007). Despite this, methods which have utilised pre-fractionation steps have shown a significant increase in the number of identifiable compounds, indicating that perhaps methods without pre-treatment may be

misrepresenting the overall complexity of these mixtures. Rowland *et al.* (2014b) and Nyakas *et al.* (2013) used SPE and offline ultra-HPLC respectively, to pre-fractionate OSPW NA to avoid ion suppression of certain species caused by competing components; both techniques revealed extended series of NA.

The most recently developed methods utilising ultra-high resolution FTICR- and Orbitrap-MS for the analysis of NA involved interfacing the advanced mass spectrometers with chromatographic instrumentation, as opposed to a separate fractionation step before analysis. Ortiz *et al.* (2014) and Barrow *et al.* (2014) both developed techniques, interfacing gas chromatography with FTICR-MS. The instrumentation described by Ortiz *et al.* (2014) separated components through a GC column which were then ionised by EI or CI. Ions were then directed via a triple-quadrupole into the FTICR-MS (Ortiz *et al.*, 2014). Barrow *et al.* (2014) separated the compounds in a similar manner, through a GC column, which was coupled to an APCI source, which was then coupled to a FTICR-MS. Combination of GC with ultra-high mass resolution allowed characterisation of isomer classes as a function of retention time, not only separating isobaric compounds by high mass resolution but also separating isomers of the same class by GC.

Pereira *et al.* (2013a) interfaced HPLC with Orbitrap-MS to analysis AEO from two types of OSPW; process water used in surface mining operations and re-used process water from *in-situ* extraction methods (e.g. SAGD). Orbitrap-MS data could only be used to show the differences in compound classes present. However, combination with HPLC provided retention time data; therefore compounds with the same molecular formula could also be separated (Pereira *et al.*, 2013a). Pereira and Martin (2014) developed their method further and integrated an online SPE step with their HPLC-Orbitrap method to remove the need of sample preparation before analysis.

The advantage of coupling a chromatographic step with ultra-high resolution mass spectrometer achieves effectively, two modes for distinguishing NA species. Three dimensional plots of the relative abundance of accurate mass m/z values, or of extracted ions of isobaric species, can be plotted against retention times. The HPLC or GC steps give what is described by Barrow *et al.* (2014) as an additional 'dimension' for characterising complex mixtures.

Despite this additional separation achieved by GC and UPLC coupled with FTICR-MS and Orbitrap-MS, the structural elucidation of NA using such techniques has not been demonstrated. The most structural detail obtained by such techniques was achieved by Rowland *et al.* (2014a), who utilised FTICR-MS and UPLC-Orbitrap-MS to partially identify polar species isolated from OSPW NA after Ag-Ion pre-fractionation, eluting the retained, more polar, organics with methanol. The compounds in the methanol eluate were non-amenable for study by gas chromatographic techniques due to insufficient solubility in GC compatible solvents (Rowland *et al.*, 2014a). By performing collision-induced dissociation (CID) and high-energy collision-dissociation (HCD) experiments on ions corresponding to SO_3 species (C_{17-22}, DBE = 3-8), detected in positive mode ESI, losses of H_2O, methanol and methyl formate and formation of product ions containing sulphur without oxygen indicated that some NA species were aromatic sulphur-containing species with hydroxy and carboxylic acid functional groups (as methyl ester derivatives) such as dibenzothiophene hydroxy acids (Rowland *et al.*, 2014a). Saponification of the methylated fraction led to the appearance of corresponding [M-H]⁻ ions in negative mode ESI, not observed in the methylated fraction; this was strong evidence that the SO_3 species were carboxylic acids and not sulfoxides.

1.3.3 Multidimensional gas chromatography with mass spectrometry

An alternate technique for the analysis of NA, especially for 'classical' NA and aromatic NA soluble in GC compatible solvents, which is complementary to the methods described by Barrow *et al.* (2014) and Pereira *et al.* (2013a), is GC×GC-MS. The coupling of two GC columns with phases of differing polarity means complex NA mixtures experience two 'dimensions' of separation, typically followed by EI-MS detection; usually a time-of-flight mass spectrometer is necessary to achieve the fast acquisition rates needed (Mondello *et al.*, 2008).

FTICR-MS was shown to have unrivalled mass accuracy and resolution. However other investigations have shown the potential application of GC×GC-MS to characterise NA in OSPW. GC×GC appears to be a technique with unparalleled chromatographic resolution and peak capacity to date. Unlike many previous methods, GC×GC-MS can produce high resolution separation of many individual components with 'medium polarity'. Unit resolution or accurate mass, mass spectra for individual compounds can then be obtained for structural identification. Compounds possessing the same retention time, co-eluting in conventional GC-MS, are separated in the second dimension by GC×GC. Therefore GC×GC-MS produces a two-dimensional (2D) chromatogram; a contour plot using colour to represent the relative intensity of compounds which can also be visualised as a three-dimensional (3D) plot, as opposed to the single dimensional 'hump' of peaks observed for unresolved complex mixtures by GC-MS (Hao *et al.*, 2005; Booth *et al.*, 2006; Sutton *et al.*, 2005; Frysinger *et al.*, 2003).

1.3.3.1 Principle of GC×GC-MS

Multidimensional or two-dimensional gas chromatography (GC×GC) involves the separation of analytes in two or more chromatographic columns possessing stationary phases of different selectivity; thereby separating the compounds in two or more dimensions (Vendeuvre *et al.*, 2007). Comprehensive multidimensional gas chromatography involves separation of the entire sample in all dimensions, as opposed to 'heart-cutting' multidimensional separations, involving the transfer of a small section of compounds separated in the first dimension onto a secondary column.
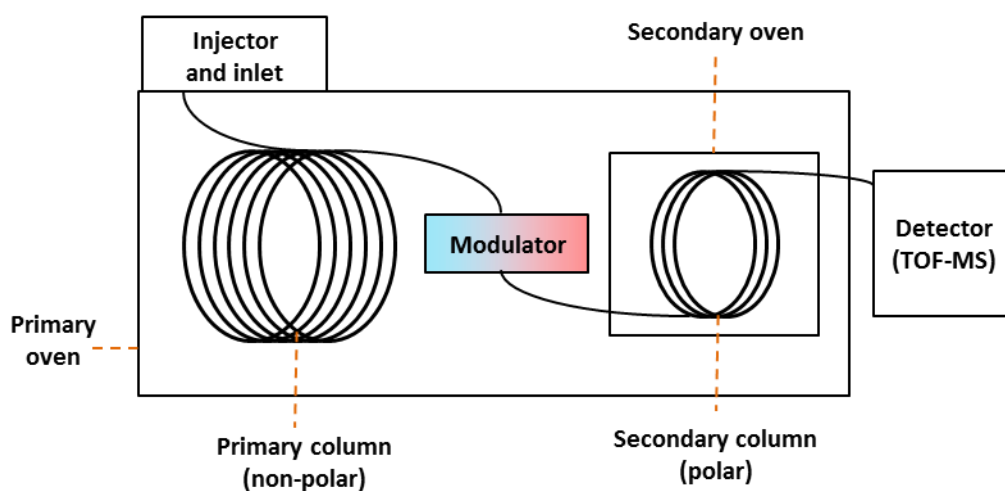
Figure 1-7: Schematic diagram of GC×GC-MS instrumentation.

Comprehensive GC×GC-MS involves joining two columns of different selectivity with a thermal or flow modulator between the columns (Figure 1-7). There are several different modulator designs (Edwards *et al.*, 2011). However, one modulation device frequently employed for the analysis of NA methyl esters by GC×GC (e.g. Rowland *et al.* (2011c) and Lengger *et al.* (2015)) is a two stage cooled loop-modulator. The modulator consists of a hot and cold jet offset at a 90 ° angle with a modulation loop passing twice between the two jets creating two cold spots (Figure 1-8). The modulation loop consists of a short length of coiled, non-phase, deactivated fused silica column, joined at one end to the primary column and joined at the other to the secondary column (Figure 1-8).
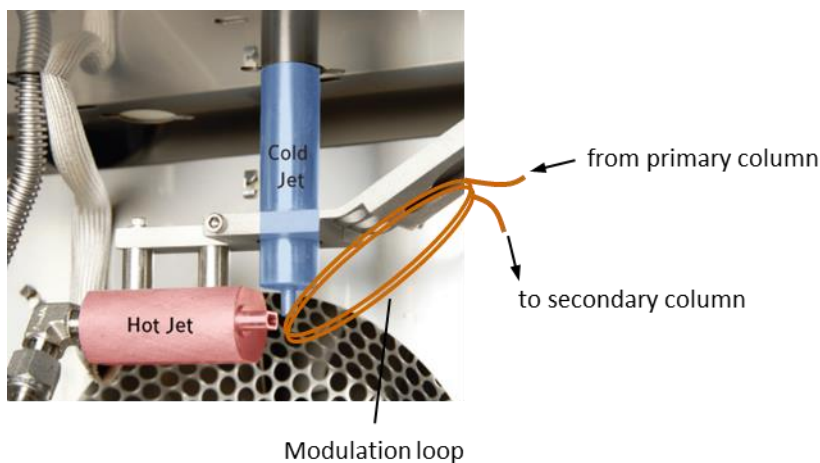
Figure 1-8: Diagram of a two stage loop modulator (image adapted from Zoex (2015)).

The cold jet continuously cools the modulation loop with cooled, compressed N_2 gas (approx. -90 °C). Analytes which have separated in the primary column based on their affinity with the non-polar phase, enter the modulation loop. The cooled modulation loop traps a small portion of analytes for a short time, dependent on the modulation period (s). This traps and re-focuses the small section of analytes into a narrow band. The hot jet then quickly turns on and off, momentarily heating the modulation loop (ms), remobilising the trapped analytes and effectively 're-injecting' the analytes onto a shorter secondary column for them to then be separated based on their affinity with the polar phase.

The modulation period is short and constantly cycling throughout the GC run, thereby providing a constant flow of analytes which separate very quickly in the shorter secondary column. The analytes eluting from the secondary column are then detected in a mass spectrometer, usually capable of fast acquisition rates such as a time-of-flight mass spectrometer (TOF-MS). The continuous data recorded by the MS is then 'sliced' according to the length of the modulation period during the exporting process (Figure 1-9). These 'slices' of data are then transposed onto each other, reconstructing the data into a two-dimensional gas chromatogram (Figure 1-9).
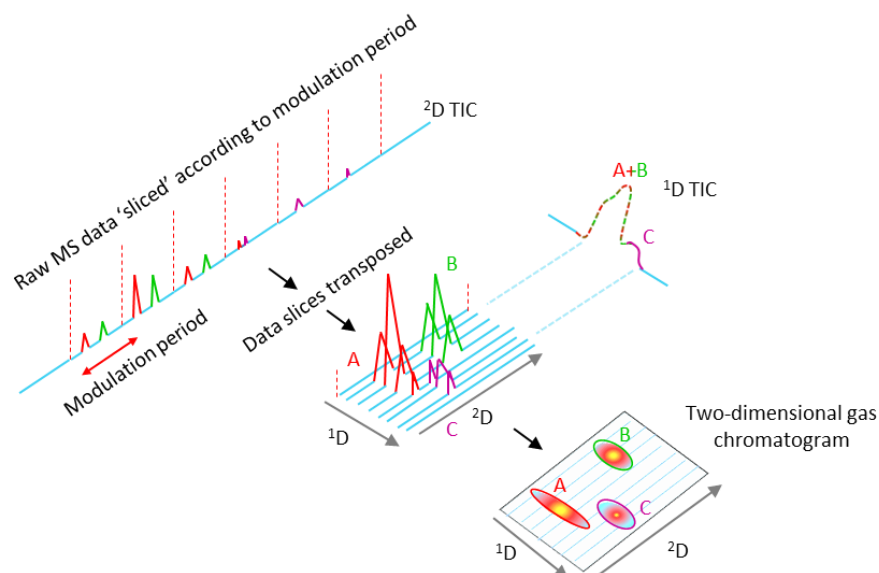
Figure 1-9: Schematic showing the export process, 'slicing' the raw one-dimensional chromatogram according to the modulation period to produce a two-dimensional chromatogram showing the separation of analytes which co-elute in the first dimension.

The two-dimensional chromatogram is usually portrayed as a coloured contour plot, with each compound observed as a coloured ellipse (Figure 1-10; A). The contour plot can then be represented as a 3D image showing the relative intensities of the peaks (Figure 1-10; B).
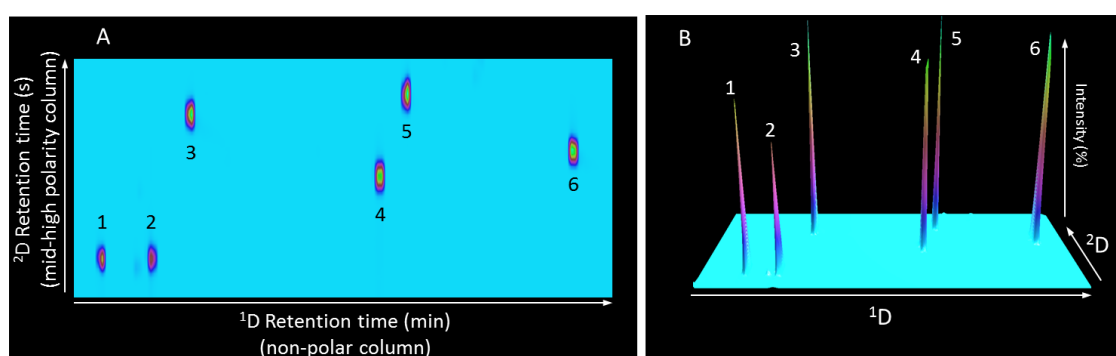
Figure 1-10: Example of (A) a two-dimensional chromatogram represented as a coloured contour plot showing six compounds and (B) a 3D representation of the same chromatogram showing the relative intensities of the peaks.

Numerous reviews and example applications of GC×GC-MS, used for the analysis of complex organic extracts from environmental and petrochemical samples, have been reported previously (Shellie *et al.*, 2002; Frysinger *et al.*, 2003; Ávila *et al.*, 2010; Vendeuvre *et al.*, 2007; Edam *et al.*, 2005).

1.3.3.2   GC×GC-MS for the analysis of NA

Hao *et al.* (2005) analysed two commercial and one OSPW NA extract as the methyl esters by GC×GC-MS. Extracted ion, two-dimensional GC×GC chromatograms of the expected molecular ions of the methyl esters were examined for patterns and differences between samples. However, the GC×GC method only allowed sufficient resolution of z = 0 and -2 NA methyl esters, with poor separation of individual isomers within the same carbon number for z = -4, -6 and -8 NA. The lack of separation reduced the structural detail attainable from mass spectra and the spectra were not used to assign specific structures to any of the NA detected. This convinced many workers to dismiss the method as useful for NA identification.

However, later GC×GC-MS studies of commercial, crude oil and OSPW NA (as methyl esters) achieved much better separation than the above initial study, which led to the first identifications of several individual NA as methyl esters (e.g. Rowland *et al.* (2011c), Rowland *et al.* (2011e) and West *et al.* (2014a)). To date, acids identified or tentatively identified have included mono- to pentacyclic (z = -2 to -10) alicyclic acids (Rowland *et al.*, 2011c; Rowland *et al.*, 2011g; Rowland *et al.*, 2011e; Wilde *et al.*, 2015), mono- to tetracyclic aromatic acids (Rowland *et al.*, 2011f; Rowland *et al.*, 2011d; Bowman *et al.*, 2014; West *et al.*, 2014a), sulphur-containing acids (West *et al.*, 2014b) possible hydroxy acids (Rowland *et al.*, 2014a) and tricyclic diacids (Lengger *et al.*, 2013) (Figure 1-11).

Optimum separation by GC×GC-MS is highly dependent on optimising the separation of compounds in the first GC dimension. Therefore 'normal' phase GC×GC-MS, with a non-polar first column and mid-high polarity second column, generally leads to optimum separation of alicyclic acids. Improved separation between alicyclic and aromatic NA was demonstrated by Rowland *et al.* (2011f) using 'reverse phase' GC×GC-MS; they used a polar phase (e.g. VF-WAXms) in the first dimension, coupled to a mid-polarity column (e.g. BPX50) in the second dimension (Figure 1-12). Individual monocyclic, monoaromatic NA (e.g. 4-ethylphenylethanoic acid), were identified by comparison with synthesised reference compounds, NIST reference mass spectra and by mass spectral interpretation (Rowland *et al.*, 2011f).
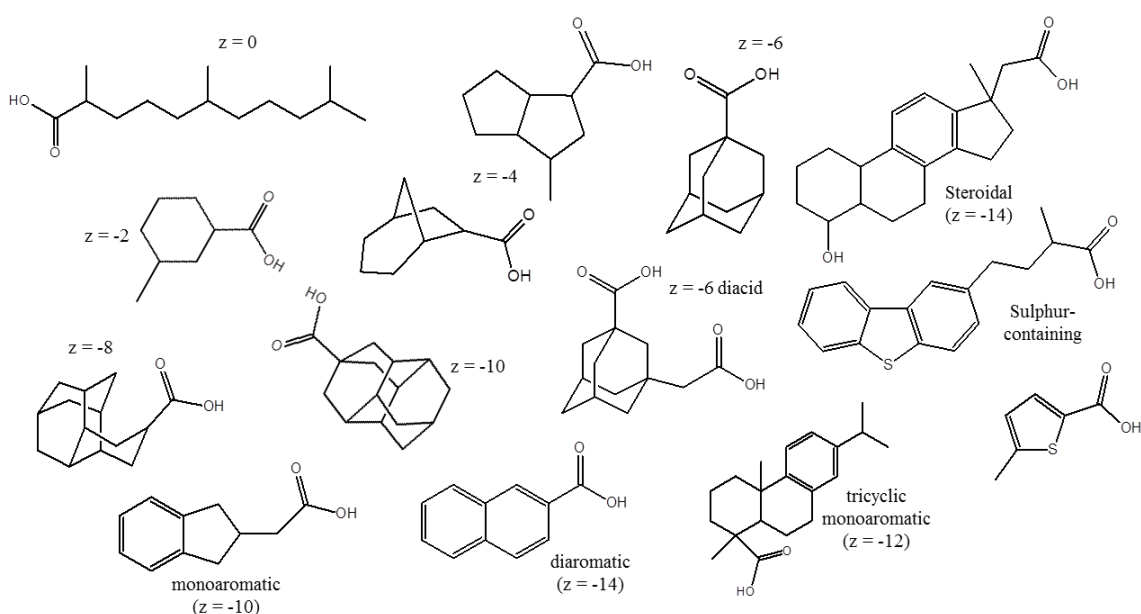
Figure 1-11: Examples of alicyclic, aromatic and sulphur-containing NA identified or tentatively assigned in commercial, crude oil, pore water or OSPW acid extracts by GC×GC-MS analysis of the methyl ester derivatives (Rowland *et al.*, 2011e; Rowland *et al.*, 2011g; Wilde *et al.*, 2015; Bowman *et al.*, 2014; West *et al.*, 2014b; West *et al.*, 2014a; Lengger *et al.*, 2013; Rowland *et al.*, 2011d).
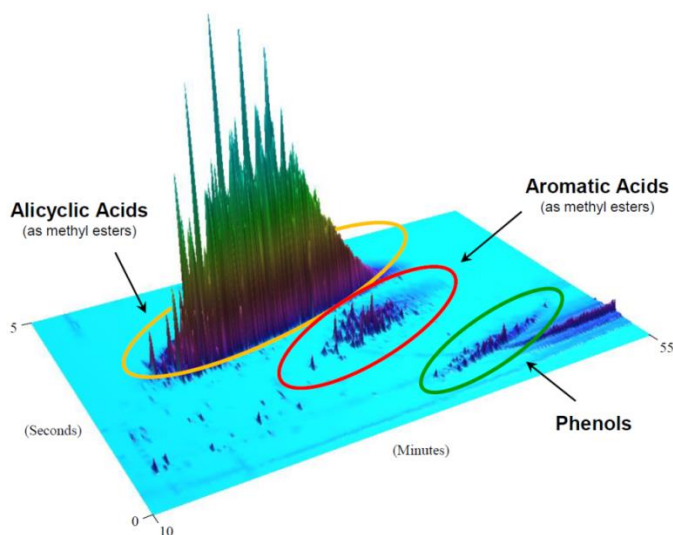
Figure 1-12: 3D representation of a GC×GC-MS chromatogram, showing the separation of alicyclic and aromatic acids in a commercial acid mixture as methyl esters (Rowland *et al.*, 2011f). Note the detection of minor amounts of phenols, indicating that commercial NA are not comprised exclusively of acids.

Pre-fractionation of methylated OSPW NA by silver-ion (Ag-Ion) or argentation chromatography developed and utilised by Jones *et al.* (2012), allowed the GC×GC-MS conditions (column selection, modulation parameters, oven temperatures) then to be modified and optimised for the type of NA being analysed (i.e. alicyclic or aromatic, high or low molecular weight, NA). For example, further separation of the fractionated aromatic acids was achieved by use of an ionic liquid column in the first dimension, showing unparalleled separation of aromatic acid constituents within OSPW as methyl esters (Figure 1-13) (Reinardy *et al.*, 2013). Figure 1-14 shows a GC×GC chromatogram displaying the optimised separation of alicyclic acids isolated by a large scale Ag-Ion fractionation procedure, using a long non-polar primary column (Jones *et al.*, 2012; Wilde and Rowland, 2015). Removal of the aromatic acid methyl esters by argentation chromatography reduced co-elution with the alicyclic compounds (discussed later in Chapter 5, Section 5.3.1, page 209).
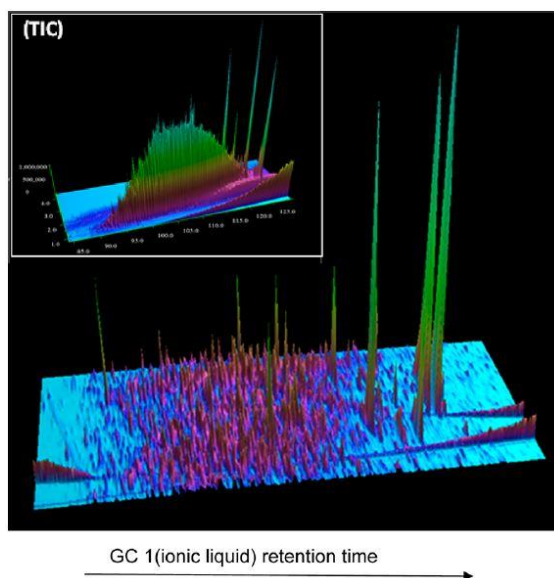
Figure 1-13: 3D representation of TIC GC×GC chromatogram showing improved

separation of an aromatic acid methyl ester fraction, isolated by argentation

chromatography, using an ionic liquid column in the first dimension (Reinardy *et al.*,

2013). Insert of TIC shows separation of same aromatic fraction by normal phase

GC×GC-MS (Jones *et al.*, 2012).
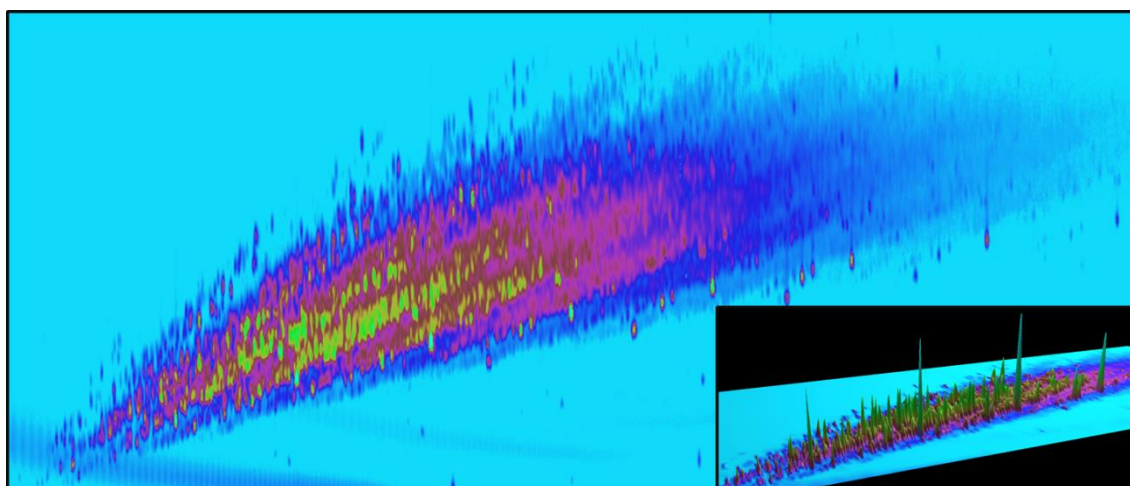
Figure 1-14: TIC GC×GC chromatogram (contour plot) showing the separation of an

alicyclic NA fraction isolated from a commercial NA extract. Insert shows 3D

representation of TIC.

The unparalleled separation achieved using GC×GC-MS, provides a new insight into the composition of complex organic mixtures, overcoming the problem of insufficient separation which limited much of the early research into NA (Chapter 1, Section 1.2). However, the analysis of compounds with polar functional groups requires derivatisation of the sample and despite the improved separation, extremely complex mixtures still require pre-fractionation and sample preparation, which increases the time required for analysis. Secondly, not all compounds within the NA extracts are GC amenable, as shown by Rowland *et al.* (2014a) and the lack of reference mass spectra for NA esters requires the synthesis of reference compounds to confirm identification. This is time-consuming and impractical for large numbers of compounds. Nonetheless, understanding of the mass spectral fragmentation patterns of esters of known specific structures and the relative retention positions, can be extrapolated for the assignment of homologous series' and group-type characterisations.

Most studies of NA involving the use of GC×GC-MS have been qualitative, focusing on structural identification (Rowland *et al.*, 2011c; Lengger *et al.*, 2013; West *et al.*, 2013). However, following the identification of interesting and abundant acids present in OSPW, knowledge of the structures has been used in recent studies for other applications, such as source characterisation (Frank *et al.*, 2014), monitoring short-term compositional changes within OSPW (Lengger *et al.*, 2015) and comparing compositional data for OSPW from different industries (Rowland *et al.*, 2012), as well as to direct, arguably more pertinent, toxicological investigations (Jones *et al.*, 2011; Reinardy *et al.*, 2013; Scarlett *et al.*, 2013; Swigert *et al.*, 2015).

1.4 Toxicity, biodegradation and remediation

Concern over the toxicity of NA in OSPW, contaminated ground and river waters and oil platform produced waters has spurred interest in investigations monitoring the changes in toxicity with compositional changes in the AEO, upon biodegradation and bio- and chemical remediation treatments.

As mentioned (Section 1.1.2), OSPW have been shown to be toxic to several organisms (Clemente and Fedorak, 2005; He *et al.*, 2012). The toxicity has been attributed to the NA content. Indeed some NA and metal naphthenates have been shown to be toxic; the toxicity of individual synthesised reference acids (Jones *et al.*, 2011; Frank *et al.*, 2009), commercially available acid mixtures (Rockhold, 1955; Kamaluddin and Zwiazek, 2002; Tollefsen *et al.*, 2012) and NA extracted from OSPW, have all been measured (Rogers *et al.*, 2002; Marentette *et al.*, 2015b; Marentette *et al.*, 2015a; Mohseni *et al.*, 2015).

However, the toxicity of an acid mixture is dependent on the composition of the extract. The composition of an NA mixture has been shown to be highly dependent on its source (West *et al.*, 2011; West *et al.*, 2013) and the extraction procedures used to obtain it (Huang *et al.*, 2015b; Rowland *et al.*, 2014b). High-resolution mass spectrometry coupled with various ionisation techniques has shown that the AEO fraction from OSPW contains an extensive range of compounds, beyond simply 'classical' $C_nH_{2n+z}O_2$ species (Barrow *et al.*, 2010; Barrow *et al.*, 2015a). The multitude of experiments using NA mixtures obtained from different sources by different extraction methods raises uncertainty about the toxicity being measured. Questions arise as to whether the toxicity of OSPW and OSPW NA extracts can be solely attributed to the NA, to the total NA concentration or to a few individual NA with high toxicities, to a type of NA species or a combination of several influences.

Recent efforts have focused on linking measured toxicity and changes in toxicity, to biodegradation and remediation treatments (Frank *et al.*, 2008; Reinardy *et al.*, 2013). This approach has included selective fractionation of the NA to isolate specific acid species, such as the aromatic acids by silver-ion chromatography, to observe the toxic effects of limited groups of compounds (Scarlett *et al.*, 2013). Determination of the NA composition and monitoring any changes after remediation treatment, such as the appearance of more oxidized acid species after ozonation, has been achieved using advanced chromatographic instrumentation, such as ultra-high performance liquid chromatography (UPLC) coupled with high-resolution mass spectrometry (Gamal El-Din *et al.*, 2011) and ion-mobility mass spectrometry (Klamerth *et al.*, 2015; Bauer *et al.*, 2015).

Interestingly, analyses of the produced water from SAGD extraction by GC-MS (Kawaguchi *et al.*, 2012), GC×GC-MS (Petersen and Grade, 2011), HPLC-Orbitrap-MS (Pereira *et al.*, 2013a) and FTICR-MS (Schaub *et al.*, 2007) all showed that although such waters contained similar classes to that of OSPW (e.g. O_x, SO_x and NO_x species), the composition, especially of the acidic $C_nH_{2n+z}O_2$ species was chemically distinct from the AEO and NA within the OSPW from surface mining operations (Pereira *et al.*, 2013a). This is important for future concerns regarding the toxicity of oil sands wastewaters. As previously stated, surface mining operations are reportedly capable of only recovering 20% of the available bitumen (Alberta-Energy, 2013). Therefore the increased projections for oil sands production, presumably involving the extraction of the remaining ~80% of deep surface bitumen by *in-situ* methods such as SAGD operations, means the AEO and NA composition of SAGD produced waters, chemical nature of its components, the toxicity and composition compared to that of OSPW currently stored from surface mining, should be important considerations for future remediation plans.

Similarly, as observed for the OSPW, the composition of the AEO from produced waters from SAGD operations shows high heterogeneity, depending on the location, industry and the part of the process from which samples are taken.

GC-MS analysis of the NA as tBDMS esters, extracted from produced water from varying stages of a SAGD process, showed the presence of only C_{4-18}, z = 0 (acyclic) and -2 (monocyclic) alicyclic monoacids, as well as some z = -8 (benzoic) monoacids and $C_nH_{2n+z}O_3$ and $C_nH_{2n+z}O_4$ species, potentially 'oxo-' and dicarboxylic acids (Kawaguchi *et al.*, 2012). This was supported by GC×GC analysis of NA extracted from SAGD produced water reported by Petersen and Grade (2011). A selected ion chromatogram (SIC) from the GC×GC-MS analysis of the free acids, resulting in poor peak shape, showed a relatively simple, resolved NA mixture dominated by acyclic acids ($C_nH_{2n}O_2$) (Petersen and Grade, 2011). The SIC reported by Petersen and Grade (2011) was substantially different to those previously reported for OSPW NA as methyl esters (Jones *et al.*, 2012; Wilde *et al.*, 2015), which have been shown to contain numerous alicyclic, aromatic and heteroatom-containing acids.

Pereira *et al.* (2013a) detected $C_nH_{2n+z}O_2$ species in both OSPW from surface mining and process water from *in-situ* extraction methods, by HPLC with negative mode ESI-Orbitrap-MS. Carbon numbers ranged from C_{7-21} with 1 − 8 DBE in *in-situ* OSPW and C_{10-21} with 3 − 10 DBE in OSPW from surface mining. However, their HPLC method provided insufficient separation to allow inference of structural differences of the components based on retention time (Pereira *et al.*, 2013a). Use of HPLC coupled with Orbitrap-MS did however show that the $C_nH_{2n+z}O_2$ species detected in positive ion mode, possessed significantly different retention times to those detected when run in negative mode, indicating the presence of non-acidic $C_nH_{2n+z}O_2$ species in both OSPW samples, potentially indicating the presence of hydroxy- and keto- compounds.

The differences in NA composition between OSPW from surface mining and produced waters from SAGD procedures could be due to the differences in pH of the water used in both processes. The pH of SAGD produced water reported by Kawaguchi *et al.* (2012) was 7.2 with a total NA concentration of 53 mg L^{-1} which was neutral and low compared with the recycled produced water and tailings pond water at pH 10.4 with total NA concentrations >120 mg L^{-1}. Klamerth *et al.* (2015) and Barrow *et al.* (2015b) recently demonstrated the influence of pH on the extraction of organics from OSPW, showing that pH does effect the composition of AEO, as observed by HRMS.

Current remediation plans include long-term storage of the OSPW in large open settling ponds designed, apparently, to allow enhanced biodegradation of the toxic components, evaporation of the water and consolidation of the suspended tailings; many new technologies focused on the reclamation of the residing solid tailings are being developed by Canada's Oil Sands Innovation Alliance (COSIA, 2015). Other remediation treatments which are focused on direct, faster methods for reducing the toxicity of the OSPW include photolysis, phytoremediation, nano-filtration, adsorption and ozonation (Headley and McMartin, 2004; Gamal El-Din *et al.*, 2011; Brown and Ulrich, 2015; Mohamed *et al.*, 2015). Several publications have summarised the numerous studies on biodegradation, remediation and corresponding effects on the toxicity of 'model', commercial and OSPW NA (Headley and McMartin, 2004; Clemente and Fedorak, 2005; Kannel and Gan, 2012).

The biodegradation of NA has shown to be structure specific, with the position of the carboxylated side chain, the cyclicity and extent of alkyl branching effecting bio-resistance (Han *et al.*, 2008; Smith *et al.*, 2008; Misiti *et al.*, 2014). The origin of NA in Athabasca bitumen and OSPW is believed, in part, to be due to the partial biodegradation of the more recalcitrant hydrocarbons present in the heavily biodegraded

bitumen and potentially biodegradation of unrecovered bitumen within the OSPW; this is reflected in the recalcitrant nature of the OSPW NA towards bioremediation compared with commercial and model NA (Han *et al.*, 2008; Toor *et al.*, 2013a).

Biodegradation of petroleum hydrocarbons under aerobic conditions (Watson *et al.*, 2002) and anaerobic conditions e.g. in deep subsurface reservoirs (Aitken *et al.*, 2004), has been shown to result in the formation of carboxylic acids including mono- and diacids. Formation of the acids is believed to be initiated by oxidation of the alkyl side chain of a petroleum hydrocarbon via alcohol and aldehyde intermediates (Watson *et al.*, 2002) or under anaerobic conditions; via either direct carboxylation or by fumarate addition forming succinic acid intermediates (Aitken *et al.*, 2004). The succinic acids are proposed to undergo further biodegradation, either via α- or β-oxidation or aromatization to form the carboxylic acids (Blakley, 1974; Aitken *et al.*, 2004; Kannel and Gan, 2012; Agrawal and Gieg, 2013).
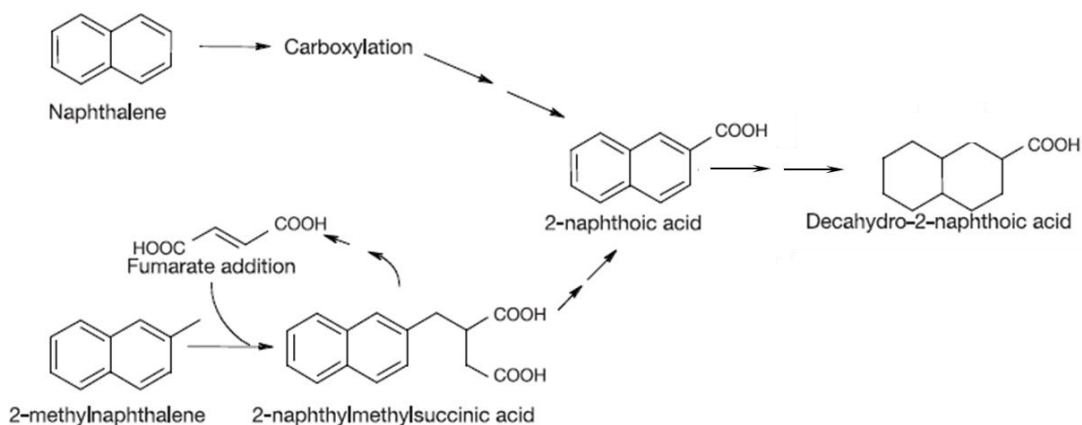
Figure 15: Proposed mechanisms for the biodegradation of petroleum hydrocarbons under anaerobic conditions resulting in the formation of carboxylic acids. (Image adapted from (Aitken *et al.*, 2004).

The toxicity studies, remediation plans, current understanding of the biodegradation mechanisms and the composition of the residual NA and by-products after chemical treatments are limited by the lack of knowledge of the exact structures of NA.

1.5 Present investigation

The need to identify individual NA within complex acid-extractable organic mixtures, including historical needs (e.g. to increase understanding of corrosion and to enhance understanding of the geochemical significance of acids) as well as more recent, topical issues (e.g. improved knowledge of toxicity and environmental contamination and monitoring of NA), have been reviewed above. Although there have been significant advances in analytical technologies and methodologies to detect and characterise NA by molecular formula based on accurate mass data, there is a paucity of knowledge regarding the structures, numbers of isomers and nature of NA within both petroleum and OSPW NA extracts.

Although techniques such as high resolution mass spectrometry, have indicated the number of individual compound classes (e.g. O_x, S_xO_x, N_xO_x) present within OSPW AEO, most investigations have shown that O_x species (Headley *et al.*, 2015; Nyakas *et al.*, 2013), particularly $C_nH_{2n+z}O_2$ species or so-called naphthenic acids (NA) (Barrow *et al.*, 2010; Headley *et al.*, 2011a), are most abundant. Within these species, investigations focusing specifically on NA have shown that the z = -4, alicyclic bicyclic acids are the major class (Figure 1-16) (Bataineh *et al.*, 2006; Martin *et al.*, 2008; Barrow *et al.*, 2010; Hindle *et al.*, 2013), comprising approximately 30% of the relative abundance of z = 0 to -12 $C_nH_{2n+z}O_2$ NA in OSPW (Figure 1-16; B-D) (Martin *et al.*, 2008; Grewer *et al.*, 2010; Barrow *et al.*, 2010). The alicyclic bicyclic acids also appear to be the most abundant acids in many other matrices, such as crude oils (Dzidic *et al.*, 1988; Barrow *et al.*, 2003; Mapolelo *et al.*, 2011) and petroleum-derived commercial NA (Figure 1-16; A) (Damasceno *et al.*, 2014). Indeed, Damasceno *et al.* (2014) showed recently that >120 bicyclic acids were present in each of two commercial NA samples although none were identified.
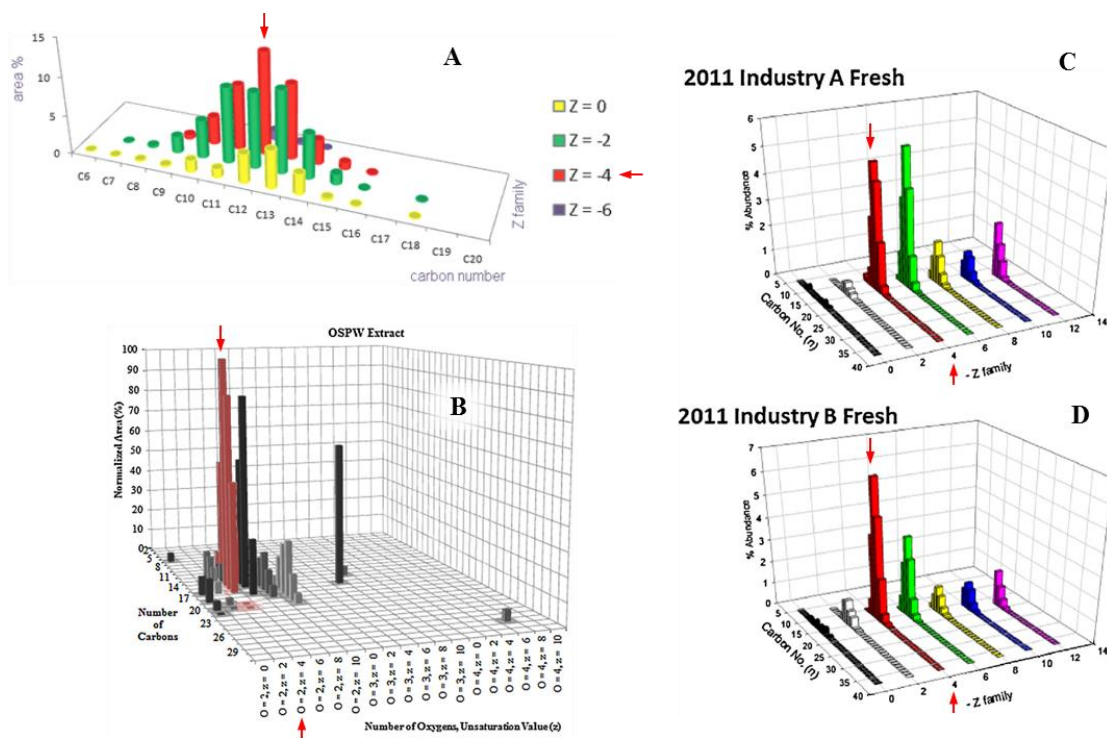
Figure 1-16: Distribution 'profiles' of NA extracts showing abundant bicyclic NA as a major acid class in (A) commercial NA and (B-D) OSPW, analysed by a range of techniques including (A) GC×GC-MS, (B) HPLC-qTOF-MS and (C and D) Orbitrap-MS, previously reported by (and images adapted from) Damasceno *et al.* (2014), Hindle *et al.* (2013) and Marentette *et al.* (2015a), respectively.

In fact, despite the abundance of alicyclic bicyclic NA, very few have been identified in crude oil and none had been identified in OSPW prior to the present study. The only bicyclic NA to have been identified in petroleum NA are alkyl substituted, fused cyclohexyl structures possessing bicyclo[4.4.0]decane (Figure 1-17; B) or bicyclo[4.3.0]nonane (Figure 1-17; C) also known as decalin (decahydronaphthalene) and perhydroindane structures (Rowland *et al.*, 2011e). A few studies have reported the presence of a C_{16} sesquiterpane acid (a penta-alkyl substituted bicyclo[4.4.0]decane e.g. Figure 1-17; A) in bitumen and crude oil by GC-MS (Cyr and Strausz, 1984; Nascimento *et al.*, 1999).
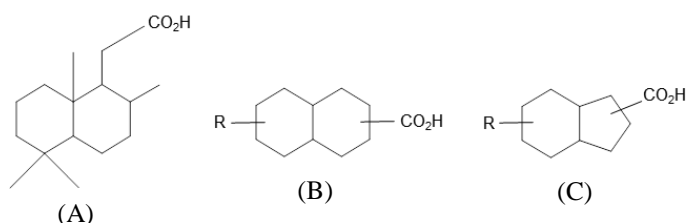
Figure 1-17: Bicyclic acid structures, including (A) a drimane acid previously identified in crude oil (Nascimento *et al.*, 1999) and bitumen (Cyr and Strausz, 1984) and (B) bicyclo[4.4.0]decane and (C) bicyclo[4.3.0]nonane acids identified in commercial NA (Rowland *et al.*, 2011e). The latter (B and C) have often been assumed, usually without justification, to be typical or representative structures of bicyclic NA in OSPW (Headley *et al.*, 2013b; Brown and Ulrich, 2015).

The few bicyclic acids to have been identified thus far in crude oil and commercial NA, have all possessed fused cyclohexyl and cyclopentyl rings, as have the few monocyclic NA previously identified (Brient *et al.*, 2000; Lochte and Littmann, 1955). These structural features are also observed in many natural products and petroleum hydrocarbons. NA are also believed to at least partially originate from the biotransformation of petroleum hydrocarbons (Aitken *et al.*, 2004; Atlas, 1984). Therefore it is often presumed that the few bicyclic NA that have been identified within crude oil and petroleum are representative of the bicyclic NA within OSPW. However, the NA compositions of crude oil and petroleum are different from those in OSPW (Bataineh *et al.*, 2006; Scott *et al.*, 2005; Grewer *et al.*, 2010; Hindle *et al.*, 2013). Alkyl substituted bicyclo[4.4.0]decane and bicyclo[4.3.0]nonane acids (Figure 1-17; B and C) are often cited as 'typical' or representative of the bicyclic acids in OSPW, but no justification has ever been given for this assumption (Headley *et al.*, 2013b; Brown and Ulrich, 2015). These assumptions are also contradictory to the concluding results from the (albeit limited) early investigations (Section 1.2, page 11). Dehydrogenation experiments and structural details interpreted from comparison of the physical

properties of isolated NA with those of synthesised reference acids, suggested that the majority of NA did not contain fused cyclohexyl rings (Zelinsky, 1911; 1924).

Jones *et al.* (2011) measured the toxicity of thirty five individual acids, including several which had been identified in commercial and OSPW NA. Although no bicyclic NA in OSPW had then been identified, Jones *et al.* (2011) measured the toxicity of bicyclo[4.4.0]decane-2-carboxylic, -2-ethanoic and -1-propanoic acid since these had been identified by Rowland *et al.* (2011e) in commercial NA. The results from the Microtox assay showed these bicyclic acids were some of the most toxic acids measured. Bicyclo[4.4.0]decane-2-propanoic acid had an EC_{50} (effective concentration at which 50% of the population are affected) of 0.004 mM (0.84 mg L^{-1}).

There is clearly a gap in knowledge regarding the structures of bicyclic NA, particularly in OSPW, but also in crude oil and commercial NA. The structures may have important implications for the toxicity, corrosivity, origins and other potential uses of NA (e.g. as biocides).

1.5.1 Aims

The aim of the current investigation was to identify at least some of the bicyclic acids typically present in petroleum and oil sands process-affected water acid extracts. As multidimensional gas chromatography-mass spectrometry has arguably shown most potential for structural elucidation of individual NA, previously demonstrated by the successful identification of other acid species within very complex NA mixtures (Rowland *et al.*, 2011c), it was chosen and utilized in the present investigation, for the identification of bicyclic NA.

The first objective was to attempt to identify bicyclic NA as their methyl esters, using GC×GC-MS to separate individual bicyclic acids as their methyl ester derivatives in

various samples of OSPW and petroleum NA. Achieving separation and chromatographic resolution of individual isomers by GC×GC-MS might allow the true complexity and number of isomers of bicyclic NA to be assessed. If the separation of individual bicyclic NA could be achieved, the mass spectra obtained for individual components might be used for identification by comparison with spectra for commercially available and synthesised, reference bicyclic acids.

Previous efforts have shown that the identification of bicyclic NA by GC×GC-MS, as methyl esters, has proved challenging. For example, only a few bicyclic NA could be firmly identified by Rowland *et al.* (2011e) in petroleum NA. Therefore an alternative method for the identification of NA was investigated herein. Taking inspiration from early investigations into petroleum NA and the substantial progress made even in the absence of the advanced analytical instrumentation available today, the second objective was to plan and develop an alternative method for the identification of NA by chemical transformation of carboxylic acids to hydrocarbons whilst retaining the 'core' bicyclic structures. After successfully reducing the petroleum NA to the corresponding hydrocarbons, the aim was to achieve clear separation of highly resolved, individual bicyclic hydrocarbons and compare the mass spectra and retention positions of the bicyclanes with those reference mass spectra and known elution orders of bicyclic hydrocarbons readily available in the literature.

The three-step procedure previously adopted by Seifert *et al.* (1969) for the conversion of petroleum acids to hydrocarbons was used as a starting point. The aim was to first develop and perform the new, optimised conversion on model bicyclic acids. Structural elucidation of the model bicyclic acids, intermediates and final hydrocarbon products by available analytical techniques (e.g. gas chromatography-mass spectrometry (GC-MS)

and nuclear magnetic resonance spectroscopy (NMR)), would be used to validate and assess the usefulness of the method.

If conversion of the model acids to hydrocarbons proved feasible, the next objective was to apply this new conversion, combined with the use of GC×GC-MS of the resulting hydrocarbon products, for the identification of bicyclic acids in petroleum and then OSPW NA.

Chapter 1

Chapter 2

General Experimental and Analytical Procedures

All laboratory glassware and apparatus were cleaned by soaking in Decon 90 (liquid detergent, Fisher), rinsing with hot water followed by cold deionised water, oven drying, solvent washing and oven drying at 110 °C before use.

2.1 Instrumentation

2.1.1 Infrared Spectroscopy

Fourier transform infrared spectroscopy (IR) was performed using a Bruker Alpha FT-IR spectrometer with a Platinum ATR module. The spectra were obtained at 4 cm^{-1} resolution using a DTGC detector, running 16 scans per spectrum.

When the quantity of sample was limited, IR spectra were obtained using a Bruker IFS 66 spectrometer attached to a Hyperion FT-IR microscope, allowing the analysis of < 1 mg quantities.

2.1.2 Gas chromatography-flame ionisation detection

Samples analysed by gas chromatography with flame ionisation detection (GC-FID) were dissolved in either DCM or hexane and diluted to 0.1 - 0.25 mg mL^{-1}. The instrument used was an Agilent Gas Chromatograph 7890A equipped with a 7683 Series Autosampler and 7683B Series Autoinjector. The column was a 5% phenylmethylpolysiloxane Agilent HP5 (30 m × 0.320 mm × 0.25 μm). The carrier gas was nitrogen with a flow rate of 1.2 mL min^{-1} and the inlet temperature was 250 °C. Attached was a flame ionisation detector at 300 °C, hydrogen flow rate of 40 mL min^{-1}, air flow rate of 400 mL min^{-1} and nitrogen (make-up) flow rate of 15 mL min^{-1}. The temperature programme consisted of 40 – 300 °C at 10 °C min^{-1} and held at 300 °C for

10 min. The chromatograms were recorded using Chemstation™ (Revision B.03.01, May 2007) software.

2.1.3 Gas chromatography-mass spectrometry

Samples analysed by gas chromatography-mass spectrometry (GC-MS) were diluted in hexane or DCM to 0.01 – 0.025 mg mL^{-1}. The instrument used was an Agilent GC-MSD; 7890A Gas Chromatograph fitted with a 7683B Autosampler and a 5975A quadrupole mass selective detector. The column was changed during the period of the investigation. Column A was (5% phenyl)-methylpolysiloxane HP5-ms (30 m × 0.25 mm × 0.25 μm). Column B was a 100% dimethylpolysiloxane Restek Rxi®-1ms (30 m × 0.25 mm × 0.25 μm). The helium carrier gas was kept at a constant flow rate of 1.0 mL min^{-1} and a 1.0 μL sample was injected into a splitless injector at typically 300 °C; however analyses were also performed where specified at 225 °C and 250 °C. The oven programme was 40 – 300 °C at 10 °C min^{-1} and held at 300 °C for 10 min. The ion source was at 230 °C and the quadrupole detector was at 150 °C, producing an ionisation energy of 70 eV. The chromatograms were recorded using Chemstation™ and the instrument operated in full scan mode, with a scan range of *m/z* 50 – 500.

2.1.4 Multidimensional gas chromatography-mass spectrometry

Comprehensive multidimensional gas chromatography-mass spectrometry (GC×GC-MS) analyses were conducted using an Agilent 7890A gas chromatograph (Agilent Technologies, Wilmington, DE) fitted with a Zoex ZX2 two stage cooled loop GC×GC modulator and secondary oven (Houston, TX, USA) interfaced with an Almsco BenchTOFdx™ time-of-flight mass spectrometer with an electron impact ionisation source (Almsco International, Llantrisant, Wales, UK).

The column diameters were changed during the period of the investigation. Column set A: the first dimension column was a 100% dimethyl polysiloxane (60 m × 0.25 mm ×

0.25 μm) Rxi®-1ms (Restek, Bellefonte, USA), followed by a 1 m × 0.1 mm deactivated fused silica modulation loop. The second-dimension column was a 50% phenyl polysilphenylene siloxane (2.5 m × 0.1 mm × 0.1 μm) BPX50 (SGE, Melbourne, Australia). Column set B: the first dimension column was kept the same as column set A, with a 100% dimethyl polysiloxane (60 m × 0.25 mm × 0.25 μm) Rxi®-1ms (Restek, Bellefonte, USA), followed by a 0.7 m × 0.25 mm deactivated fused silica modulation loop. The second-dimension column was a 50% phenyl polysilphenylene siloxane (1.4 m × 0.25 mm × 0.25 μm) BPX50 (SGE, Melbourne, Australia).

Helium was used as carrier gas and the flow was kept constant at 1.0 mL min^{-1}. 1 μL samples were injected at 275 °C and 300 °C splitless. Different temperature programmes for the oven, modulator and ion source were used to achieve optimum separation and detection of the various samples analysed (e.g. acid methyl esters, fractionated acid methyl esters or hydrocarbons). Therefore the specific oven, modulator and ion source temperatures and conditions used are specified in the method section of each of the relevant chapters; however, a typical programme was as follows: the primary oven was programmed from 30 °C, held for 1 min, then heated to 120 °C at 5 °C min^{-1}, to 220 °C at 0.8 °C min^{-1}, to 280 °C at 5 °C min^{-1} and to 320 °C at 10 °C min^{-1} and then held for 10 min. The secondary oven was programmed to track the primary oven at 40°C above. The hot jet was programmed to start 30 °C above the primary oven temperature until 150 °C, it was then ramped to 260 °C at 1.3°C min^{-1} and then to 400 °C at 4°C min^{-1}. The modulation period was set at 2, 4 or 6 s. The MS transfer line temperature was 290 °C and ion source 250°C or 300 °C. The scan range was *m/z* 50 – 550 and the data rate was 50 Hz. The ionisation energy was 70 eV.

Data processing was conducted using GC Image v2.3 (Zoex, Houston, TX). Obtaining a mass spectrum for a particular peak (per pixel or average spectrum of a defined peak

area known as a 'blob') involved clicking on the two-dimensional gas chromatogram. The software allowed the data to be processed in multiple ways e.g. background removal (Reichenbach *et al.*, 2003), template matching and batch processing (Reichenbach *et al.*, 2004). Data visualisation processing (e.g. Hollingsworth *et al.* (2006)) included the 3D spectral colourisation tool, where the 3D chromatogram was colourised based on the mass spectra of each individual pixel. Individual colours were assigned to specific ions, allowing compounds with characteristic ions to be visualised as different colours (e.g. Figure 5-2; Chapter 5, Section 5.3.1, page 211). An additional feature was the Computer Language for Identifying Chemicals (CLIC) expression tool, which was used to aid the location of compounds or for determining the presence or absence of compounds. CLIC expressions are a powerful tool for producing advanced extracted ion chromatograms with the option to apply additional constraints, such as specifying the relative intensity of specific ions, the mass of the base peak ion and only show peaks between specific retention times (e.g. Figure 6-8; Chapter 6, Section 6.3.3.1, page 280). The CLIC expression tool is similar to the LECO ChromaTOF mass spectral filters which use Microsoft Visual Basic Scripting. The use and application of CLIC expressions for the interpretation of GC×GC chromatograms of complex mixtures has been described previously (Reichenbach *et al.*, 2005; Jennerwein *et al.*, 2014; Weggler *et al.*, 2014).

2.1.5 Nuclear magnetic resonance spectroscopy

Samples were analysed by nuclear magnetic resonance spectroscopy (NMR) using a JEOL ECP-400 NMR spectrometer. All spectra, including ^1H and ^{13}C, DEPT ^{13}C, COSY, CHSHF (carbon-hydrogen shift correlation) and COLOC spectra, were obtained in deuterated chloroform or deuterated acetone (Cambridge Isotope Laboratories, Inc., US). The chemical shifts were measured relative to the solvent (CDCl$_3$; ^1H: 7.24 ppm; ^{13}C: 77.0 ppm). For samples of limited quantity an NMR insert tube (Coaxial insert assembly, Wilmad-Labglass) was used. The NMR insert tube allowed analysis of sample quantities 0.1 – 5 mg.

2.2 Extraction, derivatisation and fractionation of naphthenic acids

During the present work, a number of OSPW acid fractions were made available for study from scientists at Environment Canada. Such samples have rarely been made available before. These included samples from two oil sands industries' tailings ponds or settling basins. Unfortunately, some details of the sampling locations etc. cannot be published herein for legal reasons. The samples were usually received as the NA extract and as much detail as possible about each sample and the extraction methods used to obtain each sample are given in the method section of each of the relevant chapters. One sample, extracted from OSPW in the West-In Pit (WIP) tailings pond within industry A, was received as the sodium salts. An overview of the extraction of the NA from the WIP sample and the back extraction performed to obtain the free acids is provided below.

2.2.1 Extraction of NA from OSPW

Three 1 L samples of concentrated naphthenate solution, extracted from oil sands process-affected water (OSPW), which had undergone a prior clean-up procedure involving weak anion exchange chromatography, was received from Environment Canada, Burlington, CA. The extraction and clean-up procedure was developed and reported by Frank *et al.* (2006) for the bulk preparation of a NA stock solution for multiple, subsequent investigations. Briefly, 2000 L of OSPW collected from industry A, West In-Pit (WIP) tailings pond in 2009 was acidified to pH 2, the precipitated acids were separated, re-dissolved and centrifuged to remove sands and clay (Frank *et al.*, 2006). The naphthenates were passed through a diethylaminoethyl-cellulose column to remove humic acid substances and washed with DCM to remove neutral compounds (Frank *et al.*, 2006). The cleaned-up, concentrated naphthenates received a final wash with acidified water before being reconstituted in 0.05 N NaOH to make 14 L of ~2500

mg mL^{-1} NA solution (Frank *et al.*, 2006). The procedure outlined by Frank *et al.* (2006) is depicted in Appendix Figure 1, as a flow diagram with the four main stages of preparation highlighted.

Once received from Environment Canada, 400 mL concentrated naphthenate solution was transferred equally into two 500 mL glass separating funnels in order to be extracted as ×2 200 mL batches. The OSPW naphthenate solution was a brown, murky colour. To each separating funnel, 5 – 10 mL of concentrated HCl (<= pH 2) and 40 mL of ethyl acetate (HPLC Grade, Fisher) was added. The solution turned a milky orange/brown colour. Acidification produced the free acids which were extracted into the organic phase upon vigorous shaking for 2 min and any build-up of pressure during mixing was released. An orange/brown emulsion formed between the two layers. The orange/brown aqueous bottom layers and emulsions were drained into 500 mL glass beakers and the yellow/brown organic top layers were carefully poured through the top of the funnels and combined in a 500 mL round bottom flask.

The aqueous layers and emulsions were transferred back into the respective separating funnels and extracted two more times with 20 mL ethyl acetate. The top organic phases were combined in the round bottom flask. The smaller emulsions which formed in the 2nd and 3rd extractions were carefully separated and combined in a conical flask where the emulsion appeared to partition further. Therefore the combined emulsion solution was split between the two separating funnels and gently swirled with 40 mL ethyl acetate to extract as much of the acids as possible. The organic layers were transferred and combined with the previous organic extracts in the round bottom flask. The remaining emulsions were combined and transferred to a 22 mL vial and centrifuged. The emulsion solution separated into a clear brown top layer, above a solid brown interfacial 'pad', above a lower aqueous layer. The top organic layer was carefully

transferred and combined with the previous free acid extracts in the round bottom flask. The interfacial pad remained intact when carefully removing the lower aqueous phase to waste. The wet brown solid remaining was stored in the 22 mL vial for further analysis.

The combined free acid solution in the round bottom flask was a golden yellow colour and the original aqueous OSPW solution was a much paler and clearer after extraction. The free acid extract was concentrated by rotary evaporation at 40 °C to $1 - 2$ mL before being transferred to a pre-weighed 7 mL glass vial, rinsing the round bottom flask with solvent and collecting the rinses. The remaining solvent was removed under N_2 blowdown at 40 °C yielding 537 mg of NA extract from OSPW.

2.2.2   Derivatisation of OSPW NA extract

The free NA (537 mg) extracted from the concentrated OSPW naphthenate solution was dissolved in 8 mL DCM and split equally between four glass vials, followed by an 8 mL rinse. The DCM was then removed by N_2 blowdown at 40 °C. Next, 16 mL of 14% BF_3-methanol complex solution (Sigma Aldrich) was added to each vial and the vials heated at 70 °C for 3 hours.

The vials were allowed to cool before combining the methylated solutions in a 250 mL separating funnel. Afterwards, 30 mL of water (Chromasolv® HPLC Grade, Sigma Aldrich) and 30 mL of hexane (HPLC Grade, Rathburns Chemical Ltd.) were added and the solution shaken vigorously for 2 min. The solution separated into a cloudy brown lower aqueous layer and a clear brown top layer with a small brown emulsion at the bottom of the top layer. The lower aqueous layer and emulsion were drained into a beaker and the top organic layer transferred into a round bottom flask. The aqueous layer and emulsion was re-extracted with two more 30 mL aliquots of hexane. The combined organic extracts were concentrated by rotary evaporation to $1 - 2$ mL before

being transferred to a 15 mL glass vial. The methyl ester solution was dried over anhydrous Na_2SO_4 ($\geq$ 99.0%, Sigma Aldrich) overnight.

The dried extract was filtered into a pre-weighed 7 mL glass vial and the remaining solvent removed by N_2 blowdown at 40 °C, yielding 443.4 mg of methylated NA extracted from OSPW.

2.2.3 Derivatisation of commercial NA extract

A sample of a commercially prepared NA mixture was received as a gift in 2009 from the Merichem Company (Batch No. CN/138) and later subsampled in 2010. The Merichem Company developed a proprietary method for the efficient extraction of NA from high TAN crude oils, jet fuel, kerosene and condensates (Forero *et al.*, 1996). Instead of standard extraction by mixing a hydrocarbon feedstock with caustic soda (NaOH), with the extraction efficiency being directly related to droplet size and the inherent problem of emulsion formation, Merichem Co. developed the Fibre-Film® Contactor which passes the hydrocarbon feedstock containing naphthenic acids over metal fibres covered with a running film of NaOH (Forero *et al.*, 1996). The concurrent flow of the two phases creates a greater surface area and faster rate of extraction without the formation of soap emulsions, enabling efficient recovery of both neutralised hydrocarbons and naphthenates (Forero *et al.*, 1996).

A large scale fractionation of commercial NA was required to produce large enough quantities of individual fractions for multiple investigations (e.g. West *et al.* (2014a)). Prior to fractionation by argentation chromatography, the free acids required derivatisation to the methyl esters. Therefore 40 - 50 mg of commercial NA mixture was transferred into ten glass vials each (430 mg in total), followed by the addition of 8 mL BF_3-methanol complex solution (Sigma Aldrich). The vials were placed in a heater block at 70 °C and left to derivatise for 1 hour 20 min. After the vials had cooled, a 2

mL aliquot of water was added followed by 2 mL hexane (HPLC Grade, Rathburn Chemicals Ltd., UK). The top organic layers were carefully transferred and combined in a round bottom flask. Each aqueous phase was extracted a further two times with 2 mL aliquots of hexane, combining the organic layers in the round bottom flask.

The combined methylated NA solution was dried over anhydrous Na_2SO_4 ($\geq$ 99.0%, Sigma Aldrich) and then transferred into another round bottom flask. The NA methyl esters were concentrated to 1 – 2 mL by rotary evaporation at 40 °C before being transferred to a glass vial with rinses and taken to dryness under a stream of N_2 at 40 °C, yielding at least 310 mg of methylated commercial NA.

2.2.4 Derivatisation of reference and model carboxylic acids and alcohols

Polar compounds analysed by gas chromatography often require derivatisation prior to analysis by GC to improve their chromatographic properties. Therefore the carboxylic acids were analysed as their methyl or trimethyl silyl esters and the alcohols were analysed as their trimethyl silyl ethers. The methyl esters of the reference and model carboxylic acids were obtained by reacting the acids with BF_3-methanol complex (15%, Sigma Aldrich) or 10% HCl in methanol at 70 °C for 30 – 60 min. The reactions were quenched with an aliquot of water and the methylated acids extracted with three aliquots of hexane or cyclohexane (HPLC Grade, Rathburn Chemical Ltd., UK). The organic solutions were dried over $MgSO_4$ (>99.0%, Sigma Aldrich) before being filtered into pre-weighed vials. The solvent was removed by N_2 blowdown at 25 – 40 °C. The alcohols were derivatised with BSTFA (Sigma Aldrich) at 70 °C for 30 min and diluted with hexane or DCM (HPLC Grade, Rathburn Chemical Ltd., UK) to an appropriate concentration for GC-MS or GC×GC-MS analysis (Sections 2.1.3 and 2.1.4).

2.2.5 Fractionation of methylated commercial NA extract

The large scale fractionation procedure, previously reported by Scarlett *et al.* (2013) was developed based on the small scale procedure using silver-ion (Ag-Ion) SPE cartridges (Discovery®) previously developed by Jones *et al.* (2012) for the separation and study of aromatic acids from OSPW NA. A large glass column (length: 65 cm, I.D: 0.4 cm) with a fixed sintered glass bed and stopcock was dry-packed with 37.5 g of Ag-Ion phase (Discovery®) with a piece of filter paper (Whatman™ 1: 42.3 mm) placed on top of the phase to reduce disturbance of the top layer during the addition of solvent. The column was washed with three 300 mL aliquots of hexane (HPLC Grade, Rathburns Chemical Ltd.), the final wash was collected in a 500 mL round bottom flask to be analysed, to observe any contamination from the column.

The commercial NA methyl esters (310 mg) were dissolved in 2 mL of hexane and loaded onto the top of the phase in the column with three rinses of the vial with hexane. The NA methyl esters were eluted through the phase with an eluotropic series of solvents; 300 mL aliquots of solvent were carefully poured down the inside of the column and the eluate collected in 500 mL glass round bottom flasks producing individual fractions. When the solvent level was just above the top of the phase, to prevent the phase from drying out, the stopcock was quickly closed and the round bottom flask exchanged for the next fraction before re-opening the stopcock and carefully pouring the next aliquot of solvent down the inside of the column, collecting the next fraction. The solvent and solvent mixtures were increased in polarity, eluting the less polar analytes first (i.e. aliphatic and alicyclic acid methyl esters in hexane) and gradually the more polar acid methyl esters (i.e. aromatics and heteroatom-containing acid methyl esters). Four fractions were eluted with 100% hexane, followed by three 5% diethyl ether (Glass Distilled Grade, Rathburns Chemical Ltd.), 95% hexane fractions,

one 10% diethyl ether, 90% hexane fraction, one 100% diethyl ether fraction and finally

one 100% methanol (Chromasolv® HPLC Grade, Sigma Aldrich) fraction (Table 2-1).

The 10 individual fractions and the wash prior to loading were concentrated by rotary

evaporation to 1 – 2 mL and transferred to pre-weighed 7 mL glass vials. The mass of

each fraction is detailed in Table 2-1.

Table 2-1: Summary of the fractions obtained by Ag-Ion fractionation of the

commercial NA methyl esters.

Fraction	Eluent	Mass of eluate / mg
Wash	Hexane	0.2
1	100% hexane	110.0
2	100% hexane	125.0
3	100% hexane	12.4
4	100% hexane	0.6
5	5% diethyl ether : 95% hexane	20.1
6	5% diethyl ether : 95% hexane	2.6
7	5% diethyl ether : 95% hexane	2.9
8	10% diethyl ether : 90% hexane	11.8
9	100% diethyl ether	21.6
10	100% methanol	135.5
	Total	442.5
	Total (excluding F10)	307.0

2.2.6 Fractionation of methylated OSPW NA extract

In order to obtain enough material for several concurrent investigations into the nature of various classes of OSPW NA (e.g. Rowland *et al.* (2014a)), the large scale fractionation was performed twice, on two quantities of OSPW NA methyl esters which had been extracted from the WIP OSPW sample (Section 2.2.1, page 58). The procedure used was the same as the large scale fractionation performed on the commercial NA methyl esters, based on the procedure developed by Jones *et al.* (2012), previously described in Section 2.2.5. The mass of OSPW NA methyl esters loaded onto the phase in the first fractionation was 296 mg, and 300 mg in the second fractionation. A summary of the fractions for each fractionation is given in Table 2-2 and Table 2-3.

Table 2-2: Summary of the fractions collected in the first Ag-Ion fractionation of the OSPW NA methyl esters.

Fraction	Eluent	Mass of eluate / mg
Wash	Hexane	0.4
1	100% hexane	20.1
2	100% hexane	76.8
3	100% hexane	7.4
4	100% hexane	1.7
5	5% diethyl ether : 95% hexane	61.3
6	5% diethyl ether : 95% hexane	30.8
7	5% diethyl ether : 95% hexane	9.2
8	10% diethyl ether : 90% hexane	11.5
9	100% diethyl ether	29.6
10	100% methanol	52.1
Total		300.9
Total (excluding F10)		248.8

Table 2-3: Summary of the fractions collected in the second Ag-Ion fractionation of the

OSPW NA methyl esters.

Fraction	Eluent	Mass of eluate / mg
Wash	Hexane	0.3
1	100% hexane	7.7
2	100% hexane	96.7
3	100% hexane	16.7
4	100% hexane	2.1
5	5% diethyl ether : 95% hexane	50.0
6	5% diethyl ether : 95% hexane	38.2
7	5% diethyl ether : 95% hexane	12.9
8	10% diethyl ether : 90% hexane	15.1
9	100% diethyl ether	36.1
10	100% methanol	222.9
	Total	498.4
	Total (excluding F10)	275.5

2.3   Conversion Reactions

The conversion steps involved in the chemical transformation of carboxylic acids and their methyl ester derivatives to the corresponding hydrocarbons was based upon the preliminary investigation of Seifert *et al.* (1969), who proposed the formation and reduction of the tosyl esters via the alcohols, as opposed to previous attempts via the iodide intermediates (Zelinsky, 1924; Knotnerus, 1957). During attempts at reproducing the procedure outlined by Seifert *et al.* (1969) on model alicyclic, bicyclic acids several problems were encountered and new reaction procedures were investigated and used to optimise the conversion (Figure 2-1). For example, tosylation in pyridine did not always produce the tosyl ester in high yields and reduction of the tosyl ester with lithium aluminium hydride (LAH) did not always yield the corresponding hydrocarbon but instead, yielded the original alcohol.

However, the first reduction step using LAH, based on the method of Seifert *et al.* (1969), proved efficient at producing the primary alcohols. The formation of the tosyl esters with tosyl chloride (TsCl) in the presence of 4-(dimethylamino)pyridine (DMAP) as a catalyst and triethylamine (TEA) as a base, was instead based on the methods by Ding *et al.* (2011) and Yoshida *et al.* (1999). Final reduction of the tosyl esters to the hydrocarbons using lithium triethylborohydride (LiEt$_3$BH) (Super-Hydride®) was inspired by the procedures outlined by Krishnamurthy and Brown (1976) and Brown *et al.* (1980).
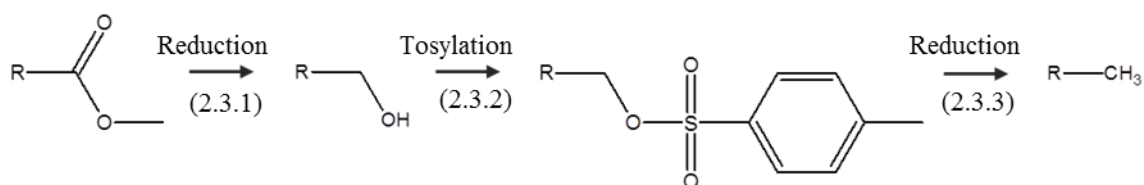
Figure 2-1: General overall reaction scheme for the conversion of carboxylic acids and their methyl ester derivatives to the corresponding hydrocarbons. Details of the procedure for each step can be found under relevant section numbers.

General methods are now given for the individual conversion steps performed on the model carboxylic acids, commercial NA methyl esters and OSPW NA methyl esters. Any minor differences for individual samples are discussed within the appropriate chapters.

2.3.1   General method for the reduction of acid methyl esters to alcohols
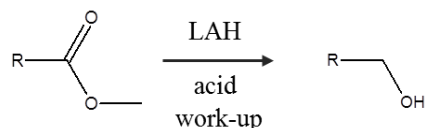
Figure 2-2: Reaction scheme for the reduction of carboxylic acids and methyl esters to primary alcohols using LAH. R = hydrocarbon 'backbone' of acid structure.

The reduction of carboxylic acids with lithium aluminium hydride (LAH) (Figure 2-2) is a moisture sensitive reaction. Therefore a reflux apparatus, consisting of a 10 mL two-neck round bottom flask within a rota-mantle and fitted with a condenser, was assembled whilst hot (Figure 2-3). The condenser was fitted with a $CaCl_2$ guard tube and a magnetic stirrer added before fitting the side arm with a rubber suba-seal (Figure 2-3). The reaction vessel was purged with N_2 to create an inert atmosphere.
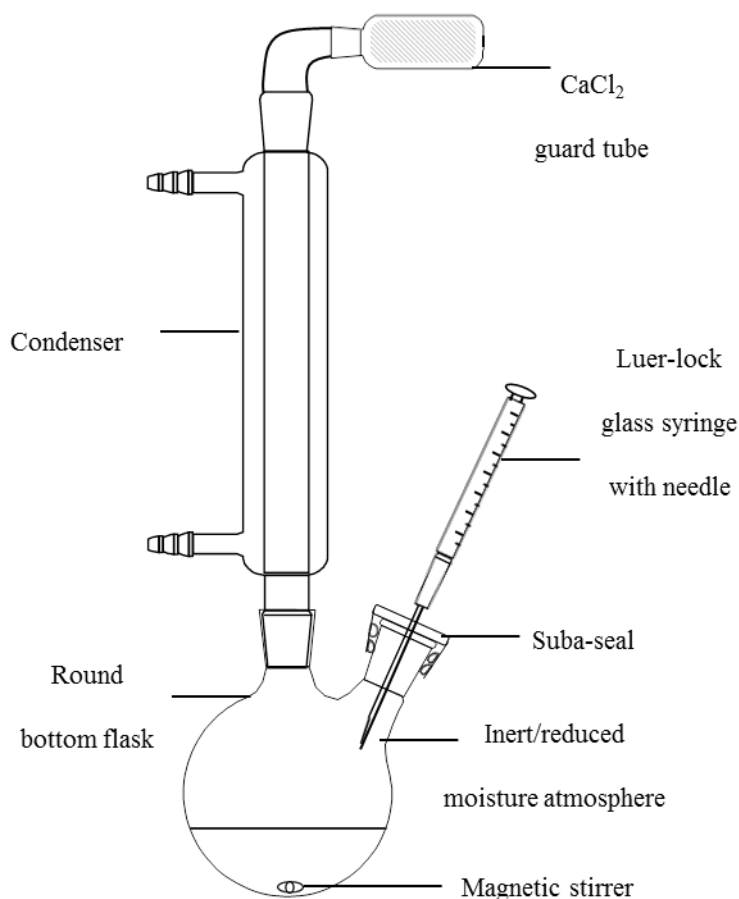
Figure 2-3: Reflux apparatus assembly for the reduction of carboxylic acids and methyl ester derivatives under a reduced moisture atmosphere.

First, the model carboxylic acids, extracted OSPW NA, or commercial NA mixtures (5 - 50 mg) were transferred into the round bottom flask under a stream of N_2. The acids were dissolved in 1.0 mL anhydrous diethyl ether (Chromasolv® HPLC Grade, inhibitor-free, Sigma Aldrich) and heated (50-70 °C). Then, LAH solution (1.0 M in diethyl ether, Sigma Aldrich) was added in excess (5 molar equivalents) and the reaction left to reflux for 30 min. Upon addition of LAH solution, the reaction mixture vigorously effervesced and a grey precipitate formed. Additional aliquots of anhydrous solvent were added if necessary to avoid the reaction running dry. In the interest of retaining semi-volatile components, it was found that the reduction was as efficient when carried out at room temperature (15-20 °C) with a longer reaction time 2+ hours.

The reaction was quenched dropwise with 10% H_2SO_4 to decompose excess hydride. A white precipitate formed and then re-dissolved. The mixture was transferred to a reaction vial (Wheaton V-Vial; Sigma Aldrich), rinsing the round bottom flask with aliquots of diethyl ether. Two clear phases were observed, the lower aqueous phase was carefully pipetted from beneath, to a separate reaction vial.

The aqueous phase was extracted three times with diethyl ether and the upper organic layer carefully pipetted into the previous reaction vial each time. The combined ethereal solution was washed with 5% $NaHCO_3$ solution and water (HPLC Grade; Fisher Scientific) to neutralise the organic phase and then washed with dilute 6% brine (technical ~26%, Sigma Aldrich). The solution was then dried over anhydrous $MgSO_4$ ($\geq$ 99.5 %, Sigma Aldrich).

The solution was filtered through a rinsed Pasteur pipette plugged with defatted cotton wool into a pre-weighed vial, rinsing the reaction vial and plugged pipette with diethyl ether. The solvent was removed under a stream of N_2 at 25 °C and the yield recorded.

2.3.2 General method for the conversion of alcohols to tosyl esters
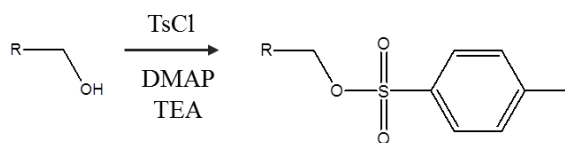
Figure 2-4: Reaction scheme for the derivatisation of primary alcohols to tosyl ester derivatives using TsCl in the presence of DMAP and TEA. R = hydrocarbon 'backbone' of original acid structure.

The alcohol (5 - 50 mg) was dissolved and transferred into a 5 or 10 mL reaction vial in a minimum volume of DCM (HPLC Grade; Rathburns Chemical Ltd.). The reaction vial was placed in an ice bath and cooled whilst stirring. Then 4-(dimethylamino)pyridine (DMAP) ($\geq$ 99 %, Sigma Aldrich) was transferred into the reaction vial (1 molar equivalent) followed by p-toluenesulfonyl chloride (TsCl) ($\geq$ 99 %, Sigma Aldrich) in slight excess (1.2 molar equivalent) and finally an aliquot of triethylamine (TEA) (1 molar equivalent) ($\geq$ 99 %, Sigma Aldrich) (Figure 2-4). It was found the addition order of the reagents was important to the success of the reaction. The reaction vial was closed and the solution left to react for 12 hours.

The reaction was quenched with diethyl ether and water (HPLC Grade; Fisher Scientific) and stirred for 15 min. A white precipitate formed upon addition of diethyl ether and cleared again upon addition of water. The lower aqueous phase was carefully pipetted into a separate reaction vial and extracted with three aliquots of diethyl ether. The extracts were combined in the original reaction vial and the ethereal solution washed with HCl (2.0 M), 5% NaHCO$_3$ solution and finally dilute 6% brine (technical ~26%, Sigma Aldrich) to remove unreacted TEA and neutralise the organic phase. The solution was then dried over anhydrous MgSO$_4$ ($\geq$ 99.5 %, Sigma Aldrich).

The solution was filtered through a rinsed Pasteur pipette plugged with defatted cotton wool into a pre-weighed vial. The solvent was removed under a stream of N_2 at 25 °C and the yield recorded.

2.3.3 General method for the reduction of tosyl esters to hydrocarbons
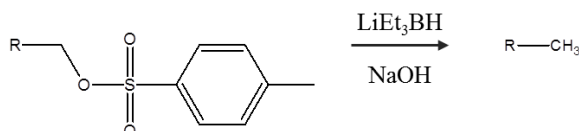
Figure 2-5: Reaction scheme for the reduction of tosyl ester derivatives to defunctionalised hydrocarbons using LiEt$_3$BH. R = hydrocarbon 'backbone' of original acid structure.

Reduction reactions with lithium triethylborohydride (LiEt$_3$BH or Super-Hydride®) (Figure 2-5) are moisture sensitive, therefore the assembly of the reflux apparatus was the same as for the first reduction with LAH (Figure 2-3; Section 2.1.3, page 69) to create an inert atmosphere. The tosylate (5 - 50 mg) was dissolved and transferred into the round bottom flask in anhydrous diethyl ether (Chromasolv® HPLC Grade, inhibitor-free, Sigma Aldrich) under a stream of N_2. Then LiEt$_3$BH solution (1.0 M in THF; Sigma Aldrich) was added in excess (15 molar equivalents). The reaction was left stirring at room temperature for 2+ hours.

The reaction flask was then placed in an ice bath to cool, before being quenched with the dropwise addition of 20% NaOH solution to decompose the excess hydride. The reaction was stirred for 30 min. The reaction mixture was transferred into a 5 or 10 mL reaction vial with anhydrous diethyl ether. Two clear phases were observed. The lower aqueous phase was transferred into a separate reaction vial, extracted with three aliquots of hexane (HPLC Grade; Rathburns Chemical Ltd.) and combined in the original

reaction vial. The combined organic phase was washed with HCl (2.0 M) and dilute 6%

brine (technical ~26%, Sigma Aldrich) to neutralise the organic phase. The solution was

dried over anhydrous $MgSO_4$ ($\geq$ 99.5 %, Sigma Aldrich) and filtered through a rinsed

Pasteur pipette plugged with defatted cotton wool into a pre-weighed vial.

When the volatility of the product was of concern (i.e. if the sample contained low

molecular weight hydrocarbons), a Kuderna-Danish apparatus (Section 2.3.4) was used

instead of removing the solvent under a stream of N_2 at 25 °C.

2.3.4 General method for the concentration of hydrocarbons using a Kuderna-Danish concentrator followed by silica chromatography

A Kuderna-Danish (KD) concentrator consisting of three main components was

assembled. These were: a graduated receiver flask fitted below an inverse conical-

shaped KD flask with a Vigreux or Synder column fitted above (Figure 2-6). A micro

Dean-Stark receiver with a condenser attached was fitted to the top of the Vigreux

column (Figure 2-6). The apparatus was lowered so that only the graduated receiver

flask was submerged in a water bath, consisting of a two-neck round bottom flask

containing a magnetic stirrer filled with water in a Rota-mantle (Barnstead heating and

stirring mantle), with a thermometer attached through the side-arm to measure the

temperature of the water (Figure 2-6).
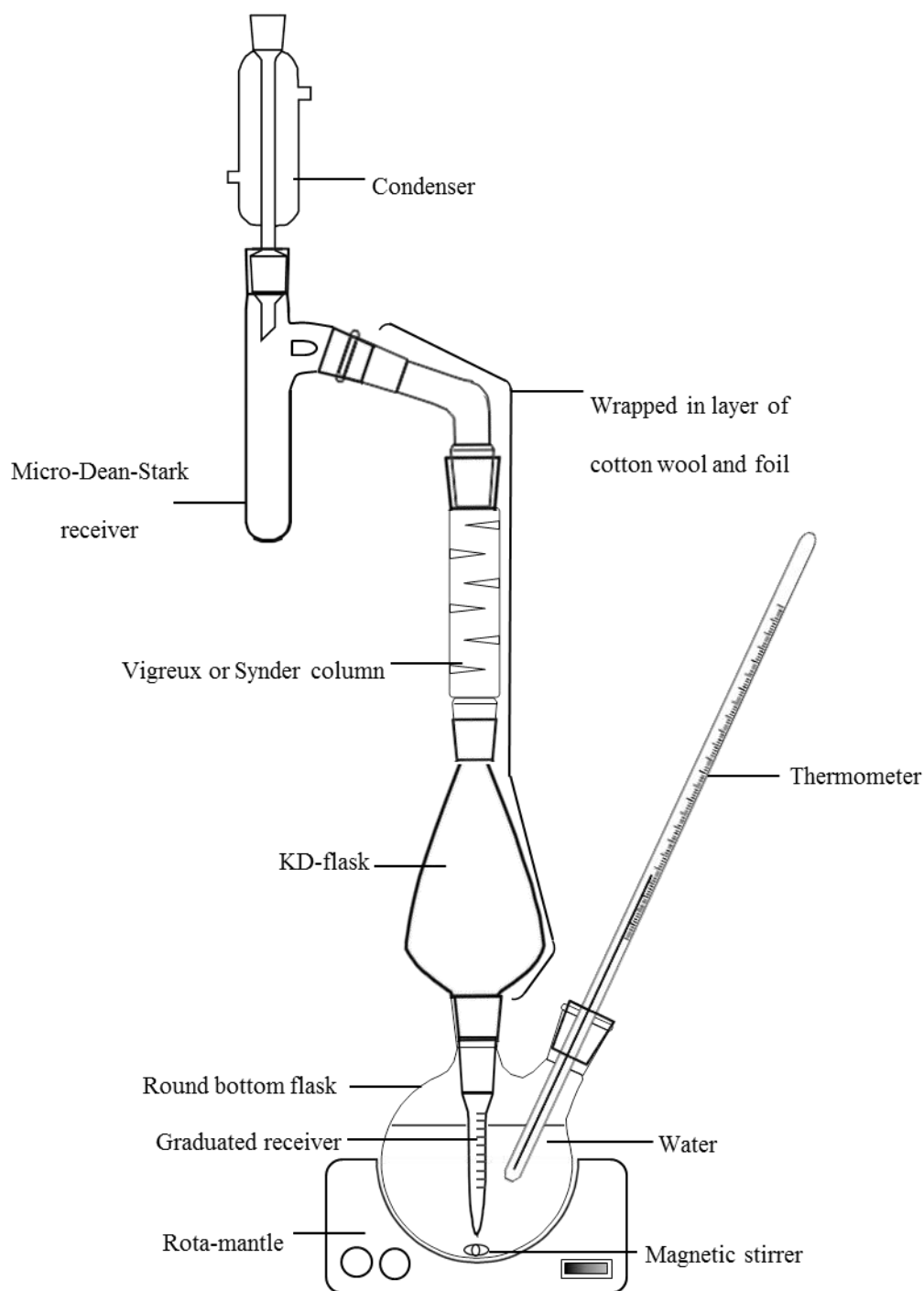
Figure 2-6: Kuderna-Danish apparatus assembly for the concentration of the final

hydrocarbon product following the reduction of the commercial and OSPW NA methyl

esters.

The ethereal solution containing the hydrocarbon product, obtained after reduction of

the tosyl esters with $LiEt_3BH$, was transferred into the graduated receiver flask attached

to the KD-flask, adding 2 – 3 Soxhlet extracted anti-bumping granules. Next, the

Vigreux column and remaining apparatus was assembled as previously described (Figure 2-6). The temperature of the water bath was slowly increased until the solution began to gently reflux, observed by a constant stream of bubbles in the graduated receiver. When the level of the solution had decreased to approximately 0.8 mL, the water bath was removed and the apparatus allowed to cool, aided by briefly lowering the receiver flask into an ice bath. This allowed the remaining vapour in the apparatus to condense and wash back down into the receiver flask resulting in a final volume of ~1 mL.

The concentrated hydrocarbon product contained two major by-products of the hydride reduction, observed in the gas chromatograms as boroxin and butylated hydroxy toluene (BHT), present as a stabiliser in the tetrahydrofuran of the $LiEt_3BH$ solution. Therefore a silica chromatography clean-up was performed to remove the majority of impurities. However, following careful concentration of the product using the Kuderna-Danish apparatus, the clean-up step had to involve minimum solvent addition. Therefore 300 μL of concentrated product solution was applied dropwise onto ~1.2 g of activated silica (600 A mesh, activated at temp 200°C for 12 hours) in an aluminium weighing boat, allowing the excess solvent to absorb or evaporate between applying each drop (Figure 2-7; A). The loaded silica was then transferred into a shortened column (cut glass Pasteur pipette) containing a bed of activated silica plugged with defatted cotton wool (Figure 2-7; B). The hydrocarbons were eluted through with hexane until 100 μL was collected in an insert vial ready for analysis.
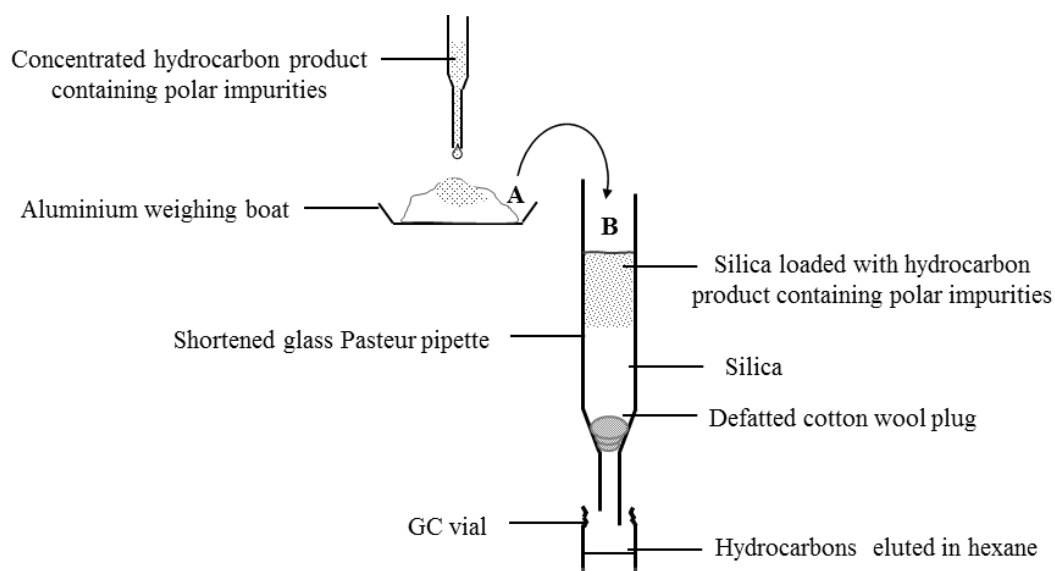
Figure 2-7: Outline of 'clean-up' procedure involving (A) the concentrated hydrocarbon product applied dropwise to activated silica allowing solvent to evaporate before (B) transferring loaded silica into a shortened column and eluting the hydrocarbons with hexane.

2.4 Additional Reactions

2.4.1 General method for hydrogenation

Selective catalytic hydrogenation of aromatic rings and unsaturated bonds for the synthesis of reference compounds was performed using a H-Cube® (ThalesNano Nanotechnology Inc., Budapest), fitted with a HPLC Pump (Model 300, Gynotek) and Rheodyne injector. The H-Cube® is a flow reactor which produces an online supply of hydrogen from the electrolysis of water and reacts the substrate with H_2 in the presence of a catalyst at controlled pressures and temperatures up to 100 bar and 100 °C. The catalysts come pre-packed in metal cartridges (CatCarts®).
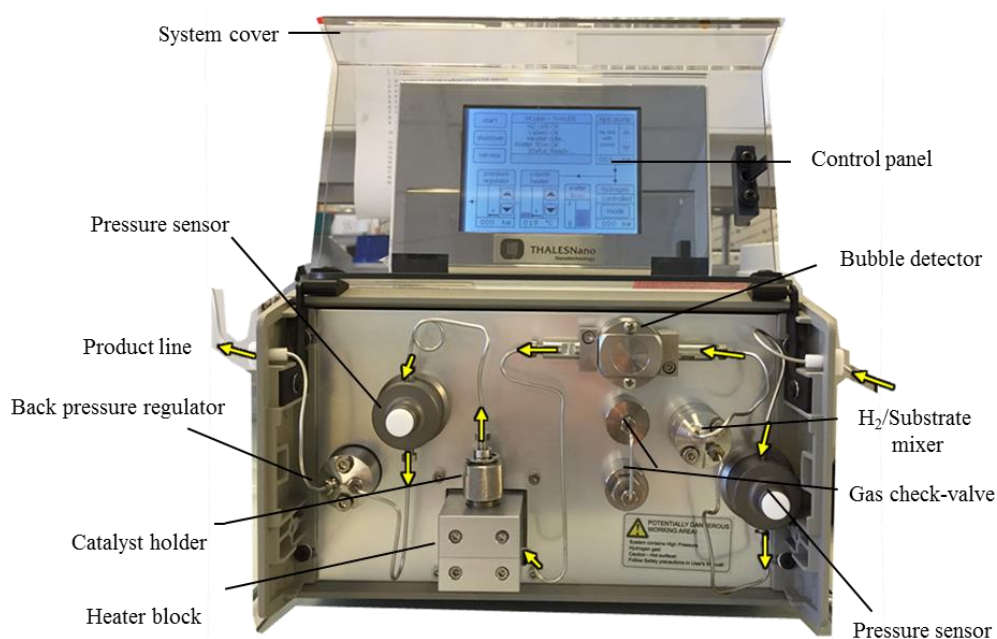
Figure 2-8: Components of an H-Cube® hydrogenation flow reactor (ThalesNano Nanotechnology Inc., Budapest).

An aliquot of sample dissolved in hexane or cyclohexane was injected into the Rheodyne injector, the injector was turned from the 'load' to 'inject' position, introducing the sample into the solvent flow of cyclohexane at $0.1 - 1.0$ mL min^{-1} through the H-Cube®. After passing through the catalyst under pre-set conditions, between $60 - 100$ °C and $60 - 100$ bar, the hydrogenated product was collected in a pre-weighed vial. The solvent was removed under a stream on N_2 at $25 - 40$ °C and the yield recorded. If the hydrogenation resulted in partial reduction and complete hydrogenation was required, the sample was re-injected and hydrogenated further.

Chapter 3

Identification of bicyclic acids by multidimensional gas chromatography-mass spectrometry of methyl ester derivatives

Chapter 3 describes the structural identification of alicyclic bicyclic acids, which is a major class of naphthenic acids (NA) within some commercial NA mixtures and in acid extracts from oil sands process-affected waters (OSPW).

A well-accepted toxicity screening assay had indicated previously that some bicyclics were the most acutely toxic acids known, but despite this toxicity and despite the high abundance of the bicyclics in petroleum acids and OSPW, very few had been identified at the inception of the present work.

Examination herein of esterified acid extracts from samples of OSPW and a sample of commercial petroleum-derived acids, by GC×GC-MS showed that >100 C_{8-15} bicyclic acids were present. Synthesis or purchase of reference bicyclic acids allowed the GC×GC retention times of the methyl esters of several structural isomers to be established. The mass spectra of these and comparison with the published spectra of some additional bicyclic acids (methyl esters), allowed identification of numerous C_{8-11} fused-ring and several novel, bridged bicyclic acids, for the first time in OSPW and indeed in any petroleum related mixture. Delimitation of possible bicyclic structures for which no reference compounds were available, or where the data for reference compounds did not match those of acids present in the commercial or OSPW NA, was also made. Mass spectra of the co-occurring bicyclic C_{12-15} acid methyl esters suggested many were simply analogues of the C_{8-11} acids identified, but with longer alkanoate chains and/or alkyl substituents.

Chapter 3

The main findings included and discussed in this chapter have been published in:

Wilde, M. J., West, C. E., Scarlett, A. G., Jones, D., Frank, R. A., Hewitt, L. M. and Rowland S. J. (2015) Bicyclic naphthenic acids in oil sands process water: Identification by comprehensive gas chromatography-mass spectrometry. *Journal of Chromatography A*, 1378, 74-87.

3.1 Introduction

The composition of the acid-extractable organic (AEO) fractions of OSPW have been investigated previously using a range of analytical techniques as described in Chapter 1. Despite slight differences in composition dependent on extraction, ionisation, chromatographic separation and resolution of the mass spectrometric techniques employed, most investigations have shown that O_x species (Headley *et al.*, 2015; Nyakas *et al.*, 2013), particularly $C_nH_{2n+z}O_2$ species or 'classical' naphthenic acids (NA) (Barrow *et al.*, 2010; Headley *et al.*, 2011a), are most abundant. Investigations focusing specifically on NA have shown that the $z = -4$, alicyclic bicyclic acids are usually the major class in OSPW, crude oil and petroleum-derived commercial NA (Bataineh *et al.*, 2006; Martin *et al.*, 2008; Barrow *et al.*, 2010; Hindle *et al.*, 2013; Dzidic *et al.*, 1988; Barrow *et al.*, 2003; Mapolelo *et al.*, 2011). Damasceno *et al.* (2014) showed that >120 bicyclic acids were present in each of two commercial NA samples, though none were identified. This lack of knowledge of the structures of the bicyclic NA has important implications for the toxicity, corrosivity, origins and potential uses of NA (as reviewed in Chapter 1).

GC×GC-MS has shown great potential for the identification of individual bicyclic acids. For example, Rowland *et al.* (2011e) confirmed the presence of two bicyclo[4.3.0]nonane carboxylic acids, two bicyclo[4.4.0]decane-3-carboxylic acid isomers and an isomer of bicyclo[4.4.0]decane-3-ethanoic acid, in a commercial NA mixture by comparison of the mass spectra with published mass spectra and GC×GC retention positions of synthesised reference compounds. Mass spectral interpretation and comparison of relative retention positions also led to the more tentative assignment of several bicyclo[4.3.0]nonane ethanoic acids, methyl substituted homologues and a bicyclo[4.4.0]decane-3-propanoic acid.

West *et al.* (2014a) and Bowman *et al.* (2014) subsequently used GC×GC-MS to identify some bicyclic mono- and diaromatic acids (i.e. naphthalene, indane and tetrahydronaphthalene and tetrahydroindane acid isomers) in crude oil and pore water from a composite tailings deposit respectively, again by comparison of the mass spectra of methyl esters with those of synthesised reference compounds.

Given the former studies it was worth considering the reasons for the paucity of information on the structures of the alicyclic bicyclic acids. Damasceno *et al.* (2014) showed by GC×GC-MS that over 120 acids were present in commercial NA, yet Rowland *et al.* (2011e) only identified a few bicyclics in similar commercial NA.

The maximum number of isomers for the simplest (C_{8-11}) acids, assuming that at least one (necessarily), and sometimes two, carbon atoms would be associated with the carboxylate/alkanoate chain was calculated herein. The latter assumption is reasonable based on the identifications of ethanoate side chains of the co-occurring tricyclic and pentacyclic acids (Rowland *et al.*, 2011a; Rowland *et al.*, 2011c; Rowland *et al.*, 2011g) and what is known of the biodegradation processes from which the acids originate (Smith *et al.*, 2008; Rowland *et al.*, 2011b; Johnson *et al.*, 2011).

For a C_{11} acid, for example, at most ten carbons are left for formation of the bicyclic 'core' of the acid, once the carboxylated carbon is discounted. If any alkyl substituents were present, the number of carbon atoms in the 'core' would be less than ten and more alkylation would be present. Since alkyl groups identified or tentatively established in OSPW acids to date have not exceeded those comprising four carbon atoms in total (e.g. a combination of ethyl and methyl groups), it is reasonable to assume that the smallest number of atoms in the bicyclic 'core' would then probably be six.

Three structural types exist for acids with a C_6 'core'. These have cyclopropyl or cyclobutyl rings; the former are present in carane- and thujane-type compounds and the

latter present in bicyclo[3.1.1]heptanes (pinanes), bicyclo[4.2.0]octanes and bicyclo[2.2.0]hexanes, which are known in the ladderane acids (Rush *et al.*, 2011). For the acids with a C_7 'core' and the requisite substituents, there are four structural types (examples are given in Figure 3-1; *I-III*), for the C_8 'core' acids, six (e.g. Figure 3-1; *IV-VII*), for the acids with a C_9 'core', seven (e.g. Figure 3-1; *VIII-XI*) and for the acids with a C_{10} 'core', nine possible structures (where there are two bridgehead carbons, e.g. Figure 3-1; *XII-XVI*). Spiro- and non-fused structures were also considered, such as spiro[4.5]decane carboxylic acid (Figure 3-1; *XVII*), fused at one carbon atom and the non-fused cyclopentylcyclopentane carboxylic acid (Figure 3-1; *XVIII*).

Therefore, the empirical calculations above suggest that even the simplest acids in OSPW or commercial NA samples might comprise over 30 structural types and for each of these, many stereoisomers are possible. Examples of some of these bicyclic structural types are given in Figure 3-1; most ring types have been identified within natural products.

Thus, in theory, it is certainly possible to account for the >100 bicyclic acids observed in commercial acids (*cf.* Damasceno *et al.* (2014)). The analytical challenge is to identify what at least some of these actually are, particularly in OSPW fractions.

(I)

Bicyclo[2.2.1]heptane acids

(II)

Bicyclo[3.1.1]heptane acids

(III)

Bicyclo[4.1.0]heptane acids

(IV)

Bicyclo[2.2.2]octane acids

(V)

Bicyclo[3.2.1]octane acids

(VI)

Bicyclo[3.3.0]octane acids

(VII)

Bicyclo[4.2.0]octane acids

(VIII)

Bicyclo[3.3.1]nonane acids

(IX)

Bicyclo[3.2.2]nonane acids

(X)

Bicyclo[4.3.0]nonane acids

(XI)

Bicyclo[4.2.1]nonane acids

(XII)

Bicyclo[4.2.2]decane acids

(XIII)

Bicyclo[5.3.0]decane acids

(XIV)

Bicyclo[4.4.0]decane acids

(XV)

Bicyclo[5.2.1]decane acids

(XVI)

Bicyclo[3.3.2]decane acids

(XVII)

Spiro[4.5]decane acids

(XVIII)

Cyclopentylcyclopentane acids

Figure 3-1: Examples of generalised structures and names of possible C_{11} bicyclic acids.

3.1.1 Aims and Objectives

The aims of the current investigation were to use GC×GC-MS to chromatographically resolve individual bicyclic acids as their methyl ester derivatives in various samples of OSPW NA and a commercially available, petroleum NA. Secondly, to utilise the separation afforded by GC×GC-MS to assess the true complexity of the bicyclic acid methyl esters mixtures present in samples of OSPW NA and a petroleum NA mixture. Thirdly, to use the mass spectra obtained for individual components in these NA mixtures, for the identification of C_{8-11} bicyclic acids as their methyl ester derivatives. Identification was reliant on comparison of the retention position and mass spectra of the bicyclic NA in OSPW and petroleum acid extracts with those of synthesised or purchased reference bicyclic acids, reference mass spectra and logical mass spectral interpretation. Finally, the mass spectra of the reference bicyclic acid methyl esters were to be evaluated for generic trends which could be correlated with key structural features for the tentative assignment and interpretation of the mass spectra of $C_{11}+$ bicyclic acid methyl esters.

3.2 Methods

3.2.1 Acid extract samples

Six acid extracts were analysed in total; one (sample #1) analysed previously (Wilde *et al.*, 2015) and five (sample #2 – #6) analysed herein. The six acid extracts included three different OSPW acid extracts from industry A, one from industry B, one commercially prepared petroleum acid extract and one acid extract from a well water sample within the oil sands mining area of industry A. Details of the NA extracts are summarised in Table 3-1.

Table 3-1: Summary of the OSPW NA and commercial NA sample details.

Sample No. #	Sample Type	Originator	Details
1	OSPW	Industry A	Collected 2004
2	OSPW	Industry A	Collected 2009, isolated concentrated naphthenates 2011
3	OSPW	Industry B	Collected 2011
4	OSPW	Industry A	Collected 2013
5	Commercial Naphthenic acids	Merichem	Batch no. CN/138 CAS# 1338-24-5
6	Well Water	Environment Canada	Collected 2013, Proximal B #4

The NA extracts included two from oil sands industry A (#1 and #2; Table 3-1) which were both extracted from OSPW collected from the West In-Pit (WIP) tailings pond; sample #1 was collected in 2004 and used in the identification of tri-, tetra- and pentacyclic diamondoid acids by Rowland *et al.* (2011c) and Rowland *et al.* (2011g) and #2 was sampled in 2009 and used in more recent studies (Scarlett *et al.*, 2013; Reinardy *et al.*, 2013). Although several Canadian researchers have reported the source of OSPW for their investigations as WIP (Frank *et al.*, 2009; Pereira *et al.*, 2013b; Brunswick *et al.*, 2015), little information has ever been reported about sampling

procedures, the location of the WIP or the inputs of OSPW into the WIP. However, one detailed insight into the transfer and storage of OSPW within industry A and the input of OSPW into the WIP was reported by Han *et al.* (2009). Briefly, OSPW produced directly from the main extraction plant in industry A is stored in one of three settling basins; the Mildred Lake Settling Basin (MLSB), the South End Pond (SEP) or Southwest Sand Settling Basin (SWSB) (Han *et al.*, 2009). OSPW from the SEP and SWSB are then transferred to the WIP. Clarified OSPW (i.e. after a period of settling), from the WIP is then either mixed with clarified OSPW from MLSB and recycled in in the main extraction plant or is mixed with tailings from a secondary site and recycled in a secondary extraction plant (Han *et al.*, 2009). Therefore, it is presumed that studies into OSPW often include OSPW collected from the WIP, firstly, because access is easy and secondly due to its continuous use as storage and recycling of OSPW within industry A.

Sample #1 was isolated using the method reported by Frank *et al.* (2006), described in Chapter 2, Section 2.2.1 (Appendix Figure 1), and extracted and analysed previously (Wilde *et al.*, 2015). Sample #2 was isolated using the same clean-up method in Spring 2011 and extracted using the methods described in Chapter 2, Section 2.2.1.

Sample #3 was an NA extract isolated from OSPW collected from a tailings pond from industry B, as described by Lengger *et al.* (2015). The extract selected was the north east (NE) sample from the spatial study conducted by Lengger *et al.* (2015); the sample site was closest to the inlet pipe with a high concentration of particulate matter, chosen due to its higher abundance of low molecular weight acids (C_{8-15}) compared to the other sites. Sample #4 was extracted from unprocessed, raw OSPW collected from the Mildred Lake Settling Basin (MLSB) from industry A in 2013. The raw OSPW was acidified ($< pH\ 2$) and extracted with ethyl acetate as described in Chapter 2, Section

2.2.1. The lack of sample clean-up and concentration steps meant it was potentially the most representative of the NA present in OSPW but as a result contained other non-acid species such as polycyclic aromatic hydrocarbons (PAHs).

A commercially prepared acid mixture, gifted in 2009 from Merichem Co., was derivatised and fractionated as described in Chapter 2, Sections 2.2.3 and 2.2.5 and is also discussed in Chapter 5, Section 5.3.1. Fractionation by argentation chromatography (Ag-Ion) severely reduced the complexity of the commercial NA and the 'alicyclic' Ag-Ion fraction was included in the analysis. Commercial NA are often used as a comparison in investigations of OSPW NA. However previous studies have shown distinct differences in the commercial NA compositions (Grewer *et al.*, 2010; Hindle *et al.*, 2013). Finally an NA extract from an OSPW related well water, collected as part of a 'plume' investigation by Environment Canada was examined. The well water extract was chosen from several samples due to its high abundance of low molecular weight acids; the sample was collected from a well adjacent to the MLSB such as those described by Frank *et al.* (2014).

3.2.2   Reference acids

Authentic bicyclo[2.2.1]heptane-2-ethanoic acid (Figure 3-3; Structure Ib), 2,6,6-trimethylbicyclo[3.1.1]heptane-3-carboxylic acid ((+)-3-pinane-carboxylic acid) (IIa), bicyclo[2.2.2]octane-2-carboxylic acid (IVa), 4-pentylbicyclo[2.2.2]octane-1-carboxylic acid (IVc), bicyclo[3.3.0]octane-2-carboxylic acid (VIa), 4-methylbicyclo[3.3.0]octane-2-carboxylic acid (3-methyl-octahydro-pentalene-1-carboxylic acid) (VIb) and bicyclo[3.3.1]nonane-1-carboxylic acid (VIIIa) were purchased from Sigma (Poole, UK). Authentic bicyclo[2.2.1]heptane-1-carboxylic acid (Ia), bicyclo[2.2.2]octane-1-carboxylic acid (IVb), bicyclo[3.3.1]nonane-3-carboxylic acid (VIIIb) and 5-methyl-

bicyclo[3.3.1]nonane-1-carboxylic acid (VIIIc) were purchased from Molport (Riga, Latvia).

Bicyclo[3.2.1]octane-6-carboxylic acid (Va) had been previously synthesised from 2-hydroxybicyclo[3.2.1]octane-6-carboxylic acid (Sigma) by base catalysed dehydration followed by hydrogenation as described previously by Rowland *et al.* (2011a). Bicyclo[4.3.0]nonane-3-carboxylic acid (Xa), 7-methylbicyclo[4.3.0]nonane-8-carboxylic acid (Xb) and bicyclo[4.4.0]decane-2-propanoic acid (XIVe) were synthesised previously by catalytic hydrogenation as previously described by Rowland *et al.* (2011e).

Bicyclo[4.4.0]decane-2-carboxylic (XIVa), -3-carboxylic (XIVb), -2-ethanoic (XIVc) and -3-ethanoic acid (XIVd) (numbers refer to position of alkanoate substituents on bicyclic core) were synthesised from 1- and 2-(5,6,7,8-tetrahydro)naphthoic acid and 1- and 2-naphthalene ethanoic acid respectively as well as 7-methylbicyclo[4.2.0]octane-7-carboxylic acid (VIIa) from 1-methyl-1,2-dihydrocyclobutabenzene-1-carboxylic acid methyl ester by hydrogenation over 20% Pd(OH)$_2$/C and Raney Nickel catalysts at 100 °C and 100 bar using a Thalesnano H-Cube® as described in Chapter 2, Section 2.4.1.

3.2.3   GC×GC-MS

The GC×GC-MS instrumentation used is described in Chapter 2, Section 2.1.4. Samples were analysed using two different temperature programmes (referred to as conditions A and B). The GC×GC-MS conditions A involved the primary oven programmed from 30°C, held for 1 min, then heated to 120°C at 5°C min^{-1}, to 220°C at 0.8°C min^{-1}, to 280°C at 5°C min^{-1} and to 320°C at 10°C min^{-1} and then held for 10 min. The secondary oven was programmed to track the primary oven at 40°C above. The hot jet was programmed to start 30°C above the primary oven temperature until 150°C, it was then

ramped to 260°C at 1.3°C min^{-1} and then to 400°C at 4°C min^{-1}. The modulation period

was set at 4 or 6 s. The GC×GC-MS conditions B involved the primary oven

programmed from 35 °C, held for 1 min, then heated to 120°C at 5°C min^{-1}, to 220°C at

0.8°C min^{-1}, 280 °C at 2 °C min^{-1} and to 320 °C at 5°C min^{-1} and then held for 10 min.

The secondary oven was programmed to track the primary oven at 40 °C above. The hot

jet was programmed to start 30 °C above the primary oven and finish 100 °C above the

primary oven over the period of the run; programmed from 65 °C, held for 1 min, then

heated to 150 °C at 5 °C min^{-1}, to 260 °C at 1.3 °C min^{-1} and then to 400 °C at 3 °C min^{-1}

^{1}. The modulation period was set at 6 and 3 s.

3.3 Results and Discussion

The major focus of the present work was to identify (in many cases for the first time), series of bicyclic naphthenic acids in petroleum-related samples.

Whilst a few bicyclic acids had been identified in one commercial NA batch at the inception of this work (Rowland et al., 2011a), none had ever been identified in oil sands process-affected water (OSPW), despite the high abundance of bicyclic ($z = -4$) acids in OSPW reported by numerous Canadian workers (e.g. Martin *et al.* (2008) and Hindle *et al.* (2013)). Mainly this lack of successful identification was a result of the extreme complexity of the NA mixtures in substrates such as OSPW, but this was also due to the fact that very few OSPW samples had ever been released for study outside of Canada, with the consequence that only methods available to Canadian scientists had been employed. Until 2011, with perhaps only one published exception in which no acids were identified (Hao *et al.*, 2005), this did not involve use of a comprehensive GC×GC chromatographic approach: yet such methods probably have the highest chromatographic resolving power reported to date. Even since 2011, the use of GC×GC methods to study OSPW fractions (Rowland *et al.*, 2011c; Rowland *et al.*, 2011g) surprisingly has not involved study of the alicyclic bicyclic acids of OSPW, although recently Bowman *et al.* (2014) identified several monoaromatic bicyclic acids in OSPW-related samples and Damasceno *et al.* (2014) reported resolution, but no identification, of alicyclic bicyclic acids, in two commercial NA samples.

During the present work, a number of OSPW acid fractions were made available for study from scientists at Environment Canada. Such samples have rarely been made available before and certainly no studies of the bicyclic acids have been made or at least, published. These included samples from two oil sands industries' tailings ponds or settling basins and a well water within the oil sands mining area (sample details

discussed in Section 3.2.1 and summarised in Table 3-1). Unfortunately, details of the sampling locations etc. cannot be published herein for legal reasons. Whilst this means that detailed explanations and interpretations of any differences and similarities cannot be made, such samples still provided a unique opportunity for the present author to attempt to identify some of the acids for the first time using GC×GC-based techniques.

3.3.1   GC×GC separation of acid methyl esters

The NA mixtures analysed included four different OSPW extracts (#1-4), one commercial NA mixture (#5) and one acid extract from a well water sample within the oil sands mining area (#6). Previous studies have shown that NA extracts show a degree of heterogeneity, with the NA composition being dependent on several factors, probably including: sample origin, location, treatment and extraction as discussed previously (Chapter 1, Section 1.3). Despite this, the alicyclic bicyclic acids are repeatedly reported as one the most abundant $C_nH_{2n+z}O_2$ acid classes, not only in OSPW, but also in commercially prepared NA and crude oil acid extracts, yet little is known about their structures (Chapter 1, Section 1.5, page 47) (Dzidic *et al.*, 1988; Martin *et al.*, 2008).

Therefore multiple OSPW samples (#1-4), a commercial NA sample (#5) and an oil sands well water sample (#6) were examined herein to maximise the possibility of identifying any bicyclic acids, to provide new understanding and improve upon the current paucity of knowledge regarding bicyclic acids structures. The OSPW samples were collected by workers at Environment Canada as part of several other investigations (Frank *et al.*, 2009; Brunswick *et al.*, 2015) and their detailed selection was outside of the control of the present author. Nonetheless they are considered representative of typical industry process waters and the results of this investigation can be compared somewhat with other experimental data for similar samples obtained by other techniques (e.g. Hindle *et al.* (2013), Frank *et al.* (2014) and Brunswick *et al.* (2015)).

The GC×GC extracted ion chromatograms (EICs) of the five NA samples examined

herein, showed separation of the acid methyl esters by carbon number (Figure 3-2).
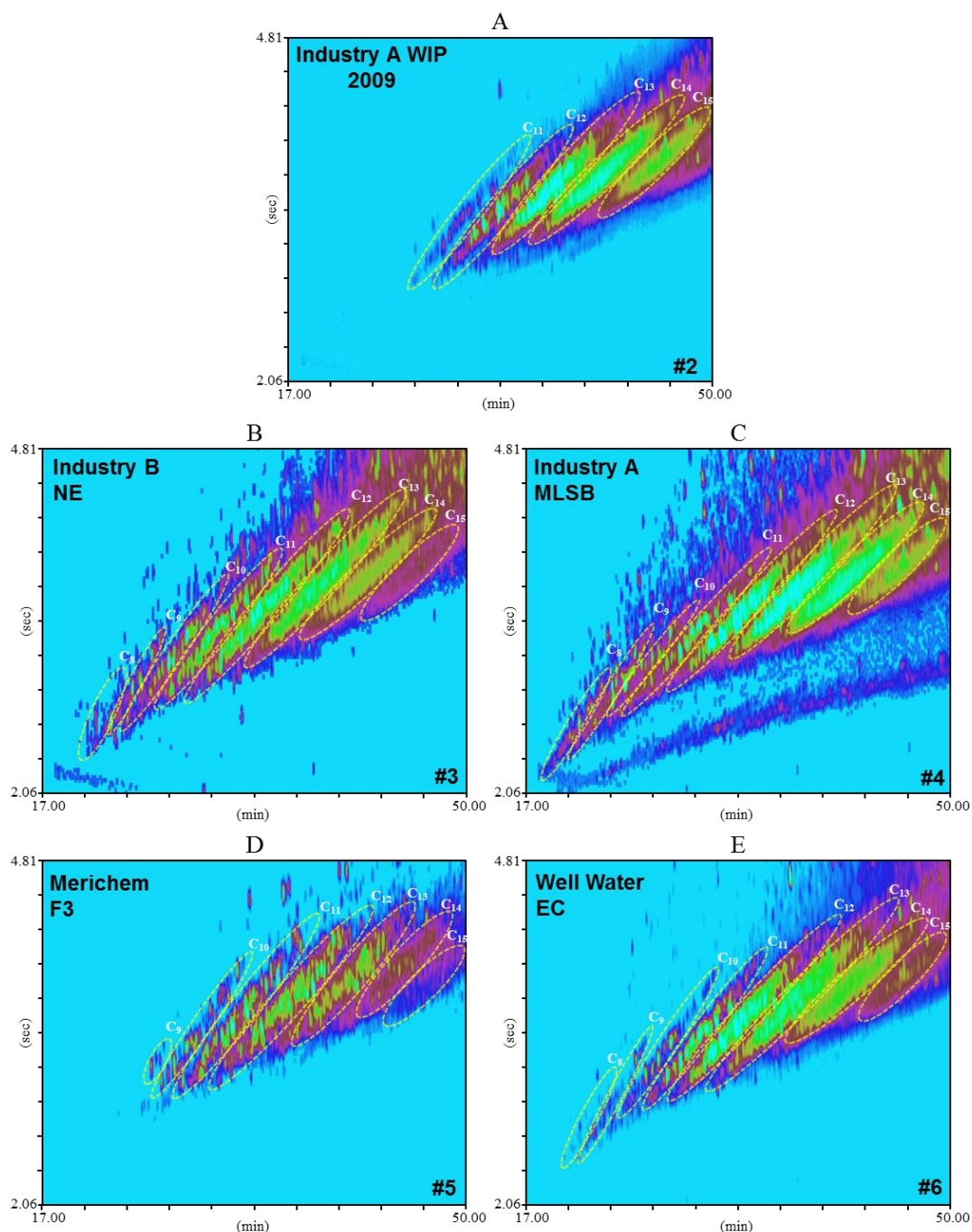
Figure 3-2: EICs (*m/z 154 (+14 Da).- 252*) showing bicyclic acid methyl ester

distributions (C_{8-15}) within (A) an OSPW acid extract from industry A (WIP) collected

in 2009, (C) an OSPW acid extract from industry B, (D) a different OSPW acid extract

from industry A (MLSB), (E) an alicyclic Ag-Ion fraction of Merichem NA and (F) an

acid extract from OSPW related well water. (Column set A, Conditions A).

93

Examination of the GC×GC-MS data of the six NA extracts as the methyl esters, using extracted ion chromatograms of the expected molecular ions, confirmed the presence of bicyclic acids with carbon numbers ranging from at least C_{11-15} in all the samples (#1-#6) (Figure 3-2; A-E and Appendix Figure 2) with an extended range of C_{8-15} bicyclic acids in samples #3 and #4. Furthermore, the GC×GC-MS data gave an insight into the true complexity of the OSPW NA mixtures, showing large numbers of individually resolved isomers. The exact number of isomers for each carbon number series varied between samples. For instance, sample #3 contained at least nineteen C_9, twenty seven C_{10}, forty C_{11} and numerous more peaks corresponding to C_{11+} bicyclic acids (Figure 3-2; C). The EIC of the NA extract from the raw MLSB OSPW (Figure 3-2; D) was even more complex, which was expected due to the lack of sample clean-up and pre-treatment, especially compared with the EICs of the NA extracted from samples #1 and #2 (WIP OSPW) which underwent extensive extraction procedures which may have removed the lower molecular weight acids.

Damasceno *et al.* (2014) recently analysed two commercial acid mixtures by GC×GC-MS characterising groups of NA by their hydrogen deficiency due to cyclicity (z-value). They detected 132 (Miracema-Nuodex NA) and 124 (Sigma Aldrich NA) peaks with molecular ions consistent with C_{9-16} bicyclic acids (z = -4) (Damasceno *et al.*, 2014). The EIC of the fractionated, commercial NA mixture (#5) analysed herein was more complex, containing a greater number of peaks (>200) corresponding to C_{9-15} bicyclic acids. The OSPW samples and related well water acid extracts (#1-#4 and #6) also showed greater complexity than the commercial mixtures reported by Damasceno *et al.* (2014), with a similar number of isomers comparable with the commercial NA analysed herein (#5).

The large number of isomers observed was strong evidence for the presence of many different structural types of bicyclic acids, or at least considerably more than the two fused cyclohexyl (decalin) and cyclopentyl (perhydroindane) structures routinely cited as examples (Holowenko *et al.*, 2001; Clemente and Fedorak, 2005; Headley *et al.*, 2009a).

3.3.2   Reference bicyclic acids

Based on the delimited, potential bicyclic structures considered (Figure 3-1), a limited range of bicyclic acids was synthesised or purchased. The structures of the reference acids are displayed in Figure 3-3. The reference acids that were synthesised included XIVa-d and VIIa and those previously synthesised, but no longer available included Va, Xa-b and XIVe. Despite the limited availability, those purchased included several different bicyclic cores, of different carbon numbers and substituted at different ring positions.

Synthesis of fused alicyclic acids via the hydrogenation of the aromatic precursors, for example bicyclo[4.4.0]decane-2- and 3-carboxylic acid (XIVa-b) and bicyclo[4.4.0]decane-2- and 3-ethanoic acid (XIVc-d) from the tetrahydronaphthalene and naphthalene precursors, resulted in the production of multiple isomers of each alicyclic acid. For example, the bicyclo[4.4.0]decane acids can show *cis-/trans-*isomerism at the bridgehead carbons and *cis-/trans* isomerism at the alkyl-substituted carbon, resulting in four possible isomers e.g. *cis-cis*, *trans-cis*, *cis-trans* and *trans-trans*. Synthesis of the desired structures was confirmed by GC-MS, based on the expected number of isomers, corresponding molecular ions and mass spectral interpretation.

(Ia) Bicyclo[2.2.1]heptane-1-carboxylic acid

(Ib) Bicyclo[2.2.1]heptane-2-ethanoic acid

(IIa) 2,6,6-trimethylbicyclo[3.1.1]heptane-3-carboxylic acid

(IVa) Bicyclo[2.2.2]octane-2-carboxylic acid

(IVb) Bicyclo[2.2.2]octane-1-carboxylic acid

(IVc) 4-pentylbiyclo[2.2.2]octane-2-carboxylic acid

(Va) Bicyclo[3.2.1]octane-6-carboxylic acid

(VIa) Bicyclo[3.3.0]octane-2-carboxylic acid

(VIb) 4-methylbicyclo[3.3.0]octane-2-carboxylic acid

(VIIa) 7-methylbicyclo[4.2.0]octane-7-carboxylic acid

(VIIIa) Bicyclo[3.3.1]nonane-1-carboxylic acid

(VIIIb) Bicyclo[3.3.1]nonane-3-carboxylic acid

(VIIIc) 5-methylbicyclo[3.3.1]nonane-1-carboxylic acid

(Xa) Bicyclo[4.3.0]octane-8-carboxylic acid

(Xb) 7-methylbicyclo[4.3.0]octane-8-carboxylic acid

(XIVa) Bicyclo[4.4.0]decane-2-carboxylic acid

(XIVb) Bicyclo[4.4.0]decane-3-carboxylic acid

(XIVc) Bicyclo[4.4.0]decane-2-ethanoic acid

(XIVd) Bicyclo[4.4.0]decane-3-ethanoic acid

(XIVe) Bicyclo[4.4.0]decane-2-propanoic acid

Figure 3-3: Structures of purchased or synthesised reference bicyclic acids.

Previous comparison of the retention positions of bicyclic NA in sample #1 with the retention positions of some of the reference acids did not result in any firm assignments (Appendix Figure 2; Wilde *et al.* (2015)). However the elution order of the reference acids and comparison of their relative retention positions with the bicyclic NA, was a useful indication as to whether isomers with the same bicyclic cores as those which eluted closely to the bicyclic NA, could be considered likely components of OSPW NA.

A systematic examination of the retention positions and mass spectra of the >100 individual GC×GC peaks in sample #2 - #6 were compared with those of the reference compounds. Since interpretation of the data for the lower homologues was likely to be simplest and might give clues to the identities of the presumably more alkylated higher homologues, the C_{8-10} acids were examined first (Sections 3.3.3 - 3.3.6).

3.3.3   C$_8$ bicyclic acids

C$_8$ acids were present in the OSPW acid extracts #3 and #4 and the well water #6. Two peaks within samples #3, #4 and #6 displayed retention positions and molecular ions (*m/z 154*) consistent with that of C$_8$ bicyclic acid methyl esters. The peak labelled 1a (Figure 3-4; A-C) was identified as bicyclo[2.2.1]heptane-2-carboxylic acid methyl ester after comparison with a NIST library spectrum. When compared with the reference mass spectra reported by Curcuruto *et al.* (1991), it became clear that the isomer was most likely exo-bicyclo[2.2.1]heptane-2-carboxylic acid due to the low intensity of the M-32 ion (*m/z* 122) (Figure 3-5). The mass spectral data reported by Curcuruto *et al.* (1991) showed the endo- isomer with a strong M-32 ion (*m/z* 122; 84 %) (Figure 3-5; A), which was postulated as the loss of methanol from the methoxy group of the methyl ester via a hydrogen rearrangement from the carbon in the 6-position of the bicyclic core. The loss of methanol via this mechanism would be expected to be greater in the endo- position due to the closer vicinity of the methyl ester moiety to the γ-hydrogen (Curcuruto *et al.*, 1991).

Interpretation of the mass spectrum of the second peak labelled 1b (Figure 3-4; A-C) resulted in the identification of bicyclo[2.2.1]heptane-1-carboxylic acid methyl ester, which was confirmed by comparison of the GC×GC retention time and mass spectrum with that of an authentic sample (Figure 3-4; F and G). The assignment of the 1-carboxylic acid isomer with a reference compound also supported the identification of the 2-isomer due to the relative retention position. Examination of the elution order of the reference acids showed that acids substituted at a bridgehead position, elute earlier than ring substituted homologues (e.g. bicyclo[3.3.1]nonane-1- and -3-carboxylic acid methyl esters (Figure 3-9; Section 3.3.5, page 109 and Appendix Figure 2) and bicyclo[2.2.2]octane-1- and -2-carboxylic acid methyl esters (Figure 3-6; Section 3.3.4, page 101)).

There was no mass spectral and retention position match with authentic bicyclo[2.2.1]heptane-2-ethanoic acid (Figure 3-5; C). However examination of the mass spectrum and retention behaviour, particularly in the second dimension (Appendix Figure 2; Wilde *et al.* (2015)), indicated other bicyclo[2.2.1]heptane acids, potentially more alkylated isomers, were present. Literature data were also available for the retention indices of some more highly methyl-substituted C_{8-11} isomers on apolar and polar phases (Heintz *et al.*, 1976). These also suggested that bicycloheptane acids were possibilities for the unknowns.
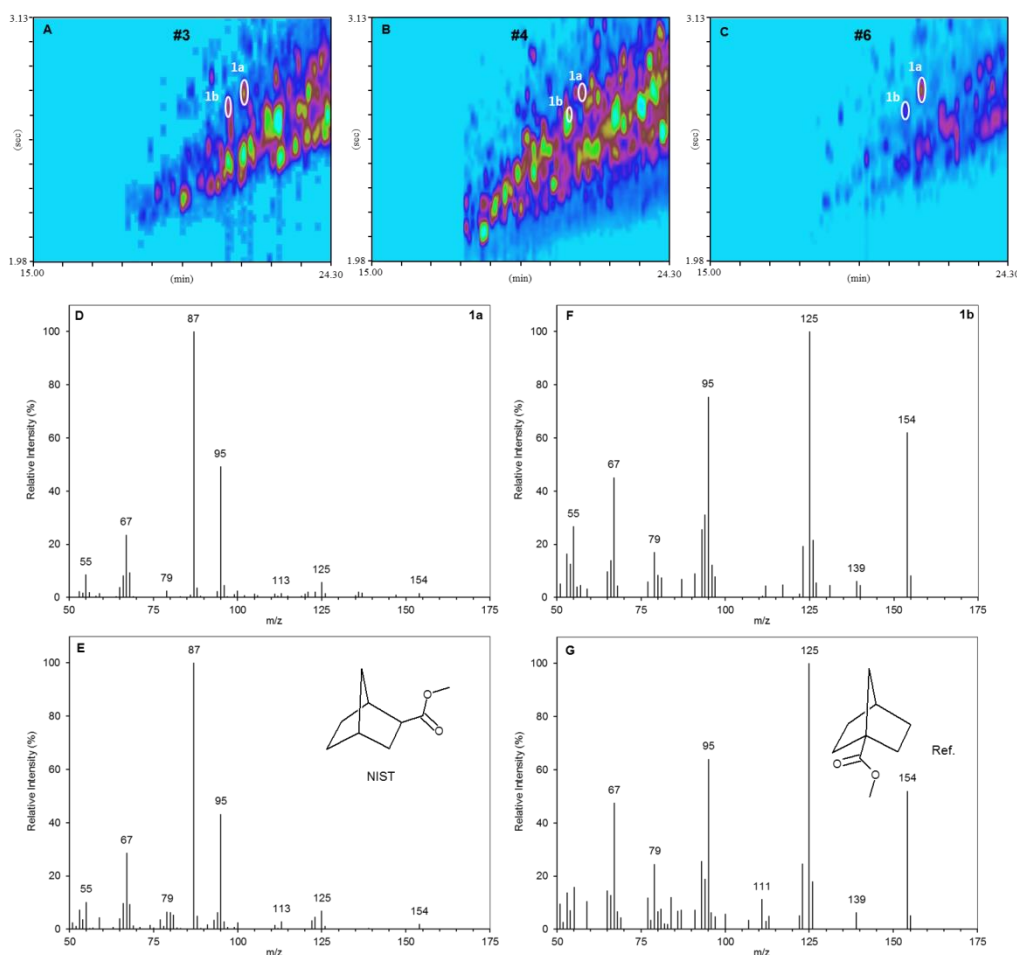
Figure 3-4: EICs (*m/z* 154, 125, 95 and 87) of (A and B) two OSPW acid extracts (#3 and #4) and (C) a well water acid extract (#6), analysed by GC×GC-MS. Peaks labelled 1a and 1b were identified by comparison of their mass spectra (D and F) with (E) a NIST library spectrum of bicyclo[2.2.1]heptane-2-carboxylic acid methyl ester and (G) a purchased reference standard of bicyclo[2.2.1]heptane-1-carboxylic methyl ester.
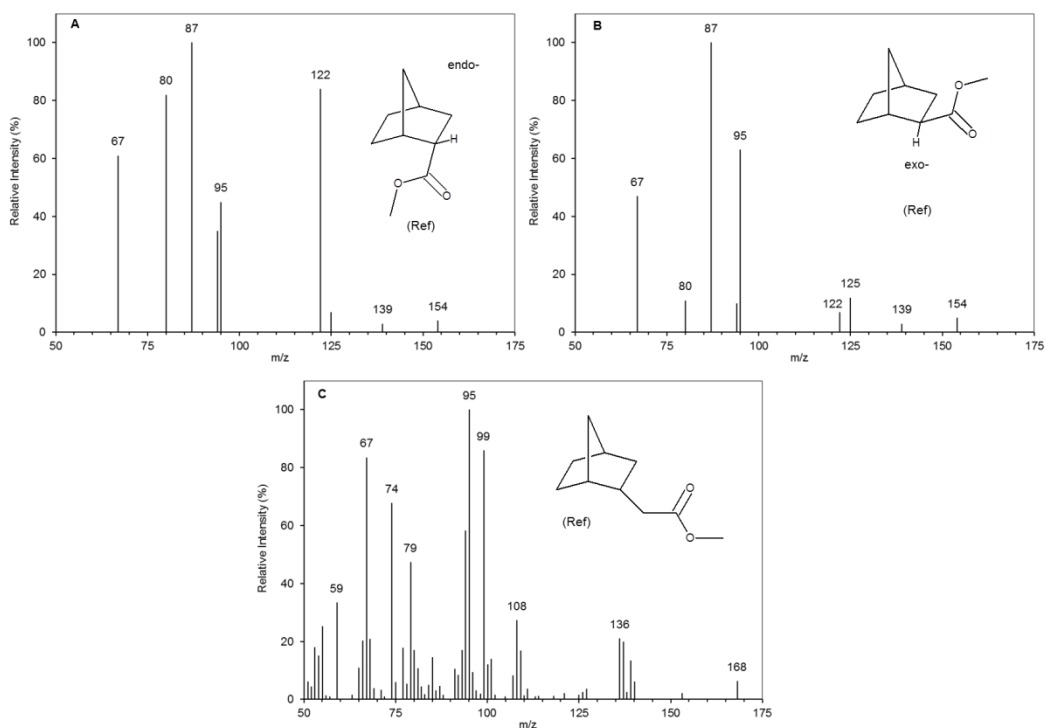
Figure 3-5: Reference mass spectra of (A and B) endo- and exo-bicyclo[2.2.1]heptane-2-carboxylic acid methyl ester replotted from tabulated values reported by Curcuruto *et al.* (1991) and (C) authentic bicyclo[2.2.1]heptane-2-ethanoic acid methyl ester.

Compounds with bicyclo[2.2.1]heptane skeletons (Figure 3-1; *I*, e.g. norbornane and bornane), are well-known in nature and are most often encountered as derivatives of camphor. Thus, there is precedence for the biosynthesis of compounds with this skeleton and numerous analogues have been studied. Seifert and Teeter (1969) suggested that naphthenic acids from a Californian petroleum might include such structural types. GC retention indices on apolar and polar phases and mass spectra or partial spectra of the methyl esters of isomers of C_{8-11} acids have been published (Heintz *et al.*, 1976; Manabe and Nishino, 1983; Curcuruto *et al.*, 1991).

The GC×GC retention position of authentic 2,6,6-trimethylbicyclo[3.1.1]heptane-3-carboxylic acid methyl ester was similar to that of the C_{11} OSPW NA in sample #1 (Appendix Figure 2), indicating other isomers were also a possibility for the identities of some of the unknowns, but no exact match was found in the spectra of the OSPW

NA methyl esters in samples #2 - #6. The most common compounds found with bicyclo[3.1.1]heptane (Figure 3-1; *II*) skeletons are pinenes; trimethyl- monterpenes produced by plants, particularly abundant in resin from pine trees (e.g. turpentine oil). The mass spectrum of 2,6,6-trimethylbicyclo[3.1.1]heptane-3-carboxylic acid methyl ester (3-pinane-carboxylic acid methyl ester) is complex (Appendix Figure 3), perhaps as a result of the bridged structure which contains a cyclobutane ring within the core. The cyclobutane ring makes the bicyclic acid liable to ring-opening and subsequent rearrangement in the ion source. This is supported by the very low intensity of the molecular ion (<2%) at *m/z* 196 (Appendix Figure 3). Distinguishable features of the mass spectrum included a strong (95%) M-60 ion at *m/z* 136 corresponding to loss of the methyl carboxylate group with a hydrogen transfer and a base peak ion was observed at *m/z* 81, as well as an intense ion at *m/z* 83 consistent with cyclic $C_6H_9^+$ and $C_6H_{11}^+$ ions respectively.

3.3.4   C$_9$ bicyclic acids

The GC retention positions of commercially available C_9 and C_{14} bicyclo[2.2.2]octane acids were examined (Figure 3-3; IVa-c). When compared with the retention positions of the bicyclic acids within all four OSPW acid extracts (#1 - #4) all three reference acids had relatively long retention times in the second dimension, relative to their respective carbon number homologues and were not identical to any of the unknowns (e.g. Appendix Figure 2). Interestingly however, bicyclo[2.2.2]octane-1-carboxylic acid and bicyclo[2.2.2]octane-2-carboxylic acid methyl esters (Figure 3-3; IVb) were both identified within the well water sample (#6) (Figure 3-6; A) and bicyclo[2.2.2]octane-1-carboxylic acid methyl ester was present in the commercial acid extract (#5) (Figure 3-6; B). All three identifications had matching retention positions and mass spectra to that of the authentic reference compounds (Figure 3-6; C-F).
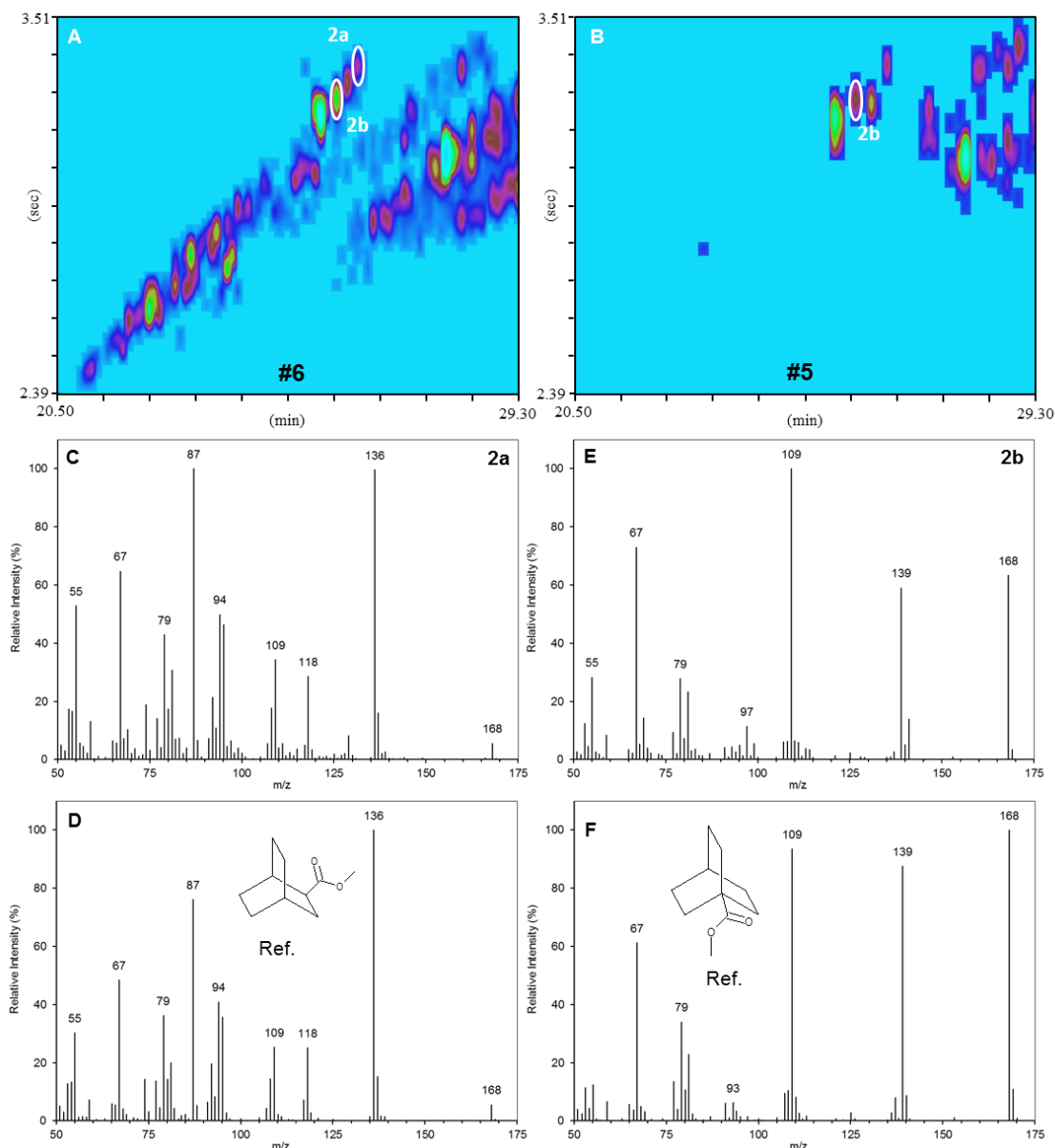
Figure 3-6: EICs (*m/z* 168) of (A) the commercial acid extract (#5) and (B) well water acid extract (#6) and the mass spectra (C and E) of peaks 2a and 2b identified by comparison with (D and F) the mass spectra and retention positions of authentic bicyclo[2.2.2]octane-1-carboxylic acid and bicyclo[2.2.2]octane-2-carboxylic acid methyl esters.

Compounds with the bicyclo[2.2.2]octane (Figure 3-1; *IV*) skeleton are found as stable, cage-like skeletons in natural products such as eremolactone isolated from *Eremophila fraseri* (Kuo *et al.*, 1998; Asaoka *et al.*, 1983) and (−)-seychellene found in patchouli oil, extracted from *Pogostemon cablin* (Srikrishna and Ravi, 2008). Whilst the mass

spectrum of bicyclo[2.2.2]octane-2-carboxylic acid methyl ester (Figure 1*A*; *IVa*) was characterised by a small molecular ion (*m/z* 168) and base peak ion (*m/z* 136) due to loss of methanol from the latter (Figure 3-6; D), the mass spectrum of bicyclo[2.2.2]octane-1-carboxylic acid methyl ester (Figure 3-6; F) contained pronounced molecular and M-29 ions, similar to those of some of the unknowns, as did the mass spectrum of the 4-methyl-1-carboxylic acid isomer (free acid, NIST library) perhaps due to the loss of $\cdot C_2H_5$. The mass spectrum of the C_{14} 4-pentylbicyclo[2.2.2]octane-1-carboxylic acid methyl ester (Appendix Figure 4) also showed a fairly abundant molecular ion (*m/z* 238) and the loss of M-29 and M-28 (*m/z* 209 and 210). Denisov *et al.* (1977d) reported the mass spectra of a range of substituted bicyclo[2.2.2]octanes with many showing loss of an ethyl group ($\cdot C_2H_5$, 29 Daltons) from the molecular ion. They proposed a mechanism for the loss of ethyl from a monocyclic intermediate brought about by the rupture of a bond at a bridgehead carbon coupled with a hydrogen transfer (Denisov *et al.*, 1977d) (discussed further in Chapter 4, Section 4.4.3.3).

GC×GC-MS revealed that two of the OSPW acid extracts containing low molecular weight acids (#3 and #4) and the well water sample (#6) all had a peak (3a) sharing the same retention position and a mass spectrum to bicyclo[3.2.1]octane-6-carboxylic acid methyl ester, identified after comparison with the reference acid (Figure 3-7; A-D and F). An isomer present as an impurity in the authentic bicyclo[2.2.2]octane-1-carboxylic acid had a matching retention position and mass spectrum with a peak (3b) present in the commercial NA and well water sample (#5 and #6) (Figure 3-7; E-H). After examination of the mass spectrum and comparison with those of other quaternary substituted, bridged bicyclic acid methyl esters (Figure 3-4; G and Figure 3-6; F), the isomer and peak within the samples was postulated to be bicyclo[3.2.1]octane-1-carboxylic acid methyl ester. The mass spectrum of the suspected bicyclo[3.2.1]octane-

1-carboxylic acid methyl ester was consistent with the other mass spectra, dominated by four main intense ions. These four ions observed in both the reference mass spectra of bicyclo[2.2.2]octane-1-carboxylic acid methyl ester and bicyclo[2.2.1]heptane-1-carboxylic acid methyl ester, corresponded to an intense molecular ion, an abundant M-29 ion due to fragmentation across the largest ring, an abundant M-59 due to the loss of the acid methyl ester group and a relatively abundant m/z 67 corresponding to a $C_5H_7^+$ ion (Figure 3-4; G and Figure 3-6; F). Low intensity M-15 and M-29 were observed in the mass spectra of bicyclo[2.2.1]heptane-1-carboxylic acid methyl ester and peak 3b, respectively, potentially due to fragmentation across the smallest ring. This was not observed in the mass spectrum of bicyclo[2.2.2]octane-1-carboxylic acid methyl ester as the rings are all equal, leading to a more abundant M-29 ion. Peak 3b, in samples #5 and #6 (Figure 3-7; E and F), also eluted earlier than the identified as bicyclo[3.2.1]octane-6-carboxylic acid, which was again consistent with the previous observations that bicyclic acid methyl esters substituted at a quaternary bridgehead carbon elute earlier than those substituted at secondary carbon positions (Figures 3-4, 3-6 and 3-9 and Appendix Figure 2).
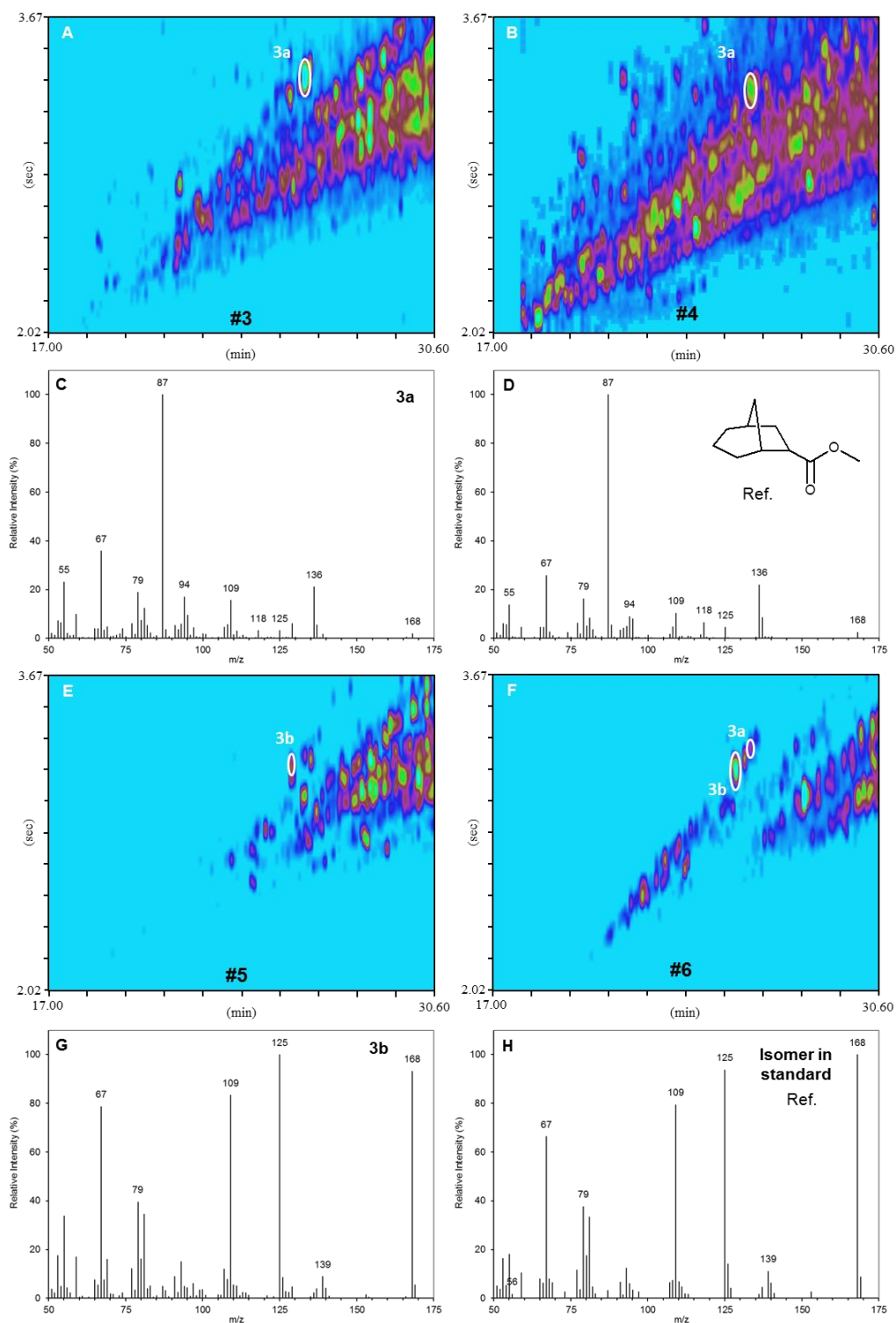
Figure 3-7: EICs (*m/z* 168 and 87) of (A and B) OSPW acid extracts from two different

industries (#3 and #4) and (C and D) the mass spectrum of peak 3a identified as

bicyclo[3.2.1]octane-6-carboxylic acid methyl ester after comparison with the reference

acid. EICs (*m/z* 168 and 87) of (E and F) the commercial acid mixture and well water

extract and (G and H) the speculative assignment of bicyclo[3.2.1]octane-1-carboxylic

acid after comparison with an isomer within a purchased reference sample.

Compounds with the bicyclo[3.2.1]octane-type skeleton (Figure 3-1; *V*) are common in several natural products (Presset *et al.*, 2012). However the hydrocarbon, bicyclo[3.2.1]octane and alkyl substituted homologues have also long been known in petroleum (Sokolova *et al.*, 1989; Mair *et al.*, 1958b). The mass spectrum of bicyclo[3.2.1]octane-6-carboxylic acid (Figure 3-7; D) contained a small molecular ion at *m/z* 168, an ion at *m/z* 136 attributed to the loss of methanol and a base peak ion typical of methyl esters at *m/z* 87.

Similarly, *cis*-bicyclo[3.3.0]octane was identified in petroleum over 50 years ago (Mair *et al.*, 1958b). Previously, 4-methylbicyclo[3.3.0]octane-2-carboxylic acid (Figure 3-3; VIb) was identified in a commercial NA by comparison of the mass spectrum with that of a purchased reference sample (Rowland *et al.*, 2011e). Since then the C_9 parent acid, bicyclo[3.3.0]octane-2-carboxylic acid (two isomers) had become commercially available (Figure 3-3; VIa) and comparison of the mass spectra and GC×GC retention times led to the identification herein of the corresponding methyl esters within the commercial acid mixture (#5) (Figure 3-8; A-E).
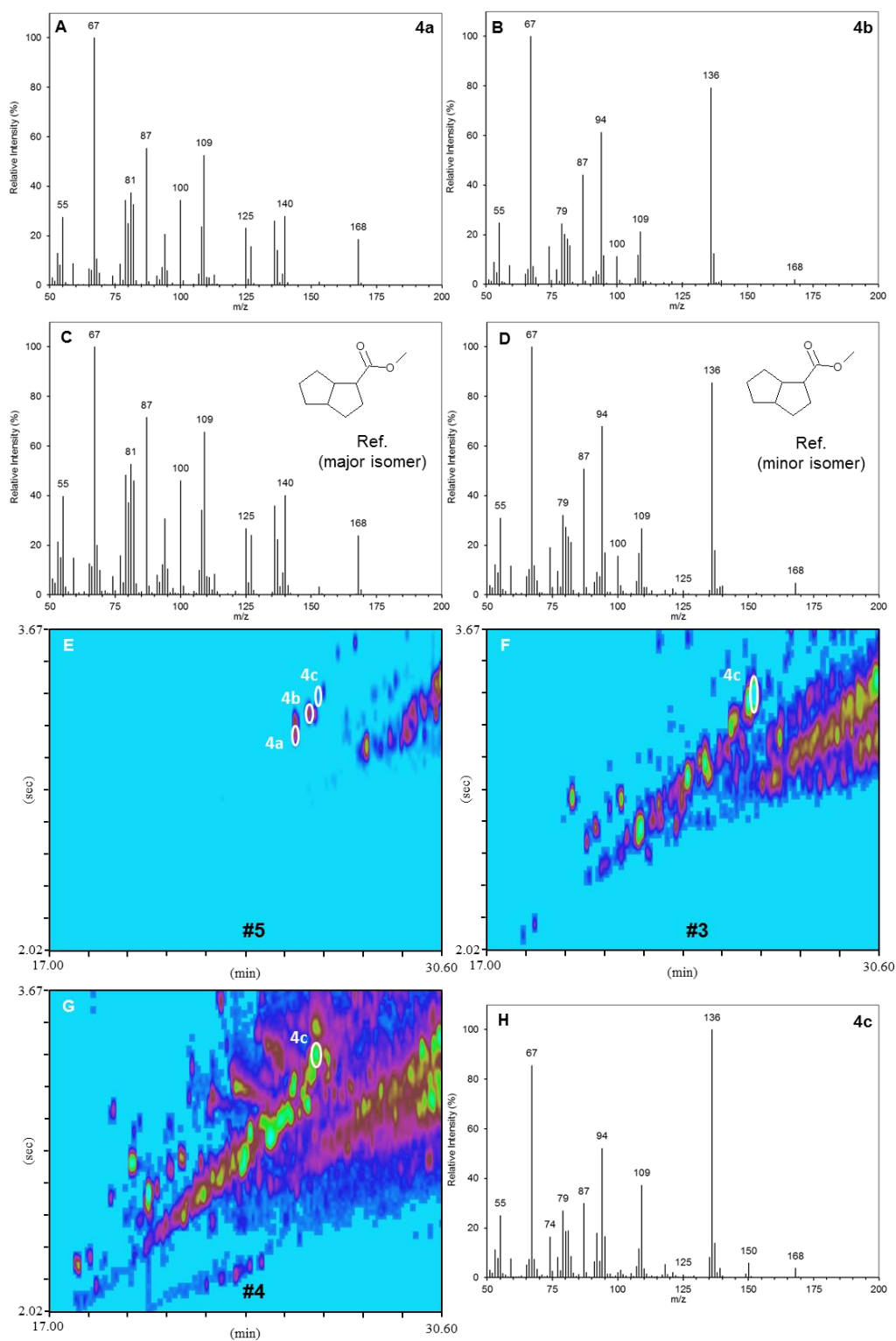
Figure 3-8: (A-D) Mass spectra of peaks 4a and b identified as isomers of bicyclo[3.3.0]octane-2-carboxylic acid methyl ester. (E) EIC (*m/z* 168 and 136) of the commercial NA (#5) showing peak 4c, present in (F and G) OSPW NA from industries A and B (#3 and #4), tentatively assigned as bicyclo[3.3.0]octane acid isomer after comparison of (H) the mass spectrum with (D) the minor reference isomer.

Another unknown compound (4c) within the commercial NA, not detected in the well water but present in the OSPW acid extracts from industry B (#3) and a different tailings from industry A (#4), had a very similar retention position and mass spectrum to that of the minor bicyclo[3.3.0]octane-2-carboxylic acid, methyl ester, isomer (Figure 3-8; E-H). However, the retention time of the unknown was different from the authentic reference acids and thus the unknown was postulated to be a different isomer. The mass spectrum of peak 4c contained an M-18 ion (*m/z* 150), attributed to the loss of water (Figure 3-8; H). The loss of water is often observed in the mass spectra of non-derivatised acids, keto- or hydroxy acids and not common in spectra of methyl esters. However, loss of water (M-18 ion) was observed in the mass spectra of some bicyclo[4.4.0]decane acid methyl esters and again appears to be specific to certain isomers (Rowland *et al.*, 2011e). The mass spectrum of the unknown displayed an ion at *m/z* 74 (Figure 3-8; H), also a characteristic ion of methyl esters, suggesting it was not a non-methylated C_{10} acid. The molecular ion did not show multiple isotopic peaks, suggesting the compound did not contain sulphur and the lack of tailing in the chromatogram often observed for non-derivatised or more polar compounds indicated it was not a keto- or hydroxy acid and was most likely a different isomer of bicyclo[3.3.0]octane-2-carboxylic acid.

3.3.5 C_{10} bicyclic acids

Comparison of the mass spectra and retention positions of bicyclo[3.3.1]nonane-1- and 3-carboxylic acid methyl esters (Figure 3-3; *VIIIa* and *b*) with the NA extracts, showed that these acids were absent from OSPW samples #2 and #4 from industry A. Wilde *et al.* (2015) showed the bicyclo[3.3.1]nonane acids were also absent from another OSPW sample from industry A (sample #1; Appendix Figure 2).. Conversely,

bicyclo[3.3.1]nonane-1-carboxylic acid methyl ester was detected in the well water sample (#6) (Figure 3-9; A, C and D) and both isomers were identified in the commercial acid mixture (#5) (Figure 3-9; B-D). The retention position of bicyclo[3.3.1]nonane-1-carboxylic acid methyl ester, matched that of a peak in the OSPW acid extract from industry B (#3); however, the peak was clearly co-eluting with another compound, complicating the mass spectrum. After analysis of sample #3 under different GC×GC conditions (GC×GC-MS conditions B, column set B; Chapter 2, Section 2.1.4), separation of the previously unresolved peaks was achieved and the peak was identifiable as bicyclo[3.3.1]nonane-1-carboxylic acid methyl ester.
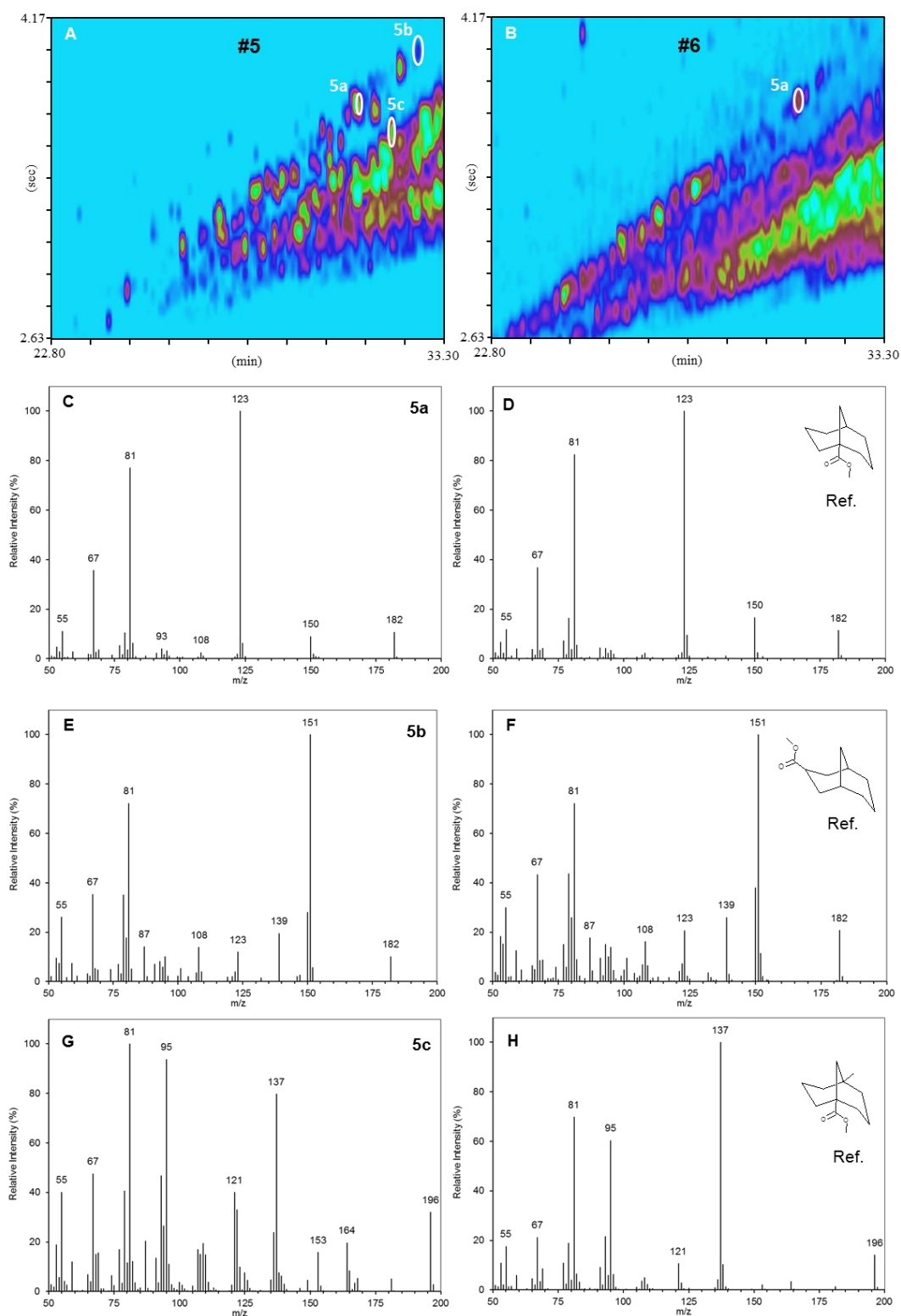
Figure 3-9: EICs (*m/z* 182, 151 and 123) of (A) the commercial acid mixture (#5) and

(B) the well water sample (#6) and (C-H) the identification of bicyclo[3.3.1]nonane

acids by comparison with authentic reference compounds.

The GC×GC retention position and mass spectrum of authentic 5-methylbicyclo[3.3.1]nonane-1-carboxylic acid methyl ester was similar to that of a peak present in both samples #3 and #5. However, co-elution, even under different GC×GC conditions (conditions B, Section 3.2.3), meant the assignment was tentative due to differences in ion intensities (Figure 3-9; G and H). Previously it has been speculated that biodegradation of adamantanes might produce ring-opened acids with the bicyclo[3.3.1]nonane skeleton, since this process occurs in the biodegradation of adamantan-2-one (Rowland *et al.*, 2011c; Selifonov, 1992). Indeed given the (albeit tentative) identification above, this seems to be possible, at least for some of the present samples (e.g. #3, #5 and #6). The data suggest the acids in the OSPW extracts (and some commercial acids) sometimes included bicyclo[3.3.1]nonane carboxylic acids.

Bicyclo[4.3.0]nonane carboxylic acids (Figure 3-1; *X*) were identified previously in a commercial NA mixture, by comparison of the mass spectra with a literature mass spectrum of bicyclo[4.3.0]nonane-7-carboxylic acid (perhydroindane-1-carboxylic acid) (Rowland *et al.*, 2011e). Wilde *et al.* (2015) reported the synthesis of bicyclo[4.3.0]nonane-8-carboxylic acid (Figure 3-3; *X*a) and a 7-methylbicyclo[4.3.0]nonane-8-carboxylic acid isomer (or 2-methyl-3-perhydroindane carboxylic acid) (Figure 3-3; *X*b). The retention times of the bicyclo[4.3.0]nonane acid standards were generally greater in the second dimension, than those of most of the NA in OSPW from industry A (Appendix Figure 2; Wilde *et al.* (2015)). However, examination of a few of the peaks within an OSPW acid extract from industry B (#3), the well water sample (#6) and the commercial acid extract (#5) analysed herein, displayed mass spectra very similar to those previously identified as C_{10} bicyclo[4.3.0]nonane carboxylic acids (methyl esters) in a commercial acid mixture (Rowland *et al.*, 2011e; Ranade *et al.*, 2000) (Peaks a-c; Figure 3-10) as well as those of

the synthesised standards (Wilde *et al.*, 2015). These data suggest the acids in the

OSPW extracts include bicyclo[4.3.0]nonane carboxylic acids.
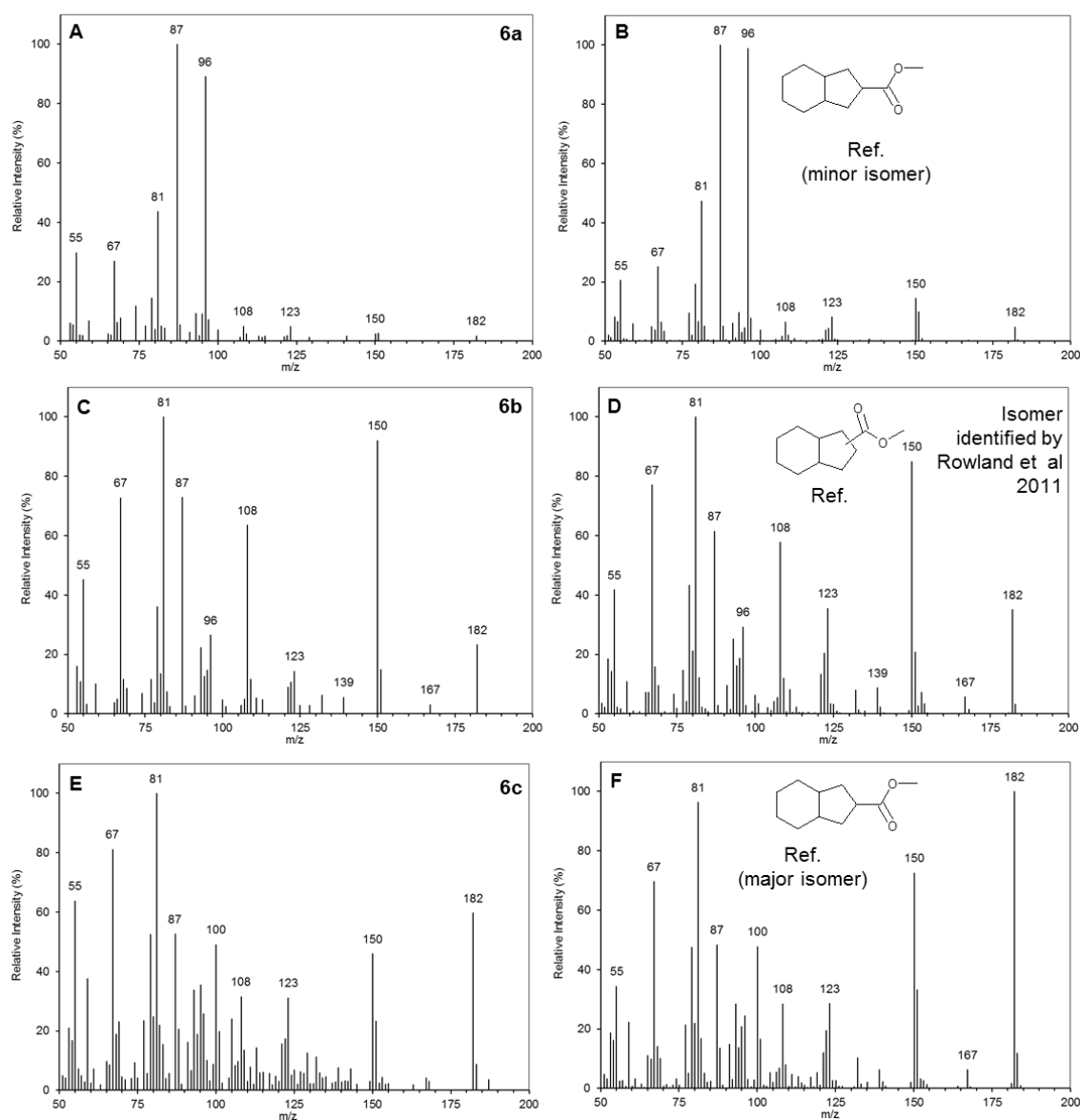
Figure 3-10: (A, C and E) Example mass spectra of three peaks (6a-c) within an OSPW,

well water and commercial acid extract (samples #3, #5 and #6) identified by

comparison with the mass spectra of (B and F) two isomers of synthesised

bicyclo[4.3.0]nonane-8-carboxylic acid methyl ester and (D) an isomer previously

identified in commercial NA (Rowland *et al.*, 2011e) (most likely a 7-isomer due to

similarity to mass spectrum reported by Ranade *et al.* (2000)).

The mass spectra of the bicyclo[4.3.0]nonane acids within the commercial acid mixture were characterised by medium intensity molecular ions (ca 20%) and ions due to loss of methanol at *m/z* 150 and an ion at *m/z* 87 typical of acid methyl esters (Ranade *et al.*, 2000; Rowland *et al.*, 2011e). The mass spectra of the isomers of the synthesised bicyclo[4.3.0]nonane-8-carboxylic acid methyl esters varied considerably (Figure 3-10; B and F). Thus in the major isomer (69% of total resolved peaks) the molecular ion was abundant (80%), whereas in more minor isomers the molecular ion was only <5% abundant (Figure 3-10; B and F). The mass spectra of the 8-isomers were easily distinguished from those reported for the 7- isomers (Rowland *et al.*, 2011e; Ranade *et al.*, 2000). Comparison of the mass spectra of several bicyclic NA (e.g. 6a-c; Figure 3-10) with the reference mass spectra was evidence of both 8-isomers and almost certainly 7-isomers being present in OSPW NA.

Wilde *et al.* (2015) reported the GC×GC retention position of 4-methylbicyclo[3.3.0]octane-2-carboxylic acid (Figure 3-3; VIb) was similar to those of the NA within the OSPW acid extract from industry A (sample #1; Appendix Figure 2). However, similarly to the C_9 parent acid isomers, there was no exact retention time or mass spectral match with any NA from the OSPW samples. Conversely, 4-methylbicyclo[3.3.0]octane-2-carboylic acid methyl ester was identified in the fractionated commercial NA herein (Figure 3-11), as previously reported by Rowland *et al.* (2011e).
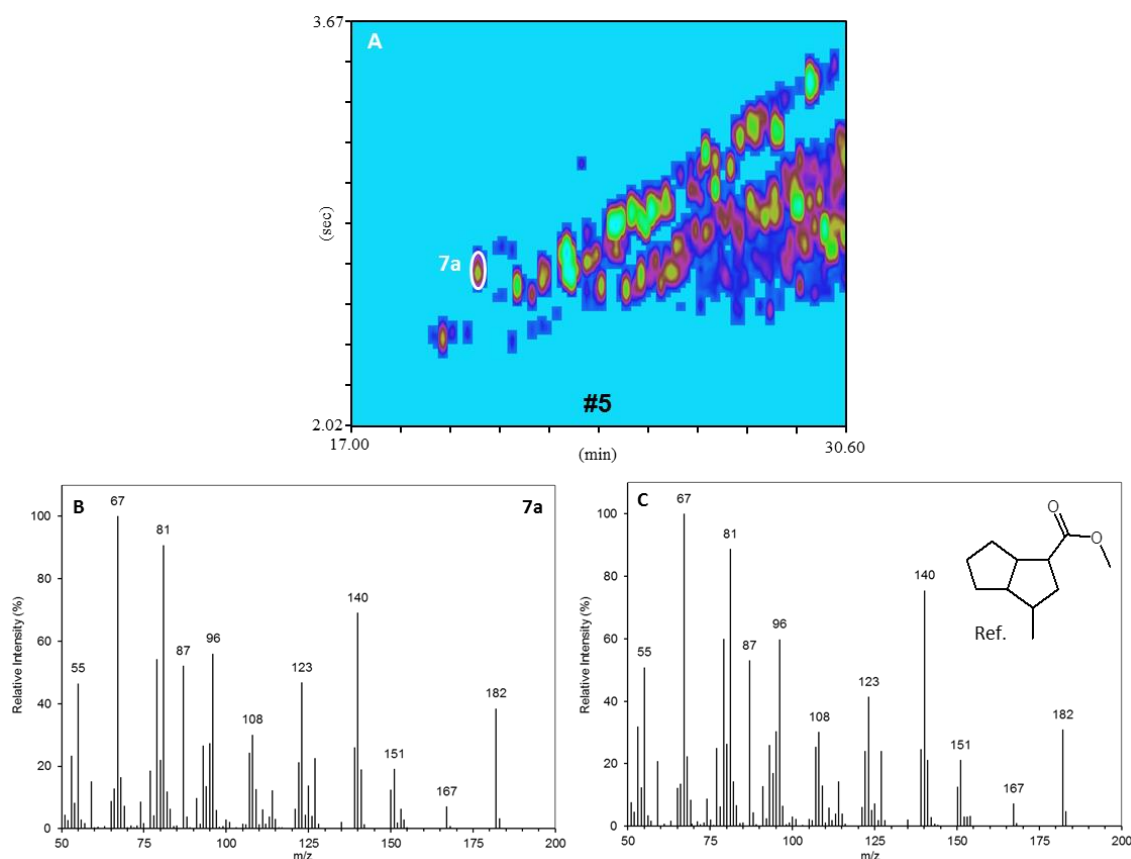
Figure 3-11: EIC (*m/z* 168) of (A) the commercial acid extract and (B) the mass spectrum of peak 7a identified by comparison with (C) authentic 4-methylbicyclo[3.3.0]octane-2-carboxylic acid methyl ester.

The mass spectrum of the C_{10} 4-methylbicyclo[3.3.0]octane-2- carboxylic acid methyl ester (Figure 3-11; C) was characterised by a relatively strong (30%) molecular ion and multiple fragment ions, including the ion at *m/z* 140 (70%) assumed to be due to loss of a propene moiety, likely via a cycloreversion/retro-Diels-Alder rearrangement, typical of cyclic hydrocarbons (Dass, 2007; McLafferty and Tureček, 1993). The retention position of the C_{10} authentic acid methyl ester relative to the OSPW NA reported by Wilde *et al.* (2015) (Appendix Figure 2), coupled with the tentative identification of a C_9 isomer in OSPW NA (Figure 3-8; H) suggested that some of the acids present in the OSPW might have this skeleton.

7-methylbicyclo[4.2.0]octane-7-carboxylic acid methyl ester eluted closely to the bicyclic acids in the OSPW acid extracts (#1-#4), but there was no exact match for the particular isomers synthesised. Bicyclo[4.2.0]octane carboxylic acids contain a fused cyclobutane ring (Figure 3-1; *VII*), similar in structure to short-chain ladderane fatty acids previously identified as degradation products of ladderane lipids (Rush *et al.*, 2011). Ladderane lipids are specific for bacteria capable of anaerobic ammonium oxidation (anammox) and therefore the acids can be used as biomarkers for anammox bacteria (Sinninghe Damsté *et al.*, 2005). The mass spectra of both 7-methylbicyclo[4.2.0]octane-7-carboxylic acid methyl ester isomers (Appendix Figure 5) displayed weak molecular ions (*m/z* 182), as expected for alicyclic acids containing a highly strained, fused cyclobutane ring. The base peak at *m/z* 101 was attributed to the fragmentation across the cyclobutane ring.

3.3.6   C$_{11}$+ bicyclic acids

Bicyclic NA, believed to be products of biodegradation, have frequently been assumed to possess bicyclo[4.4.0]decane structures (Holowenko *et al.*, 2001; Clemente and Fedorak, 2005; Headley *et al.*, 2009b). The occurrence of such acids has been shown within at least one commercial acid mixture (Rowland *et al.*, 2011e).

The retention positions of the synthetic bicyclo[4.4.0]decane (decalin) carboxylic, ethanoic and propanoic acid methyl esters substituted in either the 2- or 3- positions on the decalin core showed that these acids were absent, or had a very low relative abundance, in some of the samples of OSPW acids which were examined (e.g. #1 and #2), supported by the late elution of these acids in the second dimension (Appendix Figure 2; Wilde *et al.* (2015).

A small number of bicyclo[4.4.0]decane acids were tentatively identified within another OSPW from industry B (#3), based on mass spectral comparison with the synthesised

reference acids (Appendix Figures 6 - 9) and those previously reported in a commercial acid mixture (Rowland *et al.*, 2011e), such as an isomer of bicyclo[4.4.0]decane-3-carboxylic acid methyl ester, as well as bicyclo[4.4.0]decane-1-carboxylic acid methyl ester which was compared with a NIST library mass spectrum (Figure 3-12). Due to co-elution and insufficient separation of the acid methyl esters, the assignments could not be confirmed by comparison with the retention positions of the synthetic reference acids.
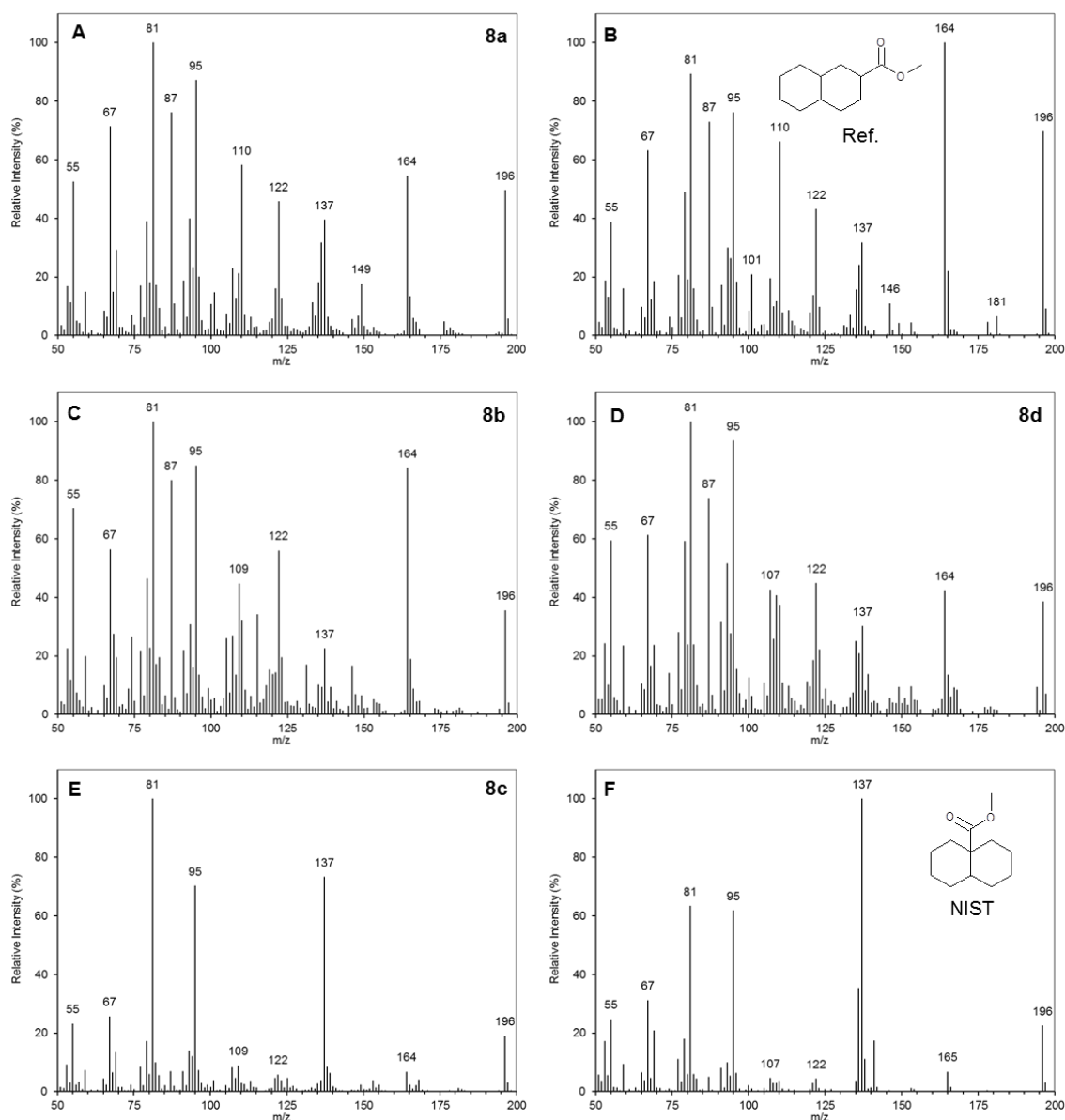
Figure 3-12: (A, C, D and E) Example mass spectra of NA within OSPW from industry B (#3), tentatively identified by comparison with (B and D) the mass spectra of previously identified bicyclo[4.4.0]decane acid methyl esters (Rowland *et al.*, 2011e).

Petroleum hydrocarbons and related compounds possessing bicyclo[4.4.0]decane cores such as drimanes, cadinanes and eudesmanes have been well studied (Alexander *et al.*, 1984; Alexander *et al.*, 1983; Gordadze *et al.*, 2011). Fused cyclohexyl rings are common in biologically derived compounds e.g. hopanes. Therefore, bicyclic sesquiterpenes can be reasonably postulated to be biodegradation products of higher terpenes (Alexander *et al.*, 1983).

Although samples of bicyclo[3.2.2]nonane (Figure 3-1; *IX*), bicyclo[4.2.1]nonane (*XI*), bicyclo[4.2.2]decane (*XII*), bicyclo[5.3.0]decane (*XIII*), bicyclo[5.2.1]decane (*XV*), bicyclo[3.3.2]decane (*XVI*), spiro[4.5]decane (*XVII*) or cyclopentylcyclopentane (*XVIII*) carboxylic acids were not available, when the reported NIST GC retention indices of the hydrocarbons bicyclo[5.3.0]decane and cyclopentylcyclopentane, were examined, it was clear that these eluted well after decalin (bicyclo[4.4.0]decane). Since the acid methyl esters would be expected to have the same relative retention orders and bicyclo[4.4.0]decane acids, when present, were the latest eluting acids; these acids were fairly confidently ruled out in these samples of OSPW. Since we could find no sources of bicyclo[4.2.1]nonane, bicyclo[3.2.2]nonane, bicyclo[4.2.2]decane, bicyclo[3.3.2]decane or spiro[4.5]decane carboxylic acids to allow study of the mass spectra or GC retention behaviour, and the retention indices of the alkanes appear not to have been published, these could not be ruled out as possibilities.

3.3.7 Mass spectral features of bicyclic acids

Examination of the mass spectral features observed for the authentic reference compounds (Figure 3-3) were used to postulate structural features of the unknown acids. For example, methyl esters of acids in which the methylated carboxylic group is substituted onto the ring, creating a tertiary carbon atom e. g. in the mass spectra of the

esters of bicyclo[4.4.0]decane-2- or 3- carboxylic acid (Figure 3-12 and Appendix Figures 6 and 7) or bicyclo[4.3.0]nonane-2- (Rowland *et al.*, 2011e) or -3- carboxylic acids (Figure 3-10), commonly lose a neutral methanol molecule, or methoxy radical (M-31/32), (though the spectra of stereoisomers vary; Figure 3-10).

In contrast, methyl esters of acids in which the methylated carboxylic group is substituted onto the ring via a longer alkanoate chain e. g. in the mass spectra of the esters of bicyclo[4.4.0]decane-2- or 3-ethanoic or propanoic acids (Appendix Figures 8 and 9) or bicyclo[2.2.1]heptane-2-ethanoic acid (Figure 3-4; C), commonly lose a $\cdot CH_2CO_2CH_3$ radical (mass 73 and mass 74 with occurrence of hydrogen transfer).

Methyl esters of acids in which the methylated carboxylic group is substituted onto the bridgehead carbon, creating a quaternary carbon atom e. g. in the NIST mass spectrum of the esters of bicyclo[4.4.0]decane-4a-carboxylic acid (Figure 3-12; F) or mass spectrum of bicyclo[3.3.1]nonane-1-carboxylic acid (Figure 3-9, D), commonly lose a methylated carboxy radical $\cdot CO_2CH_3$ radical (mass 59 and sometimes mass 60 with the occurrence of hydrogen transfer).

Abundant lower mass fragment ions such as *m/z* 55, 67, 79 and 81 present in many of the reference compound mass spectra are common ions observed in the mass spectra of cycloalkanes/polycycloalkanes, particularly those containing substituted cyclohexyl and cyclopentyl rings (McLafferty and Gould, 2012). Therefore these ions were postulated to originate from fragmentations within the bicyclic core via more complex mechanisms and rearrangements i.e. corresponding to $C_4H_7^+$, $C_5H_7^+$, $C_6H_7^+$ and $C_6H_9^+$ fragment ions respectively. Fragmentation within a bicyclic core requires fission of at least two bonds. Mass spectral studies of cycloalkanes, specifically bicyclic hydrocarbons, suggest that electron ionisation results in the fission of one of the bonds at a tertiary carbon

bridgehead, followed by subsequent rearrangement and fragmentation (Denisov *et al.*, 1977d; Denisov *et al.*, 1977b; Denisov *et al.*, 1977a).

The mass spectra of the C_{11} unknowns in the OSPW samples exhibited some of the above features. In general they were also characterised by abundant molecular ions (*m/z* 196) and ions at *m/z* 81, 95 and 107 were often predominant (Appendix Figure 10). In some spectra, ions, which may indicate losses of ethyl (M-29) and other alkyl (e.g. M-57, butyl) substituents, were present. To contain alkyl substituent groups of this size (e.g. C_4), a C_{11} acid would require a bicyclic core to contain only six carbons (e.g. C_4-bicyclo[2.2.0]hexane carboxylic acids). Spectra of the methyl esters of such acids are distinctive and do not match those observed here (Rush *et al.*, 2011). Thus, the apparent C_3/C_4 losses from the unknown C_{11} acid methyl esters represent losses from the rings, as observed in the spectrum of the methyl ester of authentic 4-methylbicyclo[3.3.0]octane-2-carboxylic acid, which shows an M-42 ion due to the loss of propene (Figure 3-11; C).

Although a number of structural features can be observed from the mass spectra of the methyl esters of the C_{12-16} acids, including molecular ions, ions due to losses of methanol (M-32) and to losses of alkyl groups or alkene moieties (e.g. M-15, M-28 and 29) from the molecular ion and ions due to losses of ethanoate (M-73) and propanoate (M-87) side chains, no more rigorous assignments of the structural types could be made for the C_{11} acids. Thus based on the structures identified, it was postulated that these were mostly higher homologues of the bicyclo[2.2.1]heptane, bicyclo[2.2.2], [3.2.1], [3.3.0]octane, bicyclo[3.3.1] and [4.3.0]nonane and some bicyclo[4.4.0]decane skeleta, with possibly bicyclo[4.2.1]nonane, bicyclo[3.2.2]nonane, bicyclo[3.3.2]decane or spiro[4.5]decane carboxylic acids represented also.

3.4 Conclusions

Consideration of the GC retention behaviour, numbers of structural types and comparison of the electron ionisation mass spectra of the methyl esters of a number of synthetic and purchased bicyclic carboxylic acids, allowed identification of various bicyclic acids in OSPW and commercial acids, many for the first time.

More than one hundred C_{8-15} bicyclic acids were shown to be present in each OSPW extract. Synthesis or purchase allowed identification of bicyclo[2.2.1]heptane, bicyclo[3.2.1]octane, bicyclo[4.3.0]octane and bicyclo[3.3.1]octane acids in OSPW and a bicyclo[2.2.2]octane acid in a commercial acid mixture. The retention positions of authentic bicyclo[3.3.0]octane and bicyclo[4.2.0]octane carboxylic acid methyl esters and published retention indices, showed these were also possibilities, as were bicyclo[3.1.1]heptane acids. In most OSPW acid extracts analysed, the bicyclo[4.4.0]decane carboxylic (decalin) acids which have always been assumed to be present in OSPW (Frank *et al.*, 2008; Headley *et al.*, 2009b), were relatively minor components. Bicyclo[5.3.0]decane and cyclopentylcyclopentane carboxylic acids were ruled out on the basis that the corresponding alkanes eluted well after bicyclo[4.4.0]decane (latest eluting acids). Bicyclo[4.2.1]nonane, bicyclo[3.2.2]nonane, bicyclo[3.3.2]decane, bicyclo[4.2.2]decane and spiro[4.5]decane carboxylic acids could not be ruled out or in, as no authentic compounds or literature data were available. Mass spectra of the methyl esters of the higher bicyclic C_{12-15} acids suggested that many were simply analogues of the above, with longer alkanoate chains and/or alkyl substituents. Based on the results, it is hypothesised that, at least, some of these acids represent the biotransformation products of the initially somewhat more bio-resistant bicyclanes of petroleum. Remediation studies suggest at least some bicyclic acids can be relatively quickly removed from suitably treated OSPW (Martin *et al.*, 2010), but a closer

examination of which isomers are degraded will now be possible using the methods demonstrated here. This may be deemed important as some bicyclic acids are more acutely toxic than others (Jones *et al.*, 2011).

Clearly many bicyclic acids remained to be identified. Since a wider literature of mass spectra of bicyclic hydrocarbons (e.g. Denisov *et al.* (1977d), Denisov *et al.* (1977c), Denisov *et al.* (1977a), Brodskii *et al.* (1977), Lukashenko *et al.* (1973), Golovkina *et al.* (1984)) was available than was extant for the acids, a useful approach formerly adopted by Zelinsky (1924) and Seifert *et al.* (1969) involving conversion of the acids to the hydrocarbons might prove a valuable complementary method to that employed here. Combining this older approach with the separation power of modern chromatography methods such as GC×GC-MS, as demonstrated for the acid methyl esters herein, might potentially be useful for furthering the investigation into the structural identification of bicyclic petroleum acids. Such an approach is described in the following chapter.

Chapter 4

Development of a method for the conversion of bicyclic naphthenic acids to hydrocarbons

Chapter 4 describes the development of a synthetic route for the conversion of carboxylic acids to the corresponding hydrocarbons. The method was tested on three 'model' bicyclic acids in order to optimise yields and to ensure that the structural integrity of the acids was maintained without extensive rearrangements.

The trial conversion method consisted of a three-step transformation encompassing reduction of the acids to alcohols, esterification of the alcohols to the tosyl esters (tosylates) and reduction of the tosyl esters to hydrocarbons. The products of each step were characterised by infrared spectroscopy (IR), gas chromatography-mass spectrometry (GC-MS) and nuclear magnetic resonance spectroscopy (NMR). Interpretation of the resultant data showed that the integrity of the bicyclic 'cores' was maintained in the corresponding bicyclic hydrocarbons (bicyclanes). The method therefore showed potential for use with unknown complex acid mixtures for the identification (by inference from the identified bicyclanes) of bicyclic naphthenic acids (NA), in matrices such as commercial NA and oil sands process-affected waters (OSPW).

The method developed herein and characterisation data for the reduced model acids (i.e. bicyclanes) discussed in this chapter have been published in part:

Wilde, M. J. and Rowland, S. J. (2015) Structural Identification of Petroleum Acids by Conversion to Hydrocarbons and Multidimensional Gas Chromatography-Mass Spectrometry. *Analytical Chemistry*, 87, 16, 8457-8465.

4.1 Introduction

The separation power of multidimensional gas chromatography-mass spectrometry (GC×GC-MS) has proved valuable in the structural elucidation of some bicyclic NA as their methyl ester derivatives for both commercial NA and for NA extracted from oil sands process-affected waters (OSPW) (Chapter 3; Wilde *et al.* (2015)). GC×GC-MS led to the identification of several fused-ring and several novel, bridged, bicyclic acids in petroleum related mixtures, as described in Chapter 3.

Although GC×GC-MS affords sufficient separation of numerous individual NA (as methyl esters) even in complex mixtures (e.g. Rowland *et al.* (2011c)), identification of bicyclic NA to date has been somewhat limited by the lack of reference mass spectra for known, authenticated, acid methyl esters (Wilde *et al.*, 2015). Such limitations led some early researchers to adopt alternative complementary approaches involving conversion of acids to compounds deemed likely to be more amenable to identification by mass spectrometry, such as hydrocarbons (Braun *et al.*, 1933; Zelinsky, 1924; Seifert *et al.*, 1969). Many more reference mass spectra exist for petroleum hydrocarbons than for the esters of the acids. The lack of functional groups in the hydrocarbons means that mass spectral fragmentation is wholly dependent on the bicyclic 'core', often making interpretation of the reference mass spectra of the hydrocarbons somewhat simpler (though not in all cases). However, the lack of sufficient chromatographic separation of the complex hydrocarbon mixtures produced in these earlier studies meant identification of individual compounds was still limited.

The present investigation aimed to investigate the hypothesis that a combination of the historical approach of converting the petroleum acids to the hydrocarbons, plus the use of improved chromatographic separations afforded by GC×GC-MS, might allow more unknown acids (by inference, following identification of the bicyclanes) to be identified.

4.1.1 Aims and Objectives

The aims of the current investigation involved planning and developing a synthetic route for the chemical transformation of carboxylic acids to hydrocarbons whilst retaining the 'core' bicyclic structure. The three-step procedures previously adopted by early researchers (e.g. Seifert *et al.* (1969)) for the conversion of petroleum acids to hydrocarbons were used as a starting point. The aims were initially tested by attempting an optimised conversion procedure on three 'model' bicyclic acids. The structures of the 'model' bicyclic acids, intermediates and final hydrocarbon products were then characterised using infrared spectroscopy (IR), gas chromatography-mass spectrometry (GC-MS) and nuclear magnetic resonance spectroscopy (NMR) to investigate the efficiency of each stage of the conversion.

4.2   Synthetic route for conversion of acids to hydrocarbons

Historically, synthetic routes adopted for conversion of NA to their hydrocarbon counterparts tended to consist of three-step transformations: reduction of the carboxylic acids (Seifert *et al.*, 1969), or their methyl (Zelinsky, 1924; Knotnerus, 1957; Anbrokh *et al.*, 1972) or ethyl (Goheen, 1940) esters, to the corresponding primary alcohols, followed by formation of tosyl or other derivatives and reduction of the tosyl (Seifert *et al.*, 1969), mesyl (Koike *et al.*, 1992; Nascimento *et al.*, 1999) or iodide (Zelinsky, 1924; Goheen, 1940; Knotnerus, 1957; Anbrokh *et al.*, 1972) intermediates to the hydrocarbons (*cf.* Figure 4-1). An alternative, direct deoxygenation of petroleum acids was attempted by hydrogenolysis of the methyl esters over a nickel catalyst (Chernyavskaya *et al.*, 1983).

The initial reduction has usually been carried out with lithium aluminium hydride (LAH) and that method was retained herein.

 The deoxygenation of the resultant primary alcohols is possibly the most versatile step of the whole acids to hydrocarbons conversion, with a variety of derivative options available. Tosylation reactions are usually carried out in the presence of an amine base, classically pyridine with either chloroform or pyridine as the solvent (Seifert *et al.*, 1969; Kabalka *et al.*, 1986). However, investigations involving the formation of tosyl and mesyl esters have reported the production of the corresponding chlorides and alkenes (Dimmler *et al.*, 1984; Kabalka *et al.*, 1986; Ding *et al.*, 2011). Therefore, catalytic tosylation in the presence of 4-(dimethylamino)pyridine (DMAP) with triethylamine (TEA) as the base, was utilised herein, as an alternative to refluxing in pyridine; this method allowed for milder conditions to be employed and resulted in improved yields of tosylate formation (Chapter 2, Section 2.3.2).

Alternative reductions via the formation of iodides have been achieved by heating the alcohols with hydroiodic acid (Knotnerus, 1957; Anbrokh *et al.*, 1972). However, studies investigating the ring structures of such acids concerned about possible isomerisation, used iodine and red phosphorus as an alternative (Zelinsky, 1924; Zelinsky and Pokrowskaja, 1924). Reduction of the iodides is usually carried out over zinc dust, in the presence of hydrochloric acid (Knotnerus, 1957; Goheen, 1940).

The final reduction of other intermediates is often a repetition of the first step using LAH (Fafet *et al.*, 2008). However, since the earlier studies, the use of lithium triethylborohydride (LiEt$_3$BH) also often called 'Super-hydride®', has been advocated for the more efficient reduction of tosylate derivatives (Krishnamurthy and Brown, 1976; Holder and Matturro, 1977; Krishnamurthy, 1978). This was therefore utilised herein.

Overall therefore, the scheme utilised herein (Figure 4-1) was a substantial refinement and potential improvement on the method reported by Seifert *et al.* (1969) and others. Overall, production of the hydrocarbons from the acids, involved reduction of the free acids or esters (both were used) with LAH, derivatisation to the tosylates in the presence of DMAP and TEA and "Super-hydride®" reduction to the hydrocarbons (Figure 4-1).
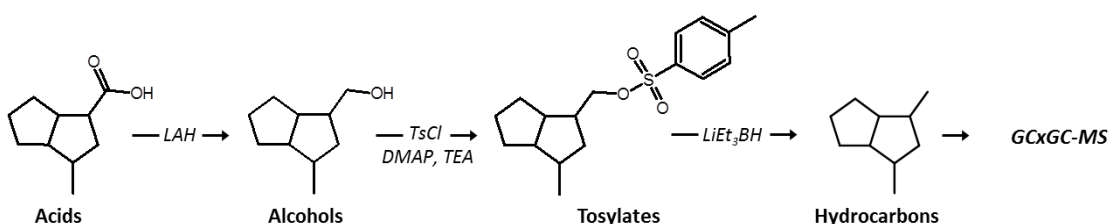
Figure 4-1: Route of conversion of the acids to the corresponding hydrocarbons used herein. Model compound 4-methylbicyclo[3.3.0]octane-2-carboxylic acid is shown as an example.

4.3 Methods

4.3.1 Experimental Details

Authentic 4-methylbicyclo[3.3.0]octane-2-carboxylic acid (3-methyloctahydro-pentalene-1-carboxylic acid) (**Ia**), 2,6,6-trimethylbicyclo[3.1.1]heptane-3-carboxylic acid ((+)-3-pinane-carboxylic acid) (**IIa**) and 4-pentylbicyclo[2.2.2]octane-1-carboxylic acid (**IIIa**) were purchased from Sigma (Poole, UK).

The general procedures for each step of the conversion, for the reduction of three model bicyclic acids to hydrocarbons, via the formation of the alcohol and tosylate intermediates are described in Chapter 2, Section 2.3 and specific experimental details and results are described below in Sections 4.4.1, 4.4.2 and 4.4.3.

4.3.2 Analytical Procedures

The instrumentation used for the structural characterisation of the acids, intermediates and hydrocarbon products, including IR, GC-MS and NMR are described in detail in Chapter 2, Section 2.1.

4.4   Results and Discussion

4.4.1   Synthesis of 2,4-dimethylbicyclo[3.3.0]octane

4.4.1.1   Synthesis and characterisation of 4-methylbicyclo[3.3.0]octane-2-methanol

4-methylbicyclo[3.3.0]octane-2-carboxylic acid (**Ia**) was successfully reduced to 4-methylbicyclo[3.3.0]octane-2-methanol (**Ib**) by reacting with excess LAH under an inert atmosphere with anhydrous diethyl ether as the solvent (Figure 4-2). Subsequent acid work-up using 10% H_2SO_4 resulted in a clear liquid product, with an average yield of $86 \pm 3\%$ (n = 3). GC-MS of the product, derivatised with BSTFA, followed by integration of the areas of the GC peaks showed **Ib**, as its trimethylsilyl (TMS) ether, present with 98 % purity (Figure 4-3).
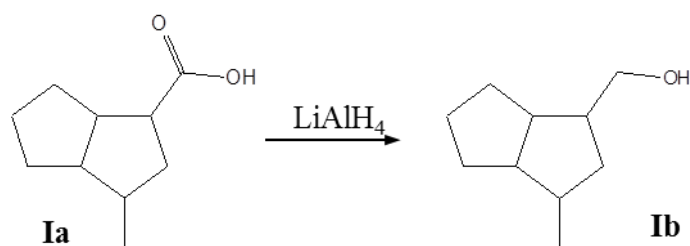
Figure 4-2: Reduction of 4-methylbicyclo[3.3.0]octane-2-carboxylic acid, **Ia** to 4-methylbicyclo[3.3.0]octane-2-methanol **Ib**.

Characterisation of the product was achieved by interpretation of the IR, GC-MS and NMR spectra, as well as comparison to the corresponding data for the original acid. The first indication of a successful reduction was the difference in the GC retention time of the derivatised suspected alcohol product to that of the initial derivatised acid (Figure 4-3). The derivatised product **Ib** had a retention time of 11.3 min compared to that of the derivatised acid **Ia**, at 12.5 min (Figure 4-3).
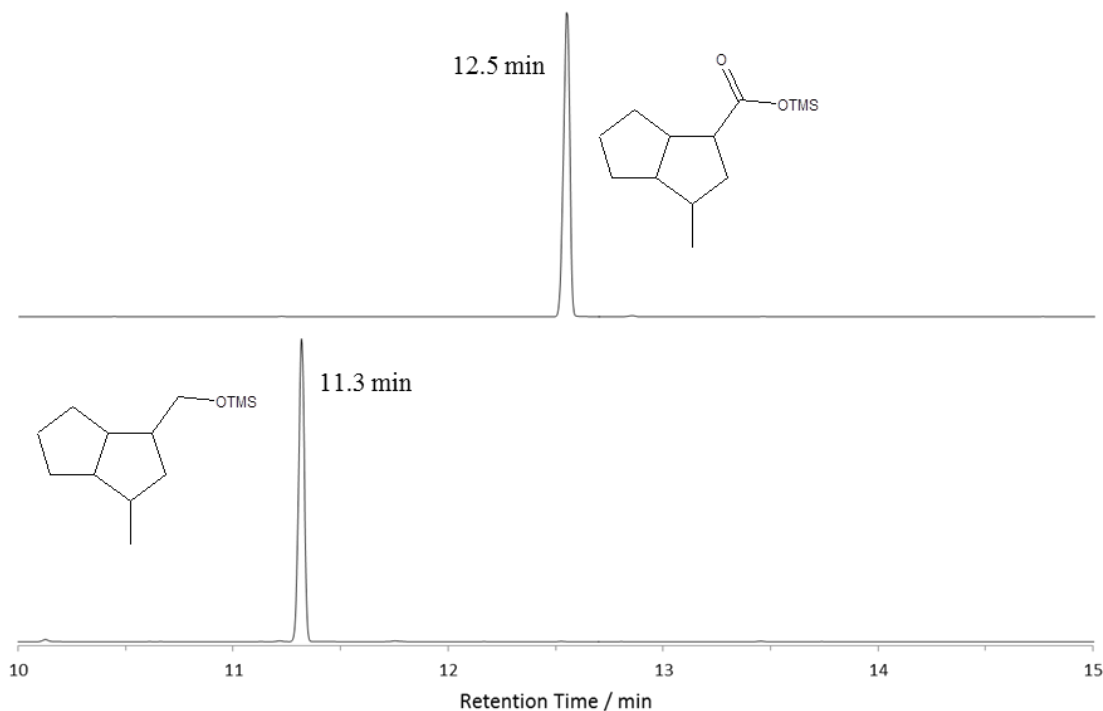
Figure 4-3: Comparison of total ion current (TIC) chromatograms showing differences in retention times of precursor acid **Ia** and reduction product **Ib**, as TMS ester and ether derivatives respectively. (Column A, inlet temperature 300 °C; Chapter 2, Section 2.1.3).

The infrared spectrum of the carboxylic acid showed transmissions with typical broadening between 3026-2692 cm^{-1} assigned to the carboxylic hydroxyl group and an intense transmittance at 1702 cm^{-1} assigned to the C=O stretch in the carboxyl group (Figure 4-4; top). The disappearance of these features in the infrared spectrum of **Ib**, coupled with the appearance of a broad, medium intensity band at 3357 cm^{-1} assigned to the O-H stretch in an alcohol hydroxyl group, suggested the product was an alcohol and that the reduction had been successful (Figure 4-4; bottom and Table 4-1).
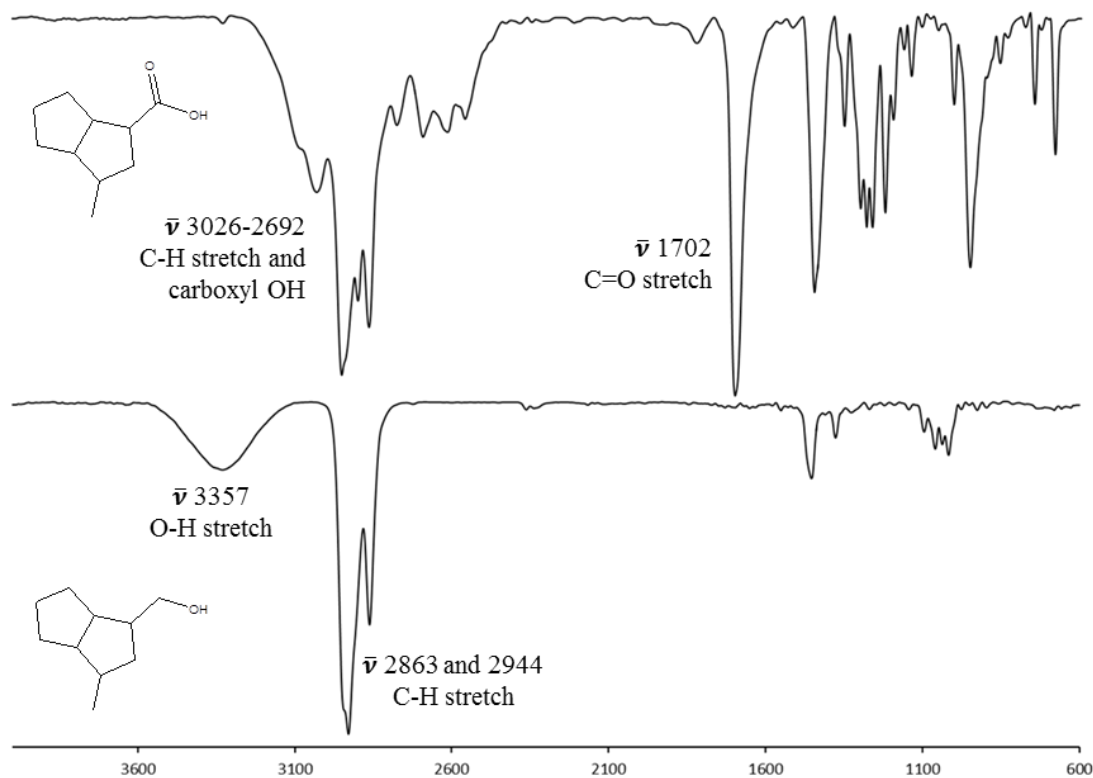
Figure 4-4: Comparison of the IR spectra of acid **Ia** (top) and alcohol product **Ib**

(bottom).

Table 4-1: Summary of features of the IR spectra of 4-methylbicyclo[3.3.0]octane-2-

carboxylic acid, **Ia** and 4-methylbicyclo[3.3.0]octane-2-methanol, **Ib**.

Ia			Ib		
$\bar{\nu}$ (cm^{-1})	Assignment	Comment	$\bar{\nu}$ (cm^{-1})	Assignment	Comment
3026-2692	Carboxyl OH	Broadening of peaks	3357	Alcoholic OH	O-H Stretch, broad
2951, 2898, 2864	CH$_3$, CH$_2$, CH saturate alkyls	C-H stretch, med. > 3000	2944	CH$_3$, CH$_2$, CH saturate alkyls	C-H stretch, med-str. >3000
			2863		
1450		C-H def.	1450		C-H def., weak
1702	Carboxyl C=O	C=O stretch, str.	1377		
900-1300	Carboxyl C-OH	fingerprint	1016	Alcoholic C-OH	C-O stretch, med.

Analysis by GC-MS provided data which supported the conclusions drawn from the IR spectra. The mass spectrum of the alcohol product (**Ib**) as the TMS ether, showed a molecular ion at *m/z* 226, fourteen Da less than the molecular ion of the reactant acid at *m/z* 240 (Figures 4-5 and 4-6). The reduction in mass was expected given the removal of oxygen within the carboxyl group and the gain of hydrogen from LAH.

Derivatisation of polar functional groups such as carboxylic acids and alcohols using BSTFA, dramatically improves their gas chromatographic behaviour on non-polar stationary phases; the chromatographic peaks of free acids and alcohols often show extensive tailing. However, the mass spectra of TMS derivatives are typically dominated by a few intense ions often from facile fragmentation of the TMS group, making structural details difficult to interpret.

The exact structure of the alcohol (**Ib**) could not be determined from the mass spectrum of the trimethyl silyl ether alone, as the dominant ions observed e.g. *m/z* 211 and 75 (Figure 4-6), were assigned as losses derived from the trimethylsilyl (TMS) group (e.g. M-15 and $HO^+=Si(CH_3)_3$). The mass spectra of TMS derivatives typically show intense ions at *m/z* 73 and 75, as seen in Figure 4-5 and Figure 4-6, due to the fragmentation of $(CH_3)_3Si^+$ and $(CH_3)_2Si=O^+H$ respectively (Zaikin and Halket, 2009; Eglinton *et al.*, 1968). An abundant M-15 ion was seen in both spectra, consistent with the losses of methyl fragments from the TMS groups (Figures 4-5, 4-6 and 4-7; A).

Alternatively, the ion assigned as the M-15 ion could also be justified by the loss of methyl at the 4-position after hydrogen rearrangement from the bicyclic ring followed by α-cleavage (Figure 4-7; B). Hydrogen rearrangement after ionisation and subsequent bond cleavage is a mechanism suggested for the occurrence of many ions in functionalised bicyclic compounds (Denisov *et al.*, 1977c; Golovkina *et al.*, 1979; Curcuruto *et al.*, 1991). Hydrogen transfer from alkyl carbons to form protonated

oxygen species in alicyclic alcohols, aldehydes and esters is energetically favourable and therefore considered likely to occur (McLafferty and Tureček, 1993).

The base peak ion at *m/z* 135 in the mass spectrum of **Ib** TMS ether (Figure 4-6) was difficult to assign from simple cleavage of the molecular ion and was attributed to the secondary fragmentation of the ion at *m/z* 211 (Figure 4-7). Fragmentation of a cation to another cation via the loss of a neutral fragment is a known fragmentation mechanism, energetically more favourable than fragmentation of a cation to a radical cation (McLafferty and Tureček, 1993). Determination of whether the alcohol retained the bicyclo[3.3.0]octane 'core', required NMR spectroscopy.
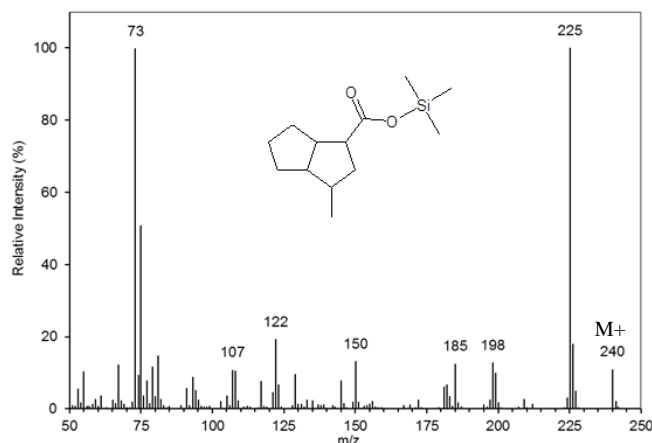
Figure 4-5: Mass spectrum of **Ia** TMS ester.
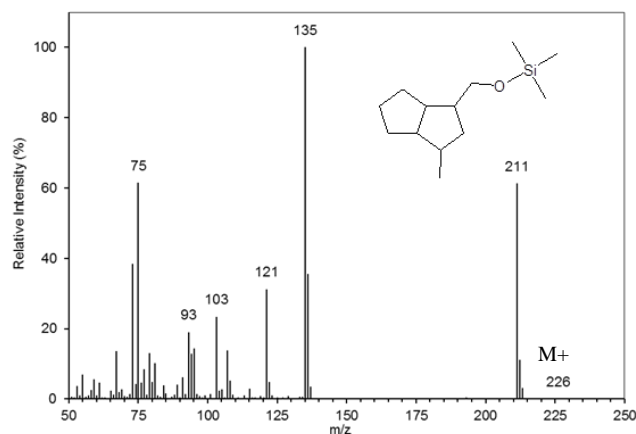
Figure 4-6: Mass spectrum of **Ib** TMS ether.
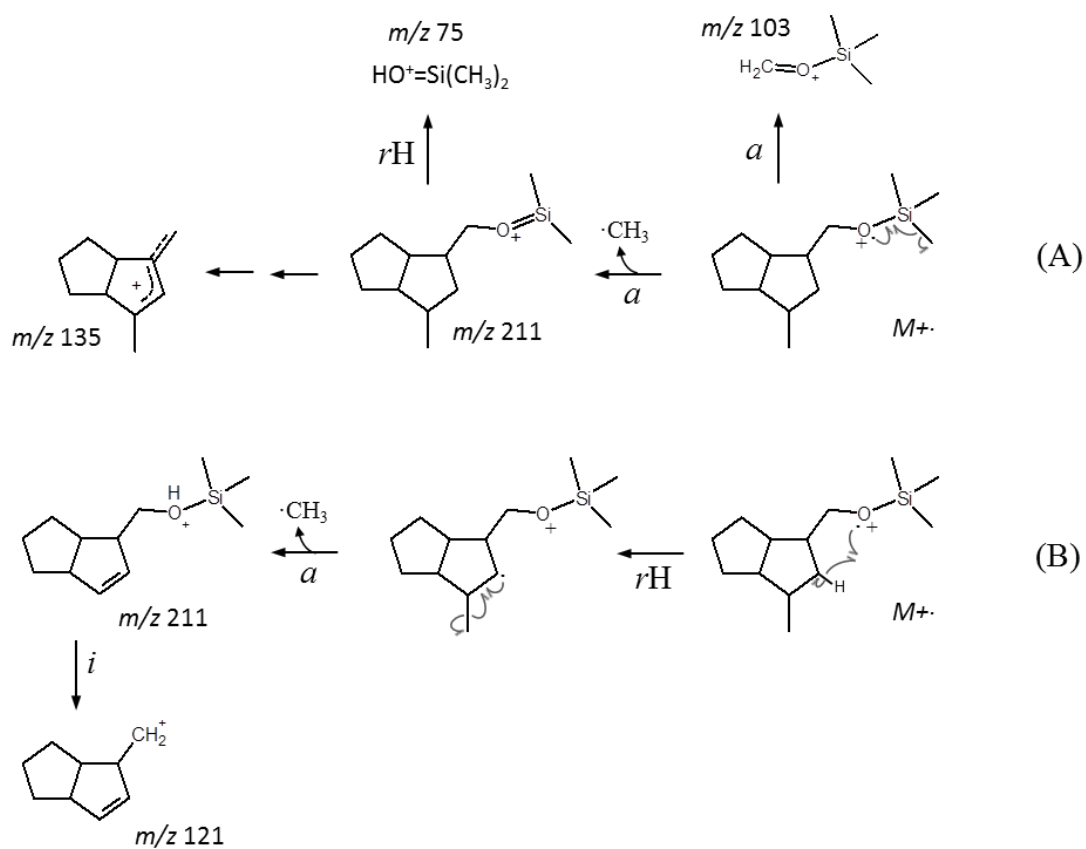
Figure 4-7: Postulated mass spectral fragmentations (A and B) to account for the principal ions in the mass spectrum of **Ib** TMS ether. (*a*, alpha-cleavage; *i*, inductive cleavage; *r*H, hydrogen rearrangement).
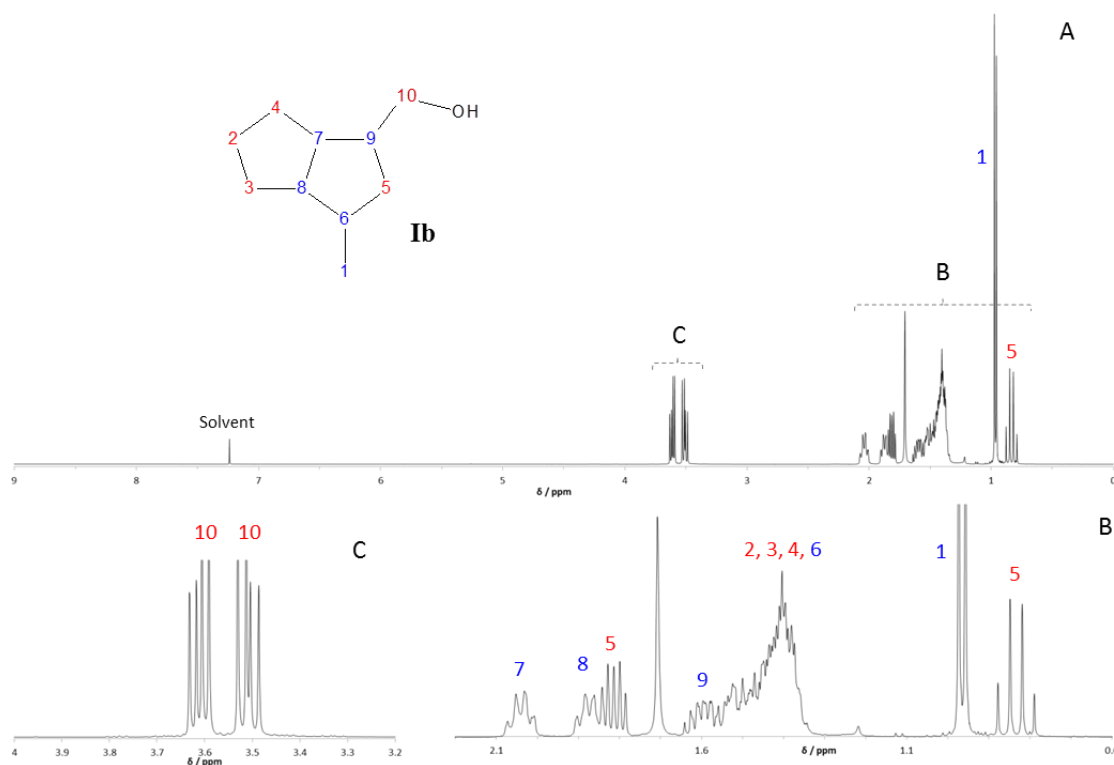
Figure 4-8: (A) ^{1}H-NMR spectrum of **Ib**. (B and C) Focused spectra showing detail between chemical shift ranges 0.5 – 2.5 and 3.2 – 4.0 ppm.

The ^{1}H-NMR spectrum of **Ib** displayed some distinct, identifiable, resonances. However, the majority of the proton signals were observed as complex multiplets between 1.20 – 2.10 ppm, which were attributed to the methylene groups of similar magnetic equivalence in the bicyclic ring system. Therefore it was not possible to elucidate the complete structure of **Ib** from the data shown in ^{1}H-NMR spectrum alone (Figure 4-8). However, the intense doublet (*d*) seen at 0.98 ppm with an integral of 3.0 was attributed to the protons of the methyl substituent at position 1 (Figure 4-8). The doublet observed was attributed to the presence of a single neighbouring proton at position 6.

The multiplets at 3.53 and 3.63 ppm, each integrating to 1.0, were each a doublet of doublets (*dd*), and were attributed to the protons on the methylene group at position 10. The splitting pattern (Figure 4-8; C) was attributed to the fact that the two protons at position 10 were diastereotopic and each magnetically inequivalent relative to the

proton at position 9, which was situated at a chiral centre. The magnetic inequivalence

of the protons at position 10 is best portrayed as a Newman projection (Figure 4-9).

Although protons H_a and H_b are on the same carbon (Figure 4-9) their positions are not

interchangeable and therefore the protons are magnetically inequivalent.
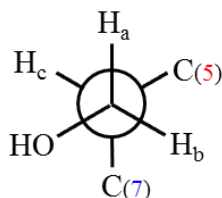
Figure 4-9: Newman projection demonstrating magnetic inequivalence of diastereotopic

protons H_a and H_b relative to the chiral proton H_c.

Therefore each proton at position 10 is split by the proton at position 9 and the other

proton on position 10, resulting in two doublet of doublets at similar chemical shifts.

The coupling constants were $^3J = 7.1$ and 10.5 Hz (3.53 ppm) and 5.8 and 10.5 Hz (3.63

ppm); the shared coupling constant of 10.5 Hz is consistent with the above.

The multiplet at 0.83 ppm (Figure 4-8; B), seemingly a quartet (*q*), in fact had a

coupling constant of 11.8 Hz, which was higher than the typical 7 Hz observed for a

quartet. The equal spacing between the peaks ruled out the possibility that the multiplet

was a doublet of doublets. However the quartet could still have arisen from three

protons on different carbons, two of which might possess the same, high coupling

constant (e.g. an overlapping triplet of doublets (*td*)). Further assignment of individual

protons required further analysis by homonuclear decoupling experiments.

Homonuclear decoupling involves irradiating the compound at a specific frequency (i.e.

targeting protons at a specific chemical shift). This removes the coupling effects of

these protons on the surrounding proton environments. Therefore any observable

changes in the splitting patterns of the remaining signals, results in the identification of

adjacent environments (e.g. Figures 4-10 and 4-11). The newly identified protons can be

targeted and the adjacent protons identified. This approach can dramatically increase the structural information obtainable from a ^{1}H-NMR spectrum containing complex multiplets.

Only a few distinct multiplets were useful for homonuclear decoupling experiments in the ^{1}H-NMR spectrum of **Ib**. If two multiplets share a similar chemical shift, irradiation at that frequency can result in the decoupling of multiple environments, decreasing the selectivity of the experiment and making it difficult to link specific signals. The irradiation strength can be lowered to reduce the possibility of decoupling multiple environments with similar chemical shifts; however this reduces the observable changes in the spectrum.

A summary of the results from the homonuclear decoupling experiments of **Ib** is given in Table 4-3 (page 143). Although six of the proton signals were unresolved within the complex multiplet between 1.31 − 1.56 ppm, some structural detail could be obtained and used tentatively to assign other signals in the spectrum. For example, the ^{1}H-NMR spectrum of **Ib** contained nine main multiplets, as seen in Figure 4-8. Irradiation of the signals at 3.53 and 3.63 ppm already identified as the diastereotopic protons at position 10 were expected to change only one other signal in the spectrum, thus identifying the chiral proton at position 9. The only difference in the spectrum after decoupling the doublet of doublets at 3.53 and 3.63 ppm was a small change seen in the multiplet at 1.58 ppm, which overlapped with the large complex multiplet between 1.31 - 1.56 ppm. The identification of the proton on position 9 at 1.58 ppm was also supported in the COSY spectrum of **Ib** (Appendix Figure 11); the assignment of the proton at position 9 was then used to identify the positions of other protons.

Decoupling the signal at 1.58 ppm might have resulted in decoupling protons within the large overlapping multiplet. Therefore the other resolved signals were decoupled to see if any affected the signal at 1.58 ppm. Three other signals with integrals of 1.0, in addition to the doublet of doublets at 3.53 and 3.63 ppm, were observed to be coupling with the proton at position 9; the doublet of doublets at 2.05 ppm and what appeared to be a quintet (*quint*) and quartet (*q*) at 1.83 ppm and 0.83 ppm, limiting them to the three protons at positions 5 and 7.

After decoupling the 'quartet' at 0.83 ppm, the multiplets at 1.58, 1.83 and 1.31-1.56 ppm were all observed to change, indicating the environment was adjacent to three other proton environments (Figure 4-10; A). Decoupling the 'quintet' (*quint*) at 1.83 ppm resulted in the same signals being affected, plus the quartet (*q*) at 0.83 ppm (Figure 4-10; C). Therefore the signals at 0.83 ppm and 1.83 ppm both couple with the same two environments (1.58 and 1.31-1.56 ppm); one being the proton at position 9 (1.58 ppm), the other potentially the proton at position 6 (1.31-1.56 ppm), and to each other. Consequently, the multiplets at 0.83 ppm and 1.83 ppm were assigned as the two protons on the methylene group in position 5. This was also supported by a large coupling constant ~11.6 Hz in both multiplets, corresponding to the coupling between the protons on the same carbon at position 5. The assignment of the two multiplets at 1.83 ppm and 0.83 ppm as the protons at position 5 was confirmed by the two resonances correlating in the COSY spectrum of **Ib** (Appendix Figure 12).
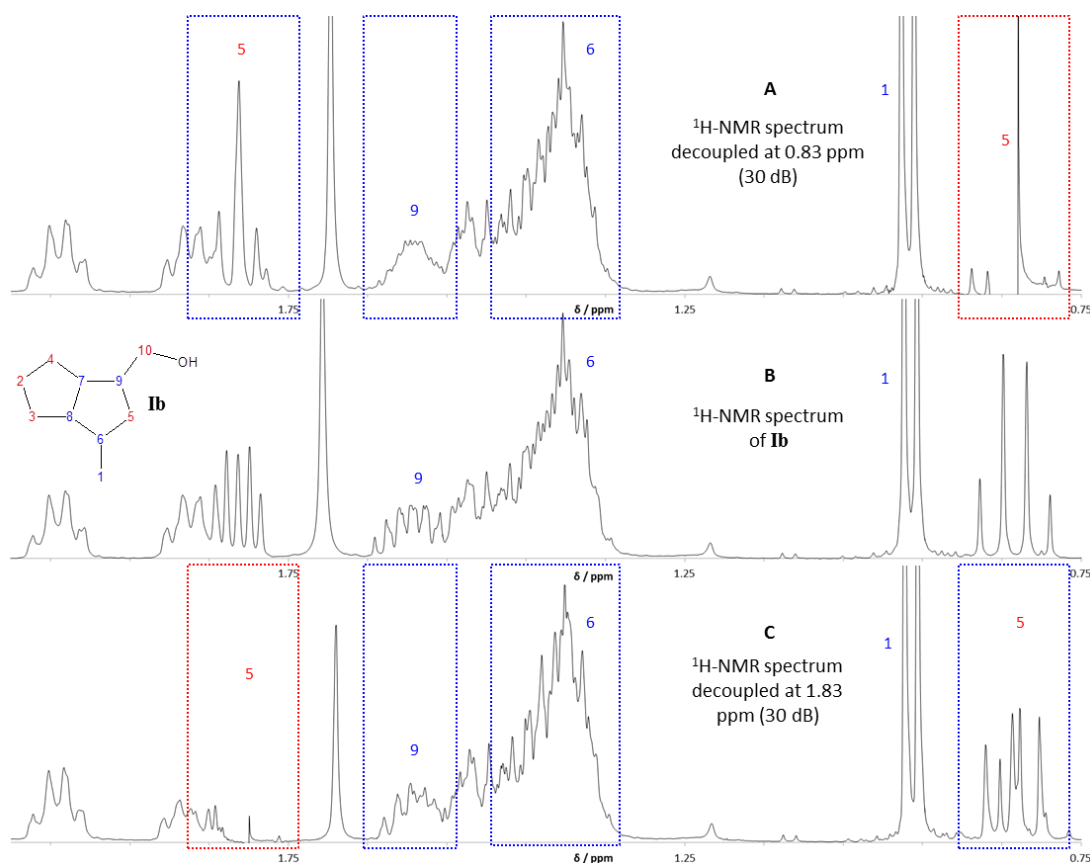
Figure 4-10: Comparison of ^{1}H-NMR spectra of **Ib** (A) decoupled at 0.83 ppm, (B) non-decoupled ^{1}H spectrum and (C) decoupled at 1.83 ppm (red; irradiated, blue; affected).

The two multiplets at 1.88 ppm and 2.05 ppm resembled doublets of doublets (*dd*). When decoupled, they affected each other and the large multiplet between 1.31 − 1.56 ppm (Figure 4-11; A and C). Decoupling the signal at 2.05 ppm also affected the multiplet at 1.58 ppm, assigned as the proton at position 9. Therefore the multiplets at 1.83 and 2.05 ppm were assigned as the protons on the bridgehead carbons in positions 7 and 8. This assignment was also supported by the signals at 1.83 and 2.05 ppm, correlating with two carbon resonances in the heteronuclear correlation (CHSHF or 'HETCOR') spectrum of **Ib** (Appendix Figure 13), which showed 'upwards' phasing in the DEPT ^{13}C spectrum of **Ib** (Figure 4-14). This confirmed the protons responsible for the resonances at 1.85 ppm and 2.05 ppm (both integrating to 1.0) were both CH groups within the molecule, supporting their assignment as protons at positions 7 and 8, ruling out other possibilities such as one of the protons at position 4 and 7.
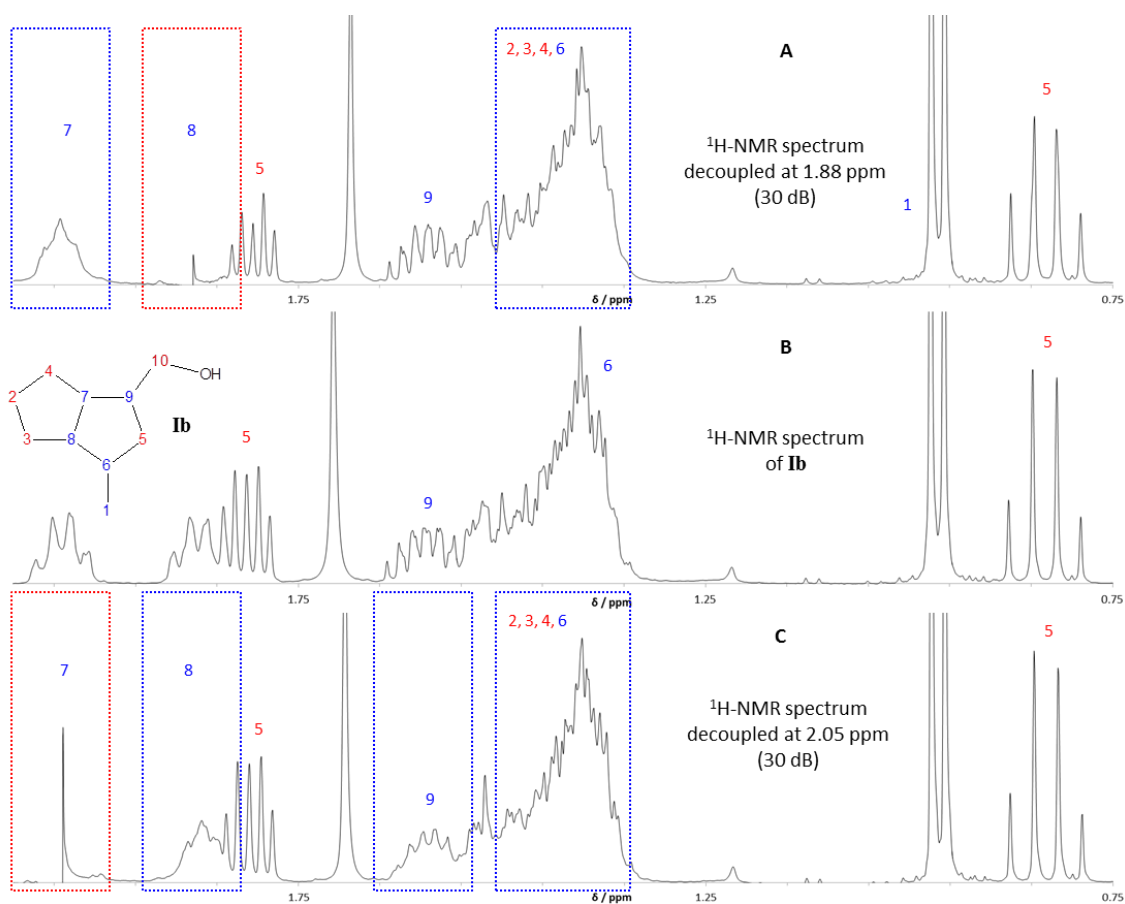
Figure 4-11: Comparison of ^{1}H-NMR spectra of **Ib** (A) decoupled at 1.88 ppm, (B) non-decoupled ^{1}H spectrum and (C) decoupled at 2.05 ppm (red; irradiated, blue; affected).

The large multiplet between 1.31 − 1.56 ppm had an integral of 7.0. When the signal was irradiated at 1.40 ppm, several signals changed as expected (Table 4-3, page 143). However the multiplet at 2.05 ppm remained relatively unaffected even though the signal at 2.05 ppm coupled with at least one proton within the multiplet at 1.31 − 1.56 ppm. This was attributed to the multiplet not being fully decoupled, without decoupling the signal at 1.58 ppm as well.

Based on logical deductions from the results of the decoupling experiments (summarised in Table 4-3) and the ^{1}H and COSY spectra (Figures 4-10 and 4-11 and Appendix Figures 11-13), assignment of each signal in the ^{1}H spectrum (Figure 4-8) was made and correlated with the structure of **Ib**. The six protons on the three methylene groups, positions 2, 3 and 4, were expected to show complex splitting with

very similar chemical shifts. Therefore they were tentatively assigned as producing the complex multiplet between 1.31 – 1.56 ppm. This was supported by the multiplet integrating to 7.0, accounting for the six methylene protons, plus the single proton on position 6, also known to be amongst the multiplet from the decoupling of the protons of the methyl group at position 1 and observed correlation with the doublet in the COSY spectrum (Appendix Figure 12). The large multiplet was decoupled at 1.40 ppm, resulting in changes to all the signals apart from those at 3.53 and 3.63 ppm, assigned as the protons at position 10, 1.58 ppm, assigned as the proton at position 9 and, interestingly, the multiplet at 2.05 ppm assigned as the proton at position 7. Overall, the decoupling experiments detailed in Table 4-3 proved useful in refining the structural detail obtained from the original interpretation (Table 4-2, page 142).

The ^{13}C-NMR spectrum (Figure 4-13) supported the above assignments of the expected structure of **Ib** (Table 4-3). The chemical shifts were comparable with values given by Whitesell and Minton (1987), who detailed the chemical shifts in the ^{13}C spectra of many alicyclic compounds, including a series of bicyclo[3.3.0]octanes. The list of structures included endo- and exo-2-methylbicyclo[3.3.0]octane and endo- and exo-bicyclo[3.3.0]octane-2-methanol; the net chemical shifts of the two exo- structures (Figure 4-12; A and B) related remarkably well to the ^{13}C-NMR spectrum in Figure 4-13.
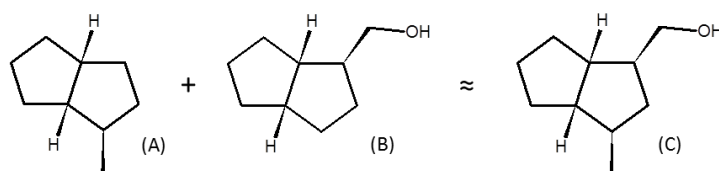
Figure 4-12: Structures of (A) exo-2-methylbicyclo[3.3.0]octane and (B) exo-bicyclo[3.3.0]octane-2-methanol; the net ^{13}C-NMR chemical shifts reported by Whitesell and Minton (1987) were similar to those in the spectrum of (C) **Ib** in Figure 4-13.

The ^{13}C-NMR spectrum contained ten signals, which was expected, as **Ib** possessed no symmetry. The DEPT ^{13}C-NMR spectrum showed five signals with opposite phasing relative to the other five signals, confirming that the product contained 5 methylene groups (labelled red in Figure 4-14). The number of secondary carbons (CH$_2$ groups) was equal to the combined number of primary and tertiary carbons (CH$_3$ and CH groups; labelled blue in Figure 4-14). Therefore the methylene signals were identified by the higher frequency of the branched methylene carbon at position 10, at 67.44 ppm. The electronegative oxygen within the hydroxyl group has a negative inductive effect on the adjacent carbon, causing the methylene carbon in position 10 to have a higher chemical shift. Conversely, the peak at the lowest chemical shift, 19.51 ppm was attributed to the methyl substituent in position 1 furthest from the hydroxyl moiety, supported by its orientation in the DEPT spectrum (Figures 4-13 and 4-14). The assignment of the peaks at 19.51 ppm and 67.44 ppm as carbon positions 1 and 10 was confirmed in the CHSHF spectrum of **Ib**, correlating with the doublet at 0.98 ppm and the doublet of doublets at 3.53 and 3.63ppm, respectively, in the ^{1}H spectrum (Appendix Figure 13).
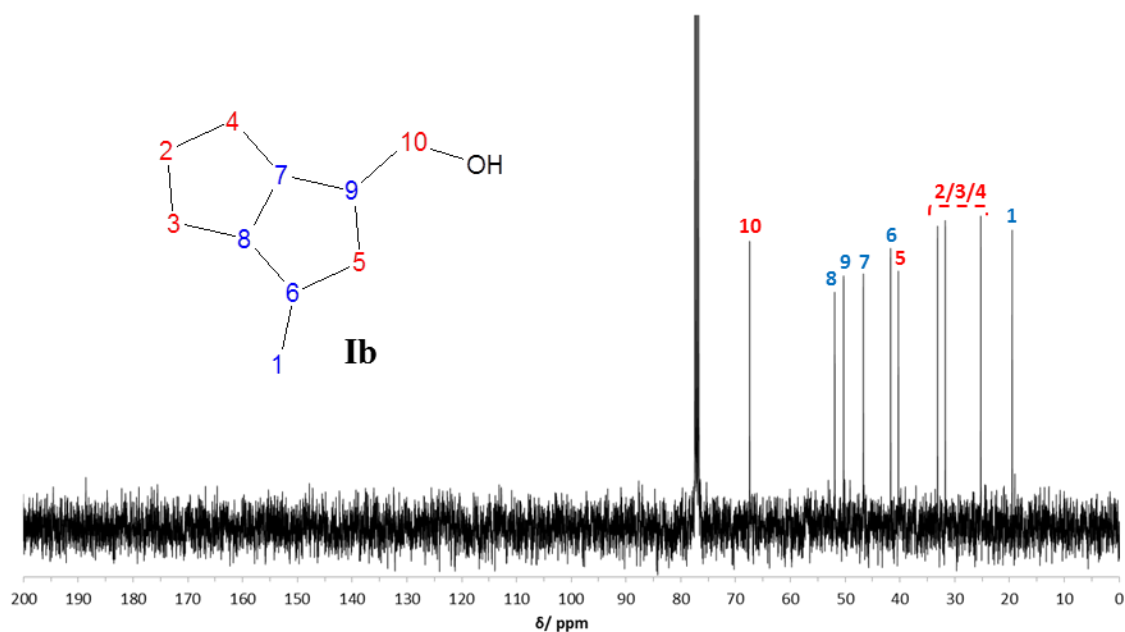
Figure 4-13: ^{13}C-NMR spectrum of alcohol product **Ib**.
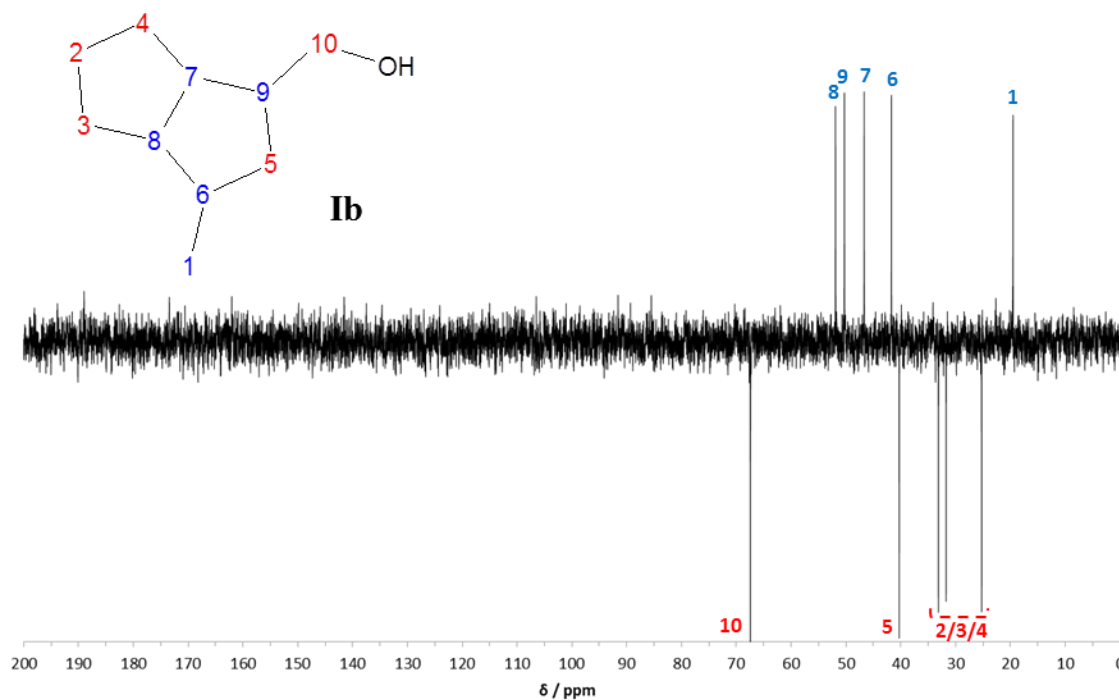
Figure 4-14: DEPT ^{13}C-NMR spectrum of alcohol product **Ib**.

The remaining carbon signals corresponding to CH groups (positions 6, 7, 8 and 9), observed in the DEPT ^{13}C-NMR spectrum at 41.71, 46.68, 50.28 and 51.91 ppm, were assigned based on the correlations observed in the CHSHF spectrum of **Ib** (Appendix Figure 13) and confirmed by the additional 2 and 3-bond heteronuclear correlations observed in the **co**rrelation through **lo**ng-range **c**oupling (COLOC) spectrum of **Ib** (Appendix Figure 14). For example, the multiplet at 2.05 ppm attributed to the proton at position 7 correlated in the COLOC spectrum of **Ib**, with the carbon signal at 51.91 ppm, assigned as the carbon in position 8, the reciprocal correlation was also observed (Appendix Figure 14). The carbon signals corresponding to the methylene groups at positions 2, 3 and 4 (25.24, 31.72 and 33.13 ppm) could not be differentiated. However, the methylene group in position 5 at 40.28 ppm was identified based on its correlation with the proton signals at 0.83 ppm (*d*) and 1.83 ppm (*m*) (Appendix Figures 13 and 14), previously assigned as the protons at position 5, based on the homonuclear decoupling experiments and COSY spectrum (Appendix Figure 12).

Table 4-2: Summary of ^{1}H and ^{13}C-NMR spectra of alcohol product **Ib**.

Position	^{1}H chemical shifts / ppm (multiplicity)	^{1}H integral	^{13}C chemical shifts / ppm			
			Primary (CH)	Secondary (CH$_2$)	Tertiary (CH$_3$)	Quaternary (C)
1	0.98 (*d*)	3.0			19.51	
2				25.24[a]		
3				31.72[a]		
4	Determined by			33.13[a]		
5	homonuclear			40.28		
6	decoupling experiments	41.71				
7	in Table 4-3	46.68				
8		51.91				
9		50.28				
10	3.53 (*dd*)	1.0		67.44		
	3.63 (*dd*)	1.0				

[a] peaks assigned positions 2, 3 and 4 are interchangeable

The combined spectrometric and spectroscopic data confirmed the successful reduction of the acid and the formation of a primary bicyclic alcohol with the same structure as the acid. The IR and mass spectral data confirmed the formation of a bicyclic alcohol and the NMR spectra confirmed that the product possessed a di-substituted bicyclo[3.3.0]octane core; the same as that of the original acid.

Table 4-3: Summary of the ^{1}H-NMR homonuclear decoupling experiments of **Ib**.

Position	[1]H chemical shifts / ppm	Multiplicity	[1]H integral	J values / Hz	Homonuclear Decoupling Experiments		
					Irradiated / ppm	Affected / ppm	[1]H within Structure (red – [1]H irradiated blue – [1]H affected)
1	0.98	*d*	3.0	6.6	0.98	1.31 - 1.56	
2	1.31-1.56	*multiplet*	6 of 7.0	-	1.40	0.83, 0.98, 1.83, 1.88	
3				-			
4				-			
5	0.83	*q*	1.0	11.8	0.83	1.31 – 1.56, 1.58, 1.83	
	1.83	*quint*	1.0	5.6, 11.6	1.83	0.83, 1.31 – 1.56, 1.58	
6	1.31-1.56	*multiplet*	1 of 7.0	-	1.40	0.83, 0.98, 1.83, 1.88	
7	2.05	*dd/multiplet*	1.0	-	2.05	1.31 - 1.56, 1.58, 1.88	
8	1.88	*dd/multiplet*	1.0	-	1.88	1.31 - 1.56, 2.05	
9	1.58	*multiplet*	1.0	-	1.60	0.83, 1.83, 2.05, 3.53, 3.63	
10	3.53	*dd*	1.0	7.1, 10.5	3.53	1.58	
10	3.63	*dd*	1.0	5.8, 10.5	3.63	1.58	

4.4.1.2 Preparation and characterisation of 4-methylbicyclo[3.3.0]octane-2-methanol tosyl derivative

4-methylbicyclo[3.3.0]octane-2-methanol (**Ib**) was successfully converted to the 4-methylbicyclo[3.3.0]octane-2-methanol tosyl derivative (**Ic**) (Figure 4-15) by catalytic tosylation using tosyl chloride (TsCl) in the presence of 4-(dimethylamino)pyridine (DMAP) and triethylamine (TEA). The procedure was adapted from various methods (Ding *et al.*, 2011; Goodenough *et al.*, 2004; Hwang *et al.*, 1984). The addition order of the reagents and choice of base was found to affect the outcome of the reaction. The method included the use of TEA as the base instead of pyridine, producing an average yield of 90 ± 5 % (n = 3). Attempts at refluxing in pyridine produced low yields and undesired products, such as the chloride.

The purity of the product was difficult to ascertain from the gas chromatogram because the tosylate underwent elimination of p-toluene sulfonic acid during gas chromatography, due to hot injection at 300 °C (Figure 4-16). Even with the inlet temperature lowered to 250 °C and 225 °C, decomposition was still observed, albeit it was significantly less (as seen for all the tosylate products, Appendix Figures 15 and 23). The chromatogram contained a peak at 22.3 min showing slight tailing, which was assigned as the tosylate. The earlier eluting peaks, between 5.9 – 7.9 min, with molecular ions at *m/z* 136 were tentatively identified as $C_{10}H_{16}$ olefins, produced by the elimination of p-toluene sulfonic acid. The relative abundance of these earlier peaks was directly related to the injection temperature (Appendix Figures 15 and 23). GC-MS was useful in determining if any other by-products had formed; for example, whether there was unreacted alcohol and whether excess TsCl was present, in the form of p-toluenesulfonyl-N-diethylamide, after reacting with TEA. Where impurities were present, the tosylate products were cleaned over silica, eluting with 30:1, hexane : ethyl acetate (Chapter 2, Section 2.3.4).
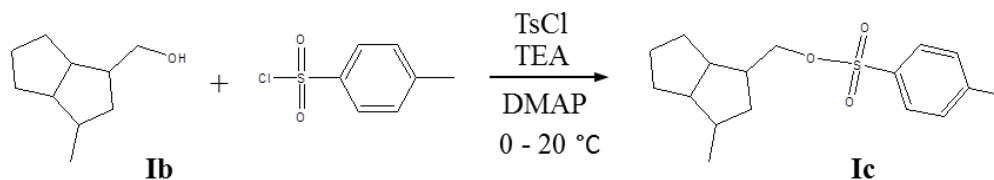
Figure 4-15: Reaction scheme for the tosylation of **Ib** to **Ic**.
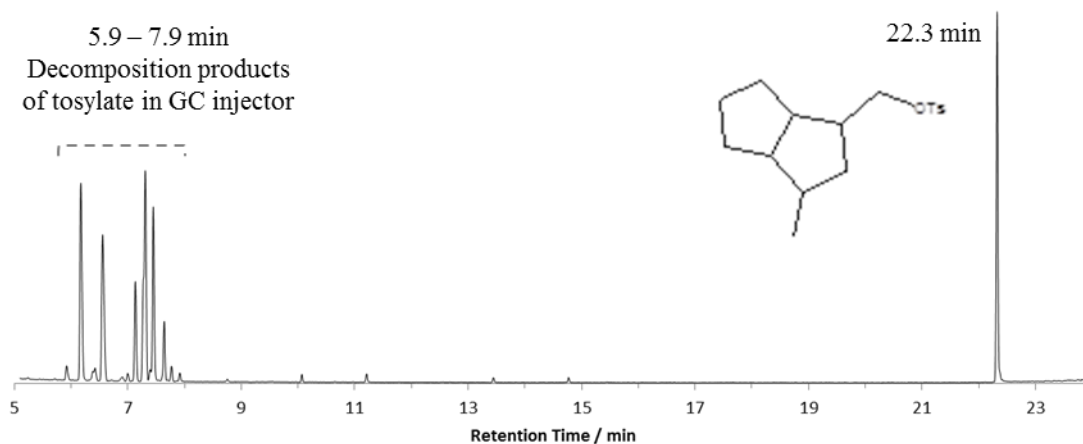
Figure 4-16: Gas chromatogram of tosylate product, **Ic**. The product underwent partial

decomposition in the hot GC inlet. (Column A, inlet temperature 300 °C).

The mass spectrum of **Ic** (Figure 4-17) did not display distinguishing features that

allowed the elucidation of the tosylate structure. Instead, confirmation of the formation

of the tosylate relied on the interpretation of NMR spectra. However, the high retention

time and tailing of the peak at 22.3 min in the chromatogram suggested a polar, low

volatility compound had been produced. The m/z 155 ion in the mass spectrum was

assigned as due to the fragment ion $CH_3(C_6H_4)S^+O_2$ (Figure 4-17). The m/z 136 ion was

attributed to the loss of $CH_3(C_6H_4)SO_3H$ resulting in an odd-electron radical cation,

$[C_{10}H_{16}]^{+\cdot}$ most likely explained by hydrogen rearrangement and inductive cleavage of

the C-O bond. The majority of low mass fragment ions such as m/z 121, 107 and 93

were tentatively identified as due to secondary fragments from the m/z 136 radical

cation (Figure 4-17). However, the ion at m/z 91 was thought to originate from the tosyl

group; attributed to the toluene cation, $C_7H_7^+$ (sometimes termed the tropylium cation).

145
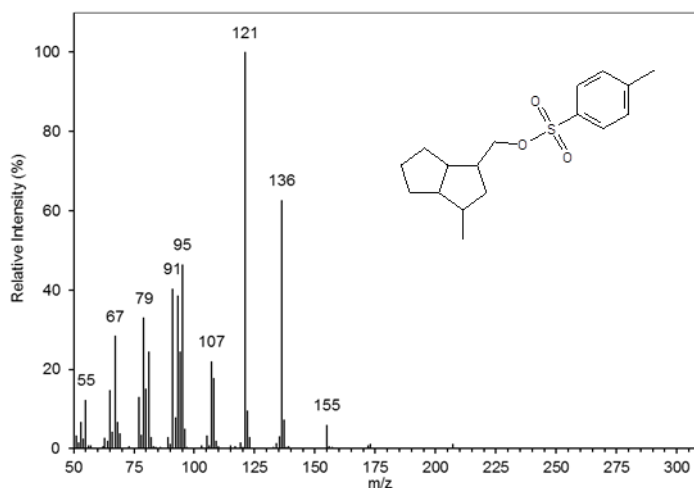
Figure 4-17: Mass spectrum of tosylate product **Ic**.

The ^{1}H-NMR spectrum of **Ic** showed very similar signals to that of **Ib**, which was strong evidence that the bicyclic part of the compound had retained the bicyclo[3.3.0]octane structure. For instance, the two doublet of doublets (*dd*) at 3.95 ppm were assigned to the diastereotopic protons at position 11 (Figure 4-18; C). The intense doublet at 0.94 ppm was attributed to the methyl substituent on the bicyclic structure at position 1 (Figure 4-18; D). The slight differences observed in chemical shift were due to the differences in polarity of the p-toluenesulfonyl ester relative to the hydroxyl moiety of the alcohol. Therefore the signals in the ^{1}H-NMR spectrum of **Ic** were assigned based on those previously deduced from the decoupling experiments and two-dimensional NMR spectra acquired for **Ib**.

Additional signals observed in the ^{1}H-NMR spectrum of **Ic** were assigned as the protons on the tosyl ester. For example, the ^{1}H-NMR spectrum contained two doublets seen at 7.32 and 7.76 ppm, each integrating to 2.0. The signals were assigned as the aromatic protons at positions 12 and 13 (Figure 4-18; B). The intense singlet (*s*) at 2.43 ppm with an integral of 3.0, absent in the alcohol spectrum, was assigned as due to the protons on the methyl substituent on the tosyl group (Figure 4-18; position 2). No splitting was observed since the adjacent position comprised a quaternary aromatic carbon atom

(Figure 4-18). These assignments were supported by those made based on the correlations observed in the COSY, CHSHF and COLOC spectra acquired for the tosyl ester products of the other 'model' compounds (e.g. Appendix Figure 22).
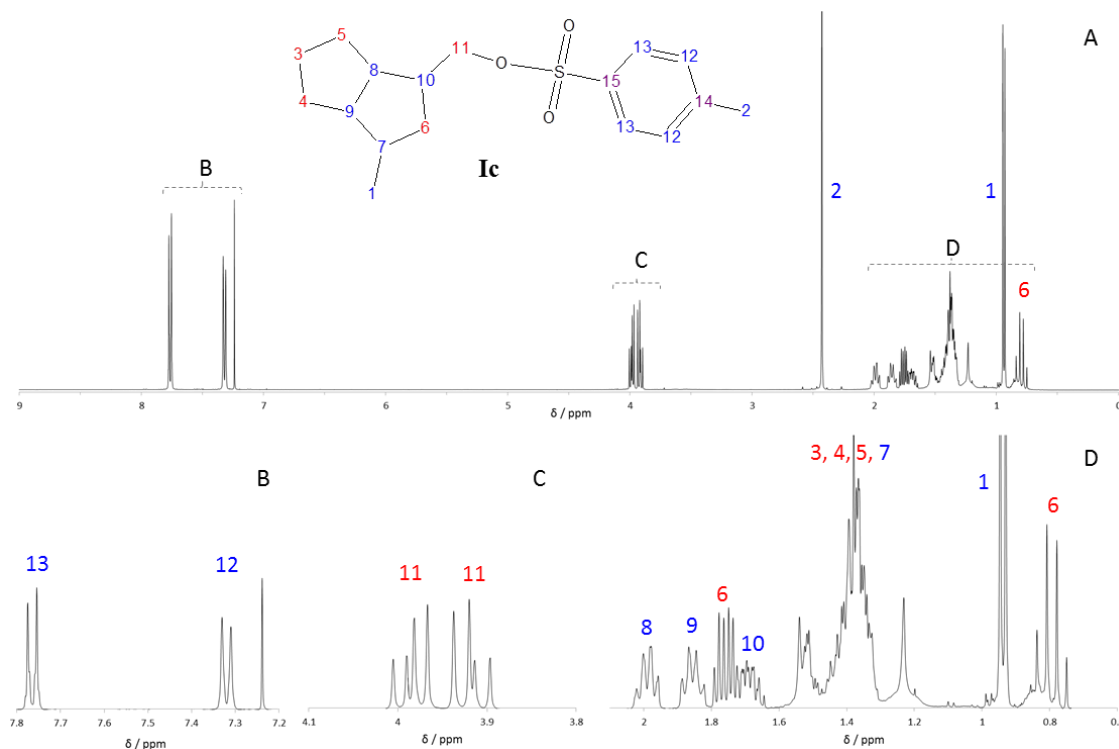
Figure 4-18: (A) ^{1}H-NMR spectrum of **Ic**. (B, C and D) Focused spectra showing detail between chemical shift ranges 0.6 – 2.1 ppm, 3.8 – 4.1 and 7.2 – 7.8 ppm.

The ^{13}C-NMR and DEPT ^{13}C-NMR spectra confirmed successful conversion of **Ib** to **Ic**. The tosylate product **Ic** showed no symmetry, resulting in fifteen peaks observed in the ^{13}C-NMR spectrum (Figure 4-19). The low intensity peaks at 144.61 and 133.38 ppm in the ^{13}C-NMR spectrum were typical of those of quaternary aromatic carbons, identified as positions 14 and 15. This assignment was supported by their disappearance in the DEPT ^{13}C-NMR spectrum (Figure 4-20). The peaks at 129.84 and 127.94 ppm were assigned to positions 12 and 13; the intensities were almost twice the height of the other peaks because each signal accounted for two magnetically equivalent environments (Figure 4-19). The exact labelling of the signals attributed to positions 12, 13, 14 and 15

were based on the correlations observed in the COLOC spectra of **IIc** and **IIIc** (e.g. Appendix Figure 21).
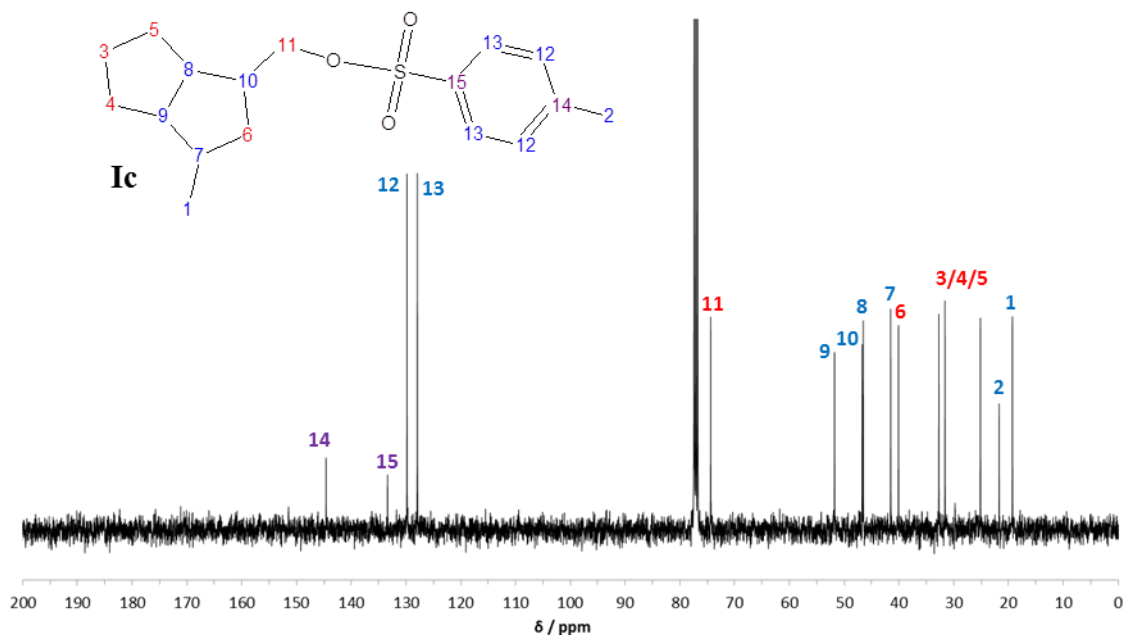
Figure 4-19: ^{13}C-NMR spectrum for tosylate product **Ic**.

The methylene carbon at position 11 (Figure 4-19), was assigned as the higher frequency resonance at 51.77 ppm, due to the proximity of position 11 being close to the sulfonate group. The methylene carbons in the bicyclic 'core' were differentiated from the CH environments based on their opposite phasing in the DEPT ^{13}C-NMR spectrum; their exact assignments were based on those determined for **Ib**, with the signals attributed to positions 3, 4 and 5, being interchangeable (Table 4-4). The two methyl substituents, positions 1 and 2, were assigned as the peaks at 19.29 and 21.71 ppm accordingly. All the signals which corresponded to part of the bicyclic structure, apart from position 11, appeared at a lower chemical shift than in the ^{13}C-NMR spectrum of the alcohol. Therefore the peak at 21.71 ppm was assigned as the methyl substituent on the tosyl group (Figure 4-20; position 2).
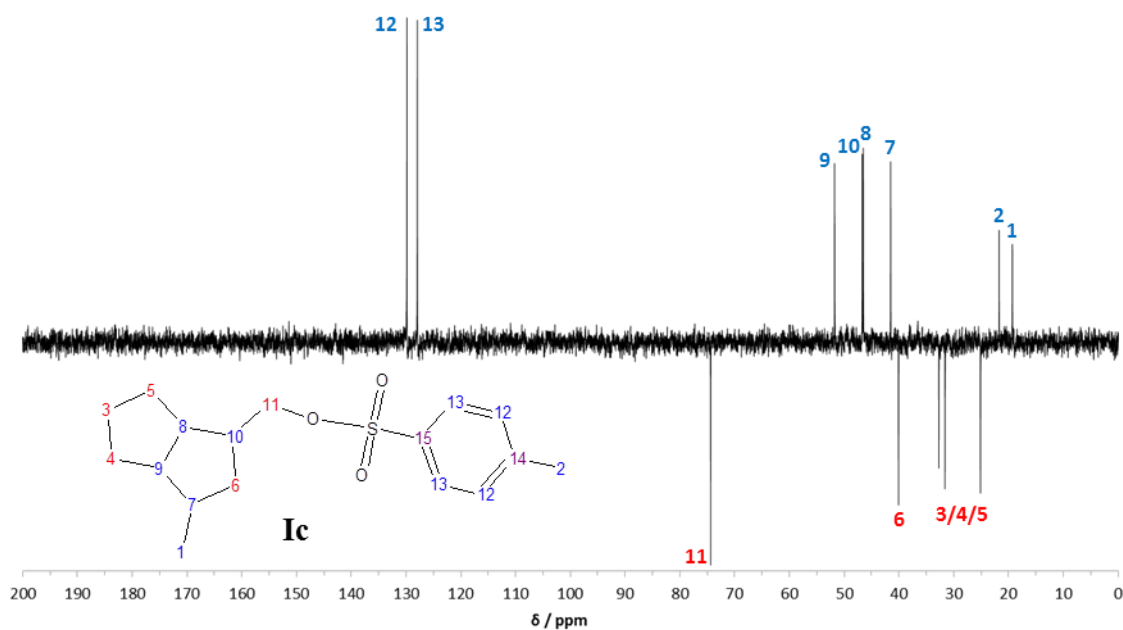
Figure 4-20: DEPT ^{13}C-NMR spectrum of tosylate product **Ic**.

Table 4-4: Summary of ^{1}H and ^{13}C-NMR spectra for tosylate product **Ic**.

Position	^{1}H chemical shifts / ppm (multiplicity)	^{1}H integral	J value / Hz	^{13}C chemical shifts / ppm			
				Primary (CH)	Secondary (CH$_2$)	Tertiary (CH$_3$)	Quaternary (C)
1	0.94 (*d*)	3.0	6.6			19.29	
2	2.43 (*s*)	3.0	-			21.72	
3					25.12[a]		
4	1.30 – 1.53	6 of 7.0	-		31.59[a]		
5					32.72[a]		
6	1.76 (*m*)	1.0	-		40.08[b]		
7	1.30 – 1.53	1 of 7.0	-	41.52[b]			
8	1.99 (*dd*)	1.0	-	46.52[b]			
9	1.86 (*dd*)	1.0	-	46.70[b]			
10	1.69 (*m*)	1.0	-	51.76[b]			
11	3.92 (*dd*)	1.0	6.9, 9.3		74.39		
	3.98 (*dd*)	1.0	6.0, 9.3				
12	7.32 (*d*)	2.0	8.1	129.84[b-]			
13	7.76 (*d*)	2.0	8.3	127.94[b]			
14	-	-	-				144.61[b]
15	-	-	-				133.38[b]

[a] peaks assigned positions 3, 4 and 5 are interchangeable
[b] peaks labelled based on the assignments determined for **Ib**

4.4.1.3   Preparation and characterisation of 2,4-dimethylbicyclo[3.3.0]octane

The tosyl derivative **Ic** was successfully reduced to 2,4-dimethylbicyclo[3.3.0]octane

(Figure 4-21; **Id**) by reacting with excess lithium triethylborohydride ('Super-

Hydride®') at room temperature, under an inert atmosphere. Anhydrous tetrahydrofuran

(THF) and diethyl ether were used as solvents and the reaction was completed with a

basic work-up using 20% w/v NaOH, yielding the hydrocarbon **Id** (Figure 4-21).

Concentration of the hydrocarbon product was achieved using a Kuderna-Danish

apparatus, described in Chapter 2, Section 2.3.4, to reduce evaporative losses since

concentration of the product under a less controlled stream of N_2 resulted in significant

evaporative losses of the product, even at 15 °C. A mixture containing C_{10-15} n-alkanes

and C_{10} tricyclic adamantane, was analysed before and after concentration using the

Kuderna-Danish concentrator in 5 mL of THF to determine the efficiency of the method

for retention of low molecular weight hydrocarbons. The approximate average recovery

of n-C_{10-15} and adamantane was 95%.

Reduction using lithium aluminium hydride was also attempted, using the method of

Seifert *et al.* (1969). However, only the original alcohol was obtained. Obtaining a

product of high purity was difficult due to the consistent presence of butylated

hydroxytoluene (BHT) (Figure 4-22). BHT is often present as an inhibitor or chemical

stabiliser in reagents and solvents. The Super-Hydride® solution was suspected as the

source of BHT, since inhibitor-free diethyl ether and THF solvents were used herein.
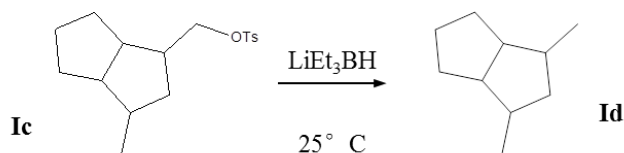
Figure 4-21: Reaction scheme for the Super-Hydride® reduction of **Ic** to **Id**.

The BHT was well separated from the model hydrocarbon product in the GC-MS chromatogram (Figure 4-22). However, it was anticipated that for more complex acid mixtures, the BHT may co-elute or interfere with other analytes of interest. Therefore a clean-up step involving silica chromatography of the product by elution of the hydrocarbons with 100% hexane was introduced following the concentration of the more complex commercial and OSPW reduced acid mixtures (Chapter 2, Section 2.3.4 and Chapter 5, Section 5.2.2).
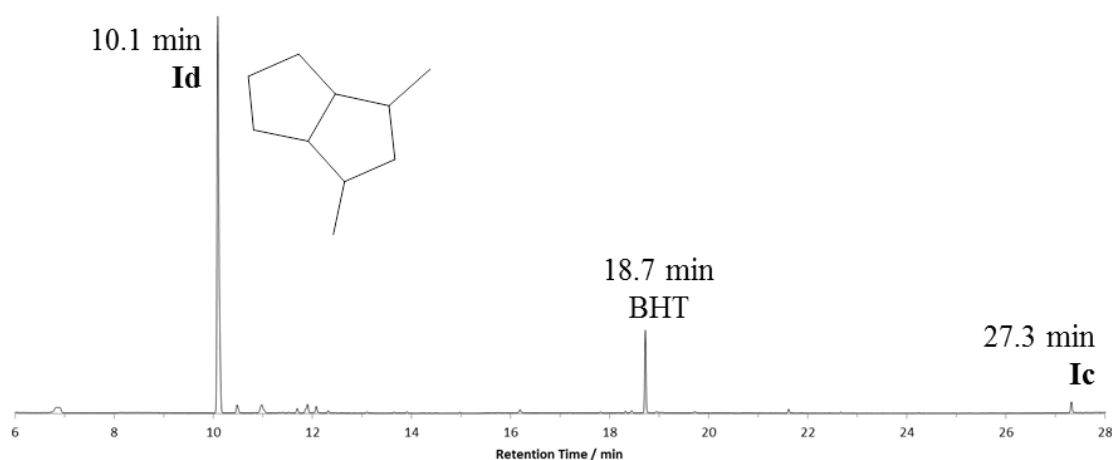
Figure 4-22: Gas chromatogram of 2,4-dimethylbicyclo[3.3.0]octane, **Id.** (Column A, inlet temperature 300 °C).

Confirmation of the final hydrocarbon was achieved by comparing the mass spectrum with that reported previously by Jørgensen *et al.* (1990) and Denisov *et al.* (1977c). The latter authors published data for the exo-exo-, exo-endo/endo-exo and endo-endo-isomers of 2,4-dimethylbicyclo[3.3.0]octane (Figure 4-23). The exo-endo- endo-exo-isomers are enantiomers and would not be separated on achiral GC stationary phases. All three isomers possessed very similar mass spectra, each containing a relatively low intensity molecular ion at *m/z* 138, a base peak ion at *m/z* 96 and an intense ion at *m/z* 67 (Figure 4-23). However, the isomers were distinguishable by comparing the ratios of the *m/z* 96/95 intensities. The hydrocarbon product **Id** was identified as the exo-exo-

isomer based on the relatively intense *m/z* 95 ion (Figure 4-23; A and B). Therefore the intensity of the *m/z* 95 ion appears to be dependent on the stereochemistry of methyl substituents.

The mass spectrum of **Id** (Figure 4-23) had a molecular ion at *m/z* 138, expected for a C_{10} bicyclic hydrocarbon. The base peak ion at *m/z* 96 was attributed to the loss of a neutral propene molecule, C_3H_6 (M-42). The bicyclic nature of the compound means a loss greater than M-15 requires cleavage of two bonds. For example, the M-42 ion can be justified by a cleavage on the dimethyl substituted ring, followed by α-cleavage resulting in the loss a neutral molecule (Figure 4-24).
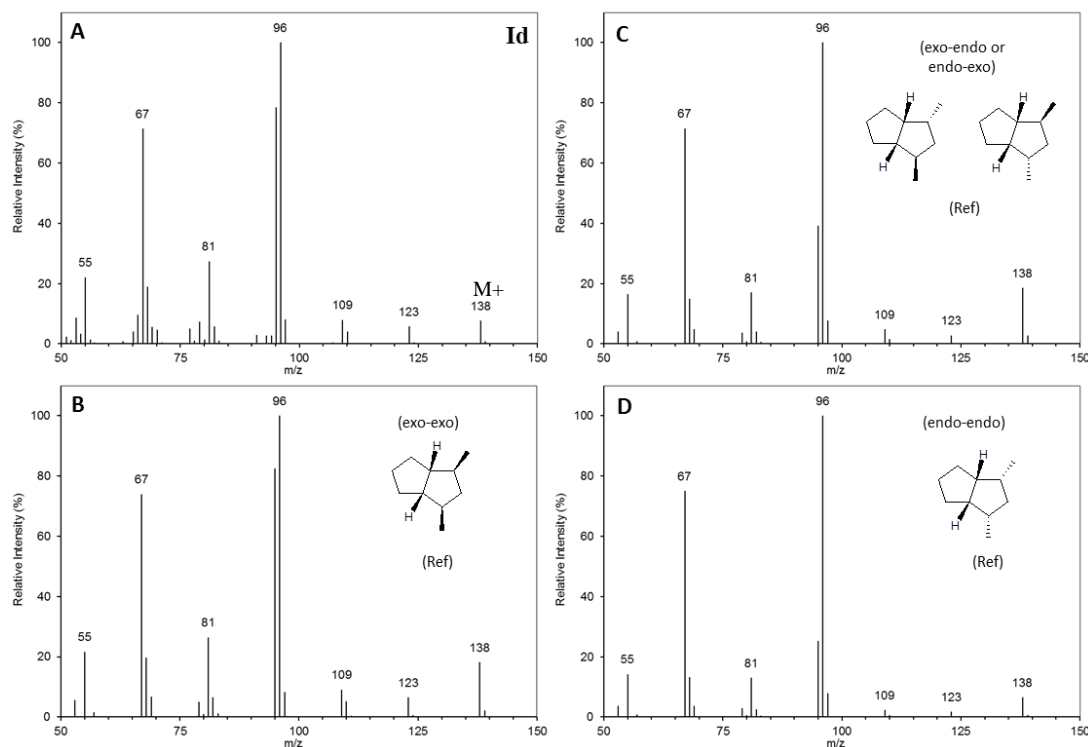
Figure 4-23: (A) Mass spectrum of **Id** identified as exo-exo-2,4-dimethylbicyclo[3.3.0]octane by comparison with (B-D) mass spectra replotted from tabulated data reported by Denisov *et al.* (1977c).
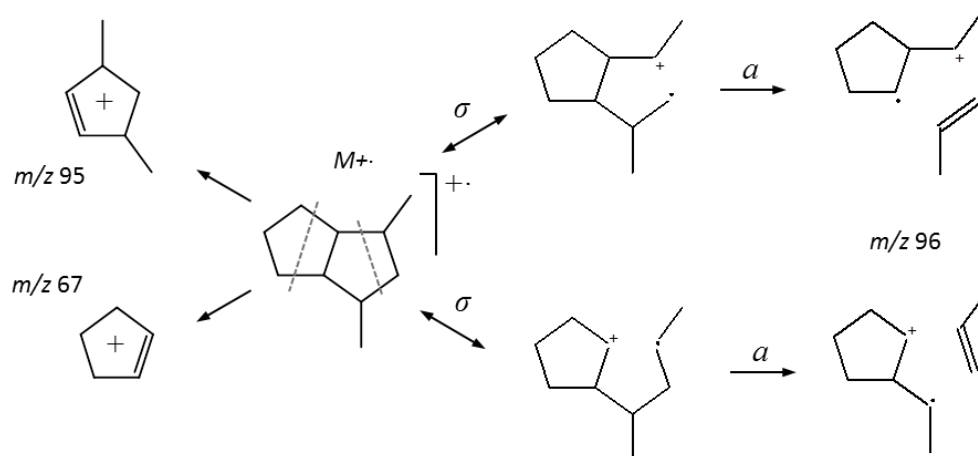
Figure 4-24: Example of mass spectral fragments proposed for the principal ions in the mass spectrum of **Id** from the cleavage of two bonds within the bicyclic compound.

The fragmentation mechanisms proposed above, for 2,4-dimethylbicyclo[3.3.0]octane, were supported by the synthesis, and interpretation of the mass spectrum, of deuterated 2,4-dimethylbicyclo[3.3.0]octane (**Ie**) (Figure 4-25). The use of lithium aluminium deuteride (LAD) in first the step of the conversion instead of LAH, resulted in the addition of two deuterium atoms on the carboxyl carbon atom. The remaining steps of the conversion, including esterification of the deuterated alcohol to the tosyl ester and the reduction of the tosylate, resulted in the synthesis of deuterated 2,4-dimethylbicyclo[3.3.0]octane with two deuterium atoms on the methyl group in the 2-position (i.e. the original carboxyl carbon).

Therefore, fragment ions in the mass spectrum of **Ie** (Figure 4-25; B), involving the methyl group in the 2-position, could be differentiated from those produced by the fragmentation of the other methyl group, or ions originating from fragmentation of the unsubstituted cyclopentyl ring. As the structure of 2,4-dimethylbicyclo[3.3.0]octane is symmetrical, the intensity of the ions produced by the fragmentation of either methyl group, would be expected to be the same, as they would be expected to occur from the same fragmentations and be equally energetically favourable.

The mass spectrum of **Ie** (Figure 4-25) displayed a molecular at *m/z* 140, two Da higher

than **Id**, due to the presence of two deuterium atoms on the 2-methyl substituent. Based

on the appearance of several '+2 ions' in the mass spectrum of **Ie** (e.g. *m/z* 55 and 57,

m/z 96 and 98, *m/z* 123 and 125), it became apparent that the deuterated methyl group

was involved in the fragmentation, or at least partially contributing to the abundance, of

the M-15, M-42, M-57 and M-83 ions (Figure 4-25; B).
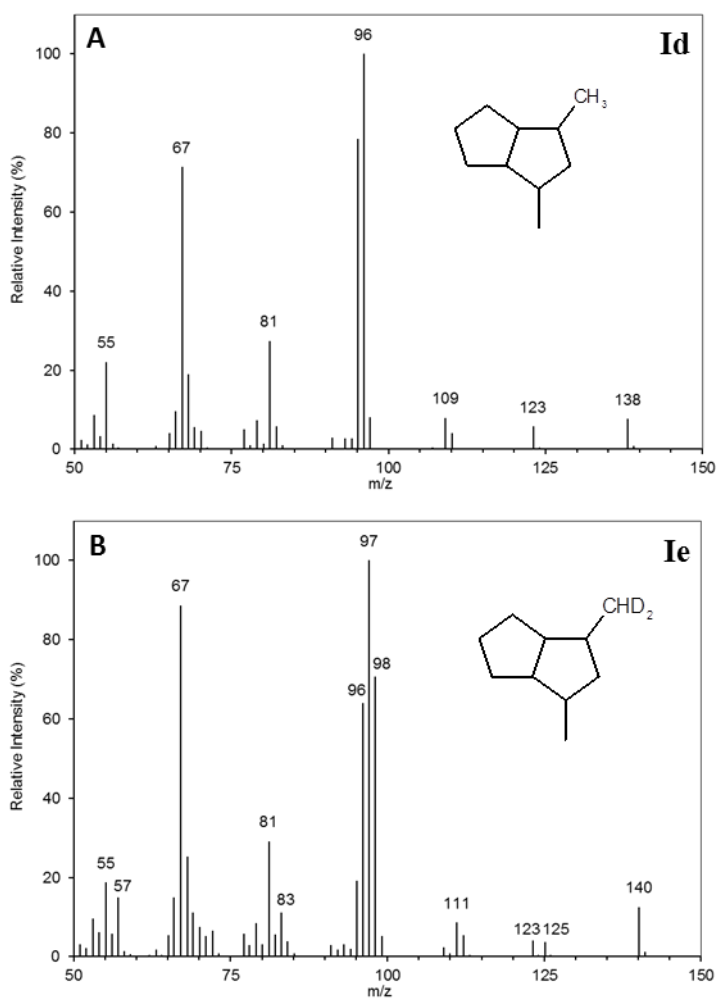
Figure 4-25: Mass spectra of (A) 2,4-dimethylbicyclo[3.3.0]octane, **Id**, synthesised

using LAH and (B) deuterated 2,4-dimethylbicyclo[3.3.0]octane, **Ie**, synthesised using

LAD.

Interestingly, the base peak ion in the mass spectrum of **Ie** increased by only 1 Da (*m/z* 96 in **Id**, to *m/z* 97 in **Ie**) (Figure 4-25). This supports the fragmentation mechanisms proposed for **Id** (Figure 4-24), in which the *m/z* 96 (M-42) ion in the mass spectrum of **Id**, is formed by the fragmentation within the substituted cyclopentyl ring, involving the loss of either methyl group, whereas formation of the *m/z* 95 ion (M-43) was proposed to originate from fragmentation of the non-substituted, cyclopentyl ring.

If the *m/z* 96 ion in the mass spectrum of **Id** (Figure 4-25; A) is formed equally from the fragmentation of both methyl groups, via cleavage at the bridgehead carbons and subsequent α-cleavage resulting in the loss of a neutral propene molecule (Figure 4-24), when one of the methyl groups is deuterated, two ions of similar intensity would be observed at *m/z* 96 (loss of propene including deuterated methyl group; M-45) and *m/z* 98 (loss of propene including non-deuterated methyl group; M-45). This is observed in the mass spectrum of **Ie** (Figure 4-25; B). If the *m/z* 95 ion, in the mass spectrum of **Id** (Figure 4-25; A), is formed from the fragmentation on the non-substituted cyclopentyl ring, the intensity of the M-43 would be unaffected in the mass spectrum of **Ie**. This observation was also made in the mass spectrum of **Ie** (Figure 4-25; B), with *m/z* 97 (M-43) becoming the base peak ion.

4.4.2 Synthesis of 3-methylpinane

4.4.2.1 Preparation and characterisation of 3-pinane-methanol

3-pinane-carboxylic acid (**IIa**) was successfully reduced to 3-pinane-methanol (Figure 4-26; **IIb**) by refluxing with excess LAH under an inert atmosphere with anhydrous diethyl ether as the solvent. Subsequent acid work-up using 10% H_2SO_4 produced an average yield of 95 ± 7% (n = 3) with a purity of >99 % determined by the integration of the areas of the peaks in the gas chromatogram of **IIb**, as the TMS ether (Figure 4-27). As seen with the previous conversion of **Ia** to **Ib**, the retention time of **IIb** (12.0 min) was less than that of the original acid, **IIa** (13.0 min) (Figure 4-27).
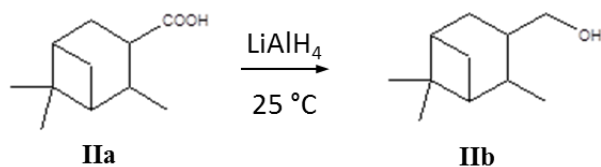
Figure 4-26: Reaction scheme for the reduction of **IIa** to 3-pinane-methanol, **IIb**.
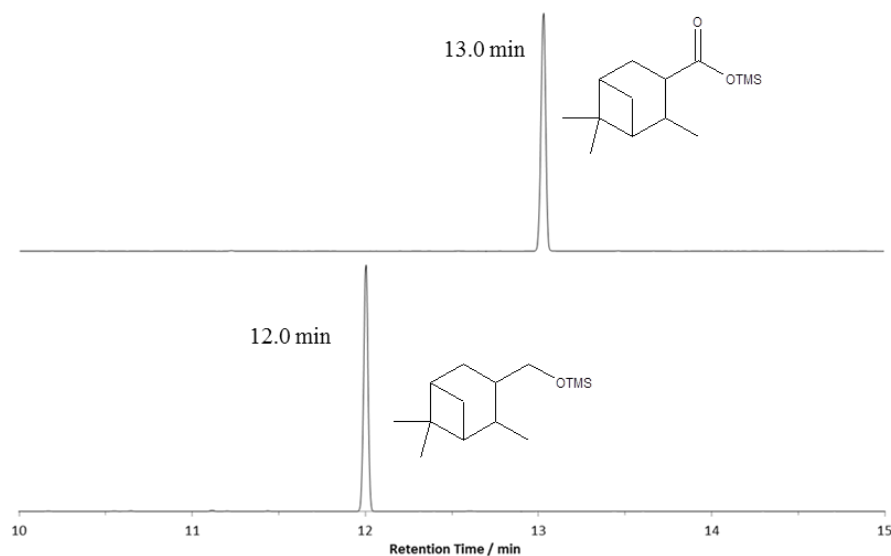
Figure 4-27: Comparison of TICs showing the differences in retention times of precursor acid **IIa** and reduction product **IIb**, as TMS ester and ether derivatives respectively. (Column A, inlet temperature 300 °C).
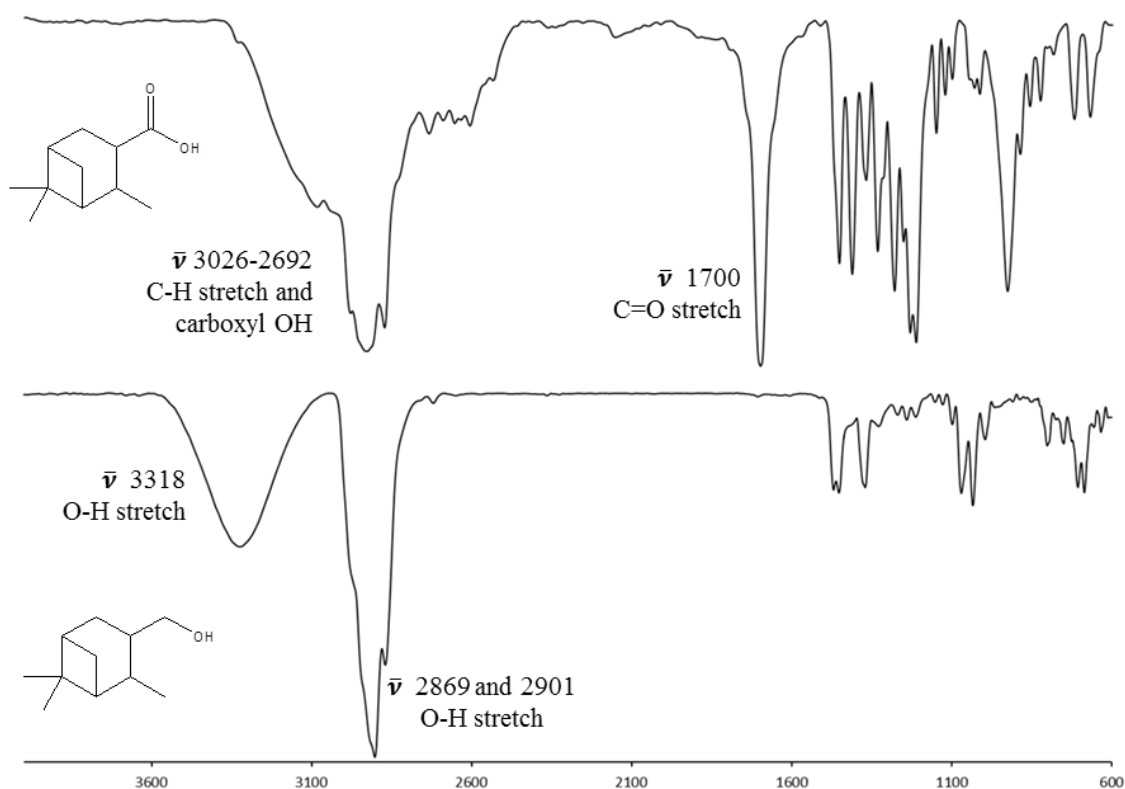
Figure 4-28: Comparison of the IR spectra of the acid, **IIa** (top) and alcohol product **IIb** (bottom).

Table 4-5: Summary of IR spectra of 3-pinane-carboxylic acid, **IIa** and reduction product 3-pinane-methanol, **IIb**.

IIa			IIb		
$\overline{v}$ (cm^{-1})	Assignment	Comment	$\overline{v}$ (cm^{-1})	Assignment	Comment
3026-2692	Carboxyl OH	Broadening of peaks	3318	Alcoholic OH	O-H Stretch, broad
2923,2872 ,	CH$_3$, CH$_2$, CH saturate alkyls	C-H stretch, med. > 3000	2901	CH$_3$, CH$_2$, CH saturate alkyls	C-H stretch, med-str. >3000
			2869		
1454		C-H def.	1452		C-H def., weak
1700	Carboxyl C=O	C=O stretch, str.	1372		
900-1413	Carboxyl C-OH	Fingerprint	1016	Alcoholic C-OH	C-O stretch, med.

The intense signal at 1700 cm^{-1} in the spectrum of the acid (Figure 4-28; top) was assigned as due to a C=O stretch within a carboxyl group. Broadening was observed in the carboxylic acid spectrum between 2500 – 3300 cm^{-1} incorporating the intense peaks at 2923 and 2872 cm^{-1}, representing C-H stretching in alkyl groups (Table 4-5). The disappearance of these features in the spectrum of the product **IIb** (Figure 4-28; bottom), with intense narrow bands at 2901 and 2869 cm^{-1}, suggested that the reduction had gone to completion. Furthermore, the appearance of a broad, medium intensity band observed at 3318 cm^{-1} was consistent with the formation of an alcohol and attributed to an alcohol O-H stretch (Table 4-5).

The mass spectra of **IIa** (Figure 4-29) and **IIb** (Figure 4-30) as their TMS derivatives were very different from each other. The spectra of both the acid and alcohol had very low intensity molecular ions at *m/z* 254 and 240, respectively. The molecular ion of the alcohol was fourteen Da less than that of the acid, which was strong additional evidence that the reduction had been successful. The presence of *m/z* 75 and 73 ions was typical of the spectra of some TMS derivatives, as was the loss of a methyl group to produce an ion at *m/z* 239 in the spectrum of the acid TMS ester (Figure 4-29). The mass spectra of both compounds (**IIa** and **b**) had M-90 ions attributed to the loss of $Si(CH_3)_3OH$.

The mass spectrum of the alcohol TMS ether had a low intensity M-15 ion and a base peak ion at *m/z* 95 (Figure 4-30). This suggests that in the case of the alcohol, fragmentation results in the charge being retained on the alicyclic hydrocarbon part of the molecule, in contrast to the spectrum of the acid (TMS ester), which showed more abundant ions where the charge was retained on the functionalised part of the molecule with loss of alkyl fragments (e.g. *m/z* 239 (M-15), *m/z* 199 (M-55), *m/z* 183 (M-71)).

Bicyclo[3.1.1]heptanes are inherently strained due to the cyclobutane ring; this may account for rearrangements during electron impact ionisation. Assignment of fragment ions is therefore speculative. Mass spectral studies of the parent pinane and α- and β-pinene structures also reported uncertainties in the origin of the ions observed, suggesting some ions may originate from a cleavage of a bond around the bridgehead carbons producing a monocyclic cation (McLafferty, 1963).
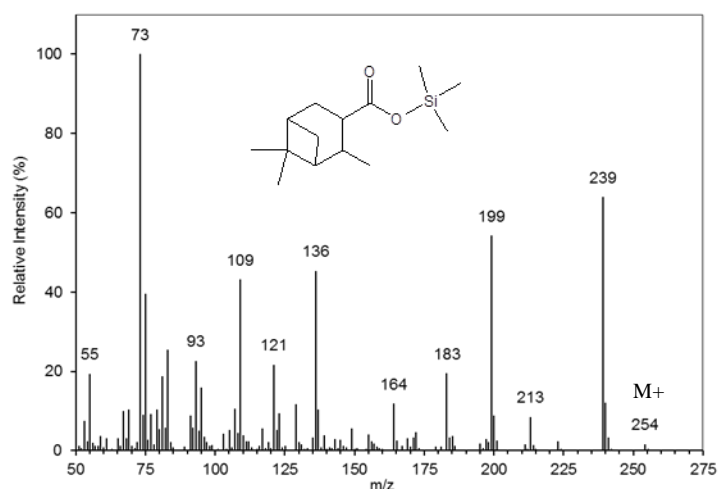
Figure 4-29: Mass spectrum of **IIa** TMS ester.
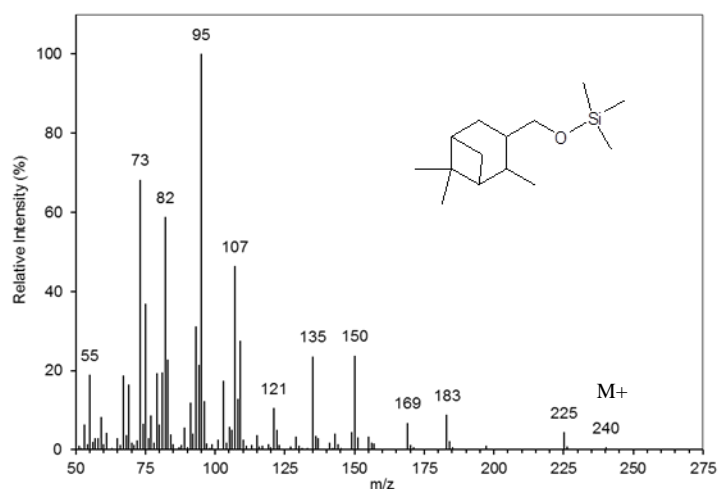
Figure 4-30: Mass spectrum of **IIb** TMS ether.

The ^{1}H-NMR spectrum of **IIb** showed two intense singlets each integrating to 3.0 at 0.99 ppm and 1.18 ppm, assigned to the gem-dimethyl substituents; positions 1 and 2 (labels are interchangeable; Figure 4-31). The methyl substituent at position 3 was attributed to producing the intense doublet at 1.05 ppm, split by the single proton in position 9. The doublet had a coupling constant of 7 Hz distinguishing it from the signal at 0.72 ppm, which also appeared as a doublet but had a higher coupling constant of 9 Hz and integral of 1.0 (Figure 4-31; B). The two doublet of doublets at 3.58 and 3.45 ppm corresponded with the diastereotopic protons at position 11, since they are adjacent to the proton on the chiral carbon at position 10 (Figure 4-31; C). The pair of doublet of doublets around 3.5 ppm appeared to be a feature of all of the primary alcohols studied herein formed from bicyclic acids in which the carboxyl group is substituted directly to the ring at a 3° carbon.
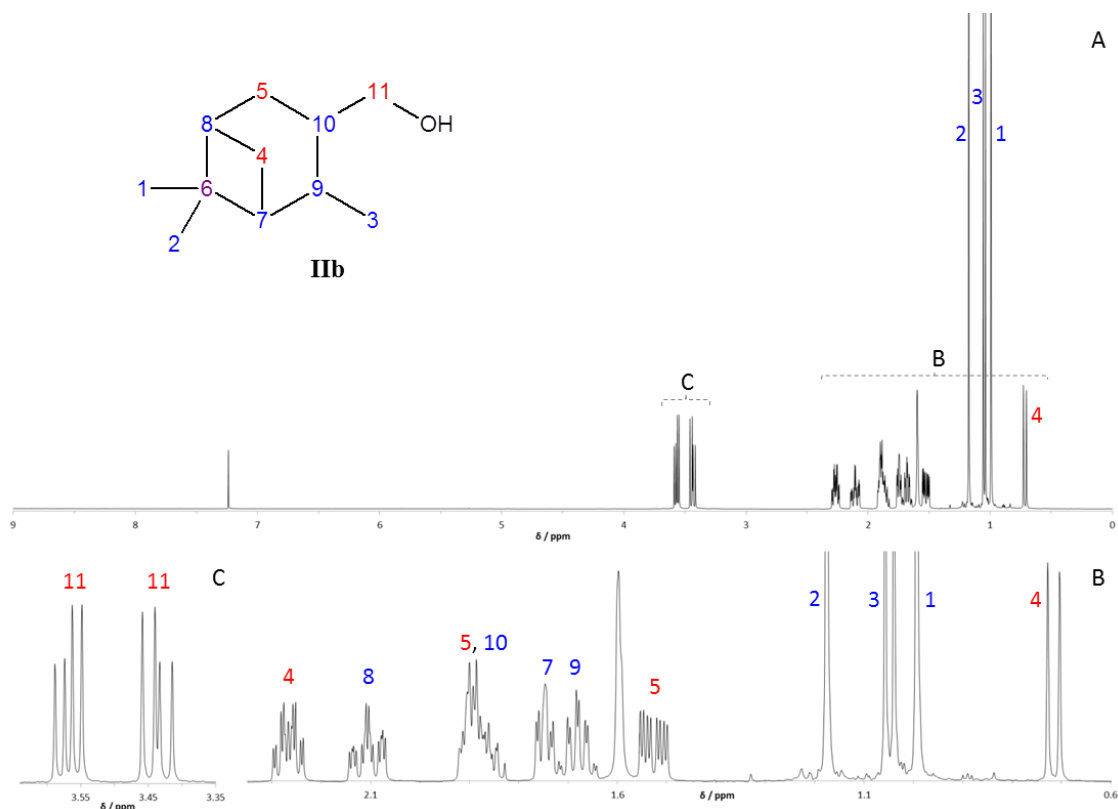
Figure 4-31: (A) ^{1}H-NMR spectrum of **IIb.** (B and C) Focused spectra showing detail between chemical shift ranges 0.60 – 2.35 and 3.35 – 3.64 ppm.

The ^{1}H-NMR spectrum of **IIb** contained a series of complex multiplets, which were well resolved compared to those seen in the ^{1}H-NMR spectrum of **Ib** (Figure 4-31). Therefore a series of homonuclear decoupling experiments was performed on **IIb** in an attempt to identify as many proton environments as possible. For example, decoupling of the doublet of doublets (*dd*) corresponding to the diastereotopic protons at position 11, resulted in a change in the multiplet at 1.88 ppm with an integral of 2.0, identifying one of the two protons as due to the proton at position 10.

Decoupling the doublet (*d*) at 1.05 ppm, (i.e. the methyl substituent at position 3), resulted in the assignment of the proton at position 9 as producing the quintet of doublets (*quint d*) at 1.68 ppm (Figure 4-32; B). The splitting pattern could be explained by the three methyl protons and one of the protons in either position 7 or 10 having the same coupling constant of 7.0 Hz, creating a quintet which is split further by the remaining proton (2.0 Hz).
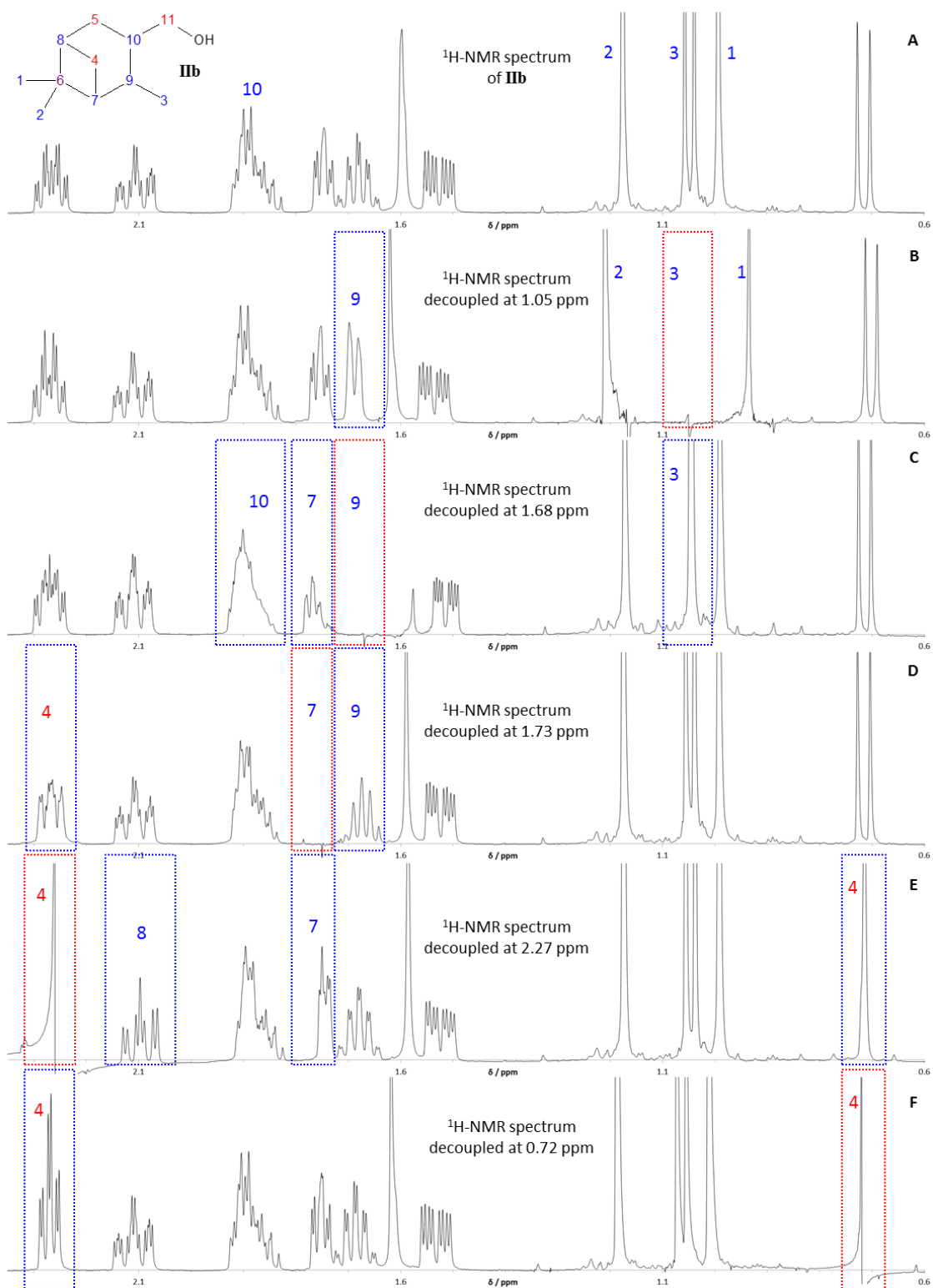
Figure 4-32: Comparison of (A) the ^{1}H-NMR spectrum of **IIb** with the ^{1}H-NMR spectra decoupled at (B) 1.05 ppm identifying position 9, (C) 1.68ppm identifying position 7, (D) 1.73 ppm identifying a proton on position 4, (E) 2.27 ppm identifying position 8 and the other proton on position 4 and (F) 0.72 ppm, confirming the assignment of the two protons on position 4 (red area; irradiated, blue area; affected).

After assigning the two chiral protons at positions 9 and 10, the remaining protons within the bicyclic structure could be assigned by decoupling the remaining resonances. For example, irradiating the quintet of doublets (*quint d*) with a low irradiation strength resulted in a change in the splitting patterns of the signals corresponding to the protons in positions 3 and 10, as expected and the multiplet at 1.73 ppm (Figure 4-32; C). Therefore by deduction, the multiplet at 1.73 ppm was assigned as the proton at position 7.

Decoupling the multiplet at 1.73 ppm (*m*) affected the quintet of doublets at 1.68 ppm and one other signal at 2.27 ppm (*m*) with an integral of 1.0 (Figure 4-32; D). This indicated the proton in position 7 only coupled with one of the protons of the methylene group in position 4. Irradiating the multiplet at 2.27 ppm affected the multiplet at 1.73 (*m*), doublet at 0.72 (*d*) and the triplet of doublets of doublets (*tdd*) at 2.13 ppm (Figure 4-32; E). Subsequent decoupling of the doublet at 0.72 ppm (J = 9.6 Hz) resulted in one change to the multiplet at 1.73 ppm (Figure 4-32; F). Therefore logical deduction meant the doublet and multiplet at 0.72 and 2.27 ppm could be assigned as due to the two inequivalent protons at position 4 and the triplet of doublets of doublets (*tdd*) at 2.13 ppm was assigned as due to the proton at position 8 (Table 4-7).

The remaining two protons were on the methylene group in position 5. Decoupling of the proton at position 8 affected one of the protons at position 4 and 10 (2.27 ppm and 1.88 ppm) as expected, as well as the doublet of doublets of doublets (*ddd*) at 1.52 ppm, thus identifying one proton in position 5 (Figure 4-33; B). Therefore, the remaining proton on position 5 could be assigned as the other proton within the complex multiplet at 1.88 ppm with an integral of 2.0, confirmed by decoupling the doublet of doublets of doublets at 1.52 ppm (Figure 4-33; C).

The series of homonuclear decoupling experiments proved particularly useful in the structural elucidation of **IIb**, importantly, clearly demonstrating that the compound had retained the bicyclo[3.1.1]heptane core. This was further supported by interpretation of the ^{13}C-NMR spectra.
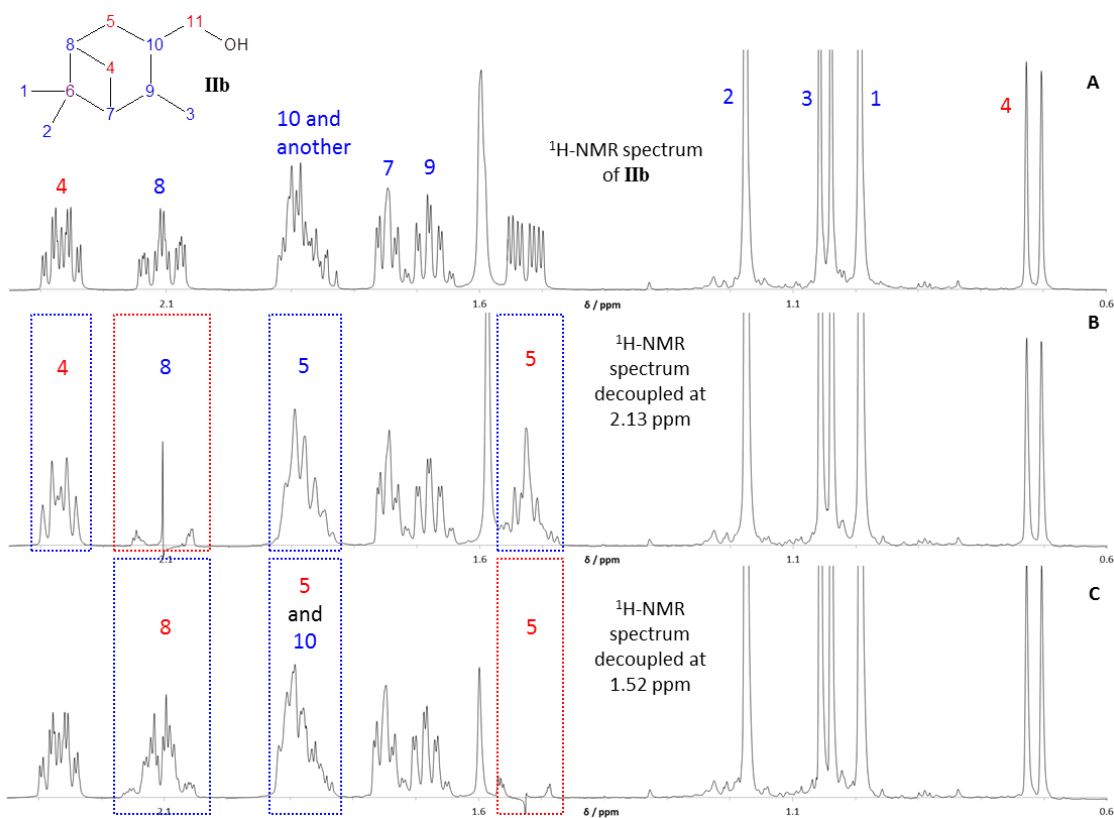
Figure 4-33: Comparison of (A) the ^{1}H-NMR spectrum of **IIb** with the ^{1}H-NMR spectra decoupled at (B) 2.13 ppm identifying the protons at position 5 and (C) 1.52ppm confirming the assignment of the protons at position 5 (red area; irradiated, blue area; affected).

The ^{13}C-NMR spectrum of **IIb** showed eleven signals matching the expected structure of **IIb**, which possesses no symmetry (Figure 4-34). The quaternary carbon at position 6 had a chemical shift of 38.99 ppm, seen as a low intensity shoulder of the peak at 39.02 ppm (Figure 4-34 insert). The half peak height and disappearance in the DEPT ^{13}C-NMR confirmed the assignment to the quaternary carbon in position 6 (Figure 4-35 insert).

The three methyl substituents, positions 1, 2 and 3, were assigned as the three signals in the typical range for methyl groups, with chemical shifts of 22.15, 22.94 and 28.03 ppm. Based on the similarity that was observed between the ^{13}C-NMR spectra of the alcohol and tosyl ester products of **Ib** and **Ic** (Figures 4-13 and 4-19), positions 1 and 2 in the alcohol were assigned as producing the peaks at 22.94 and 28.03 ppm, after their assignment in CHSHF spectrum later obtained for the tosyl ester product (**IIc**; Appendix Figure 20). The carbon signal at 22.15 ppm was assigned as due to the methyl group at position 3. The methylene group adjacent to the hydroxyl moiety, position 11, was identified at 70.10 ppm, at a lower field relative to the other alkyl environments.

The remaining two methylene groups within the structure, positions 4 and 5 at 31.24 and 33.49 ppm, were assigned based on their opposite phasing in DEPT spectrum (Figure 4-35 and Table 4-6) with their exact assignment based on those observed in the CHSHF spectrum of **IIc** (Appendix Figure 20). The remaining CH groups, at positions 7, 8, 9 and 10, confirmed by the upwards phasing in the DEPT ^{13}C-NMR spectrum (Figure 4-35), could not be differentiated based on the ^{1}H-NMR and ^{13}C-NMR spectra for **IIb**. However the signals were later assigned within the structure of **IIc**.
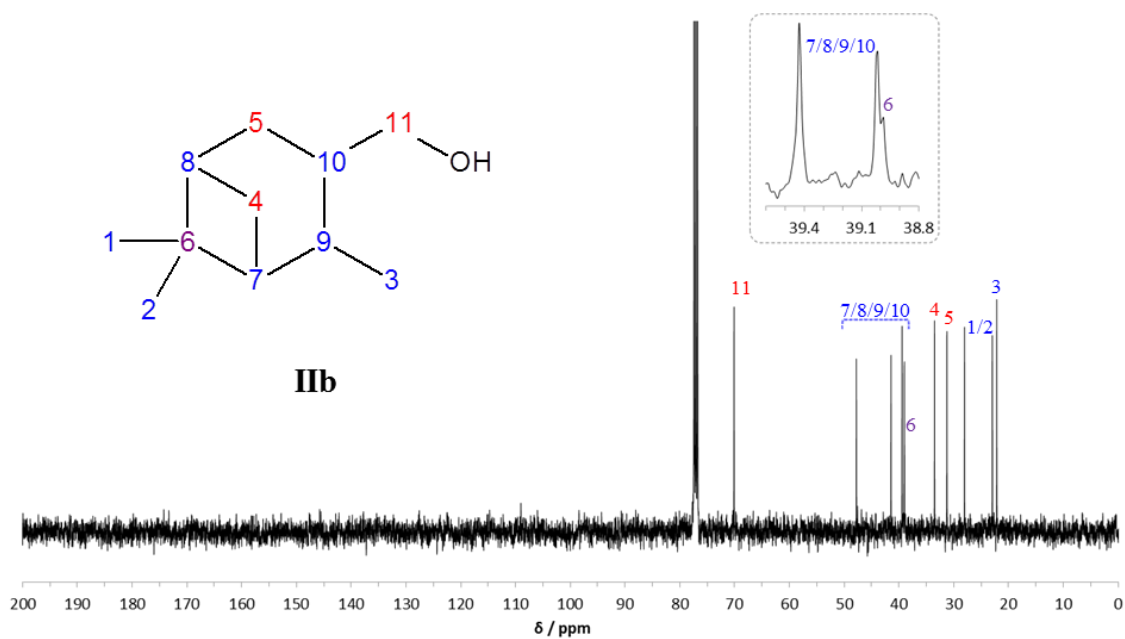
Figure 4-34: ^{13}C-NMR spectrum of alcohol product **IIb**.
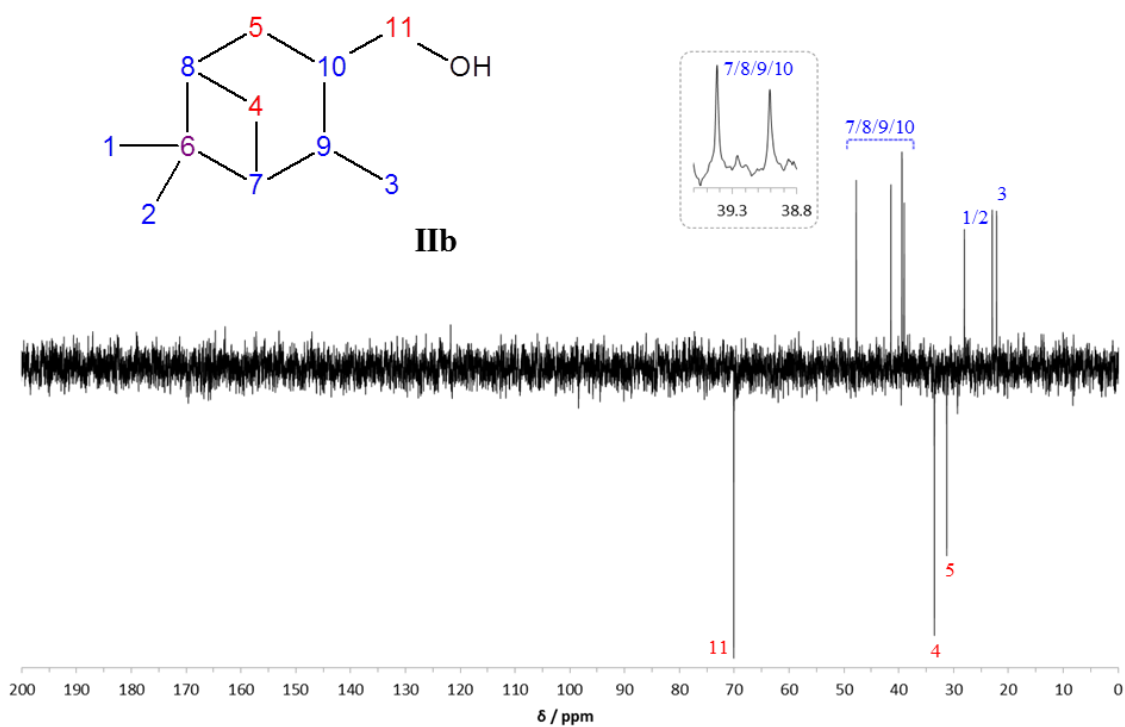
Figure 4-35: DEPT ^{13}C-NMR spectrum of alcohol product **IIb**.

Table 4-6: Summary of ^{1}H and ^{13}C-NMR spectra of **IIb**.
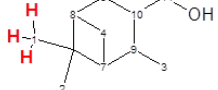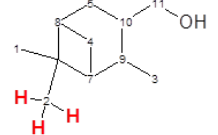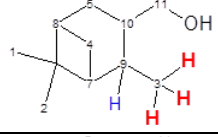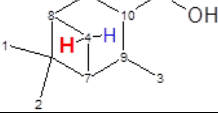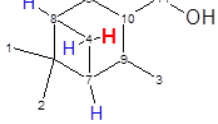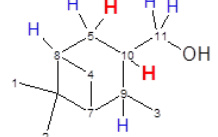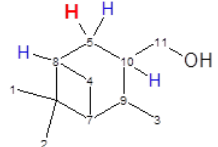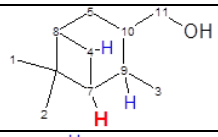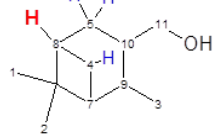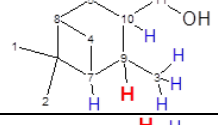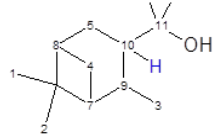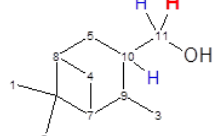
Position	^{1}H chemical shifts / ppm	^{1}H integral	J value / Hz	^{13}C chemical shifts / ppm			
				Primary (CH)	Secondary (CH$_2$)	Tertiary (CH$_3$)	Quaternary (C)
1	0.99 (*s*)	3.0	-			22.94[a]	
2	1.18 (*s*)	3.0	-			28.03[a]	
3	1.05 (*d*)	3.0	7			22.15	
4					33.49		
5					31.24		
6	Determined by homonuclear decoupling experiments in Table 4-7						38.99
7				39.02[b]			
8				39.43[b]			
9				41.45[b]			
10				47.78[b]			
11	3.45 (*dd*)	1.0	7.4, 10.3		70.10		
	3.58 (*dd*)	1.0	5.7, 10.3				

[a] peaks assigned positions 1 and 2 are interchangeable
[b] peaks assigned positions 7, 8, 9 and 10 were based on the assignments determined for **IIc**.

Table 4-7: Summary of the ^{1}H-NMR homonuclear decoupling experiments of **IIb**.

Position	^{1}H chemical shifts / ppm	Multiplicity	^{1}H integral	J values / Hz	Homonuclear Decoupling Experiments		
					Irradiated / ppm	Affected / ppm	^{1}H within Structure (red – ^{1}H irradiated, blue – ^{1}H affected)
1	0.99	s	3.0	-	0.99	-	
2	1.18	s	3.0	-	1.18	-	
3	1.05	d	3.0	7	1.05	1.68	
4	0.72	d	1.0	9.6	0.72	2.27	
4	2.27	multiplet	1.0	-	2.27	0.72, 1.73, 2.13	
10	1.88	multiplet	2.0	-	1.88	2.13, 3.445, 3.575, 1.68	
5				-			
5	1.52	ddd	1.0	2.7, 5.8, 13.4	1.52	2.13, 1.88	
6	Quaternary carbon does not appear in ^{1}H-NMR spectrum						
7	1.73	multiplet	1.0	-	1.73	1.68, 2.27	
8	2.13	multiplet (tdd)	1.0	-	2.13	1.52, 1.88, 2.27	
9	1.68	quint d	1.0	2.0, 7.0	1.68	1.05, 1.73, 1.88	
11	3.45	dd	1.0	7.6, 10.2	3.445	1.88	
11	3.58	dd	1.0	5.7, 10.2	3.575	1.88	

4.4.2.2   Preparation and characterisation of 3-pinane-methanol tosyl derivative

3-pinane-methanol (**IIb**) was successfully converted to the tosyl ester (**IIc**; Figure 4-36) using tosyl chloride (TsCl) in the presence of triethylamine (TEA) as the base and a catalytic amount of 4-(dimethylamino)pyridine (DMAP). The tosylation method had proved successful for **Ib** and as **IIb** was a bicyclic primary alcohol, the conditions optimised for **Ib** were considered suitable for the tosylation of **IIb**. The reaction yield of **IIb** was 80 ± 4% (n = 3) but again determination of the purity from the gas chromatogram was difficult as the tosylate underwent decomposition and elimination of p-toluene sulfonic acid in the hot GC inlet (Figure 4-37 and Appendix Figures 15 and 23). Figure 4-37 showed a late eluting peak at 22.7 min identified as the tosylate and a mixture of peaks between 6.1 – 9.0 min with molecular ions of m/z 150, consistent with alkenes produced upon elimination. The tosylate product was purified by silica chromatography to remove the tosyl by-product prior to NMR analysis (Chapter 2, Sections 2.3.4 and 2.1.5).
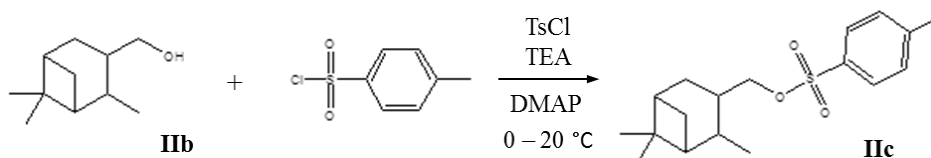
Figure 4-36: Reaction scheme for the tosylation of 3-pinane-methanol, **IIb** to **IIc**.
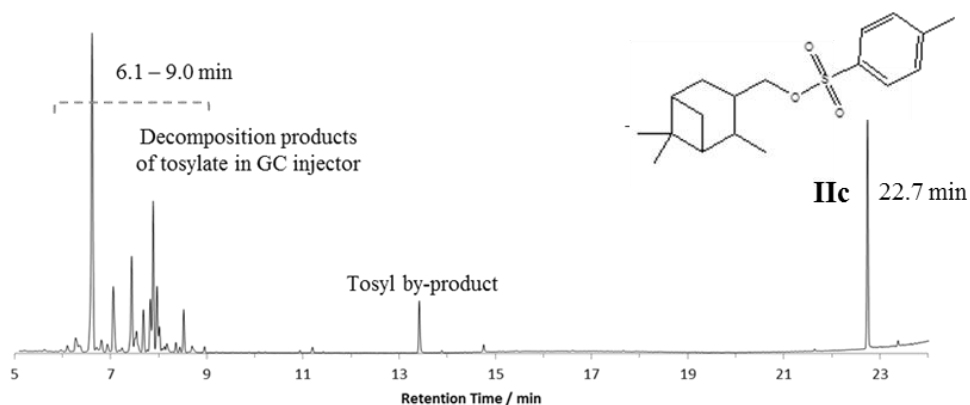
Figure 4-37: Gas chromatogram of tosylation product **IIc**, with partial decomposition in the hot GC inlet. (Column A, inlet temperature 300°C).
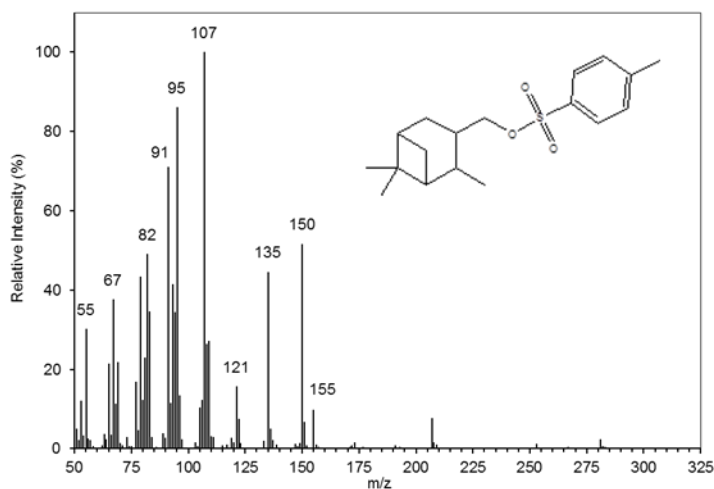
Figure 4-38: Mass spectrum of tosylate product **IIc**.

The mass spectrum of the peak at 22.7 min in the gas chromatogram (Figure 4-38) showed similar fragment ions to those seen in the mass spectrum of the previous tosylate product **Ic** (Figure 4-17). The absence of a molecular ion meant identification of the compound began with the assignment of the ions at m/z 155 and m/z 150. The m/z 155 ion was identified as the fragmentation of $CH_3(C_6H_4)S^+O_2$, as previously seen in the mass spectrum of **Ic** (Figure 4-17). Therefore the ion at m/z 150 corresponded to the loss of $CH_3(C_6H_4)SO_3H$, resulting in an odd-electron radical cation, $[C_{11}H_{18}]^{+\cdot}$ (Figure 4-38). The rest of the ions observed, (e.g. m/z 135, 121, 107 and 95), appeared to originate from secondary fragmentation of the bicyclic ring from the radical cation m/z 150, supported by the presence of the ions in the mass spectrum of the original alcohol **IIb** (Figure 4-30).
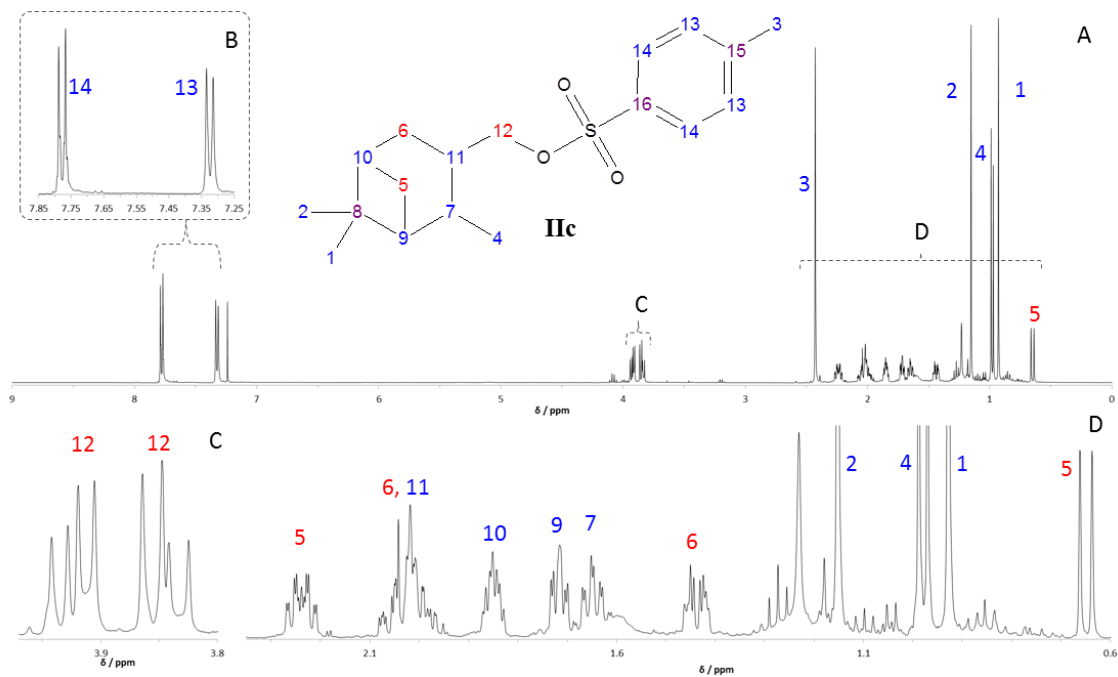
Figure 4-39: ^{1}H-NMR spectrum of the tosylate product **IIc**.
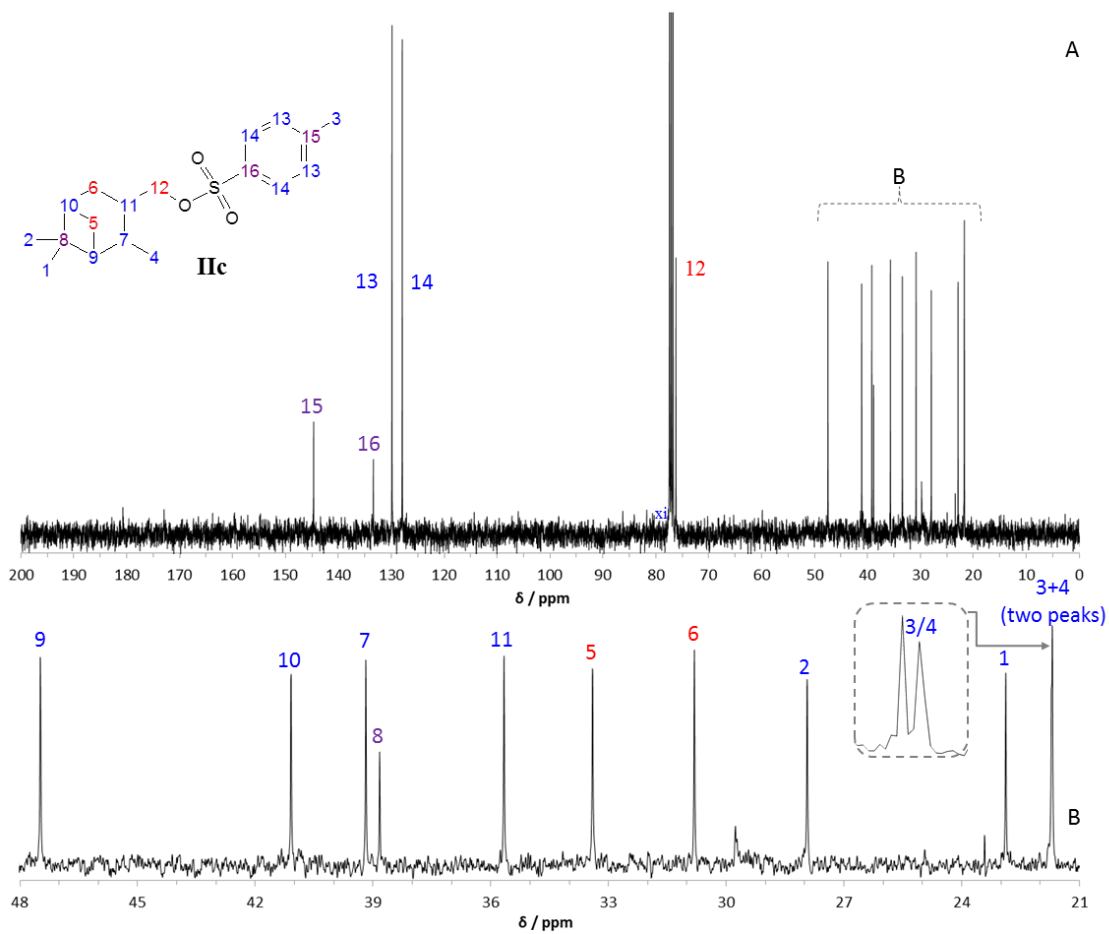
Figure 4-40: ^{13}C-NMR spectrum of tosylate product **IIc**.

The ^{1}H-NMR spectrum of the tosylate product **IIc** (Figure 4-39), displayed two, low field doublets at 7.32 and 7.77 ppm each integrating to 2.0. These doublets were attributed to the aromatic protons on the tosyl group in positions 13 and 14 (Figure 4-39; B). Three singlets, each with an integral of 3.0, were observed; two at 0.93 and 1.15 ppm and one at a higher chemical shift at 2.43 ppm. The higher field singlets were assigned as due to the protons of the two methyl groups at positions 1 and 2 and the lower field singlet was assigned as the protons on the methyl group within the tosyl group. The higher chemical shift of the methyl group within the tosyl moiety is typical for a methyl group substituted on an aromatic ring, as seen in the ^{1}H-NMR spectrum of tosyl chloride (Appendix Figure 16). The higher chemical shift can be explained by the external magnetic field inducing a local ring current involving the delocalised π-electrons in the aromatic ring. This localised ring current, results in the methyl group becoming 'deshielded' (i.e. the protons experience a larger magnetic field and thus appear at a higher chemical shift).

Many of the signals attributed to protons on the bicyclic structure previously identified in the ^{1}H-NMR and homonuclear experiments of **IIb**, were present at slightly different chemical shifts in the ^{1}H-NMR spectrum of **IIc**. For example, the ^{1}H-NMR spectrum of **IIc** (Figure 4-39; C) showed two doublet of doublets at 3.85 and 3.93 ppm, which were attributed to the diastereotopic protons at position 12. These similarities were strong evidence that **IIc** had retained the bicyclo[3.1.1]heptane core during the reaction. Repeat homonuclear decoupling experiments were performed and a COSY spectrum of **IIc** was obtained (Appendix Figure 17), which confirmed the assignment of the signals detailed in Table 4-8 (page 175).

The only signals that were different to those observed in the ^{1}H-NMR spectrum of the alcohol were the multiplet at 2.02 ppm with an integral of 2.0 and the multiplet at 1.85

ppm with an integral of 1.0 (Figure 4-39). Deductions based on the repeated homonuclear decoupling experiments and COSY spectrum, limited the three protons to one of the protons on position 6 and the protons at positions 10 and 11. Decoupling of the diastereotopic protons at 3.85 and 3.93 ppm allowed the proton at position 11 to be identified as one of the two protons in the multiplet at 2.02 ppm. The proton at position 10 was assigned as the multiplet at 1.85 ppm, correlating very faintly with one of the protons at position 5 in the COSY spectrum (Appendix Figure 18). The remaining proton in position 6 was assigned as the other proton at 2.02 ppm, correlating with the other proton assigned at a position 6 in the COSY spectrum (Appendix Figure 18).
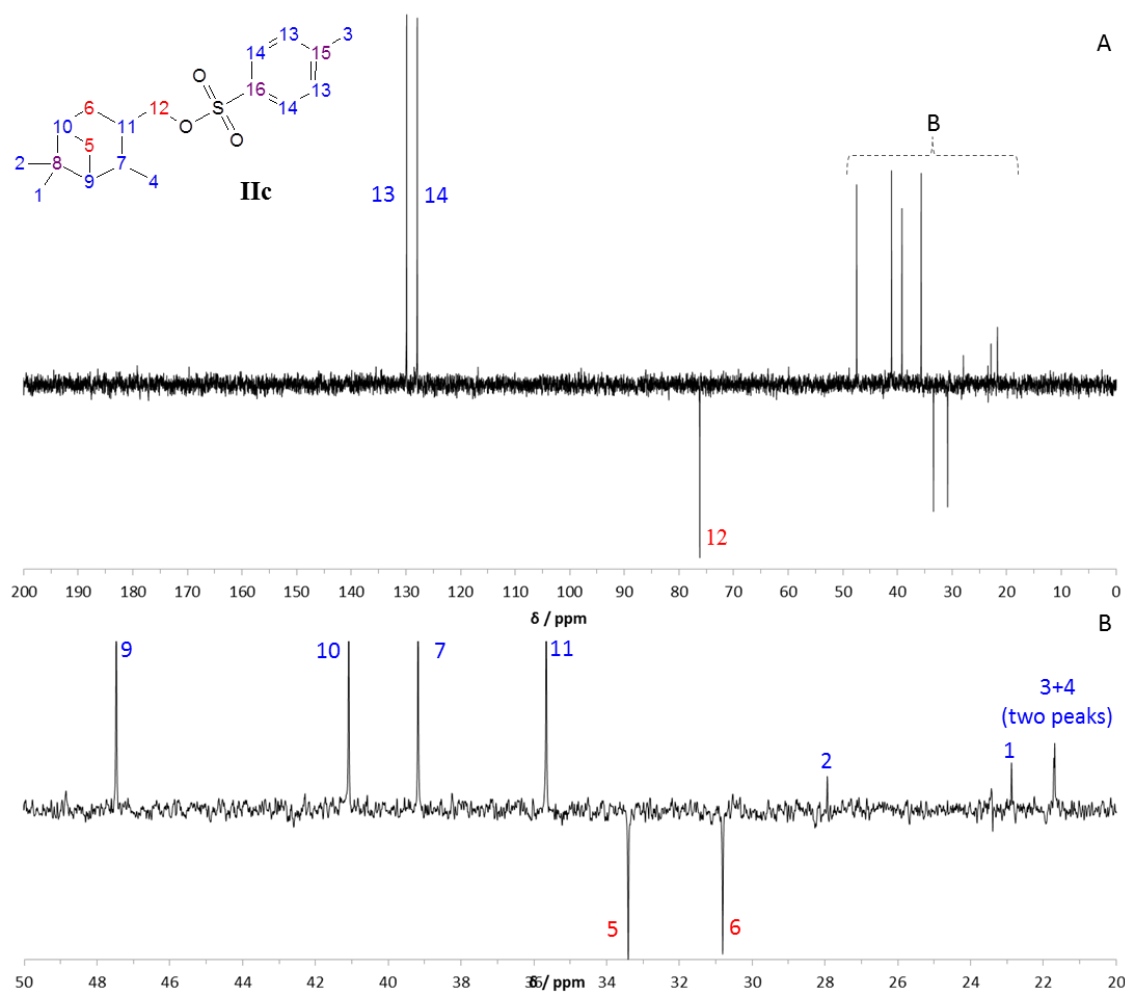
Figure 4-41: DEPT ^{13}C-NMR spectrum of tosylate product **IIc**.

The ^{13}C-NMR and DEPT ^{13}C-NMR spectra provided complementary evidence for the successful tosylation of **IIb** to **IIc**. The quaternary aromatic carbons in the tosyl group, at positions 15 and 16, were identified at 133.5 and 144.6 ppm by their low field chemical shift, half peak height and disappearance in the DEPT spectrum (Figures 4-40 and 4-41). The aromatic CH groups within the tosyl group (positions 13 and 14) were identified by their low field chemical shifts at 127.9 ppm and 129.8 ppm and twice peak heights. The assignment of positions 13 and 14 was also confirmed by correlations with the two low field doublets in the ^{1}H spectrum, observed in the CHSHF spectrum of **IIc** (Appendix Figures 19 and 20; A). The exact labelling of the signals attributed to the aromatic carbons, was based on the correlations observed in the COLOC spectrum of **IIc** (Appendix Figure 21); the signals at 129.8 and 144.6 ppm correlated with the protons at position 3 (Appendix Figure 22).

The 'peak' at 21.6 ppm, upon closer inspection, was found to be two peaks, with very similar chemical shifts (Figure 4-40; B insert). These two peaks were assigned as due to the 2-methyl substituent in the bicyclic part of the molecule (position 4) and the methyl group on the aromatic ring (position 3), based on the correlations observed in the CHSHF spectrum of **IIc** (Appendix Figure 20). The peaks at 21.6 ppm correlated with the high field doublet at 0.98 ppm and the lower field singlet at 2.43 ppm, previously assigned above in the ^{1}H-NMR spectrum as the protons at positions 4 and 3, respectively.

The methylene group in position 12 was assigned as producing the peak at 76.17 ppm based on its high chemical shift, and adjacency to the electron-withdrawing tosylate group and opposite phasing in the DEPT spectrum (Figure 4-41). This assignment was confirmed by the peak correlating with the two doublet of doublets at about 3.9 ppm in the CHSHF spectrum of **IIc** (Appendix Figure 19).

The DEPT ^{13}C-NMR spectrum confirmed the assignment of the peaks at 30.81 and 33.41 ppm as due to the methylene groups at positions 6 and 5, respectively (Figure 4-41). These were differentiated in the CHSHF spectrum, with the peak at 33.41 ppm correlating with the two separate proton resonances at 0.65 and 2.24 ppm assigned as the protons at position 5. The quaternary carbon (position 8) was assigned as the peak at 38.8 ppm, confirmed by its non-appearance in the DEPT spectrum (Figures 4-40 and 4-41). The remaining CH groups at positions 7, 9, 10 and 11, could be assigned as the peaks at 39.2, 47.5, 41.1 and 35.7 ppm based on the correlations observed in the CHSHF spectrum (Appendix Figure 20; B). All the assignments based on the NMR data are summarised in Table 4-8.

Table 4-8: Summary of ^{1}H and ^{13}C-NMR spectra of the tosylate product **IIc**.

Position	^{1}H chemical shifts / ppm	^{1}H integral	J value / Hz	^{13}C chemical shifts / ppm			
				Primary (CH)	Secondary (CH$_2$)	Tertiary (CH$_3$)	Quaternary (C)
1	0.93 (*s*)	3.0	-			22.85	
2	1.15 (*s*)	3.0	-			27.94	
3	2.43 (*s*)	3.0	-			21.67	
4	0.98 (*d*)	3.0	7.2			21.67	
5	0.65 (*d*)	1.0	9.8		33.41		
	2.24 (*m*)	1.0	1.8, 2.4, 6.3, 9.8				
6	1.43 (*m*)	1.0	-		30.81		
	2.02 (*m*)	1 of 2.0	-				
7	1.65 (*quint d*)	1.0	2.0, 7.1	39.21			
8	Quaternary carbon						38.8
9	1.72 (*m*)	1.0	-	47.54			
10	1.85 (*m*)	1.0	-	41.13			
11	2.02 (*m*)	1 of 2.0	-	35.71			
12	3.85 (*dd*)	1.0	6.8, 9.1		76.17		
	3.93 (*dd*)	1.0	5.6, 9.1				
13	7.32 (*d*)	2.0	8.3	129.84			
14	7.77 (*d*)	2.0	8.0	127.91			
15	Quaternary carbon						144.63
16	Quaternary carbon						133.51

4.4.2.3 Preparation and characterisation of 3-methylpinane

3-methylpinane (**IId**) was successfully synthesised by the reduction of **IIc** (Figure 4-42) using lithium triethylborohydride (Super-Hydride®), under an inert atmosphere with THF and diethyl ether as the solvent. The reaction was performed at room temperature, followed by a basic work-up using 20% w/v NaOH. Concentration of the product under N_2, even at room temperature, resulted in considerable losses (~40% yield). To reduce evaporative losses of the volatile C_{11} hydrocarbon, a Kuderna-Danish apparatus was employed (Chapter 2, Section 2.3.4).

The gas chromatogram showed the product was relatively pure; integration of the peak area at 11.42 min (Figure 4-43) gave a purity of 82%. Small peaks between 10-13 min with molecular ions of *m/z* 150 suggested there was a small quantity of unreacted tosylate present and BHT was observed, as with the previous use of 'Super-Hydride®' (Figure 4-22, page 151). This emphasised the need for a clean-up step with silica chromatography, during the conversion of the complex NA mixtures.
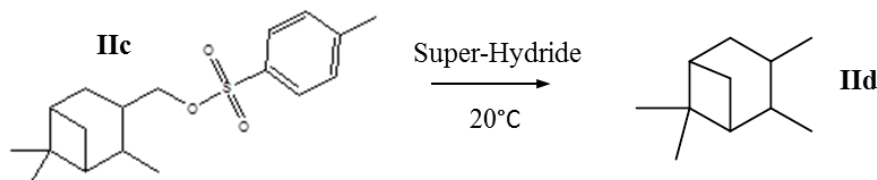
Figure 4-42: Reaction scheme for the Super-Hydride® reduction of **IIc** to **IId**.
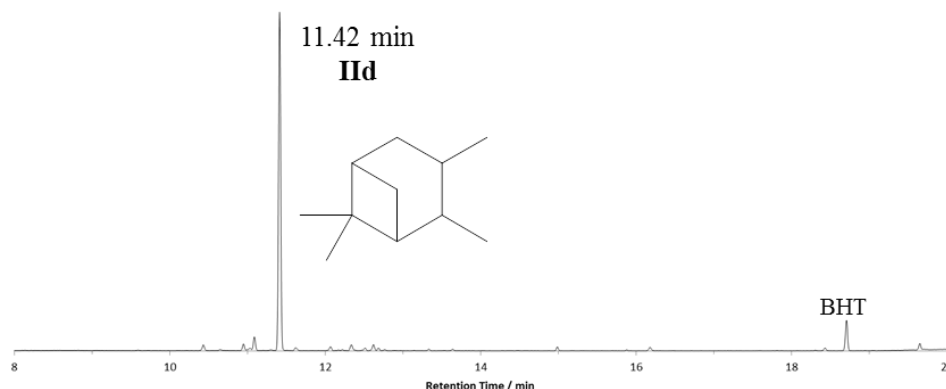
Figure 4-43: Gas chromatogram of 3-methylpinane, **IId**. (Column A, inlet temperature 300 °C).
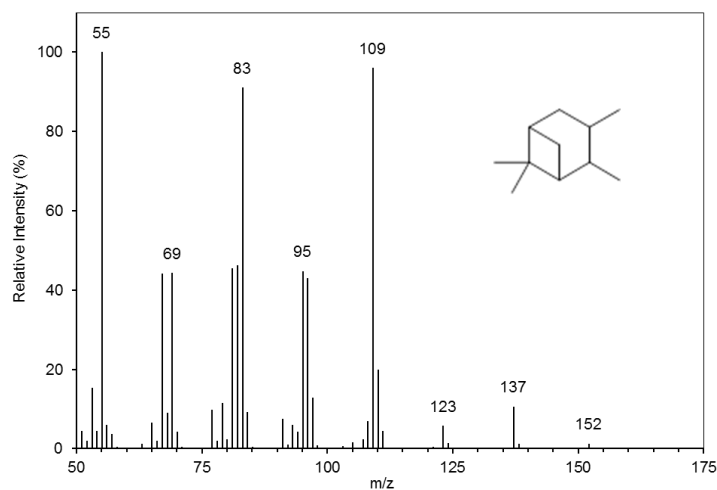
Figure 4-44: Mass spectrum of 3-methylpinane, **IId**.
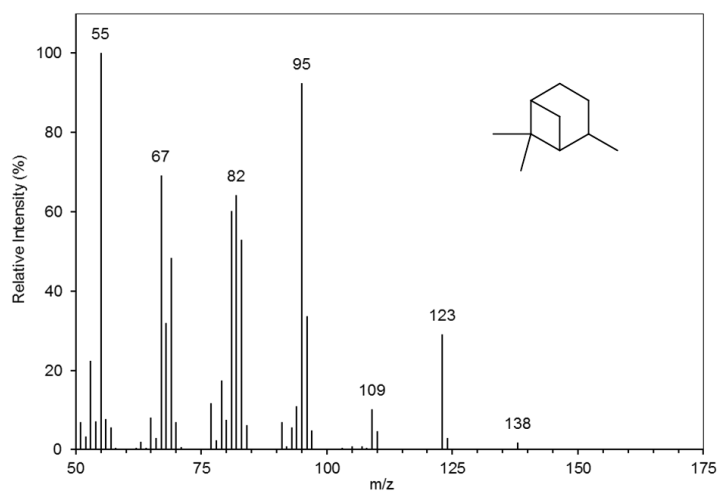
Figure 4-45: NIST mass spectrum of pinane.

GC-MS was used to characterise the final hydrocarbon product **IId** based on the mass spectrum (Figure 4-44). The mass spectrum of **IId** was assigned as due to 3-methylpinane. The spectrum displayed a molecular ion at *m/z* 152, consistent with a C_{11} bicyclic hydrocarbon (Figure 4-44). The low intensity of the molecular ion was expected for the structure of **IId**, attributed to the highly strained nature of the compound, which possesses a cyclobutane ring. The mass spectrum of **IId** was similar to that of the reference NIST spectrum of C_{10} pinane, both having a base peak ion at *m/z* 55 corresponding to a $C_4H_7^+$ cation and strong M-43 ions corresponding to the loss of $\cdot C_3H_7$ (Figures 4-44 and 4-45). The mass spectrum of the 3-methylpinane product

and the reference spectrum of pinane, displayed similar clusters of ions (e.g. M-56/57 ions and M-69/70/71 ions), suggesting the compounds undergo multiple fragmentations upon ionisation, involving hydrogen rearrangement.

Little appears to be known about the exact mass spectral fragmentation mechanisms that occur during the electron impact ionisation of bicyclo[3.1.1]heptanes. However, the mass spectral fragmentation of pinane has been postulated to begin via the cleavage of one of the bonds at the bridgehead carbons, most likely in the cyclobutane ring, followed by loss of the gem-dimethyl substituted carbon as a $\cdot C_3H_7$ (McLafferty, 1963). Correspondingly, the M-43 ion in the mass spectrum of 3-methylpinane, could originate from initial fission of the cyclobutane ring and hydrogen rearrangement, followed by subsequent α-cleavage resulting in the loss of a propyl radical (Figure 4-46).
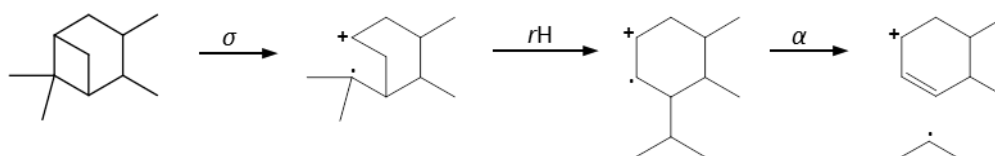
Figure 4-46: Postulated fragmentation of **IId** demonstrating the possibility of ions occurring from fragmentation of the cyclobutane ring at the bridgehead carbon.

The complex fragmentation pattern displayed in the mass spectrum of **IId** made it distinct from those of the spectra of many other bicyclic hydrocarbons (Golovkina *et al.*, 1984). This was considered useful for the identification of bicyclo[3.1.1]heptanes later when performing the conversion of more complex mixtures of NA to the corresponding hydrocarbons for identification (*vide infra*).

4.4.3 Synthesis of 1-methyl-4-pentylbicyclo[2.2.2]octane

4.4.3.1 Preparation and characterisation of 4-pentylbicyclo[2.2.2]octane-1-methanol

Reduction of 4-pentylbicyclo[2.2.2]octane-1-carboxylic acid (**IIIa**) with excess LAH produced 4-pentylbicyclo[2.2.2]octane-1-methanol (**IIIb**; Figure 4-47). The reaction was carried out under an inert atmosphere with diethyl ether as the solvent, using a 10% H_2SO_4 acid work-up. The yield of the reaction was $92 \pm 15\%$ (n = 3) and the purity, determined from the integration of the peak areas in the gas chromatogram was >99 % (Figure 4-48).
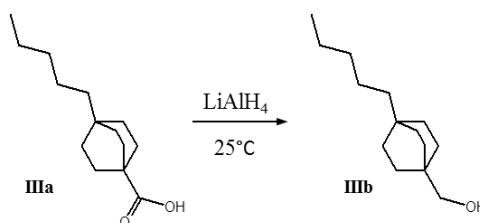
Figure 4-47: Reaction scheme for the reduction of **IIIa** to 4-pentylbicyclo[2.2.2]octane-1-methanol, **IIIb**.
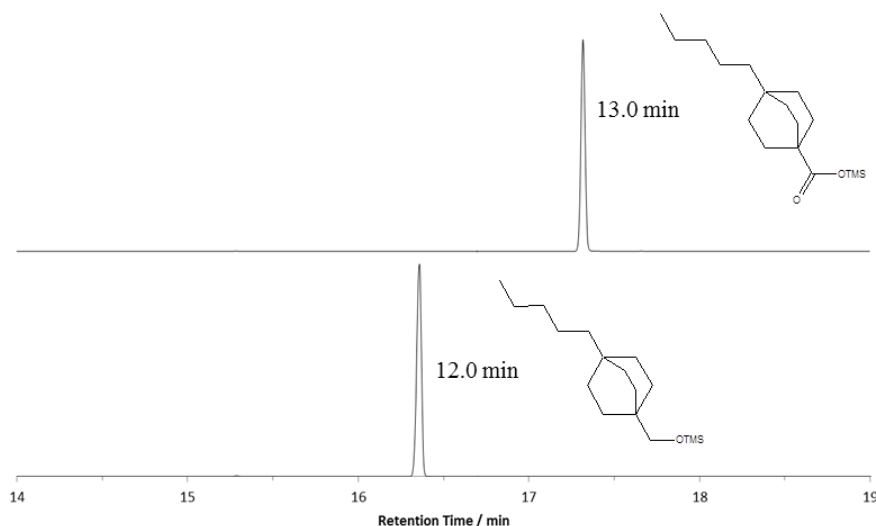
Figure 4-48: Comparison of TICs showing the retention times of the precursor acid **IIIa** and the alcohol product **IIIb**, TMS ester and ether, respectively. (Column A, inlet temperature 300 °C).
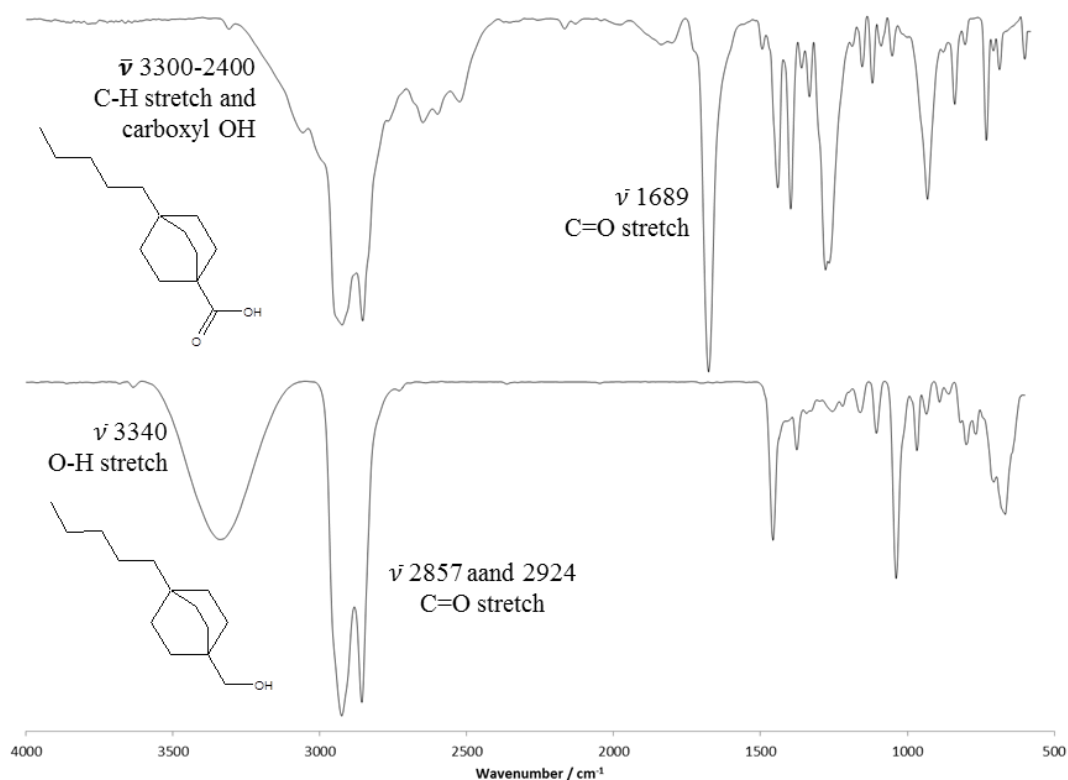
Figure 4-49: Comparison of the IR spectra of **IIIa** and **IIIb**.

The IR spectrum of **IIIb** provided preliminary evidence that the reduction had gone to completion (Figure 4-49). This was evident by the disappearance of the broadening seen in the carboxylic acid spectrum at about 3000 cm^{-1} and the absence of an intense peak at 1689 cm^{-1} attributed to the C=O stretch in the carboxyl group. The broad, medium intensity band at 3340 cm^{-1} in the spectrum of **IIIb**, was assigned as the hydroxyl O-H stretch, which was strong evidence for the formation of an alcohol (Table 4-9).

Table 4-9: Summary of the IR spectra of **IIIa** and **IIIb**.

IIIa			IIIb		
$\overline{\nu}$ (cm^{-1})	Assignment	Comment	$\overline{\nu}$ (cm^{-1})	Assignment	Comment
3300-2400	Carboxyl OH	Broadening of peaks	3340	Alcoholic OH	O-H Stretch, broad
2929,2860, 2657	CH$_3$, CH$_2$, CH saturate alkyls	C-H stretch, med. > 3000	2924	CH$_3$, CH$_2$, CH saturate alkyls	C-H stretch, med-str. >3000
1455		C-H def.	2857		
1689	Carboxyl C=O	C=O stretch, str.	1455		C-H def., weak
800-1450	Carboxyl C-OH	fingerprint	1377		
			1038	Alcoholic C-OH	C-O stretch, med.
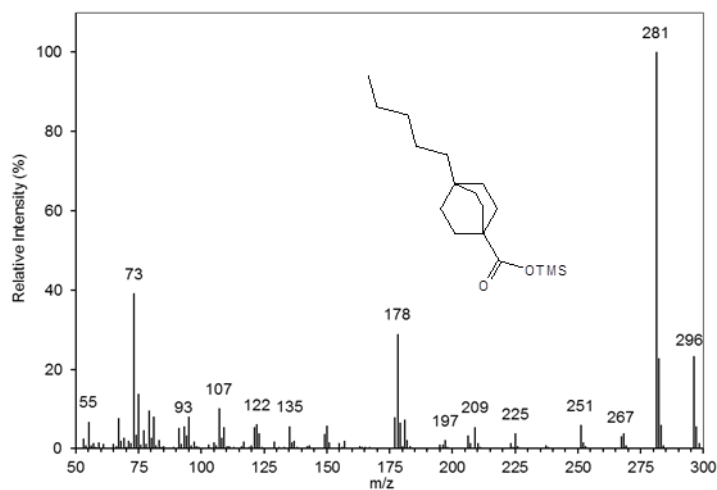
Figure 4-50: Mass spectrum of **IIIa** TMS ester.
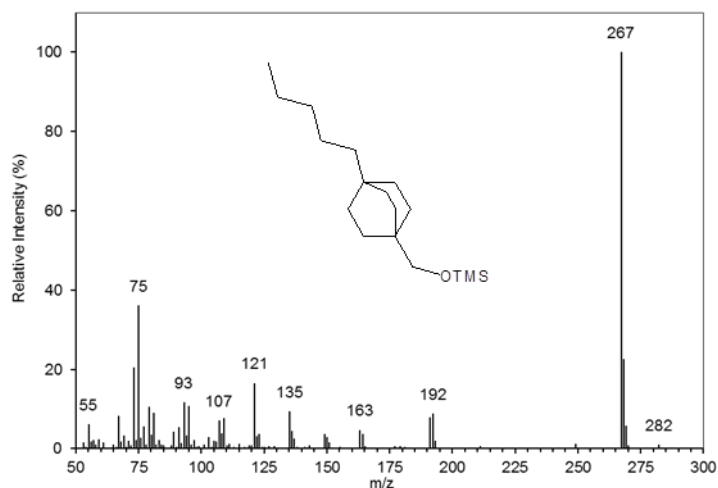
Figure 4-51: Mass spectrum of **IIIb** TMS ether.

The mass spectra of **IIIa** and **IIIb** TMS ester and ethers respectively, only displayed a few dominant ions (Figures 4-50 and 4-51). This was attributed to the stability of the cage-type, bicyclo[2.2.2]octane 'core'. The dominant ions in the spectra of the derivatised acid and alcohol were assigned to fragmentation involving losses from the TMS groups. The spectrum of the acid derivative displayed a molecular ion at *m/z* 296 which was relatively intense for a TMS ester (Figure 4-50). The base peak ion at *m/z* 281 was attributed to the loss of a methyl group from the TMS group. The medium

intensity ion at *m/z* 178 was assigned as $[C_{13}H_{22}]^{+.}$ resulting from fragmentation at the 1-position quaternary bridgehead carbon and the loss of $HCO_2Si(CH_3)_3$.

The most probable site of ionisation would be the non-bonding electrons on either oxygen of the carboxyl moiety, which is supported by the low abundance of ions originating from fragmentation of the bicyclic structure, such as the loss of the pentyl group assigned to the low intensity ion at *m/z* 225. Therefore, for fragmentation to occur at the quaternary carbon resulting in a radical cation (*m/z* 178), the mechanism must involve hydrogen rearrangement and charge migration to the bicyclic part of the structure, possibly via inductive cleavage.

It was difficult to determine structural detail of **IIIb** from the mass spectrum of the TMS ether (Figure 4-51). The molecular ion at *m/z* 282 was 14 Da less than that of the acid (Figure 4-50), confirming the conclusions made from the IR spectra that the reduction had been successful. The base peak ion at *m/z* 281 in the mass spectrum of **IIIb** was assigned as due to the loss of a methyl group, most likely from the TMS group. The M-90 ion (*m/z* 192) was attributed to the loss of $Si(CH_3)_3OH$ as seen in the mass spectrum of **IIb** (Figure 4-30, page 159) and the *m/z* 75 ion was assigned as due to $HO^+{=}SiCH_2$, as seen in the mass spectrum of **Ib** (Figure 4-6, page 131).

The ^{1}H-NMR spectrum of **IIIb** was indicative of a highly symmetrical compound; this was a good indication that the structure of the bicyclo[2.2.2]octane, substituted at carbon positions 1 and 4, had been maintained. Symmetry in a molecule is often observed in ^{1}H-NMR spectra as a low number of signals with high integrals. The ^{1}H-NMR spectrum of **IIIb** was dominated by one complex multiplet between 1.0 – 1.4 ppm with an integral of 22.0 (Figure 4-52).

The protons on the methylene group at position 10, adjacent to the hydroxyl group, were not diastereotopic as they were adjacent to a quaternary carbon. This was unlike

those observed in the structures and ¹H-NMR spectra of **Ib** and **IIb**. Therefore the protons at position 10 were expected to produce a low field singlet, as seen at 3.21 ppm with an integral of 2.0 (Figure 4-52; C). The triplet at highest field with a chemical shift of 0.84 ppm and integral of 3.0 was assigned as due to the protons on the methyl group at position 1, the splitting pattern attributed as due to the two neighbouring protons at position 2 (Figure 4-52; B).
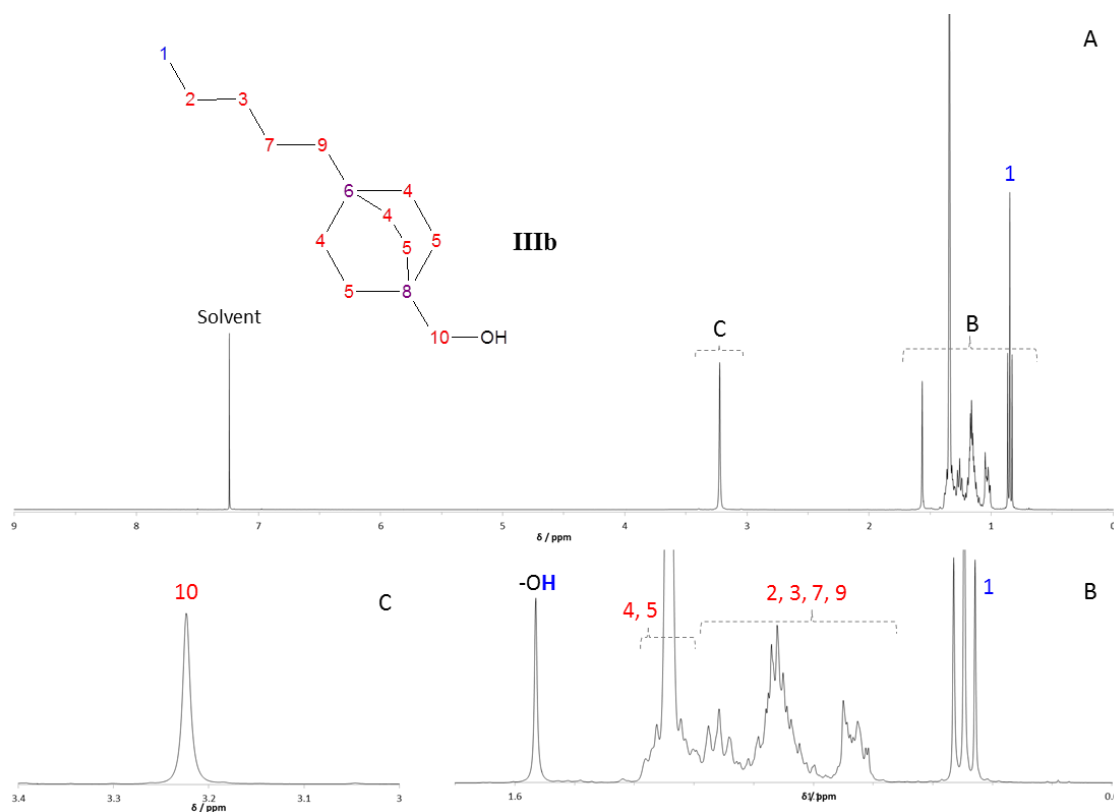
Figure 4-52: (A) ¹H-NMR spectrum of **IIIb** and (B and C) focused spectra showing detail between chemical shifts 0.8 – 1.7 ppm and 3.0 – 3.5 ppm.

The strongest signal between 1.30 – 1.40 ppm was not clearly resolved but was tentatively assigned as due to the 12 protons at positions 4 and 5, producing two overlapping triplets (Figure 4-52; B). The signal integrated to 12.2 corresponding with the 12 protons within the cage-like 'core', supporting the expected structure of **IIIb** (Table 4-10). The remaining resonances, observed as a multiplet between 1.0 – 1.3 ppm, appeared to be three overlapping signals and by means of deduction, the signals were

assigned as due to the methylene protons on the pentyl chain (positions 2, 3, 7 and 9) (Figure 4-52; B).

The singlet at 1.55 ppm had an integral of 1.0, indicating that it was due to an environment within the structure of **IIIb** and not due to an impurity from the reaction or residual solvent (Figure 4-52; C). Therefore it was assigned tentatively as due to the hydroxyl proton. Protons within alcoholic hydroxyl groups are not always present in ^{1}H-NMR spectra. However, in the spectrum of **IIIb**, it may be observed due to the highly compact, symmetrical structure and the relatively exposed position of the hydroxyl moiety.

The ^{13}C-NMR spectrum of **IIIb** was dominated by two peaks at 28.34 and 30.84 ppm, approximately three times the intensity of any other peak (Figure 4-53). These were assigned as the methylene carbons at positions 4 and 5. The methyl group in position 1 was assigned based on its low frequency and opposite phasing in the DEPT ^{13}C-NMR spectrum (Figure 4-54). The two quaternary carbons, at positions 6 and 8, appeared at 31.03 and 33.31 ppm, confirmed by their non-appearance in the DEPT ^{13}C spectrum (Figure 4-54). The lowest field signal at 71.89 ppm was assigned as due to the methylene group at position 10, bonded to the hydroxyl group (Table 4-10 and Figure 4-53). The remaining signals at 22.78, 23.42, 32.95 and 41.71 ppm were attributed to the methylene carbons along the pentyl chain (positions 2, 3, 7 and 9). Based on the ^{1}H-NMR and ^{13}C-NMR spectra alone, the exact assignment of each signal was not possible. However, after examination of the COLOC spectrum for **IIIc** (Figure 4-61; Section 4.4.3.2, page 194), full characterisation was achieved.
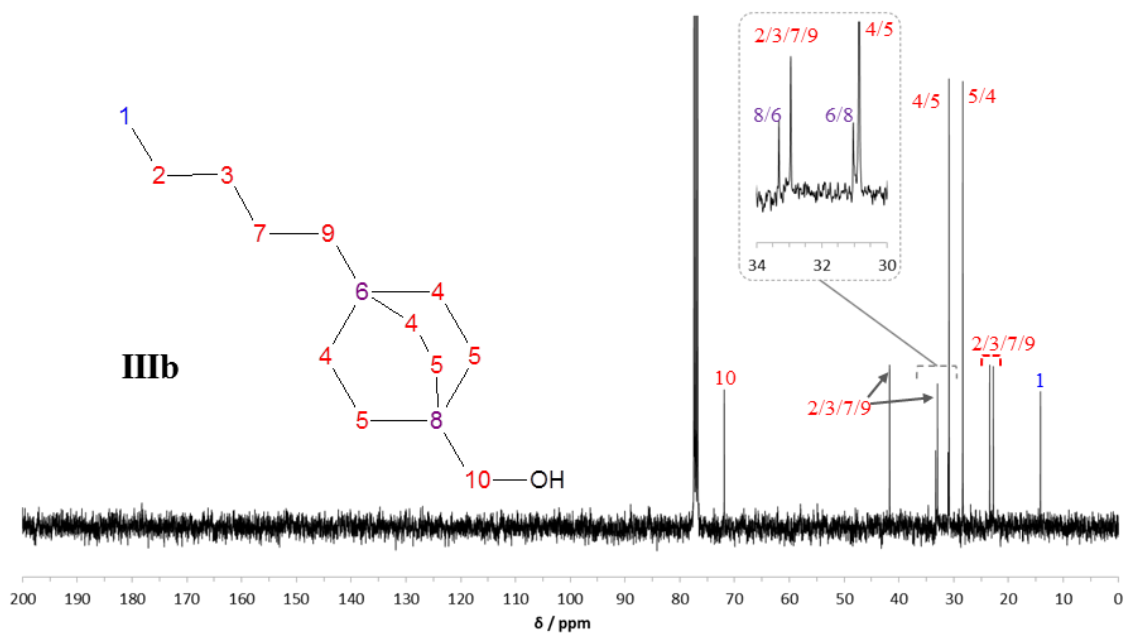
Figure 4-53: ^{13}C-NMR spectrum of **IIIb**.
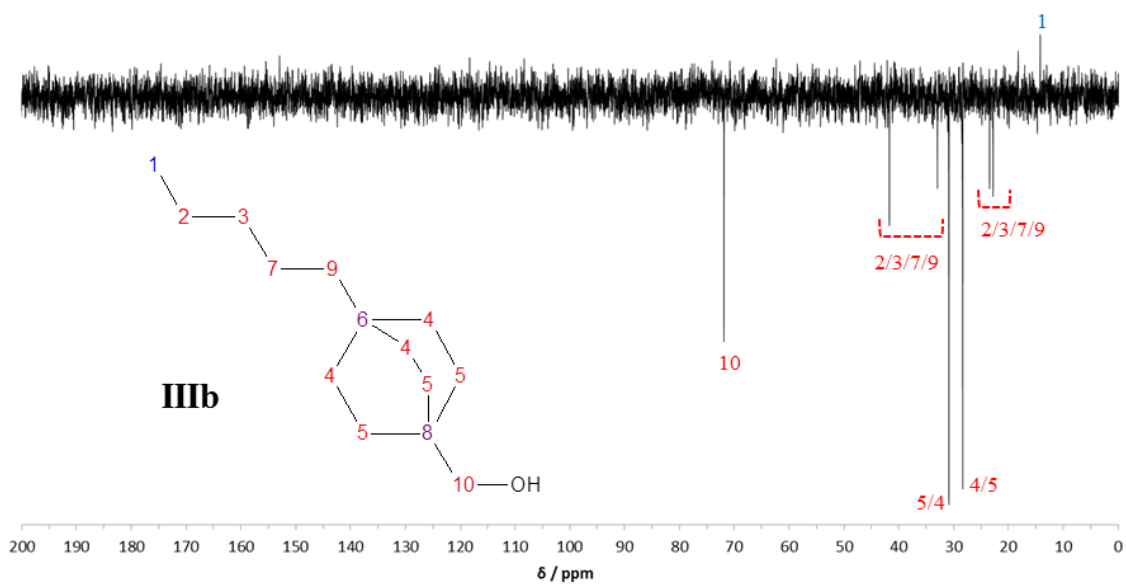
Figure 4-54: DEPT ^{13}C-NMR spectrum of **IIIb**.

Table 4-10: Summary of ^{1}H and ^{13}C spectra of alcohol product **IIIb**.

Position	^{1}H chemical shifts / ppm	^{1}H integral	J value / Hz	^{13}C chemical shifts / ppm			
				Primary (CH)	Secondary (CH$_2$)	Tertiary (CH$_3$)	Quaternary (C)
1	0.85 (*t*)	3.0	7.3			14.17	
2	1.00 – 1.30 (*m*)	-	-		22.78[a]		
3	1.00 – 1.30 (m)	-	-		23.42[a]		
4	1.30 – 1.40 (*m*)	12.2	-		28.34[b]		
5			-		30.85[b]		
6	Quaternary carbon						31.03[c]
7	1.00 – 1.30 (*m*)	-	-		32.95[a]		
8	Quaternary carbon						33.31[c]
9	1.00 – 1.30 (*m*)	-	-		41.71[a]		
10	3.22 (*s*)	-	-		71.89		

[a,b,c] peaks assigned positions 2, 3, 7 and 9; 4 and 5; 6 and 8 are interchangeable based on ^{1}H and ^{13}C-NMR data alone. Later confirmed in tosylate product (Table 4-11).

4.4.3.2 **Preparation and characterisation of 4-pentylbicyclo[2.2.2]octane-1-methanol tosyl derivative**

The catalytic tosylation of 4-pentylbicyclo[2.2.2]octane-1-methanol (**IIIb**) using tosyl chloride (TsCl) produced the tosylate **IIIc** (Figure 4-55). The use of triethylamine (TEA) and 4-(dimethylamino)pyridine (DMAP) produced **IIIc** in a yield of 88 ± 2 % (n = 3). The gas chromatogram of the tosylate product **IIIc** was consistent with the previous tosylate products, with early eluting peaks displaying molecular ions at *m/z* 192 again attributed to the decomposition of the tosylate in the hot GC injector (Figure 4-56 and Appendix Figures 15 and 23). The chromatogram also showed three small peaks, with small molecular ions at *m/z* 228 and strong M-35 ions (*m/z* 193), which suggested the loss of a chloride radical from some chloride by-products. The product was purified by silica chromatography prior to analysis by NMR.
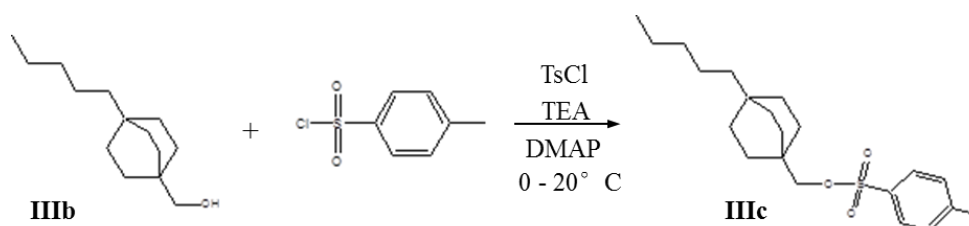
Figure 4-55: Reaction scheme for the tosylation of 4-pentylbicyclo[2.2.2.]octane-1-methanol **IIIb** to **IIIc**.
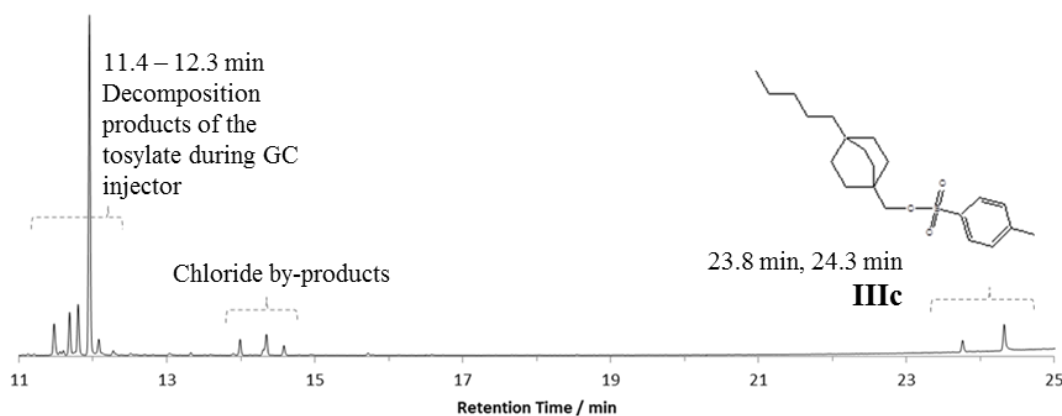

Figure 4-56: Gas chromatogram of tosylate product **IIIc** showing partial decomposition in the hot GC inlet. (Column A, inlet temperature 300 °C).
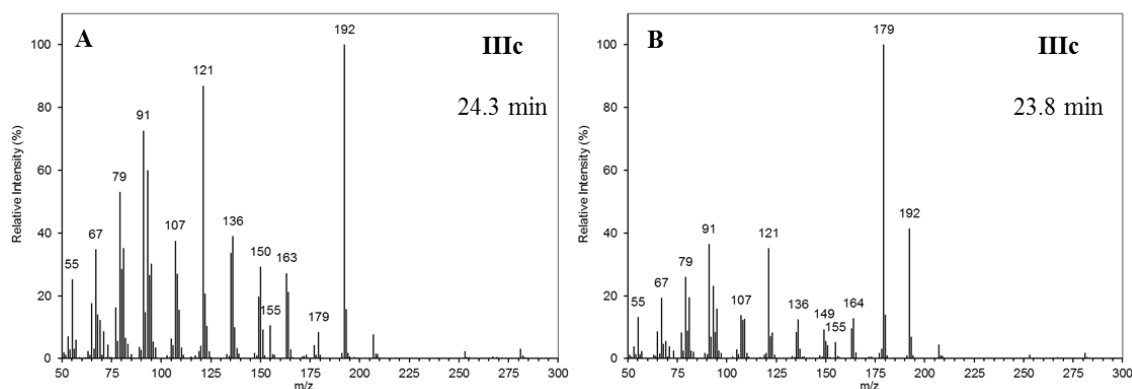
Figure 4-57: (A) Mass spectrum of the tosylate product **IIIc** at 24.8 min and (B) a rearrangement product due to the hot GC inlet temperature at 23.8 min.

The chromatogram of the tosylate product (Figure 4-56) showed two late eluting peaks at 23.8 and 24.3 min with similar mass spectra (Figure 4-57). This was unexpected as the previous tosylate products (e.g. **Ic** and **IIc**) only showed one later eluting peak. The structure of **IIIc** cannot display any geometric isomerism and it was considered unlikely that the compound would undergo rearrangement during the reaction because of the high stability of the cage-like structure and mild reaction conditions utilised. Lowering the GC inlet temperature to 250 °C and 225 °C clarified that the peak at 24.3 min was the tosylate product, since this peak increased in intensity as the inlet temperature reduced (Appendix Figure 23). The other peak at 23.8 min was assigned as a rearrangement product caused during the hot injection of the sample and not a rearrangement artefact produced during the reaction.

The ^{1}H-NMR spectrum was very similar to that of the alcohol product **IIIb**, but with the appearance of additional signals due to the protons in the tosyl group (Figure 4-58). The ^{1}H-NMR spectrum of **IIIc** showed a high field triplet with an integral of 3.0 at 0.83 ppm, this was attributed to the protons on the methyl group at position 1 and the singlet with an integral of 2.0 at 3.59 ppm, was assigned as due to the protons of the methylene group in position 11.
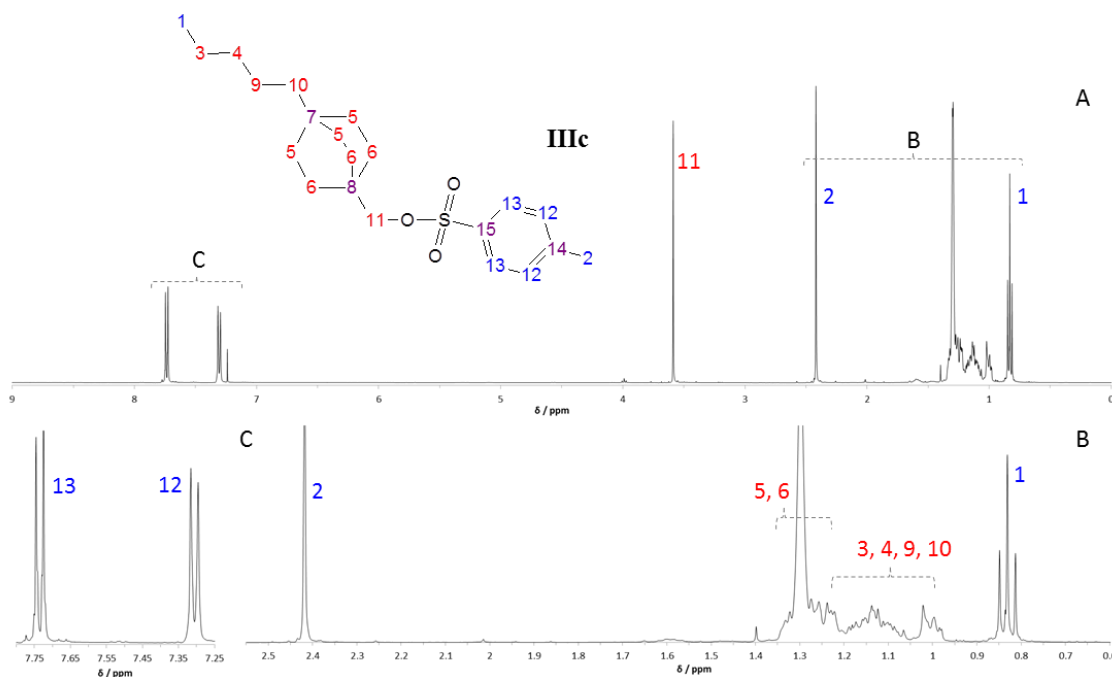
Figure 4-58: [^1]H-NMR spectrum of tosylate product **IIIc**.

The intense multiplet observed between 1.25 – 1.35 ppm with an integral of 12.1, was assigned as due to the protons in the methylene groups within the bicyclo[2.2.2]octane core at positions 5 and 6. These overlapped with a multiplet between 0.96 – 1.25 ppm attributed to the protons in the methylene groups of the pentyl chain at positions 3, 4, 9 and 10 (Figure 4-58; B). Additional signals not observed in the spectrum of the alcohol but present in the spectrum of the tosylate, included a singlet with an integral of 3.0 at 2.42 ppm. This singlet was attributed as due to the protons on the methyl group within the tosyl group at position 2. The assignment was confirmed in the COLOC spectrum of **IIIc** (Figure 4-61, page 194), with the singlet correlating with a quaternary aromatic carbon at 144.58 ppm and an aromatic CH group at 129.82 ppm. The two doublets at 7.31 and 7.35 ppm (Figure 4-58), each integrating to 2.0, were assigned as the aromatic protons at positions 12 and 13. The exact assignment of the protons at position 12 as the doublet at 7.31 ppm was based on the correlations observed in the COLOC spectrum of **IIIc** (Figure 4-61). The doublet at 7.31 ppm correlated with the same aromatic CH signal, at 129.82 ppm, as the singlet assigned as the protons within the methyl group at

189

position 2. Therefore the protons at 7.31 ppm must be within the long-range coupling

distance relative to the protons at position 2.
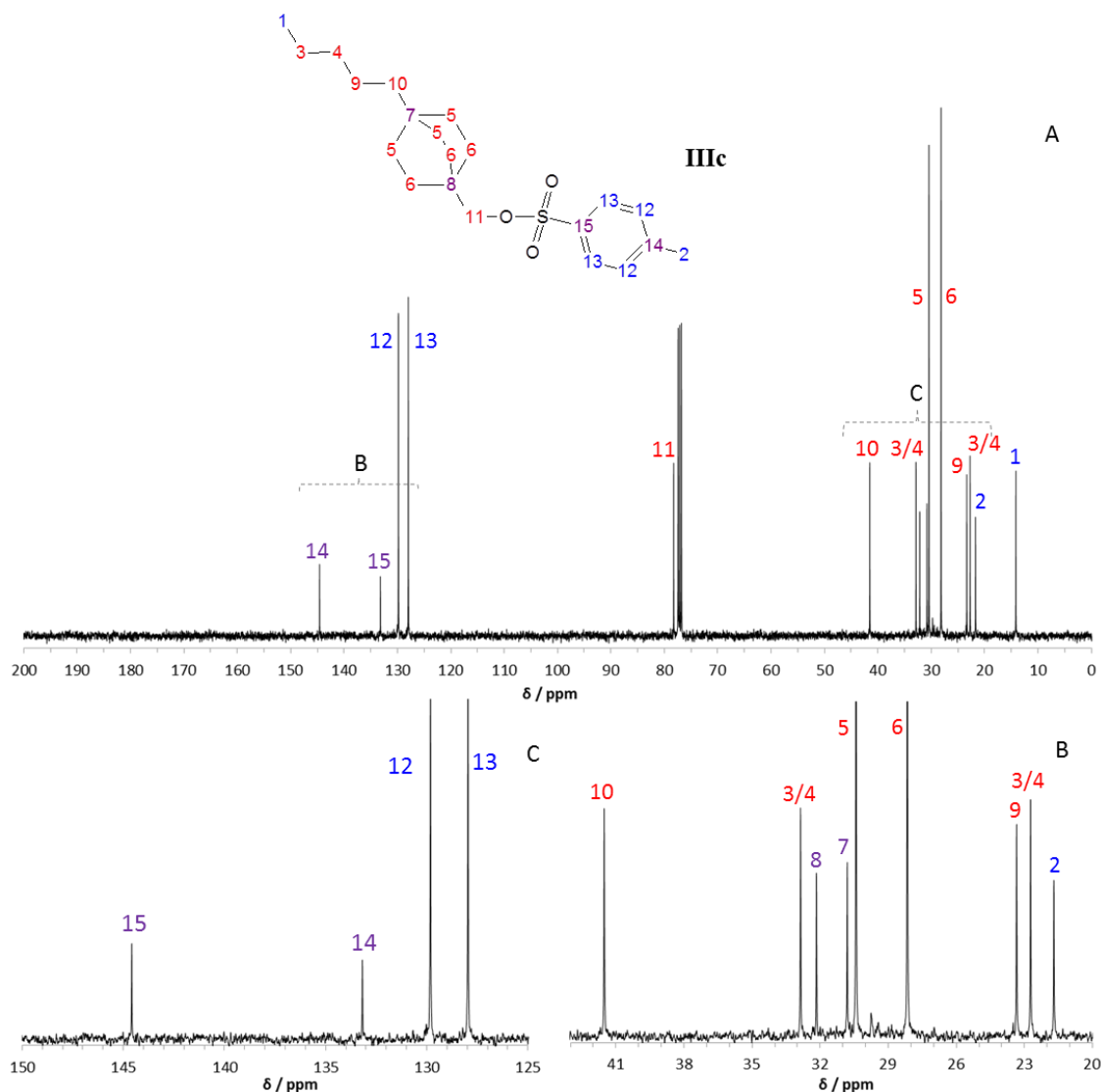
Figure 4-59: (A) ^{13}C-NMR spectrum of tosylate product **IIIc** and (B and C) focused

spectra displaying detail between chemical shifts 125 - 150 ppm and 27 - 43 ppm.

The ^{13}C-NMR spectrum confirmed the tosylate product **IIIc** had retained its structure.

The spectrum showed 15 peaks (Figure 4-59), accountable due to the symmetry of **IIIc**.

The peak at 78.25 ppm, showing opposite phasing in the DEPT 13C-NMR spectrum

(Figure 4-60), was assigned as due to the methylene carbon bonded to the tosylate group.

This was confirmed by its correlation in the CHSHF spectrum (Appendix Figure 24),

with the singlet at 3.59 ppm assigned as the protons at position 11.

The two intense peaks at 28.17 and 30.43 ppm showing opposite phasing in the DEPT spectrum (Figure 4-60), were assigned as due to the methylene groups at positions 5 and 6. This was confirmed in the CHSHF spectrum of **IIc** (Appendix Figure 25); both peaks were observed correlating with the intense multiplet assigned as the 12 methylene protons in positions 5 and 6, at 1.25 – 1.35 ppm. The peak at 28.17 ppm was assigned as due to the methylene carbon at position 6 because it was observed correlating with the singlet at 3.59 ppm, assigned as the protons at position 11 in the COLOC spectrum (Figure 4-62, page 195).
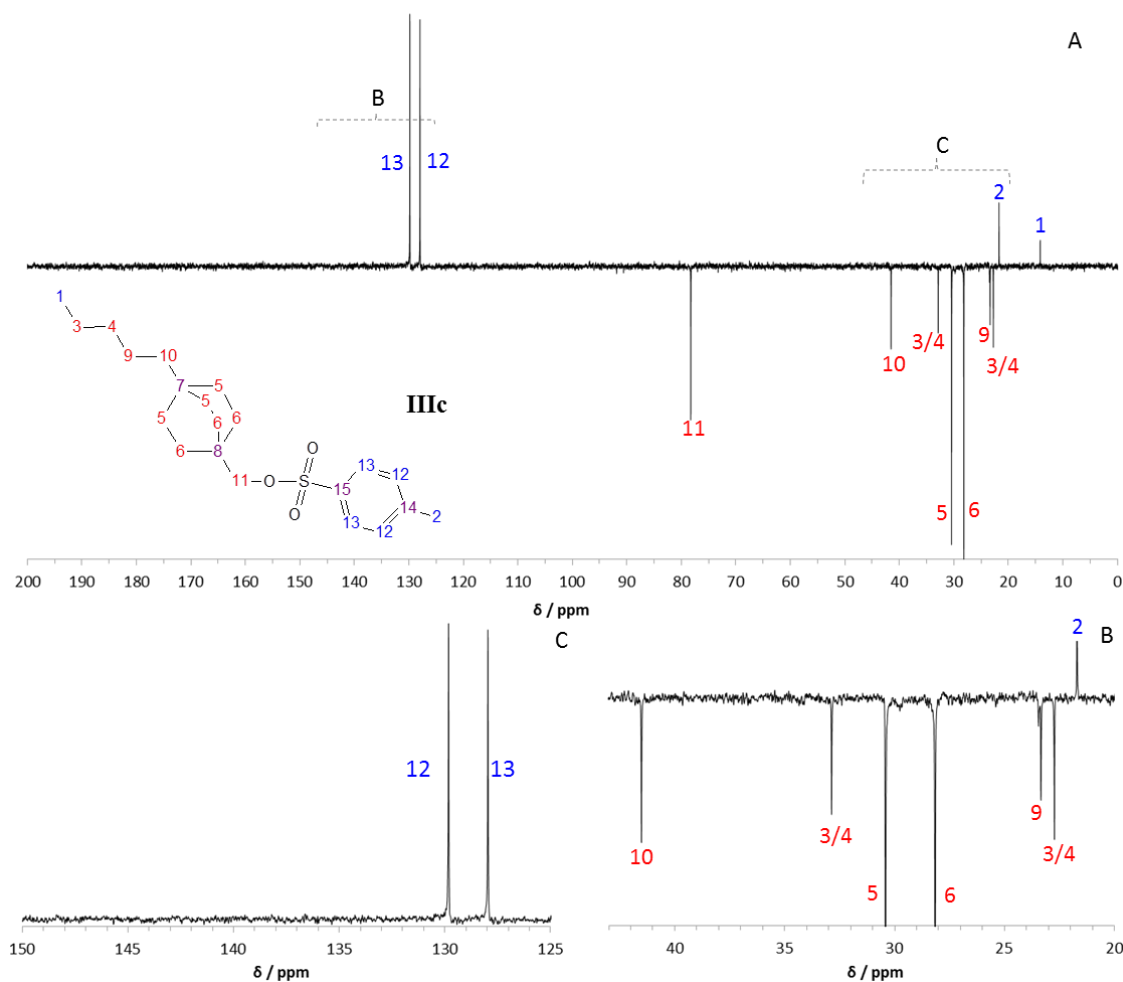
Figure 4-60: (A) DEPT ^{13}C-NMR spectrum of tosylate product **IIIc**. (B and C) Focused spectra showing detail between chemical shifts 27 - 43 ppm and 125 – 150 ppm.

Four quaternary carbons were assigned, based on their non-appearance in the DEPT ^{13}C-NMR spectrum (Figure 4-60). These included the two aromatic carbons at positions 14 and 15 with high chemical shifts at 133.18 and 144.58 ppm and the two bridgehead carbons in the bicyclic 'core', at positions 7 and 8 at 30.80 and 32.16 ppm. The presence of the latter was further evidence that the compound had maintained its structure; structural rearrangement from a bicyclo[2.2.2]octane substituted at both bridgeheads would result in fewer quaternary carbons.

The quaternary carbon at 32.16 ppm was assigned as the bridgehead carbon closest to the tosylate group in position 8, based on its correlation with the protons in position 11, observed in the COLOC spectrum of **IIIc** (Figure 4-62). Similarly, the aromatic quaternary carbon at 144.58 ppm and the aromatic CH group at 129.82 ppm were assigned as the carbon atoms at positions 14 and 12 respectively because both peaks correlated with the protons in position 2 in the COLOC spectrum (Figure 4-61).

The two signals at 14.14 and 21.70 ppm were attributed to the methyl groups at positions 1 and 2 based on their upwards phasing in the DEPT 13C-NMR spectrum of **IIIc**. The signal at 21.70 ppm was attributed to the methyl substituent in the tosyl group (position 2) based on its correlation in the CHSHF spectrum with the singlet at 2.42 ppm attributed to the protons at position 2 (Appendix Figure 25). Likewise, the methyl group at position 1, at the end of the pentyl chain, was assigned based on its low chemical shift and correlation with the high field triplet observed in the CHSHF spectrum of **IIIc** (Appendix Figure 25).

Of the remaining methylene carbons in the pentyl chain, two were differentiated following careful examination of the COLOC spectrum (Figure 4-62). The methylene group at position 10, bonded to the bridgehead carbon, was assigned as the peak at 41.5 ppm as the peak correlated with the intense multiplet attributed to the protons at

positions 5 and 6 (Figure 4-62). Assignment of the methylene carbon at position 11 previously, supported its assignment as the carbon atom at position 10. The signals at 22.79 and 32.86 ppm both showed correlations with the protons within the terminal methyl group at position 1 (Figure 4-62). Therefore these signals were assigned as the methylene carbons in positions 3 and 4. By deduction, the remaining peak at 23.34 ppm was assigned as the methylene carbon at position 9, which was supported by the correlation of the signal with the multiplet between 0.96 ppm (Figure 4-62). All of the NMR data are summarised in Table 4-11.

Table 4-11: Summary of ^{1}H and ^{13}C-NMR spectra of the tosylate product **IIIc**.

Position	^{1}H chemical shifts / ppm	^{1}H integral	J value / Hz	^{13}C chemical shifts / ppm			
				Primary (CH)	Secondary (CH$_2$)	Tertiary (CH$_3$)	Quaternary (C)
1	0.83 (*t*)	3.0	7.3			14.14	
2	2.42 (*s*)	3.0	-			21.70	
3	0.96 – 1.25 (*m*)	-	-		22.79^a		
4	0.96 – 1.25 (*m*)	-	-		32.86^a		
5	1.25 – 1.35 (*m*)	12.1	-		30.43		
6					28.17		
7	Quaternary carbon						30.80
8	Quaternary carbon						32.16
9	0.96 – 1.25 (*m*)	-	-		23.34		
10	0.96 – 1.25 (*m*)	-	-		41.50		
11	3.59 (*s*)	2.0	-		78.25		
12	7.31 (*d*)	2.0	7.9	129.82			
13	7.35 (*d*)	2.0	8.3	127.95			
14	Quaternary carbon						144.58
15	Quaternary carbon						133.18

^{a} peaks assigned positions 3 and 4.
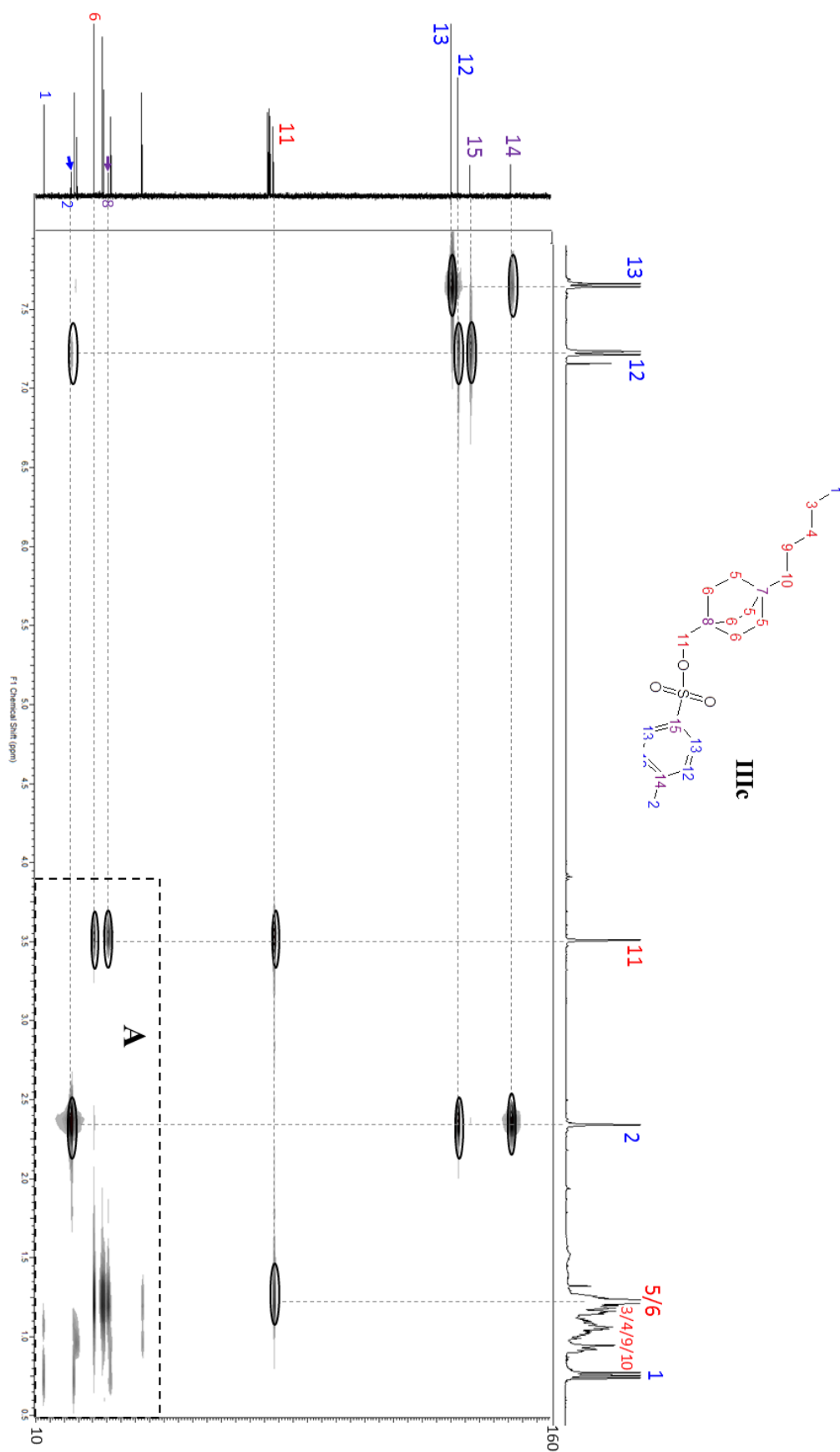
Figure 4-61: COLOC spectrum of **IIIc**.
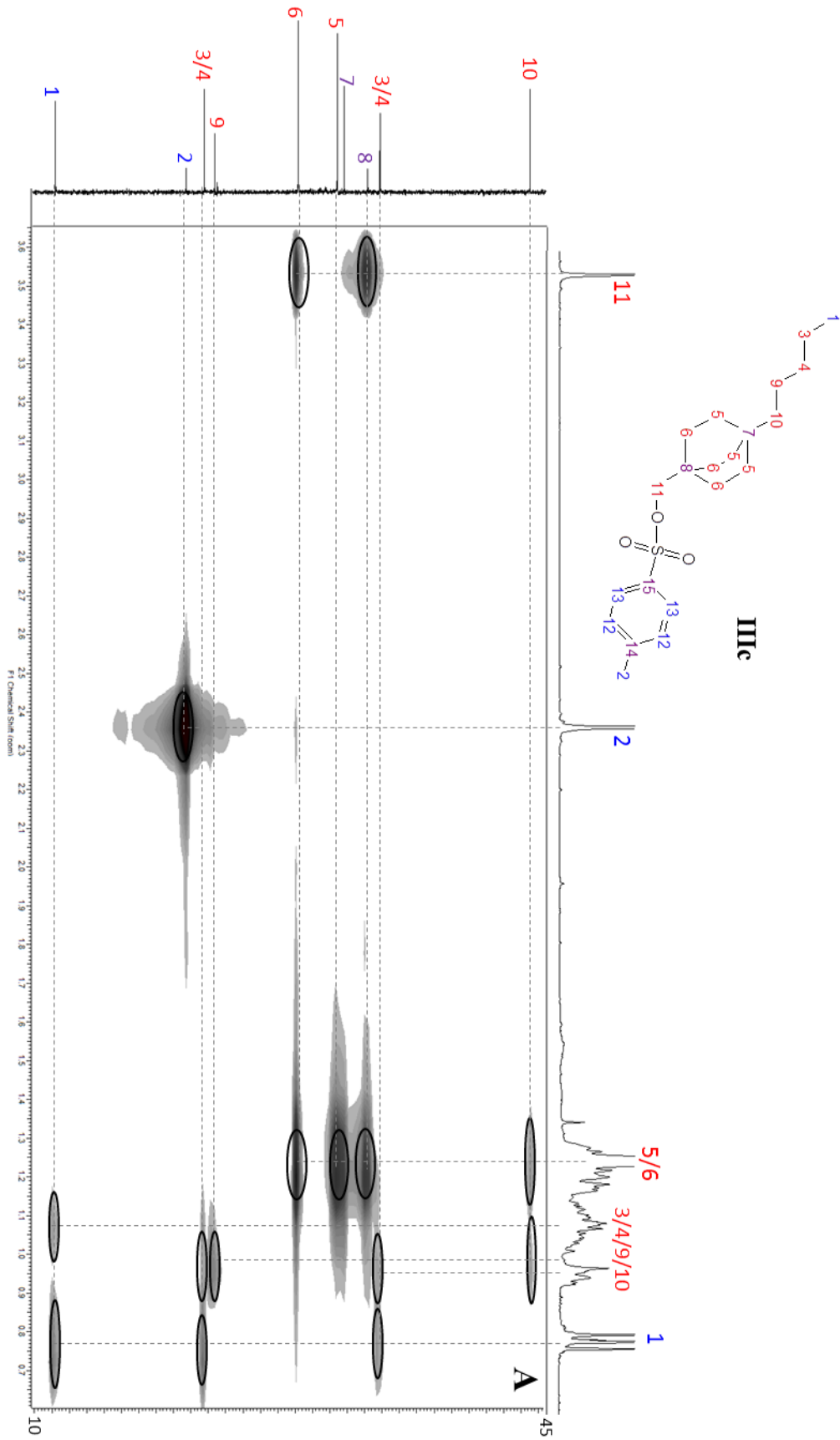
Figure 4-62: Zoomed COLOC spectrum of **IIIc**.

4.4.3.3   Preparation and characterisation of 1-methyl-4-pentylbicyclo[2.2.2]octane

The 4-pentylbicyclo[2.2.2]octane-1-methanol tosyl derivative (**IIIc**) was reduced using excess lithium triethylborohydride to 1-methyl-4-pentylbicyclo[2.2.2]octane (Figure 4-63; **IIId**). The reaction was carried out under an inert atmosphere at room temperature using THF and diethyl ether as the solvent. Although the hydrocarbon product had a higher molecular weight than that of the previous 'model' compounds, significant losses were still observed during concentration, requiring the use of a Kuderna-Danish apparatus (Chapter 2, Section 2.3.4).
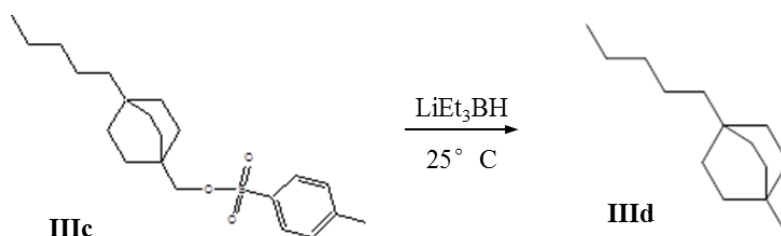

Figure 4-63: Reaction scheme for the Super-Hydride® reduction of **IIIc** to **IIId**.

Figure 4-64: Gas chromatogram of 1-methyl-4-pentylbicyclo[2.2.2]octane, **IIId**.

(Column B, inlet temperature 250 °C).

The mass spectrum of **IIId** contained a molecular ion at *m/z* 194, consistent with that of a bicyclic hydrocarbon with the molecular formula $C_{14}H_{26}$ (Figure 4-65). The molecular ion was relatively abundant for a bicyclic hydrocarbon, suggesting the compound had retained its stable cage-like 'core' (Figure 4-65; A). A reference mass spectrum for the direct comparison of **IIIc** was not available in the literature. However, Denisov *et al.* (1977d) reported the mass spectra for a series of other alkyl substituted bicyclo[2.2.2]octanes. These included that of 1,4-dimethylbicyclo[2.2.2]octane, a hydrocarbon with the same bicyclic 'core', substituted at both bridgehead carbons (Figure 4-65; B).
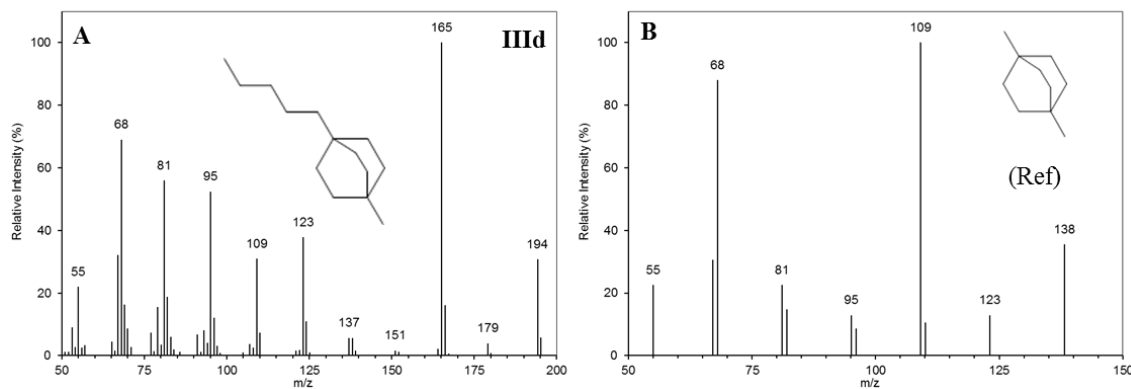
Figure 4-65: (A) Mass spectrum of **IIId**, identified as 1-methyl-4-pentylbicyclo[2.2.2]octane and (B) the mass spectrum of 1, 4-dimethylbicyclo[2.2.2]octane replotted from tabulated values reported by Denisov *et al.* (1977d).

The base peak ion in the mass spectra of both 1,4-dimethylbicyclo[2.2.2]octane and 1-methyl-4-pentylbicyclo[2.2.2]octane hydrocarbon product was the M-29 ion (*m/z* 165, Figure 4-65; A), which was attributed to the loss of an ethyl radical ($\cdot C_2H_5$). If the bicyclo[2.2.2]octane structure underwent a retro-Diels Alder type fragmentation, as proposed by McLafferty and Tureček (1993) for the fragmentation of some cyclic structures such as cyclohexane, the expected loss would be the ejection of a neutral

ethene molecule (M-28) i.e. loss of a C_2 bridge between carbons 1 and 4. The loss of an ethyl radical suggested the bicyclo[2.2.2]octane structure in fact undergoes a mechanism similar to that postulated by Denisov *et al.* (1977d) with cleavage first occurring at a bridgehead carbon and a hydrogen rearrangement followed by α-cleavage (Figure 4-66), as observed for other bicyclic hydrocarbons.
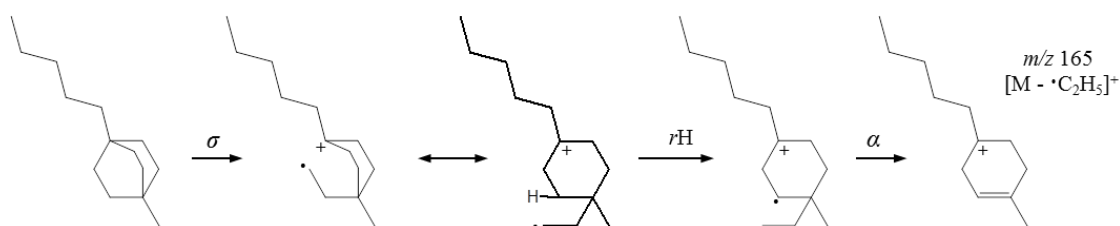
Figure 4-66: Postulated mechanism for the loss of an ethyl radical from **IIIc**, adapted from the mechanism reported by Denisov *et al.* (1977d).

The high intensity of the lower mass ions e.g. *m/z* 109, 95 and 81 was typical of mass spectra of alicyclic hydrocarbons and the increased abundance of the ion *m/z* 123 was tentatively assigned as due to the loss of the pentyl chain.

4.5 Conclusions

An alternative method for the identification of petroleum acids to that described in Chapter 3, via conversion to the corresponding hydrocarbons, was developed herein, based on the historical approach previously utilised by Seifert *et al.* (1969). Reference mass spectra of petroleum hydrocarbons are more readily available and the mass spectral fragmentation patterns are better understood, making interpretation easier. There is a lack of reference mass spectra of acid methyl esters, which in any case tend to be dominated by fragmentation of the carboxyl groups, making structural elucidation difficult.

The final optimised method developed herein involved reproducible reactions resulting in high yields of the desired products. Structural characterisation of each of the alcohol and tosylate intermediates by IR, GC-MS and NMR and of the final hydrocarbon products by GC-MS, confirmed the successful conversion of all three model bicyclic acids, possessing different bicyclic cores, to the corresponding hydrocarbons. The mass spectra of the resulting bicyclanes were all comparable to those of relevant reference hydrocarbons. The results of the current investigation provided evidence for the development of a successful method for the conversion of acids to the corresponding hydrocarbons; such detailed proof has not before been reported in previous investigations attempting to achieve a similar aim.

The conversion method developed herein can now be attempted for the conversion of more complex mixtures of petroleum NA and OSPW acids to the corresponding hydrocarbons, in an attempt to identify unknown bicyclic acids as their bicyclane equivalents (Chapter 5).

Chapter 4

Chapter 5

Structural identification of bicyclic petroleum acids by conversion to hydrocarbons and multidimensional gas chromatography-mass spectrometry

Chapter 5 describes application of the method developed in Chapter 4 (for 'model' acids), to the conversion of unknown petroleum acids to hydrocarbons, followed by analysis using multidimensional gas chromatography-mass spectrometry (GC×GC-MS).

A commercially prepared petroleum-derived acid mixture, was derivatised and first separated by argentation chromatography into two 'alicyclic' acid methyl ester fractions. The fractions were converted to the corresponding hydrocarbons using the three step transformation described in Chapter 4. Subsequent analysis of the hydrocarbon products by GC×GC-MS resulted in the separation of numerous individual hydrocarbons, reflecting the vast complexity of the original acid mixture, displaying highly resolved homologous series' of >150 C_{9-15} bicyclic hydrocarbons (bicyclanes).

Comparison of the individual mass spectra of the corresponding bicyclanes with a mass spectral database of petroleum hydrocarbons collated from the literature, led to the identification of more than forty individual bicyclanes. The bicyclic hydrocarbons identified and by inference the structures of the original bicyclic acids, included fused and bridged structures possessing methyl, dimethyl, ethyl and propyl alkyl substituents, as well as some terpenoid-derived acids. The study provides the most comprehensive analysis of a major class of petroleum acids to date.

Chapter 5

Many of the results and methods described in this chapter have been published:

Wilde, M. J. and Rowland, S. J. (2015) Structural Identification of Petroleum Acids by Conversion to Hydrocarbons and Multidimensional Gas Chromatography-Mass Spectrometry. *Analytical Chemistry*, 87, 16, 8457-8465.

5.1 Introduction

The identification of individual bicyclic acids in complex naphthenic acids (NA) mixtures has been hindered to date by the chromatographic properties of the acids and derivatives, the lack of mass spectral databases for the relevant acids and derivatives and the lack of reference compounds for identification. Advanced analytical instrumentation is often used and indeed has been proved necessary for examination of the acid mixtures (as discussed in Chapter 1). Most investigations reporting mass spectral data for commercial NA only report group-type classifications (e.g. acyclic, mono-, bicyclic etc.) based on hydrogen deficiency ('z' values), with bicyclic or so-called 'z = -4' acids, frequently reported as one of the most abundant classes (Damasceno *et al.*, 2014; Scott *et al.*, 2005; Clemente *et al.*, 2003; Martin *et al.*, 2008).

The use of GC×GC-MS for the analysis of NA as the methyl ester derivatives recently led to the identification of several bicyclic acids in both petroleum-derived acids, as well as those extracted from oil sands process-affected water (OSPW), by comparison of the mass spectral and retention position data of the unknowns with those of reference compounds (as discussed in Chapter 3; Wilde *et al.* (2015)). This approach resulted in the identification of some individual bicyclic acids for the first time in NA mixtures (op cit). However the number of identifications possible was still limited by the sparsity of current mass spectral databases for relevant acid methyl esters (Wilde *et al.*, 2015).

An historical approach, formerly adopted by Seifert *et al.* (1969) and others, involved converting the petroleum acids to compounds more amenable for study; for example, defunctionalisation of the acids to the corresponding hydrocarbons. A wider range of petroleum hydrocarbons are known, due to the early petroleum research projects which developed methods for their isolation and characterisation (Denisov *et al.*, 1977a; Golovkina *et al.*, 1984; Petrov, 1987; Sanin, 1976). The aim of the present conversion

methods developed herein was to achieve identification of the acids by comparison of the reduced acid products with the abundant data available for petroleum hydrocarbons (e.g. chromatographic properties and mass spectra). Structural assignment of individual hydrocarbons after conversion from the acids was limited in the earlier studies (e.g. Seifert *et al.* (1969)), due to the lack of chromatographic resolution using the available GC techniques but it was proposed that use of GC×GC methods might improve on this.

Therefore, the current investigation aimed to combine both the historical approach of converting the acids to hydrocarbons with subsequent analysis of the hydrocarbons by GC×GC-MS, affording the mass spectra of individual bicyclanes. It was hypothesised that comparison of the mass spectra with the abundant reference mass spectra of bicyclic hydrocarbons collated from the literature and relevant retention position data, would allow identification of the bicyclanes and by inference the original bicyclic acids.

The general synthetic route for the conversion of the acids to the hydrocarbons was developed based on the method previously reported by Seifert *et al.* (1969), involving reduction of the acids via a tosylate intermediate (Figure 5-1).
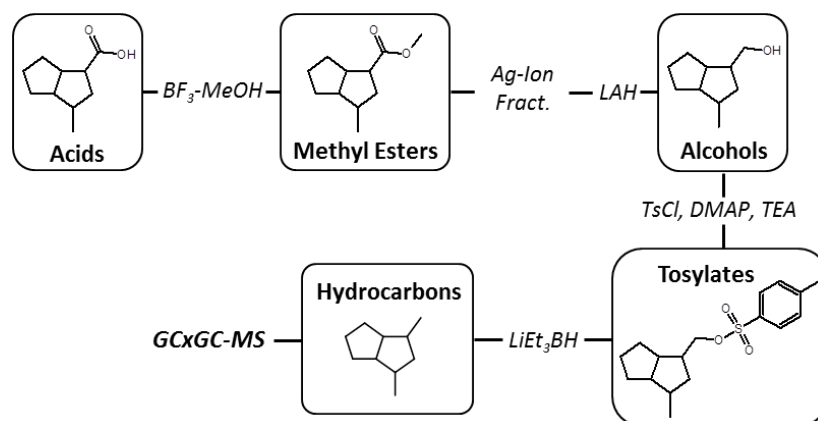
Figure 5-1: Route of conversion of the acids, via derivatisation and fractionation of the acid methyl esters, to the corresponding hydrocarbons. Model compound 4-methylbicyclo[3.3.0]octane-2-carboxylic acid is shown only as an example.

The conversion was first optimised on three 'model' bicyclic acids during which the individual steps including the reagents and conditions used were modified to improve yields and to involve milder conditions (as discussed in Chapter 4). Characterisation of the 'model' alcohol and tosylate intermediates and the final hydrocarbon products by infrared spectroscopy (IR), nuclear magnetic resonance spectroscopy (NMR) and gas chromatography-mass spectrometry (GC-MS), confirmed that the 'model' compounds retained their structural integrity throughout the conversion, showing the potential for this method to be applied to unknown complex acid mixtures. The mild conditions and use of a Kuderna-Danish apparatus reduced the loss of volatile C_{10-11} hydrocarbon products which was considered important for identification purposes when performing the conversion on unknown acid mixtures. Retaining the most volatile hydrocarbons was important because many of the reference mass spectra were known for C_{10-11} bicyclic hydrocarbons and also because C_{9-11} acids are reported in many studies (though seldom if ever, identified) of NA mixtures (Damasceno *et al.*, 2014; Wilde *et al.*, 2015).

Previous studies have utilised argentation chromatography of the acid methyl esters prior to GC×GC-MS analysis in order to reduce the overall complexity of the mixtures analysed (Jones *et al.*, 2012; Scarlett *et al.*, 2013; Reinardy *et al.*, 2013). Petroleum-derived NA have been shown previously to contain aromatic species (Knotnerus, 1957). Argentation chromatography was utilised by Wilde *et al.* (2015) to obtain a less complex 'alicyclic' acid methyl ester fraction in which bicyclic acids were abundant. Therefore, fractionation of the acid methyl esters by argentation chromatography was also performed on some samples herein, prior to converting them to the corresponding hydrocarbons and analysis by GC×GC-MS.

5.1.1 Aims and Objectives

The aims of the current investigation were to apply the method developed in Chapter 4, for the conversion of NA to hydrocarbons, to alicyclic acids isolated from petroleum NA. After successfully reducing the petroleum NA to the corresponding hydrocarbons, the aim was to achieve clear separation of highly resolved individual bicyclic hydrocarbons and compare the mass spectra of the bicyclanes and retention positions with reference mass spectra and known elution order of bicyclic hydrocarbons collated from the literature.

The first objective was to reduce the initial complexity of the NA mixture by derivatisation of the acid extract to the methyl esters followed by fractionation of the acid methyl esters by Ag-Ion chromatography. Secondly, to achieve a controlled concentration of the final hydrocarbon product, in order to retain the low molecular weight bicyclanes, using a Kuderna-Danish apparatus. Numerous reference mass spectra were replotted from tabulated mass spectral data, which had been collated from the literature. The majority of reference mass spectra available for bicyclic hydrocarbons exist for C_{9-11} bicyclanes and it was therefore important to retain and separate by GC×GC-MS, the low molecular weight bicyclic hydrocarbons.

5.2 Methods

5.2.1 Derivatisation and fractionation of petroleum NA

A commercially prepared, petroleum acid mixture was received as a gift in 2009 from Merichem Co., and was derivatised and fractionated as described in Chapter 2, Sections 2.2.3 and 2.2.5. The analysis of the acid methyl esters was discussed previously in Chapter 3.

5.2.2 Conversion of petroleum NA to hydrocarbons

The alicyclic acid methyl ester Ag-Ion fractions of the petroleum NA, were converted to the corresponding hydrocarbons using the method developed in Chapter 4. The general procedure for the conversion to hydrocarbons is described in Chapter 2, Section 2.3.

Retention of the low molecular weight hydrocarbons (C_{9-11}) was considered important for the identification of the bicyclanes and thus of the bicyclic acids. Therefore a Kuderna-Danish apparatus was used to concentrate the final hydrocarbon products of each fraction, the concentration procedure is described in Chapter 2, Section 2.3.4.

5.2.3 GC×GC-MS

The GC×GC-MS instrumentation used is described in Chapter 2, Section 2.1.4. Samples were analysed using two different temperature programmes (referred to as conditions A and B). The GC×GC-MS conditions A involved the primary oven programmed from 30°C, held for 1 min, then heated to 120°C at 5°C min^{-1}, to 220°C at 0.8°C min^{-1}, to 280°C at 5°C min^{-1} and to 320°C at 10°C min^{-1} and then held for 10 min. The secondary oven was programmed to track the primary oven at 40°C above. The hot jet was programmed to start 30°C above the primary oven temperature until 150°C, it was then ramped to 260°C at 1.3°C min^{-1} and then to 400°C at 4°C min^{-1}. The modulation period was set at 4 or 6 s. The GC×GC-MS conditions B involved the primary oven

programmed from 30°C, held for 1 min, then heated to 200°C at 1°C min^{-1} and to 320°C at 10°C min^{-1} and then held for 2 min. The secondary oven was programmed to track the primary oven at 5°C above. The hot jet was programmed to track the primary oven at 5°C above. The modulation period was set at 2 s.

5.3   Results and Discussion

5.3.1   Fractionation and GC×GC-MS of acid methyl esters

The petroleum acid mixture gifted in 2009 from Merichem Co. (Batch no. CN/138, CAS# 1338-24), was first derivatised to the acid methyl esters with BF$_3$-MeOH at 70 °C before separation by argentation (Ag-Ion) chromatography. The free acids were derivatised to the acid methyl esters prior to fractionation in order to reduce the interaction of the carboxylic functional group with the Ag-Ion phase. The separation of the acid methyl esters was thus mainly dependent on the aromatic interactions with the phase only. Derivatisation of the free acids also meant the collected fractions, after concentration, were ready for analysis by GC-MS and GC×GC-MS.

Seifert *et al.* (1969) fractionated the final hydrocarbon product obtained from the reduction of acids extracted from crude oil after the conversion by silica chromatography. However in the current study, the NA were fractionated before conversion to the hydrocarbons in order that the fractions and any acids identified in the fractions could be compared, if necessary, with previous studies on NA from commercial and OSPW sources, which have utilised the same fractionation procedure (Jones *et al.*, 2012; Reinardy *et al.*, 2013; Scarlett *et al.*, 2013; Rowland *et al.*, 2014a).

Fractionation reduced the overall complexity and allowed separation of broadly 'alicyclic' ester fractions (Figure 5-2; A-C). The 'alicyclic' fractions were the first four fractions, eluting with 100% hexane (Table 2-1, Chapter 2, Section 2.2.5). The total mass of the four alicyclic fractions collected (248 mg) accounted for 80.0% of the total mass of acid methyl esters (310 mg) loaded onto the Ag-Ion column. Fraction 1 contained 110.0 mg (35.5%), fraction 2; 125.0 mg (40.3%), fraction 3; 12.4 mg (4.0%) and fraction 4 contained 0.6 mg (0.2%).

This high proportion of non–aromatic, poorly retained (by Ag-Ion chromatography) 'alicyclic' acids methyl esters correlated well with data from previous studies using ESI-HRMS, HPLC-ESI-HRMS and Orbitrap-MS, which have also shown commercially available petroleum-derived NA to be dominated by $z = 0$ to $z = -6$, non-aromatic species (Bataineh *et al.*, 2006; Martin *et al.*, 2008; Hindle *et al.*, 2013; Marentette *et al.*, 2015a). The use of Ag-Ion chromatography also ensured that the dominant species, possessing some degree of hydrogen deficiency (e.g. $z = -2$, -4 and -6), were in fact cyclic as opposed to containing (non-aromatic) double bonds, because unsaturated compounds as well as aromatics would be retained on the Ag-Ion column.

Previously, GC×GC-MS of the methyl esters of two other commercial NA samples showed that over 100 bicyclic acids were typically present (Damasceno *et al.*, 2014). Examination of the current methyl ester fractions by GC-MS and GC×GC-MS also showed that fractions 2 and 3 contained relatively abundant, homologous series' of peaks with apparent molecular ions corresponding to those of bicyclic acid methyl esters (e.g. *m/z* 168, 182, 196, 210 etc.) (Figure 5-2; D and E). Therefore fractions 2 and 3 (F2 and F3) were selected herein for conversion to the corresponding hydrocarbons. Fraction 1 contained 35.8% of alicyclic components by mass; however EIC mass chromatograms indicated it was dominated by $z = 0$, straight chain and branched acid methyl esters.
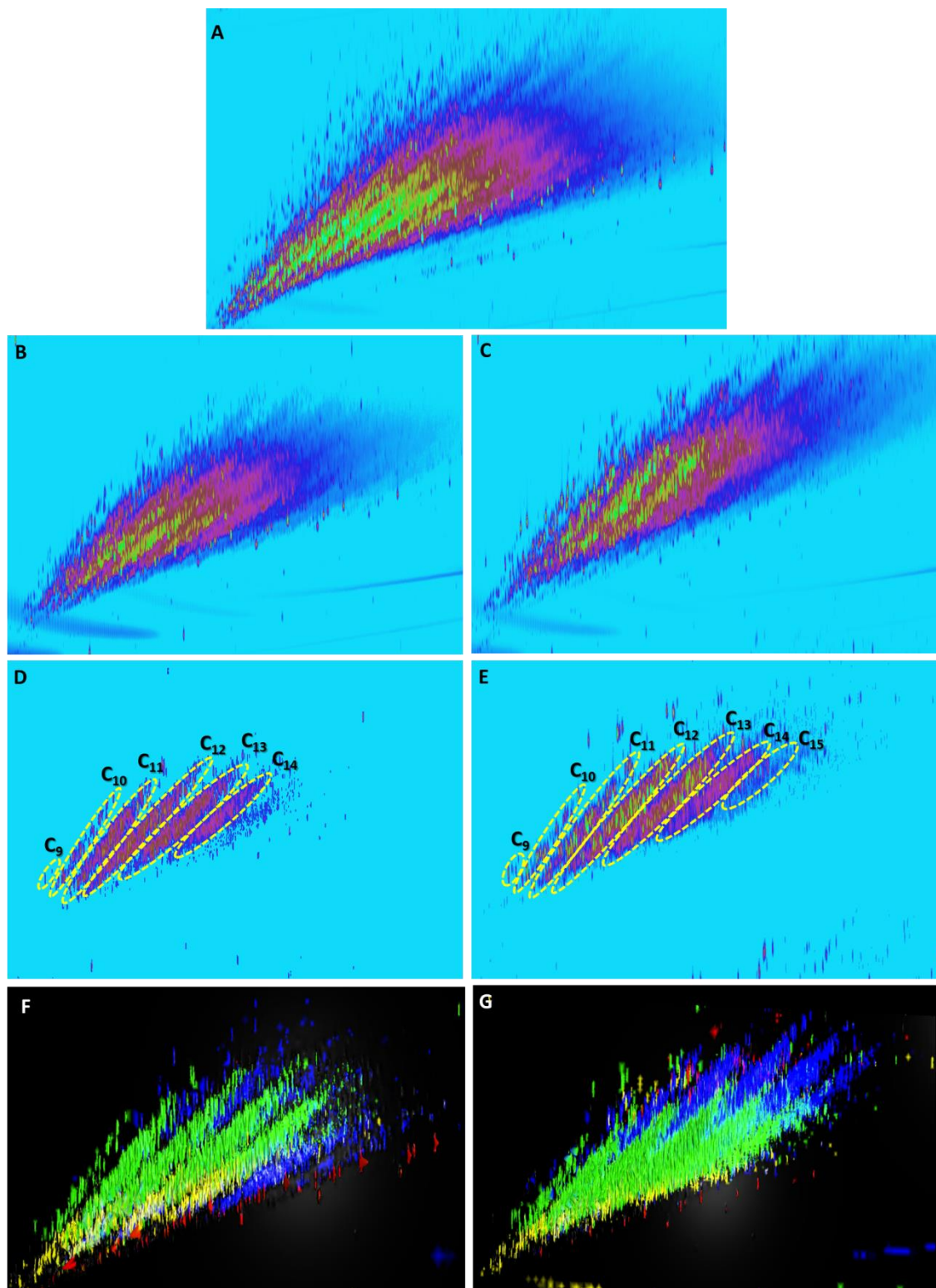
Figure 5-2: TICs (colours based on total ion intensity) of (A) unfractionated petroleum-derived NA methyl esters. (B) NA methyl esters of F2 and (C) F3 after Ag-Ion chromatography and EICs (m/z 168, 182… 252) of (D) F2 and (E) F3 showing homologous series' of C_{9-15} bicyclic acid methyl esters. TICs (colours based on molecular ions for z = 0 to -6 species; z = 0, red; -2, yellow; -4, green and -6, blue) for (D) F2 and (E) F3 highlight the separation of alicyclic acid methyl esters by carbon number in the first dimension and cyclicity in the second dimension. (Column set A, conditions A).

5.3.2 Yields of conversion

The three step conversion was performed on ~50 mg and 9 mg of fractions 2 and 3 acid methyl esters, respectively. It was anticipated that only small quantities of NA mixtures would be available for investigation in most subsequent studies and therefore the conversion was developed and tested on similar quantities of the 'model' acids (5 – 50 mg; Chapter 3 and Chapter 4). The starting masses of reactants and final masses of products for each stage of the conversions are given in Table 5-1. An approximate percent yield was determined using an approximate average molecular weight of 210 g mol^{-1} for the acid methyl esters in fractions 2 and 3, based on the carbon number range and distribution of acid methyl esters maximising at C_{12-13}. The estimated molecular weight was kept the same for fractions 2 and 3 as Ag-Ion chromatography separates the compounds based on their affinity for the phase through pi-bond interactions and not molecular weight.

Table 5-1: Summary of the masses and yields for the conversion of fractions 2 and 3 of commercial NA to the hydrocarbons.

| Starting Reactant | Starting mass and yield / mg (approx. percentage yield / %) | | | | | |
| | LiAlH$_4$ Reduction | | Tosylation | | Super-Hydride® Reduction | |
	NA methyl esters / mg	Alcohols / mg	Alcohols / mg	Tosylates / mg	Tosylates / mg	Hydrocarbons / mg*
Fraction 2	50[†]	43.5 (99%[‡])	43.5	63.8 (82%[‡])	63.8	-
Fraction 3	9[†]	8.7 (107%[‡])	8.7	11.3 (73%[‡])	11.3	-

[†]approximate masses, as methyl esters
[‡]approximate yield based on average molecular weight of acid methyl esters being 210 g mol^{-1}
* Kuderna-Danish apparatus used to concentrate to minimum volume to reduce volatile compound losses so no gravimetric weight recorded

5.3.3 GC×GC-MS of hydrocarbon products

Reduction of the 'alicyclic' (F2 and F3) ester fractions by the methods developed herein (Figure 5-1), as expected, produced mixtures of the corresponding bicyclic hydrocarbons. Examination of these by GC×GC-MS demonstrated excellent separations. Extracted ion monitoring of the expected molecular ions (e.g. *m/z* 138, 152, 166) revealed highly resolved homologous series of >150 bicyclanes (Figures 5-3 and 5-6, page 221). Fractions 2 and 3 contained bicyclanes assigned from molecular ions maximising between C_{9-15} (F2) and C_{10-15} (F3) (Figure 5-3).
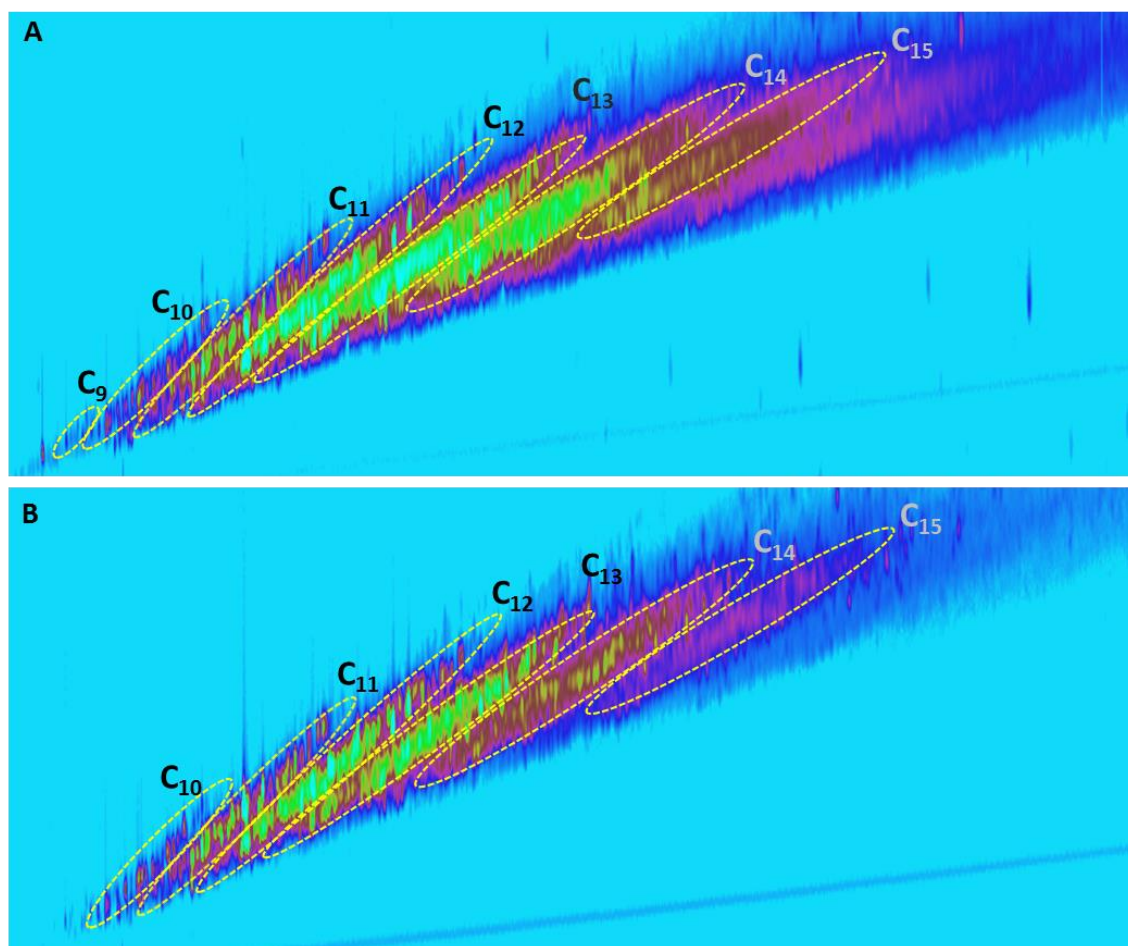
Figure 5-3: EICs (*m/z* 124, 138, 152, 166, 180, 194 and 208) of the hydrocarbon products of (A) fraction 2 and (B) fraction 3, showing abundant homologous series' of bicyclanes separated by carbon number. (Column set A, conditions A).

Separation was also observed between individual isomers of the same carbon number with and without the same hydrogen deficiency. For example, C_{10} and C_{11} bicyclanes were separated, monocyclic C_{11} and bicyclic C_{11} hydrocarbons were separated and individual C_{10} bicyclanes were resolved (Figures 5-3 - 5-6). This was achieved by careful and systematic manipulation of the GC×GC-MS conditions.

Investigations into optimisation of GC×GC-MS conditions and column set selection are usually based on maximising the separation between different classes of compounds (i.e. non-polar species such as alkanes, from aromatic and polar species such as oxygen-, nitrogen- and sulphur-containing (NSO) compounds (Omais *et al.*, 2013)). To obtain maximum separation in both GC 'dimensions', a so-called 'orthogonal' column set is recommended (Watson *et al.*, 2007). For a system to be deemed orthogonal, the mechanism of separation for each column must be independent of the other (Watson *et al.*, 2007). For example, a typical orthogonal column set is a primary GC column with a non-polar stationary phase and a secondary GC column with a mid-polarity or polar stationary phase (Edwards *et al.*, 2015). The general mechanism of separation in the primary column is 'volatility / boiling point' or more specifically, dispersive or induced-dipole interactions. The general mechanism of separation in the second dimension is 'polarity' or more specifically, dipole-dipole and dipole-induced dipole interactions. Methods for measuring the orthogonality of a GC×GC system have focused on examination of the area of chromatographic space occupied by peaks across both dimensions, relative to the maximum space and peak capacity (Omais *et al.*, 2013). Therefore an orthogonal system should utilise the maximum chromatographic space, separating the peaks in both dimensions.

However, Omais *et al.* (2013) reviewed the separation of paraffins, naphthenes, aromatics and NSO compounds in coal-derived oil using several different column sets

including orthogonal (non-polar $\times$ polar), non-orthogonal (polar $\times$ non-polar) and unconventional (polar $\times$ electrostatic polar) column sets. They showed that column sets defined as non-orthogonal based on their generic separation mechanism (e.g. polar $\times$ non-polar) showed maximum use of the two-dimensional chromatographic space. Furthermore, the unconventional column set (polar $\times$ electrostatic polar) proved particularly useful in specifically separating phenols from aromatics and NSO compounds. Therefore, it would appear that the criteria for an orthogonal system are not necessarily the same criteria required to obtain best group-type separation and best separation of specific classes.

The current investigation focused on separating compounds within the same class (i.e. acid methyl esters or hydrocarbons as opposed to group-type separation). The main separation mechanism was predicted to be non-polar, dispersive interactions. Therefore a 60 m 100% dimethylpolysiloxane (non-polar) phase was selected as the primary column to achieve optimum separation in the first dimension. The results showed the main separation in the first dimension was due to volatility/boiling point, with individual homologous series separated based on carbon number (Figure 5-3). Further separation between individual isomers of the same carbon number was also observed in the first dimension, thought to be due to the additional length of the column and slow temperature gradient. This was supported by experiments involving varying the temperature gradient; slowing the temperature gradient resulted in increased separation between C_{10} bicyclanes (Figure 5-4).

A mid-polarity, 2 m 50% phenyl dimethylpolysiloxane (BPX50) was selected as the secondary column so that any monoaromatics eluting early during the Ag-Ion chromatography, unreacted intermediates from the conversion and functionalised by-products and impurities in the reduced hydrocarbon products, would be well separated

from the analytes of interest (i.e. the bicyclic hydrocarbons). The mode of separation of the mid-polarity column on the acid methyl esters and hydrocarbons was difficult to predict, especially for the hydrocarbons, which do not possess a functional group capable of polar interactions. However, previous investigations using a similar non-polar × mid-polar column combination achieved separation between acyclic and cyclo-alkanes (Cochran and Pijpelink, 2011).

The separation observed in the second dimension appeared to be different from that observed in the first dimension but could not be described as fully orthogonal. In the second dimension, alicyclic compounds were mainly separated based on their cyclicity, with acyclic compounds eluting first (red in Figure 5-2; F and G), followed by monocyclics, bicyclics and finally tricyclics, eluting near the top of the chromatogram for both the acid methyl esters and hydrocarbons (yellow, green and blue in Figure 5-2; F and G) with some tetracyclic and monoaromatic compounds eluting even later. Separation appeared to be dependent on variations in the cyclic 'core', causing subtle differences in the interactions with the stationary phase.

Using the chosen column combination (Chapter 2, Section 2.1.4), several GC×GC-MS methods were trialled in an attempt to obtain maximum separation of both the acid methyl esters and hydrocarbons under the same run conditions for comparative purposes. The four main variables for optimisation were the primary oven temperature gradient, modulation period, secondary oven temperature offset and modulation temperature (hot jet) offset.

Changes to the modulation temperature offset and the secondary oven temperature offset mainly affected the separation in the second dimension. The secondary oven offset was kept constant at 40 °C higher than the primary oven to encourage rapid elution through the secondary column. The temperature of the hot jet during the

modulation was set 30 °C above the primary oven gradually increasing to an 80 °C offset over the length of the run to improve peak shape of higher boiling point compounds particularly for the acid methyl esters which eluted much later than the corresponding hydrocarbons.

Optimal separation of the hydrocarbons was achieved with a slow temperature gradient and short modulation time of 2 s with some 'wrapping' in the secondary dimension (Figure 5-4). The 'wrapping' phenomenon is caused when the compounds don't elute from the secondary column fast enough in the short modulation period, and are therefore incorporated in the next modulation phase (Zoex, 2015). However these conditions were unsuitable for the acid methyl esters, which showed considerable wrapping with modulation times shorter than 4 s, even with a higher secondary and modulation temperature offset. Therefore, the optimal run conditions which gave the best separation and peak shape for the acid methyl esters along with sufficient separation of the hydrocarbons, without reduced resolution of individual isomers and hence potential for identification by mass spectral comparison, were a fast temperature gradient and a 4 or 6 s modulation (Figure 5-5).
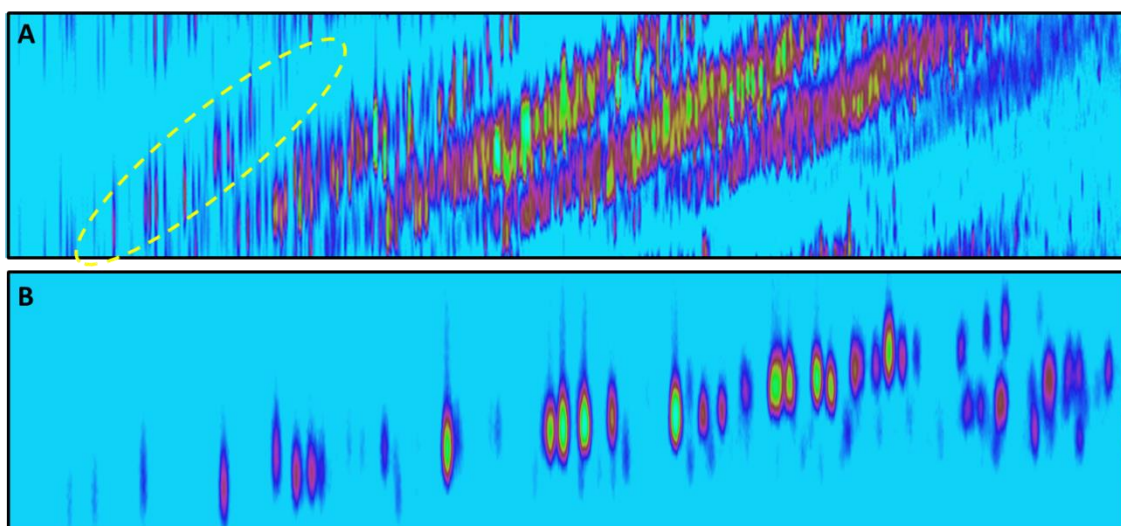
Figure 5-4: (A) EIC (*m/z* 138, 152, 166, 180, 194) showing separation of C_{10-14} hydrocarbons and (B) a region of the EIC (*m/z* 138) showing highly resolved C_{10} hydrocarbon peaks, using an optimised, slower hydrocarbon temperature program with 2 s modulation (Wilde and Rowland, 2015). (Column set A, conditions B).
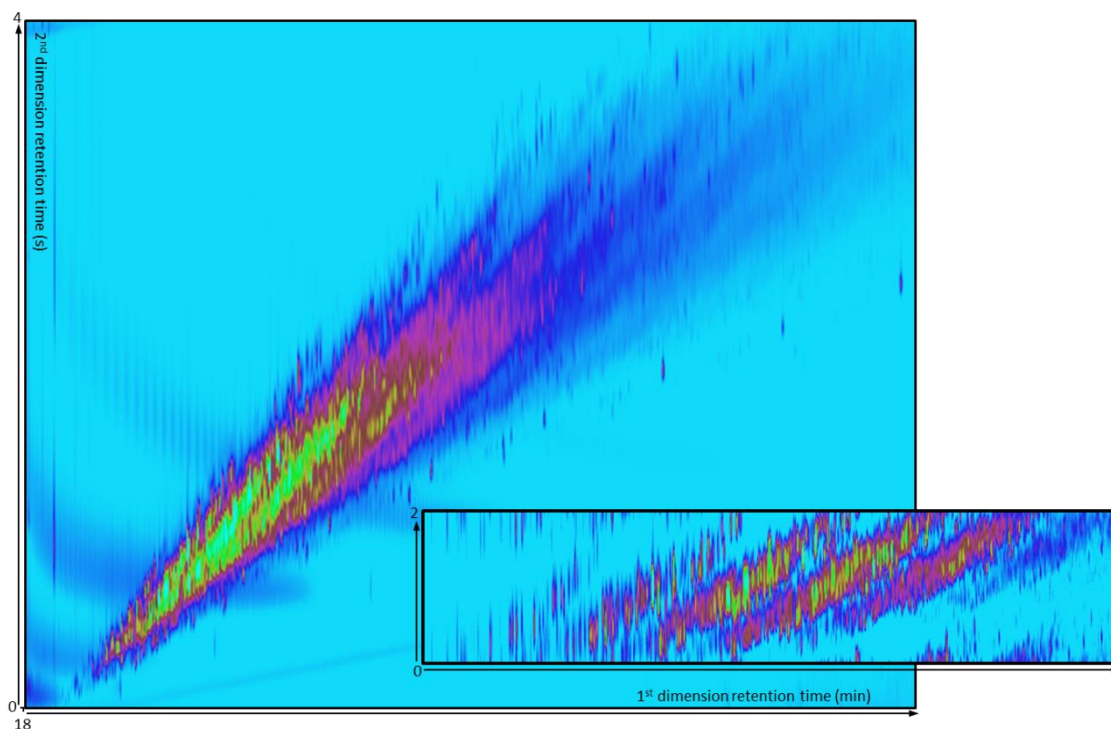
Figure 5-5: Full TIC of the F3 hydrocarbon products using the same temperature gradient optimised for the acid methyl esters with a 4 s modulation, showing minimal wrapping, sufficient separation and no loop-breakthrough of volatile components (Wilde and Rowland, 2015) (Conditions A). Insert shows EIC displaying further separation of homologous series' with a 2 s modulation with wrapping (Wilde and Rowland, 2015) (Conditions B).

The excellent GC×GC separation meant clear, distinguishable mass spectra could be obtained for individual components probably for the first time, and certainly in stark contrast to those obtained in earlier GC-MS studies (Seifert *et al.*, 1969; Seifert and Teeter, 1970b). This was crucial for assignment of individual compounds by MS.

Alongside the excellent separation provided by GC×GC-MS, fractionation by Ag-Ion chromatography of the methyl esters prior to the reduction step also aided identification, by decreasing the complexity of the final hydrocarbon products. Analysis of the hydrocarbons resulting from the transformation of each of the alicyclic NA ester fractions (F2 and F3) separately, further reduced co-elution. For example, some bicyclic hydrocarbons, which co-eluted with monocyclic hydrocarbons in F2, were identifiable in F3, where the monocyclics were absent. Separation of the different alicyclic acids (e.g. acyclic, mono-, bi- and tricyclic acid methyl esters) by Ag-Ion chromatography in fractions 2 and 3 was observed in Figure 5-2; F and G. Fraction 3 showed the disappearance of acyclic (red) and monocyclic (yellow) acids and an increase in tricyclic (blue) acids (Figure 5-2; G).

Recovery of the volatile, lower carbon number (e.g. C_{9-11}) bicyclanes was attributed to the mild reaction conditions employed and effective use of the Kuderna-Danish apparatus to reduce evaporative losses (Scarlett *et al.*, 2011). Retaining these low molecular weight bicyclics was important for the subsequent identifications because the majority of published studies report the mass spectra of low molecular weight alkanes (Denisov *et al.*, 1977d; Denisov *et al.*, 1977c; Denisov *et al.*, 1977b; Denisov *et al.*, 1977a). A mass spectral database of bicyclic hydrocarbons was collated herein and spectra plotted from tabulated data in the literature, along with published retention position and elution order data, where available. Much of this mass spectral information was obtained from older literature, particularly from Russia; early Russian

investigations involved extensive research into the isolation and identification of individual petroleum hydrocarbons, which rivalled that of the famous API Project 6 (Lochte and Littmann, 1955). However, none of these studies used the approach herein to infer the structures of the corresponding bicyclic acids.

5.3.4 Identification of bicyclic petroleum NA as hydrocarbons

The combination of the separation power of GC×GC-MS, coupled with the older approach of chemical transformation of the acids (esters) to hydrocarbons, resulted in the identification of over 40 individual bicyclic NA as the corresponding hydrocarbons by mass spectral comparison with published mass spectra of known alkanes (Figure 5-6). These included bicyclo[4.4.0]decanes, bicyclo[4.3.0]nonanes, bicyclo[3.3.1]nonanes, bicyclo[2.2.2]octanes, bicyclo[3.3.0]octanes and bicyclo[3.2.1]octanes, as well as some more highly substituted terpenoid bicyclanes (Figure 5-7).
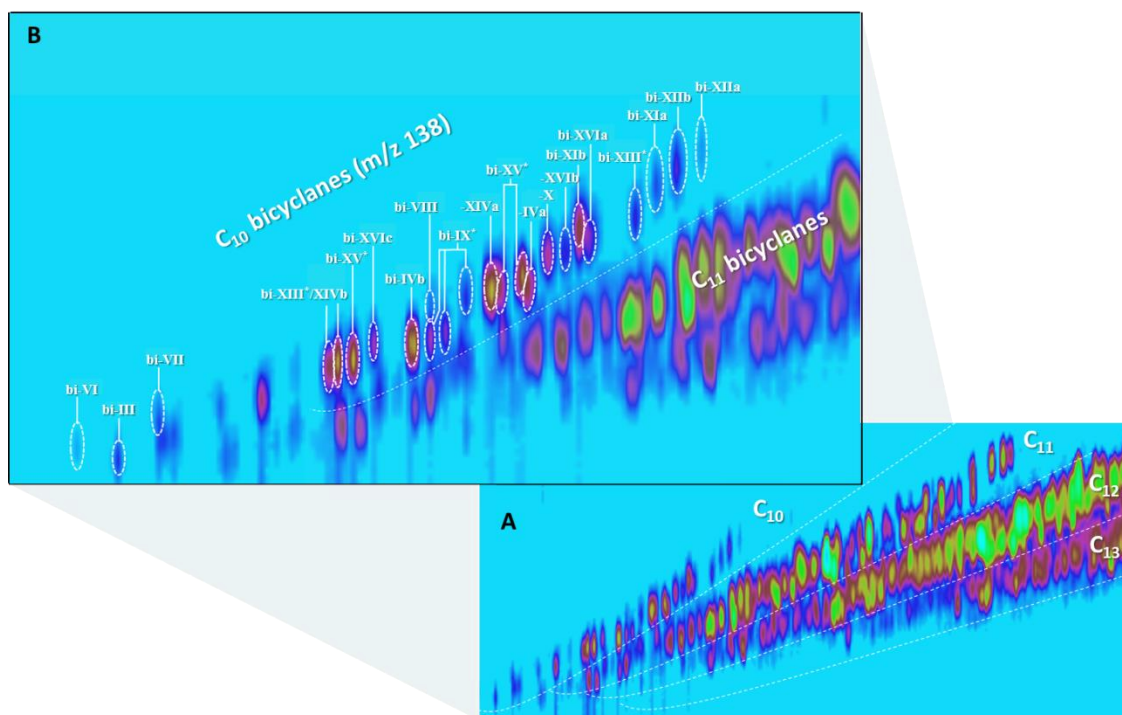
Figure 5-6: (A) EIC of C_{10-13} bicyclanes (*m/z* 138, 152, 166, 180) in the F3 hydrocarbon product showing clear separation of homologous series by carbon number (Wilde and Rowland, 2015). (B) Zoomed insert showing sufficient separation of individual C_{10} homologues for identification by comparison with literature reference mass spectra (Wilde and Rowland, 2015). Labels correspond with structures in Figure 5-7.
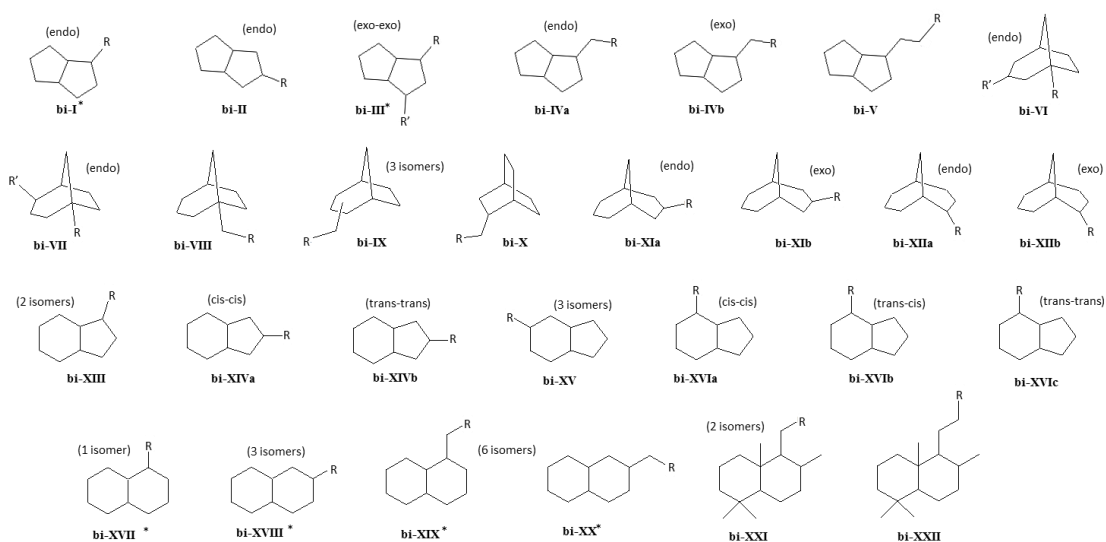
Figure 5-7: Bicyclic hydrocarbons identified by conversion of petroleum acids to alkanes and comparison of mass spectra with those of known hydrocarbons. The identification of the alkanes allows inference of the structures of the corresponding bicyclic acids, which were previously unknown for decades (*presence of acid methyl ester confirmed with reference compound). For mono-substituted bicyclics R = CH$_3$ in bicyclanes; CO$_2$H in acids. For di-substituted bicyclics R, R' = CH$_3$ in bicyclanes; R = CO$_2$H, R' = CH$_3$ or R = CH$_3$, R' = CO$_2$H in acids.

5.3.4.1 Bicyclo[3.2.1]octanes

Comparison of the mass spectra of the C$_{10}$ hydrocarbons within fractions 2 and 3 after reduction, with those reported by Denisov *et al.* (1977a), gave good matches with those of two dimethyl- and one ethyl-substituted bicyclo[3.2.1]octane (Figure 5-8; A-F). All three isomers were substituted at the quaternary bridgehead in the 1-position (Figure 5-7; **bi-VI-VIII**). The 1,3- and 1,4-dimethyl- isomers were two of the earliest eluting peaks within the C$_{10}$ homologous series and the 1-ethyl- isomer eluted later, as expected (Figure 5-6).
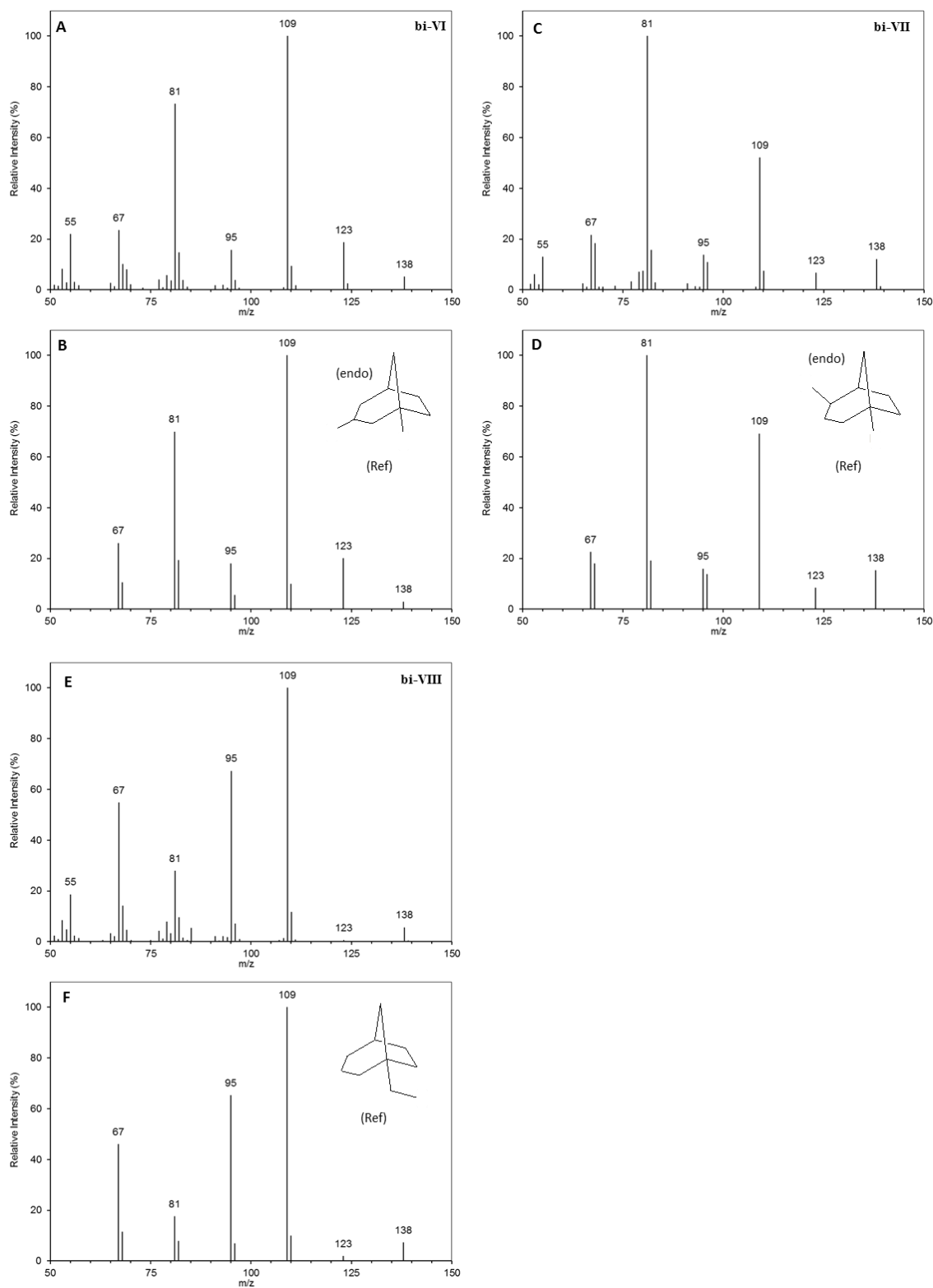
Figure 5-8: (A, C and E) Mass spectra of C_{10} bicyclo[3.2.1]octanes identified within the

F2 and F3 reduced acid products by comparison with (B, D and F) mass spectra

replotted from values previously reported in tablature by Denisov *et al.* (1977a).

The mass spectrum of **bi**-**VII** (Figure 5-8; C) was assigned as the endo- isomer, distinguished from that of the exo- isomer based on the intensity of the m/z 109 and 81 ions; the m/z 81 ion is the base peak ion in the mass spectrum of the endo- isomer, whereas the m/z 109 ion is the base peak ion in the mass spectrum of the exo-isomer similar to that of the 1,3-dimethyl isomer (Figure 5-8; C and D and Appendix Figure 26). The mass spectrum of **bi**-**VI** (Figure 5-8; A) was assigned as the 1,3-dimethyl-isomer and distinguished from that of the exo-1,4-dimethyl isomer based on the intensities of the m/z 123 ion and molecular ion (m/z 138) (Figure 5-8; A, B and Appendix Figure 26).

The mass spectra of both dimethyl- isomers showed intense M-29 and M-57 ions (m/z 109 and 81) corresponding to losses of $\cdot C_2H_5$ and $\cdot C_4H_9$. These fragment ions can be justified by a similar fragmentation route to that suggested for the 'model' bicyclic hydrocarbons (Figure 4-46; Chapter 4, Section 4.4.2.3, page 178), viz; a primary cleavage on either side of a bridgehead carbon, followed by a hydrogen rearrangement and α-cleavage. The mass spectrum of the ethyl isomer, **bi**-**VIII** (Figure 5-8; E) displayed a base peak ion at m/z 109, attributed to loss of the ethyl group due to cleavage at the bridgehead, quaternary carbon. The M-43 ion could be assigned to fragmentation across the largest unsubstituted ring.

Theoretically, a dimethyl- substituted bicyclane such as 1,4-dimethylbicyclo[3.2.1]octane could originate from an acid with the carboxylic acid group originally substituted at either methyl- position (e.g. 1-methylbicyclo[3.2.1]octane-4-carboxylic acid or 4-methylbicyclo[3.2.1]octane-1-carboxylic acid) or on both positions in the case of a diacid (e.g. bicyclo[3.2.1]octane-1,4-dicarboxylic acid). A potentially useful method for determining the original position

of the carboxyl group of a dimethyl-bicyclane, involving deuteroreduction, is discussed in detail in Chapter 7, Section 7.2.2, page 336.

5.3.4.2   Bicyclo[2.2.2]octanes

One of two peaks possessing similar mass spectra, was identified as 2-ethylbicyclo[2.2.2]octane (Figure 5-7; **bi-X**). The spectrum of the second peak resembled that of the 1-isomer but co-eluted with another unknown, making the assignment speculative. The mass spectra matched those reported by Denisov *et al.* (1977d), easily distinguished from the C_{10} dimethylbicyclo[2.2.2]octane isomers by their intense base peak ion at *m/z* 109 corresponding to the dominant loss of $\cdot C_2H_5$ (M-29) (Figure 5-9). The 1-ethyl- and 2-ethyl- isomers had similar mass spectra but could be differentiated by the intensities of the *m/z* 81 and 82 ions; the loss of $\cdot C_4H_9$ (*m/z* 81) being greater for 2-ethylbicyclo[2.2.2]octane and the loss of C_4H_8 (*m/z* 82) being greater for the 1-ethyl isomer (Figure 5-9; B and Appendix Figure 27).
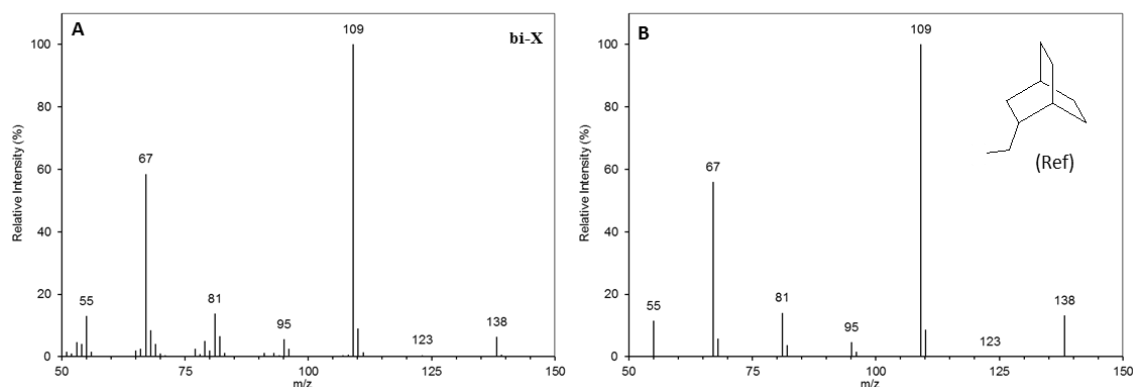
Figure 5-9: (A) Mass spectrum of a peak identified as 2-ethylbicyclo[2.2.2]octane within the F2 and F3 reduced acid products by comparison with (B) a mass spectrum replotted from values previously reported in tablature by Denisov *et al.* (1977d).

The strong intensity of the M-29 ion and the relatively low abundance of the other ions were indicative of a stable structure with a single dominant loss of the ethyl group. The virtual absence of the M-15 ion was typical of an ethyl substituted compound.

5.3.4.3   Bicyclo[3.3.0]octanes

Previously Rowland *et al.* (2011e) reported the presence of 4-methylbicyclo[3.3.0]octane-2-carboxylic acid (also called 3-methyloctahydropentalene-1-carboxylic acid) in commercial NA, but they did not report the mass spectrum. In the current study, the corresponding 2,4-dimethylbicyclo[3.3.0]octane was identified by comparison with a series of bicyclo[3.3.0]octane mass spectra (Figure 5-10; A and B) (Denisov *et al.*, 1977c).

Such assignments were made possible by the pre-fractionation of the alicyclic acid methyl esters by argentation chromatography, prior to reduction to the alkanes. Thus, 2,4-dimethylbicyclo[3.3.0]octane in the reduced hydrocarbons of F2 could not be initially firmly identified, due to co-elution with an unknown C_{10} monocyclic hydrocarbon, which made the mass spectrum less clear. However, in the reduced F3, co-elution with the monocyclic was no longer observed and the mass spectrum of the unknown was clear and similar to that of the authentic bicyclooctane, which was then assigned in both F2 and F3 (Figure 5-10; A and B). The corresponding acid methyl ester in the esterified NA was then confirmed by comparison of the mass spectrum with that of a reference compound (Figure 5-10; C and D). This showed the complementary approach of analysis of both ester and alkane fractions by GC×GC-MS (Chapter 3 and Chapter 5).
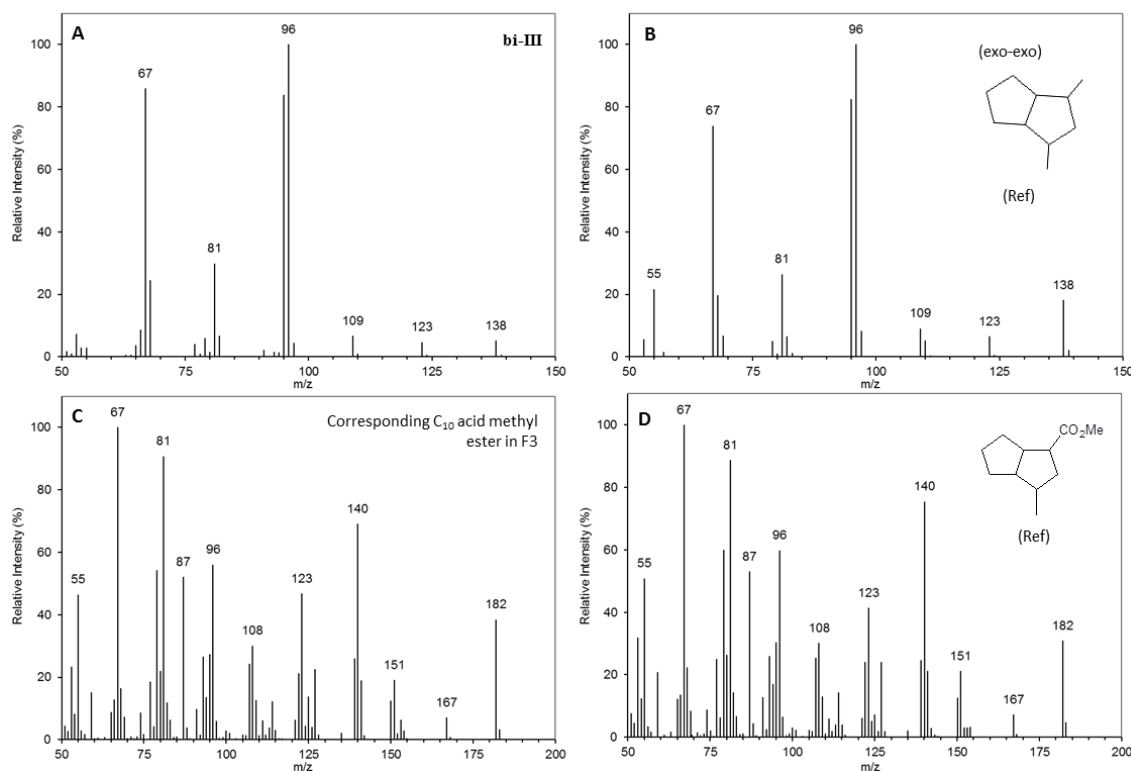
Figure 5-10: (A) Mass spectrum of a C_{10} bicyclic hydrocarbon within F2 and F3 hydrocarbon products, identified as 2,4-dimethylbicyclo[3.3.0]octane by comparison with (B) a reference mass spectrum replotted from values previously reported in tablature by Denisov *et al.* (1977c) as well as the reduced hydrocarbon product of 4-methylbicyclo[3.3.0]octane-2-carboxylic acid used a model acid. (C) The corresponding acid methyl ester was identified within the original acid methyl ester fractions and compared with (D) the mass spectrum of a commercially available reference compound.

In the alkanes, two later eluting peaks were also identified as both 2-ethylbicyclo[3.3.0]octane isomers (Figure 5-11; A and C), the exo- isomer eluting before the endo- isomer; an observation made by Jørgensen *et al.* (1990) as well as Bagrii *et al.* (1967) for the 2-methyl isomers.
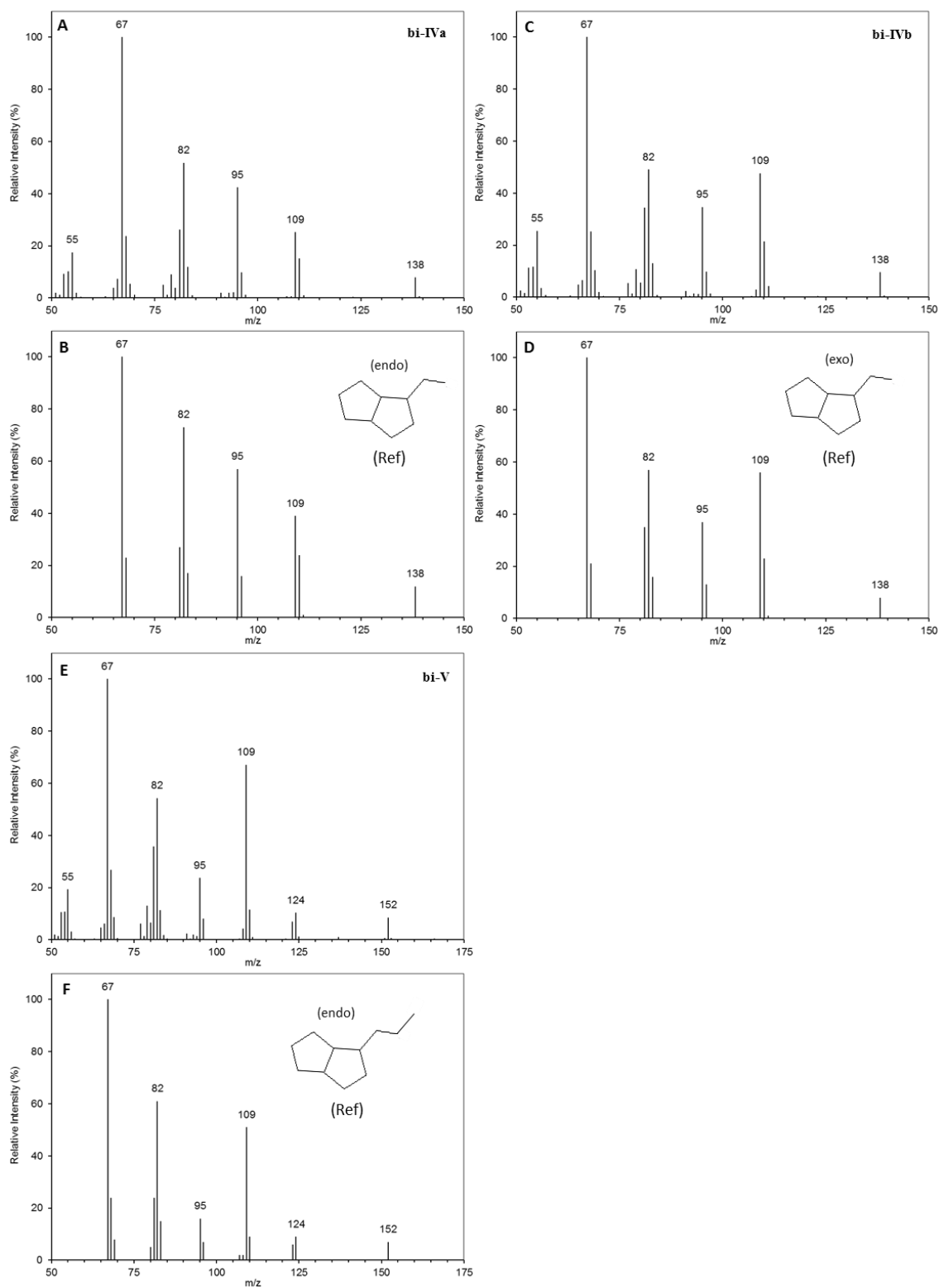
Figure 5-11: (A, C and E) Mass spectra of bicyclo[3.3.0]octanes identified within the F2 and F3 hydrocarbon products by comparison with (B, D and F) mass spectra replotted from values previously reported in tablature by Denisov *et al.* (1977c).

Concentration of the final hydrocarbon products with a Kuderna-Danish apparatus proved extremely efficient at reducing evaporative losses of the <C_{10} bicyclanes. The mass spectra of two C_9 bicyclanes were similar to those of 2-methyl and 3-methylbicyclo[3.3.0]octane (Appendix Figure 28) and comparison of the F2 acid methyl esters with that of an esterified reference compound showed bicyclo[3.3.0]octane-2-carboxylic acid methyl ester was indeed present in the NA mixture, as reported previously in another (Rowland *et al.*, 2011e; Wilde *et al.*, 2015).

Amongst the C_{11} bicyclic hydrocarbons (*m/z* 152) was a component with a mass spectrum matching that of 2-propylbicyclo[3.3.0]octane (Figure 5-11; E). This series of bicyclo[3.3.0]octanes (Figure 5-7; **bi-I-V**), with increasing alkyl chain length (from methyl to propyl) reaffirms the hypothesis that the higher carbon number homologues are more alkylated equivalents of the lower carbon number structures identified herein (Wilde *et al.*, 2015). It was also strong evidence for the current understanding of biodegradation of hydrocarbons along alkyl side chains and the occurrence of NA (Quagraine *et al.*, 2005).

5.3.4.4   Bicyclo[2.2.1]heptanes

Wilde *et al.* (2015) reported the presence of a few bicyclo[2.2.1]heptane acids in an OSPW acid extract which were absent in commercial petroleum NA after analysis of the acid methyl esters. The corresponding hydrocarbons would be expected to have the earliest retention times of the C_{10} hydrocarbons based on the relative positions of the acid methyl esters; bicyclo[2.2.1]heptane-2-ethanoic acid eluted earlier than bicyclo[3.2.1]octane-2-carboxylic acid and bicyclo[2.2.2]octane-2-carboxylic acid (Wilde *et al.*, 2015). Interestingly, no C_{10}-$_{11}$ bicyclo[2.2.1]heptanes were observed in the reduced commercial NA fractions when compared with the mass spectra of the trimethyl-/methylethyl- or tetramethyl/-dimethylethyl-bicyclo[2.2.1]heptane isomers (Rusinova *et al.*, 1981).

5.3.4.5   Bicyclo[3.3.1]nonanes

Three components, eluting the last amongst the C_{10} hydrocarbons, had mass spectra comparable with those of four methylbicyclo[3.3.1]nonane isomers (Figure 5-7; **bi-XI-XII**) reported by Golovkina *et al.* (1979) (Figure 5-12). This corresponds with previous observations of bicyclo[3.3.1]nonane-1- and 3-carboxylic acids identified in commercial NA as the methyl esters (Wilde *et al.*, 2015).

Herein, two isomers of 3-methylbicyclo[3.3.1]nonane were identified (Figure 5-12; A - D), but 1-methylbicyclo[3.3.1]nonane, which has a mass spectrum distinguished by a base peak ion at *m/z* 95, due to the loss of a propyl group (M-43), was not, despite the fact that the presence of the acid methyl ester was confirmed with a reference standard. The corresponding hydrocarbon could have remained unidentified due to co-elution or loss during evaporation. A pair of resolved peaks eluting later than the 3-methyl isomer had mass spectra matching two isomers of 2-methylbicyclo[3.3.1]nonane (Figures 5-6 and 5-12; E-H).

The mass spectra of the methylbicyclo[3.3.1]nonane isomers all possessed medium to strong intensity molecular ions (33 − 63%) (Figure 5-12), due to the relatively stable structure of the bicyclic 'core'; each ring either side of the bridgehead carbons is able to adopt a stable cyclohexyl- chair conformation. The mass spectra of the endo- and exo-3-methylbicyclo[3.3.1]nonane isomers differ significantly, with the exo- isomer showing a strong M-15 ion. The mass spectra of the 2-methyl isomers differed from those of the 3-methyl isomers by the *m/z* 95/96 intensities, with the *m/z* 96 dominant in the 2-methyl isomers, this indicated that the loss of $\cdot C_3H_7$ and C_3H_6 may originate from the substituted ring.
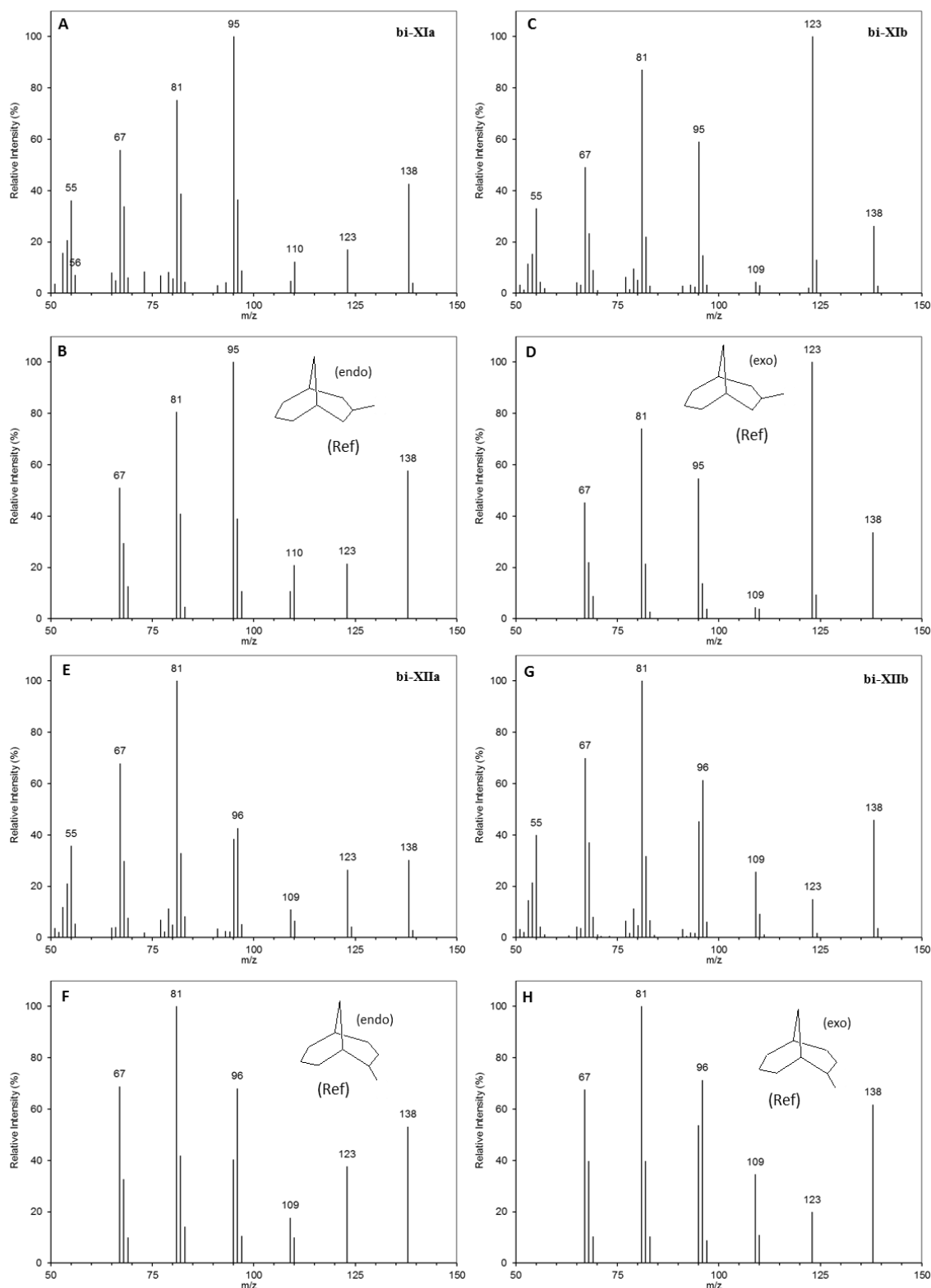
Figure 5-12: (A, C, E and G) Mass spectra of C_{10} bicyclo[3.3.1]nonanes identified within the reduced acid products of F2 and F3 by comparison with (B, D, F and H) mass spectra replotted from values previously reported in tablature by Golovkina *et al.* (1979).

5.3.4.6 Bicyclo[4.3.0]nonanes

Rowland *et al.* (2011e) tentatively identified a series of bicyclo[4.3.0]nonane carboxylic acids based on mass spectral interpretation and comparison with one available mass spectrum of the 2-carboxylic acid isomer (perhydroindane-1-carboxylic acid). They proposed the presence of several isomers. However, the lack of mass spectra available meant they were unable to confirm this or to identify the position of the carboxyl group. Reduction of the commercial NA herein resulted in several methylbicyclo[4.3.0]nonane isomers (Figure 5-7; **bi-XIII-XVI**) being identified by comparison with reference hydrocarbon mass spectra (Denisov *et al.*, 1977b) (Figures 5-13, 5-14 and 5-15).

The isomers with matching mass spectra included structures with the methyl group substituted on the cyclohexyl and cyclopentyl ring, but not on a bridgehead carbon. Methylbicyclo[4.3.0]nonanes substituted at the 7- or 8- position (on the cyclopentyl ring) showed a prominent loss of C_3H_6 (*m/z* 96) (Figure 5-15) compared to those substituted at the 2- and 3- positions (on the cyclohexyl ring) which showed a prominent loss of $\cdot C_3H_7$ (*m/z* 95) (Figures 5-13 and 5-14).
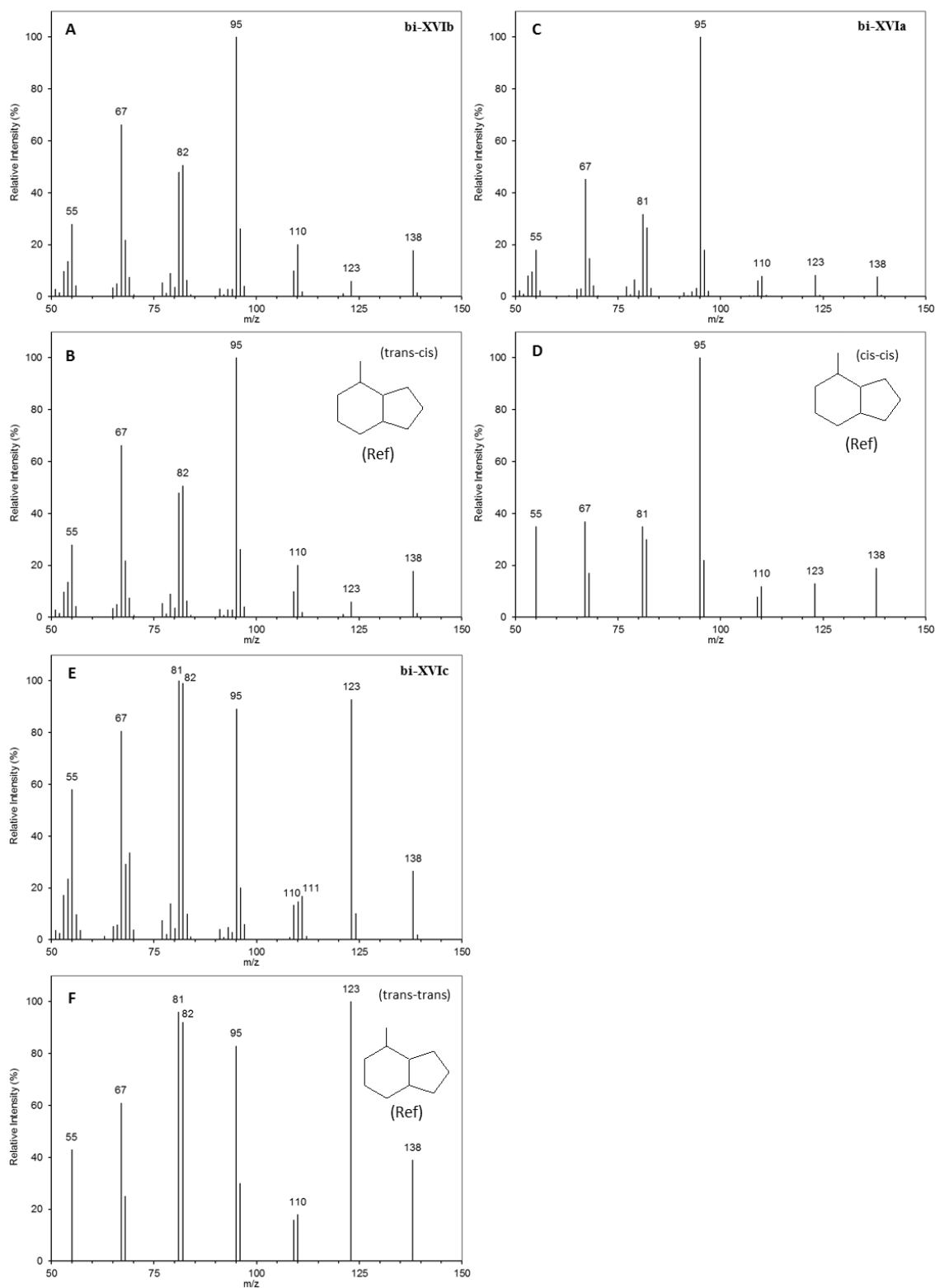
Figure 5-13: (A-F) Mass spectra of peaks identified within the F2 and F3 hydrocarbon products as 2- methylbicyclo[4.3.0]nonanes by comparison with mass spectra replotted from values previously reported in tablature by Denisov *et al.* (1977b).
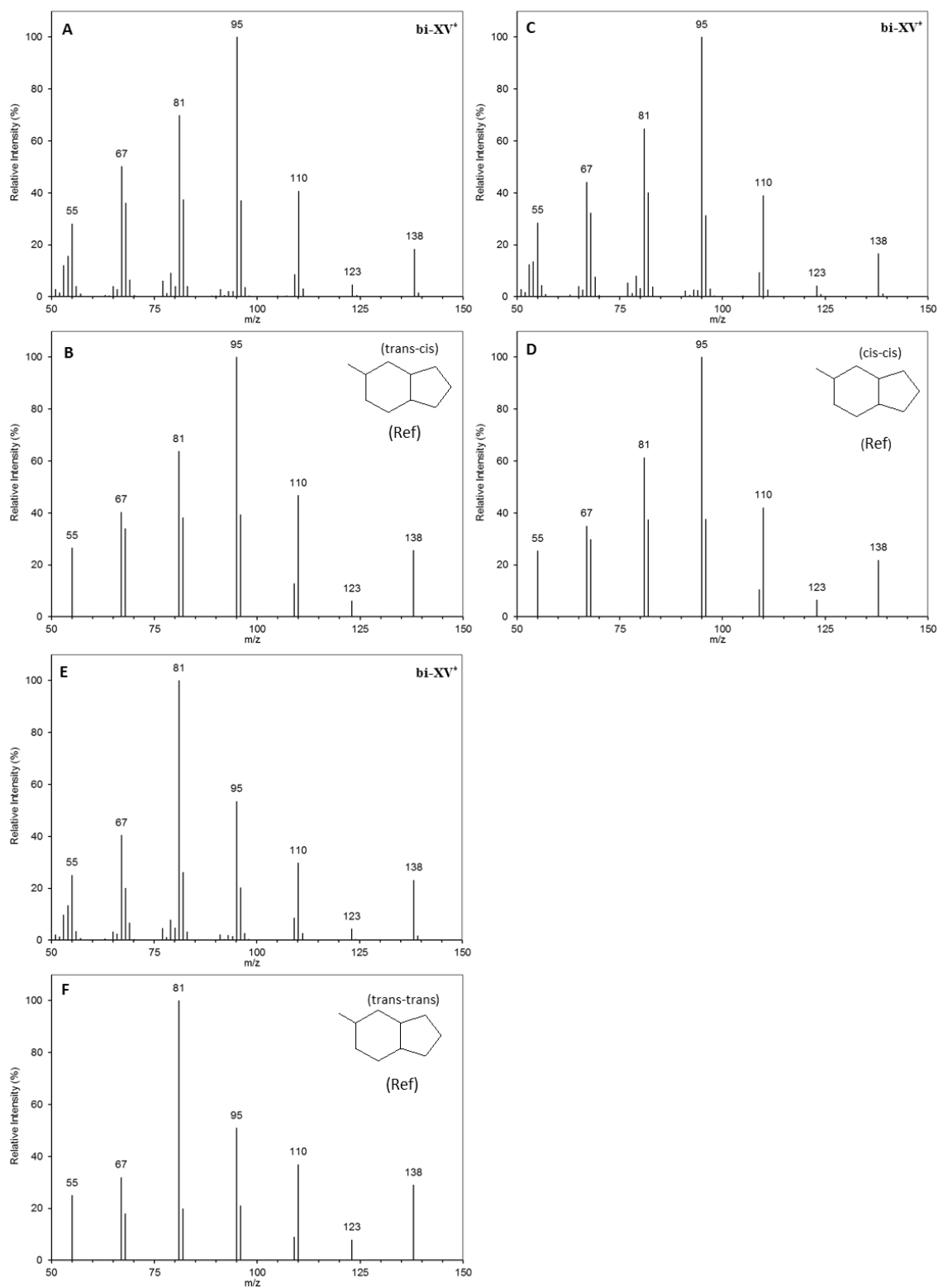
Figure 5-14: (A-F) Mass spectra of peaks identified within the F2 and F3 hydrocarbon products as 3- methylbicyclo[4.3.0]nonanes by comparison with mass spectra replotted from values previously reported in tablature by Denisov *et al.* (1977b).
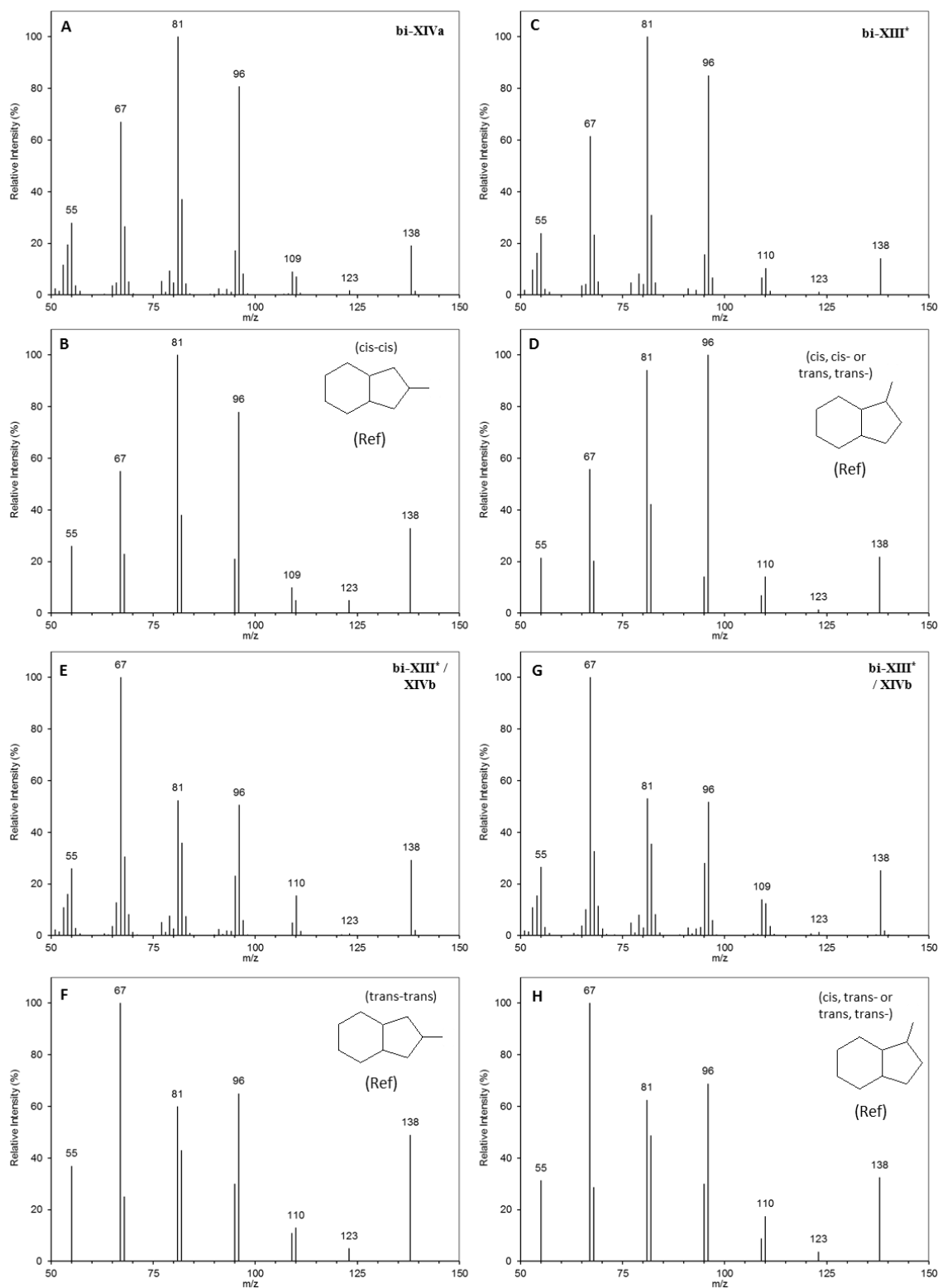
Figure 5-15: (A-H) Mass spectra of peaks identified within the F2 and F3 hydrocarbon

products as 7- and 8-methylbicyclo[4.3.0]nonanes by comparison with mass spectra

replotted from values previously reported in tablature by Denisov *et al.* (1977b).

5.3.4.7 Bicyclo[4.4.0]decanes

Bicyclo[4.4.0]decane acids (decalin acids) are probably the most studied or identifiable acids within the few studies which report EI mass spectra for individual NA. Aitken *et al.* (2004) identified two isomers of bicyclo[4.4.0]decane-3-carboxylic acid (decahydro-2-naphthoic acid) within several biodegraded oils from deep surface reservoirs and proposed they were the reduced product of the anaerobic biodegradation of naphthalene. Rowland *et al.* (2011e) also identified two isomers of bicyclo[4.4.0]decane-3-carboxylic acid and suggested that their presence could be evidence that at least some of the acids present within their commercial NA were a result of anaerobic biodegradation. They also reported that they could not detect any bicyclo[4.4.0]decane-2-carboxylic acid (decalin-1-carboxylic acid) isomers (Rowland *et al.*, 2011e), but without reporting the limits of detection of their methods.

Careful examination of the C_{11} hydrocarbon mass spectra herein and comparison with the reported mass spectra of methylbicyclo[4.4.0]decanes (decalins) (Lukashenko *et al.*, 1973) allowed the identification of three isomers of 3-methylbicyclo[4.4.0]decane and one isomer of 2-methylbicyclo[4.4.0]decane (i.e. decahydro-1- and 2-naphthalene) (Figure 5-16). Subsequent comparison of the corresponding acid methyl ester fractions with synthesised reference compounds confirmed the presence of the bicyclo[4.4.0]decane-2- and 3-carboxylic acid methyl ester isomers (i.e. decahydro-1- and 2-naphthoic acids).
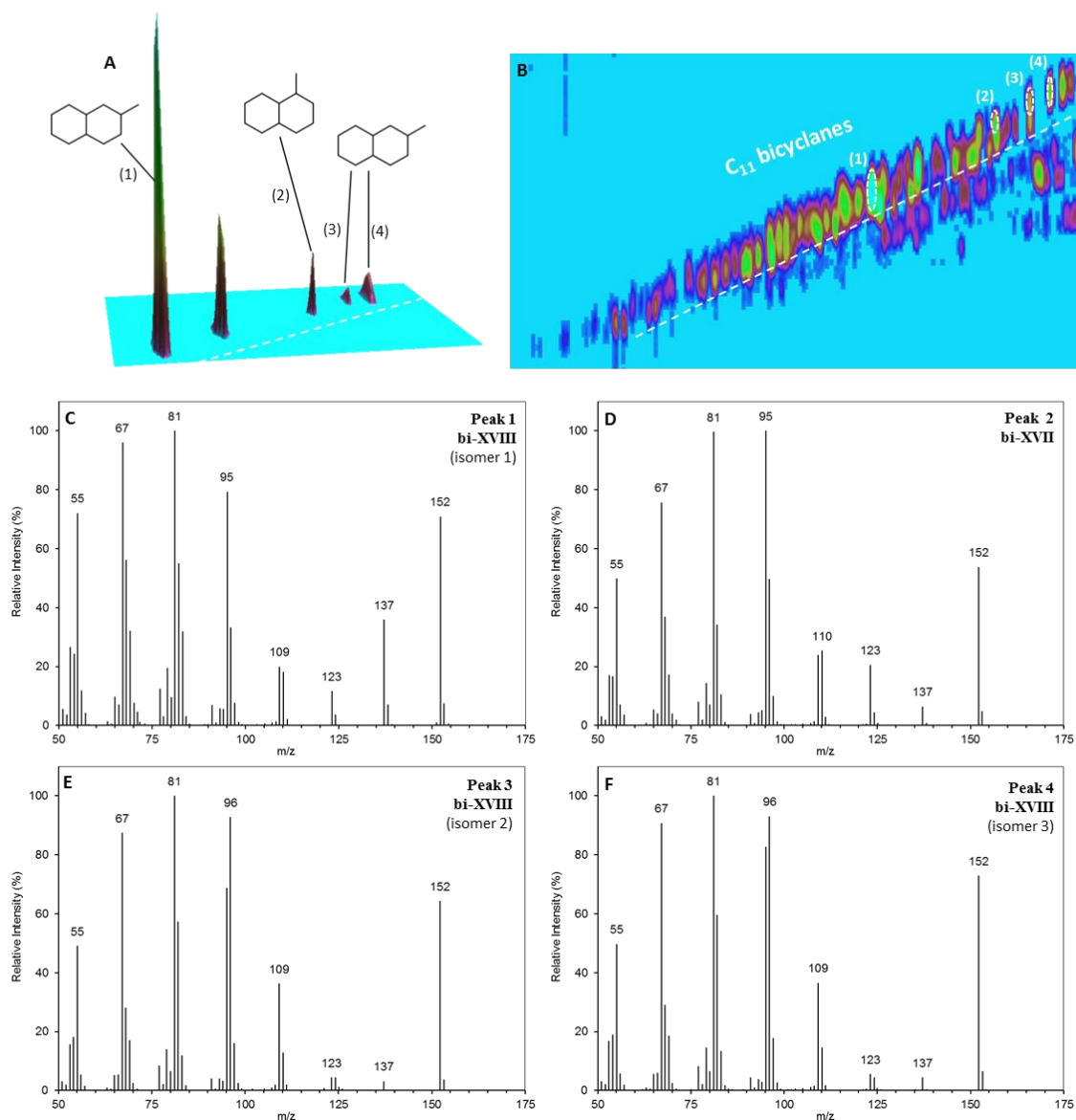
Figure 5-16: (A) 3D representation of a GC×GC chromatogram showing only 5 components after applying the CLIC expression to return data points with an *m/z* 152 ion greater than 50% relative intensity (Relative (152)>50) and (B) a contour plot of an EIC (*m/z* 152) showing the relative retention positions of the peaks. (D) Mass spectrum of one component identified as a 2-methylbicyclo[4.4.0]decane isomer and (C, E and F) the mass spectra of three components identified as 3-methylbicyclo[4.4.0]decane isomers by comparison with the reference mass spectra previously reported by Lukashenko *et al.* (1973) and comparison of the original acid methyl esters' retention positions and mass spectra with synthesised reference compounds; bicyclo[4.4.0]decane-2- and 3-carboxylic acid methyl esters.

The mass spectra of methylbicyclo[4.4.0]decanes are distinguishable from other bicyclanes by their strong molecular ions (*m/z* 152). Using the CLIC expression tool to return data points where the *m/z* 152 ion had a relative intensity greater than 50%, reduced the complexity of the image to that comprising only five peaks, making it easier to identify the methylbicyclo[4.4.0]decanes present (Figure 5-16; A).

Examination of the C_{12} bicyclane mass spectra and comparison with the mass spectra replotted from the tabulated values reported by Brodskii *et al.* (1977), led to the tentative identification of two dimethylbicyclo[4.4.0]decane isomers (Figure 5-17). Furthermore, two major peaks and four later eluting minor peaks had NIST mass spectral matches with 1- and 2-ethylbicyclo[4.4.0]decane isomers (Figure 5-18; A-F). Subsequent analysis of the acid methyl esters and synthesis of the corresponding eight possible ethanoic acid isomers confirmed the two major peaks were isomers of bicyclo[4.4.0]decane-1- and 2-ethanoic acid (methyl esters) with matching mass spectra and retention positions of the reference compounds (Figure 5-19; A-F).
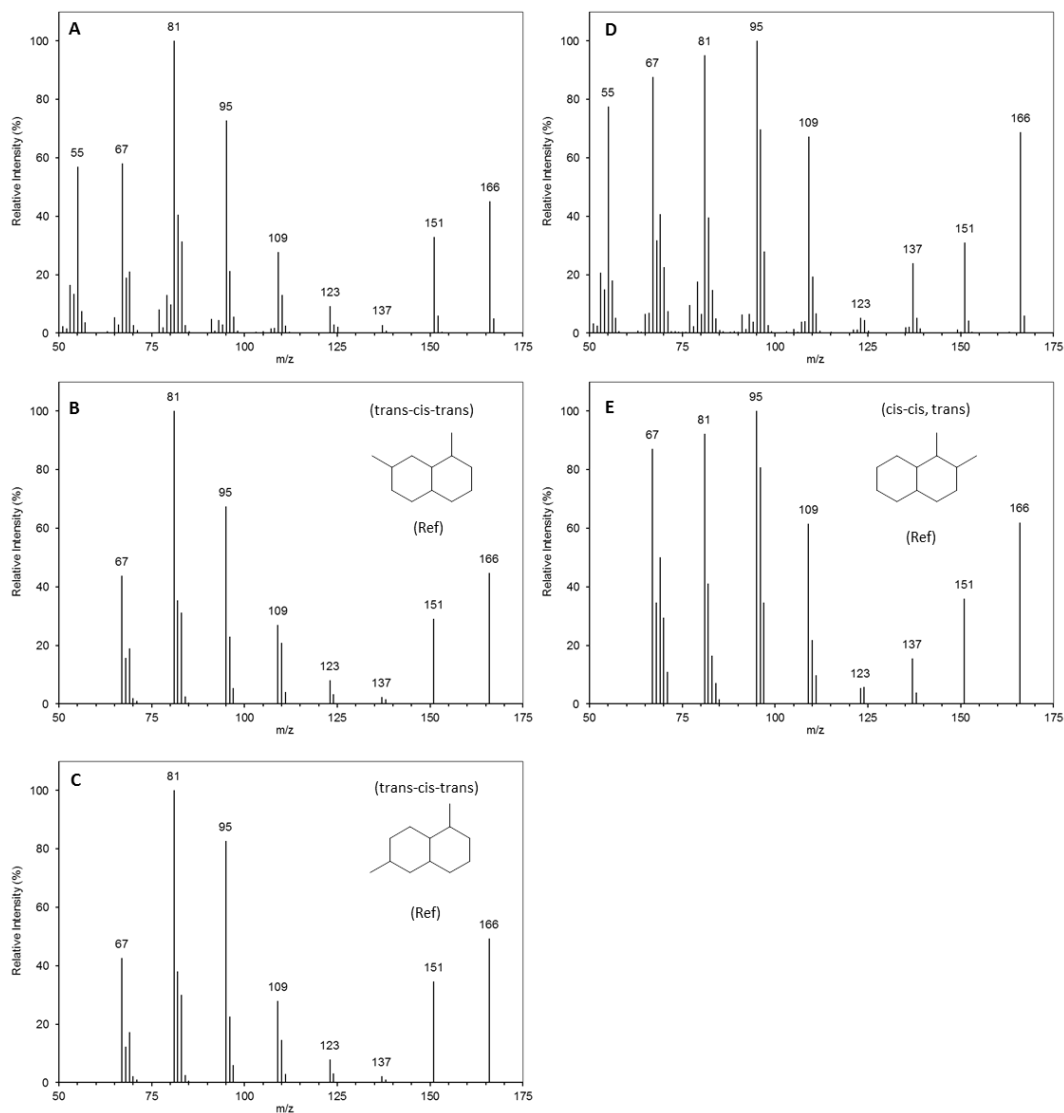
Figure 5-17: (A and D) Mass spectra of some example C_{12} bicyclanes in the F3 hydrocarbon product tentatively identified as dimethylbicyclo[4.4.0]decanes by comparison with (B, C and E) mass spectra replotted from tabulated values previously reported in tablature by Brodskii *et al.* (1977).
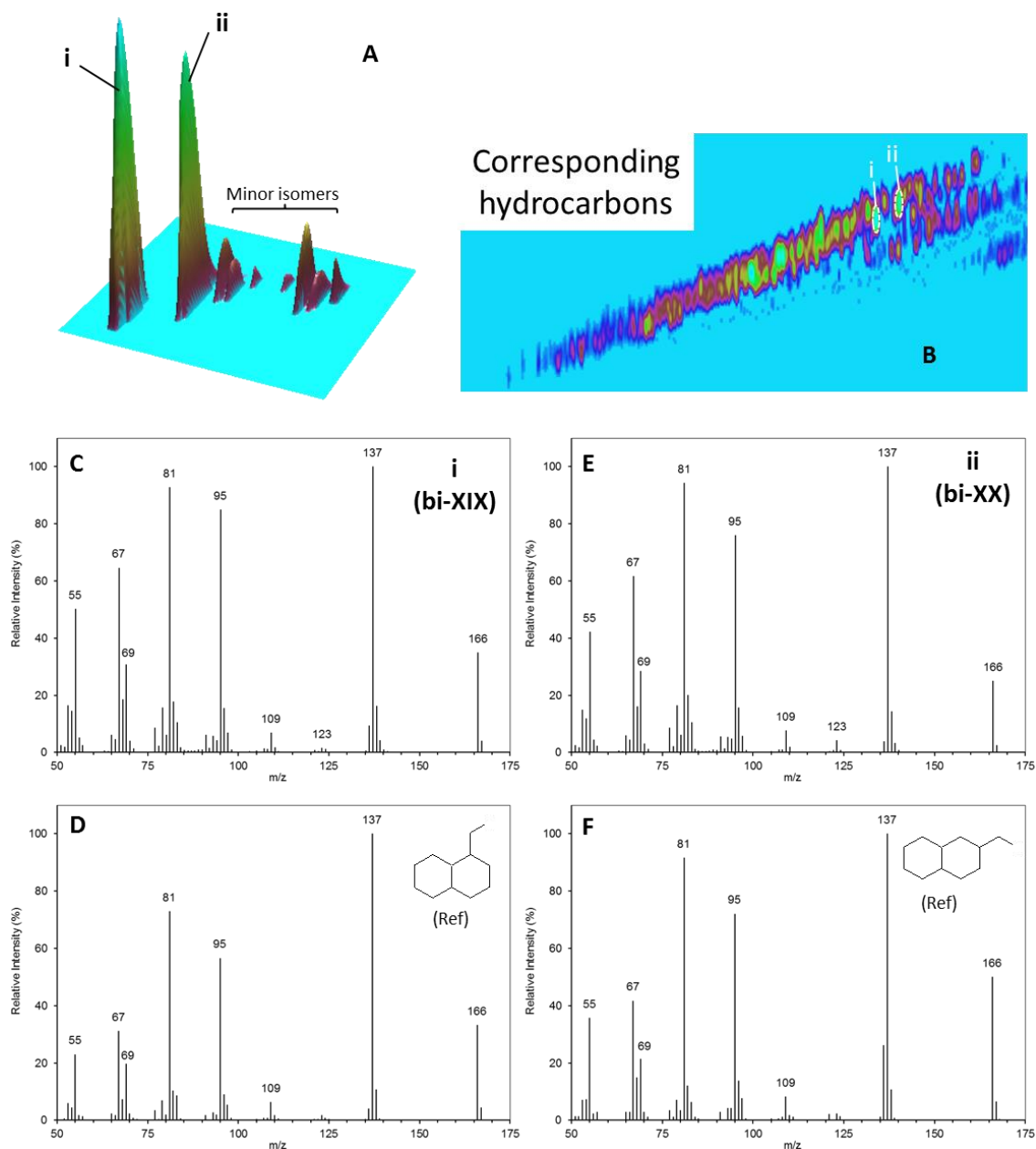
Figure 5-18: (A) 3D representation of a GC×GC chromatogram showing two major peaks in the F2 and F3 hydrocarbon products corresponding to two C_{12} bicyclanes using corresponding CLIC expression and (B) an EIC (*m/z* 166) showing their relative retention positions in relation to the C_{12} bicyclanes with (C and E) mass spectra matching (D and F) NIST library mass spectra of 1-ethyl- and 2-ethylbicyclo[4.4.0]decane isomers.
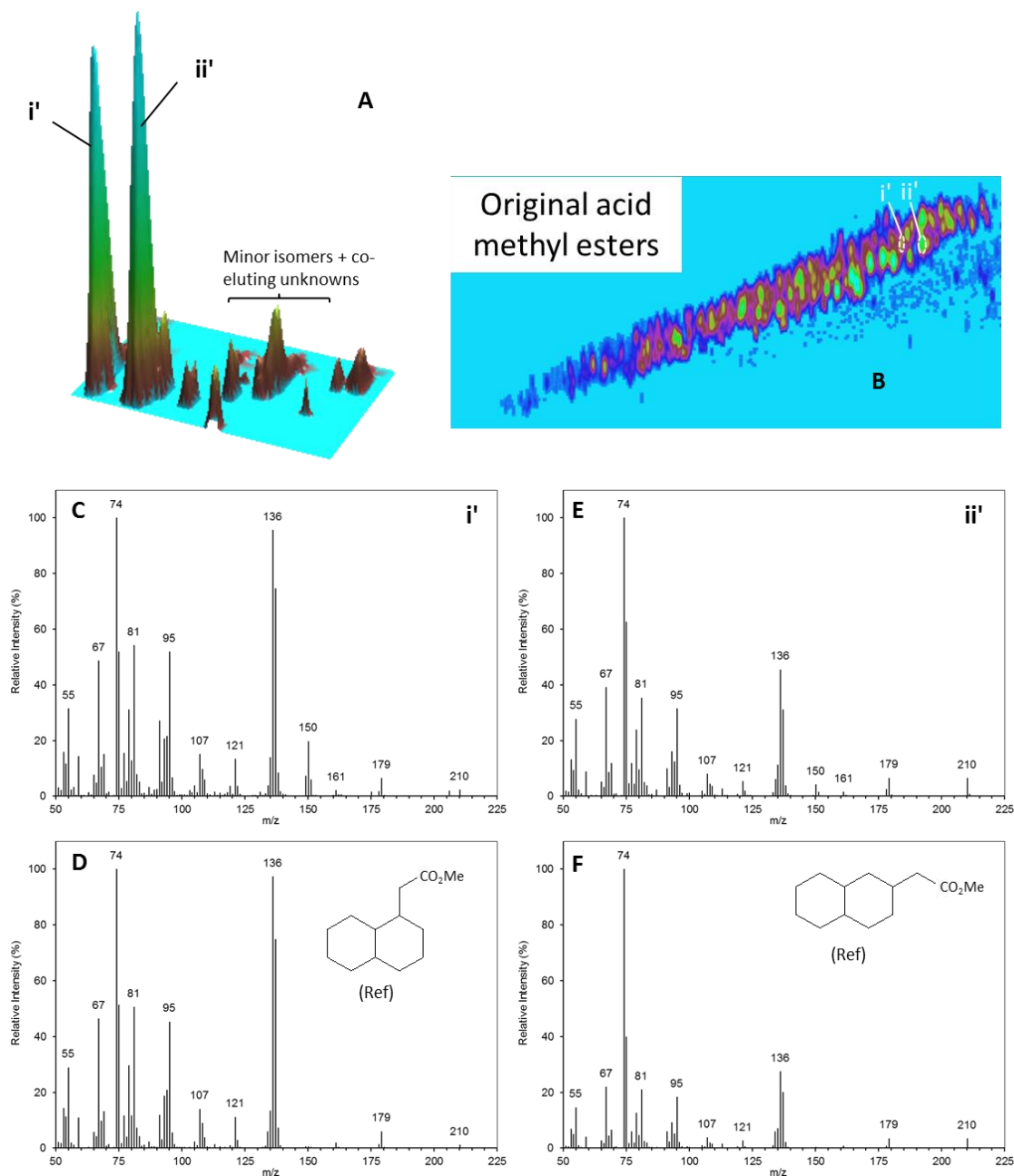
Figure 5-19: (A) 3D representation of a GC×GC chromatogram showing the equivalent two major peaks in the original acid methyl ester fractions using corresponding CLIC expression and (B) an EIC (*m/z* 210) showing their relative retention positions in relation to the C_{12} bicyclic acid methyl esters with (C and E) mass spectra and retention times matching those of (D and F) synthesised reference compounds bicyclo[4.4.0]decane-1- and 2-ethanoic acid methyl esters.

5.3.4.8 Spiro[4.5]decanes and Spiro[5.5]undecanes

Wilde *et al.* (2015) were unable to confirm or rule out the possibility of bicyclic acids in OSPW NA possessing spiro- type cores such as spiro[4.4]nonane, spiro[4.5]decane and spiro[5.5]undecane acids. However, the hydrocarbon mass spectra of a series of dimethylspiro[4.5]decanes and dimethylbicyclospiro[5.5]undecanes, reported by Rusinova *et al.* (1987), were available for comparison with the reduced petroleum NA herein. There were no mass spectral matches for the C_{11} and C_{12} bicyclanes with the reference mass spectral data reported by Rusinova *et al.* (1987), confirming, at least the absence of dimethyl substituted spiro- bicyclics in this particular petroleum NA sample.

5.3.4.9 Terpenoid-derived acids

In addition to mono- and di-substituted bicyclo[4.4.0]decanes, a few components which eluted late in chromatograms of both F2 and F3 were observed, with mass spectra matching those of bicyclic sesquiterpanes possessing drimane structures (Figure 5-20) (Dimmler *et al.*, 1984; Alexander *et al.*, 1984; Alexander *et al.*, 1983). Bicyclic sesquiterpane hydrocarbons such as drimanes, rearranged drimanes and eudesmanes have been studied and used as biomarkers in crude oils and their mass spectra are well documented (Alexander *et al.*, 1983; Stout *et al.*, 2005; Nytoft *et al.*, 2009). To the best of our knowledge, the corresponding drimane acids have not been reported in commercial NA mixtures. Cyr and Strausz (1984) reported the mass spectrum of one C_{16} bicyclic acid (methyl ester) present in the mineral-bound organic extract of the Alberta oil sands which possessed a similar mass spectrum to that of a C_{16} drimane hydrocarbon identified in Athabasca bitumen (Dimmler *et al.*, 1984). Nascimento *et al.* (1999) also identified a C_{16} bicyclic drimane acid in a heavily biodegraded oil from the Albacora oil field, Brazil, along with higher C_{19-20} labdanic acid homologues. Koike *et al.* (1992) reported the presence of one C_{16} drimane peak in the reduction product of the acids from Albacora crude oil. However, synthesis of the corresponding acid methyl

ester, based on the structure previously reported by Cyr and Strausz (1984) showed that it was absent. The mass spectrum of the synthetic C_{16} acid methyl ester reported by Koike *et al.* (1992) was slightly different to that previously reported by Cyr and Strausz (1984), with a distinct M-89 (*m/z* 177), possibly the mass spectrum of a different diastereoisomer.

In the GC×GC chromatogram of the F3 hydrocarbon product, two C_{16} bicyclic hydrocarbons ($M^+ = m/z$ 222) were observed eluting 3 min apart and one C_{17} bicyclic hydrocarbon eluting 6 min later. Their mass spectra matched those of C_{16} homodrimane and higher homologues (Figure 5-20; A, C and E) (Dimmler *et al.*, 1984; Alexander *et al.*, 1984).

The mass spectra of the drimane hydrocarbons show very characteristic fragmentation patterns, with a common loss of M-15. The mass spectra are dominated by a strong base peak ion at *m/z* 123, corresponding to fragmentation of the gem-dimethyl substituted ring (Figure 5-20). Complementary analysis of the original F3 acid methyl esters by GC×GC-MS, prompted by the identification of the bicyclanes herein, then allowed confirmation of the presence of the corresponding C_{16} and C_{17} drimane acids in the same elution order as the hydrocarbons (3 and 6 min apart) (Figure 5-20; B, D and F). Interestingly, the mass spectrum of the earlier eluting C_{16} acid methyl ester matched the mass spectrum reported by Cyr and Strausz (1984), whereas the mass spectrum of the later eluting C_{16} acid methyl ester matched the mass spectrum reported by Koike *et al.* (1992) with a more abundant *m/z* 177 ion. Using the CLIC expression tool to return data points with a base peak ion at *m/z* 123 only (CLIC expression: Ordinal(123)=1), revealed a further two later eluting peaks with mass spectra and molecular ions matching those of C_{19} and C_{20} homologues (Figure 5-21) (Dimmler *et al.*, 1984).
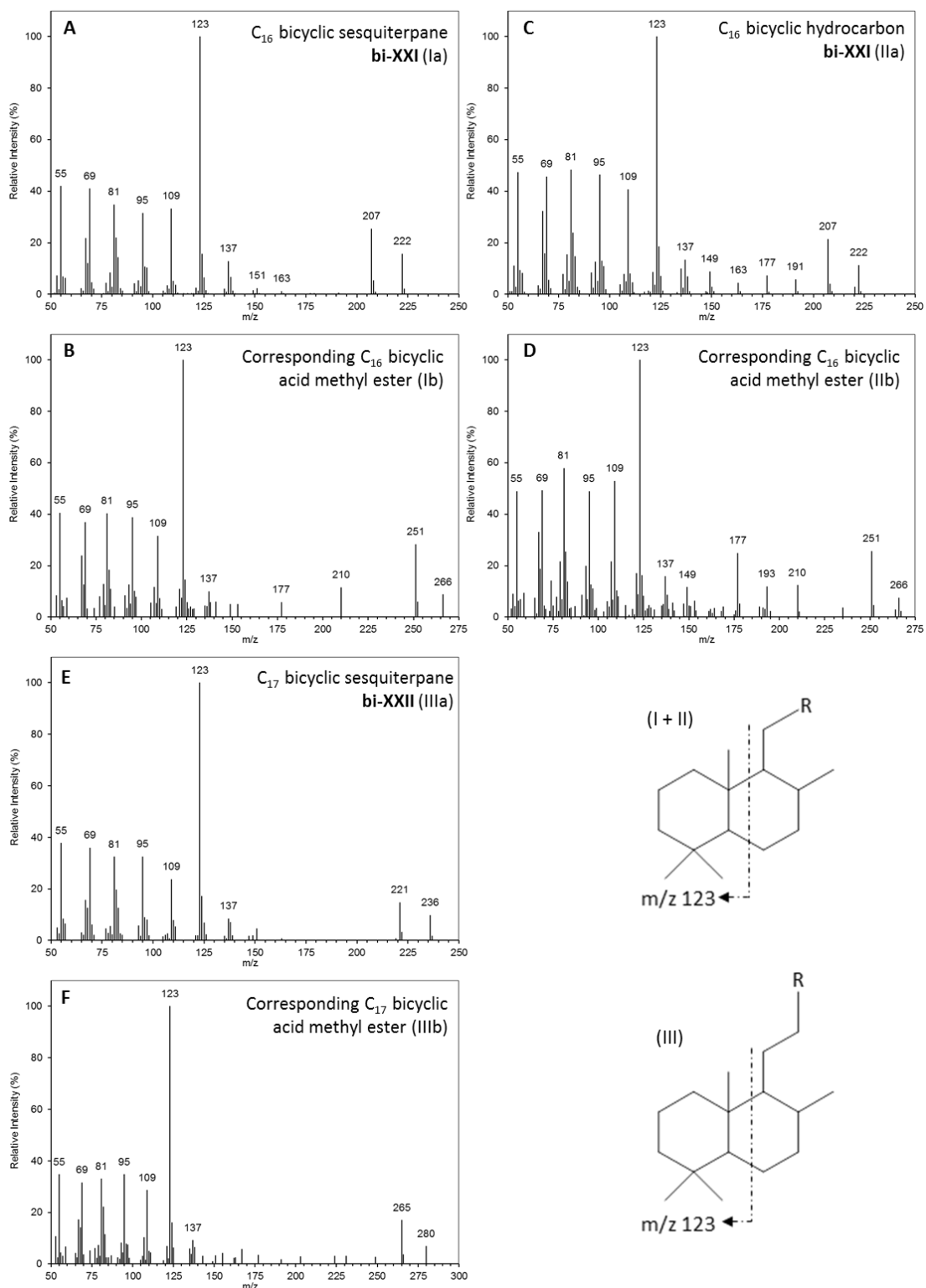
Figure 5-20: (A, C and E) Mass spectra of C_{16} and C_{17} bicyclanes identified, within both reduced fractions, as possessing terpenoid-derived drimane structures by comparison with previously reported mass spectra (Dimmler *et al.*, 1984; Alexander *et al.*, 1984) and (B, D and F) mass spectra of the corresponding methyl esters in the F2 and F3 acid methyl ester fractions (Cyr and Strausz, 1984). (I-IIIa; R = CH$_3$. I-IIIb; R = CO$_2$CH$_3$).
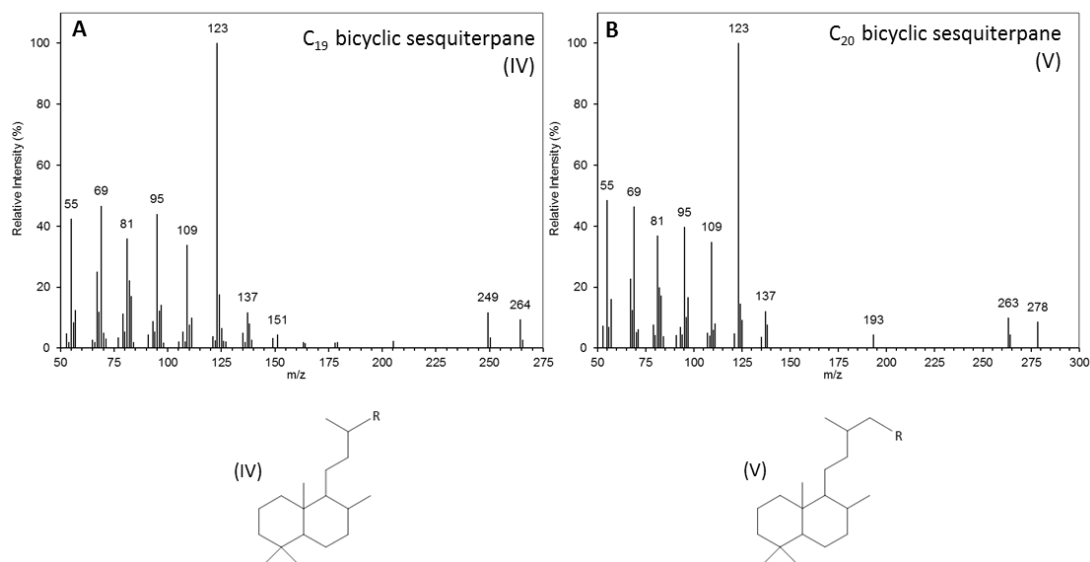
Figure 5-21: (A and B) Mass spectra of C_{19} and C_{20} bicyclanes identified within the F2 hydrocarbon product as higher labdane homologues of terpenoid-derived structures by comparison with previously reported mass spectra (Dimmler *et al.*, 1984; Nascimento *et al.*, 1999) (In hydrocarbon product; R = CH_3. I-IIIb and in the acids; R = CO_2CH_3).

5.4 Conclusions

The identifications presented herein of individual bicyclic hydrocarbons and thus, by inference, of the corresponding acids, possibly represent the most comprehensive study of bicyclic petroleum NA to date. The assignments are supported by the identification of multiple isomers of each acid type and are consistent with the (albeit sparse) previous evidence of such acids identified as the esters, in other matrices, (Wilde *et al.*, 2015). Where possible the assignments were supported by close matches with the GC×GC retention positions and mass spectra of reference compounds. Also, for various isomers, the GC×GC elution order of the hydrocarbons additionally matched those reported for other complex mixtures e.g. bicyclanes produced from the catalytic conversion of bicyclo[4.4.0]decane and bicyclo[4.3.0]nonane (Piccolo *et al.*, 2010; Bagrii *et al.*, 1970; Bagrii *et al.*, 1967; Petrov, 1987). The retention indices of the peaks in Figure 5-6, assigned as the structures in Figure 5-7 are reported in Appendix Table 1.

For decades limited identification of individual petroleum acids has hindered a detailed understanding of their role in petroleum generation and oil production processes, refinery corrosion, as wood preservatives and as environmental toxicants. The present method, based on a combination of an historical approach of converting acids to the corresponding hydrocarbons, followed by analysis by GC×GC-MS, resulted in identification of over 40 individual bicyclic acids as the bicyclane hydrocarbons. There is now clear potential for this method to be used for the structural elucidation of other unknown acids (e.g. oil sands NA) and functionalised biomarkers in complex organic extracts as described in Chapter 6.

Chapter 6

Identification of naphthenic acids in oil sands process waters by multidimensional gas chromatography-mass spectrometry, before and after conversion of acids and esters to the corresponding hydrocarbons

Chapter 6 describes the identification of naphthenic acids (NA) extracted from oil sands process water (OSPW) by multidimensional gas chromatography-mass spectrometry (GC×GC-MS), before and after conversion of either the free acids or the methyl esters, to the corresponding hydrocarbons.

The approach of converting NA (as esters) to the corresponding hydrocarbons to aid identification, using the method developed in Chapter 4, showed great potential when applied to commercially prepared, petroleum-derived NA, resulting in the identification, by inference, of over 40 individual bicyclic acids (Chapter 5).

Due to their ready availability and perhaps some naivety over their relevance (e.g. as discussed by West *et al.* (2011)), commercial NA have been used as 'model' acid mixtures in studies investigating the toxicity, remediation and fate in the environment of NA extracted from OSPW. Since numerous recent and some older investigations (e.g. Scott *et al.* (2005), Bataineh *et al.* (2006), Grewer *et al.* (2010) and Hindle *et al.* (2013)) have shown the composition of commercial and OSPW NA to be different, there is a need for greater compositional information about OSPW NA. For instance, lack of knowledge of the structures of NA in OSPW has limited attempts to calibrate methods for quantification and hindered a better understanding of toxicity, biodegradation and hence possible bioremediation mechanisms (Hindle *et al.*, 2013; Brunswick *et al.*, 2015).

Hence the approach developed for the identification of petroleum acids by conversion to hydrocarbons (Chapters 4 and 5), was applied herein to NA extracted from OSPW. GC×GC-MS of the methyl esters of the OSPW NA showed the mixtures were extremely complex, even after fractionation by argentation chromatography, although the findings of previous studies (Rowland *et al.*, 2011c; Rowland *et al.*, 2011g) were confirmed and in some cases extended. GC×GC-MS of the reduced free acids (viz: the hydrocarbon products) and of hydrocarbons produced from reduction of ester fractions of 'alicyclic', 'aromatic' and 'heteroatom-containing' fractions of OSPW NA, resulted in the confirmation of numerous bicyclic acids, adamantane and diamantane acids, as well as monoaromatic and sulphur-containing acids, as their hydrocarbon equivalents and included identification of numerous previously unidentified NA.

The main results of this chapter and methods described have been drafted for publication:

Wilde, M. J. And Rowland, S. J. (**2015**) Identification of naphthenic acids in oil sands process water by multidimensional gas chromatography-mass spectrometry after conversion to their corresponding hydrocarbons. To be submitted to *Analytical Chemistry*

.

6.1 Introduction

Intensive surface mining of the bituminous oil sands of Alberta, Canada, by hot water extraction, produces large volumes of oil sands process-affected waters (OSPW; Chapter 1, Section 1.1.2). Despite recycling of the caustic extraction water, large volumes of process water contaminated with high concentrations of aqueous-soluble components from the bitumen, such as NA, as well as suspended solids, continue to accumulate. The total volume is currently estimated to be between 720 to 975 million m^3, with volumes continually rising (Headley *et al.*, 2013a; Barrow *et al.*, 2015a; Alberta-Energy, 2013), covering an area estimated to be between 130 to 220 km^2 (Headley *et al.*, 2013a; Alberta-Energy, 2013). The OSPW is stored in large open 'tailings' ponds, allowing the suspended tailings to settle. Long-term reclamation plans for the land include storage of the water in so-called End-Pits, or by other measures (Quagraine *et al.*, 2005; Kavanagh *et al.*, 2009). Residual toxicity in the OSPW is a hindrance to successful reclamation by most, if not all, methods, so better identification of the toxic constituents (toxicity is largely attributed to the NA; Marentette *et al.* (2015a)), is essential in order that remediation attempts can be better directed.

OSPW have been shown to be toxic to numerous organisms ranging from bacteria to birds and fish at the concentrations found in tailings ponds (Clemente and Fedorak, 2005; He *et al.*, 2012). Since this toxicity has been attributed mainly to the NA content (Marentette *et al.*, 2015a; Mohseni *et al.*, 2015) (Chapter 1, Section 1.4), methods have been developed for monitoring NA in OSPW from surface mining, from treated OSPW, from steam-assisted gravity drainage (SAGD) produced water and from water samples taken from the local and distal environments surrounding the mining developments (Petersen and Grade, 2011; Pereira *et al.*, 2013b; Noestheden *et al.*, 2014; Frank *et al.*, 2014). Most of the latter quantitative studies have involved use of negative ion

electrospray ionisation ((-)ESI) coupled with high and ultra-high resolution mass spectrometry (HRMS) (Schaub *et al.*, 2007; Headley *et al.*, 2011a; Headley *et al.*, 2014; Yi *et al.*, 2015). Investigations using other ionisation techniques such as atmospheric pressure photoionisation ((+) and (-) APPI) and (+)ESI have also reported detection of hydrocarbon and heteroatom-containing species present in the acid-extractable organics (AEO) isolated from OSPW (Barrow *et al.*, 2010; Barrow *et al.*, 2015a). Also, methods involving fractionation procedures followed by HRMS methods have revealed that at least some OSPW samples contain, not only an extensive range of NA, but other compounds beyond so-called 'classical' $C_nH_{2n+z}O_2$ species (Rowland *et al.*, 2014b; Rowland *et al.*, 2014a).

The latest analytical methods for the characterisation of NA have often included a chromatographic separation step, such as gas chromatography (GC), or more commonly, high and ultra-high performance liquid chromatography (UPLC), followed by detection by Fourier transform ion cyclotron resonance-mass spectrometry (FTICR-MS) (Barrow *et al.*, 2014; Ortiz *et al.*, 2014), Orbitrap-mass spectrometry (Pereira *et al.*, 2013a; Pereira and Martin, 2014) or ion mobility-mass spectrometry (IMS) (Klamerth *et al.*, 2015; Huang *et al.*, 2015a). Methods involving the combination of a chromatographic separation step with HRMS enable the separation of isobaric species possessing the same molecular formulae, which can be determined very accurately by HRMS. However, beyond basic assumptions based on the retention times of unresolved isomers, these methods lack sufficient separation power for determining key structural features and have not allowed the identification of any individual acid from which toxicity data can then be obtained or modelled. Determination of the chemical nature of individual OSPW NA and AEO components would also allow monitoring methods to be devised to examine whether the bitumen-derived O_x, SO_x and NO_x species detected in OSPW and surrounding ground and river waters (Frank *et al.*, 2014) might be differentiated.

This would aid source identification and profiling studies designed to determine the extent to which OSPW is migrating/leaking into the surrounding environment. Identification of individual NA species would also aid current understanding of treatment mechanisms and remediation plans; identification could lead to targeted treatment so changes in concentration and the formation of by-products from specific NA could be monitored.

Recently, Lengger *et al.* (2015) monitored the distribution of individual tricyclic diamondoid mono- ($C_nH_{2n-6}O_2$) and di- ($C_nH_{2n-6}O_4$) acids as their methyl and dimethyl ester derivatives, to determine short-term compositional changes in, and sample variability between, replicate OSPW samples from two different industries. Similarly, Frank *et al.* (2014) used (-)ESI-Orbitrap-MS to determine $C_nH_{2n+z}O_2$: $C_nH_{2n+z}O_4$ ratios and complementary GC×GC-MS analysis to profile tentatively identified aromatic acids previously reported to be in OSPW (Rowland *et al.*, 2011d), to differentiate between AEO from OSPW and surrounding groundwater samples. Identification of NA structures has also enabled the toxicity of a number, albeit limited, of synthesised and commercially available reference acids, to be measured (Jones *et al.*, 2011; Tollefsen *et al.*, 2012). The results were used to predict the toxicity of numerous acids in OSPW and to identify those NA of most concern, based on modelled toxicity data (Scarlett *et al.*, 2012).

However, the identification of individual NA as their methyl ester derivatives is partially limited by the lack of mass spectral and retention time data and available reference compounds for confirmation. Recently, Wilde and Rowland (2015) reported a complementary, additional method for the identification of petroleum NA, after conversion of NA (as methyl esters) to the corresponding hydrocarbons (Chapter 5). This approach, based on the chemical transformation methods used in early

investigations of NA (e.g. Seifert *et al.* (1969)), coupled with analysis of the reduced acid products by GC×GC-MS, resulted in the identification of over 40 individual bicyclic petroleum NA. Identification of the bicyclic hydrocarbons, and by inference the original bicyclic acids, was achieved by comparison of the hydrocarbon mass spectra with the abundant mass spectra of known bicyclic hydrocarbons collated from (mainly) early Russian investigations into petroleum hydrocarbons (Sanin, 1976; Denisov *et al.*, 1977a; Denisov *et al.*, 1977b; Denisov *et al.*, 1977c; Denisov *et al.*, 1977d; Golovkina *et al.*, 1984; Golovkina *et al.*, 1979; Petrov, 1987).

The goal of the current investigation was now to apply the latter conversion method to NA extracted from samples of OSPW, both as free acids and as ester derivatives, in an attempt to assign specific structures to the compounds.

The study did indeed result in the identification of several new individual acids (as hydrocarbons) in OSPW. The results also confirmed numerous previous assignments, which were only tentative previously due to the lack of supporting mass spectral evidence for the acid methyl esters. The results also contradicted speculations that certain adamantane acids identified in OSPW might be entirely artefactual (Brunswick *et al.*, 2015).

6.1.1 Aims and Objectives

The aims of the current investigation were to apply the method for the conversion of NA to hydrocarbons, to NA extracted from OSPW and to conduct GC×GC-MS analysis on the resulting hydrocarbon products, to aid the identification of NA in OSPW. The conversion was to be performed on a derivatised (methyl esters), fractionated sample (#2) and underivatised, unfractionated (#7) sample of OSPW NA. To confirm if the reduction procedure was successful on the more complex unfractionated, underivatised OSPW NA, both the reduced underivatised, unfractionated NA and a reduced alicyclic fraction were each examined, to identify hydrocarbons for which the corresponding acids such as tricyclic and pentacyclic diamondoid NA, had been identified previously in OSPW NA,.

After confirming successful reduction, initial focus was placed on identification of bicyclic acids, as the corresponding bicyclanes, which had not been reported previously in OSPW NA. Following this, additional aims included examination of the reduced alicyclic, aromatic and aromatic/sulphur-containing NA fractions, to identify previously unknown NA, or NA that had only been identified tentatively previously, by comparison of the mass spectra of the resolved hydrocarbon products with reference hydrocarbon mass spectra and known elution orders.

6.2 Methods

6.2.1 OSPW acid extracts, derivatisation and fractionation

In the current investigation, two different OSPW NA extracts from industry A were analysed, the first (sample #2) provided by Environment Canada and the second (sample #7) provided by the University of Alberta. Sample #2 was an NA extract from OSPW, collected from the WIP tailings pond in 2009, and prepared as described in Chapter 2, Section 2.2.1 and discussed in Chapter 3, Section 3.2.1. The origin of sample #7 has to remain anonymous; however, it was also a NA sample extracted from OSPW in a tailings pond in industry A; the OSPW was filtered, acidified and extracted in DCM (*cf.* Pereira *et al.* (2013a)).

Sample #2, which was also analysed as a whole NA (methyl esters) mixture in Chapter 3, was now fractionated by Ag-Ion chromatography using the same large scale method used to fractionate the petroleum NA in Chapter 5 (Jones *et al.*, 2012; Scarlett *et al.*, 2013). Three fractions were selected from this procedure in order to perform the conversion to hydrocarbons; an 'alicyclic' fraction (F2) eluted in 100% hexane, an 'aromatic' fraction (F5) and an 'aromatic/sulphur'-containing fraction (F7) eluted with 95%:5% hexane : ether. To obtain enough material of each of the fractions on which to perform the conversion, the above fractionation was carried out twice. As the OSPW NA fractions were also used in other concurrent investigations (e.g. Rowland *et al.* (2014a) and West *et al.* (2014b)), the alicyclic Ag-Ion fraction (F2) was taken from the first large scale fractionation and the aromatic and aromatic/heteroatom-containing fractions (F5 and F7) were taken from the second fractionation (Chapter 2, Section 2.2.6).

Sample #7 (University of Alberta) was selected for the conversion to hydrocarbons as this had been shown to possess a higher abundance of lower molecular weight acids (e.g.

C_{10} bicyclic acids), relative to sample #2. Sample #7 was not derivatised or fractionated prior to the conversion to the hydrocarbons.

6.2.2 Conversion of OSPW NA to hydrocarbons

The acid methyl ester Ag-Ion fractions of sample #2 and of the free, underivatised, unfractionated acids of sample #7, were each converted to the corresponding hydrocarbons using the method developed in Chapter 4, previously shown to be successful on petroleum NA in Chapter 5. The general procedure for the conversion to hydrocarbons is described in Chapter 2, Section 2.3.

The hydrocarbon products of the reduced Ag-Ion fractions were concentrated under a stream of N_2. As sample #7 had been selected as a mixture known to contain low molecular weight acids (Prof J Martin, University of Alberta, personal communication), the final hydrocarbon products of the reduced, underivatised, unfractionated OSPW NA were concentrated using a Kuderna-Danish apparatus, as described in Chapter 2, Section 2.3.4.

6.2.3 GC×GC-MS

The GC×GC-MS instrumentation used is described in Chapter 2, Section 2.1.4. Samples were analysed using two different temperature programmes (referred to as conditions A and B). The GC×GC-MS conditions A involved the primary oven programmed from 30°C, held for 1 min, then heated to 120°C at 5°C min^{-1}, to 220°C at 0.8°C min^{-1}, to 280°C at 5°C min^{-1} and to 320°C at 10°C min^{-1} and then held for 10 min. The secondary oven was programmed to track the primary oven at 40°C above. The hot jet was programmed to start 30°C above the primary oven temperature until 150°C, it was then ramped to 260°C at 1.3°C min^{-1} and then to 400°C at 4°C min^{-1}. The modulation period was set 4 - 6 s. The GC×GC-MS conditions B involved the primary oven programmed from 40°C, held for 1.3 min, then heated to 200 °C at 1°C min^{-1}, to 280 °C and 5 °C

min^{-1} and to 320°C at 10 °C min^{-1} and then held for 5 min. The secondary oven was programmed to track the primary oven at 20 °C above. The hot jet was programmed to start 20 °C above the primary oven and finish 100 °C above the primary oven over the period of the run; programmed from 60 °C, held for 1 min, then heated to 200 °C at 1.1 °C min^{-1}, to 280 °C at 3 °C min^{-1} and then to 400 °C at 5 °C min^{-1}. The modulation period was set at 4 - 6 s.

6.3 Results and Discussion

6.3.1 Derivatised, fractionated and underivatised, unfractionated, OSPW NA

Sample #2 was first derivatised to the acid methyl esters with BF_3-MeOH at 70 °C before separation by Ag-Ion chromatography. The large scale fractionation procedure had proven successful in isolating a broadly 'alicyclic' fraction(s) of petroleum NA previously (Chapter 5) and had been employed in other studies investigating the composition and toxicity of OSPW NA to obtain broadly 'aromatic' and 'aromatic/sulphur'-containing fractions (Jones *et al.*, 2012; Reinardy *et al.*, 2013; Scarlett *et al.*, 2013). Therefore the approach of converting the fractionated acid methyl esters to hydrocarbons was applied to three fractions herein (F2, F5 and F7), broadly characterised as 'alicyclic', 'aromatic' and 'aromatic/sulphur'-containing NA by GC-MS and GC×GC-MS; equivalent fractions from previous investigations had been characterised additionally using elemental analysis, sulphur chemiluminescence detection (SCD) and high resolution mass spectrometry (HRMS) (Jones *et al.*, 2013; West *et al.*, 2014b). Therefore, any NA identified using the conversion approach herein could be compared, if necessary, with those identified in previous studies on OSPW isolated by the same fractionation procedures (Scarlett *et al.*, 2013; Reinardy *et al.*, 2013).

The 'alicyclic' fraction selected, was the second of the first four fractions, eluting with 100% hexane (Table 2-2; Chapter 2, Section 2.2.6, page 65). The total mass of the four hexane fractions collected in the first fractionation (106 mg) accounted for 35.8% of the total mass of acid methyl esters (296 mg) loaded onto the Ag-Ion column. Fraction 1 contained 20.1 mg (6.79%), fraction 2; 76.8 mg (25.9%), fraction 3; 7.4 mg (2.5%) and fraction 4 contained 1.7 mg (0.6%). The values of the hexane fractions from a second fractionation were very similar (Tables 2-2 and 2-3, pages 65 and 66). The lower

'alicyclic' content of the OSPW NA (35.8%) relative to the high 'alicyclic' content (80.0%) observed for petroleum NA (Chapter 5, Section 5.3.1) correlates with previous ESI-HRMS and HPLC-ESI-HRMS studies (Bataineh *et al.*, 2006; Hindle *et al.*, 2013). Almost half the 'alicyclic' NA content in petroleum NA, was collected in fraction 1, which was dominated by acyclic, $z = 0$, NA. The numerous charts that have been produced from high resolution mass spectrometric techniques, showing carbon number against z-value, all show OSPW NA to have depleted $z = 0$ and -2 NA and more abundant $z = -8$ to -12 NA, relative to commercial NA mixtures (Bataineh *et al.*, 2006; Hindle *et al.*, 2013).

The 'aromatic' (F5) and 'aromatic/sulphur-containing' (F7) fractions accounted for 16.9% and 4.4% of the total mass of NA methyl esters loaded onto the Ag-Ion column, respectively. These values were much higher than the equivalent fractions collected for petroleum NA (6.5% and 0.9%, respectively) and corresponded well with the more abundant NA species with higher z-values observed in the HRMS charts for OSPW NA (Bataineh *et al.*, 2006; Martin *et al.*, 2008; Hindle *et al.*, 2013). The lower abundance of acyclic NA in OSPW and the increased aromatic content relative to petroleum NA, has been attributed to the heavily degraded, oil sands bitumen and the increased susceptibility of smaller and monocyclic NA towards biodegradation and the more recalcitrant nature of the polycyclic and aromatic NA (Toor *et al.*, 2013b; Brown and Ulrich, 2015).

6.3.2   Yields of conversion

The three step conversion was performed on ~10 - 25 mg of the OSPW NA methyl ester Ag-Ion fractions of sample #2, dependent on the availability of material, and ~30 mg of the underivatised, unfractionated OSPW NA sample #7. The method had been developed on small quantities of 'model' acids (5 – 50 mg; Chapter 4) in preparation for the limited availability of OSPW material and had been shown to be successful on milligram quantities for the conversion of two Ag-Ion fractions of a petroleum NA extract (9 – 50 mg; Chapter 5).

The starting masses of reactants and final masses of products for each stage of the conversions are given in Table 6-1. An approximate percent yield was determined for the first two stages of the reaction for each Ag-Ion fraction, as well as the underivatised, unfractionated OSPW NA. Approximate yields were calculated using estimated average molecular weights, based on the carbon number distributions and the most abundant molecular ions observed in the average mass spectra across each chromatogram for each sample. The average molecular weight for the 'alicyclic' fraction was 250 g mol^{-1}; for the 'aromatic' fraction, 286 g mol^{-1}; for the 'aromatic/sulphur'-containing fraction, 294 g mol^{-1} and for the underivatised, unfractionated NA, 246 g mol^{-1}.

The final hydrocarbon products of the reduced Ag-Ion fractions were concentrated under a stream of N$_2$. However, it was obvious that the products still contained some remaining THF (by odour) and boroxin (observed as clear crystals). Therefore, the masses of the hydrocarbon products were all above the expected/theoretical mass of product.

Table 6-1: Summary of the masses and yields for the conversion of the Ag-Ion fractions 2, 5 and 7 of the derivatised OSPW NA and of the underivatised, unfractionated OSPW NA samples, to hydrocarbons.

Starting Reactant		Starting mass and yield / mg (approx. percentage yield / %)					
Derivatised (# sample number)	Fraction	LiAlH$_4$ Reduction		Tosylation		Super-Hydride® Reduction	
		NA methyl esters / mg	Alcohols / mg	Alcohols / mg	Tosylates / mg	Tosylates / mg	Hydrocarbons / mg
Yes (#2)	2	10[†]	9.8 (104%[‡])	9.8	13.3 (82%[‡])	12.2	20.7[*]
Yes (#2)	5	25[†]	23.0 (97%[‡])	23.0	27.9 (77%[‡])	27.9	17.2[*]
Yes (#2)	7	10[†]	9.1 (96%[‡])	9.1	10.5 (74%[‡])	10.5	6.7[*]
No (#7)	Whole	30[†]	25.0 (88%[‡])	25.0	32.3 (78%[‡])	32.0	-

[†] approximate masses, as methyl esters

[‡] approximate yield based on average molecular weight of acid methyl esters as 250 g mol^{-1} in F2, 286 g mol^{-1} in F5, 294 g mol^{-1} in F7 and 246 g mol^{-1} in the whole underivatised OSPW NA

[*] hydrocarbon product concentrated by N$_2$ blowdown resulting in evaporative losses; THF and boroxin residue present

[-] Kuderna-Danish apparatus used for concentration to reduce volatile compound losses, so no weight was recorded

6.3.3 Identification of OSPW acids as methyl esters and by reduction to hydrocarbons

The identification of hydrocarbons such as tricyclic and pentacyclic diamondoids, for which the corresponding acids had been identified previously in OSPW NA (discussed later in Sections 6.3.3.2 and 6.3.3.3), confirmed that the conversion to hydrocarbons was successful for the more complex alicyclic OSPW NA. Hence, initial focus was to identify any bicyclic acids, as the corresponding bicyclanes, which had not been reported previously in OSPW NA. Following this, the reduced 'aromatic' and 'aromatic, sulphur'-containing fractions were examined and the identification made of previously unknown NA, or NA that had only been identified tentatively, by comparison of the mass spectra of the resolved hydrocarbon products with reference hydrocarbon mass spectra and known elution orders.

6.3.3.1 Bicyclic acids

Alicyclic bicyclic acids are a major class of OSPW NA (Martin *et al.*, 2008). High- and ultra-high resolution mass spectrometric techniques often show ions corresponding to $z = -4$, $C_nH_{2n+z}O_2$ acid species with carbon numbers ranging from C_{9-20}, as the most abundant $C_nH_{2n+z}O_2$ species (Bataineh *et al.*, 2006; Barrow *et al.*, 2010). Analysis of commercial and OSPW NA methyl esters by GC×GC-MS, has shown that the ions detected by high resolution mass spectrometry represent hundreds of different structural isomers (Damasceno *et al.*, 2014; Wilde *et al.*, 2015). Based on the limited knowledge of bicyclic acids, a well-accepted screening assay reported some bicyclic acids to be the most toxic of those studied (Jones *et al.*, 2011). Scott *et al.* (2008) showed the ozonation of OSPW resulted in the removal of most $z = -4$ acids; however, nothing is known about the residual acids, or of any transformation products.

Investigations into the structural identification of bicyclic acids were previously described in Chapter 3. In summary, no or few, identifications, particularly in OSPW, had been made until that study. In the accompanying publication, Wilde *et al.* (2015) reported the identification of a few bicyclic acids in different samples of OSPW NA, following analysis of the methyl esters by GC×GC-MS and subsequent comparison of the mass spectra and retention positions with reference compounds, as described in more detail in Chapter 3. Following the development of the alternative method for the identification of NA by conversion to the hydrocarbons and analysis by GC×GC-MS (Chapter 4), Wilde and Rowland (2015) also reported the identification of over 40 individual bicyclic acids in petroleum NA, by comparison of the mass spectra and elution orders of the corresponding bicyclanes with those of known hydrocarbons (Chapter 5). These investigations resulted in the first identification of novel bridged bicyclic acids, along with several bicyclic fused and terpenoid-derived acids.

In the current investigation, analysis of the 'alicyclic' acids as methyl esters of sample #2 showed that C_{11-16} bicyclic acids were indeed present, as reported as typical of OSPW NA (Bataineh *et al.*, 2006; Hindle *et al.*, 2013). The absence of the lower molecular weight C_{8-11} acids, shown to be present in several other OSPW NA samples (Figure 3-2; Chapter 3, page 93), coupled with the additional loss of $<C_{13}$ bicyclanes after conversion to the hydrocarbons and concentration in this case without use of a Kuderna-Danish apparatus, limited the potential for the identification of such bicyclic acids in this sample. Reference spectra for bicyclic petroleum hydrocarbons mainly exist for C_{9-11} bicyclanes and therefore the absence of the lower molecular bicyclanes limited initial identification attempts.

By contrast, GC×GC-MS analysis of the acid methyl esters of sample #7 revealed homologous series of isomers with mass spectra displaying molecular ions consistent

with C_{10-15} bicyclic acid methyl esters. In this case, careful concentration of the hydrocarbon product, following reduction of the unfractionated NA, using a Kuderna-Danish apparatus and subsequent analysis by GC×GC-MS showed homologous series of C_{10-15} bicyclanes (Figure 6-1; A and B). However, the reduced sample #7, which had not been fractionated by Ag-Ion chromatography, revealed a more complex distribution of bicyclanes, with co-elution with tricyclanes and other hydrocarbons.

Despite this, comparison of the mass spectra of those bicyclanes which were not hindered by co-elution effects, resulted in the identification of bicyclo[3.2.1]octane, bicyclo[3.3.0]octane and bicyclo[4.3.0]nonane alkyl derivatives (Figure 6-1; C-H). The earliest eluting isomer (**bi-VII**) was assigned as 1,4-dimethylbicyclo[3.2.1]octane (Figure 6-1; C and D) after comparison with the reference mass spectrum reported by Denisov *et al.* (1977a). This identification was supported by the identification of the same bicyclane, and by inference the same acid, previously in petroleum-derived NA (Figure 5-8; Chapter 5, page 223).

Comparison of the mass spectrum of isomer **bi-XXIII** with the mass spectra of alkyl bicyclo[3.3.0]octanes reported by Denisov *et al.* (1977c), resulted in the identification of 1,2-dimethylbicyclo[3.3.0]octane (Figure 6-1; E and F). This assignment was supported by its retention position relative to 1,4-dimethylbicyclo[3.2.1]octane (**bi-VII**) which matched the elution order of C_{10} bicyclanes previously reported by Piccolo *et al.* (2010) and complemented the previous identification of several bicyclo[3.3.0]octane acids in petroleum-derived NA (Chapter 5, Sections 5.3.4.1 and 5.3.4.3). The bicyclo[3.3.0]octane acids previously identified in petroleum NA consisted of carboxylic, ethanoic and propanoic acid isomers and a methyl-substituted carboxylic acid isomer, all substituted at secondary carbon positions. (A similar observation was

made for the bicyclo[4.3.0]nonane petroleum acids). The result is thus the first identification of a bicyclo[3.3.0]octane acid with a substituent at a bridgehead carbon.
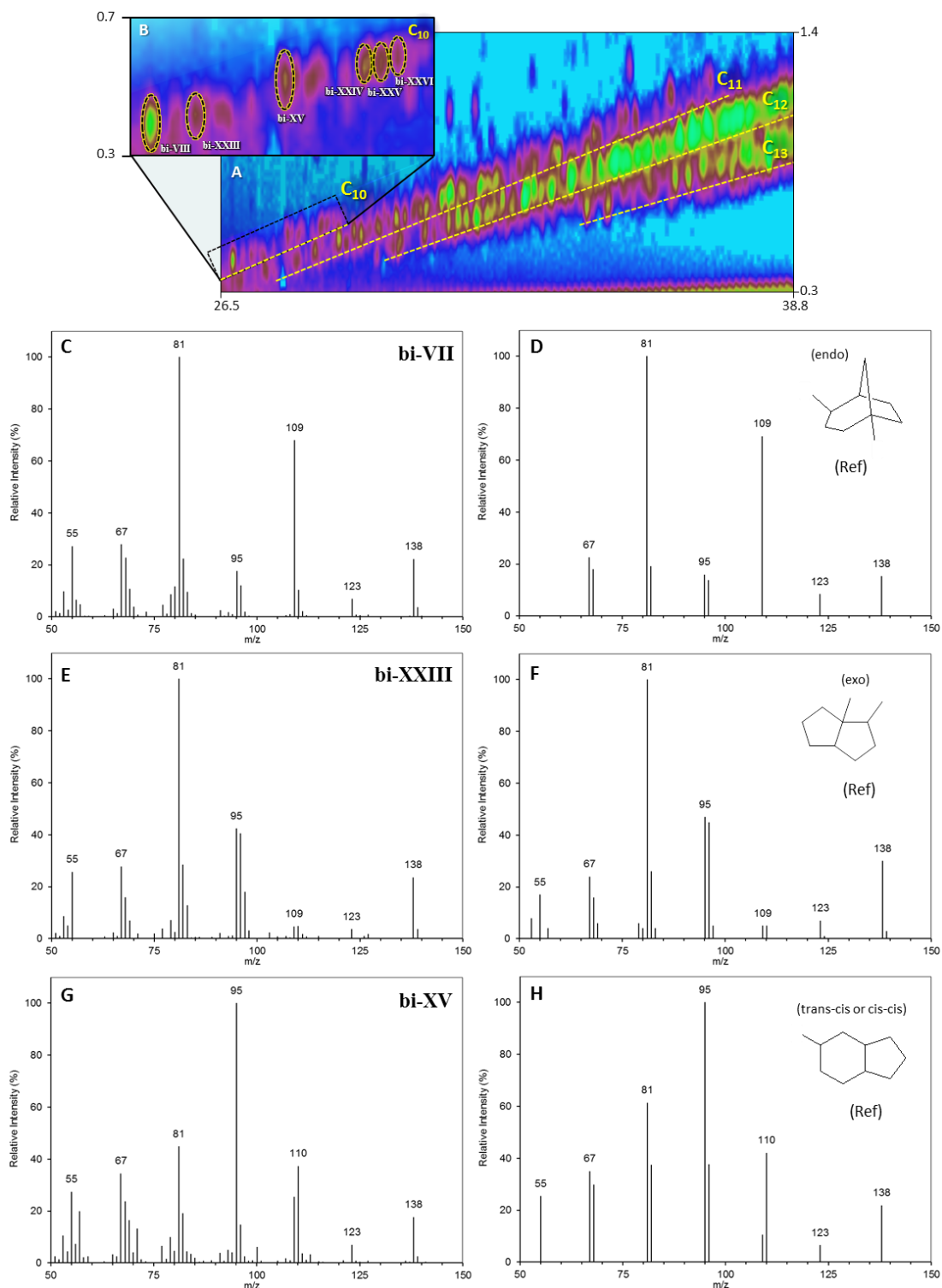
Figure 6-1: (A) EIC (*m/z* 138, 152, 166 and 180) of C_{10-13} bicyclanes in the reduced unfractionated NA (sample #7) showing separation of homologous series by carbon number. (B) Zoomed insert showing C_{10} isomers and (C-H) identification of bridged and fused bicyclanes by mass spectral comparison with reference mass spectra and elution order (Denisov *et al.*, 1977a; Denisov *et al.*, 1977c; Denisov *et al.*, 1977b).

The isomer **bi-XV** displayed a mass spectrum matching those of *cis-cis* and *trans-cis* 3-methylbicyclo[4.3.0]nonane reported by Denisov *et al.* (1977b) (Figure 6-1; G and H). Numerous methylbicyclo[4.3.0]nonanes were identified in the reduced petroleum NA (Figures 5-13 - 5-15; Chapter 5, Section 5.3.4.6, pages 233 - 235) with the isomer assigned as the *cis-cis*/*trans-cis* 3-methyl- isomer eluting earliest of all the 2- and 3-methyl- isomers.

The mass spectra of the later eluting isomers **bi-XXIV** to **XXVI** were less distinct and more difficult to assign. The isomer **bi-XXIV** was tentatively assigned as 2,6-dimethylbicyclo[3.2.1]octane based on its mass spectral match (Figure 6-2; A and B). However, there was no previous identification of this isomer in petroleum NA and no record of its retention position relative to other C_{10} bicyclanes.

The remaining bicyclanes, such as isomers **bi-XXV** and **XXVI**, were not able to be assigned as their mass spectra did not match any of the collated reference mass spectra of numerous bicyclane isomers. This contrasted with the results of the reduced petroleum NA (Chapter 5), which resulted in the identification of almost all the corresponding C_{10} bicyclic hydrocarbons.
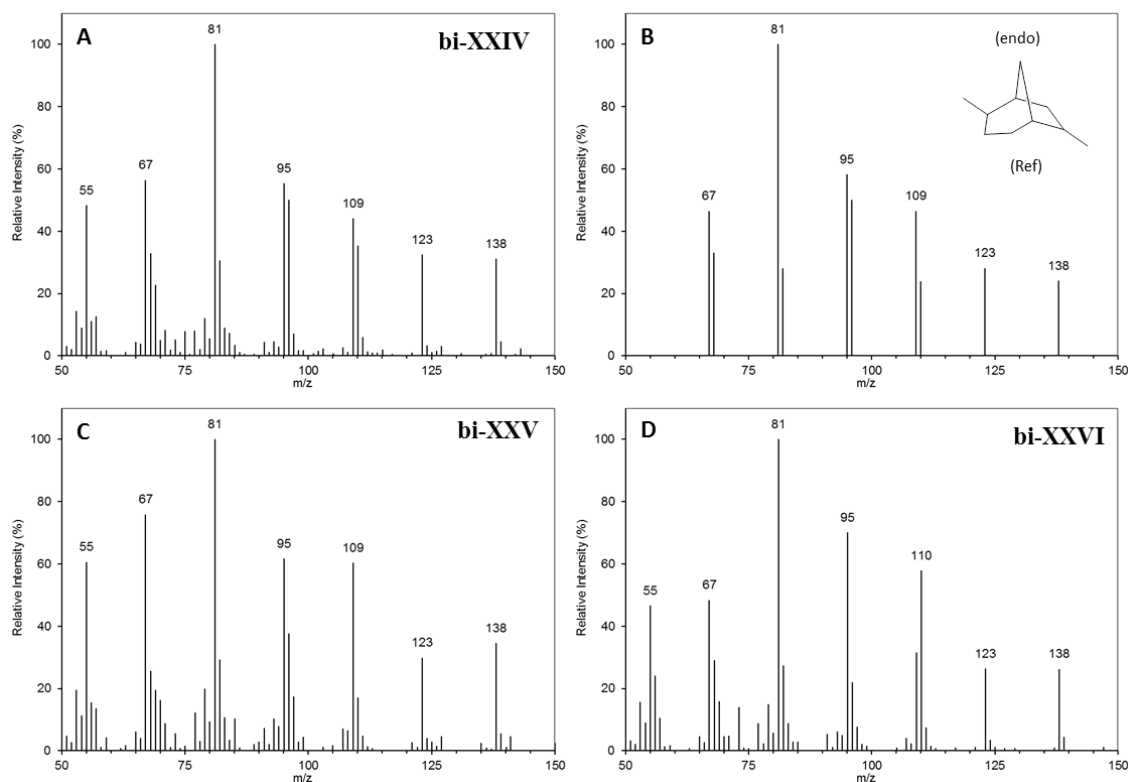
Figure 6-2: Mass spectra of C_{10} bicyclanes (**bi-XXIV** to **XXVI**) in the reduced unfractionated NA (sample #7). (A) Isomer **bi-XXIV** assigned after comparison with (B) the reference mass spectrum of endo-endo-2,6-dimethylbicyclo[3.2.1]octane. (C and D) Mass spectra of isomers **bi-XXV** and **XXVI** which did not match any reference spectra and were significantly different to those within reduced petroleum-derived acids previously reported (Wilde and Rowland, 2015).

Petroleum NA and NA extracted from OSPW have often been reported to possess significantly different compositions (Grewer *et al.*, 2010; Hindle *et al.*, 2013). These differences in compositions are often observed as a notable difference in the HPLC retention times of the unresolved NA 'humps'. The different compositions of OSPW NA, which elute slightly earlier than petroleum NA (typically in HPLC methods; e.g. Bataineh *et al.* (2006) and Han *et al.* (2008)), are often explained as due to the increased resistance to biodegradation of the OSPW NA, when compared with petroleum NA (Scott *et al.*, 2005; Frank *et al.*, 2008; Brown and Ulrich, 2015). The current

justification used by some authors to explain both of these phenomena is that the carboxylated alkyl side chains in OSPW NA, which are otherwise believed to possess alkyl substituted alicyclic structures similar to those of petroleum NA, are more highly branched in OSPW NA (example given in Figure 6-3; A) (Holowenko *et al.*, 2002; Bataineh *et al.*, 2006). It is well known that highly branched hydrocarbons, such as acyclic isoprenoid hydrocarbons, elute earlier than the equivalent carbon number, so-called 'straight chain' hydrocarbons and also that increased alkyl branching along carboxylated side chains and increased cyclicity, hinders biodegradation (Smith *et al.*, 2008; Misiti *et al.*, 2014; Quesnel *et al.*, 2011).

However, this explanation has never been supported by the identification of an acid possessing a long non-branched alkanoate chain in petroleum NA or the corresponding acid with a branched alkanoate chain in OSPW NA (such as the structures shown in Figure 6-3; A). Whilst increased cyclicity due to the presence of aromatic structures in OSPW NA, may have an important role in the differences in retention time and toxicity observed for different NA mixtures (Jones *et al.*, 2012; Rowland *et al.*, 2011d), aromaticity obviously does not explain the observations made for the alicyclic acids. This speculation that OSPW NA are simply more highly branched analogues of petroleum NA (Figure 6-3; A) is not borne out by the identifications of bicyclic acids made in both petroleum and OSPW herein (Figure 6-3; B and C).

Hypothetical differences between petroleum NA and OSPW NA.

Petroleum NA · · · · · · · · · · · · · · · · · · OSPW NA

A
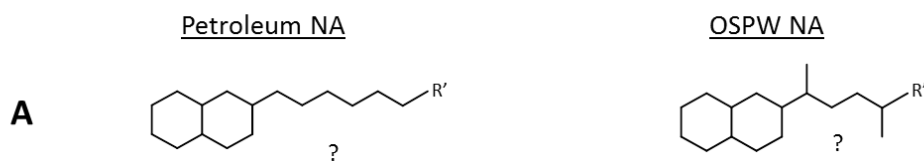
Suggested differences between petroleum NA and OSPW NA structures based on results of current study.

Petroleum NA · · · · · · · · · · · · · · · · · · OSPW NA

B
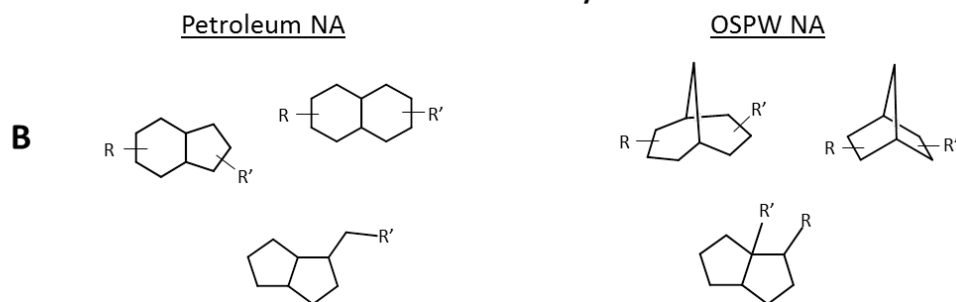
Figure 6-3: Examples of generalised structures demonstrating (A) previous

hypothesised petroleum NA and OSPW NA, suggesting that OSPW NA are more

highly branched equivalents and (B and C) a suggested hypothesis for the differences

between petroleum NA and OSPW NA based on the bicyclic NA identified in the

present study. (Structures in A are theoretical as none have been identified to support

the theory. R' = alkanoate side chain; R = alkyl substituent).

An alternative or complementary explanation is that alongside differences in alkyl

branching and aromatic content of the NA, the OSPW NA examined herein possess a

higher proportion of condensed, bridged structures, substituted at the bridgehead

position (Figure 6-3; B and C and Figure 6-4).

Following the conversion of petroleum NA to corresponding bicyclanes (Chapter 5), a

pattern in the elution orders was observed (Figure 6-4); a pattern which was also

observed for the corresponding bicyclic acid methyl esters, as shown by the analysis of

several reference acids (Wilde *et al.*, 2015). The general retention times of the

bicyclanes and reference bicyclic acids increased as follows; bicyclo[2.2.1]heptanes, bicyclo[3.2.1]octanes, bicyclo[3.3.0]octanes, bicyclo[2.2.2]octanes, bicyclo[4.3.0]nonanes, bicyclo[3.3.1]nonanes and bicyclo[4.4.0]decanes, with the more condensed-type and bridged structures eluting earlier.
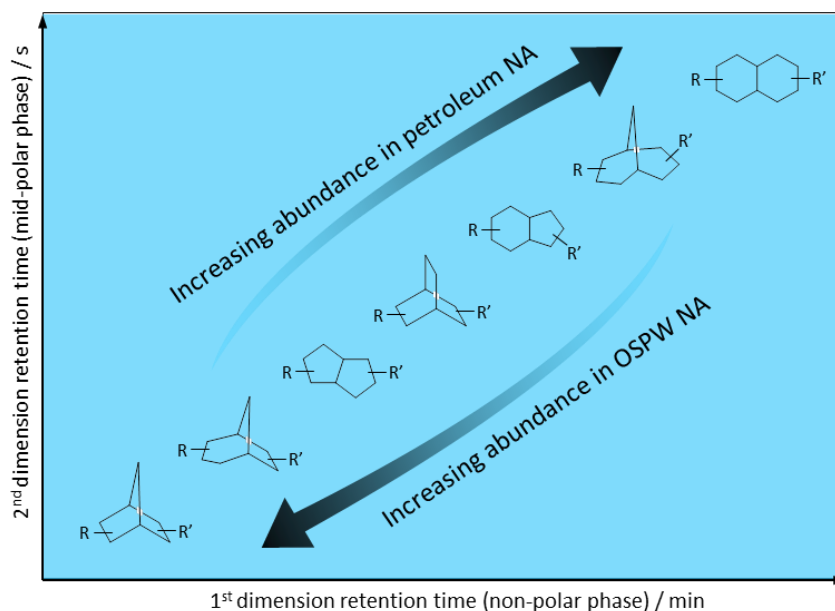
Figure 6-4: Schematic diagram showing general GC×GC elution order of bicyclic acids and bicyclanes and their relative abundance in petroleum NA and OSPW NA based on the number of structures of each identified in the present study.

Some overlap was observed, with the positions and numbers of substituents also affecting the elution order (e.g. dimethyl- isomers eluted earlier than ethyl- isomers and 1-ethylbicyclo[4.4.0]decane and the corresponding acid methyl ester eluted before 2-ethylbicyclo[4.4.0]decane and corresponding acid methyl ester (Figures 5-16 - 5-19; Chapter 5, Section 5.3.4.7). The few bicyclic acids identified in both OSPW and petroleum NA show they both contain some similar compounds: hence some overlap in overall NA retention times is to be predicted. However, there were some differences observed between the bicyclic acids identified as the corresponding bicyclanes, in petroleum NA and OSPW NA, such as the position of substituents (e.g. bridgehead

substituted isomers present in OSPW, Figure 6-3; C) as well as the presence of some unknown bicyclic acid isomers detected in OSPW, but not detected in petroleum NA (e.g. Figure 6-2; C and D). The mass spectra of the isomers **bi-V** and **-VI** in the reduced OSPW NA, did not match those of any of the reference alkanes in all the collated mass spectral data, which covered the majority of possible bridged, fused and spiro- bicyclic structures. The suggestion that OSPW NA contains more condensed, bridged structures with different substituent positions (Figure 6-3; B and C) is also supported by the identification of bicyclo[2.2.1]heptane acids in OSPW. These were the earliest eluting bicyclic acids, which were not detected in petroleum NA as the methyl esters, or corresponding bicyclanes (Wilde *et al.*, 2015; Wilde and Rowland, 2015). This explanation for the difference between petroleum NA and OSPW NA may partly explain the differences in toxicity of the two NA mixtures. Following the successful identification of the bicyclic acids, representative standards could now be used to quantify the relative proportions of different bicyclic species and measure their toxicity to confirm this (discussed in Future Work; Chapter 7, Section 7.2.1, page 334).

6.3.3.2   Adamantane Acids

Previously, Rowland *et al.* (2011c) identified a series of tricyclic diamondoid acids in OSPW, comprising 1- and 2-adamantane carboxylic acids, mono- and di-substituted alkyl adamantane carboxylic acids, as their methyl ester derivatives, using GC×GC-MS. Comparison of the mass spectra and two-dimensional retention positions with reference compounds confirmed the identification of adamantane-1-carboxylic acid and 3-ethyladamantane-1-carboxylic acid. Subsequent synthesis and purchase of more isomers and further mass spectral interpretation led to the identification and tentative identifications of numerous others (Rowland *et al.*, 2011c). Using the same technique, Bowman *et al.* (2014) reported the presence of a similar series of adamantane acids in oil sands composite tailings pore water. Most recently Lengger *et al.* (2015) confirmed the presence of several alkyl adamantane acids, including structures mainly substituted at tertiary carbon positions; structures tentatively assigned by Rowland *et al.* (2011c), which could now be confirmed using the more recently available, wider array, of reference acids. Therefore there is precedent for the identification of adamantane acids within some OSPW NA when derivatised with BF_3-methanol and examined by GC×GC-MS. Thus, if the conversion of OSPW NA methyl esters was successful for the more complex OSPW NA (free acid and esterified) mixtures herein, analysis of the final reduced acid products should lead to the identification of the corresponding alkyl adamantane hydrocarbons.

All previous identifications of adamantane acids by GC×GC-MS have involved initial derivatisation of the extracted NA to the acid methyl esters, usually by refluxing with BF_3-methanol (Rowland *et al.*, 2011c; Lengger *et al.*, 2015). When Brunswick *et al.* (2015) analysed underivatised NA in AEO extracts from fresh and aged OSPW by HPLC-MS, they were unable to detect adamantane-1-carboxylic acid in any OSPW samples, despite a limit of detection of 0.01 µg mL^{-1}. Although they acknowledged that

the concentrations of adamantane-1-carboxylic acid could be below the limits of detection of their method, they also suggested that such compounds could be artefacts produced by the derivatisation procedures, which they also suggested might be biased towards certain species (Brunswick *et al.*, 2015).

However, the occurrence of adamantane acids is known to be variable in different OSPW (Rowland *et al.*, 2012; Lengger *et al.*, 2015) and it is not clear that the particular OSPW samples examined by Brunswick *et al.* (2015) had previously been reported to contain adamantane-1-carboxylic acid (or indeed adamantane-2-carboxylic acid, since the method of Brunswick *et al.* (2015) was not reported to differentiate the two acids; Rowland *et al.* (2012)). Nonetheless, reactions involving the rearrangement of polycyclic hydrocarbons to form adamantane in the presence of Lewis acids are well documented (von R. Schleyer, 1957; Schleyer and Nicholas, 1961) and as BF_3 is also a Lewis acid and is used during the methylation of NA with BF_3-methanol, formation of rearrangement artefacts from such derivatisation procedures might be possible. The observation of methyl esters of adamantane acids in fractions esterified with other reagents (e.g. diazomethane; Bowman *et al.* (2014)) perhaps argues against this, but the identification of the adamantane hydrocarbons in the reduced, unprocessed, underivatised OSPW NA (sample #7) herein (and further identifications in sample #2) would help clarify the legitimacy of the earlier identifications of adamantane acids in OSPW derivatised with BF_3-methanol (e.g. Rowland *et al.* (2011c) and Frank *et al.* (2014)).

The lowest carbon number observed for tricyclic acid methyl esters in the 'alicyclic' methyl ester Ag-Ion fraction (F2; eluted in hexane) of sample #2 were two C_{11} acids ($M^+ = m/z$ 194). The mass spectra of the two C_{11} peaks matched those of adamantane-1- and -2-carboxylic acid methyl esters previously reported in other OSPW (Rowland *et al.*,

2011c; Rowland *et al.*, 2011a; Lengger *et al.*, 2015). Thus the identification of such acids in derivatised samples is extended to a further OSPW. However this did not negate the possibility that they were artefactual products. After reduction the lowest carbon number alkanes observed for tricyclic hydrocarbons in the reduced 'alicyclic' fraction (F2; eluted in hexane) of sample #2 were C_{13} ($M^+ = m/z$ 178), not C_{11} alkanes. This was attributed to the evaporative losses of the more volatile C_{11-12} alkanes because this hydrocarbon product mixture was not concentrated using the Kuderna-Danish apparatus, which was employed in later analyses to avoid such losses. Therefore, the expected 1- and 2-methyl adamantane were not detected in the reduced alicyclic fraction, leaving the question of aretfactual production still open; thus the reduced hydrocarbons of a non-derivatised sample (#7) was examined.

When methylated with BF_3-methanol prior to analysis of the acids by GC×GC-MS, sample #7 contained a series of C_{11} acid methyl esters, but none could be assigned as adamantane-1- or -2-carboxylic acid methyl esters. This indicated that OSPW samples vary in composition; a fact which has been used previously for differentiating different OSPW samples (Rowland *et al.*, 2012; Lengger *et al.*, 2015). The absence of adamantane-1- and -2-carboxylic acid in the derivatised samples showed that such acids are not always, if ever, consistent artefacts of BF_3-methanol treatment.

In the reduced sample #7, the lowest alkanes observed using controlled Kuderna-Danish evaporation were the expected C_{11} species ($M^+ = m/z$ 150). However, consistent with the absence of the corresponding adamantane carboxylic acids when studied as the methyl esters, none of the alkanes had mass spectra matching those of 1- or 2-methyl adamantane. These analyses were good evidence that extraction and methylation of OSPW acid methyl esters, or conversion of the acids to the corresponding hydrocarbons, does not consistently produce, via rearrangement, adamantane acids or the equivalent

hydrocarbons (*cf.* Brunswick *et al.* (2015)). If this were always the case, adamantane carboxylic acids and the corresponding methyladamantanes would have been observed in this OSPW sample. Of course it does not rule out entirely that this can never occur for any OSPW sample, but this seems unlikely given the abundance of (presumably) potential precursor C_{11} acids in the present sample and the use of typical methylation and reduction procedures herein. The statistically robust, reproducible nature of the methyl ester product distributions (Lengger *et al.*, 2015) also argues against such rearrangements, unless, that is, they too occur in a very reproducible fashion, in which case they may be equally useful for profiling.

The identity of the tricyclic C_{11} hydrocarbons in the reduced sample #7 remains unknown. However, several tricyclo-decanes, -undecanes and –dodecanes have been reported previously in petroleum and their key mass spectral features have been studied. However no partial or full mass spectra were provided (Vorob'eva *et al.*, 1971; Sanin, 1976; Golovkina *et al.*, 1984). Such structures include tricyclo[5.2.1.0^{2,6}]decane (Figure 6-5; A), tricyclo[5.4.0.0^{4,8}]undecane (B), tricyclo[5.3.1.0^{4,11}]undecane (C), tricyclo[5.3.1.0^{3,8}]undecane (homo-isotwistane) (D) and tricyclo[7.2.1.0^{2,7}]dodecane (E) (Golovkina *et al.*, 1984). The occurrence of these structures in petroleum means they could be considered as possible structures for the reduced C_{11} tricyclic acids detected herein, based on previous evidence that at least some of the NA previously identified in OSPW appear to be biotransformation products of petroleum hydrocarbons (Rowland *et al.*, 2011c; Rowland *et al.*, 2011g).

(A)   (B)   (C)   (D)   (E)
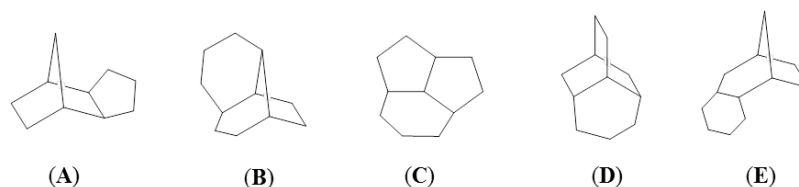
Figure 6-5: Example structures of tricyclo-decanes, -undecanes and –dodecanes previously identified in petroleum, including (A) tricyclo[5.2.1.0^{2,6}]decane, (B) tricyclo[5.4.0.0^{4,8}]undecane, (C) tricyclo[5.3.1.0^{4,11}]undecane, (D) tricyclo[5.3.1.0^{3,8}]undecane (homo-isotwistane) and (E) tricyclo[7.2.1.0^{2,7}]dodecane (Golovkina *et al.*, 1984).

An EIC of the hydrocarbons of the reduced unfractionated OSPW acids also showed a series of peaks with molecular ions consistent with C_{12} tricyclic hydrocarbons (*m/z* 164) (Figure 6-6; A). Comparison of the mass spectra for the peaks labelled **ad-I-V**, with reference mass spectra plotted from tabulated values reported by Polyakova *et al.* (1973) and those in the NIST MS library for alkyl adamantanes, supported assignment of 1-ethyl and 2-ethyladamantane (**ad-II** and **ad-V**; Figure 6-6). These were readily identified by the strong M-29 ion corresponding to the loss of ·C_2H_5. The 2-ethyl isomer was distinguished from the 1-ethyl isomer by the stronger molecular ion and later retention position (Figure 6-6; B-E). The corresponding adamantane ethanoic acids were then identified in the methyl esters by comparison of data with those for reference compounds, once more indicating the complementary nature of the two GC×GC-MS based approaches. The identification of these mono-substituted acids as the hydrocarbons, in the reduced non-methylated, unfractionated OSPW NA, finally showed that the acids are indigenous and not artefactual (*cf.* Brunswick *et al.* (2015)).

The mass spectra of alkyl adamantanes are very distinct and many reference mass spectra are readily available in the literature since diamondoid hydrocarbons are commonly used as biomarkers in petroleum geochemistry (Peters *et al.*, 2005b). The

mass spectra of alkyl adamantanes substituted at tertiary carbons display a relatively low intensity molecular ion (approx. 5 – 20%), compared with those of isomers substituted at secondary carbon positions, which display relatively intense molecular ions (approx. 30 – 50%) (Golovkina *et al.*, 1984). Typically, alkyl adamantanes substituted at the secondary carbon positions elute much later in GC (and GC×GC) than isomers substituted at the tertiary carbon positions (Petrov, 1987).

All alkyl adamantane mass spectra usually display a dominant or base peak ion corresponding to the loss of the largest alkyl group as a radical, producing an adamantyl cation (*m/z* 135) for mono-substituted isomers and corresponding alkyl adamantyl cations (e.g. *m/z* 149 and 163) in poly-substituted alkyl adamantanes. Although, from previous mass spectrometric studies of alkyl adamantanes, it is postulated that the structure of this cation does not retain that of a tricyclic adamantyl cation with the charge stabilised on the secondary or tertiary bridgehead carbon but extensively rearranges to a cyclic allyl ion (Golovkina *et al.*, 1984). Independent of its structure, the stability of the cation formed means extracted ion monitoring of the molecular ions and expected base peak ions enables alkyl adamantanes to be readily identified.

The GC elution order of many dimethyl-, ethyl-, methylethyl- and trimethyl adamantane isomers is well documented (Hála *et al.*, 1970; Wingert, 1992; Wei *et al.*, 2006; Wang *et al.*, 2013) and therefore the assignment above of the two ethyl isomers also allowed identification of numerous dimethyl- isomers (Figure 6-7) based on the comparison of their retention positions, relative to the ethyl isomers. The only two dimethyladamantane isomers reported to elute between the two ethyl isomers are the *cis-* and *trans-* isomers of 2,4-dimethyladamantane (Wang *et al.*, 2013; Wei *et al.*, 2006). In the present study this assignment was supported by the high intensity molecular ions

(50 – 60%) observed in the mass spectra of peaks **ad-III** and **ad-IV**, typical for alkyl adamantanes substituted at the secondary carbon positions (Figure 6-7; A and B).
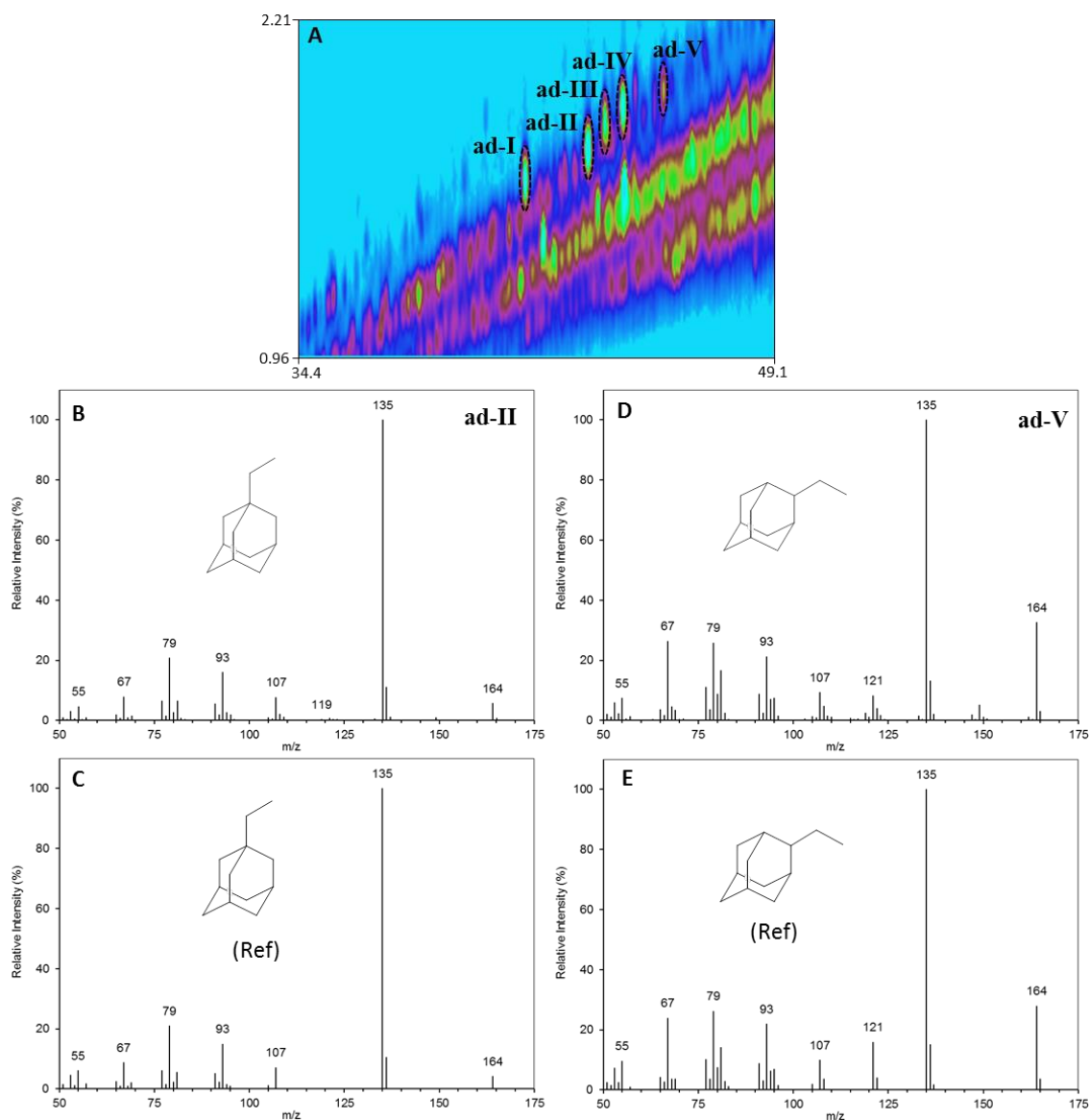
Figure 6-6: (A) EIC (*m/z* 135 and 149) of the hydrocarbon product after reduction of the underivatised, unfractioned OSPW NA and (B-D) identification of 1-ethyl and 2-ethyladamantane isomers (**ad-II** and **ad-V**) by comparison with reference mass spectra and GC elution order (Polyakova *et al.*, 1973).
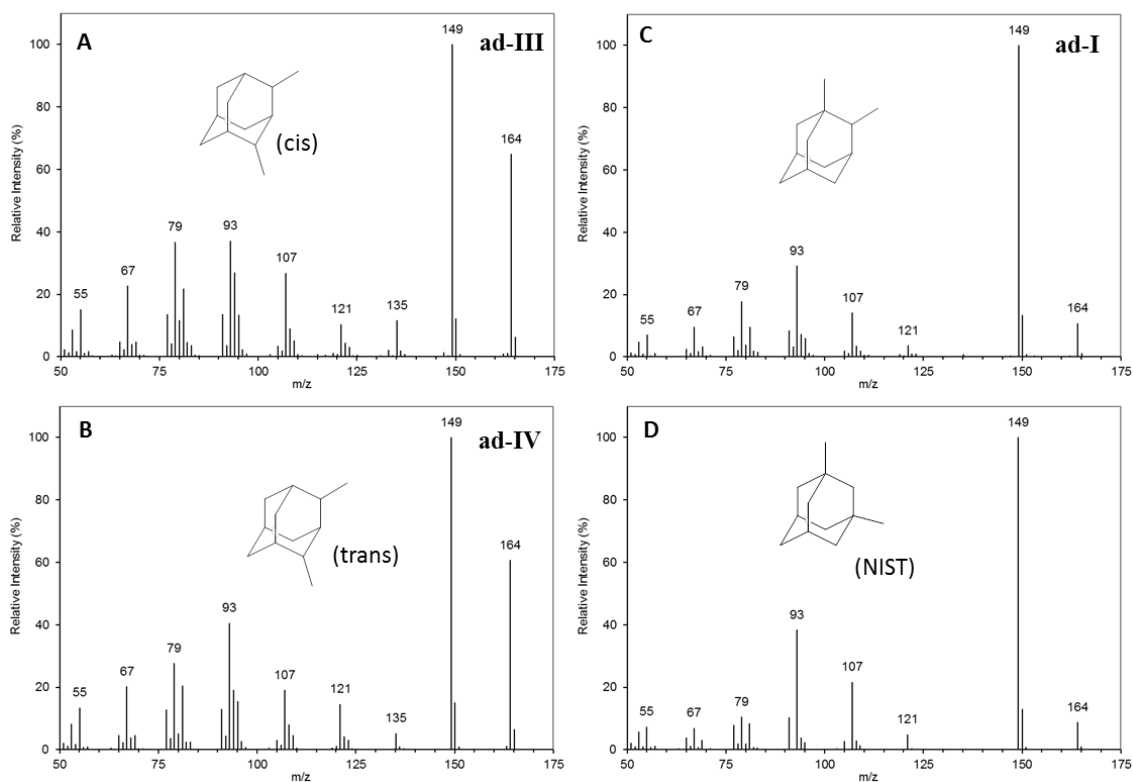
Figure 6-7: Mass spectra of isomers **ad**-**I**, **III** and **IV** (labels refer to components in EIC in Figure 6-6) assigned as dimethyladamantanes including (A and B) two isomers of 2,4-dimethyladamantane (**ad**-**III** and **IV**) and (C) 1,2-dimethyladamantane (**I**) by comparison of the known GC elution order of alkyl adamantanes relative to 1- and 2-ethyladamantane (**ad**-**II** and **V**) and by comparison with (D) reference mass spectrum of 1,3-dimethyladamantane (Polyakova *et al.*, 1973; Wang *et al.*, 2013; Wingert, 1992).

The earliest eluting peak (**ad**-**I**) had a mass spectrum which was similar to that of 1,3-dimethyladamantane (Figure 6-7; C and D) and 3-methyladamantane-1-carboxylic acid has previously been identified in OSPW NA (Lengger *et al.*, 2015), but the reported retention position for 1,3-dimethyladamantane relative to the 1-ethyl isomer was much earlier than observed for **ad**-**I** herein. Instead the retention position of **ad**-**I** more closely matched that of 1,2-dimethyladamantane. The mass spectrum of the 1,2-dimethyl isomer has not been reported fully but might be expected to be very similar to that of the 1,3-dimethyl- isomer. Wingert (1992) reported that the mass spectra of the 1,3- and 1,4-

dimethyl isomers were almost identical, suggesting they undergo a similar fragmentation mechanism and that it is the methyl group substituted at the tertiary carbon position which is preferentially lost; this is also consistent with the difference in relative intensities of the molecular ions for 1- and 2-methyladamantane. The molecular ion of the 1,2-dimethyl isomer reported by Wang *et al.* (2013) had a relative intensity of 12%, matching that of **ad**-**I** (Figure 6-7; C and D).

The assignment of the 1,2-dimethyl- isomer was also consistent with the absence of 3-methyladamantane-1-carboxylic acid methyl ester after comparison of the retention time and mass spectrum of the reference acid methyl ester with the original NA methyl esters. All five assignments were supported by comparison of the EIC in Figure 6-6; A and elution order of peaks **ad**-**I**-**V** with those reported by Wang *et al.* (2013) for the same isomers, during their investigation of diamondoid hydrocarbons in crude oil.

Extracted ion monitoring of both the reduced alicyclic fraction and reduced underivatised, unfractionated OSPW samples also showed series of peaks displaying molecular ions at *m/z* 178, corresponding to C_{13} tricyclic hydrocarbons, many of which had mass spectra matching the reference mass spectra of trimethyl- and methylethyl-adamantanes (Figures 6-8; A and Figure 6-9; A-I). However, due to the complexity of the unfractionated sample, the isomers were more difficult to distinguish. Therefore, as poly-substituted adamantanes have distinct mass spectra, a CLIC expression was applied to the chromatograms (described in Chapter 2, Section 2.1.4, page 56; Reichenbach *et al.* (2005)); the conditions of the expression were chosen to show only peaks with mass spectra possessing a base peak ion at *m/z* 135, 149 *or* 163 *and* with the relative intensity of *m/z* 93 < 55% *and m/z* 192 *and* 206 <1%. The resulting chromatogram was much simplified, and displayed more clearly a series of isomers with mass spectra fulfilling the criteria of poly-substituted alkyl adamantanes (Figure 6-8; B).
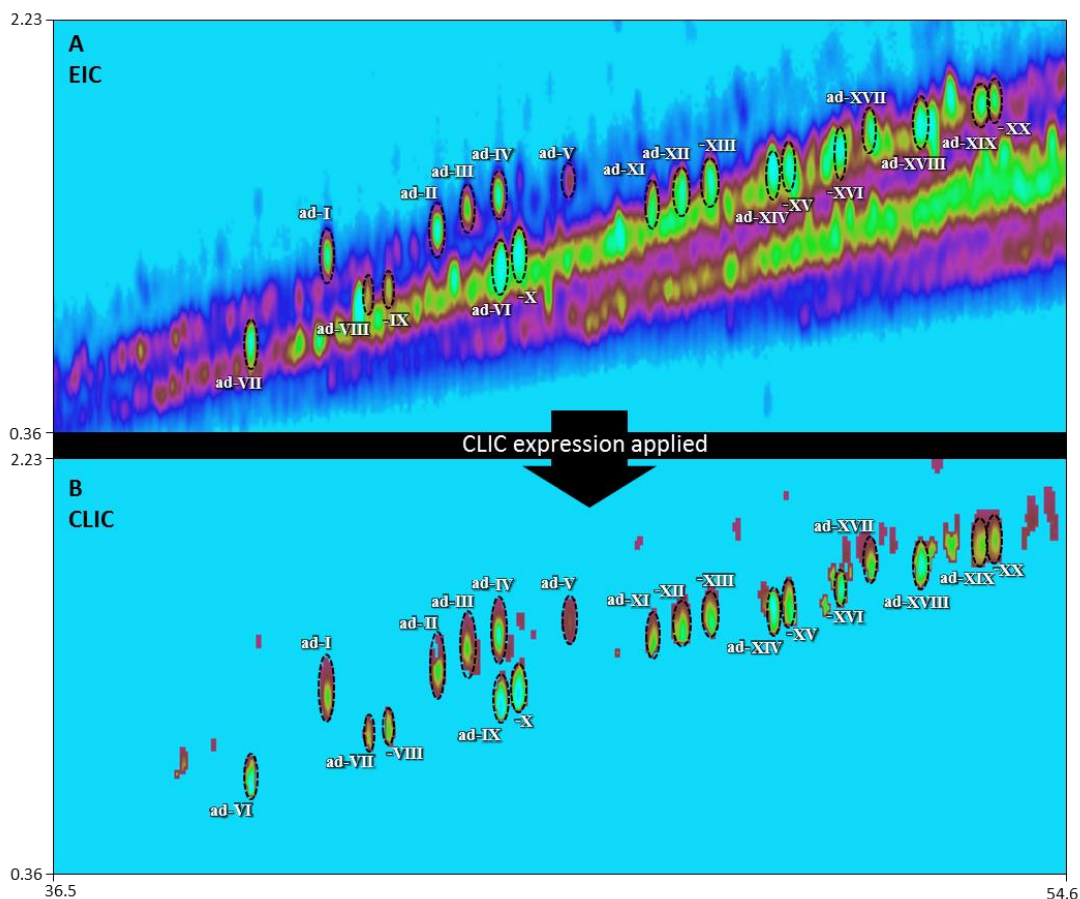
Figure 6-8: Comparison of an (A) EIC (*m/z* 135, 149, 163 and 178) and (B) chromatogram after a CLIC expression was applied (peaks only with a base peak of *m/z* 135, 149 or 163 and relative intensity of *m/z* 93 < 55% and *m/z* 192 and 206 <1%) of the reduced unfractionated OSPW sample, clearly showing the presence of three dimethyl- (**ad**-**I**, **III** and **IV**), 2 ethyl- (**ad**-**II** and **V**), 8 trimethyl- (**ad**-**VI**-**VIII**, **X**-**XIII** and **XVII**) and seven ethylmethyl-adamantane isomers (**ad**-**IX**, **XIV**-**XVI** and **XVIII**-**XX**) based on comparison with reference mass spectra (Polyakova *et al.*, 1973) and known elution order (Wang *et al.*, 2013; Wingert, 1992).

The C_{13} trimethyl- isomers were distinguished from methylethyl- isomers based on the dominant loss from the molecular ion; trimethyl- isomers displayed a base peak ion at *m/z* 163 (M-15) whereas those with an ethyl substituent displayed a base peak ion at *m/z* 149 (M-29). The additional clarification of peaks provided by the CLIC expression chromatogram, allowed comparison of the retention positions of the C_{13} adamantane isomers with those reported in the literature to aid identification.

The peak labelled **ad**-**IX** was assigned as a methylethyl- isomer based on its base peak ion at *m/z* 149 and was the earliest eluting methylethyl- isomer. The earliest eluting methylethyl- isomer and the only one reported to elute between 1-ethyl and 2-ethyladamantane (**ad**-**II** and **V**), is 1-ethyl-3-methyladamantane (Wingert, 1992; Wang *et al.*, 2013). Comparison of its mass spectrum with the reference spectrum reported by Polyakova *et al.* (1973) confirmed this identification for **ad**-**IX** (Figure 6-9; B and D).

Of course 1-ethyl-3-methyladamantane could theoretically originate from either 3-methyladamantane-1-ethanoic acid or 3-ethyladamantane-1-carboxylic acid, both of which have been previously reported in different samples of OSPW NA from different industries (Lengger *et al.*, 2015). Subsequent analysis of both reference acids as their methyl ester derivatives showed that 3-methyladamantane-1-ethanoic acid methyl ester was detected and 3-ethyladamantane-1-carboxylic acid was not detected in the unfractionated OSPW NA, indicating the 1-ethyl-3-methyladamantane in the hydrocarbon product derived from 3-methyladamantane-1-ethanoic acid.

Six other peaks (**ad**-**XIV**-**XVI** and **ad**-**XVIII**-**XX**) had mass spectra corresponding with methylethyl- isomers. However, identification of the substituent positions was not possible. Interestingly though, Wang *et al.* (2013) also reported the presence of the 1-ethyl-3-methyl- isomer in crude oil as well as six other methylethyl- isomers with retention positions later than 2-ethyladamantane, similar to that observed for peaks **ad**-**XIV**-**XVI** and **ad**-**XVIII**-**XX** in Figure 6-8.

Based on the relative retention positions and elution order of the eight peaks identified as trimethyl- isomers (**ad**-**VI**-**VIII**, **X**-**XIII** and **XVII**) compared with those reported by Wang *et al.* (2013) and Wingert (1992), the earliest eluting peak (**ad**-**VI**) was identified as 1,3,6-trimethyladamantane and its mass spectrum matched the reference mass spectrum reported by Polyakova *et al.* (1973) (Figure 6-9; A and C).
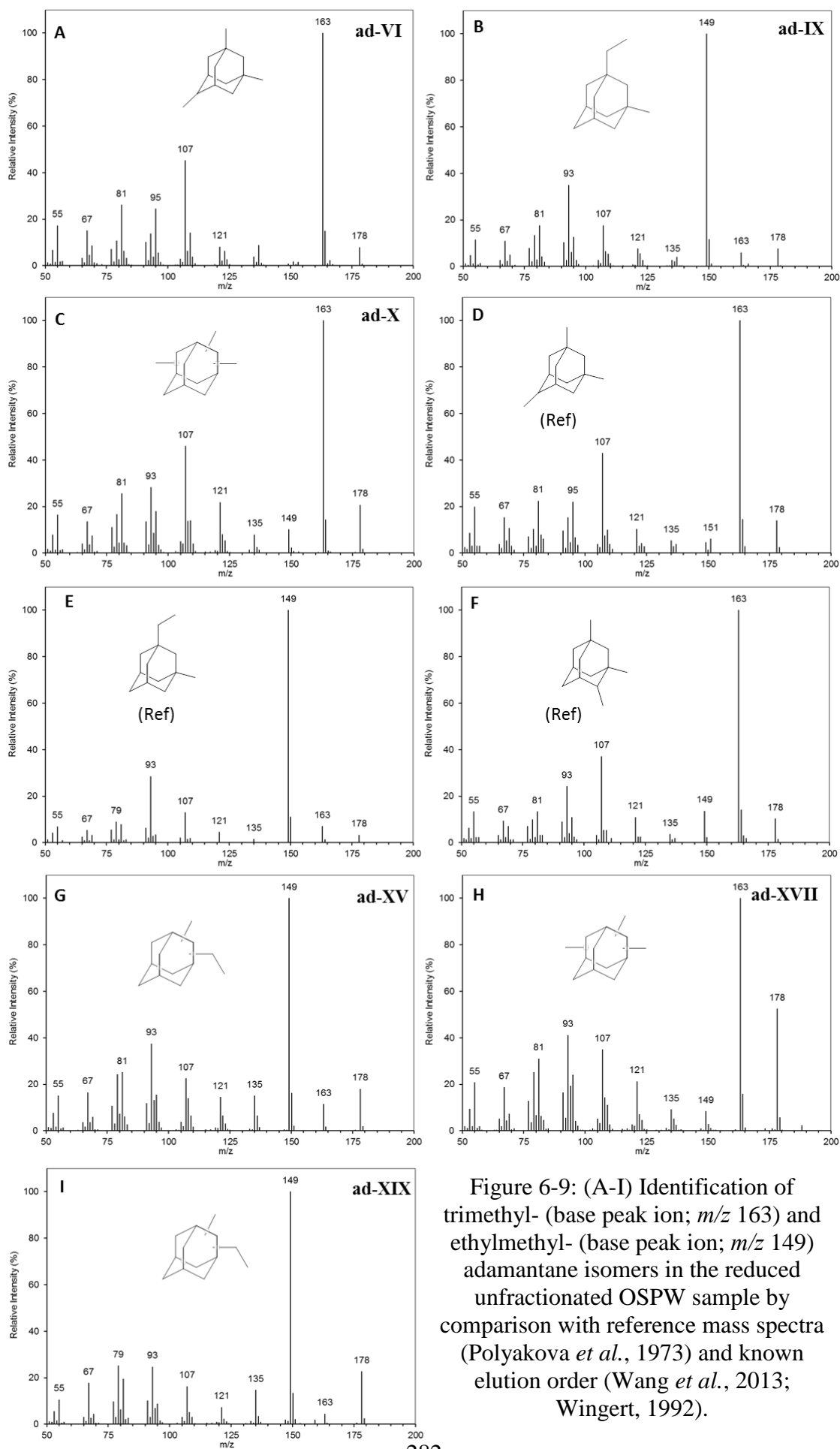
Figure 6-9: (A-I) Identification of trimethyl- (base peak ion; *m/z* 163) and ethylmethyl- (base peak ion; *m/z* 149) adamantane isomers in the reduced unfractionated OSPW sample by comparison with reference mass spectra (Polyakova *et al.*, 1973) and known elution order (Wang *et al.*, 2013; Wingert, 1992).

The only other trimethyl- isomer reported to elute before 1,2-dimethyladamantane (**I**) is 1,3,5-trimethyladamantane. However, subsequent comparison of the original NA methyl esters with the retention position and mass spectrum of the reference acid, 3,5-dimethyladamantane-1-carboxylic acid methyl ester, showed it was absent, supporting the above alternative assignment as the 1,3,6-trimethyl- isomer. Wang *et al.* (2013) and Wingert (1992) both reported that only two isomers eluted between 1,2-dimethyladamantane and 1-ethyladamantane (**ad**-**I** and **II**), such as the peaks **ad**-**VII** and **VIII** in Figure 6-8. These were the *cis*- and *trans*- isomers of 1,3,4-trimethyladamantane. Comparison of the retention position of the remaining isomer **X** indicated that it could be 1,2,3-trimethyladamantane (Wang *et al.*, 2013). The positions of the alkyl groups in the remaining trimethyl- isomers (**ad**-**XI**-**XIII** and **XVII**) which eluted after 2-ethyladamantane (**ad**-**V**) were not assignable. However, based on their late retention positions and the high intensity of the molecular ions observed in some of the mass spectra, such as in the mass spectrum of **ad**-**XVII** (Figure 6-9; H), they were postulated to be substituted at one or more of the secondary carbon positions.

In summary, analysis of the hydrocarbon products of both derivatised (methylated) fractionated (sample #2) and underivatised, unfractionated OSPW NA (sample #7) from different OSPW samples resulted in the identification of numerous alkyl adamantanes in each (Figures 6-6 - 6-9). The identifications of alkyl adamantane acids were supported by subsequent comparison of data for the original OSPW NA methyl esters with those of the esters of reference acids.

These results confirm that the conversion of OSPW NA mixtures to the corresponding hydrocarbons was successful, despite the increased complexity compared to the petroleum acid mixtures previously analysed in Chapter 5.

Secondly, the identification of numerous isomers of monoalkyl- adamantanes and therefore by inference, monoalkyl- adamantane acids, in both the unfractionated, underivatised OSPW NA and the derivatised fraction of a second OSPW sample (as acid methyl esters), is strong evidence that these were indeed present as authentic components of OSPW NA, and are at least, not all (if indeed any), artefacts of derivatisation procedures. This was further supported by the identification of alkyl adamantanes substituted mainly at secondary carbon positions. Isomers substituted solely at the tertiary carbon positions, which are deemed most stable and hence most likely to form during Lewis acid catalysed reactions, were largely absent or more minor. The absence of adamantane-1- and 2- carboxylic acids in one sample of OSPW even after methylation (and of the corresponding hydrocarbons on reduction), and in the presence of other C_{11} acids, also shows that adamantane acids are not ubiquitous artefacts of methylation or reduction processes.

Finally, due to the extensive reports of reference mass spectra and the known elution order of alkyl adamantanes, conversion of the OSPW NA to their corresponding hydrocarbons has confirmed the presence of several structures that were only tentatively assigned previously when based on the acid methyl ester mass spectra. This also resulted in the identification of several new alkyl adamantane acids. Synthesis, or purchase when available, of the newly identified alkyl adamantane acids means these structures could be added to the adamantane acids used previously to profile OSPW NA variability and source characterisation (Lengger *et al.*, 2015). The adamantane acids profiled by Lengger *et al.* (2015) were almost exclusively isomers substituted at the tertiary carbon positions, most likely due to availability of commercial reference compounds for confirmation. However, the results of this investigation suggest that it would be worthwhile to synthesise and use some isomers with alkyl groups and

carboxyl groups substituted at the secondary carbon positions in profiling investigations, as it appears they are indeed present in some OSPW NA.

Alkyl adamantane hydrocarbons have been identified in various crude oils (Sanin, 1976). The relative abundance of the different isomers in crude oil were different to those observed when formed at equilibrium by isomerisation over an alumina catalyst (Sanin, 1976). If the relative abundance of the individual alkyl adamantane acids was measured relative to the total alkyl adamantane acids detected, the ratios may indicate the type of conditions under which the acids were formed, aiding source characterisation.

6.3.3.3 Tricyclic terpenoid acids

Apart from the tricyclic diamondoid acids previously discussed (Section 6.3.3.1), few alicyclic tricyclic acids have been identified in OSPW. The abundance of isomers within the homologous series observed in EICs of the lower molecular weight tricyclics (Figures 6-6; A and 6-8), suggested numerous different structures were possible. However, when examining the mass spectra of the higher molecular weight compounds, a clear series of peaks (**tt-I** to **-VI**) with molecular ions corresponding to C_{20-24} tricyclic hydrocarbons, were observed eluting late in the chromatogram of the reduced alicyclic Ag-Ion fraction of OSPW NA (Figure 6-10; A and B). Their elution in the alicyclic Ag-Ion fraction and their mass spectral fragmentation, strongly supports their assignment as alicyclic, tricyclic hydrocarbons and not other compounds with the same nominal mass, such as tricyclic triaromatic hydrocarbons.

The mass spectra of isomer **tt-I** to **-VI** all displayed a similar fragmentation pattern, characterised by low-medium intensity molecular ions and M-15 ions and dominated by strong base peak ions at *m/z* 191 (Figure 6-10). The mass spectra of isomers **tt-I** to **-VI** were characteristic of those of tricyclic terpane hydrocarbons (Figure 6-10; F and H). Tricyclic terpanes are known petroleum hydrocarbons, often used as biomarkers, due to their abundance in petroleum and sediments (Moldowan *et al.*, 1983; Anders and Robinson, 1971). Ekweozor and Strausz (1982) reported the identification of a series of C_{19-30} tricyclic terpanes present in bitumen from the Athabasca oil sands. Most tricyclic terpane hydrocarbons have been reported to possess a cheilanthane 'core', with the branched alkyl side chain substituted at position 14 (Figure 6-10; F), increasing in chain length as carbon number increases.
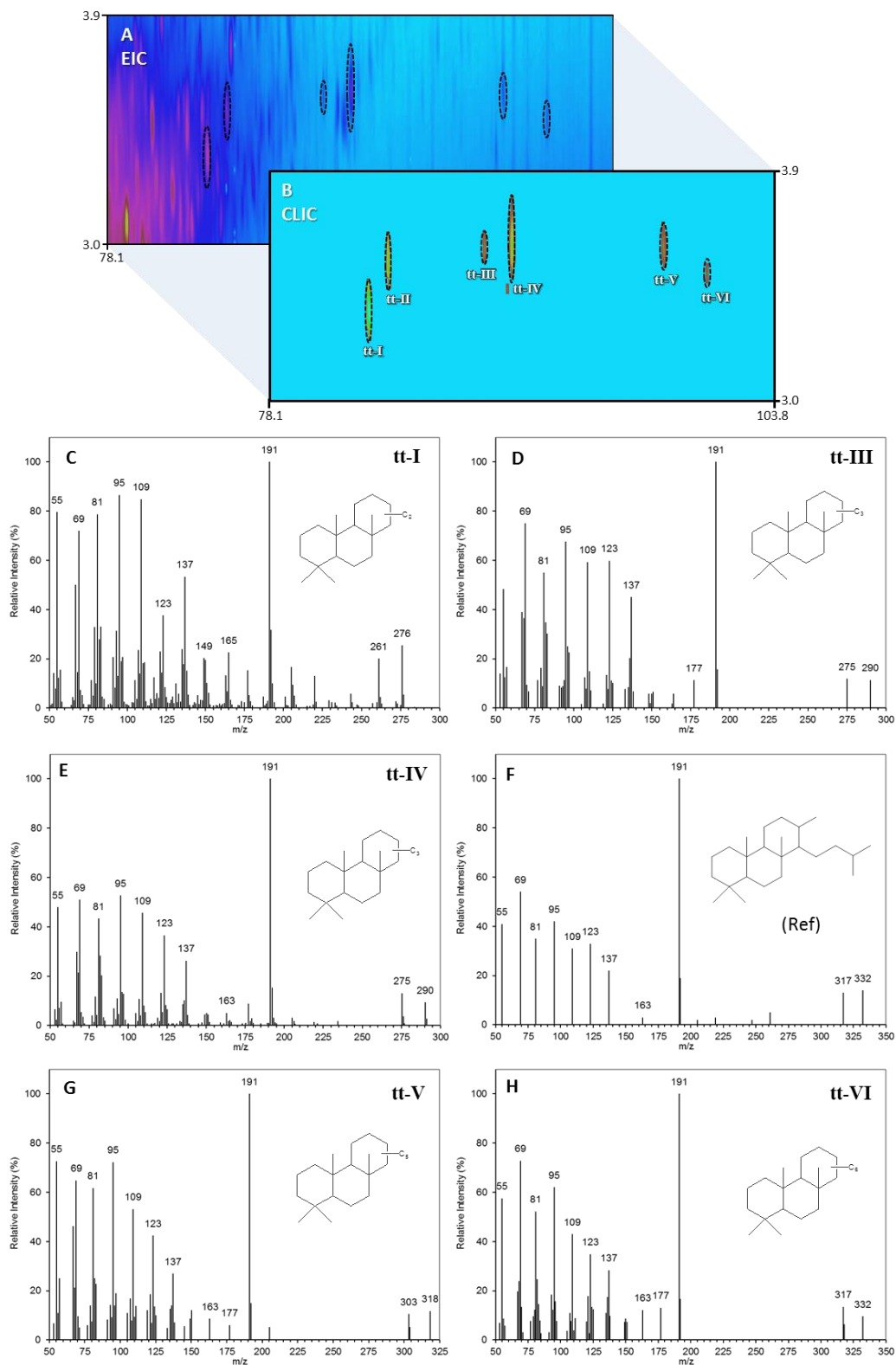
Figure 6-10: (A) EIC (*m/z* 191) and (B) CLIC expression chromatogram revealing series of isomers assigned as (C-H) C_{20} (**tt-I** and **II**), C_{21} (**tt-III** and **-IV**), C_{23} (**tt-V**) and C_{24} (**tt-VI**) tricyclic terpanes by comparison with reference mass spectra (Chicarelli *et al.*, 1988; Cyr and Strausz, 1983; Philp, 1985; Hall and Douglas, 1981).

Tricyclic terpenoid acids have not been reported in OSPW NA previously. However, they have been reported in other petroleum NA by Seifert (1975) and, perhaps more significantly in the present context, by Cyr and Strausz (1983) in bitumen from the Athabasca oil sands. Although the availability of the mass spectra for tricyclic terpenoid acid methyl esters was far more limited, the mass spectrum of the C_{24} tricyclic terpenoid acid methyl ester reported by Cyr and Strausz (1983) was used to examine the original acid methyl esters of **tt-I** to **-VI** in the original alicyclic Ag-Ion fraction of NA methyl esters. The mass spectrum of the acid methyl ester was almost identical to that of the hydrocarbon (Figure 6-10; F), again dominated by a base peak ion at *m/z* 191, with a low-medium intensity molecular ion and M-15 ion, 44 Da higher than the corresponding hydrocarbon. However, the corresponding acid methyl esters were expected to elute later than hydrocarbons, towards the end of the temperature programme and as such, only two isomers, including the first C_{20} and C_{21} acid methyl esters, with mass spectra matching those of the reference spectra, were observed.

Based on the molecular ions, in the mass spectra of **tt-I** to **-VI**, the series included two C_{20} (**tt-I** and **-II**), two C_{21} (**-III** and **-IV**), one C_{23} (**-V**) and one C_{24} (**-VI**) structure. After comparison of their mass spectra with those reported in the literature (Chicarelli *et al.*, 1988; Philp, 1985; Hall and Douglas, 1981), identification of some of the corresponding acid methyl esters and the previous evidence of such acids present in petroleum and Athabasca bitumen, **tt-I** to **-VI** were assigned as tricyclic terpanes. The structures were proposed to possess cheilanthane 'cores', methyl- substituted in the 13-position with a branched alkyl chain substituted in the 14-position. However, the structures were only tentatively assigned (Figure 6-10), because the presence of the methyl substituent in the 13-position and the structure of the alkyl chain substituted in 14-position in terpenoid acids has been debated for the lower (C_{20}) molecular acids (Cyr and Strausz, 1983).

6.3.3.4   Tetracyclic and pentacyclic diamondoid acids

The presence of tricyclic diamondoid acids in OSPW was proposed to be, at least partly, due to the biotransformation of the corresponding hydrocarbons (Rowland *et al.*, 2011c); adamantane and alkyl adamantanes are known constituents of crude oil and bitumen (Sanin, 1976; Petrov, 1987). Tetra- and pentacyclic diamondoid hydrocarbons such as diamantane and alkyl diamantanes (Figure 6-11; A and C-E) have also been reported in various crude oils (Petrov, 1987). However diamantane hydrocarbons have been found to be much more resistant to biodegradation compared to the adamantane homologues (Wang *et al.*, 2006). Adamantane hydrocarbons were reported to be relatively more biodegradable than other non-diamondoid tricyclic hydrocarbons (e.g. tricyclic terpanes; Wang *et al.* (2006)), which would explain the reported absence of adamantane and its methyl to butyl derivatives in the saturates fraction of Athabasca bitumen (Strausz *et al.*, 2010) and the numerous adamantane acids present in the OSPW, reported by Rowland *et al.* (2011c) and identified in Section 6.3.3.1.

However, Rowland *et al.* (2011g) also detected some pentacyclic diamondoid acids in OSPW, confirming the presence of diamantane-1- and -3-carboxylic acid by comparison of the OSPW NA methyl esters with the GC×GC retention positions and mass spectra of reference acid methyl esters. Mass spectral interpretation also led to the tentative identification of methyl-, dimethyl- and ethyldiamantane carboxylic acids as well as a diamantane ethanoic acid and methyl- and dimethyl- derivatives. Rowland *et al.* (2011g) suggested the occurrence of these acids was from the biodegradation of the corresponding diamantane hydrocarbons and suggested their presence was evidence for an unprecedented degree of biodegradation.

Isomers with mass spectra displaying molecular ions and fragmentation patterns corresponding to those of tetracyclic acids were also tentatively assigned based on mass spectral interpretation (Rowland *et al.*, 2011g). The tetracyclic acids were proposed to

possess a ring-opened diamantane structure (Figure 6-11; B) and were postulated to be further biodegradation products of the diamantanes. Rowland *et al.* (2011a) later synthesised some tetracyclic, ring-opened diamantane acids. However, comparison of the retention positions and mass spectra of the synthetic reference standards with those of NA within OSPW, did not confirm their identification.
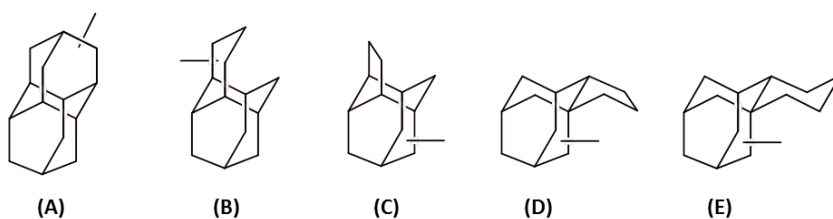
Figure 6-11: Examples of substituted pentacyclic and tetracyclic diamondoid compounds showing the structure of the skeletal core, including (A) diamantane, (B) 2,4-cyclohexano-adamantane (tetracyclic ring-opened diamantane), (C) 2,4-cyclopentano-adamantane, (D) 1,2-cyclopentano-adamantane and (E) 1,2-cyclohexano-adamantane.

Following the successful conversion and identification of the alkyl adamantane hydrocarbons herein and therefore, by inference, alkyl adamantane acids, in both the reduced alicyclic fraction of the esters and unfractionated OSPW free NA, the hydrocarbon products of each were further examined for isomers of pentacyclic and tetracyclic diamondoid hydrocarbons.

Reference spectra reported for diamantane hydrocarbons are fewer than those of the adamantanes. However, the mass spectra of alkyl diamantanes are as distinctive as those of the alkyl adamantanes due the stability of the cage-like core; the molecular ions undergo similar fragmentation patterns to those of the alkyl adamantanes. For example, the molecular ion of 3-methyldiamantane (M^+ = *m/z* 202), in which the methyl group is substituted on a secondary carbon position, is significantly more intense than the

molecular ions observed for the 1- and 4-methyl- isomers (Kuraš and Hála, 1970; Golovkina *et al.*, 1984). Comparison of the reference mass spectra of 1-, 3- and 4-methyldiamantanes reported by Kuraš and Hála (1970) and their GC elution order (Wingert, 1992; Wang *et al.*, 2013), allowed the identification of all three isomers in the unfractionated OSPW sample herein and of 3-methyldiamantane in the reduced alicyclic NA ester fraction (Figure 6-12; B).

Similar to the mass spectra of alkyl adamantanes, alkyl diamantanes display a dominant base peak ion corresponding to the loss of the largest alkyl group as a radical, producing a diamantyl cation (*m/z* 187) for mono-substituted isomers and corresponding alkyl diamantyl cations (e.g. *m/z* 201 and 215) in poly-substituted isomers.

Extracted ion monitoring of the key fragment ions then revealed the series of isomers assigned as alkyl diamantanes (**diA-I** to **diA-XXV**) ranging from C_{15-18} based on the observed molecular ions (*m/z* 202, 216, 230 and 244) (Figure 6-12). A CLIC expression, equivalent to that produced for the alkyl adamantanes (*cf.* Figure 6-8 above; page 280) was applied using the observed base peak ions and molecular ions for the alkyl diamantanes; the peaks remaining in the chromatogram supported those assigned in the EIC in Figure 6-12; A.

Interpretation of the mass spectra of the peaks labelled **diA-I** to **XXV** (examples shown in Figure 6-12; B-G) resulted in the assignment of isomers of ethyl- (Figure 6-12; D), dimethyl- (E), ethylmethyl- (F and G) and dimethylethyl- (H) diamantanes. These results provided strong supporting evidence for the array of highly substituted alkyl diamantane acids previously speculated to be present in OSPW by Rowland *et al.* (2011g).
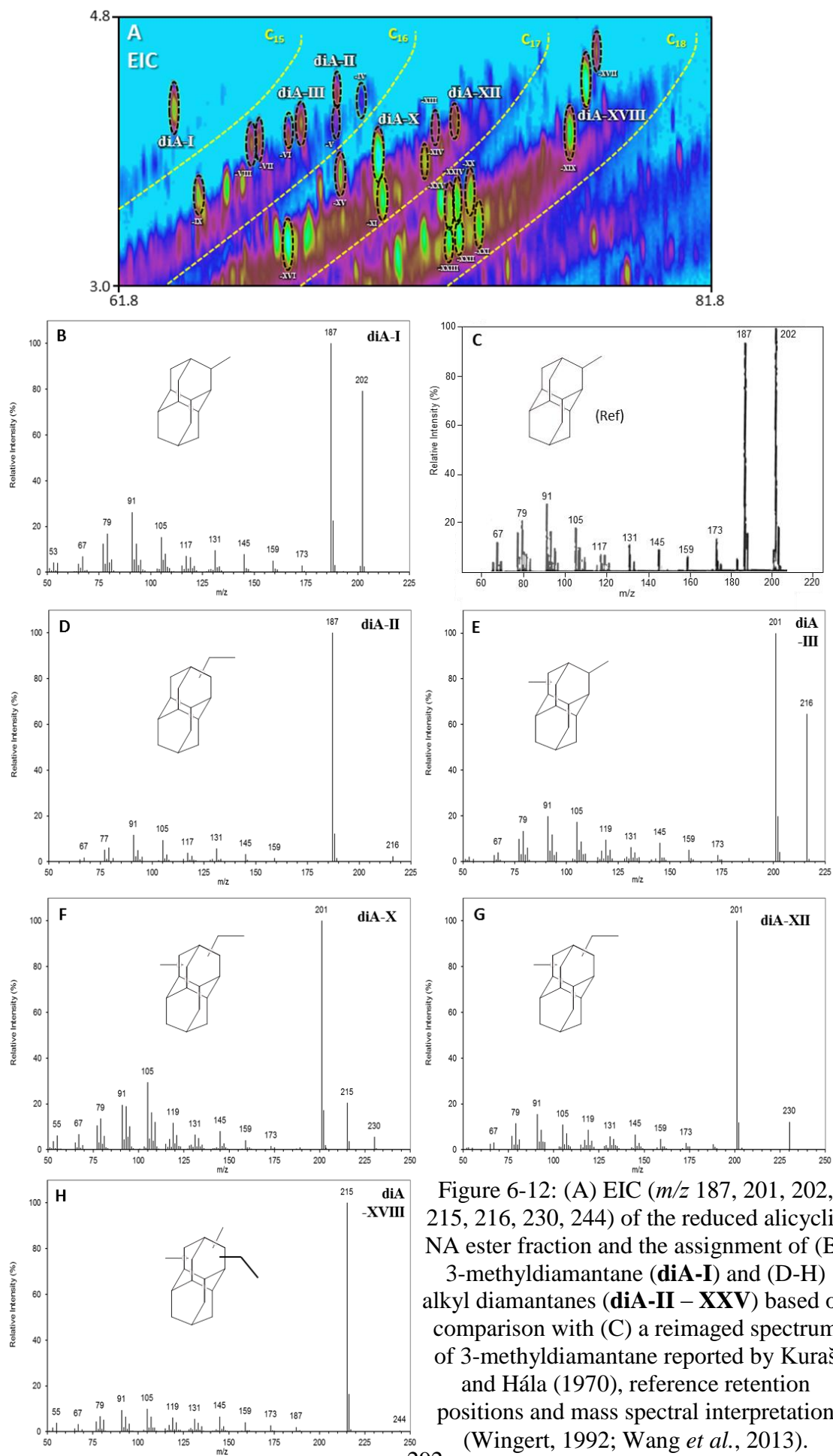
Figure 6-12: (A) EIC (*m/z* 187, 201, 202, 215, 216, 230, 244) of the reduced alicyclic NA ester fraction and the assignment of (B) 3-methyldiamantane (**diA-I**) and (D-H) alkyl diamantanes (**diA-II – XXV**) based on comparison with (C) a reimaged spectrum of 3-methyldiamantane reported by Kuraš and Hála (1970), reference retention positions and mass spectral interpretation (Wingert, 1992; Wang *et al.*, 2013).

Similarly, series of peaks were observed in the hydrocarbon products obtained from both samples #2 and #7, with molecular and base peak ions consistent with C_{14-18} tetracyclic adamantanoid hydrocarbons, and some additional C_{13} isomers present in the reduced sample #7 (Figures 6-13 and 6-14). The mass spectra were very similar to those of alkyladamantanes and alkyldiamantanes, dominated by a base peak ion, presumably corresponding to the loss of the largest alkyl substituent and suggesting a highly stable core (Figures 6-13 and 6-14). These hydrocarbons were presumed to originate from tetracyclic acids, such as those previously tentatively assigned by Rowland *et al.* (2011g). Subsequent examination of the original acid methyl esters showed isomers across the same carbon number range, with mass spectra similar to those previously reported in other OSPW samples (Rowland *et al.*, 2011g).

Interestingly, the lowest carbon number isomers displayed base peak ions of *m/z* 161 (Figure 6-13; B-C). Assuming the compounds possess adamantanoid-like structures, based on the structures of hydrocarbons previously identified in crude oils (Figure 6-11; B-E), the loss of methyl (M-15) and ethyl (M-29) groups from a C_{13} ($M^+ = 176$) and C_{14} ($M^+ = 190$) isomer would indicate a C_{12} core; *m/z* 161 (100%) corresponding with a $C_{12}H_{17}^+$ highly stable cation. The only alkyl adamantanoid structures with a C_{12} core, previously assigned in crude oils, are alkyl 2,4-cyclopentano-adamantanes (Petrov, 1987). In contrast, the 2,4-cyclohexano-adamantane structures tentatively proposed for the tetracyclic acids by Rowland *et al.* (2011g) possessed a C_{13} core; therefore, monosubstituted isomers would display a base peak ion at *m/z* 175, as shown in the mass spectra in Figure 6-14; A and B. The OSPW acids did not correspond to those 2,4-cyclohexano-adamantane acids synthesised by Rowland *et al.* (2011a) since the GC×GC retention positions were different, though the spectra were very similar. Analysis of the reduced acid hydrocarbon products herein therefore provides the first evidence for a firmer assignment of the tetracyclic acids as 2,4-cyclopentano-adamantane acids.

Subsequent re-examination of the unfractionated OSPW NA as their acid methyl esters, did indeed reveal esters with mass spectra consistent with those of the corresponding 2,4-cyclopentano-adamantane acids (Appendix Figure 29).
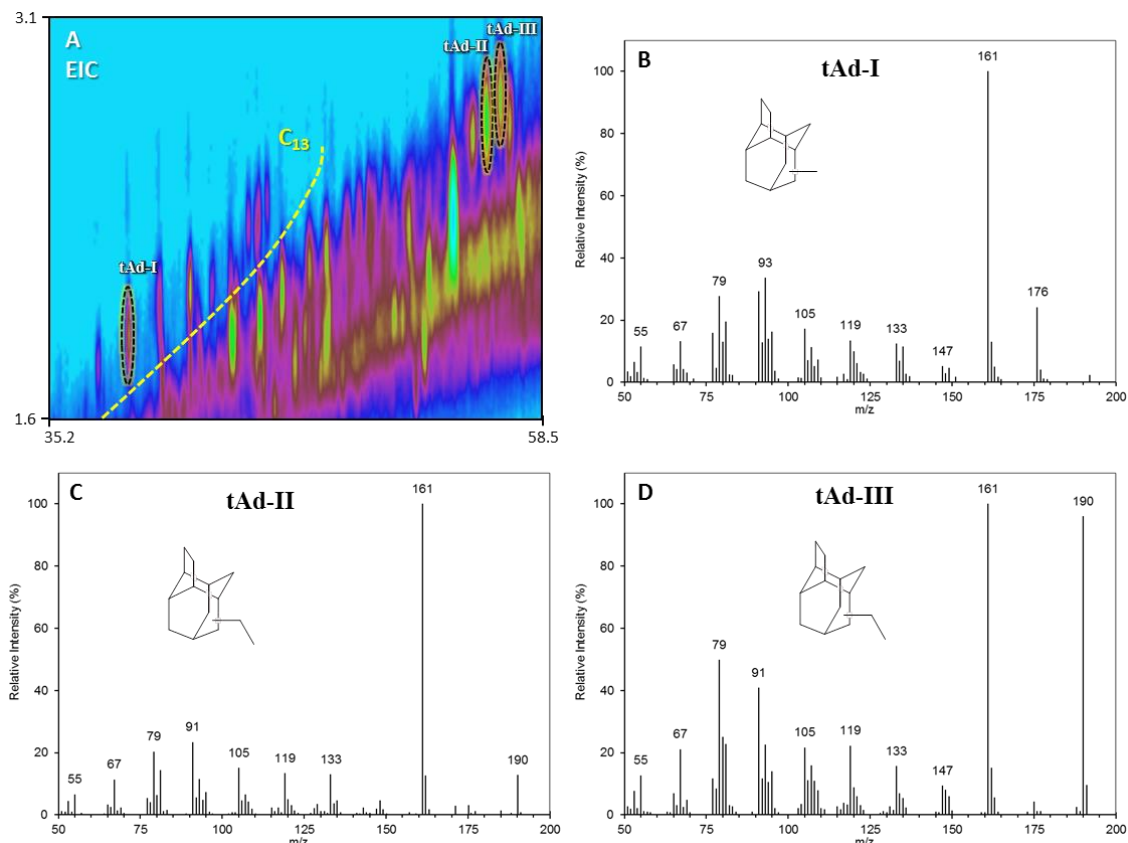
Figure 6-13: (A) EIC (*m/z* 161, 175, 176, 189, 190, 203, 217) of the reduced unfractionated OSPW NA, showing components with mass spectra containing molecular ions corresponding to C_{13} and C_{14} tetracyclic hydrocarbons, tentatively assigned as alkyl 2,4-cyclopentano-adamantanes.

Due to the lack of reference mass spectra available for tetracyclic adamantanoid hydrocarbons, specific structures could not be assigned to the higher carbon number homologues (Figure 6-14). The different types of tetracyclic adamantanoid hydrocarbons would be expected to display similar mass spectra and retention positions. Other stable, non-adamantanoid tetracyclic structures, such as bridged or highly condensed cyclohexyl or cyclopentyl structures were considered, but none would allow for isomers with carbon numbers as low as C_{13} and the few reference mass spectra

available for bridged tetracyclic diterpenoids, such as kauranes or the fused dicyclopentapentalene structures proposed by Vorob'eva *et al.* (1986), were significantly different from those observed herein.
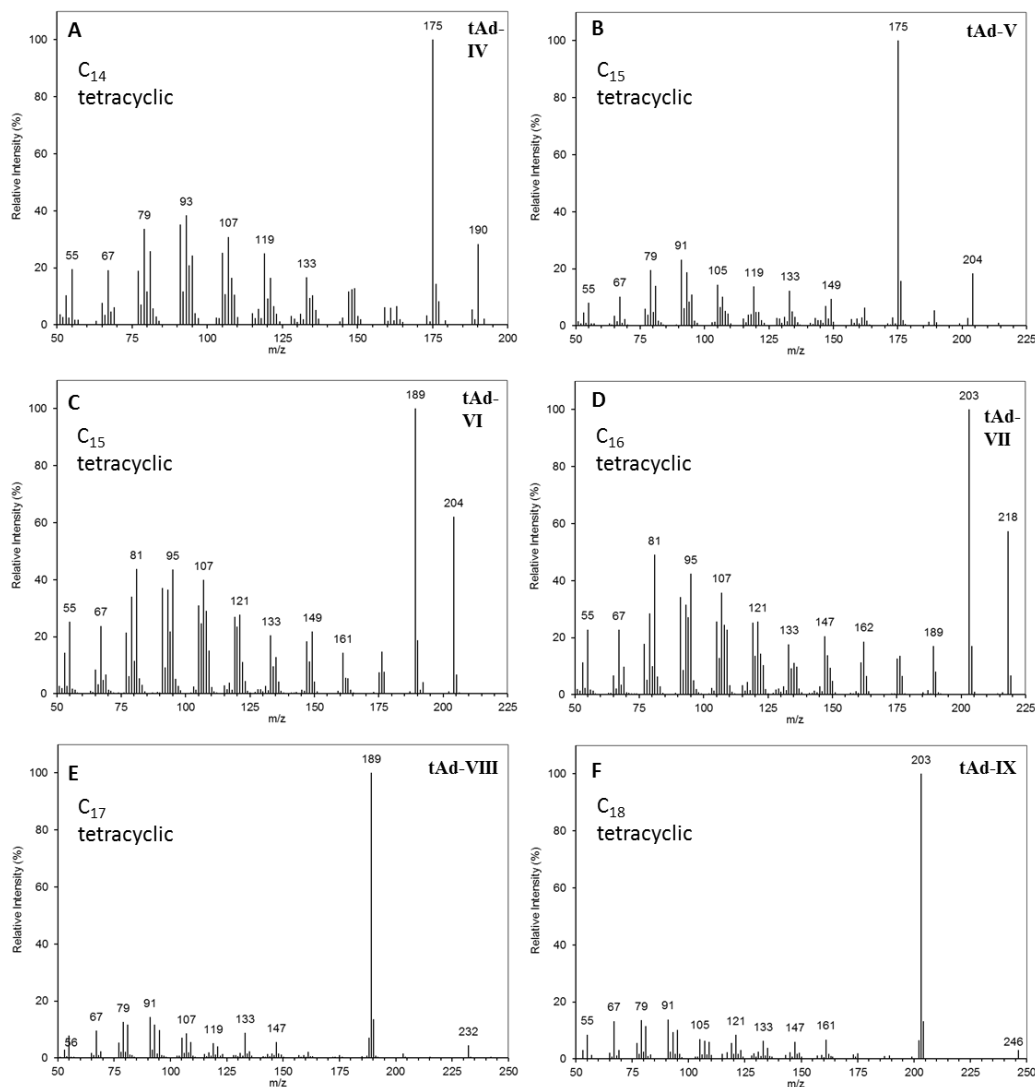
Figure 6-14: (A-F) Mass spectra of C_{14-18} alkyl tetracyclic hydrocarbons in the reduced unfractionated NA, postulated to possess adamantanoid structures (e.g. Figure 6-11; B-E).

Rowland *et al.* (2011g) suggested the tetracyclic adamantanoid acids in OSPW could be formed during the biodegradation of diamantane; this was based on previous evidence that biodegradation of tricyclic adamantanone resulted in formation of a lactone which upon secondary reactions produced a ring-opened bicyclic alcohol, bicyclo[3.3.1]nonan-

3-ol (Selifonov, 1992). However, the identifications of most NA, assigned to date, have been supported by the identification of the corresponding hydrocarbons in petroleum as possible precursors, formed by either direct carboxylation or fumarate addition and β-oxidation of the alkyl carboxylate side chain (discussed in Chapter 1, Section 1.4). The 2,4-cyclohexano-adamantane structure (Figure 6-11; B) suggested for the tetracyclic acids reported by Rowland *et al.* (2011g) has not been previously identified as the corresponding hydrocarbons in crude oils, based on the literature available (Sanin, 1976; Petrov, 1987; Musayev *et al.*, 1983; Golovkina *et al.*, 1984) and hence Rowland *et al.* (2011g) favoured a source from ring-opening of the co-occurring diamantane acids by bacteria. However, methyl substituted 2,4-cyclopentano-adamantane (Figure 6-11; C) and 1,2-cyclopentano- and cyclohexano-adamantane (Figure 6-11; D and E) have been reported to be present in crude oils (Musayev *et al.*, 1983; Golovkina *et al.*, 1984; Petrov, 1987). Considering this, coupled with the assignment of C_{13} tetracyclic adamantanoid hydrocarbons in the reduced acid products (Figure 6-13), it appears likely that the tetracyclic adamantanoid acids present in the OSPW possess cyclopentano-adamantane cores, at least for some of the higher carbon number homologues, substituted at both the 1,2- and 2,4- positions. Conclusive assignment of such structures would require synthesis of a range of alkyl substituted tetracyclic adamantanoid hydrocarbons or acids and comparison with the corresponding reduced or original NA methyl esters. Synthesis of the hydrocarbons would advance current understanding, show their mass spectral features and aid their assignment in biodegraded oils. Synthesis of the acids and analysis of the methyl esters by GC×GC-MS would allow their retention positions and mass spectra to be compared with the isomers tentatively assigned as 2,4-cyclopentano-adamantane acids in Appendix Figure 29.

6.3.3.5   Monoaromatic Acids

Fraction 5 from the large scale fractionation of the derivatised OSPW NA sample #2, detailed in Chapter 2, Section 2.2.6, eluting with 95:5%, hexane : diethyl ether, was also selected for conversion to the hydrocarbons since it was rich in aromatic acids, as exemplified by FTIR spectroscopy, strong UV absorption and adsorption to silver ions in thin layer chromatography and SPE (Jones *et al.*, 2012; Jones *et al.*, 2013). The 'aromatic' acids have been shown to have similar acute toxicity to the 'alicyclic' acids and additionally produce a weak estrogenic toxicological effect in zebrafish larvae (Scarlett *et al.*, 2013; Reinardy *et al.*, 2013). Such compounds are thus of interest for environmental as well as industrial reasons.

Early investigations of petroleum NA, rarely cited in the current literature, also showed that aromatic acids were present (Knotnerus, 1957) but the use of the term 'naphthenic' to describe the acids appears to have led most recent workers to overlook the relevance of the aromatic species. Even with this realisation, (e.g. Rowland *et al.* (2011f) and Jones *et al.* (2012)), very few aromatic acids have been firmly identified in OSPW to date.

Rowland *et al.* (2011f) synthesised numerous alkyl-substituted monoaromatic alkanoic acids for chromatographic and spectral comparison with those in OSPW, but despite these efforts, few could be assigned. Those reported recently by Bowman *et al.* (2014) in oil sands composite tailings pore water after GC×GC-MS of the methyl esters, are an exception.

However, herein using the mass spectral characteristics of the hydrocarbons to aid assignments, series of peaks with spectra containing base peak ions characteristic of aromatic species were identified. Thus, a number of components with spectra containing molecular ions consistent with C_{14-18} monoaromatic hydrocarbons (alkylbenzenes;

(McLafferty, 1963)), were observed in the reduction product of the OSPW 'aromatic' fraction of sample #2 (Figure 6-15 shows some example spectra).
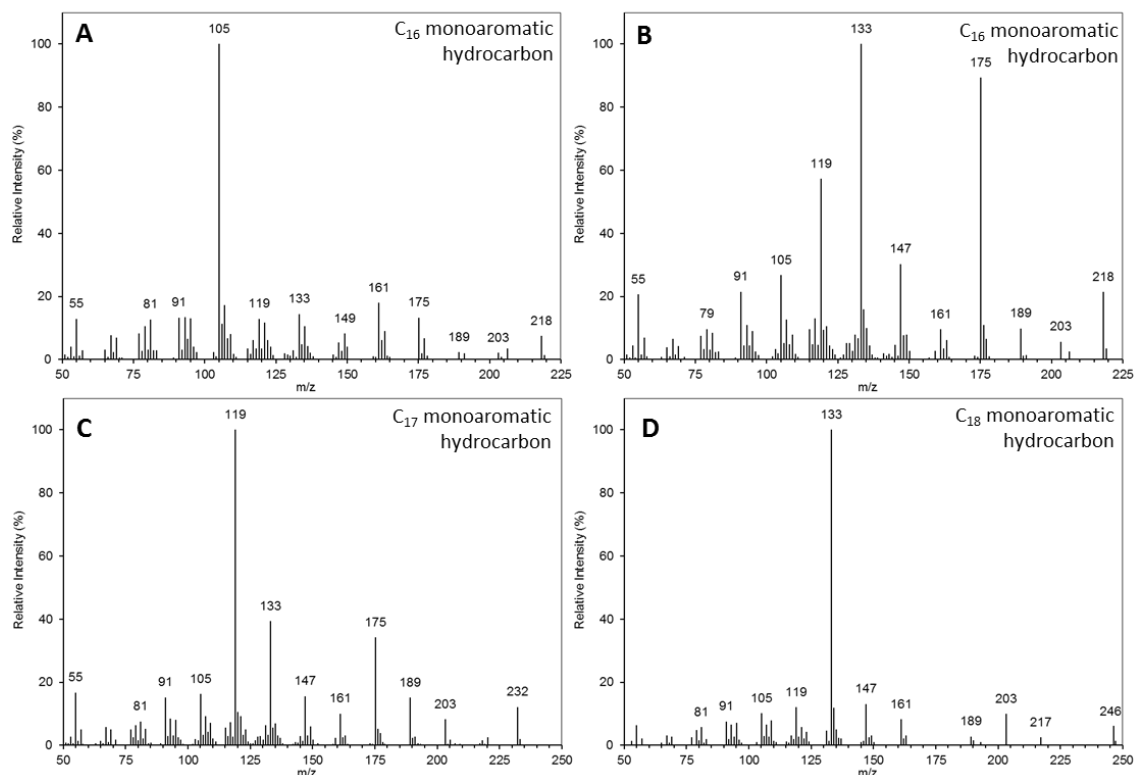
Figure 6-15: Example mass spectra of components assigned as C_{16-18} alkylbenzenes within the reduced aromatic fraction of sample #2.

The base peak ions in the mass spectra (e.g. *m/z* 105, 119, 133) suggested these consisted mainly of di-, tri- and tetramethylalkylbenzenes (Figure 6-15). The presence of many fragment ions (e.g. *m/z* 175, 161 and 147) suggested they did not possess straight n-alkyl chain substituents, since the spectra were dissimilar from those reported elsewhere for such compounds (Ji-Zhou *et al.*, 1993). The lack of intense ions at *m/z* 106, 120 and 134 (from γ-hydrogen transfer as opposed to benzylic or β-cleavage) also implied that either, the alkyl chain was not methyl-substituted at the γ-position or, that both ortho- positions on the benzene ring were substituted (Sinninghe Damsté *et al.*, 1988), such as those reported by Requejo *et al.* (1992). Some of the mass spectra closely resembled those reported by Larter *et al.* (1981) for monoaromatic hydrocarbons identified as alkylbenzenes obtained from artificially matured melanoidins. Further

structural assignments would require preparation of reference compounds. Importantly, the above arguments imply that the corresponding alkylbenzene alkanoic acids were present in the OSPW NA. These have not been reported in OSPW previously. Further structural assignments would require preparation of more reference compounds.

Since alkylbenzenes are common pollutants and might also be contaminants in the OSPW, the corresponding acid methyl esters were searched for in the esterified OSPW NA, based on the expected 12 minute retention difference observed between the acid methyl esters and the hydrocarbon products (Appendix Figure 30). Extracted ion chromatograms using the key fragment ions expected in the spectra of such acids due to benzoic cleavage (e.g. *m/z* 91, 105, 119) were used to guide the searches. The acids (methyl esters) were indeed, present. For example, Figure 6-16 shows the mass spectrum of an alkylbenzene eluting 12 min earlier than the peak tentatively identified within the F5 OSPW acid methyl esters, as the corresponding acid methyl ester. The difference between the molecular ions was 44 Da, as expected from the spectra of similar synthesised compounds (Rowland et al., 2011e), and the similarity in mass spectra indicated that the carboxylate moiety was at the end of an alkyl side chain and not directly substituted onto the benzene ring, fitting with the current understanding of bacterial degradation of branched alkyl hydrocarbons (Smith *et al.*, 2008; Han *et al.*, 2008; Misiti *et al.*, 2014). Again, this showed the complementarity of the approach used herein, via identification of the hydrocarbon analogues of the acids, coupled with a retro-search for the parent acids (methyl esters) in the OSPW extracts.
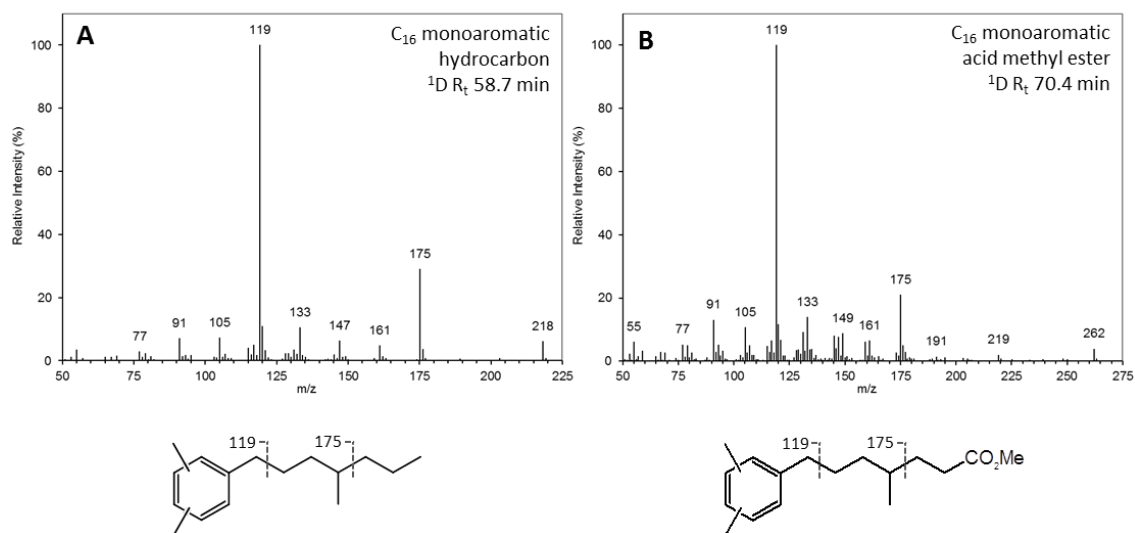
Figure 6-16: (A) Mass spectrum of a C_{16} monoaromatic hydrocarbon in the reduced aromatic fraction, assigned as a dimethyl branched alkylbenzene, based on comparison with reference spectra and mass spectral interpretation and (B) the mass spectrum of a C_{16} monoaromatic acid methyl ester, assigned as the corresponding alkylbenzene acid methyl ester before reduction in the aromatic NA methyl ester fraction. Structures given are speculative, to demonstrate the key fragment ions observed.

Recently, Bowman *et al.* (2014) identified the methyl esters of the bicyclic monoaromatic C_{11} indane-2-acetic acid and tetralin-2-carboxylic acids in oil sands composite tailings pore water, following derivatisation. Such low molecular weight acids were not present in the OSPW aromatic fraction of sample #2 under study herein and hence were not observed in the hydrocarbon reduction product. Nonetheless, series of larger C_{14-20} branched alkyl indanes and tetralins were tentatively identified by comparison of the spectra in the NIST mass spectral library and with available literature mass spectra (Booth, 2004; Booth *et al.*, 2006). The spectra contained putative molecular ions for bicyclic monoaromatic hydrocarbons with the same recurring alkyl group losses (M-43 and -57) and common fragment ions at *m/z* 145, 159, which are often characteristic of the spectra of substituted indanes and tetralins (Figure 6-17)

(Booth, 2004; Booth *et al.*, 2006). These identifications imply that the corresponding indane and tetralin alkanoic acids, not known previously, were present in OSPW.
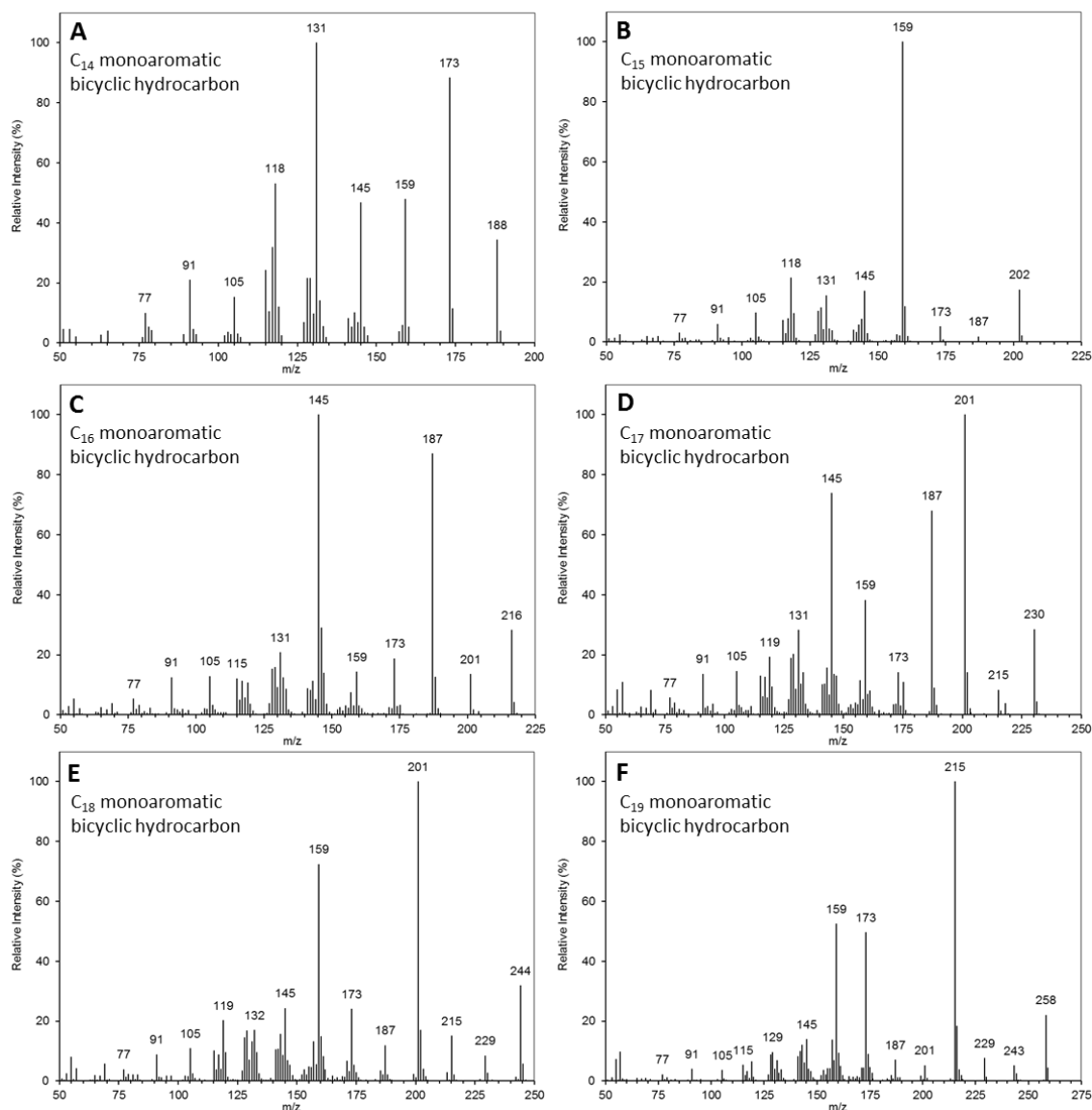
Figure 6-17: (A-F) Mass spectra of C_{14-19} monoaromatic bicyclic hydrocarbons tentatively assigned based on mass spectral comparison and interpretation.

Numerous tricyclic monoaromatic acids were present in OSPW NA, though the only acid to be assigned to date is dehydroabietic acid (DHAA); identification based on a comparison of the mass spectrum and GC×GC retention time of an authentic sample (Jones *et al.*, 2012). A compound with a mass spectrum which was similar to that of the corresponding hydrocarbon, dehydroabietane, was identified in the OSPW

hydrocarbons obtained from reduction of the 'aromatic' OSPW NA Ag-Ion fraction of sample #2 (Figures 6-18; A and B). However, the spectrum was more similar to that of the C_{19} and isomeric C_{20} hydrocarbons 13,14-dimethyl- and 13-methyl-14-ethylpodocarpa-8,11,13-triene (Figure 6-18; C and D) (Azevedo *et al.*, 1990; Azevedo *et al.*, 1992) than to that of dehydroabietane, in this OSPW sample. A subsequent retro-examination of the aromatic acid methyl esters of this fraction also failed to reveal the presence of DHAA methyl ester in this OSPW sample (*cf.* a different OSPW sample examined by Jones *et al.* (2012)).
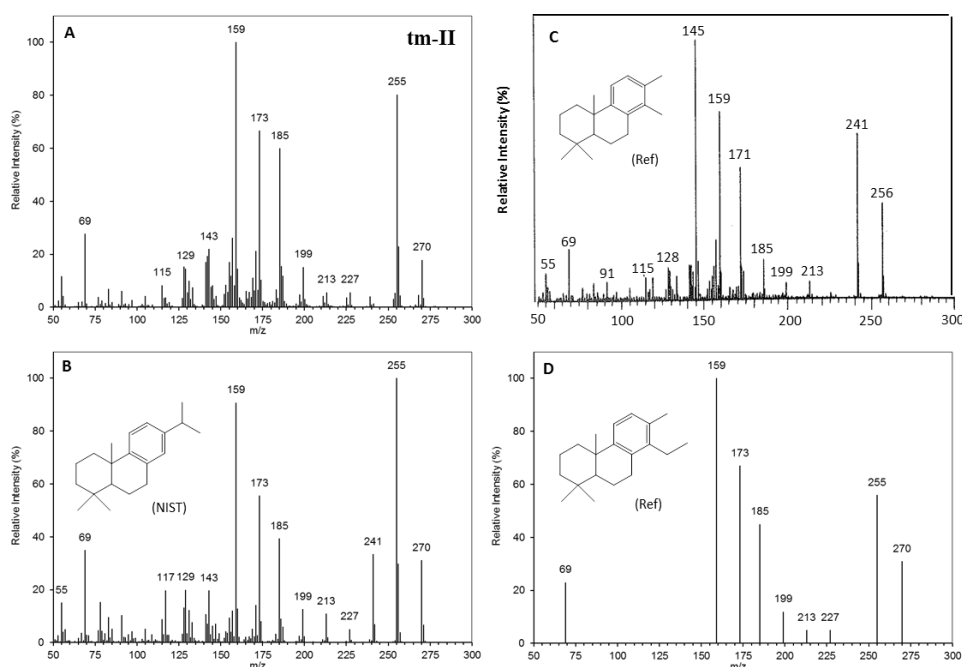
Figure 6-18: (A) Mass spectrum of isomer **tm-II**, a C_{20} tricyclic monoaromatic hydrocarbon assigned as 13-methyl-14-ethylpodocarpa-8,11,13-triene after comparison with the mass spectra of (B) dehydroabietane plotted from the NIST MS Library, (C) 13,14-dimethylpodocarpa-8,11,13-triene reimaged from the spectrum reported by Azevedo *et al.* (1992) and (D) 13-methyl-14-ethylpodocarpa-8,11,13-triene replotted from the tabulated values reported by Azevedo *et al.* (1990).

Identification of the corresponding alkyl substituted podocarpa-8,11,13-triene acid has not been previously reported in OSPW NA. However, Azevedo *et al.* (1994) reported

the presence of a series of C_{19-30} tricyclic C-ring monoaromatic carboxylic acids possessing the same structure, with the alkanoate chain in the 14-position increasing in length, in Tasmanian tasmanite (a marine type oil shale).

Interestingly, a series of non-aromatic tricyclic acids, were identified as the corresponding hydrocarbons, in the reduced 'alicyclic' OSPW NA fraction herein and in the reduced unfractionated OSPW NA sample, possessing cheilanthane-type 'cores' (Figure 6-10, discussed in Section 6.3.3.3). These structures are perhydro- equivalent structures of the podocarpa-8,11,13-triene reported in Figure 6-18.

Other monoaromatic acids tentatively identified in OSPW previously included possible de-A steroidal tricyclic acids (Rowland *et al.*, 2011d; Frank *et al.*, 2014). Rowland *et al.* (2011d) tentatively assigned a series of acids within OSPW NA, characterised by a dominant base peak ion at *m/z* 145 as de-A steroidal keto acids, suggested as possible biotransformation products from A-ring degraded steranes or keto-steranes. Accurate mass data obtained by analysis of the free acids by (-)ESI-Orbitrap-MS and analysis of expected molecular ions for the deprotonated free acids (e.g. $[C_{20}H_{27}O_2]^-$, *m/z* 299) revealed the most abundant ions had accurate masses consistent with O_3 species (*m/z* 299.1642), hence the acids were tentatively assigned as the keto acids (e.g. $[C_{19}H_{23}O_3]^-$, *m/z* 299) (Rowland *et al.*, 2011d). The base peak ion at *m/z* 145 was reasoned to be a keto ion ($C_{10}H_9O^+$) instead of a methyltetralin cation ($C_{11}H_{13}^+$) (Rowland *et al.*, 2011d). However, a later investigation into the '*m/z* 145' acid series, involving isolation of one of the abundant C_{21} isomers by GC- and GC×GC-prep and characterisation by subsequent GC-HRMS and GC×GC-HRMS, showed the acid was in fact, a tricyclic monoaromatic acid ($C_{21}H_{30}O_2$) and that the base peak ion at *m/z* 145 corresponded with a $C_{11}H_{13}^+$ cation (Rowland *et al.*, [unpublished]). NMR analysis of the isolated acid showed it possessed a methyl substituted fused aromatic ring (Figure 6-19).
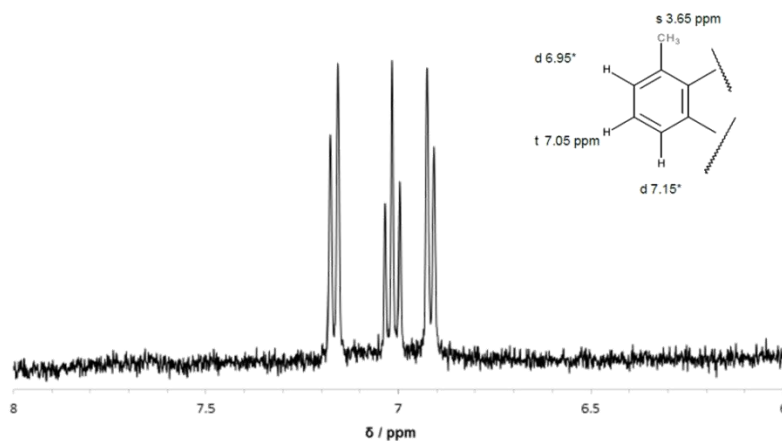
Figure 6-19: Partial ^{1}H-NMR spectrum showing the aromatic resonances for the isolated monoaromatic acid and proposed partial structure (Rowland *et al.*, [unpublished]).

Based on the accurate mass and NMR data, as well as comparison of the mass spectra and retention positions of several synthesised octahydrophenanthrene acids, the '*m/z* 145' series of acids were putatively assigned as de-A steroidal acids, such as that shown in Figure 6-20 (Rowland *et al.*, [unpublished]). However no authentic compounds or reference spectra were available for confirmation or rebuttal of these.
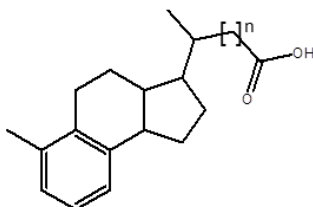
Figure 6-20: Proposed tentative structure of the '*m/z* 145' series of tricyclic monoaromatic acids.

Despite the heterogeneity observed between OSPW acid extracts, the tentative de-A steroidal acids are usually observed as consistent components in relatively high abundances in OSPW NA. Their apparent ubiquitous occurence in numerous OSPW samples and well resolved nature, when examined by GC×GC-MS as the methyl esters, allowed Frank *et al.* (2014) to monitor their presence in OSPW and in environmental samples taken from the surroundings within the oil sands industry, in an attempt to distinguish between NA from OSPW and NA from erosion of natural oil sands outcrops.

Analysis of the reduced aromatic fraction of OSPW NA and the reduced unfractionated OSPW NA herein, as expected, revealed a series of the corresponding hydrocarbons. Their relatively high abundances were not only observed in the acid methyl esters, but also in the hydrocarbon product, as shown in the TIC in Figure 6-21; A, of the reduced aromatic fraction and were clearly resolved in the EIC in Figure 6-21; B. The mass spectra of the acid methyl esters were characterised by a m/z 145 base peak ion; this feature was also observed in the putative hydrocarbon products (Figure 6-21; C-H).

Six isomers (**tm-I**, **-IV** – **VII** and **-IX**) with base peak ions at m/z 145 and mass spectra similar to those of the acids reported previously (Rowland *et al.*, 2011d), were observed in the reduced 'aromatic' fraction of sample #2, with spectra displaying molecular ions consistent with one C_{19}, three C_{20}, one C_{21} and one C_{23} isomer (Figure 6-21; C-H). A peak eluting after **tm-VII** appeared to be a seventh isomer; however, it had a very low abundance. The six isomers were also detected in the reduced sample #7, along with three additional isomers (**tm-XI** – **XIII**) spectra of which displayed molecular ions consistent with another C_{19} isomer (**tm-XI**), eluting between **tm-IV** and -**V** and two C_{20} isomers (**tm-XII** and -**XIII**) which eluted between **tm-VI** and -**VII** and **tm-VII** and -**IX,** respectively. The isomer **tm-XIII** detected in the unfractionated sample was thought to be the low intensity, seventh isomer observed in the reduced aromatic fraction sample.

Retro-analysis of the aromatic fraction of sample #2 as the acid methyl esters showed the presence of seven abundant isomers (Figure 6-22; A), with molecular ions consistent with one C_{19}, three C_{20}, one C_{21} and two C_{23} isomers. Their distribution and mass spectra were comparable with that of the same acids shown in the 3D EIC reported by Frank *et al.* (2014) and Rowland *et al.* (2011d), respectively (Figure 6-22; B and Figure 6-23). However, the seven isomers reported by Rowland *et al.* (2011d) did not contain a C_{21} isomer, but another C_{20} isomer.
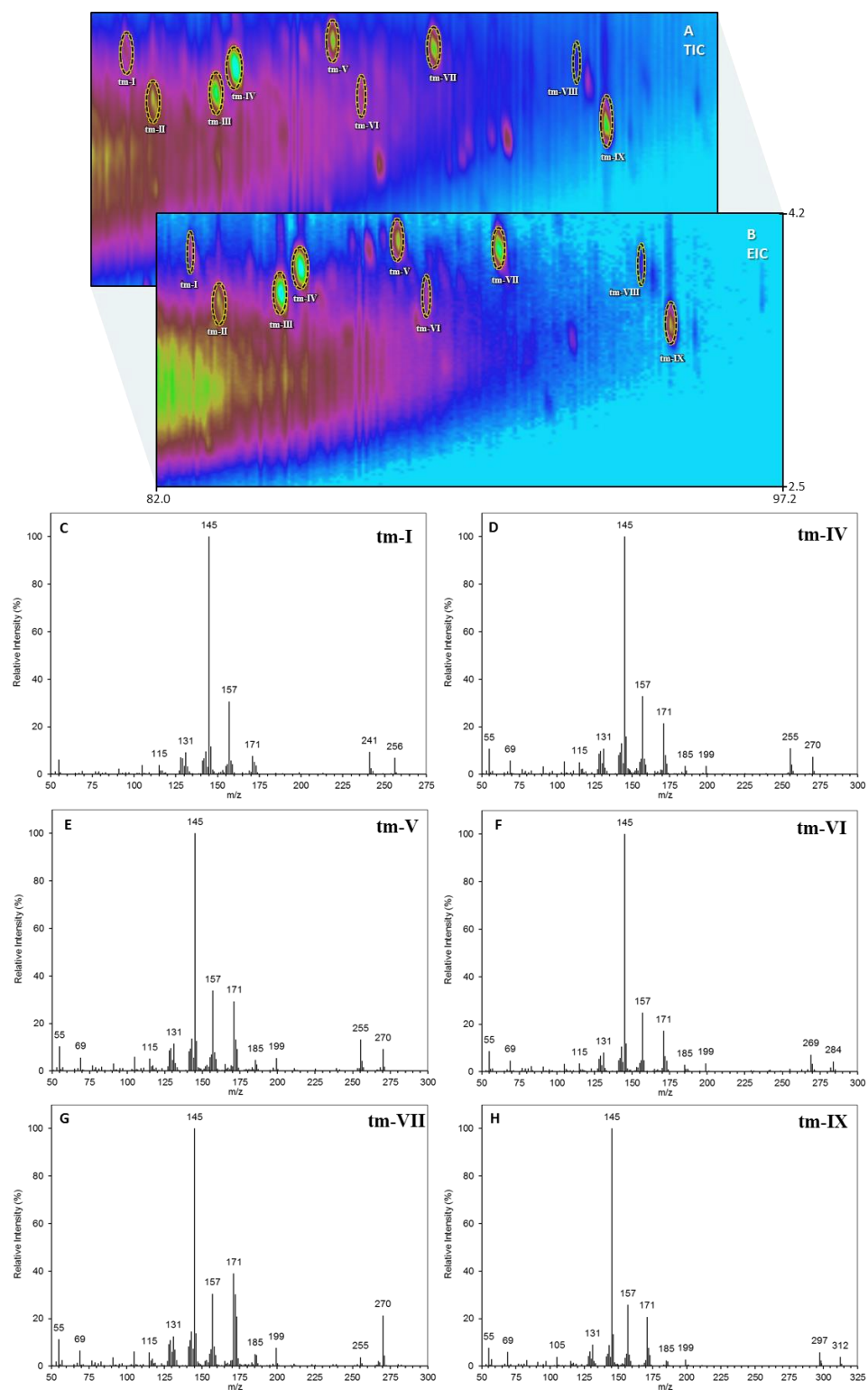
Figure 6-21: (A) TIC and (B) EIC (*m/z* 256, 270, 284, 298 and 312) of the reduced

aromatic fraction and (C-H) mass spectra of isomers assigned as C_{19-23} tricyclic

monoaromatic hydrocarbons derived from the abundant acids putatively re-assigned as

de-A (18-nor) steroidal acids (Rowland *et al.*, 2011d; Rowland *et al.*, [unpublished]).
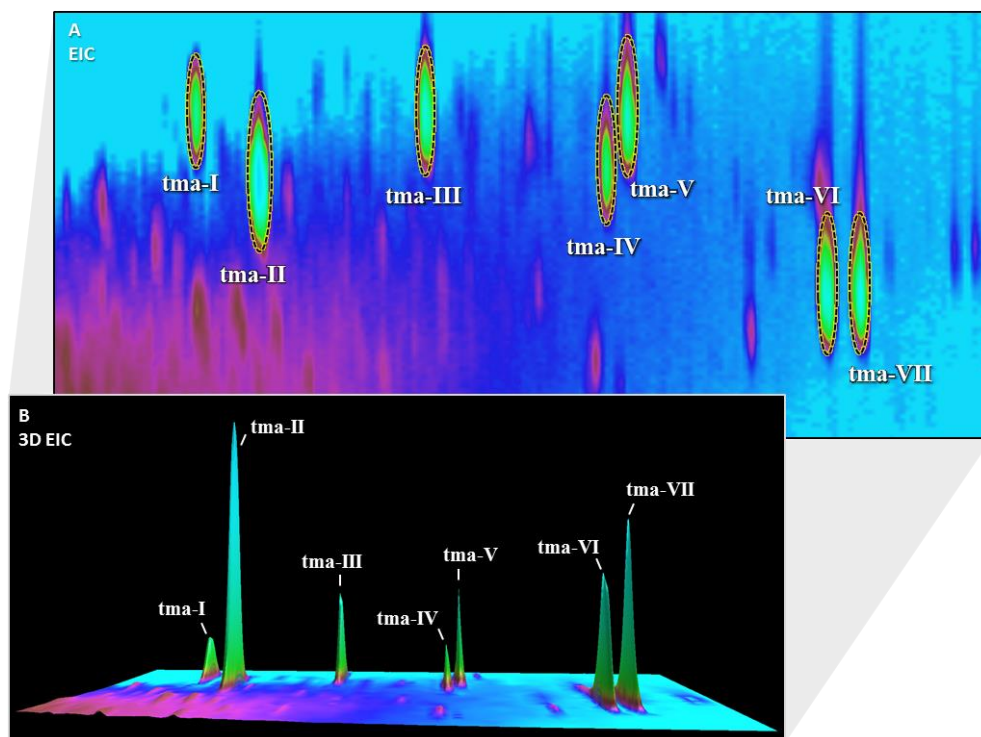
Figure 6-22: (A) EIC (*m/z* 145) of the aromatic acid methyl ester fraction showing the distribution of the '*m/z* 145' series of tricyclic monoaromatic acids and (B) a 3D representation of the EIC comparable with that reported by Frank *et al.* (2014).

The conversion of the acid methyl esters to the corresponding hydrocarbons supported the assignment of the series as $C_nH_{2n+z}O_2$ tricyclic monoaromatic acids and not keto acids. The molecular ions of the original acids (Figure 6-23) ($M^+ = $ *m/z* 300, 314, 328 and 356) all reduced by 44 mass units after the reduction, corresponding to the reduction of the acid methyl ester to a defunctionalised hydrocarbon. If a keto group was present, this would have been expected to be reduced to an alcohol and either further derivatised to the tosylate and reduced accordingly, or remain unaffected as the keto or alcohol group, dependent on its position in the structure. The mass spectra and molecular ions of reduced keto products would not produce the molecular ions observed in the mass spectra of the corresponding hydrocarbons in Figure 6-21.
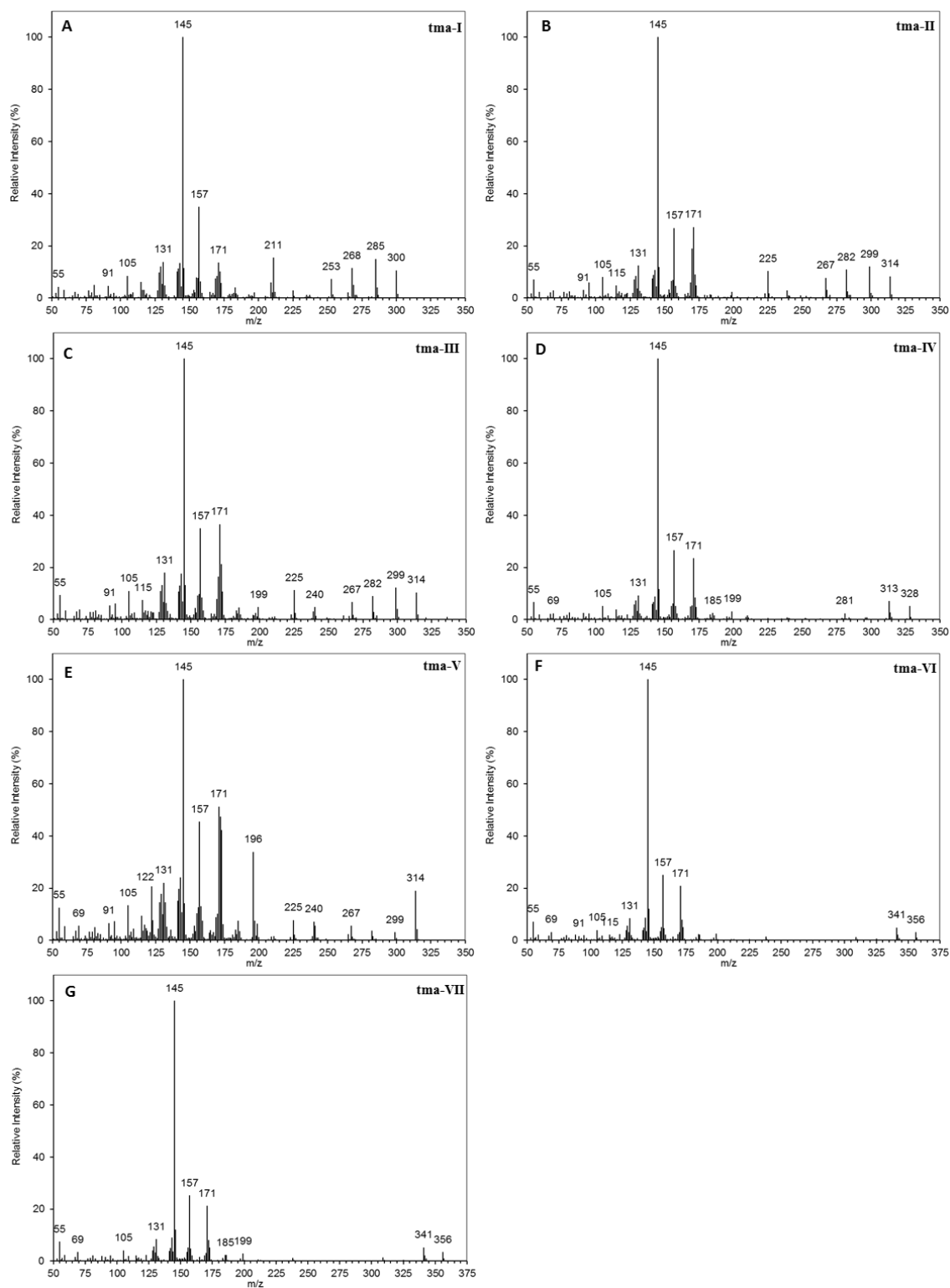
Figure 6-23: (A) Mass spectra of tricyclic monoaromatic acids in the aromatic acid methyl ester fraction, tentatively re-assigned as de-A steroidal acids (Rowland *et al.*, 2011d; Frank *et al.*, 2014).

The mass spectra of the hydrocarbons displayed a similar fragmentation pattern to those observed for the acids; an observation made for the alkyl benzene acids, suggesting the acid group was substituted at the end of an alkanoate side chain. No reference mass spectra for de-A steroidal acid methyl esters were found, but a few mass spectra were available for de-A sterane hydrocarbons with structures similar to those proposed for the corresponding hydrocarbons herein. The fragmentation patterns observed in the reference mass spectra reported by Peakman *et al.* (1986) and van Graas *et al.* (1982) for C_{23} and C_{25} de-A steranes, respectively (Figure 6-24; A), were similar to those observed for corresponding hydrocarbons in Figure 6-21, supporting the assignment of a de-A (18-nor) sterane 'core' (Figure 6-24; B). The reference mass spectra displayed a dominant base peak ion at *m/z* 157 with a smaller *m/z* 145 ion, as opposed to the *m/z* 145 base peak ion with a smaller *m/z* 131, observed herein (Figure 6-25; A-C). Therefore, it is proposed that the acids and corresponding hydrocarbons are 18-nor isomers; potentially products of further biodegradation of the hydrocarbon precursors similar to those reported by Peakman *et al.* (1986) and van Graas *et al.* (1982), observed at the severe level of biodegradation previously reported in the OSPW (Rowland *et al.*, 2011g). This is supported by the detection of these acids ('*m/z* 145 series') in severely biodegraded crude oils (Rowland *et al.*, [unpublished]).
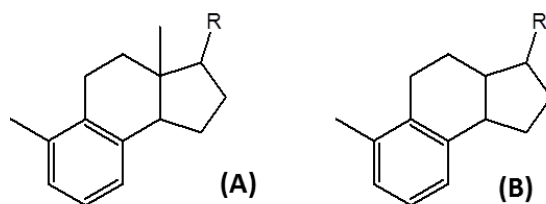
Figure 6-24: Structure of (A) a de-A sterane reported by Peakman *et al.* (1986) and van Graas *et al.* (1982) and (B) the proposed structure of the tricyclic monoaromatic, de-A (18-nor) sterane acids and corresponding hydrocarbons (R = alkyl chain in reduced hydrocarbon product; = alkanoate chain in acid methyl esters).
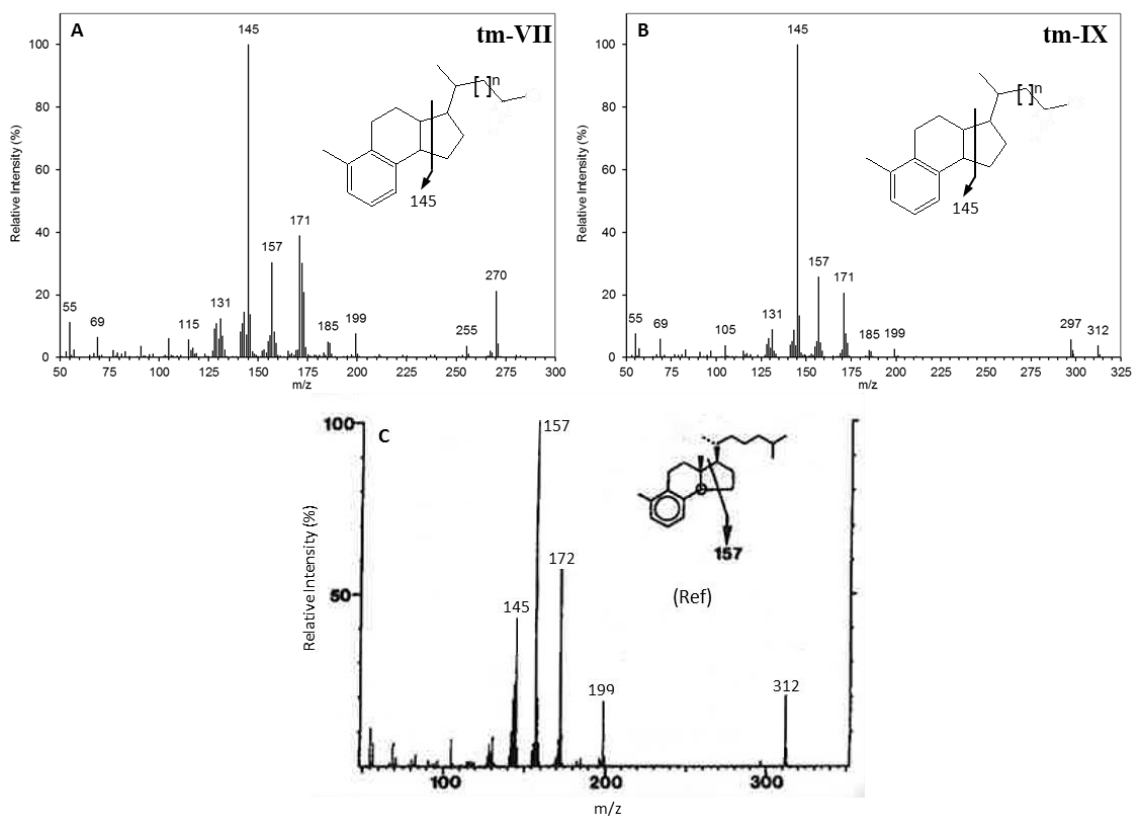
Figure 6-25: (A and B) Example mass spectra of tricyclic monoaromatic hydrocarbons in the reduced aromatic fraction of OSPW NA tentatively assigned as de-A (18-nor) steranes after comparsion with (C) the reimaged reference mass spectrum reported by Peakman *et al.* (1986) and observations reported by van Graas *et al.* (1982).

The formation of a stable *m/z* 145 ion is postulated to proceed via fission of a bridgehead bond in the terminal saturated ring (i.e. the cyclopentyl ring), followed by hydrogen rearrangement and inductive cleavage; a similar mechanism to that previously shown for other known tricyclic monoaromatic terpanes (Enzell, 1966; Azevedo *et al.*, 1990). Initial fission and resulting fragmentation across the ring, as opposed to fragmentation of the alkyl side chain, has been reported for similar tricyclic monoaromatic terpanes with long alkyl side chains (Azevedo *et al.*, 1990). The isomers reported herein possessed carbon numbers of C_{19} and higher, suggesting alkyl side chains greater than C_5 in length.
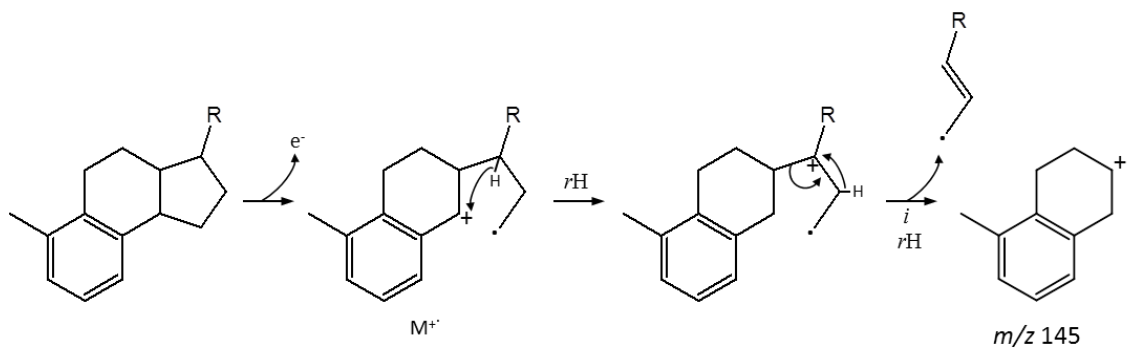
Figure 6-26: Proposed mass spectral fragmentation mechanism for the formation of the base peak ion *m/z* 145 observed in the mass spectra of the tricyclic aromatic hydrocarbons and acids, tentatively assigned as possessing de-A (18-nor) steroidal cores.

6.3.3.6 Diaromatic sulphur-containing acids

Fraction 7 from the large scale fractionation of the derivatised OSPW NA sample #2, detailed in Chapter 2, Section 2.2.6, eluting with 95%:5% hexane:diethyl ether, was selected as a sulphur-rich, aromatic fraction of OSPW NA for conversion to hydrocarbons. The fraction was known to be sulphur-rich following a previous investigation on the equivalent Ag-Ion fraction of the same OSPW NA sample; elemental analysis of the acid methyl esters showed the fraction contained 1.5% sulphur (Jones *et al.*, 2013). Jones *et al.* (2013) performed a series of spectrometric investigations of the fractionated acid methyl esters, including FT-IR, UV-Vis spectroscopy, GC×GC-HRMS and GC×GC with sulphur chemiluminescence detection (GC×GC-SCD); the results of the FT-IR and GC×GC-HRMS analyses indicated that the major SO_2 species detected were sulphur-containing aromatic carboxylic acids.

Later, West *et al.* (2014b) analysed the equivalent fraction of the same OSPW NA again by GC×GC-MS, GC×GC-SCD and GC×GC-HRMS. The accurate mass of the molecular ions of five major isomers, were consistent with C_{16-18} SO_2 species with 10 double bond equivalents (DBE) (West *et al.*, 2014b). The mass spectra of all five isomers; one C_{16}, two C_{17} and two C_{18} acid methyl esters, all displayed relatively intense (~40%) molecular ions at *m/z* 284, 298 and 312 and dominant base peak ions at *m/z* 197, 211 and 225, respectively, consistent with the loss of $C_4H_7O_2$ (West *et al.*, 2014b). Synthesised reference, mono-substituted dibenzothiophene and naphtho[2,1-b]thiophene acids, with a n-C_4 alkanoate side chain and some with branched C_5 alkanoate side chains substituted at the 2-position, were compared with the GC×GC retention positions and mass spectra of the unknown NA (West *et al.*, 2014b). Although the reference acids (methyl esters) possessed similar retention positions to those of the unknowns, none were identified. The mass spectra of the reference compounds all contained an even mass radical cation, which was attributed to loss of either M-74 and

M-88 produced by a γ-hydrogen or McLafferty rearrangement on the alkanoate side chain (McLafferty and Tureček, 1993). This rearrangement ion was absent in all the mass spectra of the unknown acids. Therefore West *et al.* (2014b) tentatively assigned the C_{16-18} diaromatic sulphur-containing acids as possessing methyl substituted dibenzothiophene or dimethylnaphthothiophenes (or dimethyldibenzothiopyrans) with methyl branched propanoate acid side chains.

Prior to the investigations by Jones *et al.* (2013) and West *et al.* (2014b), utilising GC×GC-MS, little was known about the identity of the sulphur-containing dioxygenated species in OSPW, despite the frequent reports of sulphur acid species in OSPW NA and AEO samples by other HRMS techniques (Barrow *et al.*, 2010; Headley *et al.*, 2011a). The only other sulphur-containing acids to have been identified previously were a series of mono- and disubstituted C_{6-7} thiophene acids in oil sands composite tailings pore water after analysis of the acid methyl esters by GC×GC-MS and comparison with authentic reference compounds (Bowman *et al.*, 2014).

Examination of the 'aromatic/sulphur'-containing fraction of acid methyl esters analysed herein by GC×GC-MS revealed the five C_{16-18} isomers reported by West *et al.* (2014b). Following reduction, the corresponding sulphur-containing hydrocarbons were detected with molecular ions at *m/z* 240, 254 and 268, possessing mass spectra similar to those of the acids (e.g. dominated by base peak ions at *m/z* 197, 211 and 225), corresponding to the loss of ·C_3H_7 (Figure 6-27; A and B). The five isomers (**dbt-I** to **-V**) were detectable using extracted ion monitoring. However, they were more readily detected after the simple application of a CLIC expression (intensity of base peak ions at *m/z* 197, 211 and 225 >200000 counts and relative intensity of ions at *m/z* 240, 254 and 268 > 20%) (Figure 6-27; B). This helped differentiate the isomers from minor

components with similar ions and elution times and enabled clear mass spectra to be
obtained for interpretation and comparison with reference spectra and compounds.
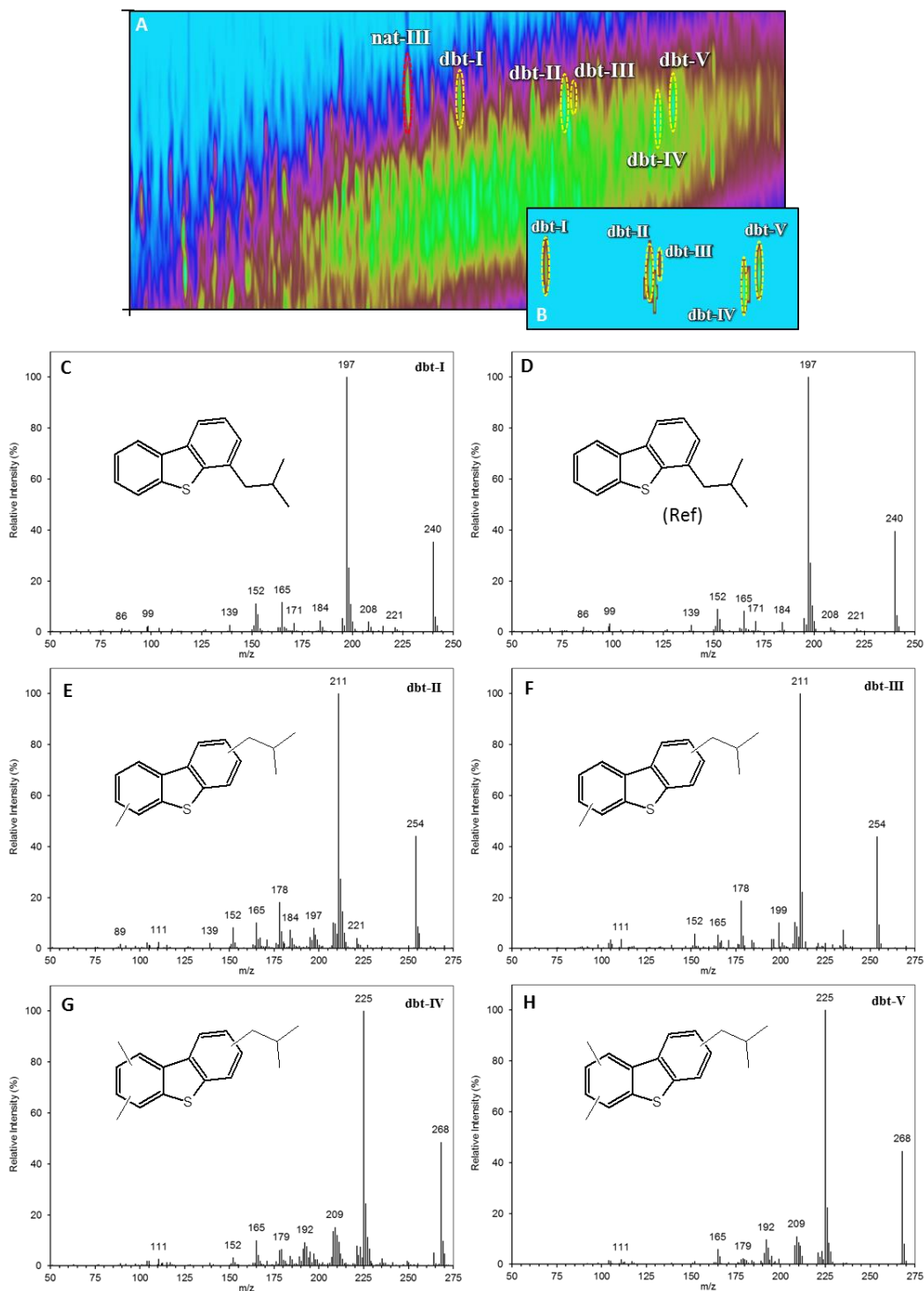
Figure 6-27: (A and B) TIC and CLIC EIC of reduced 'aromatic, sulphur' fraction of #2,
showing isomers **dbt-I** to **-V** assigned as the reduced hydrocarbons of the five methyl
esters reported by West *et al.* (2014b). (C-D) Identification of **dbt-I** after comparison
with (D) synthesised 4-isobutyldibenzothiophene (Luty, 2014) and (E-H) assignment of
dbt-II to **-V** as methyl- and dimethyl- isobutyldibenzothiophenes.

The only structure possible for the alkanoate side chain of these isomers, which would result in the consistent loss of M-87 and the absence of a radical cation produced from a McLafferty rearrangement in the mass spectra of the acid methyl esters (West *et al.*, 2014b), along with the consistent loss of $\cdot C_3H_7$ by benzylic cleavage in the mass spectra of the hydrocarbons, was that of a dibenzothiophene (or naphthothiophene) containing an isobutyl side chain.

Authentic reference dibenzothiophene or naphthothiophene acids with an isobutyric acid (C_2-methyl propanoate) side chain were not available. However authentic 4-propyl- and 4-isobutyldibenzothiophene previously synthesised by Luty (2014) was available for comparison with the corresponding hydrocarbons obtained herein. The GC×GC retention position of 4-propyldibenzothiophene matched that of two co-eluting isomers in the reduced OSPW F7 hydrocarbon product (labelled **nat-III** and **-IV** in Figure 6-27), though the mass spectra of the two isomers were different to the reference hydrocarbon. However the GC×GC retention position and mass spectrum of synthesised 4-isobutyldibenzothiophene matched that of the **dbt-I** isomer, confirming its identification (Figure 6-27; C and D), and by inference, the identification of dibenzothiophene-4-isobutanoic acid in OSPW NA for the first time, as originally postulated by West *et al.* (2014b). This is another example of how the approach of chemical transformation developed and applied herein was complementary to the analysis of the acid methyl esters; interpretation of the mass spectra of both the acid methyl esters and hydrocarbons and comparison of the hydrocarbon product with available reference compounds in the absence of available reference acid methyl esters aided the identification of unknown NA in OSPW.

West *et al.* (2014b) also reported the presence of some sulphur-containing acids with 8 and 9 DBE, eluting slightly earlier than those compounds possessing 10 DBE now

identified as dibenzothiophene acids. The identities of these acid methyl esters were not investigated further. However, examination of the OSPW F7 hydrocarbon product herein, revealed a series of isomers with spectra displaying molecular ions consistent with diaromatic sulphur-containing hydrocarbons with 8 DBE (e.g. *m/z* 214, 228, 242 and 256), eluting slightly earlier than the 10 DBE dibenzothiophenes (e.g. isomer **nat-1** in Figure 6-27).

The mass spectra of these isomers (**nat-1** to **-V**) were dominated by intense base peak ions at *m/z* 171 and 185, with very few fragment ions observed below *m/z* 171, except very low intensity ions at *m/z* 92, 115, 127, 152 and 165 present in most of the spectra (Figure 6-28). This indicated that the compounds were highly condensed, with the base peak ion most likely formed via benzylic cleavage of an alkyl substituent; similar to the mass spectra of alkyl 2H-naphtho[1,8-bc]thiophenes reported by Hawthone and Porter (1968) and the mass spectra of alkyl substituted, condensed polycyclic aromatic hydrocarbons (e.g. those of alkyl acenaphthenes and pyrenes; NIST library).

Comparison of the mass spectrum of the isomer with the lowest carbon number (**nat-I**), with reference spectra in the NIST MS Library, showed that the spectrum was similar to that of 2-methyl-2H-naphtho[1,8-bc]thiophene (Figure 6-28; A and B). The NIST mass spectrum showed a loss of M-15, attributed to fragmentation of the methyl substituent, via benzylic cleavage, as proposed previously for the fragmentation of alkyl 2H-naphtho[1,8-bc]thiophenes (Hawthone and Porter, 1968; Porter, 1985) (Figure 6-28; A). The mass spectrum of **nat-I** displayed a similar fragmentation pattern and ions to that of the NIST reference spectrum, with the base peak ion corresponding to the loss of M-43 instead, attributed to the loss of a propyl group ·C_3H_7 (Figure 6-28; B). The series of isomers (**nat-II** to **-V**) had increasing molecular ions (by 14 Da) and showed similar losses in accordance with higher carbon number homologues (Figure 6-28; C-F).
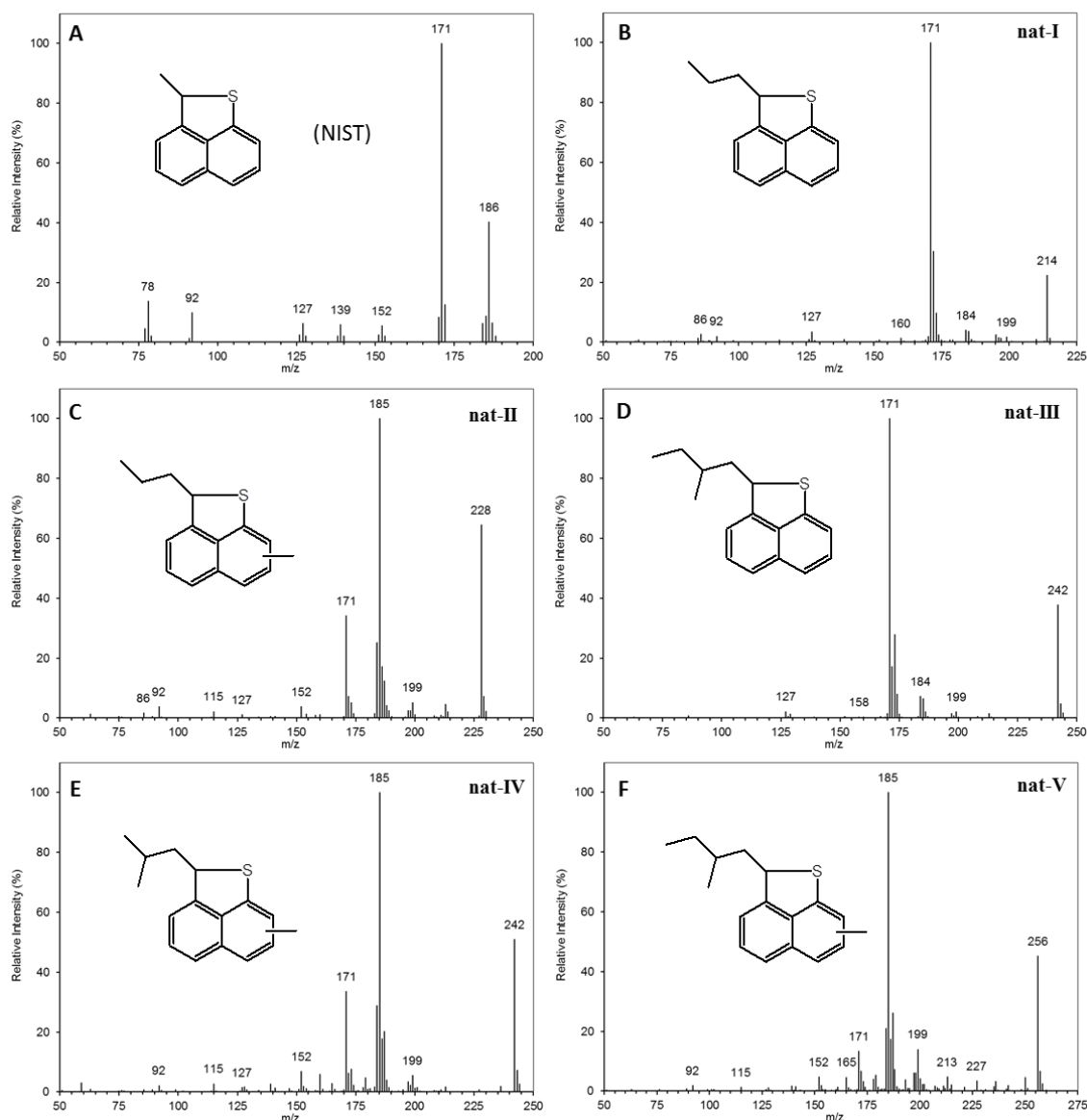
Figure 6-28: Mass spectra of a series of isomers (**nat-I** to **-V**) in the reduced 'aromatic, sulphur' fraction of sample #2, tentatively assigned, after comparison with (A) the NIST spectrum of 2-methyl-2H-naphtho[1,8-bc]thiophene and their retention positions relative to authentic 4-propyl- and isobutyl- dibenzothiophene, as (B-F) 2-alkyl (C_{3-5}) substituted 2H-naphtho[1,8-bc]thiophenes and methyl 2H-naphtho[1,8-bc]thiophenes.

As previously mentioned, the retention positions of **nat-III** and -**IV** matched that of synthesised 4-propyldibenzothiophene. A tricyclic, diaromatic sulphur-containing hydrocarbon possessing a more highly condensed ring structure such as a naphtho[1,8-bc]thiophene would be expected to elute in a similar 2nd dimension retention position to

317

that of a dibenzothiophene isomer possessing the same carbon number. The isomer with a more condensed ring structure would also be expected to possess an earlier 1st dimension retention position; both these observations matched that observed for the retention position of the **nat-I** isomer relative to the **dbt-I** isomer (Figure 6-27; A).

If the hydrocarbon isomers detected (**nat-I** to **-V)** did indeed possess condensed ring structures, such as naphtho[1,8-bc]thiophenes, the mass spectra of the original acids would be expected to display similar mass spectral fragmentation patterns (due to the stability of the condensed structure) with additional radical cations due to McLafferty rearrangement of the alkanoate side chain, involving the hydrogen on the carbon adjacent to the sulphur atom. The original acid methyl esters would also possess 9 DBE with retention positions similar to those observed by West *et al.* (2014b). Subsequent examination of the OSPW F7 NA methyl esters indeed revealed a series of peaks with mass spectra displaying fragmentation patterns similar to those of the **nat-I** to -**V** hydrocarbons, with additional even mass ions, corresponding to M-74, M-88 and M-102 ions (Figure 6-29), attributed to neutral losses from hydrogen rearrangement on the alkanoate side chain. These observations coupled with the mass spectral interpretation, similarity with the reference mass spectrum (Figure 6-28; B) and precedent for the presence of sulphur-containing acids with 9 DBE confirmed by GC×GC-SCD and HRMS (West *et al.*, 2014b), led to the tentative assignment of naphtho[1,8-bc]thiophene acids in OSPW NA herein.
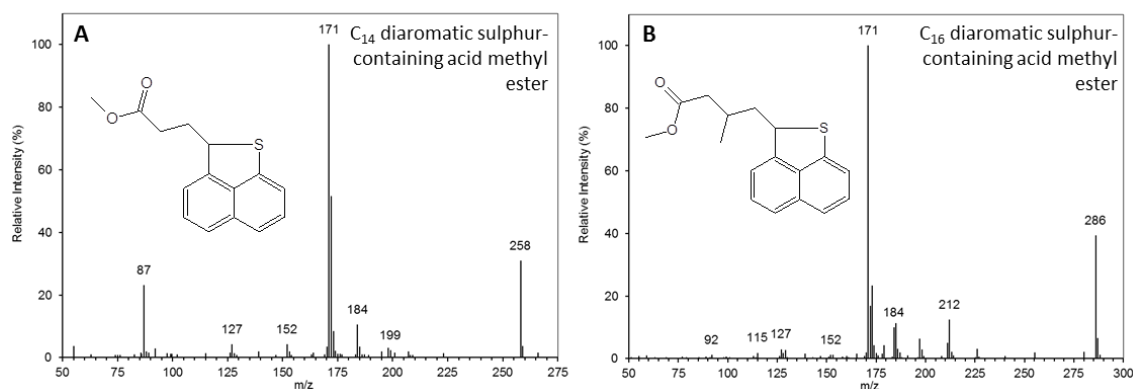
Figure 6-29: (A and B) Example mass spectra of a C_{14} and C_{16} acid methyl ester in the 'aromatic, sulphur' fraction of sample #2, with molecular ions and retention positions consistent with condensed tricyclic, diaromatic sulphur-containing acid methyl esters, tentatively assigned as naphtho[1,8-bc]thiophene acids.

Sulphur-containing hydrocarbons possess the same nominal mass as some aromatic hydrocarbons and could be mis-assigned when analysed by unit resolution mass spectrometric techniques, as highlighted by Hegazi and Andersson (2007). For example, the C_{16} sulphur-containing hydrocarbons tentatively assigned above (Figure 6-27; D and E) with molecular ions at m/z 242, possess the same nominal mass as a C_{18} tricyclic monoaromatic hydrocarbon e.g. an alkylated C_4 octahydrophenanthrene, as well as a C_{19} tetracyclic tetra-aromatic hydrocarbon (e.g. methyl benz[a]anthracene or chrysene). However, interpretation and comparison of the mass spectra of such hydrocarbons (NIST MS Library v.2.0) clearly rule them out as possibilities for those discussed above.

There is precedence for the occurrence of aromatic sulphur-containing acids in petroleum; benzothiophene-3-carboxylic acid has been shown to occur as a metabolite during the bacterial oxidation of 3-methylbenzothiophene (Kropp and Fedorak, 1998). Sulphur-containing hydrocarbons e.g. polycyclic sulphides (Payzant *et al.*, 1986) and alkylated dibenzothiophenes, have been reported as petroleum hydrocarbons and the mass spectra of several methyl and polysubstituted isomers have been reported (Zeigler

et al., 2012; Andersson and Schade, 2004; Andersson *et al.*, 2001). Polycyclic aromatic thiophenes have been used frequently as biomarkers in oil analysis, including as tracers for determining oil migration (Li *et al.*, 2014).

To confirm the identification of the methyl- and dimethyl substituted dibenzothiophene acids and the tentatively assigned naphtha[1,8-bc]thiophene acids, reference acids or hydrocarbons should now be synthesised and spectra compared with those of constituents in the OSPW NA or equivalent hydrocarbon products. Sulphur-containing species (e.g. SO_3 and SO_5 species), are also present in more polar fractions of OSPW NA e.g. in the methanol eluate (e.g. Rowland *et al.* (2014a)), and these are potentially hydroxy- or keto- equivalents of those identified in the fraction analysed herein. Therefore the identification of sulphur-containing acids has implications for the understanding of further degradation processes and, formation of more polar sulphur species, as well as for their toxic effects.

6.4 Conclusions

The identifications presented herein, including those of novel alicyclic bi-, tri-, tetra- and pentacyclic hydrocarbons; mono-, bi- and tricyclic monoaromatic hydrocarbons and diaromatic sulphur-containing hydrocarbons and thus, by inference, of the corresponding acids, extends significantly previous identifications of OSPW NA as their methyl esters (Rowland *et al.*, 2011c; Rowland *et al.*, 2011g; Rowland *et al.*, 2011d; West *et al.*, 2014b; Wilde *et al.*, 2015). The data also lend support to many previous assignments.

The assignments were all supported by the identification of multiple isomers of each acid type, easily detected by the separation achieved using GC×GC and an understanding of the elution patterns observed for higher carbon number homologues. The assignments were also supported by interpretation of the hydrocarbon mass spectra and where possible, by comparison with the known elution order of the hydrocarbons. Furthermore, the assignments were supported, where possible, by subsequent re-examination of data for the NA methyl esters and comparison of their GC×GC retention positions and mass spectra with those of reference compounds, as well as interpretation of the corresponding acid methyl ester mass spectra. Most identifications were consistent with previous evidence for the identification of the acids, or for the petroleum hydrocarbons from which the acids identified herein could derive.

The identification of numerous adamantane acids as hydrocarbons in the reduced samples #2 and #7, supported by comparison of the NA methyl esters with reference compounds, confirmed that the conversion was successful on OSPW NA despite the increased complexity. Identification of methyl, ethyl, di- and trimethyl adamantane acids in the reduced underivatised, unfractionated OSPW NA confirmed adamantane

acids were indeed authentic components of OSPW NA and not just artefacts of derivatisation with BF_3-methanol.

The identification of novel bicyclic acids in OSPW NA, by comparison of spectra with collated bicyclane mass spectra and known elution orders was achieved. Although the identification of the bicyclics was limited by the low abundance of lower molecular weight acids, and thus hydrocarbons in OSPW NA, for comparison with reference mass spectra, new structures that had not been previously identified as the acid methyl esters could still be assigned. These new structures were also consistent with those previously identified, including both novel bridged and fused bicyclic compounds. Based on the observed differences between the bicyclic acids, identified as bicyclanes and acid methyl esters in petroleum NA and those identified in OSPW NA, new conclusions about the nature of these NA mixtures (a greater majority of bridgehead-substituted condensed bicyclics, rather than branched chain substituted bicyclics) were postulated.

The conversion of acids to hydrocarbons also proved successful on aromatic and sulphur-containing NA. Reference mass spectra of aromatic hydrocarbons have been frequently reported and are well characterized and often show distinctive mass spectral fragmentation patterns. This allowed for the assignment of several new mono- to tricyclic monoaromatic NA, as well as diaromatic sulphur-containing NA. Confirmation of the identification of dibenzothiophene-4-isobutanoic acid was possible by comparison of mass spectrum and retention position of the hydrocarbon equivalent with those of an available reference hydrocarbon. An equivalent reference acid was not available in this case.

The paucity of knowledge regarding the structure of NA in OSPW has limited the understanding of toxicity, remediation and the ability to accurately quantify and profile NA for environmental monitoring purposes. Prior to the current investigation, recent

advances in the identification of individual NA had only been achieved by GC×GC-MS analysis of the methyl esters. The complementary method developed and described herein, which combined an historical approach for identifying NA by chemical transformation to hydrocarbons with the unparalleled chromatographic separation afforded by GC×GC-MS, resulted in the identification of numerous individual NA as their hydrocarbon equivalents in OSPW.

Clearly many acids remain to be identified and the data produced in the current study can be re-examined as more hydrocarbon mass spectra and reference hydrocarbons become available. However, a significant number of acids from several acid classes have now been identified (e.g. alicyclic, aromatic, sulphur-containing), as detailed in the current investigation and in previous studies (Rowland *et al.*, 2011c; Rowland *et al.*, 2014a) and these can now be used to inform environmental monitoring programs and toxicity studies. For example, representative standards, including potentially radio-labelled analogues, could be purchased or synthesised and used to measure the toxicity of specific NA, or to study the transformation of such species during chemical treatment or bioremediation, or to quantify specific classes of NA by other complementary techniques (Hindle *et al.*, 2013; Brunswick *et al.*, 2015; Pereira *et al.*, 2013a; Pereira and Martin, 2014). The current investigation has shown the successful application of the conversion method developed herein to a complex NA mixture and there is now potential for it to be applied to other organic extracts for the identification of other acids and functionalised biomarkers from environmental samples, such as sediments.

Chapter 6

Chapter 7

Conclusions

The current investigation focused on the bicyclic acids of petroleum with the primary aim of identifying at least some of the bicyclic acids typically present in petroleum and in oil sands process-affected waters (OSPW) acid extracts.

This aim was achieved, first by carrying out the analysis of petroleum and OSPW naphthenic acid (NA) extracts using the unparalleled chromatographic separation and subsequent mass spectrometric detection of the methyl esters offered by multidimensional gas chromatography-mass spectrometry (GC×GC-MS). More than one hundred C_{8-15} bicyclic acids were shown to be present in each OSPW extract. Consideration of the GC retention behaviour, numbers of structural types and interpretation and comparison of the electron ionisation mass spectra of the methyl esters of a number of synthetic and purchased bicyclic carboxylic acids allowed identification of various bicyclic acids in OSPW and commercial acids, many for the first time. The identifications included several, novel, bridged bicyclic acid structures e.g. bicyclo[2.2.1]heptane, bicyclo[3.2.1]octane, bicyclo[2.2.2]octane and bicyclo[3.3.1]nonane acids, fused bicyclic acid structures e.g. bicyclo[3.3.0]octane, bicyclo[4.3.0]nonane and bicyclo[4.4.0]decane acids. Many of the findings were published (Wilde *et al.*, 2015).

Further identifications were still limited by the lack of reference spectra and availability of reference compounds for comparison. For example, bicyclic acid structures including bicyclo[4.2.1]nonane, bicyclo[3.2.2]nonane, bicyclo[3.3.2]decane, bicyclo[4.2.2]decane and spiro[4.5]decane carboxylic acids could not be ruled out or in, as no authentic compounds or literature data were available. Interpretation of the mass spectra of the

methyl esters of the higher bicyclic C_{12-15} acids suggested that many were simply analogues of those identified, with longer alkanoate chains and/or alkyl substituents. Many bicyclic acids remain to be identified.

Since a wider literature of mass spectra of bicyclic hydrocarbons (e.g. Denisov *et al.* (1977d), Denisov *et al.* (1977c), Denisov *et al.* (1977a), Brodskii *et al.* (1977), Lukashenko *et al.* (1973), Golovkina *et al.* (1984)) was available than was extant for the acids or esters, a useful approach, formerly adopted by Zelinsky (1924) and Seifert *et al.* (1969) was investigated as an alternative approach for the identification of NA: namely, conversion of the acids to hydrocarbons.

Although this approach was adopted by early researchers (Zelinsky, 1924; Braun *et al.*, 1933; Seifert *et al.*, 1969), the lack of sufficient chromatographic separation of the complex hydrocarbon mixtures produced in these earlier studies meant identification of individual compounds was still limited. Therefore combining this older approach with the separation power of a modern chromatographic method such as GC×GC-MS, was considered potentially useful for furthering the investigation into the structural identification of bicyclic petroleum acids. A large data set of reference mass spectra for bicyclic hydrocarbons was laboriously collated from the older literature and replotted from the tabulated values. Many of these data were from early Russian investigations into the isolation and characterisation of petroleum hydrocarbons (Denisov *et al.*, 1977a; Denisov *et al.*, 1977b; Denisov *et al.*, 1977c; Denisov *et al.*, 1977d; Rusinova *et al.*, 1987; Rusinova *et al.*, 1981; Golovkina *et al.*, 1984; Golovkina *et al.*, 1979).

The optimised method, based on the historical approach involving reduction of the NA esters to hydrocarbons, was developed first on three model bicyclic acids to obtain reproducible reactions and high yields of the desired products. The multistep synthetic route involved reduction of the free acids or esters with lithium aluminium hydride;

derivatisation to the tosylates using tosyl chloride in the presence of 4-(dimethylamino)pyridine and triethylamine and in a novel modification and improvement, "Super-hydride®" reduction using lithium triethylborohydride to the hydrocarbons. Structural characterisation of each of the alcohol and tosylate intermediates by IR, GC-MS and NMR and of the final hydrocarbon products by GC-MS, confirmed the successful conversion of the model bicyclic acids, possessing different bicyclic cores, to the corresponding hydrocarbons. Data for the resulting bicyclanes were all comparable with relevant reference mass spectra. The method developed was reliable, and by carrying out full characterisation of the compounds at each stage to ensure that the structural integrity of the bicyclic core was maintained throughout the conversion, the method could then be applied with confidence to much more complex NA mixtures.

The method developed was first performed on a petroleum NA mixture. Subsequent analysis of the reduced acids by GC×GC-MS and comparison of the hydrocarbon mass spectra with the numerous reference spectra for bicyclic hydrocarbons collated from the literature, resulted in the identification of >40 individual bicyclic acids including fused, bridged and terpenoid-derived acids (Wilde and Rowland, 2015). The identification of acids, across a range of carbon numbers, with the same reoccurring bicyclic 'core' such as the identification of methyl-, dimethyl-, ethyl- and propylbicyclo[3.3.0]octanes and thus of the corresponding bicyclo[3.3.0]octane carboxylic to propanoic acids, was strong evidence in support of the previous proposal that at least some of the higher carbon acids are analogues of those identified, with longer alkanoate chains and/or alkyl substituents.

The success of the conversion and the numerous identifications achieved after careful sample concentration, fractionation and optimal separation using GC×GC-MS, and thus

by inference the corresponding acids, represents the most comprehensive study of bicyclic petroleum NA to date. Assignments were supported by the identification of multiple isomers of each acid type by close matches with the GC×GC retention positions and mass spectra of reference hydrocarbons and the bicyclic acids identified were consistent with the previous evidence of such acids in other matrices, identified as the esters (Piccolo *et al.*, 2010; Bagrii *et al.*, 1970; Bagrii *et al.*, 1967; Petrov, 1987). Many of the above results were published (Wilde and Rowland, 2015).

The method developed, for the conversion of NA to hydrocarbons followed by analysis using GC×GC-MS, was then applied to the structural elucidation of NA in OSPW. Rigorous examination of the mass spectra of individual hydrocarbons, made possible by the separation afforded by GC×GC-MS and effective use of data processing software (e.g. CLIC expressions), resulted in the identification of numerous alicyclic, aromatic and sulphur-containing acids. In addition to the identifications of acids that had previously been assigned in OSPW as methyl esters and which were used herein to confirm the successful conversion of acids to hydrocarbons, numerous identifications of other acids were made, including some NA which were only tentatively assigned in OSPW previously and many new identifications of NA in OSPW.

Although the identification of bicyclic acids, as bicyclanes, was more limited than when applied to petroleum NA, new structures that had not been previously identified as the acid methyl esters were assigned. These new structures were also consistent with those previously identified, including both novel bridged and fused bicyclic structures. Based on the observed differences between the bicyclic acids, identified as bicyclanes and acid methyl esters, in petroleum NA and those identified in OSPW NA, new conclusions about the nature of these NA mixtures were drawn.

7.1 Wider context

7.1.1 Occurrence and nature of bicyclic NA

Based on the structures of the bicyclic acids identified herein, many possessing bicyclic cores similar to bicyclic petroleum hydrocarbons, it can be hypothesised that these acids probably represent the biotransformation products of the initially somewhat more bio-resistant, bicyclanes of petroleum. This hypothesis can also be applied to several of the other NA classes identified in the OSPW NA herein (e.g. diamondoid and dibenzothiophene acids).

The identification of acids (as hydrocarbons) herein possessing more highly condensed or bridged-type structures (e.g. bicyclo[2.2.2]- and [3.2.1]octanes, adamantanes and 2,4-cyclopentanoadamantanes), makes it possible to suggest that these also likely derive from biotransformation of the corresponding alkylhydrocarbons in petroleum, rather than from ring opening of higher polycyclic terpenoids as sometimes suggested previously (Rowland *et al.*, 2011g).

Petroleum NA and NA extracted from OSPW have, in general, often been reported to possess significantly different compositions (Grewer *et al.*, 2010; Hindle *et al.*, 2013), observed most commonly as differences in the HPLC retention times of the unresolved acid 'humps'. This has typically been attributed to the increased resistance, of the OSPW NA to biodegradation (Scott *et al.*, 2005; Frank *et al.*, 2008; Brown and Ulrich, 2015). The current justification used to explain both of these phenomena is that the carboxylated alkyl side chains in OSPW NA, which are otherwise believed to possess alkyl-substituted alicyclic structures similar to those of petroleum NA, are simply longer and more highly branched in OSPW NA (Holowenko *et al.*, 2002; Bataineh *et al.*, 2006). This explanation is based on the knowledge that the branched chain acids elute before the corresponding straight chain equivalents and that branched chain are more

resistant to biodegradation (Smith *et al.*, 2008; Misiti *et al.*, 2014; Quesnel *et al.*, 2011). However, this explanation has never been supported by the identification of, for example, an acid possessing a long non-branched alkanoate chain in petroleum NA and the corresponding acid with a branched alkanoate chain in the OSPW NA.

Based on the new knowledge of bicyclic structures identified in both petroleum NA and OSPW NA herein, an alternative explanation was made for the observed differences between the retention times and biodegradation of petroleum and OSPW NA mixtures. It is proposed herein that OSPW and petroleum NA indeed contain acids with some similar structures, but that, alongside differences in alkyl branching and aromatic contents of the NA, the OSPW NA might also possess a greater abundance of more condensed, bridged structures. This is reflected in the elution order of the bicyclanes and the corresponding bicyclic acid methyl esters observed herein. The general retention times of the bicyclanes and reference bicyclic acids increased as follows: bicyclo[2.2.1]heptanes, bicyclo[3.2.1]octanes, bicyclo[3.3.0]octanes, bicyclo[2.2.2]octanes, bicyclo[4.3.0]nonanes, bicyclo[3.3.1]nonanes and bicyclo[4.4.0]decanes, with the more condensed-type and bridged structures eluting earlier.

The identification of a series of C_{9-11} bicyclo[3.3.0]octane acids with increasing alkanoate side chains supports the proposal that some of the higher carbon number analogues in OSPW NA, possess structures similar to the lower molecular weight bicyclic acids identified herein. However, the paucity of data for C_{13-15} bridged bicyclic hydrocarbons means this extrapolation of knowledge is limited. Examination of the relevant literature suggests that there has been no identification of petroleum hydrocarbons possessing small, condensed, bridged bicyclic cores e.g. bicyclo[3.2.1]octanes with alkyl chains longer than C_4 (despite the mass spectra of some

long chain >C_5 bicyclo[2.2.1]heptanes present in the NIST library). In order for the C_{13-15} bicyclic acids observed in the OSPW NA herein to simply be homologues of those observed in the petroleum NA, but with longer and more branched alkanoate chains, these condensed bridged bicyclics would have to derive from either bicyclo-octanes with >C_5 branched alkyl chains or from more complex rearrangements of higher carbon number unknown precursors. Therefore it is proposed that at least some of the higher carbon number bicyclic acids observed in the OSPW NA, and petroleum NA to less of an extent, actually possess larger bridged bicyclic cores such as the bicyclo[4.2.1]nonane, bicyclo[3.2.2]nonane, bicyclo[3.3.2]decane, bicyclo[4.2.2]decane structures which could not be ruled in or out herein due to lack of reference data and compounds.

7.1.2   Implications for future research

Now there are a significant number of acids from various acid classes identified herein (e.g. alicyclic, aromatic, sulphur-containing), or during previous studies (Rowland *et al.*, 2011c; Rowland *et al.*, 2014a), this knowledge can be used to inform other research, such as investigations into the environmental monitoring of NA or toxicity studies to target remediation of specific NA or NA classes.

Using the current and new knowledge, representative compounds can be purchased or synthesised and used to measure the toxicity of specific relevant NA. Representative standards of acids known to be components specific to OSPW NA can be purchased or synthesised, to be used for the quantification of specific NA or NA classes, using the recently developed advanced techniques such as HPLC or GC coupled with high or ultra-high resolution mass spectrometry or ion mobility mass spectrometry (Pereira and Martin, 2014; Pereira *et al.*, 2013a; Barrow *et al.*, 2014; Bauer *et al.*, 2015; Huang *et al.*, 2015a; Brunswick *et al.*, 2015).

Similar standards or radio-labelled analogues could be spiked into OSPW NA mixtures before being chemically treated to help monitor the formation of by-products to enhance current understanding of proposed short-term remediation plans. Remediation studies suggest at least some bicyclic acids can be relatively quickly removed from suitably treated OSPW (Martin *et al.*, 2010), but a closer examination of which isomers are degraded will now be possible, using the knowledge of the structures identified herein. This may be deemed important as some bicyclic acids are more acutely toxic than others (Jones *et al.*, 2011). Further investigations into the identification of OSPW NA could result in the identification of those most resistant to biodegradation in OSPW NA. The isolation of bacteria which effectively remove the most recalcitrant OSPW NA could be used for long term remediation plans.

Alternative uses of the NA identified herein, or simple transformation products or derivatives, could also be investigated. For example the medicinal properties or lubrication and surfactant properties of the ester or amine derivatives (e.g. Bagrii and Maravin (2013)). Initial interest in the extraction and identification of NA was due to their economic value. However, these mixtures were often crude NA mixtures used as additives or bulking agents (Lochte and Littmann, 1955). If a specific NA or class of NA were discovered to possess an economic value, significant quantities obtained by a targeted extraction process, could be extracted from the large volumes of stored OSPW wastewater.

Limited identification of individual petroleum acids has hindered a detailed understanding of their role in petroleum generation and oil production processes, refinery corrosion, uses as wood preservatives and as environmental toxicants, for decades. The current investigation has shown the successful application of the methods developed herein, including conversion of NA to hydrocarbons, for the identification of

numerous NA in petroleum and OSPW acid extracts. There is now potential for this to be applied to other complex NA mixtures and for the identification of other functionalised biomarkers in environmental samples such as the polar constituents of sediments or contaminated groundwaters.

7.2 Future Work

Considering the conclusions of the results and their application in a wider context, future work could involve methods to address both the limitations of the current investigation, but also investigate how the results could be used to progress future research. The three main limitations of the work included the lack of knowledge of higher carbon number analogues of bicyclic acids, the ambiguity regarding the position of the carboxyl group in poly-substituted acids and the lack of available reference compounds to confirm new identifications. Fortunately these limitations can all be addressed.

7.2.1 Reference Compounds

The synthesis of higher carbon number reference acids and hydrocarbons, guided by those identified in the current investigation, would not only extend the potential for the method developed herein in aiding the identification of higher carbon number homologues, but also be useful in future studies.

Synthesis of C_{12-15} bridged bicyclic hydrocarbons or carboxylic acids could be performed, including some with small bicyclo-octanes cores, with longer branched alkyl or alkanoate side chains, as well as those with larger bicyclic cores (e.g. bicyclo[4.2.1]nonanes and bicyclo[3.2.2]nonanes). Synthesis of the hydrocarbons may be easier than the functionalised equivalents. The synthesis of reference hydrocarbons would aid the identification of NA after conversion using the method developed herein and would enhance current knowledge of petroleum hydrocarbons.

Several procedures for the synthesis of various bridged and fused bicyclic compounds are reported in the literature. For example, Knotnerus and co-workers reported a series of investigations for the synthesis of bicyclo[3.3.0]octanes (Knotnerus and Schilling,

1964a; b), bicyclo[2.2.2]octanes (Bickel *et al.*, 1960), bicyclo[4.3.0]nonanes and bicyclo[4.4.0]decanes (Knotnerus and Bickel, 1964). The synthetic procedures usually proceed via three mains routes, including cycloaddition across a π-system (Singh *et al.*, 2006; Blaney *et al.*, 1972), via ring closure reactions (Filippini and Rodriguez, 1999), or via the rearrangement or isomerisation of other bicyclic compounds (Chow *et al.*, 1966; Bagrii *et al.*, 1970; Flego *et al.*, 2009). As novel bicyclic compounds are found in natural products, synthetic routes for the synthesis of bicyclic terpenoids could also be investigated (Cocker *et al.*, 1968; Mori *et al.*, 1972; Pavel, 1982; Filippini and Rodriguez, 1999).

Following the identification, or in some cases tentative identification, of several new acids in OSPW NA, such as several adamantane acids substituted at a secondary carbon position, tricyclic terpenoid acids and naphtha[1,8-bc]thiophene acids, a broader range of NA could be synthesised and used for profiling and source characterisation studies. Frank *et al.* (2014) demonstrated the potential use of monitoring individual acids for identifying the source of AEO in natural groundwaters and Lengger *et al.* (2015) reported the use of adamantane acid distributions to determine short-term temporal and spatial variability within OSPW tailings ponds. The eleven adamantane acids including diacids used for profiling purposes by Lengger *et al.* (2015) were all, excluding adamantane-2-carboxylic acid, isomers substituted at the tertiary carbon positions. This was most likely due to the availability of commercial reference compounds. However, the results of the current investigation suggest that it would be worthwhile to synthesise and use some isomers with alkyl groups and carboxyl groups substituted at the secondary carbon positions, as it appears they are indeed present in some OSPW NA.

7.2.2   Conversion of acids to deuterated hydrocarbons

The reduction of petroleum and OSPW NA to their corresponding hydrocarbons, resulted in the identification of several alkyl-substituted acids as dimethyl-, trimethyl, or methylethyl-substituted hydrocarbons. Although the approach resulted in the identification of the 'main' acid structures, there still remained a degree of ambiguity regarding the original positions of some of the carboxylic acid groups. For example, there were three possible precursor acids of 1,4-dimethylbicyclo[3.2.1]octane; a bicyclane identified in the reduced hydrocarbons of petroleum NA and OSPW NA (discussed in Chapter 5, Section 5.3.4.1, page 224).

Theoretically, a dimethyl- substituted bicyclane such as 1,4-dimethylbicyclo[3.2.1]octane could originate from an acid with the carboxylic acid group originally substituted at either methyl- position (e.g. 1-methylbicyclo[3.2.1]octane-4-carboxylic acid or 4-methylbicyclo[3.2.1]octane-1-carboxylic acid) or on both positions in the case of a diacid (e.g. bicyclo[3.2.1]octane-1,4-dicarboxylic acid).

An approach previously adopted by early researchers of petroleum NA, who also attempted identification by chemical transformation, was to use a metal deuteride in one of the conversion steps as opposed to a metal hydride (e.g. lithium aluminium deuteride; LAD, instead of lithium aluminium hydride; LAH) (Hoering, 1970; Seifert *et al.*, 1972). The use of a metal deuteride to produce deuterium labelled hydrocarbons is a method also used in investigations into the mass spectral fragmentation mechanisms of certain compounds (Kwart and Blazer, 1970). Incorporation of deuterium atoms onto a specific part of a compound and analysis by mass spectrometry reveals information about the mass spectral fragmentation of that molecule. However the origins of all fragment ions

observed in the mass spectra of bicyclic hydrocarbons are not always easily justified using basic rules for mass spectral interpretation.

A preliminary experiment, to investigate the use of LAD, was attempted on one of the model acids (**Ia**) to produce deuterium labelled 2,4-dimethylbicyclo[3.3.0]octane (**Ie**; Figure 4-25, Chapter 4, page 154). The use of LAD during the reduction of the acid to the alcohol intermediate, resulted in the addition of two deuterium atoms onto the carboxyl carbon atom. In the final hydrocarbon product, the methyl group derived from the original carboxyl carbon was observed as a -CHD_2 substituent instead of a -CH_3 group. The additional 2 mass units were observed in the mass spectrum as a change in the molecular ion and the fragment ions which involved the loss of the deuterated methyl group.

Whilst deuterium labelling of the carboxyl carbons would be especially useful in the detection of diacids, resulting in the molecular ion increasing by 4 mass units in the mass spectrum of the hydrocarbon products, its usefulness for the determination of the carboxyl group in dimethyl- bicyclanes derived from monoacids relies on detailed understanding and mass spectral interpretation of bicyclic hydrocarbon mass spectra, with the potential for misidentification. The mass spectrum of deuterated 2,4-dimethylbicyclo[3.3.0]octane indicated that the compound can undergo extensive rearrangement (Chapter 4, Section 4.4.1.3). A more detailed understanding of the main fragmentations of bicyclic hydrocarbons may also be better studied using a lower ionisation energy by means of a variable-energy ion source.

Following the successful deuteroreduction of a model bicyclic acid (Chapter 4, Section 4.4.1.3, page 153), this approach could now be applied first to petroleum NA and the results compared with those discussed herein (Chapter 5). Mass spectral interpretation would require clear mass spectra to be obtained by good separation of resolved,

individual hydrocarbons, previously achieved using GC×GC-MS. However, the deuteroreduction approach may be less informative when applied to more complex mixtures such as OSPW NA.

It was considered likely that for a dimethyl- bicyclane identified as the hydrocarbon herein, (e.g. 1,4-dimethylbicyclo[3.2.1]octane), both possible acid isomers (e.g. 1-methylbicyclo[3.2.1]octane-4-carboxylic acid and 4-methylbicyclo[3.2.1]octane-1-carboxylic acid), with the acid substituted at either alkyl position would be present in OSPW NA. This was observed in the instance of 3-methyladamantane-1-ethanoic acid and 3-ethyladamatane-1-carboxylic acid; both of which have been detected in some samples OSPW NA and both of which produce the same tricyclic hydrocarbon upon reduction (discussed in Chapter 6, Section 6.3.3.1, page 281). Therefore synthesis or purchase of as many possible isomers would be most beneficial for the detection of such acids in other NA matrices.

7.2.3   Continued data analysis

The large volume of data within a single, multidimensional gas chromatogram displaying the separation of a complex NA or hydrocarbon mixture, means further information can always be extracted if the data are continually processed. Future work would entail the continued collection of hydrocarbon mass spectra (i.e. those of alicyclic, aromatic and heteroatom-containing hydrocarbons), and comparison with the GC×GC-MS data of all the reduced NA mixtures discussed herein. Good use of GC×GC-MS software for the interpretation and presentation of GC×GC-MS data has been demonstrated herein, especially the application of CLIC expressions for the fast identification of specific compounds. Similar expressions could be produced and automatically applied to the analysis of other hydrocarbon and NA mixtures for the rapid screening of target compounds.

Chapter 7

Chapter 7

Appendix

Appendix Table 1: 1st dimension retention indices of the peaks assigned as C_{9-12}

bicyclanes in Figures 5-6 and 5-7.

Carbon Number	Structure/Peak Label	Retention Index ($RI_{Rxi-1ms}$)
9	Nonane	900
9	bi-II	928
9	bi-I	949
10	bi-VI	954
10	bi-III	965
10	bi-VII	974
10	Decane	1000
10	bi-XIV b	1011
10	bi-XIII* isomer 2	1014
10	bi-XV* isomer 3	1017
10	bi-XVI c	1021
10	bi-IV b	1029
10	bi-IX* isomer 3	1032
10	bi-VIII	1032
10	bi-IX* isomer 2	1035
10	bi-IX* isomer 1	1039
10	bi-XIV a	1044
10	bi-XV* isomer 2	1046
10	bi-XV* isomer 1	1049
10	bi-IV a	1051
10	bi-X	1055
10	bi-XVI b	1059
10	bi-XI b	1061
10	bi-XVI a	1062
10	bi-XIII* isomer 1	1071
10	bi-XI a	1076
10	bi-XII b	1080
10	bi-XII a	1085
11	Undecane	1100
11	bi-XVIII (peak 1)	1118
11	bi-V	1125
11	bi-XVII (peak 2)	1160
11	bi-XVIII (peak 3)	1172
11	bi-XVIII (peak 4)	1179
12	Dodecane	1200
12	bi-XIX (major isomer)	1231
12	bi-XX (major isomer)	1241
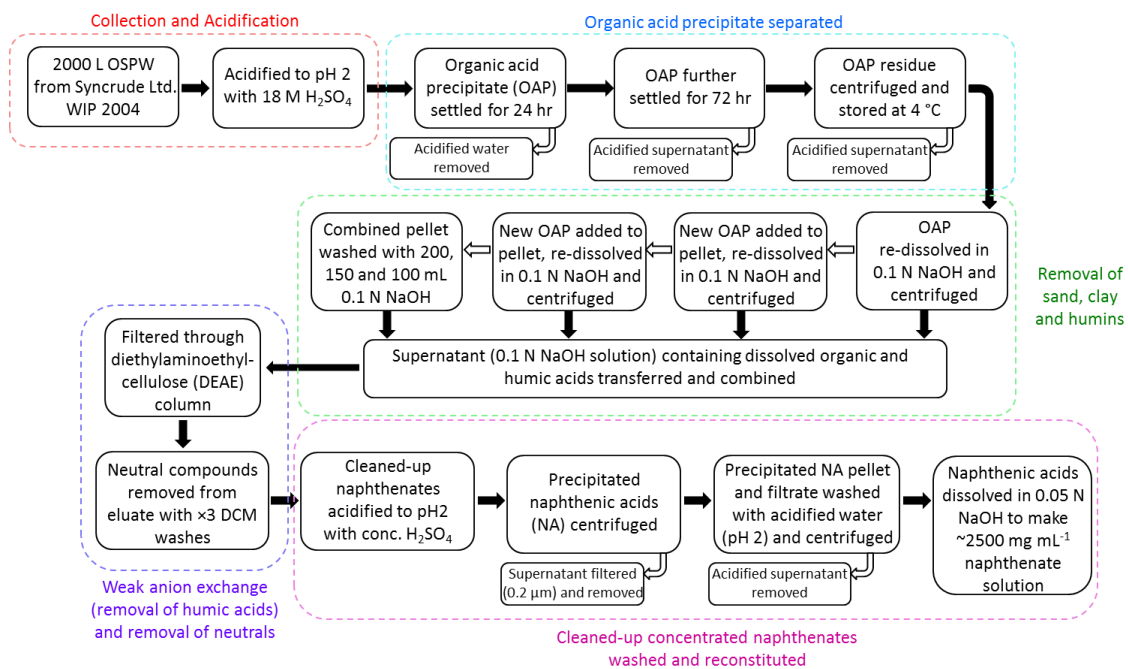
Appendix Figure 1: Flow diagram depicting extraction and clean-up procedure for naphthenic acids from OSPW as outlined by Frank *et al.* (2006).
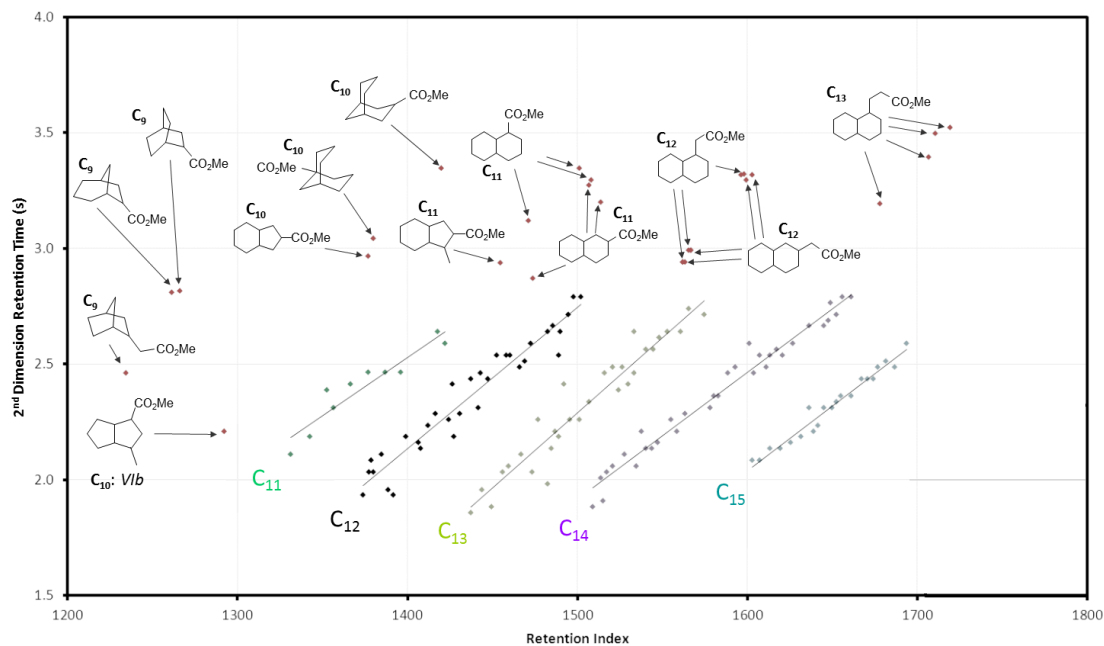
Appendix Figure 2: Schematic GC×GC EIC of sample #1 (WIP, 2004) showing the relative retention positions of the C_{11-15} bicyclic NA methyl esters compared with those of the authentic reference acid methyl esters (Wilde *et al.*, 2015).
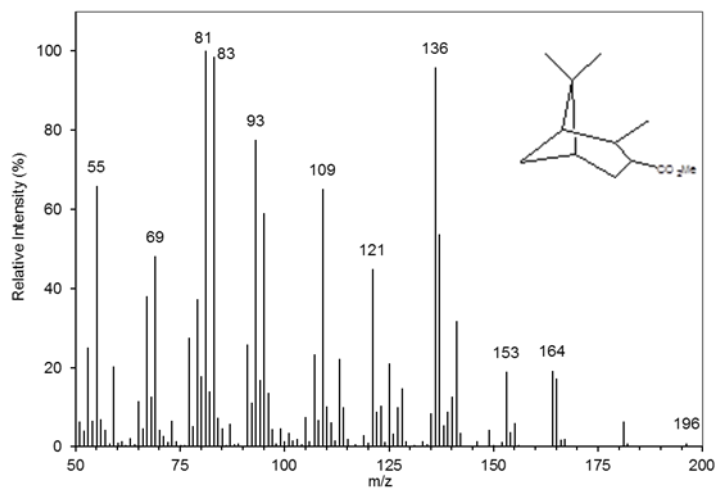
Appendix Figure 3: Electron ionisation mass spectrum of 2,6,6-trimethylbicyclo[3.1.1]heptane-3-carboxylic acid methyl ester ((+)-3-pinane-carboxylic acid methyl ester).
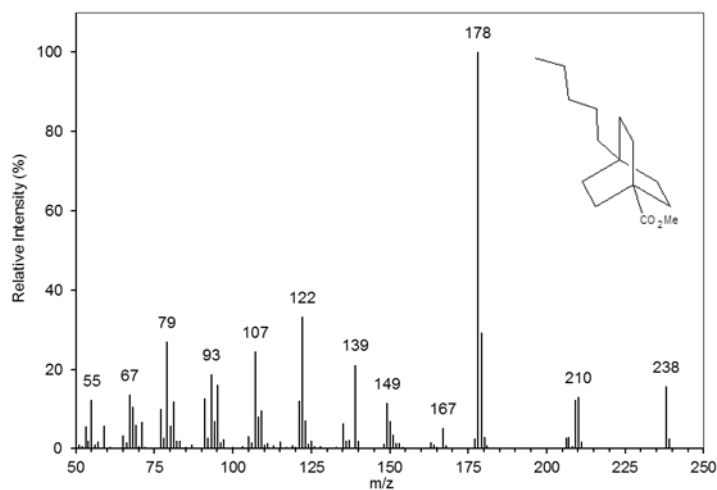
Appendix Figure 4: Electron ionisation mass spectrum of 4-pentylbicyclo[2.2.2]octane-1-carboxylic acid methyl ester.
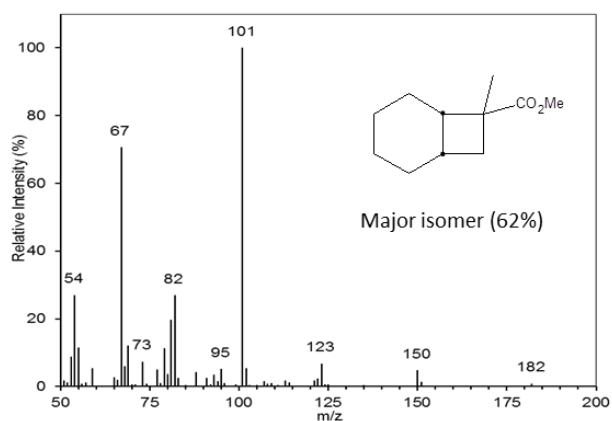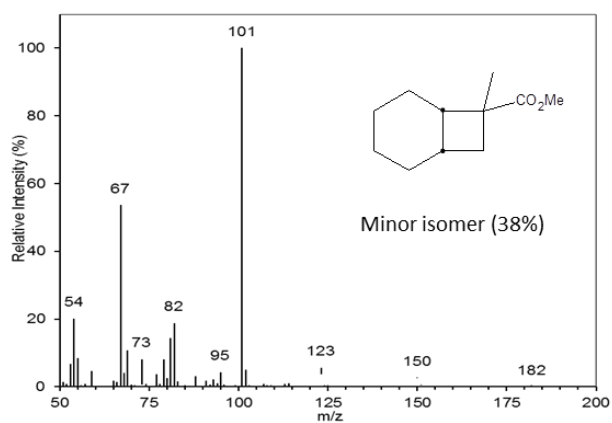
Appendix Figure 5: Electron ionisation mass spectra of two isomers of synthesised 7-methylbicyclo[4.2.0]octane-7-carboxylic acid methyl ester.
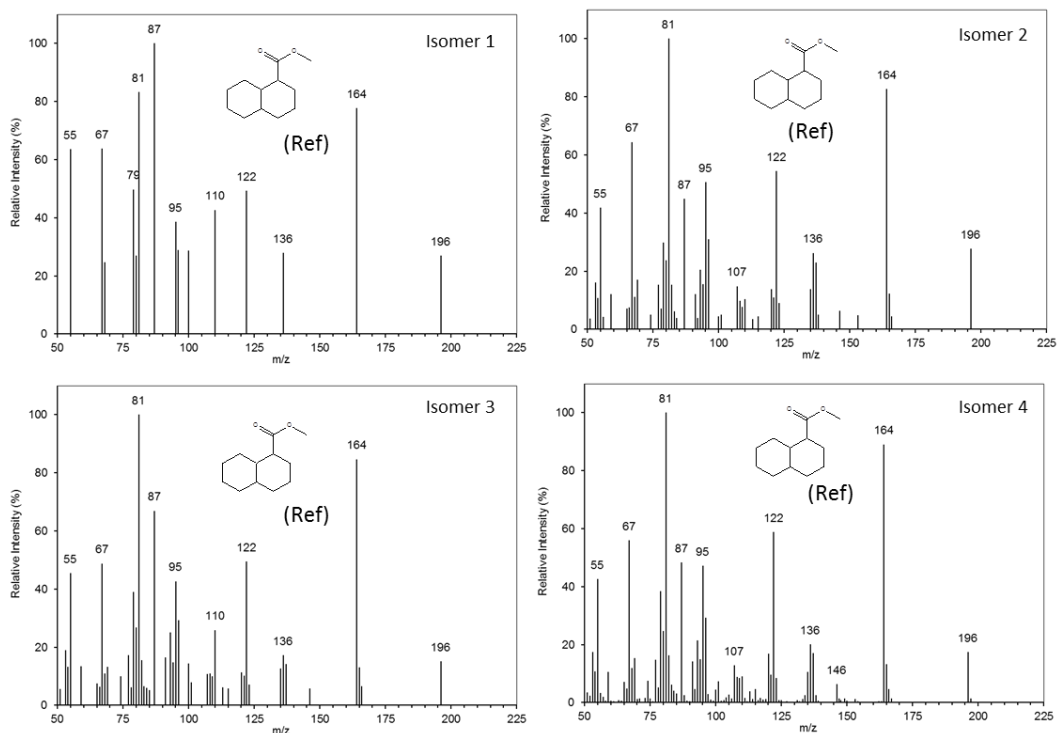
Appendix Figure 6: Electron ionisation mass spectra of four isomers of synthesised

bicyclo[4.4.0]decane-2-carboxylic acid methyl ester.
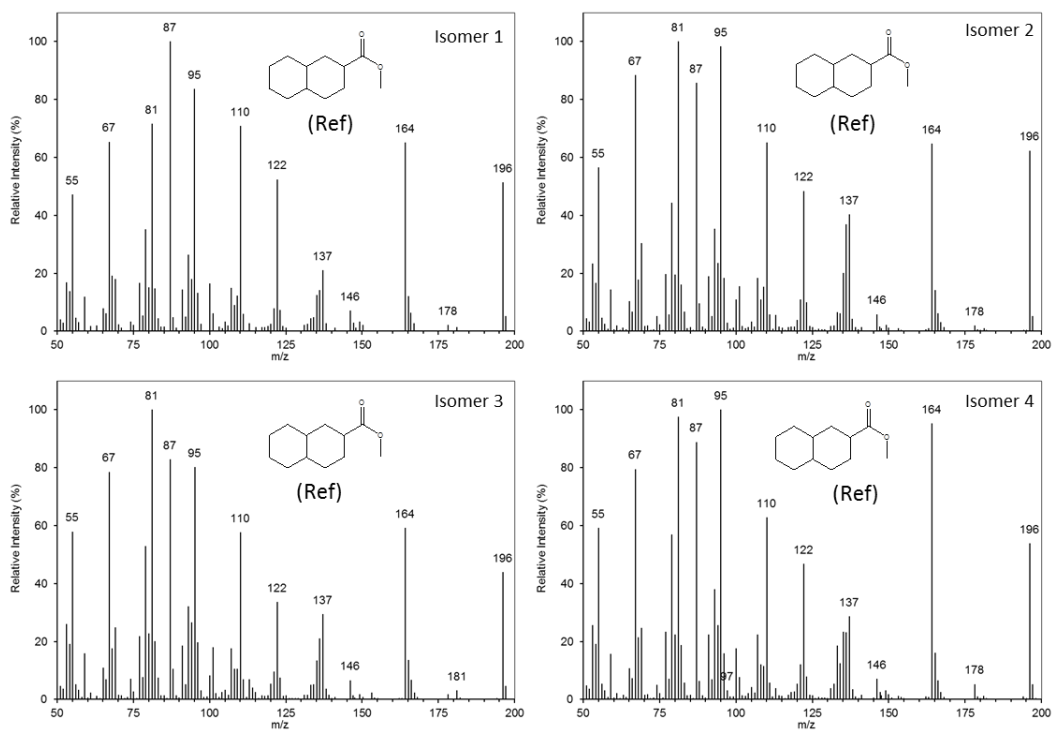
Appendix Figure 7: Electron ionisation mass spectra of four isomers of synthesised

bicyclo[4.4.0]decane-3-carboxylic acid methyl ester.
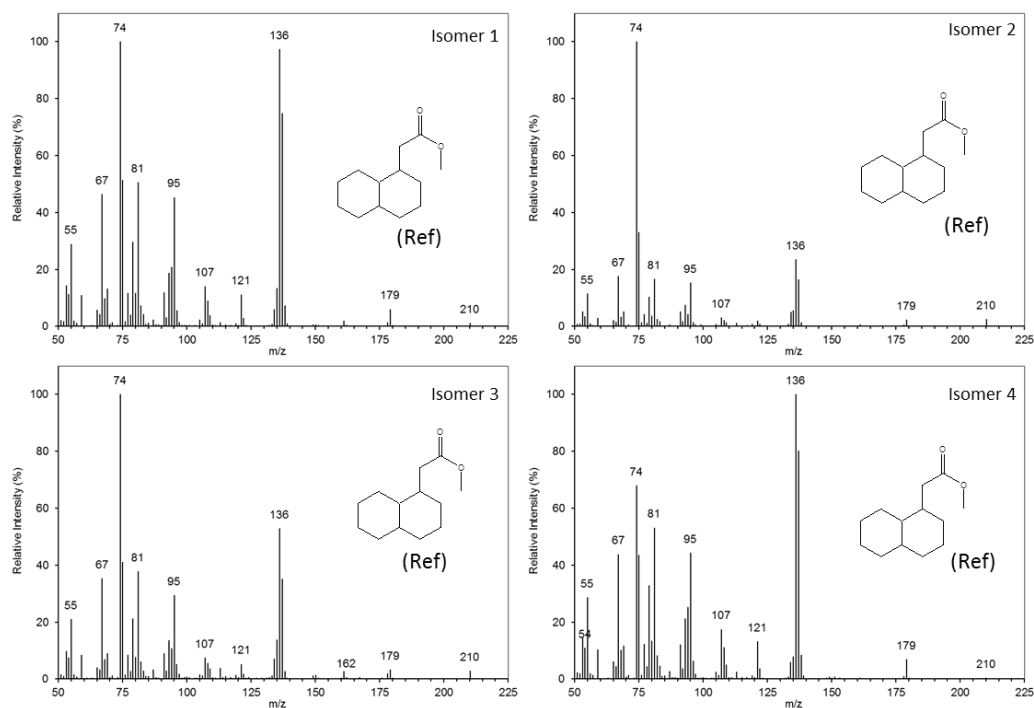
Appendix Figure 8: Electron ionisation mass spectra of four isomers of synthesised

bicyclo[4.4.0]decane-2-ethanoic acid methyl ester.
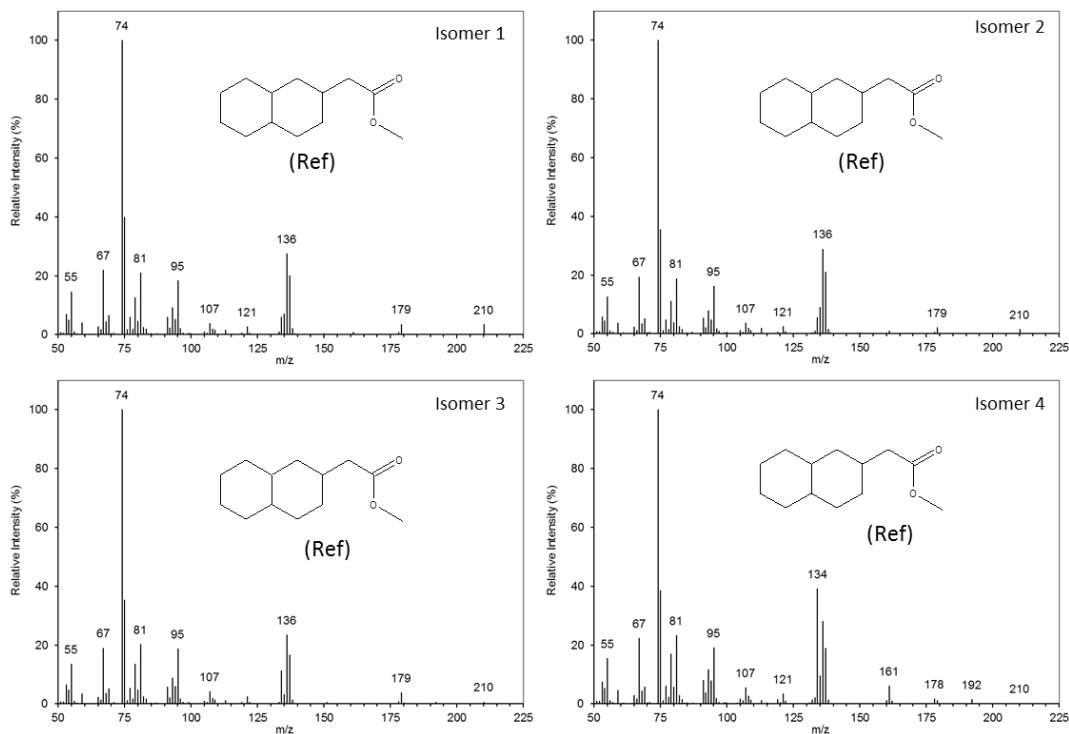
Appendix Figure 9: Electron ionisation mass spectra of four isomers of synthesised

bicyclo[4.4.0]decane-3-ethanoic acid methyl ester.
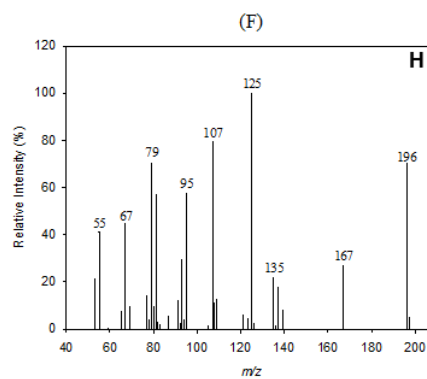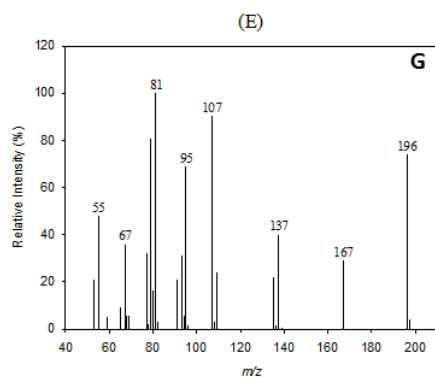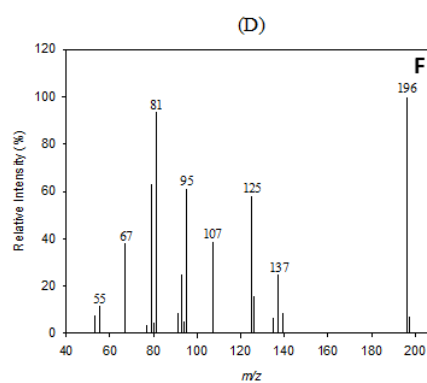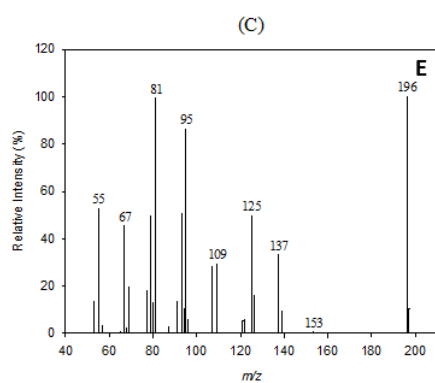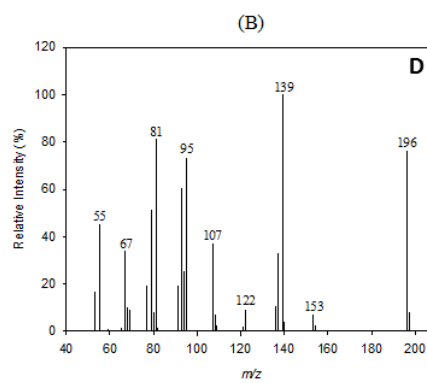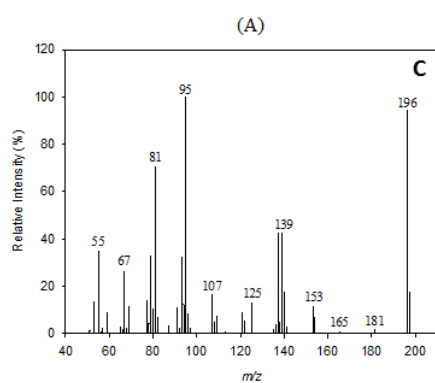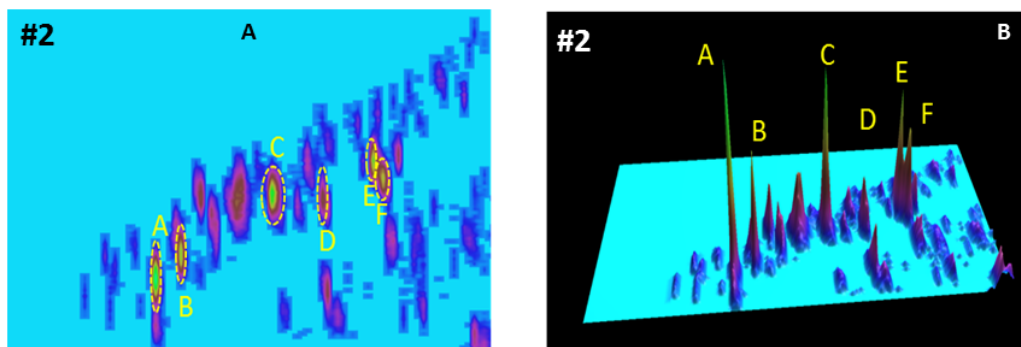
Appendix Figure 10: (A and B) EIC (*m/z* 196) and 3D representation, showing examples of C_{11} bicyclic NA in OSPW from industry A (sample #2) and (C-F) mass spectra of six peaks A-F (Wilde *et al.*, 2015).
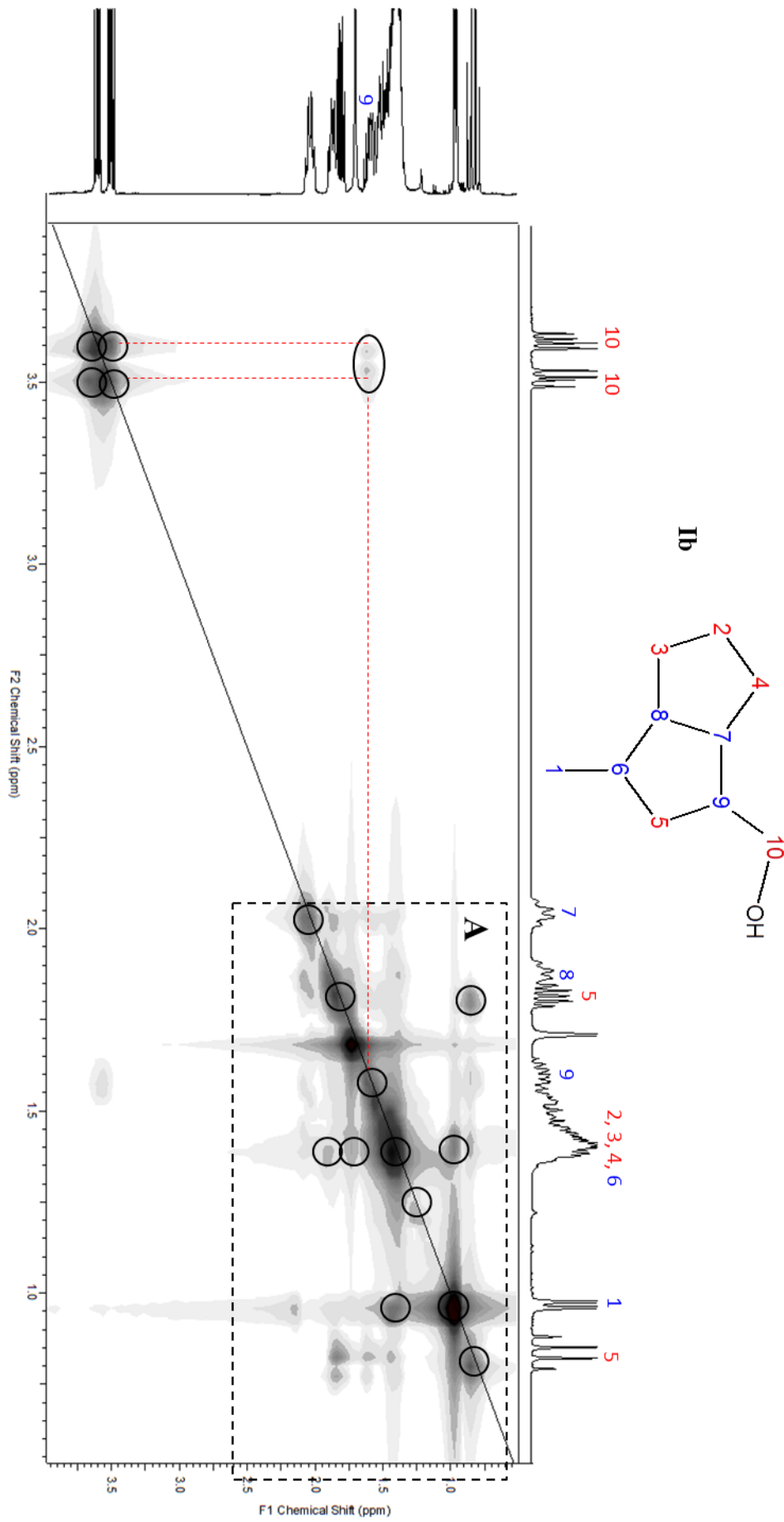
Appendix Figure 11: Correlation (COSY) spectrum of **Ib**.
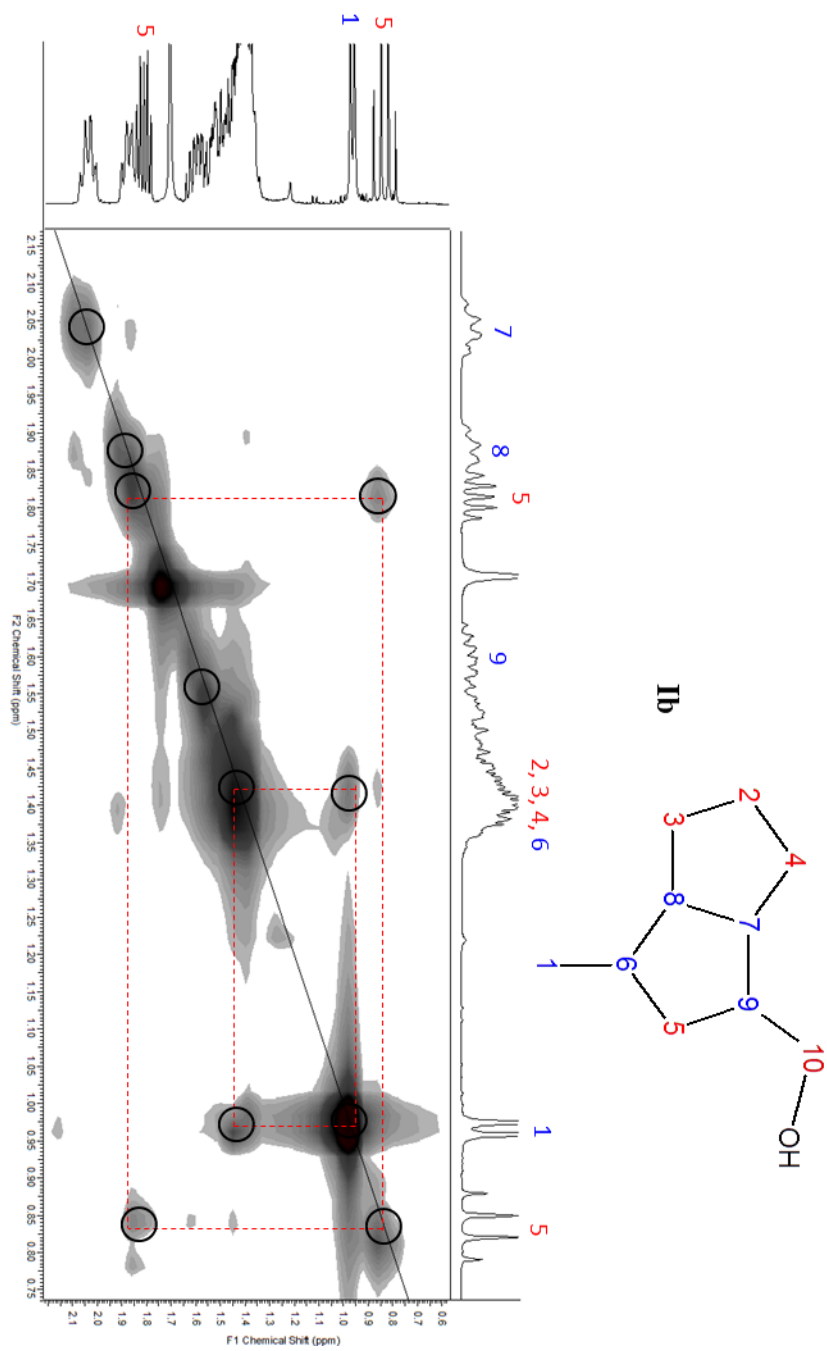
Appendix Figure 12: Zoomed COSY spectrum of **Ib**.
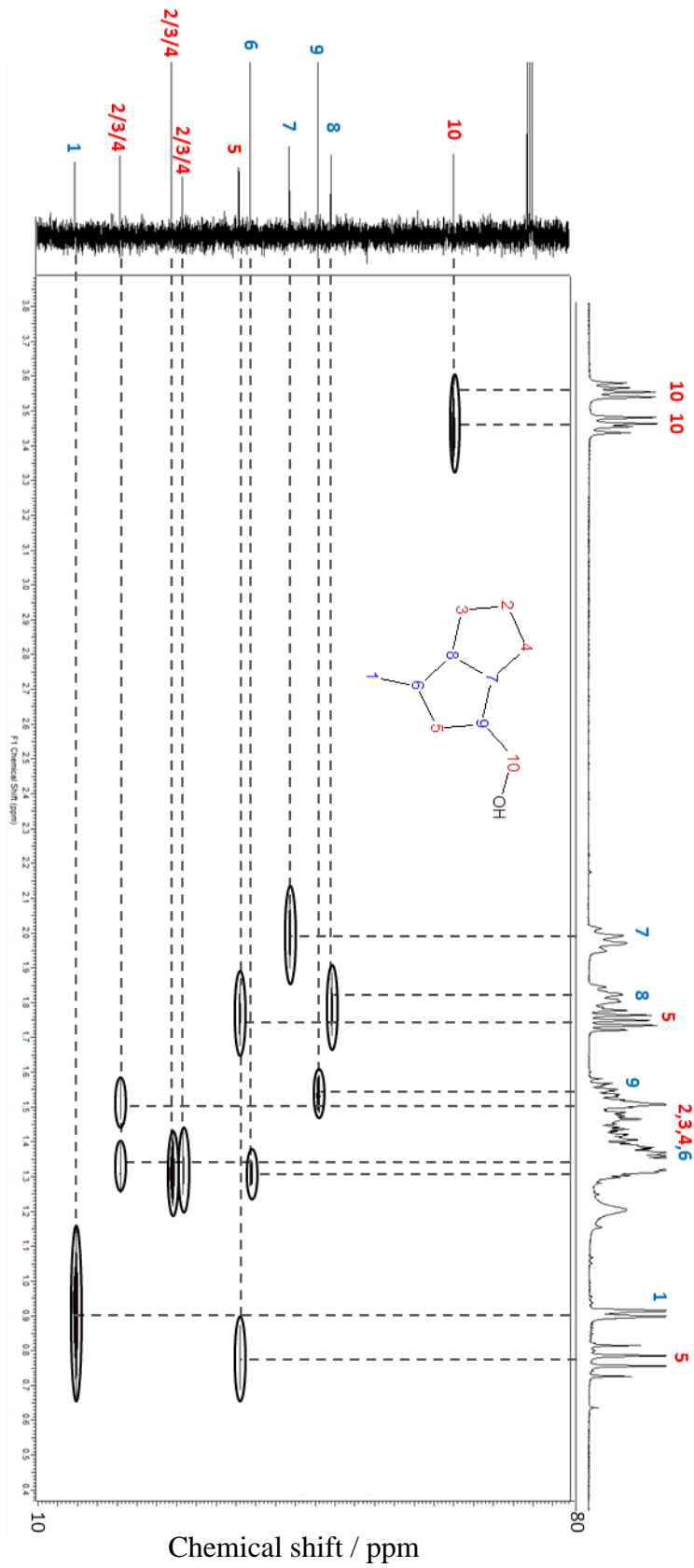
Appendix

Appendix Figure 13: Heteronuclear shift correlation (HETCOR or CHSHF) spectrum of

Ib.

350
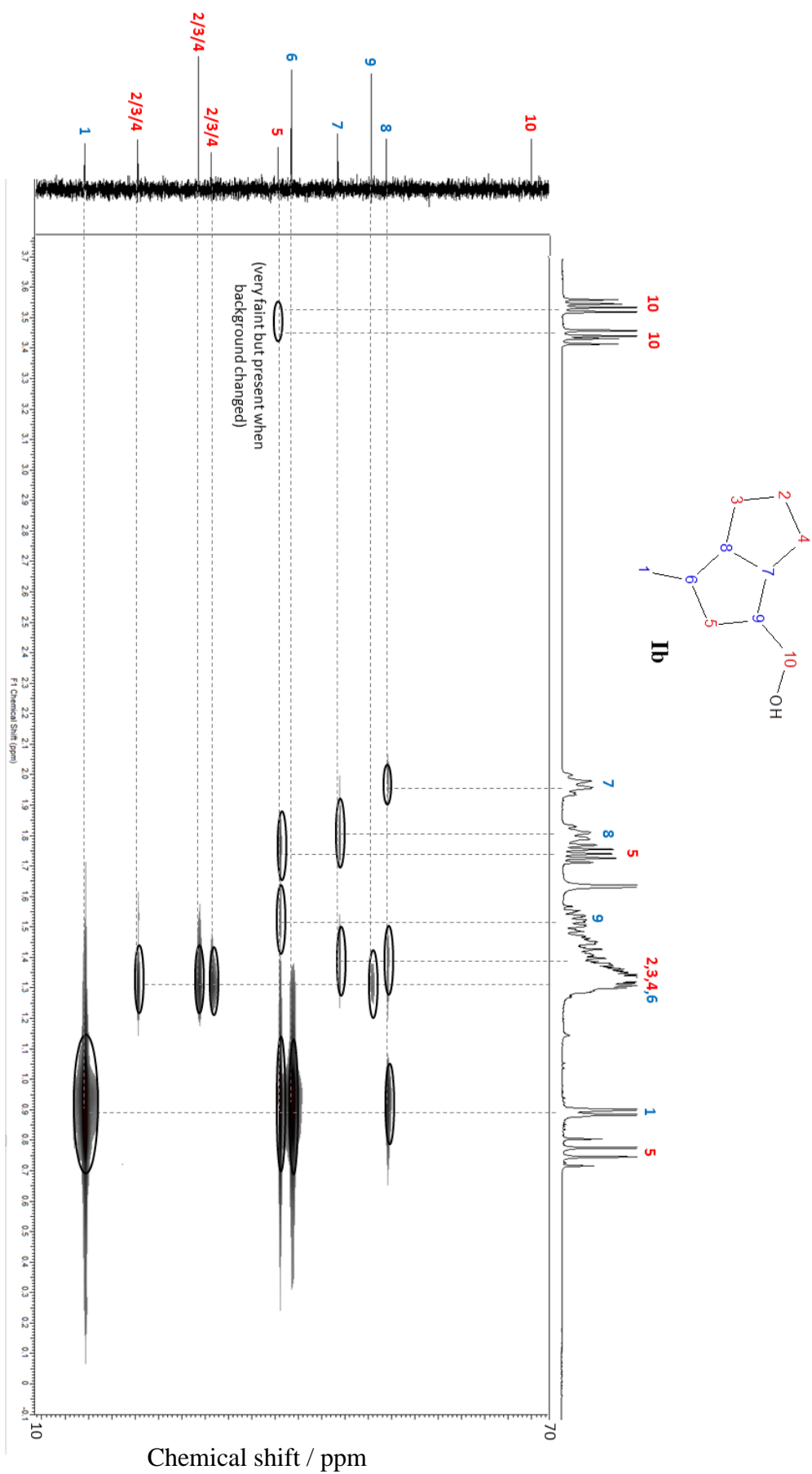
Appendix Figure 14: Correlation through long-range coupling (COLOC) spectrum of **Ib**.
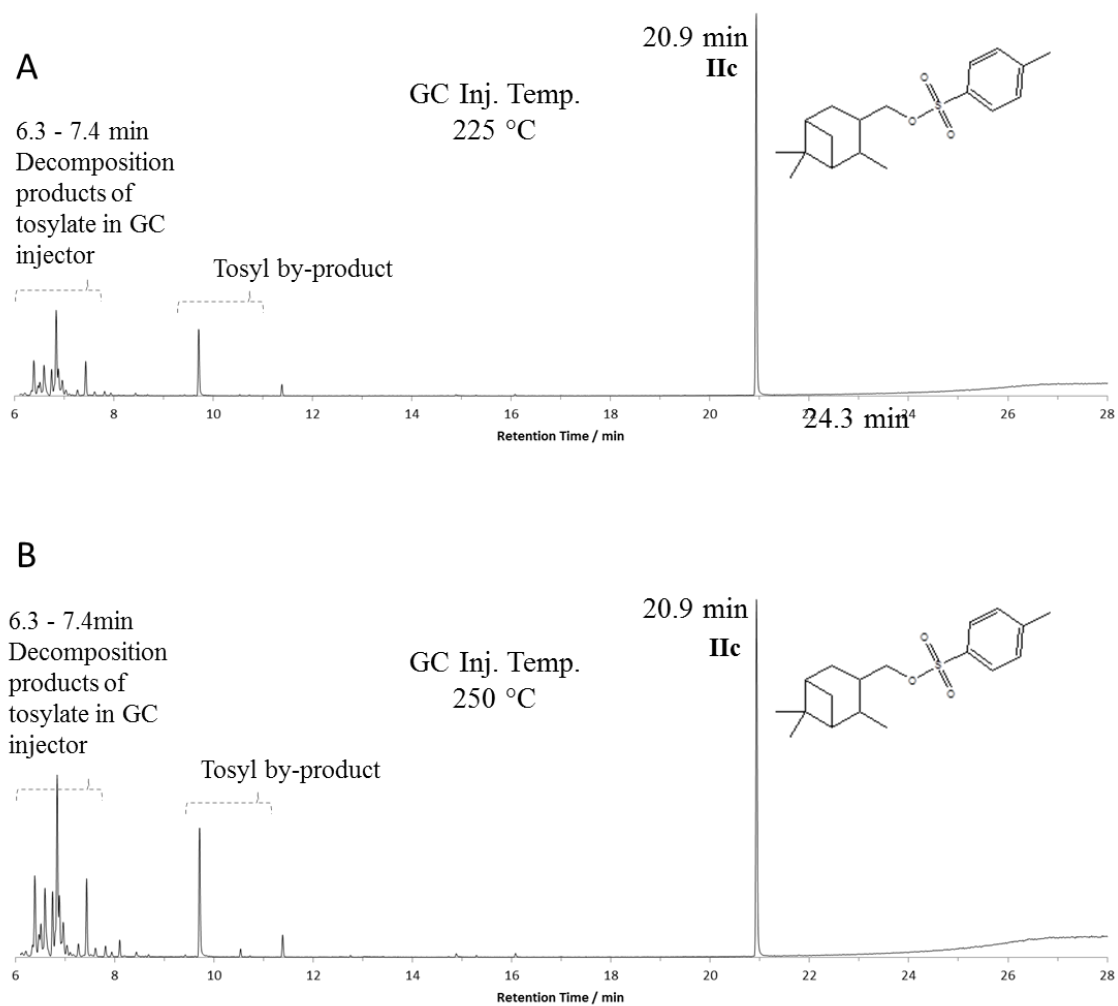
Appendix Figure 15: GC-MS chromatograms showing tosylation product **IIc** injected at

an inlet temperature of 225 and 250 °C.
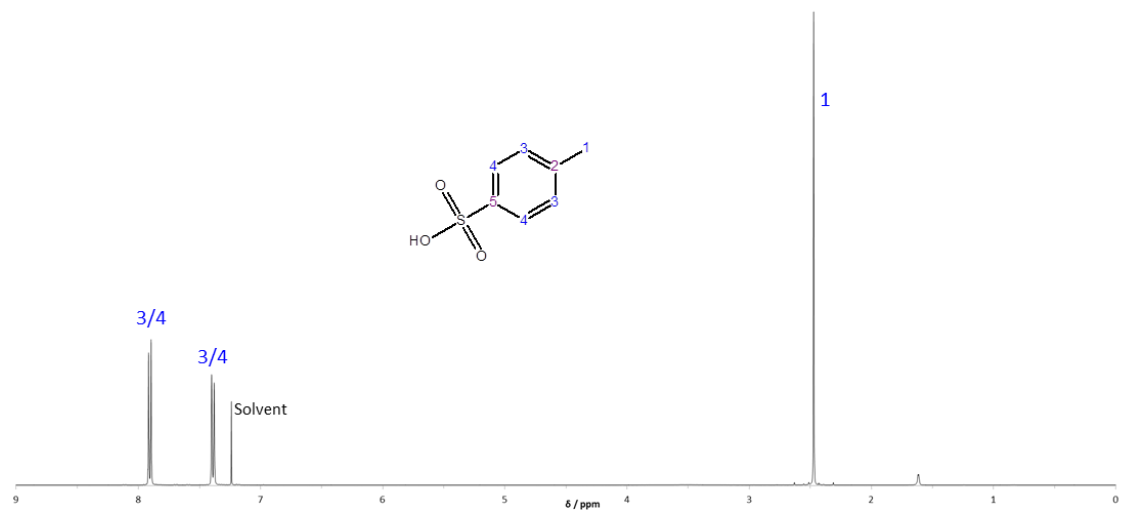
Appendix Figure 16: ^{1}H-NMR spectrum of tosyl chloride (TsCl).
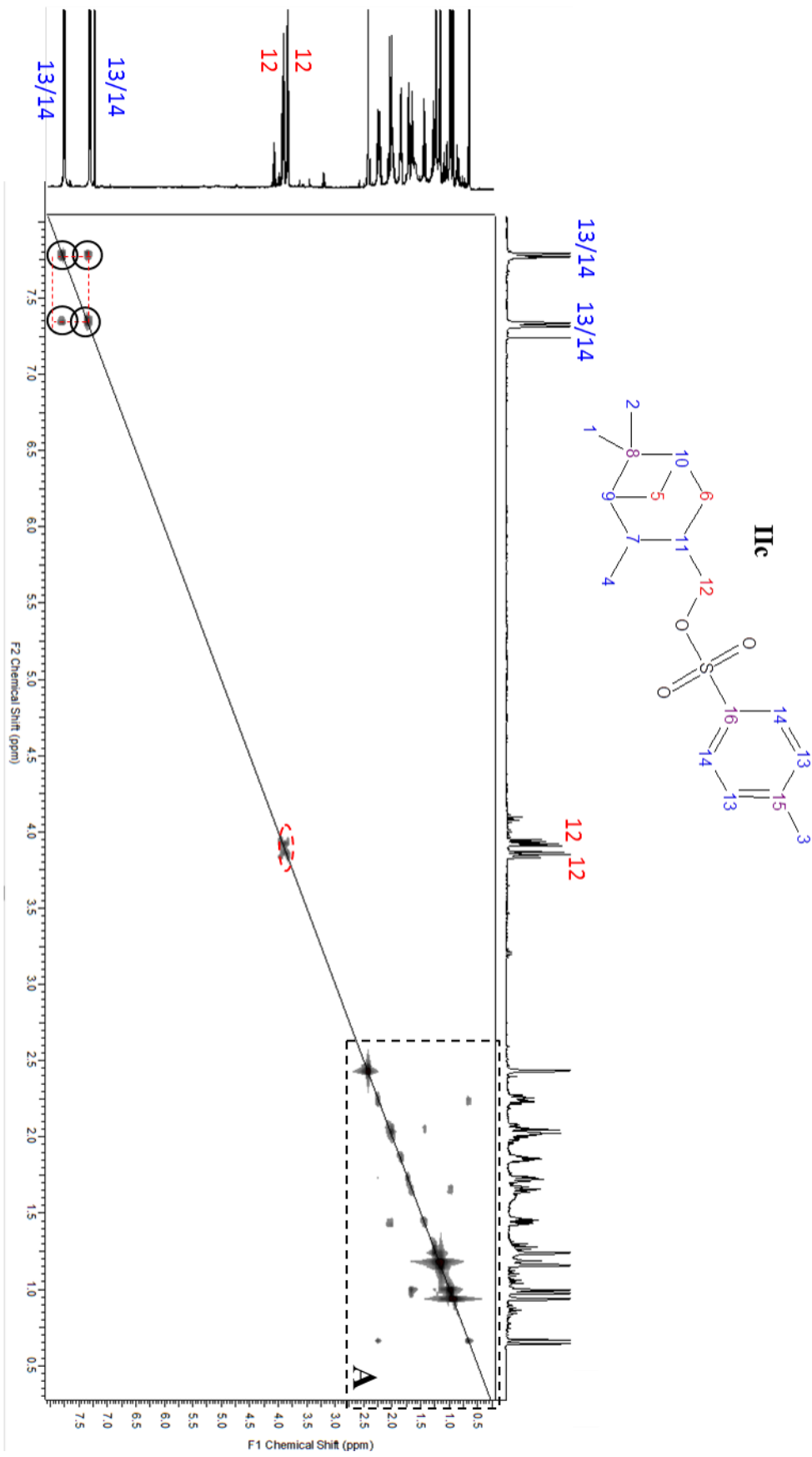
Appendix Figure 17: COSY spectrum of **IIc**.

Appendix Figure 18: Zoomed COSY spectrum of **IIc**.
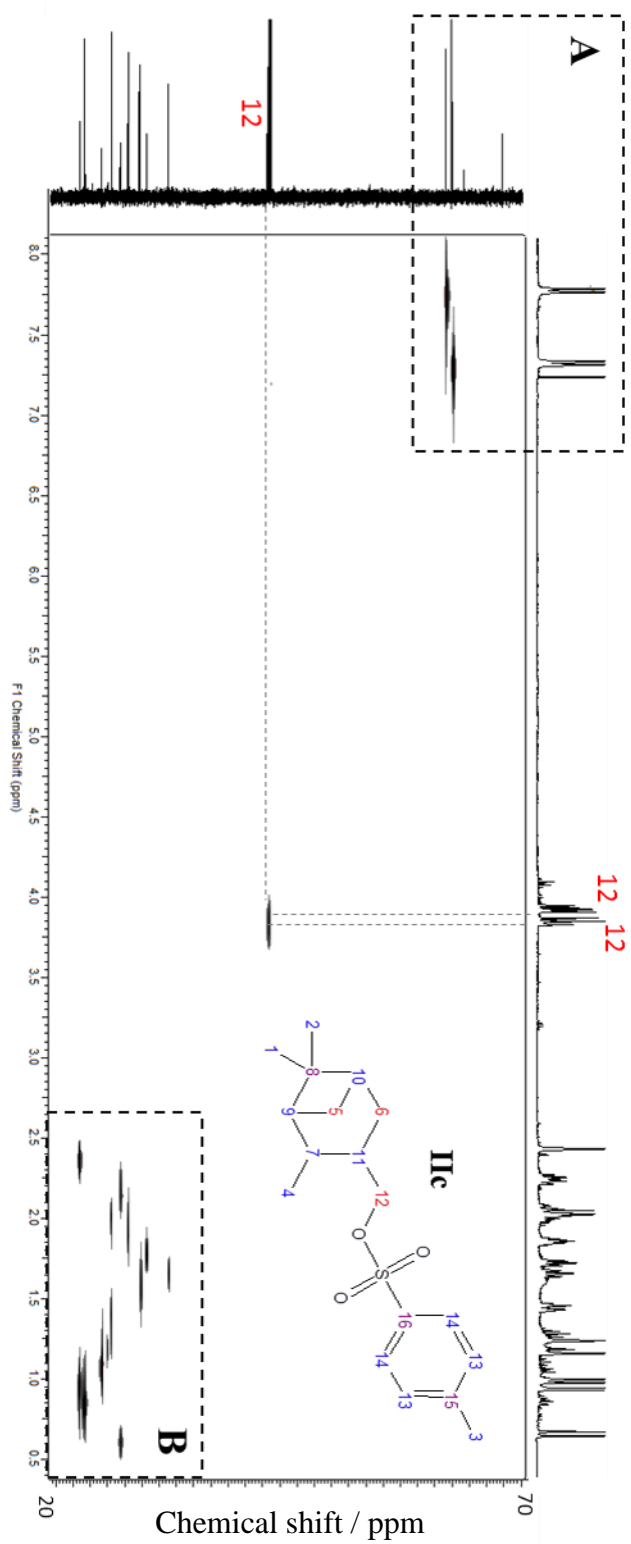
Appendix Figure 19: CHSHF (HETCOR) spectrum of **IIc**.
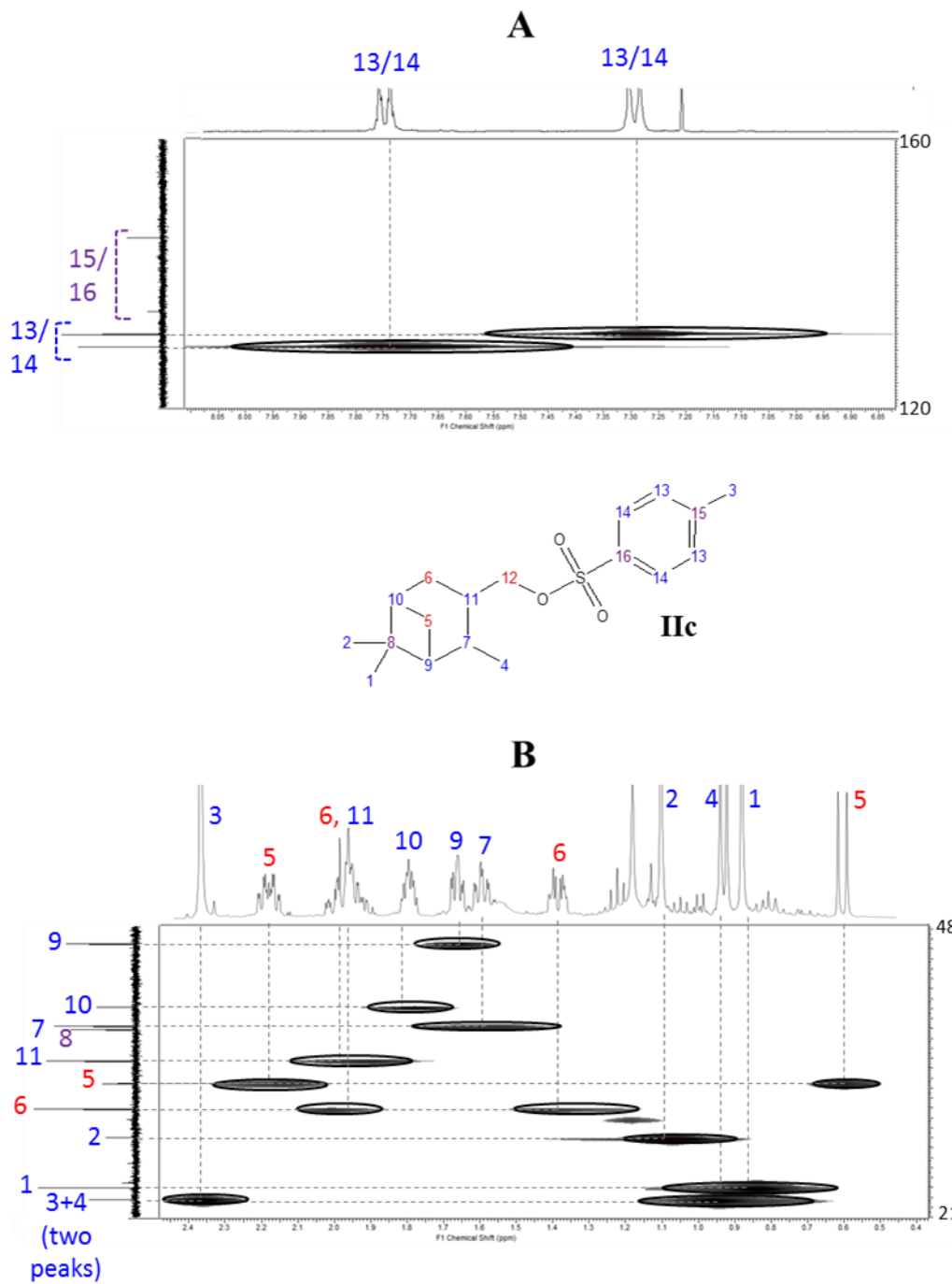
Appendix Figure 20: (A and B) Zoomed in CHSHF (HETCOR) spectra of **IIc**.
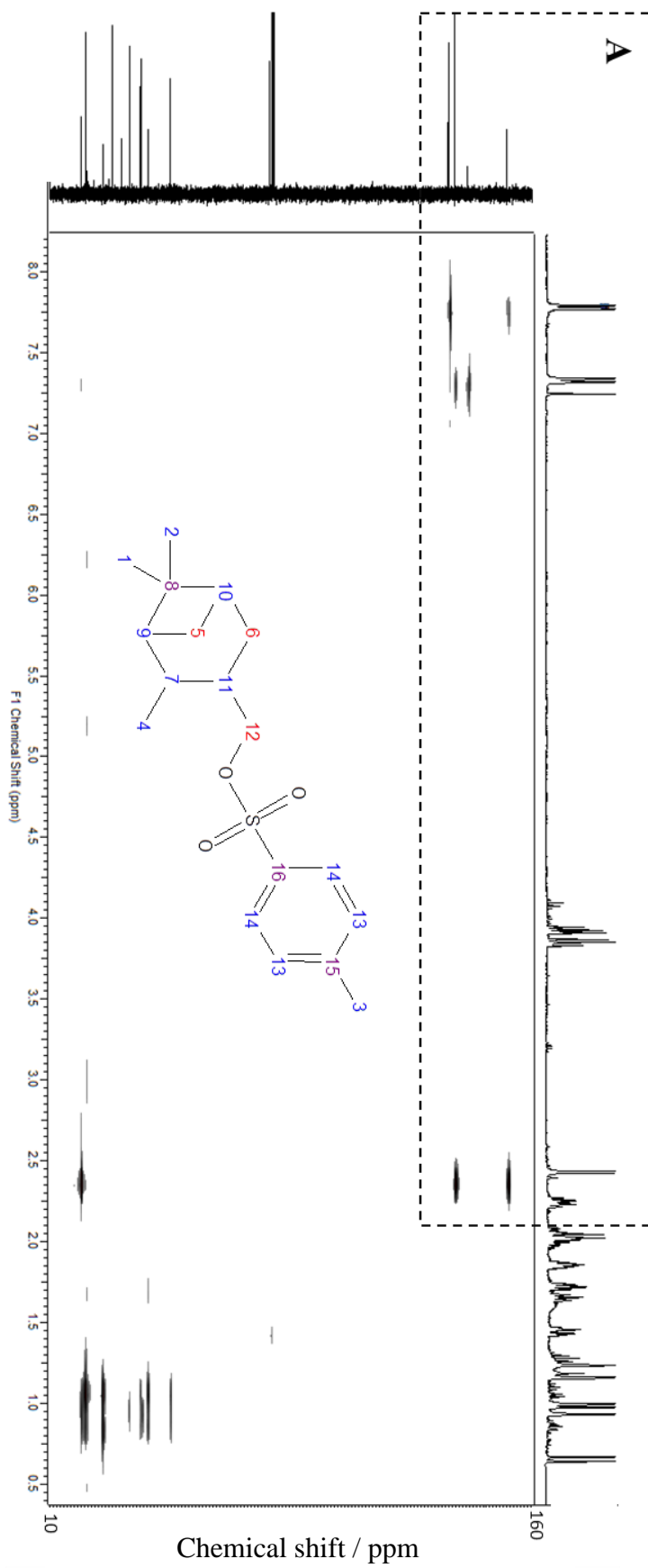
Appendix Figure 21: COLOC spectrum of **IIc**.
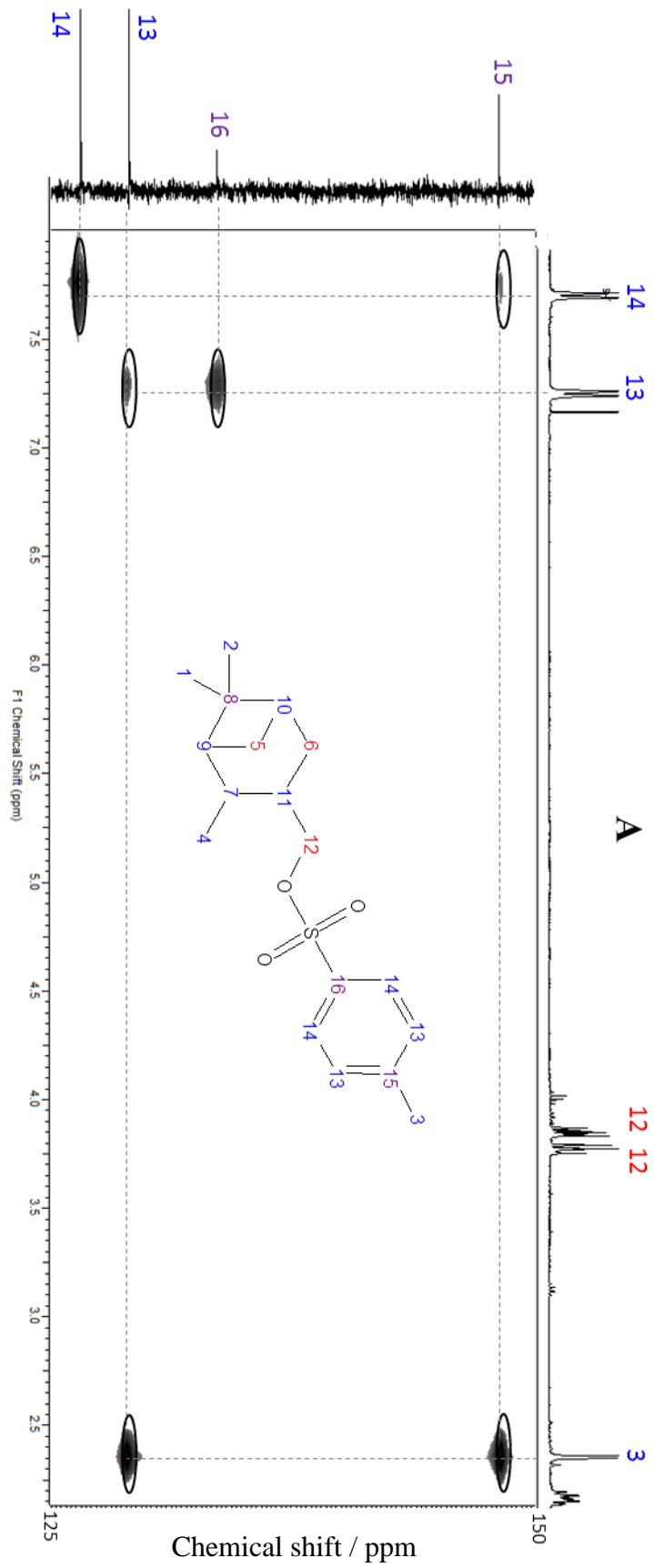
Appendix Figure 22: Zoomed COLOC spectrum of **IIc**.

A

11.4 – 11.8 min
Decomposition
products of tosylate in
GC injector

Chloride by-products

GC Inj. Temp.
225 °C

24.3 min
IIIc

23.7 min

B

11.4 – 11.8 min
Decomposition
products of tosylate in
GC injector

Chloride by-products

GC Inj. Temp.
250 °C

24.3 min
IIIc

23.7 min
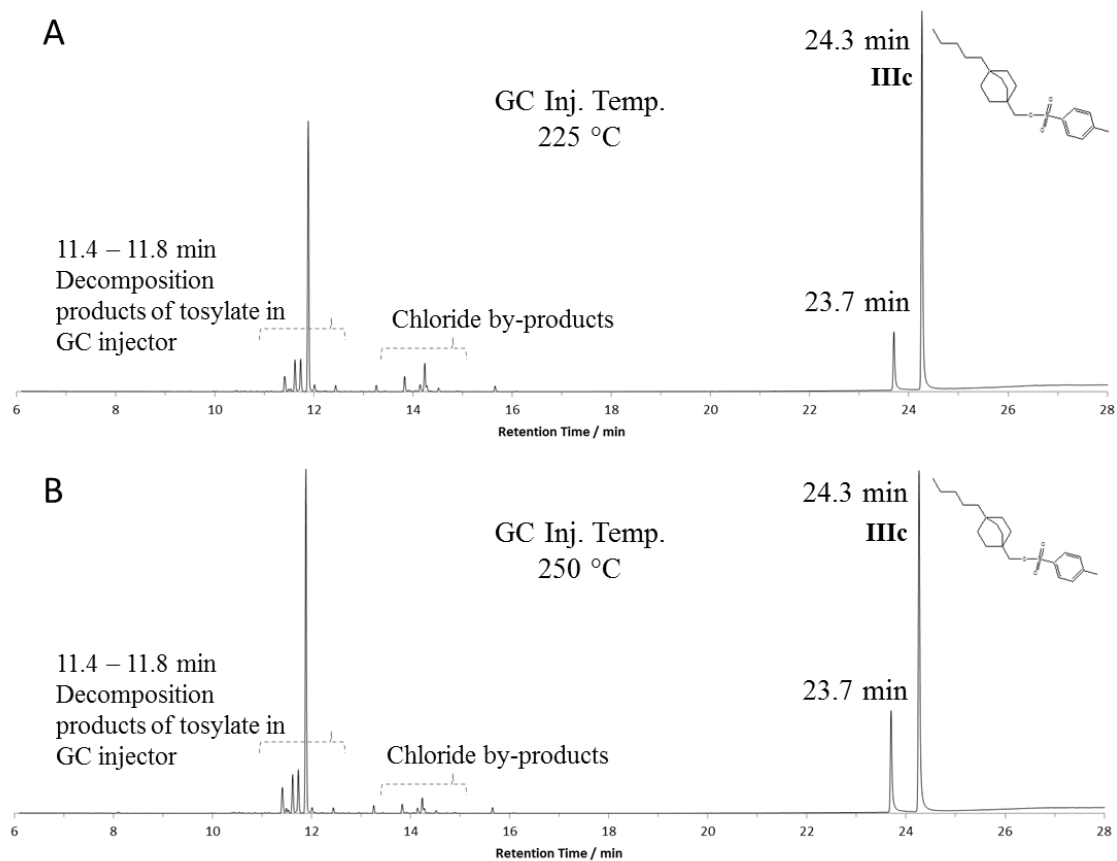
Appendix Figure 23: GC-MS chromatograms showing tosylation product **IIIc** injected

at an inlet temperature of 225 and 250 °C.
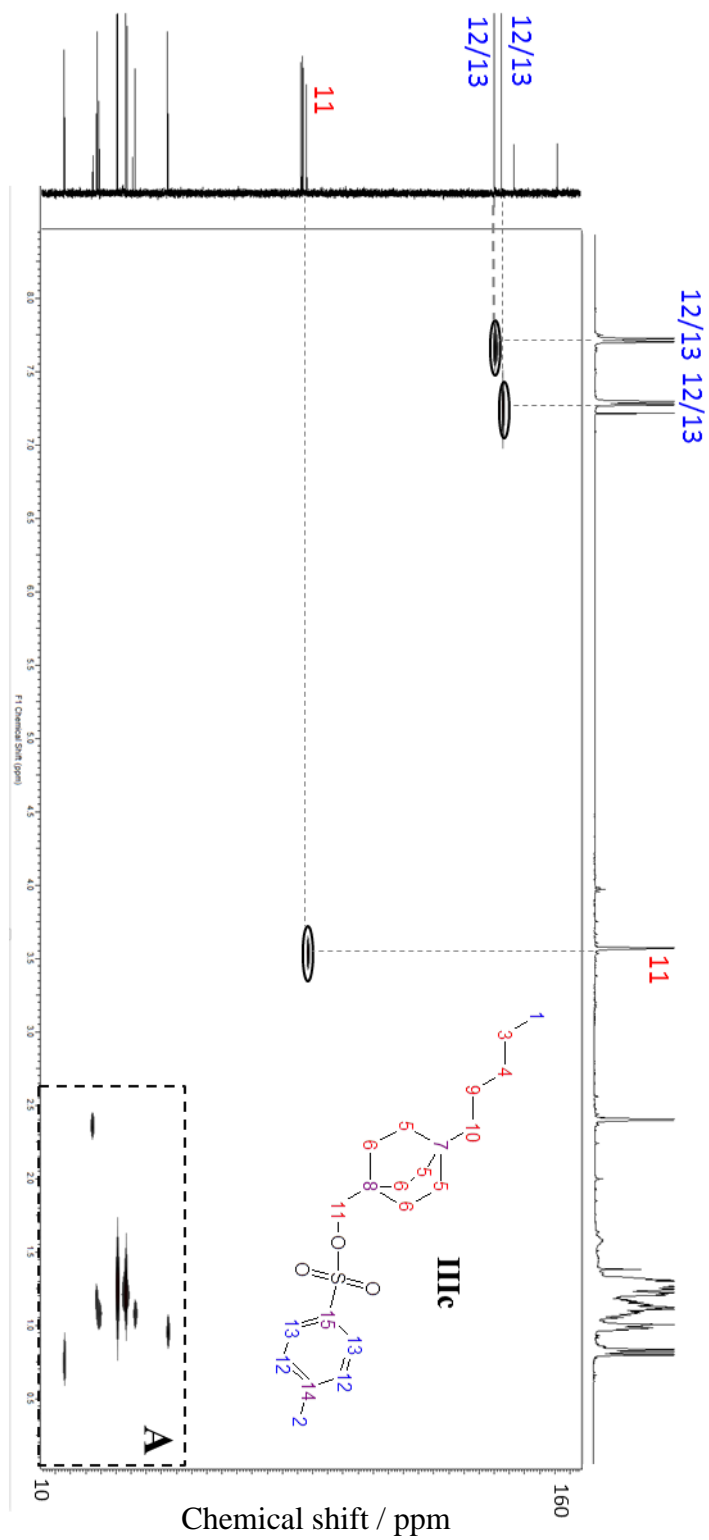
Appendix Figure 24: CHSHF (HETCOR) spectrum of **IIIc**.
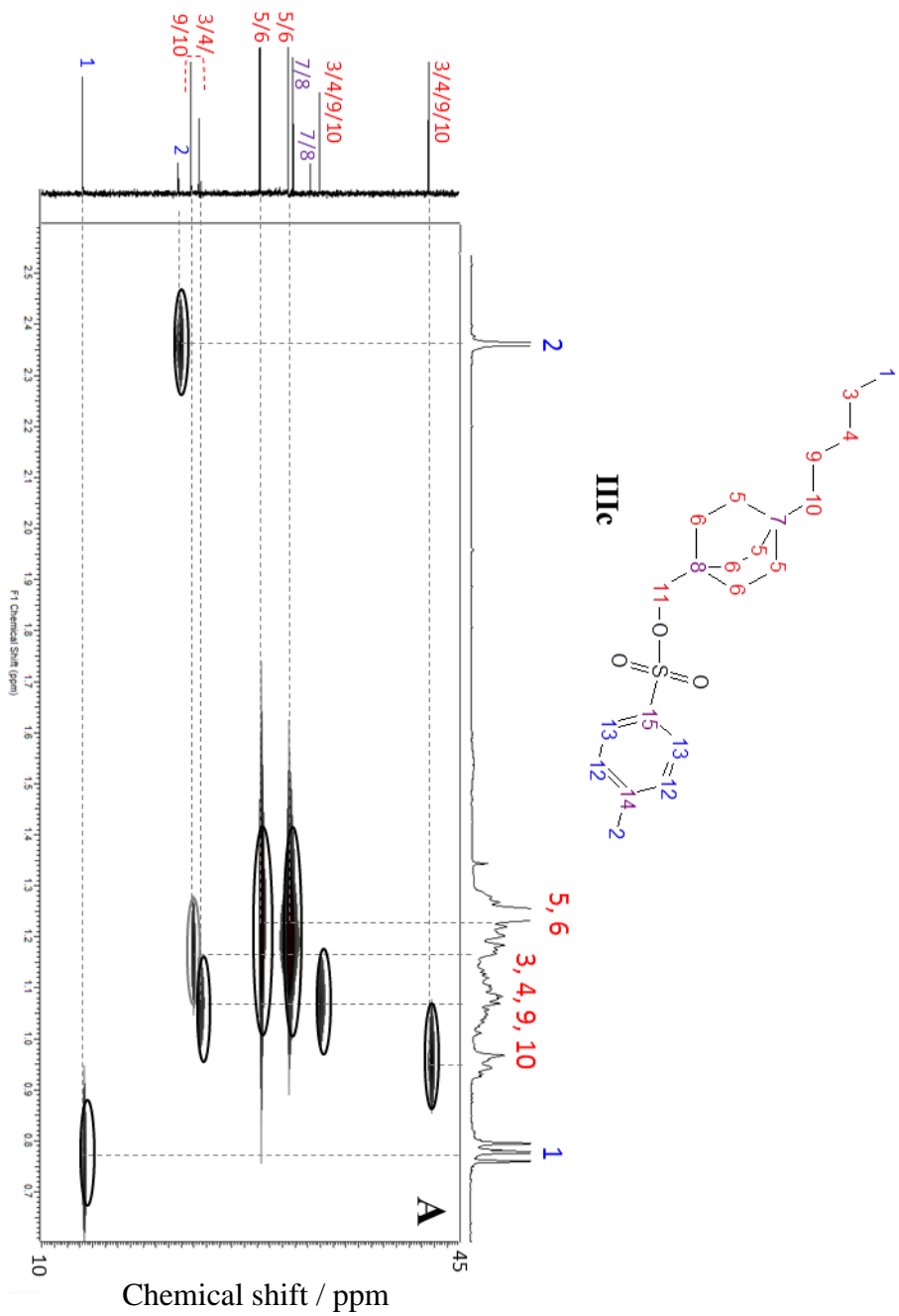
Appendix Figure 25: Zoomed CHSHF (HETCOR) spectrum of **IIIc**.
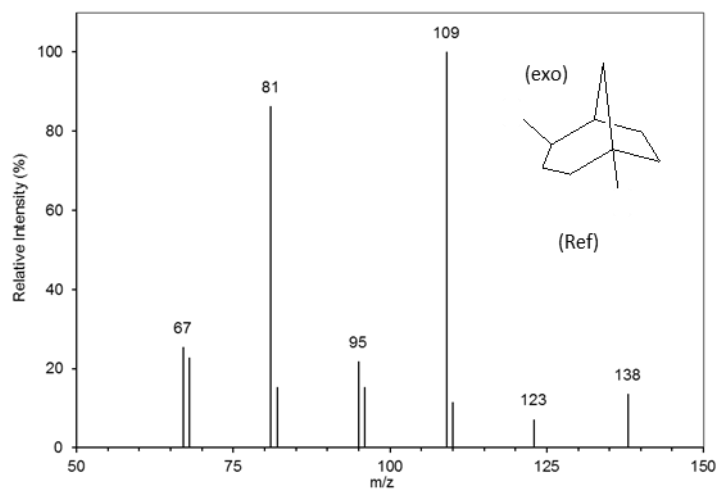
Appendix Figure 26: Electron ionisation mass spectrum of exo-1,4-

dimethylbicyclo[3.2.1]octane replotted from tabulated values reported by Denisov *et al.*

(1977a).
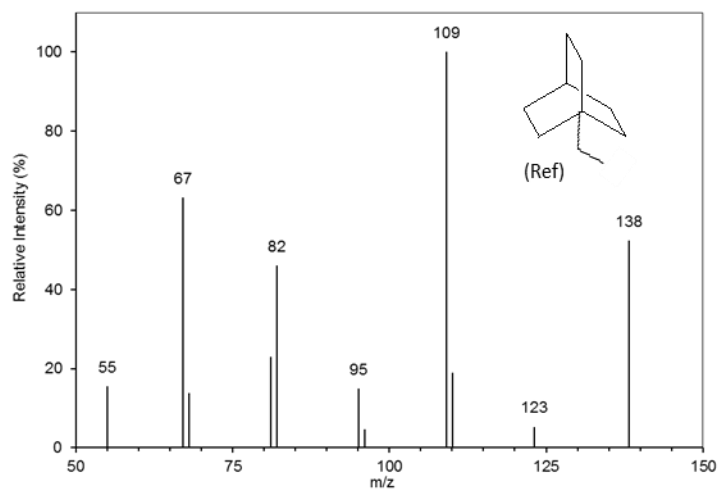
Appendix Figure 27: Electron ionisation mass spectrum of 1-ethylbicyclo[2.2.2]octane

replotted from tabulated values reported by Denisov *et al.* (1977d).
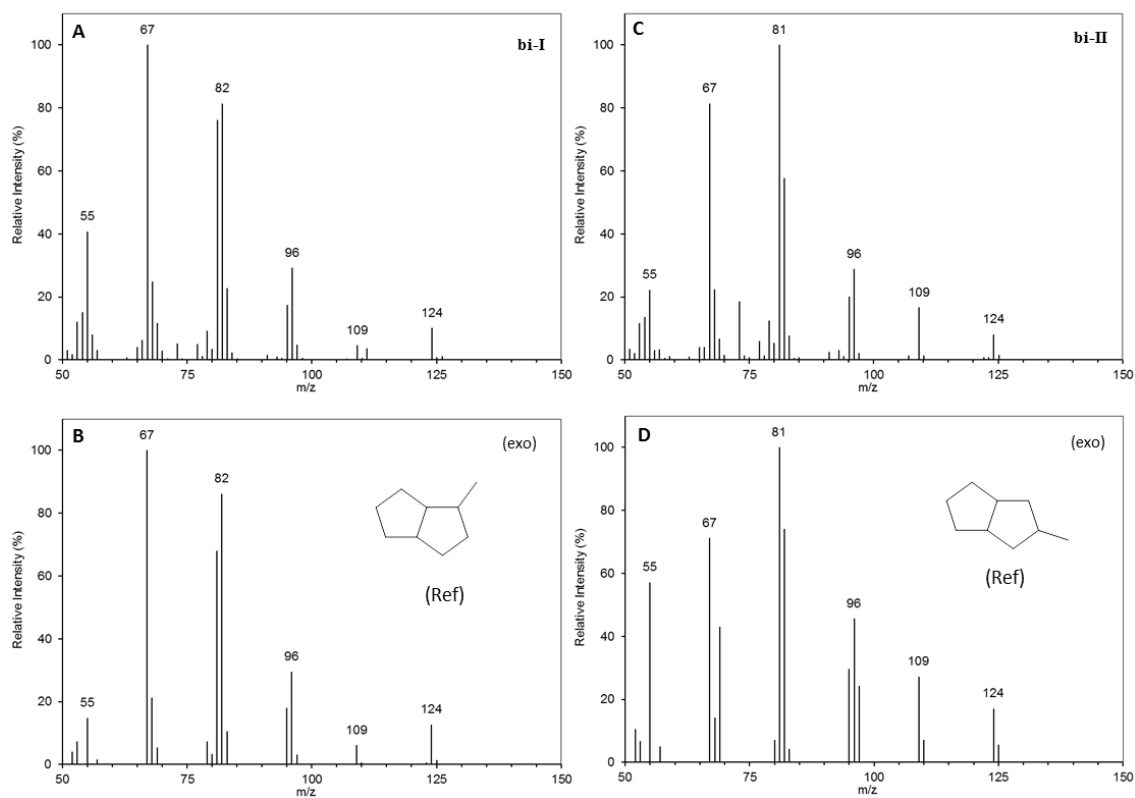
Appendix Figure 28: (A and C) Electron ionisation mass spectra of peaks **bi-I** and **bi-II** in reduced petroleum NA hydrocarbon product identified as 2- and 3-methylbicyclo[3.3.0]octane after comparison with (B and D) reference mass spectra replotted from tabulated values reported by Denisov *et al.* (1977d).
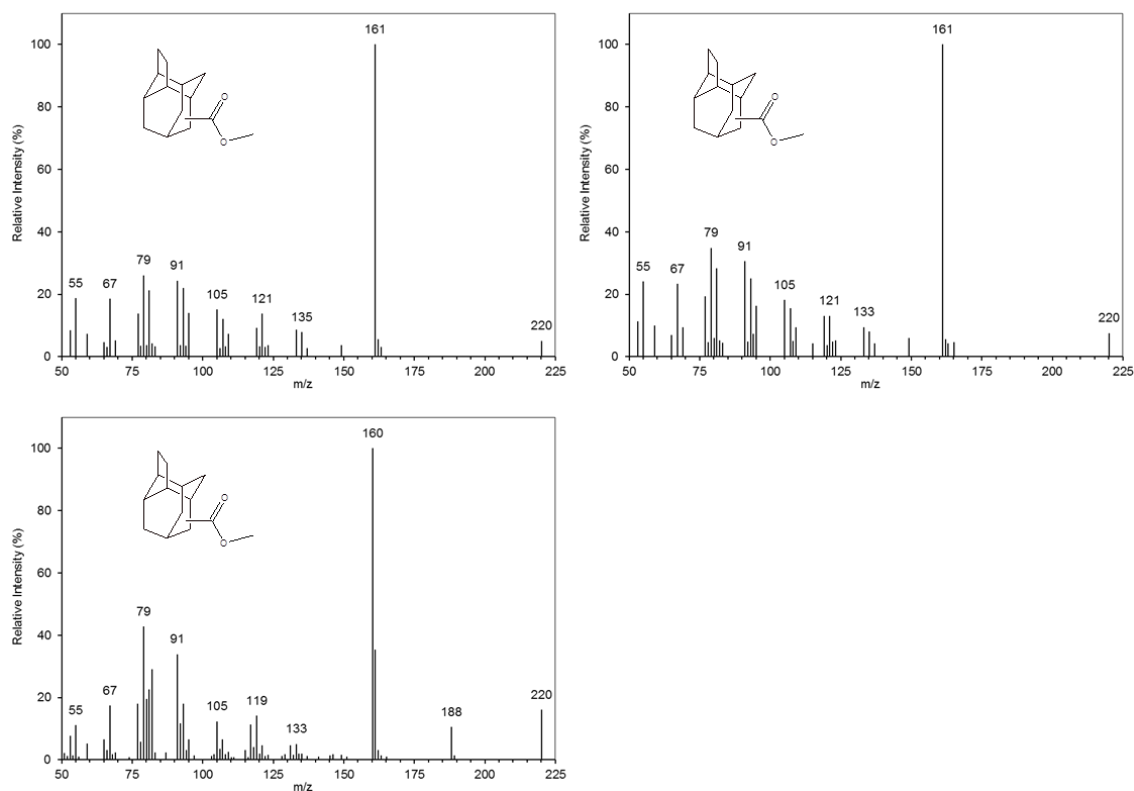
Appendix Figure 29: Electron ionisation mass spectra of components in sample #7 NA methyl esters tentatively assigned as cyclopentano-adamantane acids after examination of the mass spectra of the corresponding hydrocarbons.
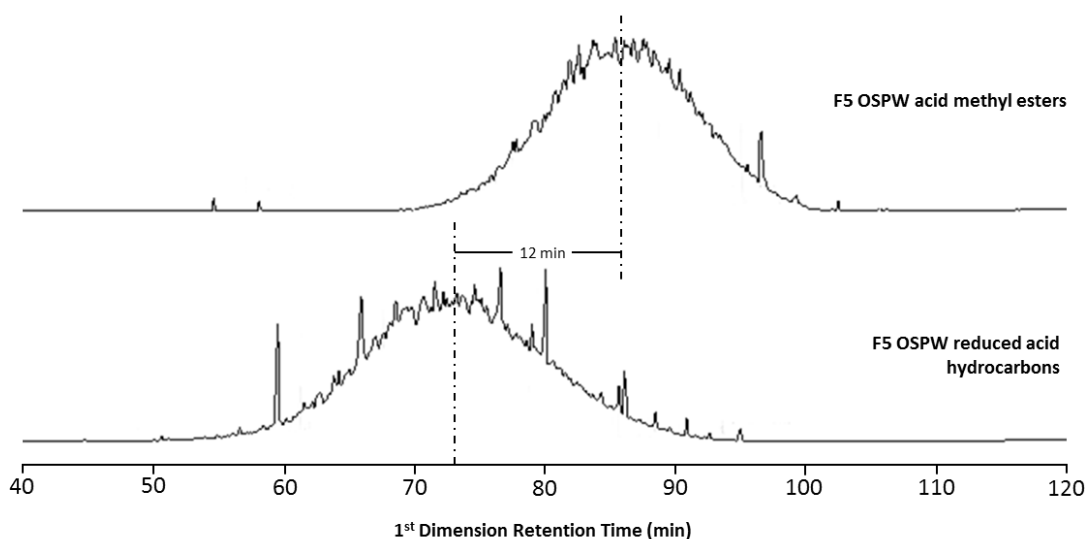
Appendix Figure 30: Comparison of the GC-MS TIC chromatograms before (top) and after (bottom) reduction of the 'aromatic' acid methyl ester Ag-Ion fraction (F5) of sample #2, to the corresponding hydrocarbons.

Appendix

References

Agrawal, A. & Gieg, L. M. 2013. In situ detection of anaerobic alkane metabolites in subsurface environments. *Frontiers in Microbiology,* 4**,** 140.

Ahad, J. M. E., Pakdel, H., Savard, M. M., Calderhead, A. I., Gammon, P. R., Rivera, A., Peru, K. M. & Headley, J. V. 2013. Characterization and Quantification of Mining-Related "Naphthenic Acids" in Groundwater near a Major Oil Sands Tailings Pond. *Environmental Science & Technology,* 47**,** 5023-5030.

Ahad, J. M. E., Pakdel, H., Savard, M. M., Simard, M.-C. & Smirnoff, A. 2012. Extraction, Separation, and Intramolecular Carbon Isotope Characterization of Athabasca Oil Sands Acids in Environmental Samples. *Analytical Chemistry,* 84**,** 10419-10425.

Aitken, C. M., Jones, D. M. & Larter, S. R. 2004. Anaerobic hydrocarbon biodegradation in deep subsurface oil reservoirs. *Nature,* 431**,** 291-294.

Alberta-Energy. 2013. *Facts and Statistics: Oil Sands* [Online]. Alberta Energy. Available: http://www.energy.alberta.ca/oilsands/791.asp [Accessed 07/03/2013].

Government of Alberta Alberta. Alberta's Oil Sands: The Facts. 2011. Available: www.oilsands.alberta.ca/FactSheets/fs_Tailings_online.pdf ['Accessed' 14/09/2015].

Alexander, R., Kagi, R. & Noble, R. 1983. Identification of the bicyclic sesquiterpenes drimane and eudesmane in petroleum. *Journal of the Chemical Society, Chemical Communications***,** 226-228.

Alexander, R., Kagi, R. I., Noble, R. & Volkman, J. K. 1984. Identification of some bicyclic alkanes in petroleum. *Organic Geochemistry,* 6**,** 63-72.

Alvisi, P. P. & Lins, V. F. C. 2011. An overview of naphthenic acid corrosion in a vacuum distillation plant. *Engineering Failure Analysis,* 18**,** 1403-1406.

Anbrokh, R. V., Bogatskii, A. V., Garbalinskii, V. A., Petrov, A. A. & Krasavchenko, M. I. 1972. Aliphatic hydrocarbons prepared from petroleum acids in diesei fuels from Romashkino and Mukhanov petroleums. *Chemistry and Technology of Fuels and Oils,* 8**,** 573-577.

Anders, D. E. & Robinson, W. E. 1971. Cycloalkane constituents of the bitumen from Green River Shale. *Geochimica et Cosmochimica Acta,* 35**,** 661-678.

Andersson, J. T. & Schade, T. 2004. Higher alkylated dibenzothiophenes in some crude oils and hydrodesulfurized fuels. *Prepr. Pap.-Am. Chem. Soc., Div. Fuel Chem,* 49**,** 338-340.

Andersson, J. T., Schräder, W., Traulsen, F. & Werlich, S. 2001. Synthesis of Seven Trimethyldibenzothiophenes. *Polycyclic Aromatic Compounds,* 18**,** 351-360.

Asaoka, M., Ishibashi, K., Yanagida, N. & Takei, H. 1983. Total synthesis of (±)-eremolactone. *Tetrahedron Letters,* 24**,** 5127-5130.

Ashumov, G. 1961. Nature of Naphthenic Acids Baku Crude Oils as a Function of the Depth of Occurrence. *International Geology Review,* 3**,** 42-48.

Atlas, R. M. 1984. *Petroleum microbiology,* New York, Macmillan.

Ávila, B. M. F., Aguiar, A., Gomes, A. O. & Azevedo, D. A. 2010. Characterization of extra heavy gas oil biomarkers using comprehensive two-dimensional gas chromatography coupled to time-of-flight mass spectrometry. *Organic Geochemistry,* 41**,** 863-866.

Azevedo, D. A., Aquino Neto, F. R., Simoneit, B. R. T. & Pinto, A. C. 1992. Novel series of tricyclic aromatic terpanes characterized in Tasmanian tasmanite. *Organic Geochemistry,* 18**,** 9-16.

Azevedo, D. A., de Aquino Neto, F. R. & Simoneit, B. R. T. 1990. Mass spectrometric characteristics of a novel series of ring-c monoaromatic tricyclic terpanes found in Tasmanian tasmanite. *Organic Mass Spectrometry,* 25**,** 475-480.

Azevedo, D. A., Neto, F. R. A. & Simoneit, B. R. T. 1994. Extended saturated and monoaromatic tricyclic terpenoid carboxylic acids found in Tasmanian tasmanite. *Organic Geochemistry,* 22**,** 991-1004.

Bagrii, E. I. & Maravin, G. B. 2013. Adamantane-containing esters as potential components of thermostable lubricating oils. *Petroleum Chemistry,* 53**,** 418-422.

Bagrii, Y. I., Dolgopolova, T. N. & Sanin, P. I. 1970. Catalytic conversions of bicyclo[4.3.0]nonane with activated alumina. *Petroleum Chemistry U.S.S.R.,* 10**,** 147-152.

Bagrii, Y. I., Sanin, P., Vorob'eva, N. & Petrov, A. A. 1967. Hydrocarbon composition of extracts obtained from petroleum fractions by extractive crystallization with thiourea. *Petroleum Chemistry USSR,* 7**,** 159-163.

Barrow, M. P., Headley, J. V., Peru, K. M. & Derrick, P. J. 2004. Fourier transform ion cyclotron resonance mass spectrometry of principal components in oilsands naphthenic acids. *Journal of Chromatography A,* 1058**,** 51-59.

Barrow, M. P., Headley, J. V., Peru, K. M. & Derrick, P. J. 2009. Data Visualization for the Characterization of Naphthenic Acids within Petroleum Samples. *Energy & Fuels,* 23**,** 2592-2599.

Barrow, M. P., McDonnell, L. A., Feng, X., Walker, J. & Derrick, P. J. 2003. Determination of the Nature of Naphthenic Acids Present in Crude Oils Using Nanospray Fourier Transform Ion Cyclotron Resonance Mass Spectrometry: The Continued Battle Against Corrosion. *Analytical Chemistry,* 75**,** 860-866.

Barrow, M. P., Peru, K. M., Fahlman, B., Hewitt, L. M., Frank, R. A. & Headley, J. V. 2015a. Beyond Naphthenic Acids: Environmental Screening of Water from Natural Sources and the Athabasca Oil Sands Industry Using Atmospheric Pressure Photoionization Fourier Transform Ion Cyclotron Resonance Mass Spectrometry. *Journal of the American Society for Mass Spectrometry,* 26**,** 1508-1521.

Barrow, M. P., Peru, K. M. & Headley, J. V. 2014. An Added Dimension: GC Atmospheric Pressure Chemical Ionization FTICR MS and the Athabasca Oil Sands. *Analytical Chemistry,* 86**,** 8281-8288.

Barrow, M. P., Peru, K. M., McMartin, D. W. & Headley, J. V. 2015b. Effects of Extraction pH on the FTICR MS Profiles of Athabasca Oil Sands Process Water. *Energy & Fuels*.

Barrow, M. P., Witt, M., Headley, J. V. & Peru, K. M. 2010. Athabasca Oil Sands Process Water: Characterization by Atmospheric Pressure Photoionization and Electrospray Ionization Fourier Transform Ion Cyclotron Resonance Mass Spectrometry. *Analytical Chemistry,* 82**,** 3727-3735.

Bataineh, M., Scott, A. C., Fedorak, P. M. & Martin, J. W. 2006. Capillary HPLC/QTOF-MS for Characterizing Complex Naphthenic Acid Mixtures and Their Microbial Transformation. *Analytical Chemistry,* 78**,** 8354-8361.

Bauer, A. E., Frank, R. A., Headley, J. V., Peru, K. M., Hewitt, L. M. & Dixon, D. G. 2015. Enhanced characterization of oil sands acid-extractable organics fractions using electrospray ionization–high-resolution mass spectrometry and synchronous fluorescence spectroscopy. *Environmental Toxicology and Chemistry,* 34**,** 1001-1008.

Baumgarten, H. E. & Gleason, D. C. 1951. Synthesis of dl-3,3,4-Trimethylcyclopentanone. *The Journal of Organic Chemistry,* 16**,** 1658-1668.

Bickel, A. F., Knotnerus, J., Kooyman, E. C. & Vegter, G. C. 1960. Bicyclanes—II : On the preparation and halogenation of bicyclo[2,2,2]octane. *Tetrahedron,* 9**,** 230-236.

Blakley, E. R. 1974. The microbial degradation of cyclohexanecarboxylic acid: a pathway involving aromatization to form p-hydroxybenzoic acid. *Canadian Journal of Microbiology,* 20**,** 1297-1306.

Blaney, F., Faulkner, D., McKervey, M. A. & Step, G. 1972. The [small pi]-route to substituted adamantanes. Part II. *Journal of the Chemical Society, Perkin Transactions 1,* 0**,** 2697-2701.

Booth, A. M. 2004. *Biodegradation, water solubility and characterisation studies of unresolved complex mixtures (UCMs) of aromatic hydrocarbons.* PhD, University of Plymouth.

Booth, A. M., Sutton, P. A., Lewis, C. A., Lewis, A. C., Scarlett, A., Chau, W., Widdows, J. & Rowland, S. J. 2006. Unresolved Complex Mixtures of Aromatic Hydrocarbons: Thousands of Overlooked Persistent, Bioaccumulative, and Toxic Contaminants in Mussels. *Environmental Science & Technology,* 41**,** 457-464.

Bowman, D. T., Slater, G. F., Warren, L. A. & McCarry, B. E. 2014. Identification of individual thiophene-, indane-, tetralin-, cyclohexane-, and adamantane-type carboxylic acids in composite tailings pore water from Alberta oil sands. *Rapid Communications in Mass Spectrometry,* 28**,** 2075-2083.

Braun, J. V. 1938. Naphthenic Acids, Oxy-Compounds, Etc: The Science of Petroleum; eds Dunstan, A.E., Nash, A.W., Brooks, B.T., Tizard, H. *vol. II***,** 1007.

Braun, J. V., Mannes, L. & Reuter, M. 1933. Untersuchungen über die Bestandteile des Erdöls, II. Mitteil.: Darstellung der ersten einheitlichen Naphthensäure. *Berichte der deutschen chemischen Gesellschaft (A and B Series),* 66**,** 1499-1505.

Brient, J. A., Wessner, P. J. & Doyle, M. N. 2000. Naphthenic Acids. *Kirk-Othmer Encyclopedia of Chemical Technology.* John Wiley & Sons, Inc.

Brodskii, Y. S., Lukashenko, I. M., Musayev, I. A., Kurashova, E. K. & Sanin, P. I. 1977. Mass-spectra of dimethylbicyclo[4.4.0]decane stereoisomers (2,3-; 2,4-; 2,8- and 2,9-dimethylbicyclo[4.4.0]decanes). *Petroleum Chemistry U.S.S.R.,* 17**,** 77-84.

Brown, H. C., Kim, S. C. & Krishnamurthy, S. 1980. Selective reductions. 26. Lithium triethylborohydride as an exceptionally powerful and selective reducing agent in organic synthesis. Exploration of the reactions with selected organic compounds containing representative functional groups. *The Journal of Organic Chemistry,* 45**,** 1-12.

Brown, L. D. & Ulrich, A. C. 2015. Oil sands naphthenic acids: A review of properties, measurement, and treatment. *Chemosphere,* 127**,** 276-290.

Brunswick, P., Shang, D., van Aggelen, G., Hindle, R., Hewitt, L. M., Frank, R. A., Haberl, M. & Kim, M. 2015. Trace analysis of total naphthenic acids in aqueous environmental matrices by liquid chromatography/mass spectrometry-quadrupole time of flight mass spectrometry direct injection. *Journal of Chromatography A,* 1405**,** 49-71.

Buchman, E. R. & Sargent, H. 1942. Naphthenic Acid Studies. I. The Synthesis of 3,3,4-trimethylcyclopentanone. *The Journal of Organic Chemistry,* 07**,** 148-153.

Cason, J. & Khodair, A. I. A. 1967a. Isolation of the eleven-carbon acyclic isoprenoid acid from petroleum. Mass spectroscopy of its p-phthalimidophenacyl ester. *The Journal of Organic Chemistry,* 32**,** 3430-3433.

Cason, J. & Khodair, A. I. A. 1967b. Mass spectra of certain cycloalkylacetates and of related unsaturated esters. *The Journal of Organic Chemistry,* 32**,** 575-581.

Canadian Energy Research Institute CERI. Canadian economic impacts of new and existing oil sands development in Alberta (2014-2038). November, 2014. ['Accessed'.

Chernyavskaya, S. V., Filimonova, T. A. & Kam'yanov, V. F. 1983. Lower carboxylic acids of West Siberian crude oil. *Petroleum Chemistry U.S.S.R.,* 23**,** 40-47.

Chicarelli, M. I., Neto, F. R. A. & Albrecht, P. 1988. Occurrence of four stereoisomeric tricyclic terpane series in immature Brazilian shales. *Geochimica et Cosmochimica Acta,* 52**,** 1955-1959.

Chow, A. W., Jakas, D. R. & Hoover, J. R. E. 1966. Preparation of 1-substituted bicyclo[3.2.1]octanes by a rearrangement reaction. *Tetrahedron Letters,* 7**,** 5427-5431.

Clemente, J. S. & Fedorak, P. M. 2005. A review of the occurrence, analyses, toxicity, and biodegradation of naphthenic acids. *Chemosphere,* 60**,** 585-600.

Clemente, J. S., MacKinnon, M. D. & Fedorak, P. M. 2004. Aerobic Biodegradation of Two Commercial Naphthenic Acids Preparations. *Environmental Science & Technology,* 38**,** 1009-1016.

Clemente, J. S., Prasad, N. G. N., MacKinnon, M. D. & Fedorak, P. M. 2003. A statistical comparison of naphthenic acids characterized by gas chromatography–mass spectrometry. *Chemosphere,* 50**,** 1265-1274.

Cochran, J. & Pijpelink, J. 2011. GCxGC Analysis of Complex Petroleum Hydrocarbons: Sulfur Speciation in Diesel. Available: http://www.restek.com/Technical-Resources/Technical-Library/Petroleum-Petrochemical/petro_pin072011.

Cocker, W., Hanna, D. P. & Shannon, P. V. R. 1968. The chemistry of terpenes. Part VI. Pyrolysis and acid-catalysed rearrangements of (+)-car-3-ene and some derivatives. *Journal of the Chemical Society C: Organic,* 0**,** 489-495.

COSIA. 2015. *Focus Areas: Tailings* [Online]. Available: http://www.cosia.ca/initiatives/tailings [Accessed 21/09/2015].

Curcuruto, O., Favrctto, D., Traldi, P., Ajo, D., Cativiela, C., Mayoral, J. A., Lorez, M. P., Fraile, J. M. & Garcia, J. I. 1991. Mass spectrometry in stereochemical problems. 6 — The case of mono and di-substituted norbornanes. *Organic Mass Spectrometry,* 26**,** 977-984.

Cyr, T. D. & Strausz, O. P. 1983. The structures of tricyclic terpenoid carboxylic acids and their parent alkanes in the Alberta oil sands. *Journal of the Chemical Society, Chemical Communications,* 0**,** 1028-1030.

Cyr, T. D. & Strausz, O. P. 1984. Bound carboxylic acids in the Alberta oil sands. *Organic Geochemistry,* 7**,** 127-140.

Damasceno, F. C., Gruber, L. D., Geller, A. M., de Campos, M. C. V., Gomes, A. O., Guimarães, R. C., Péres, V. F., Jacques, R. A. & Caramão, E. B. 2014. Characterization of naphthenic acids using mass spectroscopy and chromatographic techniques: study of technical mixtures. *Analytical Methods,* 6**,** 807-816.

Dass, C. 2007. *Fundamentals of Contemporary Mass Spectrometry*, Wiley.

Denisov, Y. V., Matveyeva, I. A., Sokolova, I. M. & Petrov, A. A. 1977a. Mass-spectrometric study of hydrocarbons of bicyclo[3.2.1]octane series. *Petroleum Chemistry U.S.S.R.,* 17**,** 85-93.

Denisov, Y. V., Sokolova, I. M. & Petrov, A. A. 1977b. Mass Spectrometric study of hydrocarbons of the bicyclo[4.3.0]octane series (In Russian). *Neftekhimiya,* 17**,** 491-497.

Denisov, Y. V., Vorob'eva, N. S. & Petrov, A. A. 1977c. Mass Spectrometric study of hydrocarbons of the bicyclo[3.3.0]octane series (In Russian). *Neftekhimiya,* 17**,** 656-662.

Denisov, Y. V., Vorobeva, N. S., Sokolova, I. M. & Petrov, A. A. 1977d. Mass Spectrometric study of hydrocarbons of the bicyclo[2.2.2]octane series (In Russian). *Neftekhimiya,* 17**,** 186-191.

Derungs, W. A. 1956. Naphthenic Acid Corrosion —An Old Enemy Of the Petroleum Industry. *Corrosion,* 12**,** 41-46.

Dimmler, A., Cyr, T. D. & Strausz, O. P. 1984. Identification of bicyclic terpenoid hydrocarbons in the saturate fraction of Athabasca oil sand bitumen. *Organic Geochemistry,* 7**,** 231-238.

Ding, R., He, Y., Wang, X., Xu, J., Chen, Y., Feng, M. & Qi, C. 2011. Treatment of Alcohols with Tosyl Chloride Does Not always Lead to the Formation of Tosylates. *Molecules,* 16**,** 5665-5673.

Droitsch, D. 2015. *New Tar Sands Water Policy from Government of Alberta Favors Industry* [Online]. Available: http://switchboard.nrdc.org/blogs/ddroitsch/new_tar_sands_water_policy_fro.html [Accessed 21/09/2015].

Dyer, S. J., Graham, G. M. & Arnott, C. 2003. Naphthenate Scale Formation - Examination of Molecular Controls in Idealised Systems. Society of Petroleum Engineers.

Dzidic, I., Somerville, A. C., Raia, J. C. & Hart, H. V. 1988. Determination of naphthenic acids in California crudes and refinery wastewaters by fluoride ion chemical ionization mass spectrometry. *Analytical Chemistry,* 60**,** 1318-1323.

Edam, R., Blomberg, J., Janssen, H. G. & Schoenmakers, P. J. 2005. Comprehensive multi-dimensional chromatographic studies on the separation of saturated hydrocarbon ring structures in petrochemical samples. *Journal of Chromatography A,* 1086**,** 12-20.

Edwards, M., Boswell, H. & Górecki, T. 2015. Comprehensive Multidimensional Chromatography. *Current Chromatography,* 2**,** 80-109.

Edwards, M., Mostafa, A. & Górecki, T. 2011. Modulation in comprehensive two-dimensional gas chromatography: 20 years of innovation. *Analytical and Bioanalytical Chemistry,* 401**,** 2335-2349.

Eglinton, G., Hunneman, D. H. & McCormick, A. 1968. Gas chromatographic—mass spectrometric studies of long chain hydroxy acids.—III.1 The mass spectra of the methyl esters trimethylsilyl ethers of aliphatic hydroxy acids. A facile method of double bond location. *Organic Mass Spectrometry,* 1**,** 593-611.

Ekweozor, C. M. & Strausz, O. P. 1982. 18,19-Bisnor-13βH, 14-αh-cheilanthane: a novel degraded tricyclic sesterterpenoid-type hydrocarbon from the athabasca oil sands. *Tetrahedron Letters,* 23**,** 2711-2714.

Enzell, C. R. 1966. Mass spectrometric studies of diterpenes 4-aromatic diterpenes. *Tetrahedron Letters,* 7**,** 2135-2143.

Fafet, A., Kergall, F., Da Silva, M. & Behar, F. 2008. Characterization of acidic compounds in biodegraded oils. *Organic Geochemistry,* 39**,** 1235-1242.

Filippini, M.-H. & Rodriguez, J. 1999. Synthesis of Functionalized Bicyclo[3.2.1]octanes and Their Multiple Uses in Organic Chemistry. *Chemical Reviews,* 99**,** 27-76.

Flego, C., Gigantiello, N., Parker Jr, W. O. & Calemma, V. 2009. A comprehensive two-dimensional gas chromatography coupled with quadrupole mass spectrometry approach for identification of C10 derivatives from decalin. *Journal of Chromatography A,* 1216**,** 2891-2899.

Forero, P., Suarez, F. J. & Dupont, A. 1996. Caustic treatment of jet fuel streams. *Petroleum Technology Quarterly***,** 43-48.

Frank, R. A., Fischer, K., Kavanagh, R., Burnison, B. K., Arsenault, G., Headley, J. V., Peru, K. M., Kraak, G. V. D. & Solomon, K. R. 2009. Effect of Carboxylic Acid

Content on the Acute Toxicity of Oil Sands Naphthenic Acids. *Environmental Science & Technology,* 43**,** 266-271.

Frank, R. A., Kavanagh, R., Burnison, B. K., Headley, J. V., Peru, K. M., Der Kraak, G. V. & Solomon, K. R. 2006. Diethylaminoethyl-cellulose clean-up of a large volume naphthenic acid extract. *Chemosphere,* 64**,** 1346-1352.

Frank, R. A., Kavanagh, R., Kent Burnison, B., Arsenault, G., Headley, J. V., Peru, K. M., Van Der Kraak, G. & Solomon, K. R. 2008. Toxicity assessment of collected fractions from an extracted naphthenic acid mixture. *Chemosphere,* 72**,** 1309-1314.

Frank, R. A., Roy, J. W., Bickerton, G., Rowland, S. J., Headley, J. V., Scarlett, A. G., West, C. E., Peru, K. M., Parrott, J. L., Conly, F. M. & Hewitt, L. M. 2014. Profiling Oil Sands Mixtures from Industrial Developments and Natural Groundwaters for Source Identification. *Environmental Science & Technology,* 48**,** 2660-2670.

Frysinger, G. S., Gaines, R. B., Xu, L. & Reddy, C. M. 2003. Resolving the Unresolved Complex Mixture in Petroleum-Contaminated Sediments. *Environmental Science & Technology,* 37**,** 1653-1662.

Gamal El-Din, M., Fu, H., Wang, N., Chelme-Ayala, P., Pérez-Estrada, L., Drzewicz, P., Martin, J. W., Zubot, W. & Smith, D. W. 2011. Naphthenic acids speciation and removal during petroleum-coke adsorption and ozonation of oil sands process-affected water. *Science of the Total Environment,* 409**,** 5119-5125.

Goheen, G. E. 1940. Conversion of Naphthenic Acids to Naphthene Hydrocarbons: Chemical Constitution. *Industrial & Engineering Chemistry,* 32**,** 503-508.

Golovkina, L. S., Rusinova, G. V. & Petrov, A. A. 1984. Mass Spectrometry of Saturated Hydrocarbons. *Russian Chemical Reviews,* 53**,** 870-887.

Golovkina, L. S., Rusinova, G. V., Sokolova, I. M., Matveeva, I. A., Gervitz, G. E. & Petrov, A. A. 1979. Structural and stereochemical factors in the mass spectrometry of mono- and dimethylbicyclo[3.3.1]nonanes. *Organic Mass Spectrometry,* 14**,** 629-634.

Goodenough, K. M., Moran, W. J., Raubo, P. & Harrity, J. P. A. 2004. Development of a Flexible Approach to Nuphar Alkaloids via Two Enantiospecific Piperidine-Forming Reactions. *The Journal of Organic Chemistry,* 70**,** 207-213.

Gordadze, G. N., Okunova, T. V., Giruts, M. V., Erdnieva, O. G. & Koshelev, V. N. 2011. Petroleum C15 polyalkyl substituted bicyclo[4.4.0]decanes (sesquiterpanes) as oil maturity indicators (illustrated by the example of Jurassic and Cretaceous oils of Kalmykia). *Petroleum Chemistry,* 51**,** 117-122.

Grewer, D. M., Young, R. F., Whittal, R. M. & Fedorak, P. M. 2010. Naphthenic acids and other acid-extractables in water samples from Alberta: What is being measured? *Science of The Total Environment,* 408**,** 5997-6010.

Gunstone, F. 2009. *The Chemistry of Oils and Fats: Sources, Composition, Properties and Uses*, Wiley.

Hála, S., Eyem, J., Burkhard, J. & Landa, S. 1970. Retention Indices of Adamantanes. *Journal of Chromatographic Science,* 8**,** 203-209.

Hall, P. B. & Douglas, A. G. The distribution of cyclic alkanes in two lacustrine deposits. *In:* BJOROY, M., ed. International Meeting on Organic Geochemistry, 1981 Bergen, Norway. Chichester: John Wiley & Sons, 576-587.

Han, X., MacKinnon, M. D. & Martin, J. W. 2009. Estimating the in situ biodegradation of naphthenic acids in oil sands process waters by HPLC/HRMS. *Chemosphere,* 76**,** 63-70.

Han, X., Scott, A. C., Fedorak, P. M., Bataineh, M. & Martin, J. W. 2008. Influence of Molecular Structure on the Biodegradability of Naphthenic Acids. *Environmental Science & Technology,* 42**,** 1290-1295.

Hancock, K. & Lochte, H. L. 1939. Acidic Constituents of a California Straight-run Gasoline Distillate. *Journal of the American Chemical Society,* 61**,** 2448-2452.

Hao, C., Headley, J. V., Peru, K. M., Frank, R., Yang, P. & Solomon, K. R. 2005. Characterization and pattern recognition of oil–sand naphthenic acids using comprehensive two-dimensional gas chromatography/time-of-flight mass spectrometry. *Journal of Chromatography A,* 1067**,** 277-284.

Harkness, R. W. & Bruun, J. H. 1940. Naphthenic Acids from Gulf Coast Petroleum: Composition Of Higher Boiling Acids. *Industrial & Engineering Chemistry,* 32**,** 499-502.

Hawthone, D. & Porter, Q. 1968. Naphtho[1,8-bc]thiophens. II. Mass spectrometry. *Australian Journal of Chemistry,* 21**,** 171-183.

He, Y., Patterson, S., Wang, N., Hecker, M., Martin, J. W., El-Din, M. G., Giesy, J. P. & Wiseman, S. B. 2012. Toxicity of untreated and ozone-treated oil sands process-affected water (OSPW) to early life stages of the fathead minnow (Pimephales promelas). *Water Research,* 46**,** 6359-6368.

Headley, J. V., Barrow, M. P., Peru, K. M., Fahlman, B., Frank, R. A., Bickerton, G., McMaster, M. E., Parrott, J. & Hewitt, L. M. 2011a. Preliminary fingerprinting of Athabasca oil sands polar organics in environmental samples using electrospray ionization Fourier transform ion cyclotron resonance mass spectrometry. *Rapid Communications in Mass Spectrometry,* 25**,** 1899-1909.

Headley, J. V., Kumar, P., Dalai, A., Peru, K. M., Bailey, J., McMartin, D. W., Rowland, S. M., Rodgers, R. P. & Marshall, A. G. 2014. Fourier Transform Ion Cyclotron Resonance Mass Spectrometry Characterization of Treated Athabasca Oil Sands Processed Waters. *Energy & Fuels.*

Headley, J. V. & McMartin, D. W. 2004. A Review of the Occurrence and Fate of Naphthenic Acids in Aquatic Environments. *Journal of Environmental Science and Health, Part A,* 39**,** 1989-2010.

Headley, J. V., Peru, K. M., Armstrong, S. A., Han, X., Martin, J. W., Mapolelo, M. M., Smith, D. F., Rogers, R. P. & Marshall, A. G. 2009a. Aquatic plant-derived changes in oil sands naphthenic acid signatures determined by low-, high- and ultrahigh-resolution mass spectrometry. *Rapid Communications in Mass Spectrometry,* 23**,** 515-522.

Headley, J. V., Peru, K. M. & Barrow, M. P. 2009b. Mass spectrometric characterization of naphthenic acids in environmental samples: A review. *Mass Spectrometry Reviews,* 28**,** 121-134.

Headley, J. V., Peru, K. M. & Barrow, M. P. 2015. Advances in mass spectrometric characterization of naphthenic acids fraction compounds in oil sands environmental samples and crude oil—a review. *Mass Spectrometry Reviews***,** n/a-n/a.

Headley, J. V., Peru, K. M., Barrow, M. P. & Derrick, P. J. 2007. Characterization of Naphthenic Acids from Athabasca Oil Sands Using Electrospray Ionization: The Significant Influence of Solvents. *Analytical Chemistry,* 79**,** 6222-6229.

Headley, J. V., Peru, K. M., Fahlman, B., Colodey, A. & McMartin, D. W. 2013a. Selective solvent extraction and characterization of the acid extractable fraction of Athabasca oils sands process waters by Orbitrap mass spectrometry. *International Journal of Mass Spectrometry,* 345–347**,** 104-108.

Headley, J. V., Peru, K. M., Janfada, A., Fahlman, B., Gu, C. & Hassan, S. 2011b. Characterization of oil sands acids in plant tissue using Orbitrap ultra-high resolution mass spectrometry with electrospray ionization. *Rapid Communications in Mass Spectrometry,* 25**,** 459-462.

Headley, J. V., Peru, K. M., Mohamed, M. H., Frank, R. A., Martin, J. W., Hazewinkel, R. R. O., Humphries, D., Gurprasad, N. P., Hewitt, L. M., Muir, D. C. G.,

Lindeman, D., Strub, R., Young, R. F., Grewer, D. M., Whittal, R. M., Fedorak, P. M., Birkholz, D. A., Hindle, R., Reisdorph, R., Wang, X., Kasperski, K. L., Hamilton, C., Woudneh, M., Wang, G., Loescher, B., Farwell, A., Dixon, D. G., Ross, M., Pereira, A. D. S., King, E., Barrow, M. P., Fahlman, B., Bailey, J., McMartin, D. W., Borchers, C. H., Ryan, C. H., Toor, N. S., Gillis, H. M., Zuin, L., Bickerton, G., McMaster, M., Sverko, E., Shang, D., Wilson, L. D. & Wrona, F. J. 2013b. Chemical fingerprinting of naphthenic acids and oil sands process waters—A review of analytical methods for environmental samples. *Journal of Environmental Science and Health, Part A,* 48**,** 1145-1163.

Hegazi, A. H. & Andersson, J. T. 2007. Limitations to GC-MS Determination of Sulfur-Containing Polycyclic Aromatic Compounds in Geochemical, Petroleum, and Environmental Investigations. *Energy & Fuels,* 21**,** 3375-3384.

Heintz, M., Gruselle, M., Druilhe, A. & Lefort, D. 1976. Relations entre structure chimique et données de rétention en chromatographie en phase gazeuse VI-Alcools et esters méthyliques de structures cycliques. *Chromatographia,* 9**,** 367-372.

Hell, C. & Medinger, E. 1874. Ueber das Vorkommen und die Zusammensetzung von Säuren im Rohpetroleum. *Berichte der deutschen chemischen Gesellschaft,* 7**,** 1216-1223.

Hell, C. & Medinger, E. 1877. Ueber die Oxydation der im Rohpetroleum enthaltenen Säure C11 H20 O2. *Berichte der deutschen chemischen Gesellschaft,* 10**,** 451-456.

Henry, J. D. 1905. *Baku: an eventful history*, A. Constable & Co., ltd.

Hindle, R., Noestheden, M., Peru, K. & Headley, J. 2013. Quantitative analysis of naphthenic acids in water by liquid chromatography–accurate mass time-of-flight mass spectrometry. *Journal of Chromatography A,* 1286**,** 166-174.

Hoering, T. 1970. The conversion of polar organic molecules in rock extracts to saturated hydrocarbons. *Carnegie Inst. Wash. Yearbook***,** 251-258.

Holder, R. W. & Matturro, M. G. 1977. Lithium triethylborohydride reduction of alkyl methanesulfonate esters. *The Journal of Organic Chemistry,* 42**,** 2166-2168.

Hollingsworth, B. V., Reichenbach, S. E., Tao, Q. & Visvanathan, A. 2006. Comparative visualization for comprehensive two-dimensional gas chromatography. *Journal of Chromatography A,* 1105**,** 51-58.

Holowenko, F. M., MacKinnon, M. D. & Fedorak, P. M. 2000. Methanogens and sulfate-reducing bacteria in oil sands fine tailings waste. *Canadian Journal of Microbiology,* 46**,** 927-937.

Holowenko, F. M., MacKinnon, M. D. & Fedorak, P. M. 2001. Naphthenic acids and surrogate naphthenic acids in methanogenic microcosms. *Water Research,* 35**,** 2595-2606.

Holowenko, F. M., MacKinnon, M. D. & Fedorak, P. M. 2002. Characterization of naphthenic acids in oil sands wastewaters by gas chromatography-mass spectrometry. *Water Research,* 36**,** 2843-2855.

Huang, R., McPhedran, K. N. & Gamal El-Din, M. 2015a. Ultra performance liquid chromatography ion mobility time-of-flight mass spectrometry characterization of naphthenic acids species from oil sands process-affected water. *Environmental Science & Technology*.

Huang, R., Sun, N., Chelme-Ayala, P., McPhedran, K. N., Changalov, M. & Gamal El-Din, M. 2015b. Fractionation of oil sands-process affected water using pH-dependent extractions: A study of dissociation constants for naphthenic acids species. *Chemosphere,* 127**,** 291-296.

Hughey, C. A., Rodgers, R. P., Marshall, A. G., Qian, K. & Robbins, W. K. 2002. Identification of acidic NSO compounds in crude oils of different geochemical

origins by negative ion electrospray Fourier transform ion cyclotron resonance mass spectrometry. *Organic Geochemistry,* 33**,** 743-759.

Hughey, C. A., Rodgers, R. P., Marshall, A. G., Walters, C. C., Qian, K. & Mankiewicz, P. 2004. Acidic and neutral polar NSO compounds in Smackover oils of different thermal maturity revealed by electrospray high field Fourier transform ion cyclotron resonance mass spectrometry. *Organic Geochemistry,* 35**,** 863-880.

Hwang, C. K., Li, W. S. & Nicolaou, K. C. 1984. Reactions of hydroxyl groups with tosylchloride-dimethylaminopyridine system. Direct synthesis of chlorides from hydroxycompounds. *Tetrahedron Letters,* 25**,** 2295-2296.

Jennerwein, M. K., Eschner, M., Gröger, T., Wilharm, T. & Zimmermann, R. 2014. Complete Group-Type Quantification of Petroleum Middle Distillates Based on Comprehensive Two-Dimensional Gas Chromatography Time-of-Flight Mass Spectrometry (GC×GC-TOFMS) and Visual Basic Scripting. *Energy & Fuels,* 28**,** 5670-5681.

Ji-Zhou, D., Vorkink, W. P. & Lee, M. L. 1993. Origin of long-chain alkylcyclohexanes and alkylbenzenes in a coal-bed wax. *Geochimica et Cosmochimica Acta,* 57**,** 837-849.

Jie, W., Cao, X., Chai, L., Liao, J., Huang, Y. & Tang, X. 2015. Quantification and characterization of naphthenic acids in soils from oil exploration areas in China by GC/MS. *Analytical Methods,* 7**,** 2149-2154.

Johnson, R. J., Smith, B. E., Sutton, P. A., McGenity, T. J., Rowland, S. J. & Whitby, C. 2011. Microbial biodegradation of aromatic alkanoic naphthenic acids is affected by the degree of alkyl side chain branching. *ISME J,* 5**,** 486-496.

Jolly, S. E., 'Naphthenic Acids' in 1985. *Concise Encyclopedia of Chemical Technology*, John Wiley & Sons.

Jones, D., Scarlett, A. G., West, C. E., Frank, R. A., Gieleciak, R., Hager, D., Pureveen, J., Tegelaar, E. & Rowland, S. J. 2013. Elemental and spectroscopic characterization of fractions of an acidic extract of oil sands process water. *Chemosphere,* 93**,** 1655-1664.

Jones, D., Scarlett, A. G., West, C. E. & Rowland, S. J. 2011. Toxicity of individual naphthenic acids to *Vibrio fischeri*. *Environmental Science & Technology,* 45**,** 9776-9782.

Jones, D., West, C. E., Scarlett, A. G., Frank, R. A. & Rowland, S. J. 2012. Isolation and estimation of the 'aromatic' naphthenic acid content of an oil sands process-affected water extract. *Journal of Chromatography A,* 1247**,** 171-175.

Jørgensen, E., Meyer, T. & Sydnes, L. K. 1990. Alkyl-substituted cis-bicyclo[3.3.0]octanes, potentially informative crude oil constituents. *Organic Geochemistry,* 16**,** 1039-1050.

Kabalka, G. W., Varma, M., Varma, R. S., Srivastava, P. C. & Knapp, F. F. 1986. The tosylation of alcohols. *The Journal of Organic Chemistry,* 51**,** 2386-2388.

Kamaluddin, M. & Zwiazek, J. J. 2002. Naphthenic acids inhibit root water transport, gas exchange and leaf growth in aspen (Populus tremuloides) seedlings. *Tree physiology,* 22**,** 1265-1270.

Kannel, P. R. & Gan, T. Y. 2012. Naphthenic acids degradation and toxicity mitigation in tailings wastewater systems and aquatic environments: A review. *Journal of Environmental Science and Health, Part A,* 47**,** 1-21.

Kavanagh, R. J., Burnison, B. K., Frank, R. A., Solomon, K. R. & Van Der Kraak, G. 2009. Detecting oil sands process-affected waters in the Alberta oil sands region using synchronous fluorescence spectroscopy. *Chemosphere,* 76**,** 120-126.

Kavanagh, R. J., Frank, R. A., Solomon, K. R. & Van Der Kraak, G. 2013. Reproductive and health assessment of fathead minnows (Pimephales promelas)

inhabiting a pond containing oil sands process-affected water. *Aquatic Toxicology,* 130–131**,** 201-209.

Kawaguchi, H., Li, Z., Masuda, Y., Sato, K. & Nakagawa, H. 2012. Dissolved organic compounds in reused process water for steam-assisted gravity drainage oil sands extraction. *Water Research,* 46**,** 5566-5574.

Kennedy, T. 1939. A Solid Naphthenic Acid from Iranian Petroleum. *Nature,* 144**,** 832.

Klamerth, N., Moreira, J., Li, C., Singh, A., McPhedran, K. N., Chelme-Ayala, P., Belosevic, M. & Gamal El-Din, M. 2015. Effect of ozonation on the naphthenic acids' speciation and toxicity of pH-dependent organic extracts of oil sands process-affected water. *Science of the Total Environment,* 506–507**,** 66-75.

Knotnerus, J. 1957. The chemical constitution of the higher naphthenic acids. *Journal of the Institute of Petrol,* 43**,** 307-312.

Knotnerus, J. & Bickel, A. F. 1964. Bicyclanes III. The acid-catalysed isomerization of perhydronaphthalene and perhydroindane. *Recueil des Travaux Chimiques des Pays-Bas,* 83**,** 400-413.

Knotnerus, J. & Schilling, H. 1964a. Bicyclanes IV. Preparation and properties of the methyl-cis-bicyclo[3.3.0]octanes. *Recueil des Travaux Chimiques des Pays-Bas,* 83**,** 414-428.

Knotnerus, J. & Schilling, H. 1964b. Bicyclanes: V. New syntheses of cis-bicyclo[3.3.0]octane and cis-bicyclo[3.3.0]oct-2-ene. *Recueil des Travaux Chimiques des Pays-Bas,* 83**,** 1185-1190.

Koike, L., Rebouças, L. M. C., Reis, F. d. A. M., Marsaioli, A. J., Richnow, H. H. & Michaelis, W. 1992. Naphthenic acids from crude oils of Campos Basin. *Organic Geochemistry,* 18**,** 851-860.

Kraft, P., Swift, K. A. D., Chemistry, R. S. o. & Industry, S. o. C. 2005. *Perspectives in Flavor and Fragrance Research*, Wiley.

Krishnamurthy, S. 1978. Rapid reduction of alkyl tosylates with lithium triethylborohydride. A convenient and advantageous procedure for the deoxygenation of simple and hindered alcohols. Comparison of various hydride reagents. *Journal of Organometallic Chemistry,* 156**,** 171-181.

Krishnamurthy, S. & Brown, H. C. 1976. Facile reduction of alkyl tosylates with lithium triethylborohydride. An advantageous procedure for the deoxygenation of cyclic and acyclic alcohols. *The Journal of Organic Chemistry,* 41**,** 3064-3066.

Kropp, K. G. & Fedorak, P. M. 1998. A review of the occurrence, toxicity,and biodegradation of condensed thiophenes found in petroleum. *Canadian Journal of Microbiology,* 44**,** 605-622.

Kuo, Y.-H., Chen, C.-H. & Huang, S.-L. 1998. A novel bicyclo [2. 2. 2] octane skeleton diterpene, obtunone, from the heartwood of Chamaecyparis obtusa var. formosana. *Chemical and pharmaceutical bulletin,* 46**,** 181-183.

Kuraš, M. & Hála, S. 1970. The use of a gas chromatograph-mass spectrometer for the analysis of complex hydrocarbon mixtures. *Journal of Chromatography A,* 51**,** 45-57.

Kwart, H. & Blazer, T. A. 1970. Analysis of mass spectral fragmentation patterns in various bicyclic alcohols. *The Journal of Organic Chemistry,* 35**,** 2726-2731.

Laredo, G. C., López, C. R., Álvarez, R. E. & Cano, J. L. 2004. Naphthenic acids, total acid number and sulfur content profile characterization in Isthmus and Maya crude oils. *Fuel,* 83**,** 1689-1695.

Larter, S. R., Solli, H. & Douglas, A. G. Phytol-containing Melanoidins and their Bearing on the Fate of Isoprenoid Structures in Sediments. *In:* BJOROY, M., ed. International Meeting on Organic Geochemistry, 1981 Bergen, Norway. Chichester: John Wiley & Sons, 513-523.

Leishman, C., Widdup, E. E., Quesnel, D. M., Chua, G., Gieg, L. M., Samuel, M. A. & Muench, D. G. 2013. The effect of oil sands process-affected water and naphthenic acids on the germination and development of Arabidopsis. *Chemosphere,* 93**,** 380-387.

Lengger, S. K., Scarlett, A. G., West, C. E., Frank, R. A., Hewitt, L. M., Milestone, C. B. & Rowland, S. J. 2015. Use of the distributions of adamantane acids to profile short-term temporal and pond-scale spatial variations in the composition of oil sands process-affected waters. *Environmental Science: Processes & Impacts*.

Lengger, S. K., Scarlett, A. G., West, C. E. & Rowland, S. J. 2013. Diamondoid diacids ('O4' species) in oil sands process-affected water. *Rapid Communications in Mass Spectrometry,* 27**,** 2648-2654.

Leung, S. S., MacKinnon, M. D. & Smith, R. E. H. 2003. The ecological effects of naphthenic acids and salts on phytoplankton from the Athabasca oil sands region. *Aquatic Toxicology,* 62**,** 11-26.

Li, M., Wang, T. G., Shi, S., Liu, K. & Ellis, G. S. 2014. Benzo[b]naphthothiophenes and alkyl dibenzothiophenes: Molecular tracers for oil migration distances. *Marine and Petroleum Geology,* 57**,** 403-417.

Lo, C. C., Brownlee, B. G. & Bunce, N. J. 2003. Electrospray-Mass Spectrometric Analysis of Reference Carboxylic Acids and Athabasca Oil Sands Naphthenic Acids. *Analytical Chemistry,* 75**,** 6394-6400.

Lochte, H. L. & Littmann, E. R. 1955. *Petroleum Acids and Bases,* New York, Chemical Pub. Co.

Lukashenko, I. M., Brodskii, Y. S., Musayev, I. A., Kurashova, E. K., Lebedevskaya, V. G. & Sanin, P. I. 1973. Mass spectra of methylbicyclo[4.4.0]decane stereoisomers. *Petroleum Chemistry U.S.S.R.,* 13**,** 38-44.

Lutnaes, B. F., Brandal, O., Sjoblom, J. & Krane, J. 2006. Archaeal C80 isoprenoid tetraacids responsible for naphthenate deposition in crude oil processing. *Organic & Biomolecular Chemistry,* 4**,** 616-620.

Lutnaes, B. F., Krane, J., Smith, B. E. & Rowland, S. J. 2007. Structure elucidation of C80, C81 and C82 isoprenoid tetraacids responsible for naphthenate deposition in crude oil production. *Organic & Biomolecular Chemistry,* 5**,** 1873-1877.

Luty, D. 2014. Synthesis of branched alkyl dibenzothiophenes. Plymouth University.

Mair, B. J., Eberly, P. E., Krouskop, N. C. & Rossini, F. D. 1958a. Separation of 132o to 138o C. Fraction of Petroleum. Bicycloparaffins in Gasoline Fraction of Petroleum. *Analytical Chemistry,* 30**,** 393-400.

Mair, B. J., Eberly, P. E., Li, K. & Rossini, F. D. 1958b. Polycycloparaffin Hydrocarbons in Petroleum. *Industrial & Engineering Chemistry,* 50**,** 115-116.

Manabe, S. & Nishino, C. 1983. Sex pheromonal activity of (+)-bornyl acetate and related compounds to the American cockroach. *Journal of Chemical Ecology,* 9**,** 433-448.

Mapolelo, M. M., Rodgers, R. P., Blakney, G. T., Yen, A. T., Asomaning, S. & Marshall, A. G. 2011. Characterization of naphthenic acids in crude oils and naphthenates by electrospray ionization FT-ICR mass spectrometry. *International Journal of Mass Spectrometry,* 300**,** 149-157.

Marentette, J. R., Frank, R. A., Bartlett, A. J., Gillis, P. L., Hewitt, L. M., Peru, K. M., Headley, J. V., Brunswick, P., Shang, D. & Parrott, J. L. 2015a. Toxicity of naphthenic acid fraction components extracted from fresh and aged oil sands process-affected waters, and commercial naphthenic acid mixtures, to fathead minnow (Pimephales promelas) embryos. *Aquatic Toxicology,* 164**,** 108-117.

Marentette, J. R., Frank, R. A., Hewitt, L. M., Gillis, P. L., Bartlett, A. J., Brunswick, P., Shang, D. & Parrott, J. L. 2015b. Sensitivity of walleye (Sander vitreus) and

fathead minnow (Pimephales promelas) early-life stages to naphthenic acid fraction components extracted from fresh oil sands process-affected waters. *Environmental Pollution,* 207**,** 59-67.

Martin, J. W., Barri, T., Han, X., Fedorak, P. M., El-Din, M. G., Perez, L., Scott, A. C. & Jiang, J. T. 2010. Ozonation of Oil Sands Process-Affected Water Accelerates Microbial Bioremediation. *Environmental Science & Technology,* 44**,** 8350 - 8356.

Martin, J. W., Han, X., Peru, K. M. & Headley, J. V. 2008. Comparison of high- and low-resolution electrospray ionization mass spectrometry for the analysis of naphthenic acid mixtures in oil sands process water. *Rapid Communications in Mass Spectrometry,* 22**,** 1919 - 1924.

McLafferty, F. W. 1963. *Mass spectrometry of organic ions,* New York, Academic Press.

McLafferty, F. W. & Gould, R. F. 2012. *Mass Spectral Correlations: Advances in Chemistry*, Literary Licensing, LLC.

McLafferty, F. W. & Tureček, F. 1993. *Interpretation of Mass Spectra*, University Science Books.

Meredith, W., Kelland, S. J. & Jones, D. M. 2000. Influence of biodegradation on crude oil acidity and carboxylic acid composition. *Organic Geochemistry,* 31**,** 1059-1073.

Misiti, T. M., Tezel, U. & Pavlostathis, S. G. 2014. Effect of Alkyl Side Chain Location and Cyclicity on the Aerobic Biotransformation of Naphthenic Acids. *Environmental Science & Technology,* 48**,** 7909-7917.

Mohamed, M. H., Wilson, L. D., Shah, J. R., Bailey, J., Peru, K. M. & Headley, J. V. 2015. A novel solid-state fractionation of naphthenic acid fraction components from oil sands process-affected water. *Chemosphere,* 136**,** 252-258.

Mohseni, P., Hahn, N. A., Frank, R. A., Hewitt, L. M., Hajibabaei, M. & Van Der Kraak, G. 2015. Naphthenic Acid Mixtures from Oil Sands Process-Affected Water Enhance Differentiation of Mouse Embryonic Stem Cells and Affect Development of the Heart. *Environmental Science & Technology,* 49**,** 10165-10172.

Moldowan, J. M., Seifert, W. K. & Gallegos, E. J. 1983. Identification of an extended series of tricyclic terpanes in petroleum. *Geochimica et Cosmochimica Acta,* 47**,** 1531-1534.

Mondello, L., Tranchida, P. Q., Dugo, P. & Dugo, G. 2008. Comprehensive two-dimensional gas chromatography-mass spectrometry: A review. *Mass Spectrometry Reviews,* 27**,** 101-124.

Mori, K., Nakahara, Y. & Matsui, M. 1972. Diterpenoid total synthesis—XIX : (±)-Steviol and erythroxydiol A: Rearrangements in bicyclooctane compounds. *Tetrahedron,* 28**,** 3217-3226.

Musayev, I. A., Bagrii, Y. I., Kurashova, E. K., Zaikin, V. G. & Sanin, P. I. 1983. Diamantane and 4-methyldiamantane in naphthalane and Russian crude oils. *Petroleum Chemistry U.S.S.R.,* 23**,** 182-185.

Nascimento, L. R., Rebouças, L. M. C., Koike, L., de A.M Reis, F., Soldan, A. L., Cerqueira, J. R. & Marsaioli, A. J. 1999. Acidic biomarkers from Albacora oils, Campos Basin, Brazil. *Organic Geochemistry,* 30**,** 1175-1191.

Noestheden, M. R., Headley, J. V., Peru, K. M., Barrow, M. P., Burton, L. L., Sakuma, T., Winkler, P. & Campbell, J. L. 2014. Rapid Characterization of Naphthenic Acids Using Differential Mobility Spectrometry and Mass Spectrometry. *Environmental Science & Technology,* 48**,** 10264-10272.

Nyakas, A., Han, J., Peru, K. M., Headley, J. V. & Borchers, C. H. 2013. Comprehensive Analysis of Oil Sands Processed Water by Direct-Infusion

Fourier-Transform Ion Cyclotron Resonance Mass Spectrometry with and without Offline UHPLC Sample Prefractionation. *Environmental Science & Technology,* 47**,** 4471-4479.

Nytoft, H. P., Samuel, O. J., Kildahl-Andersen, G., Johansen, J. E. & Jones, M. 2009. Novel C15 sesquiterpanes in Niger Delta oils: Structural identification and potential application as new markers of angiosperm input in light oils. *Organic Geochemistry,* 40**,** 595-603.

Omais, B., Crepier, J., Charon, N., Courtiade, M., Quignard, A. & Thiebaut, D. 2013. Oxygen speciation in upgraded fast pyrolysis bio-oils by comprehensive two-dimensional gas chromatography. *Analyst,* 138**,** 2258-2268.

Ortiz, X., Jobst, K. J., Reiner, E. J., Backus, S. M., Peru, K. M., McMartin, D. W., O'Sullivan, G., Taguchi, V. Y. & Headley, J. V. 2014. Characterization of Naphthenic Acids by Gas Chromatography-Fourier Transform Ion Cyclotron Resonance Mass Spectrometry. *Analytical Chemistry,* 86**,** 7666-7673.

Pavel, F. V. 1982. The Chemistry of Perfumes Based on Labdane Diterpenoids. *Russian Chemical Reviews,* 51**,** 644.

Payzant, J. D., Montgomery, D. S. & Strausz, O. P. 1986. Sulfides in petroleum. *Organic Geochemistry,* 9**,** 357-369.

Peakman, T. M., Farrimond, P., Brassell, S. C. & Maxwell, J. R. 1986. De-A-steroids in immature marine shales. *Organic Geochemistry,* 10**,** 779-789.

Pereira, A. S., Bhattacharjee, S. & Martin, J. W. 2013a. Characterization of Oil Sands Process-Affected Waters by Liquid Chromatography Orbitrap Mass Spectrometry. *Environmental Science & Technology,* 47**,** 5504-5513.

Pereira, A. S., Islam, M. D. S., Gamal El-Din, M. & Martin, J. W. 2013b. Ozonation degrades all detectable organic compound classes in oil sands process-affected water; an application of high-performance liquid chromatography/obitrap mass spectrometry. *Rapid Communications in Mass Spectrometry,* 27**,** 2317-2326.

Pereira, A. S. & Martin, J. W. 2014. On-Line Solid Phase Extraction–HPLC–Orbitrap Mass Spectrometry for Screening and Quantifying Targeted and Non-Targeted Analytes in Oil Sands Process-Affected Water and Natural Waters in the Athabasca Oil Sands Region. OSRIN Report No.

Peters, K. E., Walters, C. C. & Moldowan, J. M. 2005a. *The Biomarker Guide: Biomarkers and Isotopes in the Environment and Human History*, Cambridge University Press.

Peters, K. E., Walters, C. C. & Moldowan, J. M. 2005b. *The Biomarker Guide: Biomarkers and Isotopes in the Environment and Human History*, Cambridge University Press.

Petersen, M. A. & Grade, H. 2011. Analysis of Steam Assisted Gravity Drainage Produced Water using Two-Dimensional Gas Chromatography with Time-of-Flight Mass Spectrometry. *Industrial & Engineering Chemistry Research,* 50**,** 12217-12224.

Petrov, A. A. 1987. *Petroleum Hydrocarbons,* Berlin Heidelberg, Springer-Verlag.

Philp, R. P. 1985. *Fossil fuel biomarkers: applications and spectra*, Elsevier.

Piccolo, L., Nassreddine, S., Toussaint, G. & Geantet, C. 2010. Discussion on "A comprehensive two-dimensional gas chromatography coupled with quadrupole mass spectrometry approach for identification of C10 derivatives from decalin" by C. Flego, N. Gigantiello, W.O. Parker, Jr., V. Calemma [J. Chromatogr. A 1216 (2009) 2891]. *Journal of Chromatography A,* 1217**,** 5872-5873.

Polyakova, A. A., Khramova, E. V., Bagrii, Y. I., Tsitsugina, N. N., Lukashenko, I. M., Frid, T. Y. & Sanin, P. I. 1973. Mass spectrometric study of alkyladamantanes. *Petroleum Chemistry U.S.S.R.,* 13**,** 1-10.

Porter, Q. N. 1985. *Mass Spectrometry of Heterocyclic Compounds*, Wiley.

Presset, M., Coquerel, Y. & Rodriguez, J. 2012. Syntheses and Applications of Functionalized Bicyclo[3.2.1]octanes: Thirteen Years of Progress. *Chemical Reviews,* 113**,** 525-595.

Qian, K., Robbins, W. K., Hughey, C. A., Cooper, H. J., Rodgers, R. P. & Marshall, A. G. 2001. Resolution and Identification of Elemental Compositions for More than 3000 Crude Acids in Heavy Petroleum by Negative-Ion Microelectrospray High-Field Fourier Transform Ion Cyclotron Resonance Mass Spectrometry. *Energy & Fuels,* 15**,** 1505-1511.

Quagraine, E. K., Headley, J. V. & Peterson, H. G. 2005. Is Biodegradation of Bitumen a Source of Recalcitrant Naphthenic Acid Mixtures in Oil Sands Tailing Pond Waters? *Journal of Environmental Science and Health, Part A,* 40**,** 671-684.

Quesnel, D. M., Bhaskar, I. M., Gieg, L. M. & Chua, G. 2011. Naphthenic acid biodegradation by the unicellular alga Dunaliella tertiolecta. *Chemosphere,* 84**,** 504-511.

Ranade, V. S., Consiglio, G. & Prins, R. 2000. Functional-Group-Directed Diastereoselective Hydrogenation of Aromatic Compounds. 21. *The Journal of Organic Chemistry,* 65**,** 1132-1138.

Reichenbach, S. E., Kottapalli, V., Ni, M. & Visvanathan, A. 2005. Computer language for identifying chemicals with comprehensive two-dimensional gas chromatography and mass spectrometry. *Journal of Chromatography A,* 1071**,** 263-269.

Reichenbach, S. E., Ni, M., Kottapalli, V. & Visvanathan, A. 2004. Information technologies for comprehensive two-dimensional gas chromatography. *Chemometrics and Intelligent Laboratory Systems,* 71**,** 107-120.

Reichenbach, S. E., Ni, M., Zhang, D. & Ledford Jr, E. B. 2003. Image background removal in comprehensive two-dimensional gas chromatography. *Journal of Chromatography A,* 985**,** 47-56.

Reinardy, H. C., Scarlett, A. G., Henry, T. B., West, C. E., Hewitt, L. M., Frank, R. A. & Rowland, S. J. 2013. Aromatic Naphthenic Acids in Oil Sands Process-Affected Water, Resolved by GCxGC-MS, Only Weakly Induce the Gene for Vitellogenin Production in Zebrafish (Danio rerio) Larvae. *Environmental Science & Technology,* 47**,** 6614-6620.

Requejo, A. G., Allan, J., Creaney, S., Gray, N. R. & Cole, K. S. 1992. Aryl isoprenoids and diaromatic carotenoids in Paleozoic source rocks and oils from the Western Canada and Williston Basins. *Organic Geochemistry,* 19**,** 245-264.

Riebeek, H. 2011. *NASA Earth Observatory: Athabasca Oil Sands* [Online]. Available: http://earthobservatory.nasa.gov/Features/WorldOfChange/athabasca.php [Accessed 21/09/2015].

Rockhold, W. T. 1955. Toxicity of naphthenic acids and their metal salts. *AMA archives of industrial health,* 12**,** 477.

Rogers, V. V., Wickstrom, M., Liber, K. & MacKinnon, M. D. 2002. Acute and Subchronic Mammalian Toxicity of Naphthenic Acids from Oil Sands Tailings. *Toxicological Sciences,* 66**,** 347-355.

Ross, M. S., Pereira, A. d. S., Fennell, J., Davies, M., Johnson, J., Sliva, L. & Martin, J. W. 2012. Quantitative and Qualitative Analysis of Naphthenic Acids in Natural Waters Surrounding the Canadian Oil Sands Industry. *Environmental Science & Technology,* 46**,** 12796-12805.

Rossini, F. & Mair, B. 1958. Summary of 159 Hydrocarbons Isolated from One Representative Petroleum. *Industrial & Engineering Chemistry Chemical & Engineering Data Series,* 3**,** 141-145.

Rowland, S. J., Ahad, J. M. E., Frank, R. A., Hewitt, L. M., Lengger, S. K., Belt, S. T., Wilde, M. J., Marriott, P., Pye, T., Pureveen, J., Scarlett, A. G., Tegelaar, E. W.,

West, C. E., Henry, T. B. & Dummett, C. J. [unpublished]. Isolation, spectral identification, synthesis and influences on toxicity, of individual aromatic petorleum acids. *corresponding author institution: Petroleum and Environmental Geochemisry Group, Plymouth University.

Rowland, S. J., Clough, R., West, C. E., Scarlett, A. G., Jones, D. & Thompson, S. 2011a. Synthesis and mass spectrometry of some tri-and tetracyclic naphthenic acids. *Rapid Communications in Mass Spectrometry,* 25**,** 2573-2578.

Rowland, S. J., Jones, D., Scarlett, A. G., West, C. E., Hin, L. P., Boberek, M., Tonkin, A., Smith, B. E. & Whitby, C. 2011b. Synthesis and toxicity of some metabolites of the microbial degradation of synthetic naphthenic acids. *Science of The Total Environment,* 409**,** 2936-2941.

Rowland, S. J., Pereira, A. S., Martin, J. W., Scarlett, A. G., West, C. E., Lengger, S. K., Wilde, M. J., Pureveen, J., Tegelaar, E. W., Frank, R. A. & Hewitt, L. M. 2014a. Mass spectral characterisation of a polar, esterified fraction of an organic extract of an oil sands process water. *Rapid Communications in Mass Spectrometry,* 28**,** 2352-2362.

Rowland, S. J., Scarlett, A. G., Jones, D., West, C. E. & Frank, R. A. 2011c. Diamonds in the rough: Identification of individual naphthenic acids in oil sands process water. *Environmental Science & Technology,* 45**,** 3154-3159.

Rowland, S. J., West, C. E., Jones, D., Scarlett, A. G., Frank, R. A. & Hewitt, L. M. 2011d. Steroidal Aromatic 'Naphthenic Acids' in Oil Sands Process-Affected Water: Structural Comparisons with Environmental Estrogens. *Environmental Science & Technology,* 45**,** 9806-9815.

Rowland, S. J., West, C. E., Scarlett, A. G., Ho, C. & Jones, D. 2012. Differentiation of two industrial oil sands process-affected waters by two-dimensional gas chromatography/mass spectrometry of diamondoid acid profiles. *Rapid Communications in Mass Spectrometry,* 26**,** 572-576.

Rowland, S. J., West, C. E., Scarlett, A. G. & Jones, D. 2011e. Identification of individual acids in a commercial sample of naphthenic acids from petroleum by two-dimensional comprehensive gas chromatography/mass spectrometry. *Rapid Communications in Mass Spectrometry,* 25**,** 1741-1751.

Rowland, S. J., West, C. E., Scarlett, A. G., Jones, D., Boberek, M., Pan, L., Ng, M., Kwong, L. & Tonkin, A. 2011f. Monocyclic and monoaromatic naphthenic acids: synthesis and characterisation. *Environmental Chemistry Letters,* 9**,** 525-533.

Rowland, S. J., West, C. E., Scarlett, A. G., Jones, D. & Frank, R. A. 2011g. Identification of individual tetra- and pentacyclic naphthenic acids in oil sands process water by comprehensive two-dimensional gas chromatography/mass spectrometry. *Rapid Communications in Mass Spectrometry,* 25**,** 1198-1204.

Rowland, S. M., Robbins, W. K., Corilo, Y. E., Marshall, A. G. & Rodgers, R. P. 2014b. Solid-Phase Extraction Fractionation To Extend the Characterization of Naphthenic Acids in Crude Oil by Electrospray Ionization Fourier Transform Ion Cyclotron Resonance Mass Spectrometry. *Energy & Fuels,* 28**,** 5043-5048.

Rowling, R. 2012. *Venezuela Passes Saudis to Hold World's Biggest Oil Reserves* [Online]. Available: http://www.bloomberg.com/news/2012-06-13/venezuela-overtakes-saudis-for-largest-oil-reserves-bp-says-1-.html [Accessed 12/12/2012].

Rush, D., Jaeschke, A., Hopmans, E. C., Geenevasen, J. A. J., Schouten, S. & Damsté, J. S. S. 2011. Short chain ladderanes: Oxic biodegradation products of anammox lipids. *Geochimica et Cosmochimica Acta,* 75**,** 1662-1671.

Rusinova, G. V., Golovkina, L. S., Novikova, N. B., Sokolova, I. M. & Petrov, A. A. 1987. Mass spectrometric study of dimethyl-substituted spiro[4.5]decanes and

spiro[5.5]undecanes. *Bulletin of the Academy of Sciences of the USSR, Division of chemical science,* 36**,** 1626-1630.

Rusinova, G. V., Matveeva, I. A., Sokolova, I. M., Golovkina, L. S. & Belikova, N. A. 1981. Mass spectrometric investigation and synthesis of hydrocarbons of the bicyclo[2.2.1] heptane series with the compositions C10H18 and C11H20. *Bulletin of the Academy of Sciences of the USSR, Division of chemical science,* 30**,** 239-244.

Ruzicka, L., Seidel, C. F. & Brugger, W. 1947. Veilchenriechstoffe. 17 Mitteilung. Über den Abbau des Tetrahydro-irons. *Helvetica Chimica Acta,* 30**,** 2168-2198.

Ruzicka, L., Seidel, C. F., Schinz, H. & Pfeiffer, M. 1942. Veilchenriechstoffe. (12. Mitteilung). Über den Abbau des Irons mit Ozon und Chromsäure. *Helvetica Chimica Acta,* 25**,** 188-205.

Sanin, P. I. 1976. Petroleum Hydrocarbons. *Russian Chemical Reviews,* 45**,** 684.

Sargent, H. 1942. The Synthesis of 3,3,4-trimethylcyclopentanone. II. *The Journal of Organic Chemistry,* 07**,** 154-157.

Scarlett, A. G., Clough, R., West, C., Lewis, C. A., Booth, A. M. & Rowland, S. J. 2011. Alkylnaphthalenes: Priority Pollutants or Minor Contributors to the Poor Health of Marine Mussels? *Environmental Science & Technology,* 45**,** 6160-6166.

Scarlett, A. G., Reinardy, H. C., Henry, T. B., West, C. E., Frank, R. A., Hewitt, L. M. & Rowland, S. J. 2013. Acute toxicity of aromatic and non-aromatic fractions of naphthenic acids extracted from oil sands process-affected water to larval zebrafish. *Chemosphere,* 93**,** 415-420.

Scarlett, A. G., West, C. E., Jones, D., Galloway, T. S. & Rowland, S. J. 2012. Predicted toxicity of naphthenic acids present in oil sands process-affected waters to a range of environmental and human endpoints. *Science of The Total Environment,* 425**,** 119-127.

Schaub, T. M., Jennings, D. W., Kim, S., Rodgers, R. P. & Marshall, A. G. 2007. Heat-Exchanger Deposits in an Inverted Steam-Assisted Gravity Drainage Operation. Part 2. Organic Acid Analysis by Electrospray Ionization Fourier Transform Ion Cyclotron Resonance Mass Spectrometry. *Energy & Fuels,* 21**,** 185-194.

Schleyer, P. v. R. & Nicholas, R. D. 1961. Further examples of the adamantane rearrangement. *Tetrahedron Letters,* 2**,** 305-309.

Scott, A. C., MacKinnon, M. D. & Fedorak, P. M. 2005. Naphthenic acids in athabasca oil sands tailings waters are less biodegradable than commercial naphthenic acids. *Environ Sci Technol,* 39**,** 8388-94.

Scott, A. C., Zubot, W., MacKinnon, M. D., Smith, D. W. & Fedorak, P. M. 2008. Ozonation of oil sands process water removes naphthenic acids and toxicity. *Chemosphere,* 71**,** 156-160.

Seifert, W. K. 1969. Effect of phenols on the interfacial activity of crude oil (California) carboxylic acids and the identification of carbazoles and indoles. *Analytical Chemistry,* 41**,** 562-568.

Seifert, W. K. 1975. Carboxylic acids in petroleum and sediments. *Fortschr Chem Org Naturst,* 32**,** 1-49.

Seifert, W. K., Gallegos, E. J. & Teeter, R. M. 1972. Proof of structure of steroid carboxylic acids in a California petroleum by deuterium labeling, synthesis, and mass spectrometry. *Journal of the American Chemical Society,* 94**,** 5880-5887.

Seifert, W. K. & Howells, W. G. 1969. Interfacially active acids in a California crude oil. Isolation of carboxylic acids and phenols. *Analytical Chemistry,* 41**,** 554-562.

Seifert, W. K. & Teeter, R. M. 1969. Preparative thin-layer chromatography and high-resolution mass spectrometry of crude oil carboxylic acids. *Analytical Chemistry,* 41**,** 786-795.

Seifert, W. K. & Teeter, R. M. 1970a. Identification of polycyclic aromatic and heterocyclic crude oil carboxylic acids. *Analytical Chemistry,* 42**,** 750-758.

Seifert, W. K. & Teeter, R. M. 1970b. Identification of polycyclic naphthenic, mono-, and diaromatic crude oil carboxylic acids. *Analytical Chemistry,* 42**,** 180-189.

Seifert, W. K., Teeter, R. M., Howells, W. G. & Cantow, M. J. R. 1969. Analysis of crude oil carboxylic acids after conversion to their corresponding hydrocarbons. *Analytical Chemistry,* 41**,** 1638-1647.

Selifonov, S. A. 1992. Microbial oxidation of adamantanone by Pseudomonas putida carrying the camphor catabolic plasmid. *Biochemical and Biophysical Research Communications,* 186**,** 1429-1436.

Shang, D., Kim, M., Haberl, M. & Legzdins, A. 2013. Development of a rapid liquid chromatography tandem mass spectrometry method for screening of trace naphthenic acids in aqueous environments. *Journal of Chromatography A,* 1278**,** 98-107.

Shellie, R., Mondello, L., Marriott, P. & Dugo, G. 2002. Characterisation of lavender essential oils by using gas chromatography–mass spectrometry with correlation of linear retention indices and comparison with comprehensive two-dimensional gas chromatography. *Journal of Chromatography A,* 970**,** 225-234.

Singh, V., Pal, S. & Mobin, S. M. 2006. Cycloaddition between Electron-Deficient π-Systems, Photochemical and Radical-Induced Reactions: A Novel, General, and Stereoselective Route to Polyfunctionalized Bridged Bicyclo[2.2.2]octanes, Bicyclo[3.3.0]octanes, Bicyclo[4.2.0]octanes, and Tricyclo[4.3.1.03,7]decanes. *The Journal of Organic Chemistry,* 71**,** 3014-3025.

Sinninghe Damsté, J. S., Kock-van Dalen, A. C. & de Leeuw, J. W. 1988. Identification of long-chain isoprenoid alkylbenzenes in sediments and crude oils. *Geochimica et Cosmochimica Acta,* 52**,** 2671-2677.

Sinninghe Damsté, J. S., Rijpstra, W. I. C., Geenevasen, J. A. J., Strous, M. & Jetten, M. S. M. 2005. Structural identification of ladderane and other membrane lipids of planctomycetes capable of anaerobic ammonium oxidation (anammox). *FEBS Journal,* 272**,** 4270-4283.

Slavcheva, E., Shone, B. & Turnbull, A. 1999. Review of naphthenic acid corrosion in oilrefining. *British Corrosion Journal,* 34**,** 125-131.

Smith, B. E., Lewis, C. A., Belt, S. T., Whitby, C. & Rowland, S. J. 2008. Effects of Alkyl Chain Branching on the Biotransformation of Naphthenic Acids. *Environmental Science & Technology,* 42**,** 9323-9328.

Smith, B. E. & Rowland, S. J. 2008. A derivatisation and liquid chromatography/electrospray ionisation multistage mass spectrometry method for the characterisation of naphthenic acids. *Rapid Communications in Mass Spectrometry,* 22**,** 3909-3927.

Smith, B. E., Sutton, P. A., Lewis, C. A., Dunsmore, B., Fowler, G., Krane, J., Lutnaes, B. F., Brandal, Ø., Sjöblom, J. & Rowland, S. J. 2007. Analysis of 'ARN' naphthenic acids by high temperature gas chromatography and high performance liquid chromatography. *Journal of Separation Science,* 30**,** 375-380.

Sokolova, I. M., Berman, S. S., Abryutina, N. N. & Petrov, A. A. 1989. Natural concentrates of Bi- and tricyclic naphthenes. *Chemistry and Technology of Fuels and Oils,* 25**,** 233-235.

Srikrishna, A. & Ravi, G. 2008. A stereoselective total synthesis of (−)-seychellene. *Tetrahedron,* 64**,** 2565-2571.

St. John, W. P., Rughani, J., Green, S. A. & McGinnis, G. D. 1998. Analysis and characterization of naphthenic acids by gas chromatography–electron impact mass spectrometry of tert.-butyldimethylsilyl derivatives. *Journal of Chromatography A,* 807**,** 241-251.

Stanford, L. A., Kim, S., Klein, G. C., Smith, D. F., Rodgers, R. P. & Marshall, A. G. 2007. Identification of Water-Soluble Heavy Crude Oil Organic-Acids, Bases, and Neutrals by Electrospray Ionization and Field Desorption Ionization Fourier Transform Ion Cyclotron Resonance Mass Spectrometry. *Environmental Science & Technology,* 41**,** 2696-2702.

Stout, S. A., Uhler, A. D. & McCarthy, K. J. 2005. Middle Distillate Fuel Fingerprinting Using Drimane-Based Bicyclic Sesquiterpanes. *Environmental Forensics,* 6**,** 241-251.

Strausz, O. P., Morales-Izquierdo, A., Kazmi, N., Montgomery, D. S., Payzant, J. D., Safarik, I. & Murgich, J. 2010. Chemical Composition of Athabasca Bitumen: The Saturate Fraction. *Energy & Fuels,* 24**,** 5053-5072.

Sutton, P. A., Lewis, C. A. & Rowland, S. J. 2005. Isolation of individual hydrocarbons from the unresolved complex hydrocarbon mixture of a biodegraded crude oil using preparative capillary gas chromatography. *Organic Geochemistry,* 36**,** 963-970.

Swigert, J. P., Lee, C., Wong, D. C. L., White, R., Scarlett, A. G., West, C. E. & Rowland, S. J. 2015. Aquatic hazard assessment of a commercial sample of naphthenic acids. *Chemosphere,* 124**,** 1-9.

Tollefsen, K. E., Petersen, K. & Rowland, S. J. 2012. Toxicity of Synthetic Naphthenic Acids and Mixtures of These to Fish Liver Cells. *Environmental Science & Technology,* 46**,** 5143-5150.

Toor, N. S., Franz, E. D., Fedorak, P. M., MacKinnon, M. D. & Liber, K. 2013a. Degradation and aquatic toxicity of naphthenic acids in oil sands process-affected waters using simulated wetlands. *Chemosphere,* 90**,** 449-458.

Toor, N. S., Han, X., Franz, E., MacKinnon, M. D., Martin, J. W. & Liber, K. 2013b. Selective biodegradation of naphthenic acids and a probable link between mixture profiles and aquatic toxicity. *Environmental Toxicology and Chemistry,* 32**,** 2207-2216.

Turner, M. S. & Smith, P. C. 2005. Controls On Soap Scale Formation, Including Naphthenate Soaps - Drivers And Mitigation. Society of Petroleum Engineers.

van Graas, G., de Lange, F., de Leeuw, J. W. & Schenck, P. A. 1982. De-A-steroid ketones and de-A-aromatic steroid hydrocarbons in shale indicate a novel diagenetic pathway. *Nature,* 299**,** 437-439.

Vendeuvre, C., Ruiz-Guerrero, R., Bertoncini, F., Duval, L. & Thiébaut, D. 2007. Comprehensive Two-Dimensional Gas Chromatography for Detailed Characterisation of Petroleum Products. *Oil & Gas Science and Technology - Rev. IFP,* 62**,** 43-55.

von R. Schleyer, P. 1957. A SIMPLE PREPARATION OF ADAMANTANE. *Journal of the American Chemical Society,* 79**,** 3292-3292.

Vorob'eva, N. S., Aref'ev, O. A., Yepishev, V. I. & Petrov, A. A. 1971. Kinetics and mechanism of formation of hydrocarbons of the adamantane series from tricyclic bridged hydrocarbons. *Petroleum Chemistry U.S.S.R.,* 11**,** 37-46.

Vorob'eva, N. S., Zemskova, Z. K., Pekh, T. I. & Petrov, A. A. 1986. Diterpenoid tetracyclic hydrocarbons of petroleum. *Petroleum Chemistry U.S.S.R.,* 26**,** 69-76.

Wang, G., Shi, S., Wang, P. & Wang, T. G. 2013. Analysis of diamondoids in crude oils using comprehensive two-dimensional gas chromatography/time-of-flight mass spectrometry. *Fuel,* 107**,** 706-714.

Wang, X. & Kasperski, K. L. 2010. Analysis of naphthenic acids in aqueous solution using HPLC-MS/MS. *Analytical Methods,* 2**,** 1715-1722.

Wang, Z., Yang, C., Hollebone, B. & Fingas, M. 2006. Forensic Fingerprinting of Diamondoids for Correlation and Differentiation of Spilled Oil and Petroleum Products. *Environmental Science & Technology,* 40**,** 5636-5646.

Waples, D. W. 1985. *Geochemistry in Petroleum Exploration*, Springer Netherlands.

Watson, J. S., Jones, D. M., Swannell, R. P. J. & van Duin, A. C. T. 2002. Formation of carboxylic acids during aerobic biodegradation of crude oil and evidence of microbial oxidation of hopanes. *Organic Geochemistry, 33*, 1153-1169.

Watson, N. E., Davis, J. M. & Synovec, R. E. 2007. Observations on "Orthogonality" in Comprehensive Two-Dimensional Separations. *Analytical Chemistry, 79*, 7924-7927.

Weggler, B. A., Gröger, T. & Zimmermann, R. 2014. Advanced scripting for the automated profiling of two-dimensional gas chromatography-time-of-flight mass spectrometry data from combustion aerosol. *Journal of Chromatography A, 1364*, 241-248.

Wei, Z., Michael Moldowan, J., Dahl, J., Goldstein, T. P. & Jarvie, D. M. 2006. The catalytic effects of minerals on the formation of diamondoids from kerogen macromolecules. *Organic Geochemistry, 37*, 1421-1436.

West, C. E., Jones, D., Scarlett, A. G. & Rowland, S. J. 2011. Compositional heterogeneity may limit the usefulness of some commercial naphthenic acids for toxicity assays. *Science of The Total Environment, 409*, 4125-4131.

West, C. E., Pureveen, J., Scarlett, A. G., Lengger, S. K., Wilde, M. J., Korndorffer, F., Tegelaar, E. W. & Rowland, S. J. 2014a. Can two-dimensional gas chromatography/mass spectrometric identification of bicyclic aromatic acids in petroleum fractions help to reveal further details of aromatic hydrocarbon biotransformation pathways? *Rapid Communications in Mass Spectrometry, 28*, 1023-1032.

West, C. E., Scarlett, A. G., Pureveen, J., Tegelaar, E. W. & Rowland, S. J. 2013. Abundant naphthenic acids in oil sands process-affected water: studies by synthesis, derivatisation and two-dimensional gas chromatography/high-resolution mass spectrometry. *Rapid Communications in Mass Spectrometry, 27*, 357-365.

West, C. E., Scarlett, A. G., Tonkin, A., O'Carroll-Fitzpatrick, D., Pureveen, J., Tegelaar, E., Gieleciak, R., Hager, D., Petersen, K., Tollefsen, K.-E. & Rowland, S. J. 2014b. Diaromatic sulphur-containing 'naphthenic' acids in process waters. *Water Research, 51*, 206-215.

Whitesell, J. K. & Minton, M. A. 1987. *Stereochemical analysis of alicyclic compounds by C-13 NMR spectroscopy*, Chapman and Hall.

Wilde, M. J. & Rowland, S. J. 2015. Structural Identification of Petroleum Acids by Conversion to Hydrocarbons and Multidimensional Gas Chromatography-Mass Spectrometry. *Analytical Chemistry, 87*, 8457-8465.

Wilde, M. J., West, C. E., Scarlett, A. G., Jones, D., Frank, R. A., Hewitt, L. M. & Rowland, S. J. 2015. Bicyclic naphthenic acids in oil sands process water: Identification by comprehensive multidimensional gas chromatography–mass spectrometry. *Journal of Chromatography A, 1378*, 74-87.

Wingert, W. S. 1992. G.c.-m.s. analysis of diamondoid hydrocarbons in Smackover petroleums. *Fuel, 71*, 37-43.

Yi, Y., Birks, S. J., Cho, S. & Gibson, J. J. 2015. Characterization of organic composition in snow and surface waters in the Athabasca Oil Sands Region, using ultrahigh resolution Fourier transform mass spectrometry. *Science of The Total Environment, 518–519*, 148-158.

Yoshida, Y., Sakakura, Y., Aso, N., Okada, S. & Tanabe, Y. 1999. Practical and efficient methods for sulfonylation of alcohols using Ts(Ms)Cl/Et3N and catalytic Me3H·HCl as combined base: Promising alternative to traditional pyridine. *Tetrahedron, 55*, 2183-2192.

Zaikin, V. & Halket, J. M. 2009. *A Handbook of Derivatives for Mass Spectrometry*, IM Publications.

Zeigler, C., Schantz, M., Wise, S. & Robbat, A. 2012. Mass Spectra and Retention Indexes for Polycyclic Aromatic Sulfur Heterocycles and Some Alkylated Analogs. *Polycyclic Aromatic Compounds,* 32**,** 154-176.

Zelinsky, N. 1911. Über Dehydrogenisation durch Katalyse. *Berichte der deutschen chemischen Gesellschaft,* 44**,** 3121-3125.

Zelinsky, N. 1924. Über die chemische Natur des Naphthensäuren (I.). *Berichte der deutschen chemischen Gesellschaft (A and B Series),* 57**,** 42-51.

Zelinsky, N. & Pokrowskaja, E. 1924. Über die chemische Natur der Naphthensäuren (II.). *Berichte der deutschen chemischen Gesellschaft (A and B Series),* 57**,** 51-58.

Zhao, B., Currie, R. & Mian, H. 2012. Catalogue of Analytical Methods for Naphthenic Acids Related to Oil Sands Operations. *Oil Sands Research and Information Network, University of Alberta, School of Energy and the Environment, Edmonton, Alberta. OSRIN Report No. TR-21.*

Zoex. What is GCxGC? 2015. Available: http://zoex.com/products/zx2-thermal-modulator/ ['Accessed' 20/01/2016].